Universitat
de les Illes Balears

DOCTORAL THESIS
2024

SPONGE COMMUNITIES OF THE BALEARIC ISLANDS: ADVANCING KNOWLEDGE ON THEIR TAXONOMY, DISTRIBUTION, AND ECOLOGY

Julio Alberto Díaz Sancho

Universitat
de les Illes Balears

INSTITUTO
ESPAÑOL DE
OCEANOGRAFÍA

CSIC
CONSEJO SUPERIOR DE INVESTIGACIONES CIENTÍFICAS

DOCTORAL THESIS
2024

Doctoral Programme in Marine Ecology

SPONGE COMMUNITIES OF THE BALEARIC ISLANDS: ADVANCING KNOWLEDGE ON THEIR TAXONOMY, DISTRIBUTION, AND ECOLOGY

Julio Alberto Díaz Sancho

Thesis Supervisor: Enric Massutí Sureda
Thesis Supervisor: Francesc Ordines
Thesis Supervisor: Pere Ferriol Bunyola
Thesis tutor: Guillem Mateu Vicens

Doctor by the Universitat de les Illes Balears

¿Quién ha podido sondear jamas las profundidades del abismo?, solo dos entre todos los hombres tienen el derecho a responder ahora. El capitán Nemo y yo.

Agraiments

Aquesta tesi no hauria estat possible sense el suport dels meus directors, que des de un bon principi confiaren amb jo i que me donaren responsabilitat i llibertat per encuidarme d'aquest grup tan emprenyós d'animals. Tampoc sense la confiança que va depositar en jo el Govern de les Illes Balears quan me concediren la beca FPI.

Per suposat, la tesi tampoc hagues anat enlloc sense totes les campanyes oceanogràfiques a les que he pogut participar i que m'han permes ficar mà a unes mostres increibles. Per això, volia agrair a tots els companys que féren posible aquestes campanyes, novament a n'Enric i en Xisco, però també a na Teresa, n'Elena i n'Aída, així com a na Bea i a tot els altres companys d'equip. A més, també vui agrair el suport als capitans i les tripulacions dels vaixells de recerca *Ángeles Alvariño*, *Ramon Margalef*, *Sarmiento de Gamboa* y *Miguel Oliver* per les bones acollides i el bon treball dut a terme.

Tot i que la major part de la tesi s'ha desenvolupat a partir de mostres obtingudes a partir de campanyes oceanogràfiques, també hi ha una part important que s'ha fet a partir de mostres litorals. Durant totes aquestes excursions i sortides de busseig he tengut la sort de contar amb l'ajud desinteressat de na Bel, en Joan, en Joan Lluís, en Xavier, n'Aída (novament) i en Guillem. Inclús mumare, mumpare i n'Auba, m'han acompanyat a segons quins forats.

També he de donar les gràcies a nen Sergio i al grup de Genètica Humana, per la ajuda i la sempre bona acollida al laboratòri.

A en Pere, per introduirme al món de les esponges.

Als companys de l'estació Jaume Ferrer de Menorca, per tot lo que m'han ajudat cada vegada que hi he anat a fer un experiment.

Moltes gràcies Dr. Ferran Hierro, per les incontables hores de SEM.

I would like to express my gratitude for the warm reception I received at Uppsala University during the winter of 2020. It proved to be one of the most enriching experiences throughout my entire Ph.D., where I thoroughly enjoyed engaging in scientific discussions with Paco and contributing to the ongoing Tetractinellid chapter.

I extend my sincere thanks to Professor Jean Vacelet, who consistently offered assistance in sharing materials from the Station Marine d'Endoume. I am also grateful of Nicole Boury-Esnault, who shared kind words with me during the taxonomy workshop in Genova and to Christine Morrow and Bernard Picton, for their assistance in providing Atlantic material and offering guidance on taxonomic matters.

I finalment, moltes gràcies a total la meva familia, i sobretot a na Bel, que ha estat present tan en els bons com en els mals moments, i m'ha ajudat moltissim en acabar aquesta tesi.

Funding

The project LIFE IP INTEMARES is coordinated by the Biodiversity Foundation of the Spanish Ministry for the Ecological Transition and the Demographic Challenge and receives financial support from the European Union's LIFE program (LIFE15 IPE ES 012).

MEDITS surveys are co-funded by the European Union through the European Maritime and Fisheries Fund (EMFF), within the National Program of collection, management and use of data in the fisheries sector and support for scientific advice regarding the Common Fisheries Policy.

The project 18-ESMARES2-CIRCA, included in the program "Asesoramiento científico-técnico para la protección del medio marino: Evaluación y seguimiento de las Estrategias Marinas, Seguimiento de los espacios marinos protegidos de competencia estatal (2018-2021)", is co-funded by Spanish Ministry for the Ecological Transition and the Demographic Challenge.

The Project BIO023 "Una aproximación taxonómica integrativa para mejorar el conocimiento de la biodiversidad marina del Archipiélago Balear" was co-funded by Regional Government of the Balearic Islands and framed within the Complementary Plans Recovery, Transformation and Resilience Plan.

Julio A. Diaz was supported by a predoctoral contract co-funded by the Regional Government of the Balearic Islands and the European Social Fund (FPI/2178/2018) and received a mobility grant (MOB_008_2019) by the *Conselleria de Fons Europeus, Universitat i Cultura del Govern de les Illes Balears* that allowed J. A. Díaz to carry out a stay at the Uppsala Universiy, and a mobility grant by the Càtedra de la Mar (Fundación Iberostar), to present the results of the chapter 4.6. in the World Sponge Conference that took place in Leiden, the Netherlands.

Sergio Ramírez-Amaro was supported by a postdoctoral contract, co-funded by the Regional Government of the Balearic Islands and the European Social Fund.

Paco Cárdenas was supported in part by the SponBIODIV project, a 2021-2022 BiodivProtect joint call for research proposals, under the Biodiversa+ Partnership co-funded by the European Commission and the Swedish funding organization FORMAS (project#2022-01709) and by the European Union's Horizon 2020 research and innovation program through the SponGES project (grant agreement No. 679849).

List of Manuscripts

This Phd is a compendium of the following scientific articles:

Sponge diversity

- Díaz JA, Ramírez-Amaro S, Ordines F, Cárdenas P, Ferriol P, Terrasa B, Massutí E. 2020. Poorly known sponges in the Mediterranean with the detection of some taxonomic inconsistencies. *Journal of the Marine Biological Association of the United Kingdom*, 1008, 1247-1260. (Chapter 4.1).

- Díaz JA, Ramírez-Amaro S, Ordines F. 2021. Sponges of Western Mediterranean seamounts: New genera, new species and new records. *PeerJ*, 9, e11879. (Chapter 4.2).

- Díaz JA, Ordines F, Massutí E, Cárdenas P. 2024. From caves to seamounts: the hidden diversity of tetractinellid sponges from the Balearic Islands, with the description of eight new species. *PeerJ*., In Press. (Chapter 4.3).

- Díaz JA, Ordines F, Massutí E. Submitted. First record of the recently described *Axinella venusta* Idan, Shefer, Feldstein & Ilan, 2021 (Demospongiae: Axinellidae) in the western Mediterranean. (Chapter 4.4).

- Díaz JA. Submitted. First documented report and barcoding of the sponge *Placospongia decorticans* (Hanitsch, 1895) in the North-Western Mediterranean. (Chapter 4.5).

Sponge communities

- Díaz JA, Ordines F, Farriols MT, Melo-Aguilar C, Massutí E. 2024. Sponge assemblages in fishing grounds and seamounts of the Balearic Islands (western Mediterranean). *Deep Sea Research I*, 203, 104211. (Chapter 4.6).

Acronyms and abbreviations

AM	Ausias March
BI	Bayesian Inference
COI	Cytochrome Oxidase subunit I
EB	Emile Baudot
GSA	Geographical Sub-Area
GOC	GOC-73
LEBA	Levantino-Balear demarcation
LIW	Levantine Intermediate Water
ML	Maximum likelihood
MaC	Mallorca channel
MeC	Menorca channel
MEDITS	Mediterranean International Bottom Trawl Surveys
RD	Rock dredge
ROV	Remote operated vehicle
R/V	Research vessel
SEM	Scanning electron microscope
SAC	Special Areas of Conservation
SO	Ses Olives
SCI	Sites of Community Importance
SIMPER	Similarity Percentage
TFG	Trawl fishing grounds

Museum and collections abbreviations

BELUM: Ulster Museum Belfast (Northern Ireland, UK).
CEAB.POR.BIO: Porifera Collection at the Centre d'Estudis Avançats de Blanes (Spain).
CFM-IEOMA: Colección de Fauna Marina del Centro Oceanográfico de Málaga (Spain).
COLETA: Coleção de Referência Biológica Marinha dos Açores of the Department of Oceanography and Fisheries, University of the Azores (Portugal).
CPORCANT: Colección de Poríferos del Cantábrico del Centro Oceanográfico de Gijón (Spain).
HBOI: Harbor Branch Oceanographic Institute, Florida Atlantic University (Fort Pierce, FL, USA).
MHNCUP: Museu de História Natural e da Ciência da Universidade do Porto (Portugal).
MNCN: Museo Nacional de Ciencias Naturales (Madrid, Spain).
MNHN: Muséum National d'Histoire Naturelle (Paris, France).
MSNG: Museo Civico di Storia Naturale "G. Doria" (Genoa, Italy).
NHM: Natural History Museum (London, UK).
PC: Personal collection of P. Cárdenas, Uppsala University (Sweden).
RMNH: Rijksmuseum van Natuurlijke Historie, Naturalis Biodiversity Center (Leiden, The Netherlands).
SME: Station Marine d'Endoume (Marseille, France).
UPSZMC/UPSZTY: Zoological collections at the Museum of Evolution (Uppsala, Sweden).
ZMBN: Zoological collections at the Bergen Museum (Bergen, Norway).
ZMUC: Zoological Museum, University of Copenhagen (Denmark).

Summary

The waters surrounding the Balearic Islands exhibit high oligotrophy, primarily due to the scarcity of rainfall, the karstic composition of their soils, and the absence of rivers. Fluvial contributions and terrigenous sediment input into the sea are limited, favoring high water transparency, a factor that influences marine benthic communities. One of the most important groups within these communities is sponges, which colonize a significant portion of the Balearic Archipelago's seabed, ranging from shallow waters to great depths.

Despite considering previous studies, due to the significant biodiversity of this group and the complexity of the habitats in the Islands, the available information is still incomplete. Moreover, this lack of information becomes more evident as depth increases, as the study of the circalittoral and bathyal zones is limited by technical and logistical issues. The objective of this doctoral thesis is to improve the current knowledge of sponges in the Balearic Islands, focusing on their biodiversity. This involves providing taxonomic and molecular descriptions of new, infrequent, poorly known, or previously unreported species in this area. Additionally, the study aims to explore the biological communities they form and the influence of environmental factors and fishing exploitation.

The data and samples used come from various oceanographic research campaigns: (i) MEDITS, conducted from 2016 to 2021 using an experimental trawl net to assess demersal resources and benthic ecosystems of the continental shelf and slope of the Balearic Islands; (ii) INTEMARES, carried out from 2018 to 2020 using rock dredges, epibenthic sledges, experimental trawl nets, and ROVs to study benthic communities and habitats of the submarine mountains in the Mallorca Channel and the continental shelf of the Menorca Channel; and (iii) CIRCA-LEBA-1121, conducted in 2021 using an epibenthic sled to study the biodiversity and habitats of circalittoral and bathyal sedimentary bottoms in the Levantine-Balearic demarcation. Sponge samples have also been collected from various marine coastal caves in Mallorca through scuba diving with autonomous and lung-powered diving equipment. In total, samples have been taken at 590 stations ranging from 45 to 1068 m depth and at 7 coastal caves between 0 and 10 m depht. A collection of over 2800 samples has been established, with 350 species identified, mainly at the species and genus levels.

Sponges were identified using macroscopic, microscopic, and genetic characters. Biomass estimation was also performed, standardized to the sampled seafloor area. Multivariate analyses of species or taxon presence-absence matrices per sampling station allowed the identification and characterization of sponge communities and the species contributing most to them in terms of specific richness, biomass, and taxonomic composition. Additionally, through distance-based redundancy analysis the effects of biotic and abiotic factors and the fishing impact on these communities has been modeled.

The results highlight the limited existing information on sponges in the Mediterranean, as this thesis describes 9 new species and a new genus. Numerous species have also been cited, some of which were not previously known in the Mediterranean, its western basin, or the Balearic Islands. On the other hand, systematic inconsistencies have been

identified in several studied taxonomic groups, and modifications have been proposed to address them. Regarding communities, it has been observed that they are strongly structured bathymetrically, with maximum diversity and biomass in red algae beds, extending to depths of up to 90 m in the Balearic platform and even more than 130 m in the case of the Emile Baudot and Ausias March peaks. It also has been confirmed that other factors such as currents and fishing impact these communities. Moreover, a comparison between the insular seabeds exploited by trawl fishing and the unexploited submarine mountains has revealed differences in diversity, biomass, taxonomic composition, and bathymetric distribution of mesophotic communities.

Keywords: Benthic invertebrates, Sponges, Sponge Communities, Integrative Taxonomy, Submarine Mountains, Emile Baudot, Ausias March, Ses Olives, Menorca Channel, Mesophotic Communities, Coastal Caves.

Resum

Comunitats d'esponges de les Illes Balears: Millora del coneixement sobre la seva taxonomia, distribució i ecologia

Les aigües de les Illes Balears presenten una elevada oligotrofia, principalment a causa de la manca de pluges, la composició càrstica dels seus sòls i la falta de rius. Les aportacions fluvials i de sediments terrígens al mar són escasses, la qual cosa afavoreix una gran transparencia de les aigües, un fet que condiciona les comunitats bentòniques marines. Un dels grups més importants d'aquestes comunitats són les esponges, que colonitzen la major part dels fons de l'Arxipèlag Balear, des de les aigües més somes fins les grans profunditats.

Tot i considerant els estudis previs, a causa de la gran biodiversitat d'aquest grup i la complexitat dels hàbitats de les Illes, la informació disponible és encara incompleta. A més, aquesta manca d'informació es fa més evident a mida que s'incrementa la fondària, ja que l'estudi dels pisos circalitoral i batial es veu limitat per qüestions tècniques i logístiques. L'objectiu d'aquesta tesi doctoral és millorar el coneixement actual sobre les esponges de les Illes Balears, tant des del punt de vista de la seva diversitat, aportant descripcions taxonòmiques i moleculars d'espècies noves, infrequents, poc conegudes o no citades fins ara en aquesta àrea, com de les comunitats biològiques que conformen, i la influència que tenen sobre aquestes els factors ambientals i l'explotació pesquera.

Les dades i mostres utilitzades provenen de diverses campanyes de recerca oceanogràfica: (i) MEDITS, realitzades del 2016 al 2021 amb una xarxa de ròssec experimental per avaluar els recursos demersals i els ecosistemes bentònics de la plataforma continental i el talús de les Illes Balears; (ii) INTEMARES, realitzades del 2018 al 2020 amb draga de roca, patí epi-bentònic, xarxa de ròssec experimental i ROV, per l'estudi de les comunitats i els hàbitats bentònics de les muntanyes submarines del Canal de Mallorca i de la plataforma continental del Canal de Menorca; i (iii) CIRCA-LEBA-1121, realitzada el 2021 amb patí epi-bentònic i trineu fotogramètric, per estudiar la biodiversitat i els hàbitats dels fons sedimentaris circalitorals i batials de la demarcació Llevantina-Balear. També s'han recol·lectat mostres d'esponges a diverses coves litorals marines de Mallorca mitjançat busseig amb escafandre autònoma i a pulmó. S'han mostrejat un total de 590 estacions entre 45 i 1068 m de fondària i a 7 coves litorals entre 0 i 10 m. S'ha creat una col·lecció de més de 2800 mostres i s'han identificat 350 espècies, principalment a nivel d'espècie i de gènere.

Les esponges s'han identificat mitjançant l'ús de caràcters macroscòpics, microscòpics i genètics, i també s'ha estimat la seva biomassa, estandarditzada a la superficie de fons marí mostrejada. Les anàlisis multivariants de les matrius de presència-absència d'espècies o tàxons per estació de mostreig ha permés identificar les seves comunitats i les espècies que més hi contribueixen, i caracteritzar-les quant a la seva riquesa específica, biomassa i composició taxonòmica. A més, s'ha calculat un anàlisi de redundancia per tal d'identificar l'efecte que tenen sobre aquestes comunitats tant factors biòtics i abiòtics com l'explotació pesquera.

Els resultats posen de manifest l'escassa informació existent que es té sobre les esponges a la Mediterrània, ja que s'han descrit un gènere i 9 espècies noves per a la ciència. A més s'han citat nombroses espècies, algunes de les quals no eren conegudes fins ara a la Mediterrània, a la seva conca occidental o a les Illes Balears. D'altra banda, s'han identificat una sèrie de incongruències sistemàtiques en diversos dels grups taxonòmics estudiats i s'han proposat modificacions per solucionar-les. Pel que fa a les comunitats, s'ha observat que estan marcadament estructurades batimètricament, amb una diversitat i biomassa màximes als fons d'algues vermelles, que a la plataforma de les Balears es distribueixen fins als 90 m de fondària, i fins i tot a més de 130 m en els cims de les muntanyes submarines Emile Baudot i Ausias March. També s'ha constatat que altres factors com els corrents marins i l'explotació pesquera afecten aquestes comunitats. Per altra banda, la comparació entre els fons insulars explotats per la pesca de ròssec i els fons no explotats de les muntanyes submarines ha revelat diferències en la diversitat, biomassa, composició taxonòmica i distribució batimètrica de les comunitats mesofòtiques.

Paraules clau: Invertebrats Bentònics, Porífers, Comunitats d'Esponges, Taxonomia Integrativa, Muntanyes Submarines, Emile Baudot, Ausias March, Ses Olives, Menorca Channel, Comunitats Mesofòtiques, Coves Litorals.

Resumen

Comunidades de esponjas de las Islas Baleares: Mejora del conocimiento sobre su taxonomía, distribución y ecología

Las aguas de las Islas Baleares presentan una elevada oligotrofia, principalmente debido a la escasez de lluvias, la composición cárstica de sus suelos y la inexistencia de ríos. Las aportaciones fluviales y de sedimentos terrígenos al mar son escasas, lo que favorece una gran transparencia de las aguas, un hecho que condiciona las comunidades bentónicas marinas. Las esponjas son uno de los grupos más importantes de estas comunidades, ya que colonizan la mayor parte de los fondos del Archipiélago Balear, desde las aguas más someras hasta las grandes profundidades.

A pesar de considerar los estudios previos, debido a la gran biodiversidad de este grupo y la complejidad de los hábitats de las islas, la información disponible aún es incompleta. Además, esta falta de información se hace más evidente a medida que aumenta la profundidad, ya que el estudio de los pisos circalitoral y batial se ve limitado por cuestiones técnicas y logísticas. El objetivo de esta tesis doctoral es mejorar el conocimiento actual de las esponjas de las Islas Baleares, tanto desde el punto de vista de su biodiversidad, aportando descripciones taxonómicas y moleculares de especies nuevas, poco frecuentes, poco conocidas o incluso no citadas hasta ahora en esta área, como de las comunidades biológicas que conforman, y la influencia que tienen sobre estas los factores ambientales y la explotación pesquera.

Los datos y muestras utilizados provienen de diversas campañas de investigación oceanográfica: (i) MEDITS, realizadas del 2016 al 2021 con una red de arrastre experimental para evaluar los recursos demersales y los ecosistemas bentónicos de la plataforma continental y el talud de las Islas Baleares; (ii) INTEMARES, realizadas del 2018 al 2020 con draga de roca, patín epi-bentónico, red de arrastre experimental y ROV, para estudiar las comunidades y hábitats bentónicos de las montañas submarinas del Canal de Mallorca y la plataforma continental del Canal de Menorca; y (iii) CIRCA-LEBA-1121, realizada en 2021 con patín epi-bentónico, para el estudio de la biodiversidad y los hábitats de los fondos sedimentarios circalitorales y batiales de la demarcación Levantina-Balear. También se han recolectado muestras de esponjas en diversas cuevas litorales marinas de Mallorca mediante buceo con escafandra autónoma y a pulmón. Se han tomado muestras en un total de 590 estaciones entre 45 y 1068 m y en 7 cuevas litorales entre 0 y 10 m. Se ha creado una colección de más de 2800 muestras y se han identificado 350 especies, principalmente a nivel de especie y género.

Las esponjas se han identificado mediante el uso de caracteres macroscópicos, microscópicos y genéticos, y también se ha estimado su biomasa, estandarizada a la superficie de fondo marino muestreada. Los análisis multivariantes de las matrices de presencia-ausencia de especies o taxones por estación de muestreo han permitido identificar sus comunidades y caracterizarlas en cuanto a su riqueza específica, biomasa y composición taxonómica. Además, mediante un análisis de redundáncia se ha modelado el efecto de los factores bióticos y abióticos, como el impacto de la pesca, sobre estas comunidades.

Los resultados ponen de manifiesto la escasa información que se tiene sobre las esponjas en el Mediterráneo, ya que en esta tesis se han descrito 9 especies y un nuevo género para la ciencia. Además se han citado numerosas especies, algunas de las cuales no eran conocidas hasta ahora en el Mediterráneo, su cuenca occidental o en las Islas Baleares. Por otra parte, se han identificado incongruencias sistemáticas en varios de los grupos taxonómicos estudiados, y se han propuesto modificaciones para solucionarlas. En cuanto a las comunidades, se ha observado que están marcadamente estructuradas batimétricamente, con una biodiversidad y biomasa máximas en los fondos de algas rojas, que en la plataforma de las Baleares se distribuyen hasta los 90 m de profundidad, e incluso a más de 130 m en el caso de las cimas de Emile Baudot y Ausias March. También se ha constatado que otros factores como las corrientes y la pesca impactan en estas comunidades. Por otro lado, la comparación entre los fondos insulares explotados por la pesca de arrastre y los no explotados de las montañas submarinas ha revelado diferencias en la diversidad, biomasa, composición taxonómica y distribución batimétrica de las comunidades mesofóticas.

Palabras clave: Invertebrados bentónicos, Esponjas, Comunidades de Esponjas, Taxonomía Integrativa, Montes Submarinos, Emile Baudot, Ausias March, Ses Olives, Canal de Menorca, Comunidades Mesofóticas, Cuevas Litorales.

TABLE OF CONTENTS

GENERAL INTRODUCTION

1. General introduction

1.1. The phylum Porifera

Sponges are one of the most important and yet often overlooked components of marine benthic biocenosis (*Bell, 2008*). As the oldest extant metazoans, they have lived for at least 560 million years, surviving throughout major mass extinctions and colonizing all kinds of marine and freshwater environments. Sponges are found in many different habitats from polar to tropical and temperate waters, and from the intertidal zone to bathyal depths, including caves, rocky outcrops, muddy and sandy bottoms (*Van Soest et al., 2012*). In many ecosystems sponges play an important role, yet they can be habitat engineers, increasing the three-dimensional complexity of the grounds and providing substrate to other benthic invertebrates and refuge for fish, crustaceans and mollusks, including species of commercial interest (*Maldonado et al., 2016, Pham et al., 2019*). In certain instances, sponges aggregate forming sponge grounds or sponge gardens, singular and heterogeneous communities that boost the local diversity (*Beazley et al., 2013*). Additionallu, sponges play an important role in the food webs, acting as food supply (*Meylan, 1988*), and also participating in the benthopelagic coupling by recycling dissolved organic matter which is particulated and made available again for higher trophic levels. This sponge loop, analogous to the microbial loop, appears to be important for the functioning of biological hotspots in oligotrophic areas, such as coral reefs, where nutrients are scarce and the recycling of organic matter becomes essential for sustaining life (*de Goeij et al., 2013*).

Besides their ecological roles, sponges have been important to humans. In the Mediterranean, dating back to the time of the Egyptian civilization, sponges have been used for personal hygiene, household and metall cleaning, protection and even as a mean of drinking, as they can absorb liquid without draining. In the northern Atlantic, sponges accumulated on the beaches after storms, were also used as fertilizer for agricultural fields. Sponge fishing in Greece dates back to ancient times, mainly in the Dodecanese Islands, where Kalymnos is known as the sponge fishermen's island and sponges are referred to as "the gold of Kalymnos”. At present, they are the most prominent marine source of natural products, with a large number of potential applications in fields like medicine or industrial biotechnology (*Steffen et al., 2021*).

The sponge body plan is very simple, with tissues lacking the specialization level that characterize the rest of animals. They have an external layer, the pinacoderm; an inner layer, the mesohyl; and an aquiferous system composed of pores, canals and choanocyte chambers. Choanocyte chambers are lined by choanocytes, a special cell type with a central flagellum that regularly beats creating negative water pressure inside the chamber. This negative pressure induces the surrounding water to enter inside the sponge body, circulating through the canals and choanocyte chambers, carrying food particles that are captured by the same choanocytes. Once processed, the water flows outside and exits in large orifices called oscula (*Simpson, 1984*). In carnivorous sponges, the aquiferous system is reduced or abscent and feeding strategy has evolved

towards predation (*Vacelet, 2007*). The body structure is maintained with a network of supporting elements of organic and/or inorganic nature (collagen fibers, and calcium carbonate or silicon spicules, respectively). This simplicity often results in an ill-defined, amorphous shape, which implies a lack of a clear set of morphological diagnostic characters. Moreover, sponge morphology is influenced by environmental conditions such as exposure to sunlight, turbidity of water, currents, and depth (*Bidder, 1923; Kaandorp & De Kluijver, 1992; McDonald et al., 2002*), and modulated through complex morphogenetic pathways (*Wiens et al., 2008*).

Therefore, the morphological variability within the phylum Porifera challenges the delineation of both high and low level taxa. Often, sympatric sibling species with minor morphological differences are masked under a "species complex" name (*Blanquer & Uriz, 2008*). Conversely, in other cases, high levels of intraspecific plasticity blurs the boundaries between populations and species (*Schmitt et al., 2005*).

Besides the extreme variability in spicule shapes and sizes, they are relatively well-conserved between taxa and far more reliable than macroscopic traits such as shape or color. Hence, spicules have traditionally been used as the main character for sponge classification. The heterogeneity of spicule types present in a given species depends on its phylogenetic group: some having a large set (i.e. Class Hexactinellida, Orders Poecilosclerida and Tetractinellida) while others being very limited (i.e. Class Calcarea, Orders Haplosclerida, Suberitida). The study of skeletal architecture, or the way that the skeletal elements (spicules and organic fibers) are oriented in the body is often used to complement the identification. The last is specially important in groups like Haplosclerida which are very speciose but have paucity of spicules. Besides, some groups of sponges lack spicules, and its classification relies on the study of its organic fibers (*Hooper & Van Soest, 2002*).

However, the use of spicules in sponge taxonomy and systematics shows several limitations due to their size, shape and even presence is influenced by environmental factors such as depth, temperature and nutrient availability, and, to a certain degree, by intraspecific variability (*Uriz et al., 2003a, 2003b; Erpenbeck et al., 2006*). In recent years, the *integrative taxonomy* postulates the use of two or more sets of characters for taxonomic diagnosis, including spicules morphology, embryology, ecology, reproduction, molecular markers, chemical markers, geographic distribution, etc (*Padial et al., 2010; Cardenas et al., 2012*). Molecular markers, particulary the COI and the 28S, are the most widely used in sponge research. However, those markers have limitations, yet its rate of mutation fixation may be too low, and in some cases having no resolution at species level. Therefore, genetics must always be used together with morphology, and viceversa.

Sponge taxonomy is a challenging and time-consuming discipline that requires an extensive learning process. Additionally, taxonomic studies often face insufficient funding, and academic impact metrics tend to disadvantage taxonomic papers and journals. Consequently, the global number of sponge taxonomists remains low

(*Cárdenas et al., 2012*).This triggers a chain reaction that extends upwards all the levels of research: if no specialists are working on the faunistic lists, biodiversity is not accurately estimated, which is detrimental to biogeographical studies and the assessment of anthropogenic impacts on communities, and hence, their management.

Based on the Worl Porifera Database (www.marinespecies.org/porifera), there are 9640 valid species of recent sponges, with the vast majority (83%) belonging to the class Demospongiae (*Van Soest et al. 2012* and *de Voogd et al., 2024*). According to *Van Soest et al. (2012)*, the number of sponge taxa increases steadily at a rate of 35-87 each year. In the Mediterranean, about 680 species have been reported, including approximately 265 endemic species (*Pansini & Longo, 2003; Voultsiadou, 2009; Van Soest et al., 2012; Xavier & Van Soest, 2012*). Moreover, new species and new geographic records are periodically reported in this sea (e.g. *Vacelet et al., 2007; Corriero et al., 2015; Bertolino et al., 2013, 2015; Sitjà & Maldonado, 2014; Melis et al., 2016*). Knowledge on Mediterranean sponge fauna come mainly from species living in shallow habitats accessible through scuba diving. Less is known about the circalittoral and bathyal domains (*Danovaro et al., 2010*), although these deep ecosystems may harbour important communities of filter feeding animals, like corals or sponges.

1.2. Sponge studies from the Balearic Islands

The first taxonomic studies of the sponge fauna in the Balearic Islands date back to the late 19th and the early 20th centuries. *Lackschewitz* (*1886*) conducted a first study on the calcareous sponges from Menorca and *Ferrer-Hernández* (*1916, 1921, 1934*), after participating in pioneering surveys headed by Odon de Buen around the Palma, Cabrera Archipelago and Maó, described several new species, rising the known sponge fauna of the Islands to more than 20 species. Then, there is a gap in the literature until the 1980's, when several authors relaunched sponge research, with most of this work focusing on shallow water fauna. *Bibiloni & Gili (1982)* conducted a first study on cave sponges, mapping the sponge communities of a large cave in Cala Rajada, reporting 27 sponge species distributed on a light gradient, a research latter extended in *Bibiloni et al. (1989),* which reported 45 species from caves of the same locality. Maria Antonia Bibiloni's work culminated in her Doctoral Thesis (*Bibiloni, 1990*) which also studied the sponges from the littoral and bottom trawl fishing grounds, increasing the number of known species in the Balearic Archipelago to almost 200. Other works in the Balearic caves were conducted by *Vacelet & Uriz (1991)* and *Gràcia et al. (2005*, *2014)*. Regarding the study of deep-sea sponges, *Uriz & Rosell (1990)* collected species from 100 to 10750 m depth, reporting two new species for the Mediterranean and expanding the bathymetric range of *Polymastia tissieri* (Vacelet, 1961). *Maldonado et al. (2015)* presented a first insight into the fauna from the Mallorca Channel seamounts, also describing an interesting deep-sea reef formed by the lithistid *Leiodermatium pfeifferae* (Carter, 1873). Also noteworthy is the contribution made by *Traveset (1991)* on the report of *Epidathya fluviatilis* (Linnaeus, 1759), the only freshwater sponge cited in the Balearic Archipelago.

Regarding the study of the sponges from a community-level perspective, *Bibiloni (1990)* provided an initial approach to the bathymetric distribution of sponges, using parameters like diversity, substrate coverage, dry weight and organic matter. The results were then compared with sponge communities in Tossa de Mar and the Medes Islands, on the Catalan coast. Later, *Uriz et al. (1992)* studied the sponges from the Cabrera Archipelago, while *Martí et al., 2004* compared the sponge communities from Sa Cova Blava, a cave in the Cabrera Archipelago, with those from La Cova dels Misidacis, in the Medes Iislands and *Santin et al. (2018)* and *Santin et al. (2019)* examined the deep-sea sponge communities of the Menorca Channel. Additionally, *Díaz et al. (2020)* performed a time-series experiment with the model sponge *Aplysina aerophoba* (Nardo, 1833) and *Guzzetti et al. (2019)* reported the invasive calcareous sponge *Paraleucilla magna* Klautau, Monteiro & Borojevic, 2004.

1.3. Study area

The Balearic promontory

The Balearic Promontory, a structural elevation 348 km in length, 105 km wide and from 1000 to 2000 m high with respect to the surrounding basins, is separated from continental coast by 40-90 miles and 800-2000 m depth, being among the most isolated insular areas in the western Mediterranean. It is composed of four main islands and several islets, channels and seamounts (Fig. 1.1).

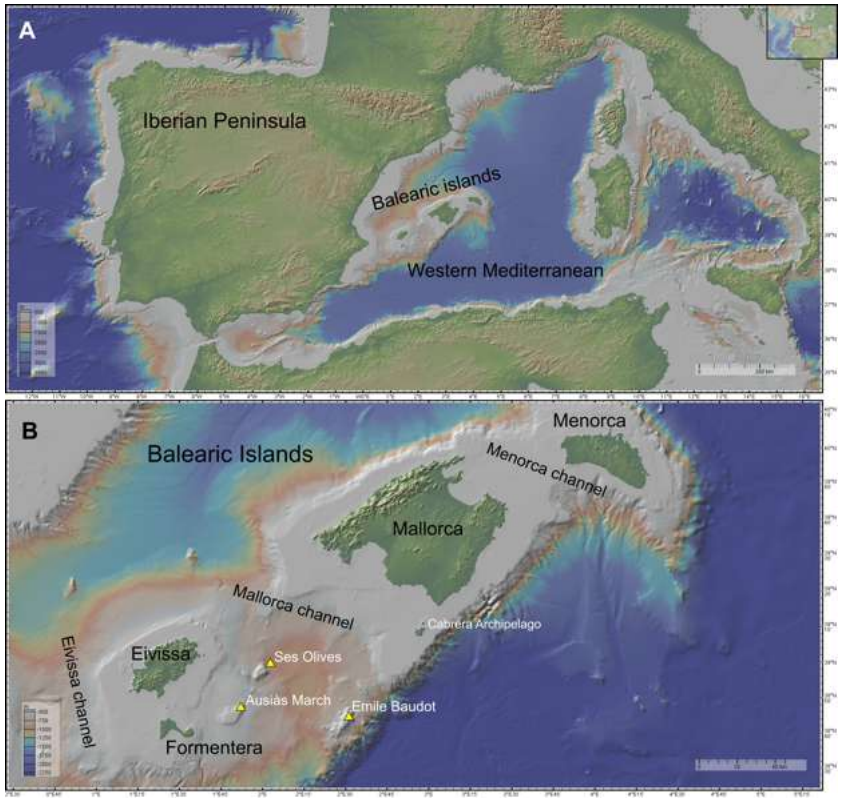

Fig. 1.1. Maps showing the western Mediterranean (A) and the Balearic Islands (B), as well as their main geomorphological features where sponges sampling was developed during the present thesis.

The shelf of the Balearic Archipelago can be divided in two, the larger Mallorca-Menorca shelf to the east, narrow on the northern side (3 km width) and wider in the south (up to 35 km width), and the smaller Ibiza-Formentera shelf to the west, from 2 km wide on the eastern side to more than 25 km wide in the west (*Acosta et al., 2002*). The slope on the western and southern sides is gentle (6º average inclination) in some parts with no clear shelf-break, while the northern and eastern sides have an abrupt slope (16º average inclination), with a clear shelf-break, several seamounts and a pronounced scarp, with depths ranging from 200 to 800 m in its shallowest part to more than 2000 m at its base. This scarpment is crossed by numerous small canyons, the biggest one situated southern Menorca (*Acosta et al., 2004*).

The Balearic Islands are characterized by clear waters, as a consequence of their oligotrohy, the lack of river runoff, the scarcity of rain and the high distance from the Iberian Peninsula, where terrigenous-muddy sediments from river discharges are widely distributed. By contrast, the sand and gravel calcareous biogenic sediments predominate in the Balearic shelf (*Alonso et al., 1988*). These oceanographic characteristics allow light intensity to reach 0.05% of surface values as deep as 110 m, allowing the growth of seaweeds in most of the continental shelf (*Canals & Ballesteros, 1997*; *Joher et al., 2012*, *2015*). As a consequence, benthic communities distribution and composition varies from that of the adjacent Iberian Peninsula and other Mediterranean areas (*Pérès & Picard, 1964, Ballesteros, 1994*).

According to *Ordines & Massutí (2009)*, seaweed communities including rhodoliths, *Peyssonnelia* spp., *Osmundaria volubilis* (Linnaeus) R.E.Norris, 1991 and *Laminaria rodriguezii* Bornet, 1888 beds predominate in the coastal shelf of the Balearic Islands, while sedimentary bottoms of the deep shelf and upper slope show some other habitats of interest, like crinoids beds. Despite the pronounced oligotrophy of this Archipelago, the red algae beds show high diversity and benthic productivity (*Ordines & Massutí, 2009*), being the sponges one of the main benthic groups associated to this algal communities (*Ordines et al., 2017*).

The Menorca and Mallorca channels

This thesis focuses on studying two of the three main channels within the Balearic Islands (Fig. 1.1): the Menorca Channel, between the islands of Mallorca and Menorca, and the Mallorca Channel, between the Pitiusas Islands (Ibiza and Formentera) and Mallorca. The third one, the Ibiza Channel, separates the Pitiusas Islands from the Iberian Peninsula. The Menorca and Mallorca channels are sited, at the north and sout areas of the Archipelago, respectively, connecting the Balearic sub-basin in the north with the Algerian sub-basin in the south, which show different oceanographic conditions (*EUROMODEL Group, 1995*). While the Balearic sub-basin is more influenced by atmospheric forcing and Mediterranean waters, which are colder and more saline, the Algerian sub-basin is affected basically by density gradients and receives warmer and less saline Atlantic waters (*Pinot et al., 2002*). The Balearic

channels play an important role in the regional circulation, serving as passages for water masses exchange between them (*Massutí et al., 2014*; and references cited therein).

The Menorca Channel is characterized by having relatively shallow waters, a consequence of the continuity of the continental shelf between Mallorca and Menorca. It is influenced by atmospheric forcing (*Monserrat et al., 2008; López-Jurado et al., 2008*) and by the Balearic Current, which flows along the northern shelf margin and upper slope of the Balearic Promontory and, jointly with frontal meso-scale events between Mediterranean and Atlantic waters and input of old northern water into the Balearic channels, can acts as external fertilization mechanism that enhance productivity off Balearic Islands (*Pinot et al., 1995; Fernández de Puelles et al., 2004*). This channel harbors rich and diverse benthic habitats (*Barberá et al., 2012; Grinyó et al., 2018*) and hence in 2014 it was declared Site of Community Importance (SCI), under the Natura 2000 framework.

Fig. 1.2. Rhodolith bed with sponges at the summit of the Emile Baudot seamount (about 130 m depth), at the Mallorca Channel.

The Mallorca Channel is a seaway composed of diverse geomorphological features, with an abyssal plain descending down to 1050 m depth, that separates the continental shelves of Mallorca-Menorca and Ibiza-Formentera. Mostly sited in the Algerian sub-basin, this channel is mainly affected by density gradients and the warmer and less saline Atlantic waters (*Monserrat et al., 2008; López-Jurado et al., 2008*) and the trophic webs of their deep water ecosystems are supported more by plankton biomass than by benthic productivity as in the Balearic sub-basin, in which suprabenthos play a more important role (*Maynou & Cartes, 2000; Cartes et al., 2001, 2008*). At the southern part of the Mallorca Channel there are three seamounts: Ses Olives and Ausias March of orogenic origin, and the Emile Baudot of volcanic origin. These seamounts have been recently studied, within the LIFE IP INTEMARES project (https://intemares.es/en) and the first results have mapped their geomorphological features, showing a high diversity of species, mainly benthic filter feeders like sponges,

and habitats of special interest for conservation, including coralligenous outcrops and maërl beds at summits (Fig. 1.2), deep- sea coral and sponge reefs at rocky escarpments of their flanks (Fig. 1.3) and *Isidella elongata* (Esper, 1788) and pockmarks fields on sedimentary bathyal bottoms (*Massutí et al., 2022*).

Fig. 1.3. Rocky outcrop colonized by coralligenous communities and dominated with sponges at the summit of the Emile Baudot seamount (about 135 m depth), at the Mallorca channel.

Marine caves

Litoral marine caves represent a vulnerable habitat of special interest for the conservationyet they remain largely unexplored in the Mediterranean. This habitat is another important and common habitat of the Balearic Archipelago (Fig. 1.4), which can have a Karstic origin, result from the abrasive action of littoral processes or a mix of both (*Gràcia et al. 1998, 2005, 2014; Ginès et al., 2013; Morató et al., 2022*).

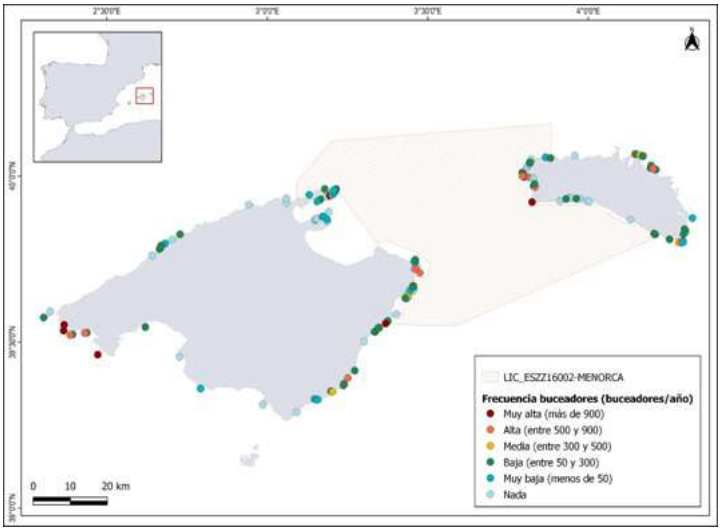

Fig. 1.4. Map of submerged and semi-submerged caves of Mallorca and Menorca (Balearic Islands). The different colors represent the frequency of divers: red (very high), orange (high), yellow (medium), green (low), blue (very low) and grey (nill). Source: *Morató et al. (2022)*.

The coastal marine caves constitute an important habitat for marine invertebrates, especially sponges (*Vicens et al., 2011*). Within caves, sponges take advantage of the lack of algae, which are the main competitors for space in well-illuminated zones (*Gerovasileiou & Voultsiadou, 2012*). In some caves sponge biodiversity is very high and mostly understudied (Fig. 1.5), yet, like in the deep sea, cave accessibility is difficult and more limited than in other littoral areas. Besides, cave sponges tend to adopt similar shapes, most of them being encrusting and minute, which makes the collection, manipulation and identification more difficult.

Fig. 1.5. Speleothem colonized by encrusting sponges at at 4-5 m depth in the marine cave "Cova de cala Sa Nau" (eastern Mallorca, Balearic Islands).

Trawl fishing grounds

Although it is not clear when the trawl fishery started in the Balearic Islands, the most probably date is during the end of the 18th century. At the beginning, this fishery was developd in coastal areas and bays, while the exploitation of fishing grounds between 100 and 300 m depth did not start until almost the beginning of the last century (*Massutí, 1959, 1973*; *Terrasa and Oliver, 2024*). Deeper fishing grounds, located between 300 and 800 m depth, which were formerly unknown or impracticable, started to be exploited in 1948, coinciding with its charting by the Instituto Español de Oceanografía (*Oliver, 1983*).

Historically, the number of trawl fishing boats has remained relatively low in the Balearic Islands, compared to other areas of the Mediterranean coast of the Iberian Peninsula (*Quetglas et al., 2012*). According to these authors, the number of vessels per potential fishing ground surface, as a simple indicator of the fishing effort exerted, is one order of magnitude lower in the Balearic Islands than in the adjacent peninsular coast. However, compared to other areas, the trawl fishing has a great relative importance in the Balearic Islands. Whereas in the adjacent coasts of the north east Iberian Peninsula this fishery represents up to 45-50% of the landings and a similar percentage is provided by the purse seine fleet, in the Archipelago the trawl fishing produces up to 70% of the landings, followed by the artisanal fleet, which contributes with up to around 20% (*Quetglas et al., 2012*).

As other areas of the western Mediterranean, most sedimentary bottoms of the continental shelf and the upper and middle slope around the Balearic Islands have been exploited by the trawling fleet for several decades (*Farriols et al., 2017*). In the Archipelago, bottom trawling is conducted from 50 to about 750 m depth (Fig. 1.6). Fishing grounds between 50 and 100 m depth overlap with red algae beds, which explains the high quantity of algae and benthic invertebrates in the discards of this fleet (*Ordines et al., 2006*).

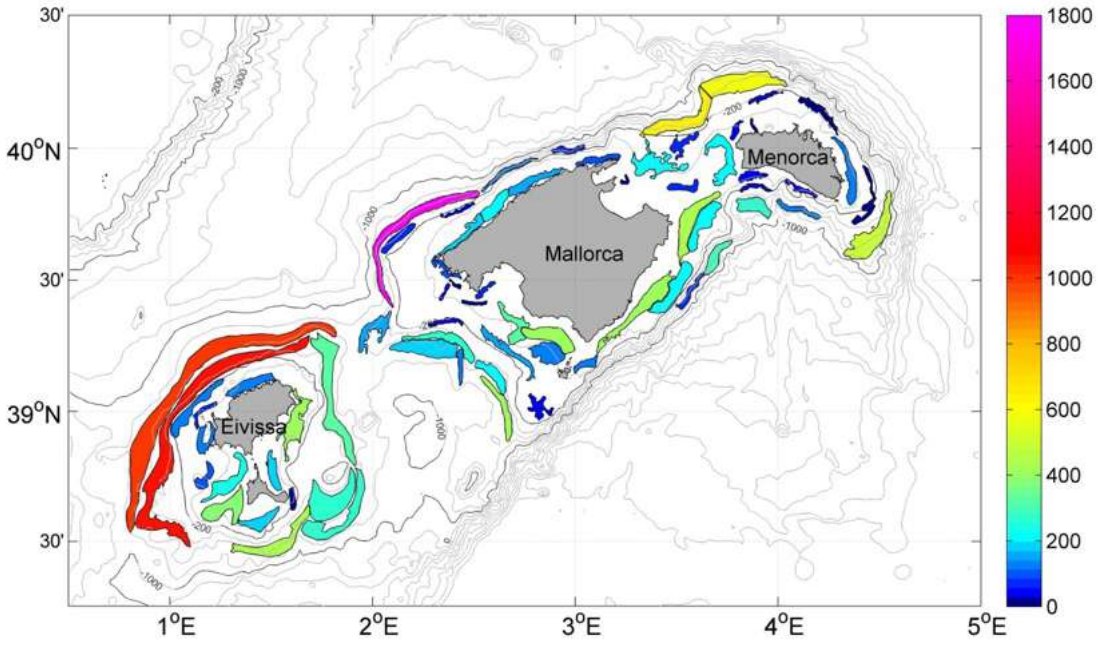

Fig. 1.6. Trawl fishing grounds around Belaric Islands mapped from Vessel Monitoring by Satellite System (VMS) signals during the period 2006-2014 and their fishing pressure, in number of fishing days per year. Source: *Guijarro et al. (2020)*.

The bottom trawl fishery developed around the Balearic Islands has a clear multi-species character, as consequence of the different fishing strategies developed by the trawling fleet (*Palmer et al., 2009*), which are quite coincident with the main communities of demersal species and resources described in the continental shelf and upper and middle slope of the Mediterranean (e.g. *Massutí and Reñones, 2005*; *Biagi et*

al., 2002; *Kallianiotis et al., 2000*). These fishing strategies, which are detailed below according to *Palmer et al. (2009)*, can be developed even during the same daily fishing trip:

- The shallow shelf (50-100 m depth), where the main target species are the striped red mullet *Mullus surmuletus* Linnaeus, 1758, the squid *Loligo vulgaris* Lamarck, 1798, the octopus *Octopus vulgaris* Cuvier, 1797, the picarel *Spicara smaris* (Linnaeus, 1758) and the "Morralla", a mixed fish category in which a great variety of small and medium sized species (e.g. *Chelidonichthys lastoviza* (Bonnaterre, 1788), *Trachinus draco* Linnaeus, 1758, *Scorpaena notata* Rafinesque, 1810, *Serranus hepatus* (Linnaeus, 1758), *Serranus cabrilla* (Linnaeus, 1758), *Chelidonichtys cuculus* (Linnaeus, 1758) and *Pagellus acarne* (Risso, 1827)) and small individuals of larger species (e.g. *Scorpanea scrofa* Linnaeus, 1758, *Pagellus erythrinus* (Linnaeus, 1758)) are gathered.

- The deep shelf (100-250 m depth), where main target species are hake (*Merluccius Merluccius* (Linnaeus, 1758)), red mullet (*Mullus barbatus* Linnaeus, 1758) and John Dory (*Zeus faber* Linnaeus, 1758).

- The upper slope (250-600 m depth), where main target species are Norway lobster (*Nephrops norvegicus* (Linnaeus, 1758)) and deep-sea rose shrimp (*Parapenaeus longirostris* (Lucas, 1846)), but where the yields of hake (*M. merluccius*), megrims (*Lepidorhombus* spp.), monkfish (*Lophius* spp.) and blue whiting (*Micromesistius poutassou* (Risso, 1827)) can also be important.

- The middle slope (600-800 m depth), where the red shrimp (*Aristeus antennatus* (Risso, 1816)) is the only target species.

While the fishing grounds around Mallorca and Menorca are exclusively expoited by the local trawl fleet, the deep water fishing grounds off Pitiusas Islands are targeted by a trawl fleet from the Iberian Peninsula (Fig. 1.7). Vessels from the ports of Dènia, Calp, Altea, La Vila Joiosa and Santa Pola undertake 3–5 days trips to fish below 150 m depth around Ibiza and Formentera. This fleet is primarily focuses on decapod crustaceans of high economic value: deep-sea rose shrimp (*P. longirostris*) and Norway lobster (*N. norvegicus*) in the upper slope and red shrimp (*A. antennatus*) in the middle slope (*García-Rodríguez & Esteban, 1999*).

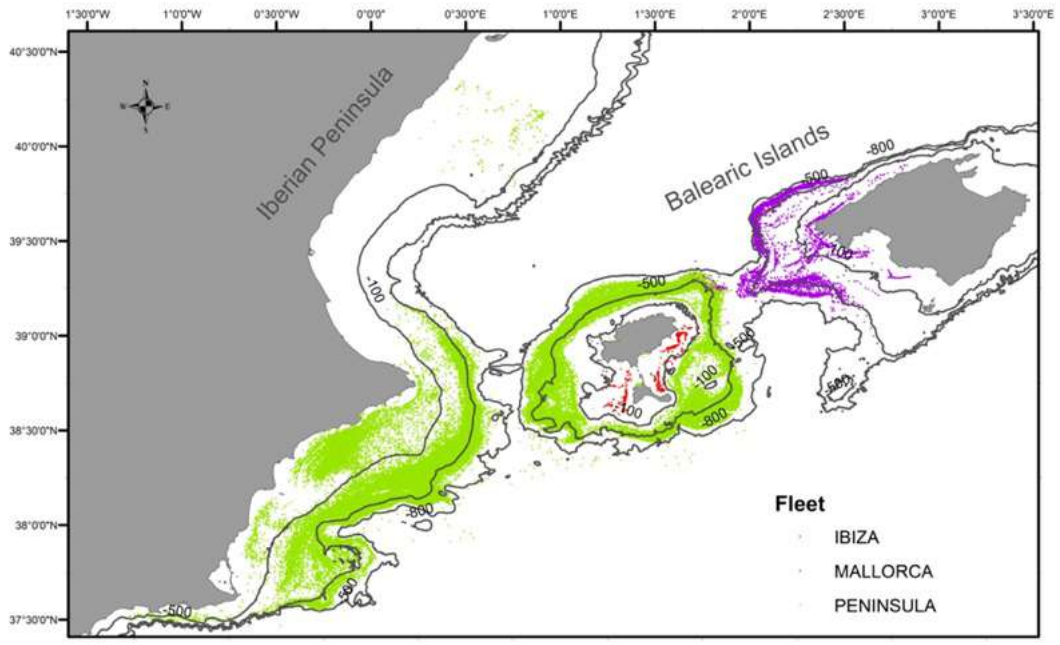

Fig. 1.7. Bottom trawl fishing activity in the seamounts of the Mallorca Channel, estimated from Vessel Monitoring by Satellite System (VMS) signals during the period 2016-2019 of the fleets that operate around Ibiza and Formentera (red: vessels from ports on these islands; green: vessels from ports on the Iberian Peninsula; violet: vessels from ports on Mallorca). Source: *Massutí et al. (2022)*.

This bottom trawl fleet exploit sedimentary bottoms adjacent to the seamounts of the Mallorca Channel, mainly Ausias March and at a lesser extent Ses Olives (Fig. 1.7), while Emile Baudot remains unexploited by the bottom trawl fleet for two decades (*Massutí et al., 2022*). Other fishery developed at the flanks and summits of these seamounts is focused on the deep-water pandalid shrimp *Plesionika edwardsi* using traps (*García-Rodríguez et al., 2000*), while commercial and recreational fishing fleets also operate more sporadically using bottom long-line and hand-lines, respectively, to capture large sparids and serranids. In this area there are also pelagic fisheries, mainly targeted to swordfish (*Xiphias gladius*) using pelagic and semi-pelagic long-lines (e.g. *Barcelona et al., 2010*) and to bluefin tuna (*Thunnus thynnus*) using purse-seine (e.g. *Gordoa et al., 2017*).

OBJECTIVES

2. Objectives

The general objective of the present thesis is to improve the knowledge on the diversity of sponges and their communities in the Balearic Islands. To achieve this, the following specific objectives were proposed:

- ✓ To describe new taxa from underexplored ecosystems such as seamounts, deep sea and littoral caves, along with the re-description of poorly known species, including the documentation of new species records for the Mediterranean, its western basin and the Balearic Islands (Chapters 4.1-4.5).
- ✓ To improve the systematics of Balearic Islands deep sea and cave Tetractinellids, through a critical review of their taxonomy (Chapters 4.3).
- ✓ To identify and characterize the sponge assemblages from the continental shelf and slope trawl fishing grounds around the Archipelago and the seamounts of the Mallorca Channel (Chapter 4.6).
- ✓ To investigate the effects of environmental variables, including fishing pressure, on the distribution and composition of these assemblages (Chapter 4.6).

MATERIAL AND METHODS

3. Material and Methods

3.1. Umbrella projects and sampling surveys

MEDITS

The MEDITS bottom trawl surveys started in 1994 from the coordination between marine research institutions of four Mediterranean countries of the European Union: France, Greece, Italy and Spain (http://www.sibm.it/MEDITS\%202011/principalemedits.htm). Later, more institutes from other new Mediterranean Member States joined the program, until reaching the 10 countries cooperating nowadays. For several years now, MEDITS surveys are included in the Data Collection Framework, regulated by the Council Regulation (EC) Nº 199/2008, of 25 February 2008, concerning the establishment of a Community framework for the collection, management and use of data in the fisheries sector and support for scientific advice regarding the Common Fisheries Policy, which Article 12 establishes that "Member States shall carry out research surveys at sea to evaluate the abundance and distribution of stocks, independently of the data provided by commercial fisheries, and to assess the impact of the fishing activity on the environment".

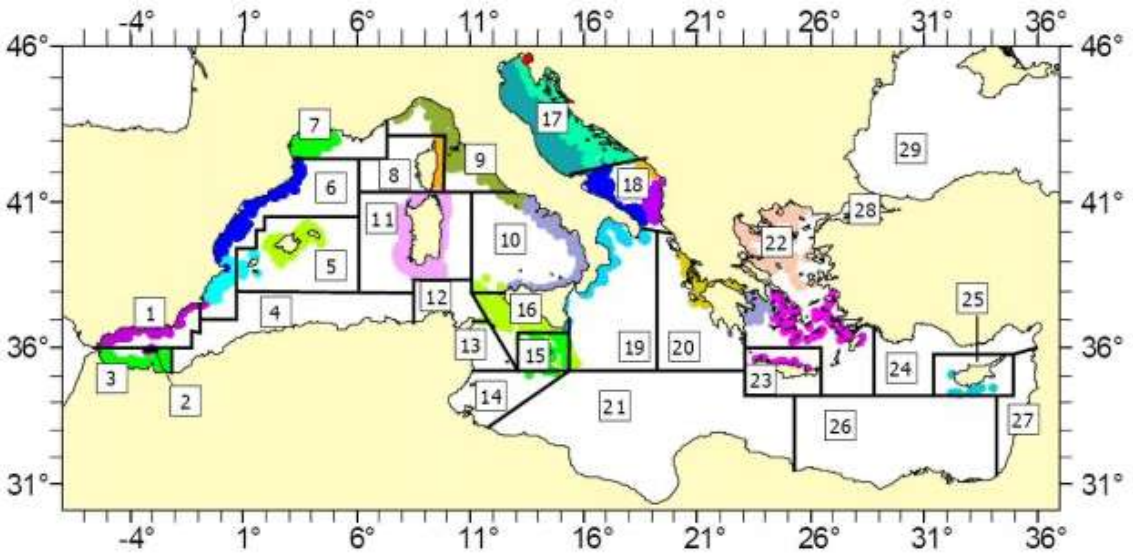

Figure 3.1. Map of the thirty Geographical Sub-Areas (GSAs) established in the Mediterranean and Black Sea by the General Fisheries Commission for the Mediterranean (GFCM): (01) Northern Alboran Sea. (02) Alboran Island. (03) Southern Alboran Sea. (04) Algeria. (05) Balearic Islands. (06) Northern Spain. (07) Gulf of Lions. (08) Corsica Island. (09) Ligurian and North Tyrrhenian Sea. (10) South and Central Tyrrhenian Sea. (11) Sardinia. (12) Northern Tunisia (13) Gulf of Hammamet. (14) Gulf of Gabes. (15) Malta Island. (16) South of Sicily. (17) Northern Adriatic Sea. (18)SouthernAdriaticSea. (19)Western Ionian Sea. (20) Eastern IonianSea. (21) Southern Ionian Sea. (22) Aegean Sea. (23)Crete. (24) North Levant. (25) Cyprus Island. (26) South Levant. (27) Levant. (28) Marmara Sea. (29) Black Sea. (30) Azov Sea. Source: *Anon (2017)*; http://www.sibm.it/MEDITS\%202011/principalegeo.htm.

More specifically, the aim of MEDITS surveys is to obtain fishery independent data on demersal resources and benthic ecosystems, mainly exploited by the trawl fishery, along

the whole northern Mediterranean (Fig. 3.1), by applying a common sampling strategy and protocol (*Bertrand et al., 2002*; *Spedicato et al., 2019*). The bathymetric range sampled is 10-800 m depth, with sampling stations following a stratified sampling scheme, which considers Geographical Sub-Areas (GSAs) established in the Mediterraenan by the General Fisheries Commission for the Mediterranean (GFCM) and five depth strata (10-50, 51-100, 101-200, 201-500 and 501-800 m) in which samples were ramdomly distributed at the begining of the MEDITS time series. The number of samples in each stratum is proportional to its surface and their position is fairly maintained from year to year.In the Balearic Islands the shallowest stratum is not samped, due to the wide distribution of *Posidonia oceanica* meadows at this depth range.

The surveys are developed yearly from late spring to middle summer, using a sampling gear specifically designed for the MEDITS program, the experimental bottom trawl GOC-73 (GOC), which has proven highly efficient for sampling nektobenthic and megabenthic species (*Fiorentini et al., 1999*; *Dremière et al., 1999*). This gear is equipped with a 15-20 mm mesh codend and has horizontal and vertical net openings of 16-22 and 2.7-3.2 m, respectively (Fig. 3.2A). The towing speed during the sampling hauls is 2.8-3 knots to ensure the net proportions are maintained during trawling. The effective trawling duration, after the net contacting the seafloor, is 20, 30 and 60' at ≤100, 101-200 and >200 m depth, respectively.

Biological data used in this thesis were obtained from the MEDITS surveys carried out between 2016 and 2021 in the GSA 5 (Balearic Islands), one of the 30 GSAs established by the GFCM. Some additional samples have also been collected off the Catalan coast, at the GSA 6 (Northern Spain), from the MEDITS survey carried out in 2020. In each MEDITS haul, all specimens captured were sorted on board, identified to species level or to the lowest posible taxonomic level, counted and weighed (Fig. 3.2B). For more details about the MEDITS sampling strategy and protocol, as well the sampling gear GOC, see *Anon (2017)*.

Figure 3.2. (A) Afterdeck stern of the R/V *Miquel Oliver*, showing the experimental bottom trawl gear GOC-73. (B) MEDITS sample sorting.

INTEMARES

The LIFE IP INTEMARES project (https://intemares.es/en) has the aim to achieve a network of efficiently managed marine Natura 2000 areas, with the active participation of the sectors involved and research as basic tools for decision-making. As a part of it, the scientific exploration of the seamounts in the Mallorca Channel aims to improve the scientific knowledge of this area, for its inclusion in the Natura 2000 network (sub-action A22_B). The tasks within the Project include mapping and characterization of the benthic habitats and species of special interest for conservation, the most important human threats and the vulnerability of the area, ini order to propose it as Sites of Community Importance (SCI), for the subsequent development of a management plan and its final declaration as Special Areas of Conservation (SAC). Those protection regimes seek to ensure the long-term preservation of the flora and fauna, as well as the sustainability of human activities.

Seamounts are isolated undersea topographical elevations on continental margins and oceanic domains, which are considered as hotspots of biological activity and biodiversity in the deep-sea (*Clarke et al., 2012*). These relevant seafloor reliefs span a broad depth range, being influenced by different oceanographic processes (*Palomino et al., 2011*) and located in diverse geodynamic settings. Therefore, they comprise heterogeneous habitat types (*Würtz & Rovere, 2015*), some of them structured by fragile, sessile, slow-growing, and long-lived species sensitive to fishing and other types of disturbance, being internationally recognized as Vulnerable Marine Ecosystems (*FAO, 2009*) that have been suggested to serve as isolated refuges for relict populations of species that previously had larger distribution ranges (*Galil & Zibrowius*, 1998).

The Mediterranean is considered as rich area in terms of presence of seamount-like features with up to about a hundred of these structures that occupy nearly 89000 km^2 (*Morato et al., 2013*). Despite this, Mediterranean seamounts are poorly known, with scientific information only available for less than 10% of them and mainly consisting of geological studies. In fact, there were almost no biological and ecological information on these structures until the end of the 20th century, except for the Erastothenes seamount in the Levant basin (*Galil & Zibrowius, 1998*; *Danovaro et al., 2010*). Hence, the scientific knowledge on Mediterranean seamounts is marked by large gaps and an asymmetry between the number of geological studies and biological ones (*Würtz & Rovere, 2015*).

Up to 60 seamounts and seamount-like structures have been identified in the western Mediterranean (*Gómez-Ballesteros et al., 2015*). Among these are Ses Olives (SO), Ausias March (AM) and Emile Baudot (EB) seamounts, sited in the Mallorca Channel (Balearic Islands) and currently studied within the INTEMARES project (Fig. 3.3). Several studies on these seamounts have analyzed the demersal fisheries targeted on deep water decapods crustaceans (*Rodíguez & Esteban, 1999*), the geomorphology and geodynamics (*Acosta et al., 2004*), and the benthic species and habitats (*OCEANA, 2011, 2015*; *Aguilar et al., 2011*; *Maldonado et al., 2015*), suggesting their high

ecological value. For this, the protection of these seamounts is recommended (*Marín et al., 2011*).

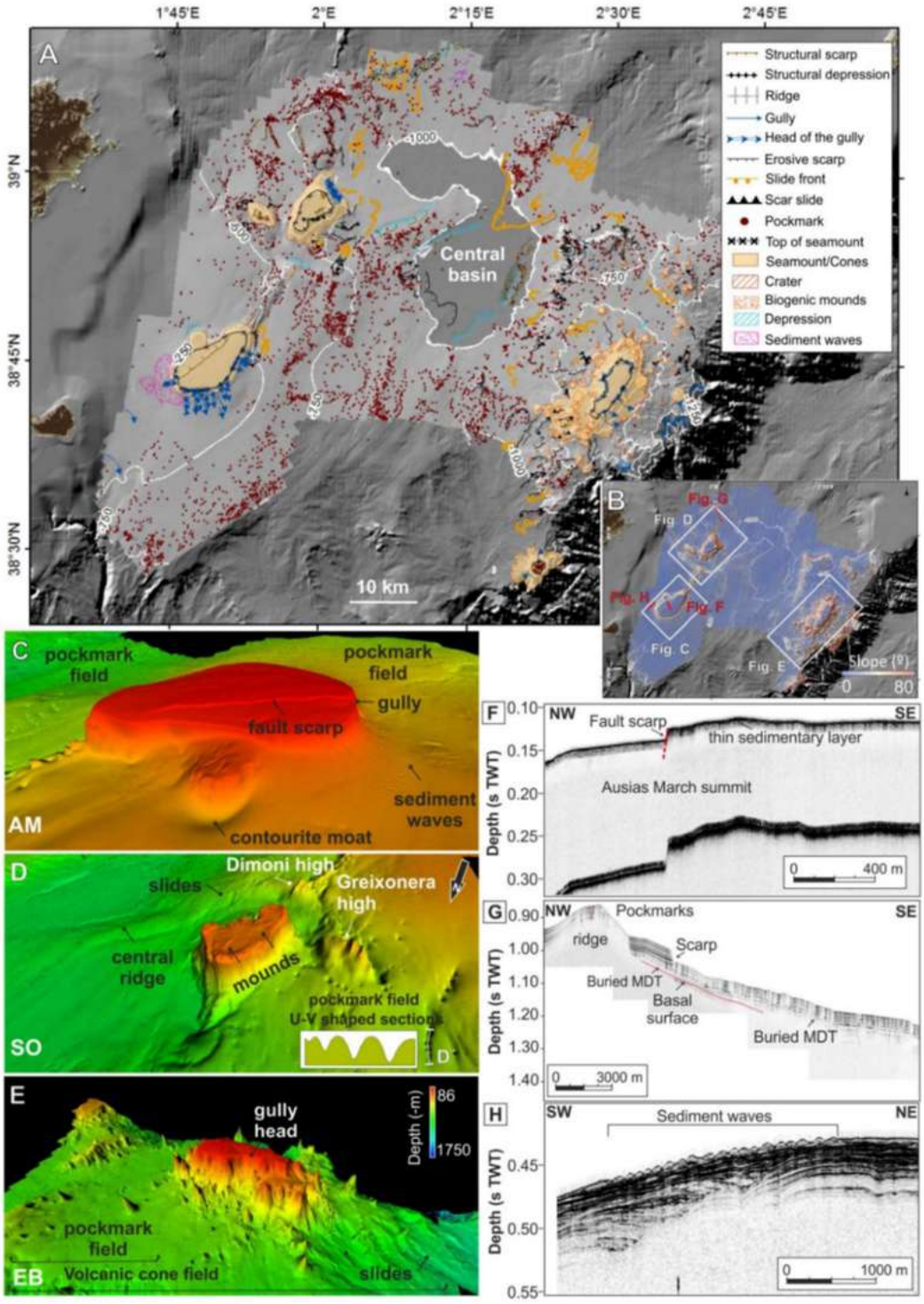

Figure 3.3. Bathymetry and geomorphology of the seafloor in the Mallorca Channel: (A) Morphological map showing the main morphological features and domains of the study area; (B) slope map showing bathymetric contours at each 250 m and the location of the 3D bathymetric models and parametric profiles; (C–E) overview 3D bathymetric map of the main edifices of the study area: Ses Olives, Ausias March, and Emile Baudot seamounts and Greixonera and Dimoni highs; (F–H) parametric profiles showing the internal structure of the main morphological features present in the study area. Source: *Massutí et al. (2022)*.

Within the framework of the INTEMARES project, a mulidisciplinary scientific approach have been developed to study these seamounts and their adjacent areas. It included both geological and biological sampling, monitoring of the fishing fleet, and compilation and review of information from existing databases on fishing landings (*Massutí et al., 2022*). Between 2018 and 2020, four INTEMARES research surveys were developed. High resolution geophysical techniques were applied to study the seafloor, while dredges, a beam trawl and the experimental bottom trawl GOC were used for sampling sediments, rocks, epi-benthic and nekton-benthic organisms, as well as demersal fishing resources (Fig. 3.4).

Figure 3.4. (A) Beam trawl used on board the R/V *Ángeles Alvariño* during the INTEMARES_1019 survey. (B) Sample sorting on board the R/V *Ángeles Alvariño* during the INTEMARES_0720 survey. (C) Sponge sorted sample. (D) On deck processing (character annotation, sampling, genetic and spicule subsampling) of the beam trawl sample.

A photogrammetric sledge and a remote operated vehicle (ROV; Fig. 3.5) were also used to take videos of the seafloor and their benthic communities. In 2020 and 2021, samples from GOC were also collected during the MEDITS surveys at the deep water trawl fishing grounds adjacent to AM and EB.

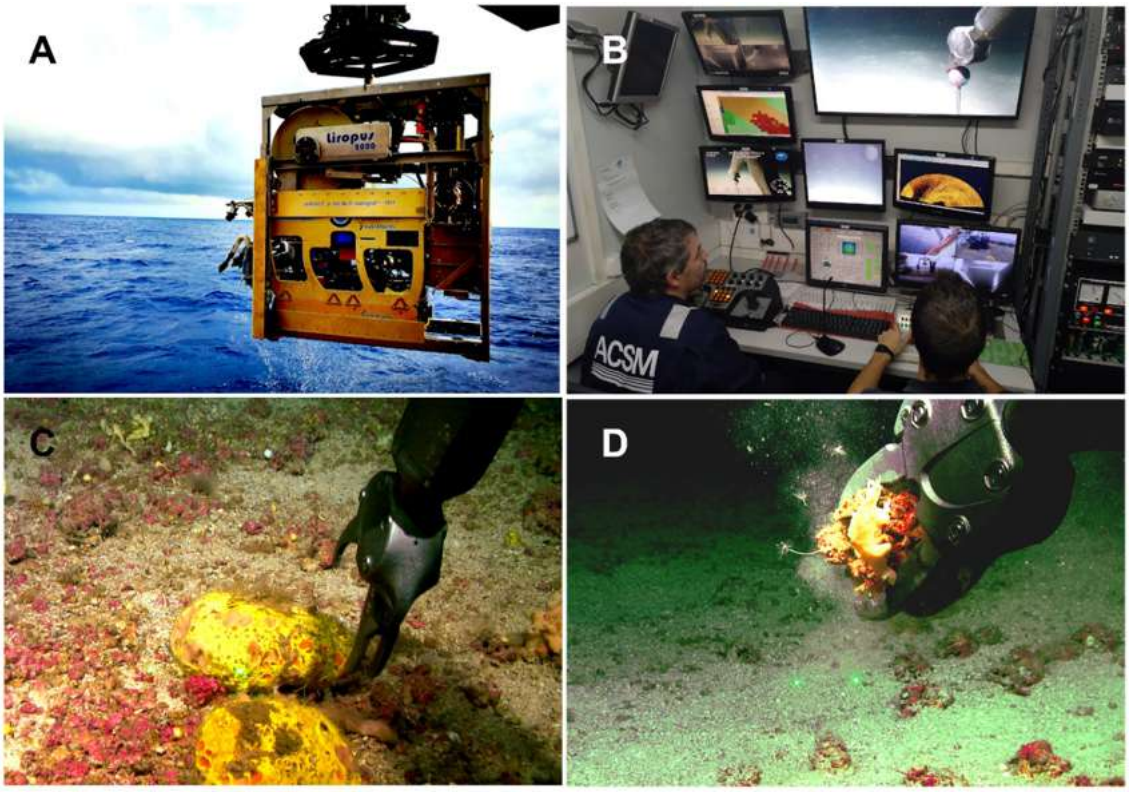

Figure 3.5. (A) Reel in of the Remote Operated Vehicle (ROV) Liropus 2000 after a dive in the Emile Baudot. (B) Control room of the Liropus 2000. (C) Collection of a *Spongosorites* sp1 specimen at the summit of the Emile Baudot. (D) Collection of a rhodolith with sponges at the summit of the Emile Baudot. All the images were taken on board of the R/V Sarmiento de Gamboa during the INTEMARES_0820 survey.

MSFD

The Directive 2008/56/EC establishing a framework for community action in the field of marine environmental policy or Marine Strategy Framework Directive (MSFD) came into force in July 2008 to protect and restore the European marine ecosystems and to achieve a good environmental status (GES) of the sea, ensuring the sustainable use of marine resources. The concept of GES is defined through 11 descriptors which describe the state of the marine environment, such as conserving biodiversity or food webs, as well as anthropogenic pressures such as commercial fisheries, marine litter, contaminants or the input of energy (*Borja et al., 2010*): 1 (Biodiversity), 2 (Non-indigenous species), 3 (Exploited fish and shellfish), 4 (Food webs), 5 (Eutrophication), 6 (Sea-floor integrity), 7 (Hydrographical conditions), 8 (Contaminants), 9 (Contaminants in fish), 10 (Marine litter) and 11 (Noise).

In Spain, the complexity of the MSFD implementation has been accentuated by the great dimension of the marine area under sovereignty or jurisdiction ($>1*10^6$ km^2). To facilitate it, five "demarcations" were stablished on the basis of particular biogeographic, oceanographic and hydrological characteristics of the different areas (*Bellas, 2014*): The Atlantic region includes the North Atlantic, the South Atlantic and

the Canary Islands demarcations, while the Mediterranean region comprises the Levantine-Balearic and the Gibraltar Strait and Alboran Sea demarcations (Fig. 3.6).

The Levantine-Balearic demarcaction is located between Cape of Gata and the geopolitical limit between the French and Spanish waters, including the Balearic Archipelago (Fig. 3.6). It is a large marine area, with about 2400 km of coast length, and harboring a high diversity of benthic habitats and species, some of which are included in international conventions and protected by regional, European, national and local regulations.

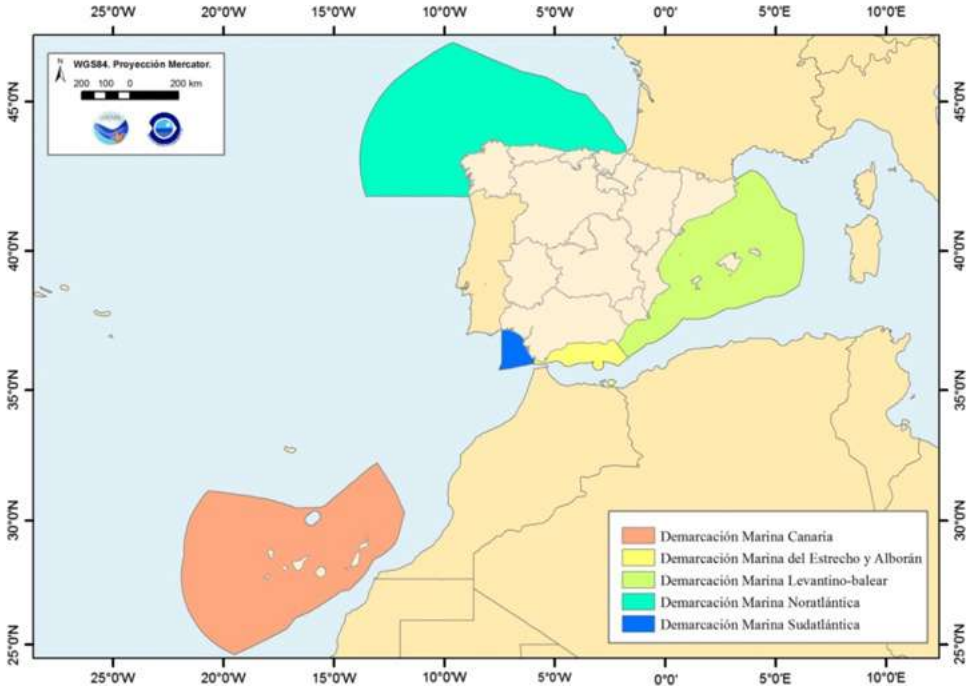

Fig. 3.6. Demarcations established in Spain within the framework of the Marine Strategy Framework Directive (modified from http://ec.europa.eu/). Source: *Bellas (2014)*.

Within this context, the Instituto Español de Oceanografía is currently developing the research project "Asesoramiento científico técnico para la protección del medio marino: Evaluación y seguimiento de las Estrategias Marinas, seguimiento de los espacio marinos protegidos de competencia estatal", commissioned by General Directorate for the Protection of the Sea of the Spanish Ministry for the Ecological Transition and the Demographic Challenge. This project is composed by different sub-projects, one of them (18-ESMARES2-CIRCA) being focussed on the scientific monitoring of the benthic habitats in sedimentary and rocky bottoms of the circalittoral and bathyal domains.

The CIRCA-LEBA-1121 research survey was developed in 2021 as part of the 18-ESMARES2-CIRCA sub-project. The aim of this survey was to characterize the benthic communities of the circalittoral and bathyal sedymentary bottoms of the Levantine-Balearic demarcation. For this purpose, one of the sampling methods used, among others, were a beam trawl for collecting benthic flora and fauna.

Litoral marine caves

Marine caves are considered vulnerable marine habitats due to their low resilience (*Vacelet et al.*, 1994) and are included in the Habitats Directive (European Union, Council Directive 92/43/EEC). One of the main threats to litoral caves is the growing pressure that recreational scuba diving, a buoyant economic activity in the Balearic Islands, is exerting on them. The impacts of this activity include direct breaking of vulnerable organisms as well as indirect impacts such as those caused by resuspension and resettlement of sediments and subsequent smoothing of organisms, and the accumulation of air from exhaled air at the ceiling of the caves, subsequently leaving organisms out of the water (*Milazzo et al.*, 2022; *Lloret et al.*, 2006)

Shallow water caves (0-10 m), located eastern ("Cova de sa Figuera", "Cova de ca'n Rafalino", "Cova de Cala Sa Nau"), northern ("Coves de Na Dana"), and western ("Cova Caló des Monjo") off Mallorca island (Fig. 3.5), were sampled by using scuba diving or free apnea techniques between 2020 and 2021. Most of them can be classified as littoral marine caves created by sea erosion.

The size of these caves is quite variable, "Cova de Cala Sa Nau" being the largest and the most important in terms of benthic organisms, with a spacious entrance and main chamber (Fig. 3.7). This cave is commonly frequented by scuba divers. In contrast, the "Cova de ca'n Rafalino" is the smallest, being a short tunnel only several meters long, with a depth of 1-2 m and between 0.5 and 3 m wide. Inland freshwater infiltration has been observed in "Cova de ca'n Rafalino" and "Coves de na Dana".

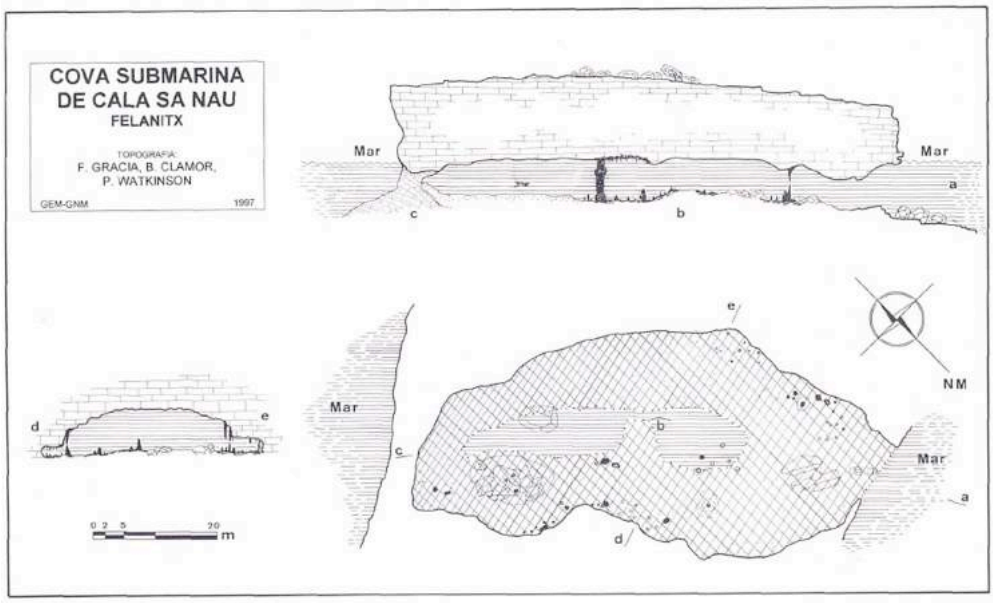

Figure 3.7. Topography of "Cova de cala sa Nau", located eastern Mallorca (Balearic Islands). Source: *Gràcia et al. (1998)*.

3.2. Sample processing

3.2.1. On board procedures and morphological analysis

In the case of the research surveys, once on board, sponges were separated from the rest of the sample and photographed with a Olympus TG5 digital camera on a graph chart (Fig. 3.8). Whole samples were preserved in absolute ethanol (EtOH). Sponges specimens were deposited in the CFM-IEOMA and in the UPSZMC/UPSZTY collections.

Figure 3.8. Images of sorted sponges. (A-B) Collected from fishing grounds around Balearic Islands. (C-D) Collected at seamounts of the Mallorca Channel.

External morphology, color and texture were annotated prior to the sample conservation, as well as the presence of epibionts. Spicules preparations and histological sections were made according to the standard methods described by *Hooper (2003)*.

Spicules were observed with a Nikon S-Ke optical microscope and photographed with a CMOS digital camera. Images were processed with the software Fiji (*Schindelin et al. 2012*). For each sample, 30 spicules per spicule class or category were counted. Spicular sizes are provided as minimum-mean-maximum in chord length and minimum-mean-maximum in width, and expressed in microns (µm). For studying the skeletal architecture, thick sections of both tangential-surface and transversal-surface sections were made with a scalpel and, when necessary, dehydrated with alcohol and cleared with xylene. Cleared sections were re-hydrated with water, included in mounting media and observed with the microscope or a Leica M165C stereomicroscope. Aliquots of suspended spicules were transferred onto aluminum foil, air dried, sputter coated with gold and observed under a HITACHI S-3400N scanning electron microscope (SEM).

The terminology applied for the morphological description follows *Boury-Esnault & Rützler (1997)*, *Hooper & Van Soest (2002)* and *Łukowiak (2022)*.

3.2.2. Genetic methods

DNA was extracted from a piece of choanosomal tissue (~2 cm^3) using the DNeasy Blood and Tissue Extraction kit (QIAGEN). Polymerase chain reaction (PCR) was used to amplify the Folmer fragment (658 bp) of the mitochondrial cytochrome c oxidase subunit I (COI) and the C1-C2 (~369 bp) or C1-D2 (~800 bp) fragments of the nuclear rDNA 28S gene.

For COI, the universal Folmer primers LCO1490/HCO2198 were used (*Folmer et al., 1994*), except for the *Craniella* species, for which we used the primer set LCO1490/COX1R1 (*Rot et al., 2006*), which amplifies a longer fragment ca. 1180 bp (Folmer + Erpenbeck fragments). When LCO1490/HCO2198 failed, the primers LCO and TetractminibarR1 were used to amplify the first 130 bp of the Folmer marker, also called the Folmer COI minibarcode (*Cárdenas & Moore, 2019*). The primers jgHCO (*Geller et al., 2013*) and ErylusCOIF2 (5'-CTCCYGGATCAATGTTGGG-3') were then used to amplify the rest of the Folmer fragment (*Cárdenas et al., 2018*).

For 28S, the primer set C1'ASTR/D2 (*Vân Le et al., 1993; Cárdenas et al., 2011*) was used to get the C1-D2 domains. When these primers failed, we used the primers C1'/Ep3 to get the shorter C1-C2 fragment.

PCR was performed in 50 µl volume reaction (34.4 µl ddH20, 5 µl Mangobuffer, 2 µl DNTPs, 3.5 $MgCl_2$, 1 µl of each primer, 1 µl BSA, 0.1 µl TAQ and 2 µl DNA). The thermal profile used for PCR amplification was the following: [94°C / 5 min; 37 cycles (94°C / 15 s, 46°C / 15 s, 72°C / 15 s); 72°C / 7 min]. The PCR products were visualized with 1% agarose gel, purified using the QIAquickR PCR Purification Kit (QIAGEN) and sequenced at Macrogen Inc. (South Korea).

Sequences were imported into BioEdit 7.0.5.2. (*Hall, 1999*) and checked for quality and accuracy with nucleotide base assignment. Sequences were aligned using Mafft (*Katoh et al., 2002*). The resulting sequences were deposited in GenBank (http://www.ncbi.nlm.nih.gov/genbank/). Eight COI minibarcodes (111-130 bp), too small to be submitted to GenBank, were deposited on the Sponge Barcoding Project instead (https://www.spongebarcoding.org; Table S4.3.2).

Phylogenetic analysis were conducted using two different approaches: Bayesian Inference (BI) and Maximum likelihood (ML), performed with the CIPRES science gateway platform (http://www.phylo.org; *Miller et al., 2010*) using MrBayes version 3.6.2 (*Ronquist et al., 2012*) and RAxML (*Stamatakis, 2014*). For MrBayes, we conducted four independent Markov chain Monte Carlo runs of four chains each, with 5 million generations, sampling every 1000^{th} tree and discarding the first 25% as burn-in, while RAxML was performed under the GTRCAT model with 1000 bootstrap iterations. Convergence was assessed by effective sample size (ESS) calculation and was visualized using TRACER version 1.5. Number of pair base differences and genetic distance (p-distance) between sequences of DNA were estimated with MEGA version 10.0.5 software (*Kumar et al., 2018*).

RESULTS

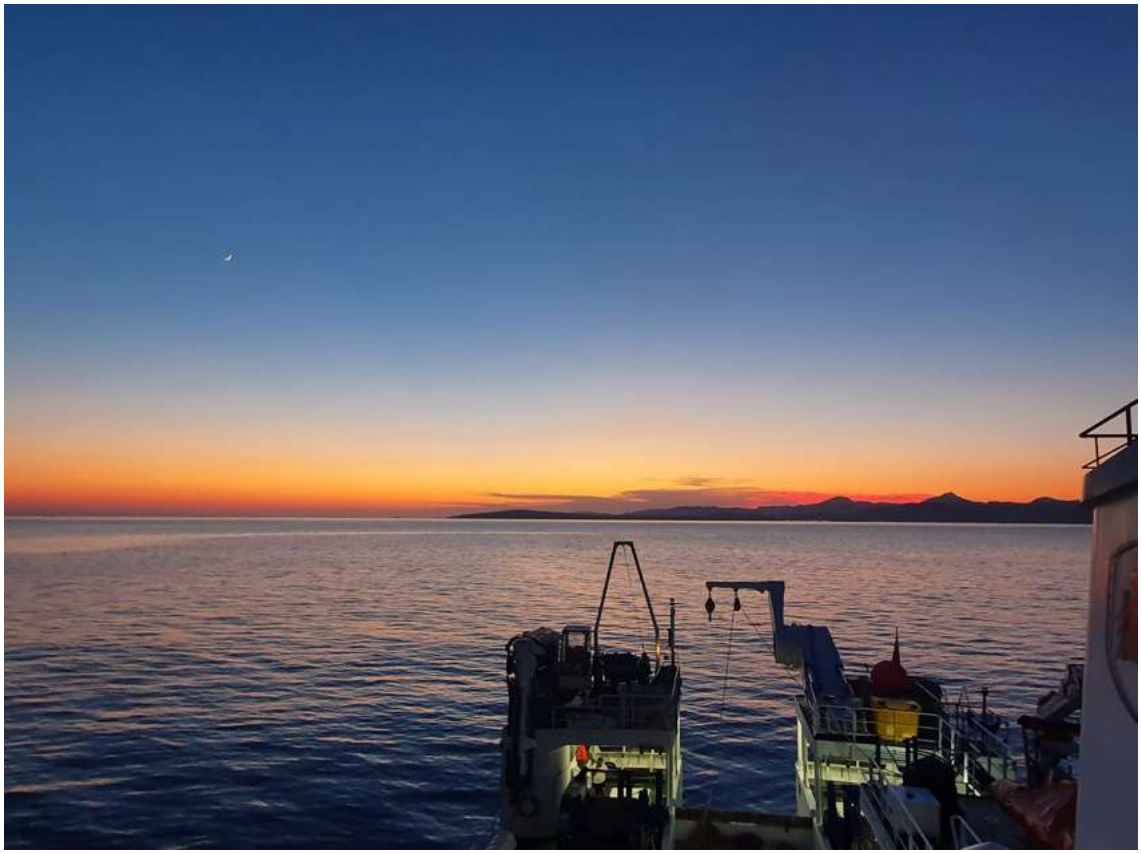

4.1. Poorly-known sponges in the Mediterranean with the detection of some taxonomical inconsistencies

Julio A. Díaz[1-4], Sergio Ramírez-Amaro[1,2], Francesc Ordines[1], Paco Cárdenas[3], Pere Ferriol[4], Bàrbara Terrasa[2] and Enric Massutí[1].

Abstract

The poorly-known sponge species Axinella vellerea *(Topsent 1904),* Acarnus levii *(Vacelet, 1960) and* Haliclona poecillastroides *(Vacelet, 1969) are reported from bottom-trawl samples off Balearic Islands, Western Mediterranean. A re-description is provided for all three species and the Folmer fragment of Cytochrome Oxidase subunit I (COI) obtained for A. levii and H. poecillastroides. This is the second report of* A. vellerea *in the Mediterranean, the first time that* A. levii *is reported outside Corsica and the first time that* H. poecillastroides *is documented outside the Gulf of Lion, France. The systematic allocation of* A. levii *and* H. poecillastroides *is discussed based on a COI phylogenetic analysis and morphology. The poorly understood phylogeny of the Haplosclerida does not permit us to find a proper allocation for* H. poecillastroides*, although its current position in the genus* Haliclona *nor the family Chalinidae is not defensible. On the other hand,* A. levii *currently fits best in the family Microcionidae, and seems related to some* Clathria *species with mixed features between* Clathria *and* Acarnus*. Considering that the species of the genus* Acarnus *shares a strong synapomorphy (the possession of Cladotylotes), it is plausible all* Acarnus *species to be Microcionids. We conclude that* H. poecillastroides *need to be reallocated to a new genus:* Xestospongia poecillastroides *comb. nov. (Petrosiidae). However, a reallocation of* A. levii *is not advisable for the moment, thus would imply major systematic changes like the reallocation of the whole genus* Acarnus *to Microcionidae, and the redescription of Microcionidae and Acarnidae*.

Keywords: *Porifera, New Records, Petrosiidae, Acarnidae, Barcoding, Balearic Islands, Mediterranean Sea*

Introduction

The Mediterranean is considered a hotspot of sponge diversity, with about 680 species reported including approximately 265 endemic species (*Pansini & Longo, 2003; Voultsiadou, 2009; Van Soest et al., 2012; Xavier & Van Soest, 2012*). Moreover, new species and new geographic records are periodically reported in this sea (e.g. *Vacelet et al., 2007; Corriero et al., 2015; Bertolino et al., 2013, 2015; Sitjà & Maldonado, 2014; Melis et al., 2016*). Knowledge on Mediterranean sponge fauna come mainly from species living in shallow habitats accessible through scuba diving. Less is known about the circalittoral and bathyal domains (*Danovaro et al., 2010*), although these deep ecosystems may harbour important communities of filter feeding animals, like corals or sponges, that can also function as habitat engineers (*Maldonado et al., 2015*). Improving

the scientific knowledge of this fauna contributes in the management of these fragile ecosystems and their protection.

The Balearic Promontory, in the Western Mediterranean, is an area of high ecological interest because of the high oligotrophy of its waters, a consequence of the lack of rivers and upwelling zones, the scarcity of rain and the karstic nature of its rocks (*Estrada, 1996; Acosta et al. 2002*). Moreover, the oceanographic fronts and currents of the Balearic Archipelago and between the Islands and the Iberian Peninsula may act as genetic barriers to the dispersal of sponges and other benthic organisms, contributing to its isolation (*Duran et al., 2004; Galarza et al., 2009; Pérez-Portela et al., 2015; Pascual et al., 2016*).

The first taxonomic studies of the sponge fauna in the Balearic Islands date back to the end of the 19th and the beginning of the 20th centuries and focus on samples collected from Maó in Menorca, Palma Bay in Mallorca and Cabrera Island (*Lackschewitz, 1886; Ferrer-Hernández, 1916, 1921*). Then, there is a gap in the literature until the 1980's, when several authors relaunched sponge research, mainly from shallow waters (*Bibiloni & Gili, 1892, Bibiloni et al., 1989; Bibiloni, 1990; Vacelet & Uriz, 1991; Martí et al., 2004; Gràcia et al., 2005; Gràcia et al., 2014; Guzzetti et al., 2019*), although with some exceptions from deeper habitats (*Uriz & Rosell, 1990; Maldonado et al., 2015*). Recently, *Santin et al. (2018)* have analysed the sponges of the Menorca Channel from a community-level perspective.

Within the ecosystem approach to fisheries, the MEDITS surveys program provides data and samples of benthic and demersal species on the sedimentary bottoms of the continental shelf and upper slopes along the northern Mediterranean (*Spedicato et al., 2020*). The aim of this work is to re-describe three poorly-known deep-sea sponge species, recorded for the first time from the circalittoral soft bottoms of the Balearic Promontory using an integrative taxonomy approach (combining morphological descriptions and molecular sequences). This is taken as an opportunity to revisit and question the phylogenetic relationships of these species.

Material and Methods

Samples

The specimens were collected during the MEDITS surveys developed off Balearic Islands (western Mediterranean), using the experimental bottom trawl gear GOC (*Bertrand et al., 2002*) (see Fig. 4.1.1 and Table 4.1.1 for sampling station details). Additional sampling with a Jennings' type beam trawl (*Reiss et al., 2006*) has been also carried out during these surveys in order to improve the sampling of benthic species. Sponges analyzed in this study have been collected with both sampling methods during the MEDITS surveys carried out in 2016, 2017 and 2018 around Mallorca and Menorca.

Once on deck, sponges were separated from the rest of the catch and photographed with a Nikon DSLR D300 digital camera on a graph chart. Whole samples were preserved in absolute ethanol (EtOH). Sponges specimens were deposited in the Marine Fauna Collection (http://www.ma.ieo.es/cfm/; CFM-IEOMA) based at the Centro Oceanográfico de Málaga (Instituto Español de Oceanografía) with the following identification reference numbers: CFM-IEOMA-6390-6399.

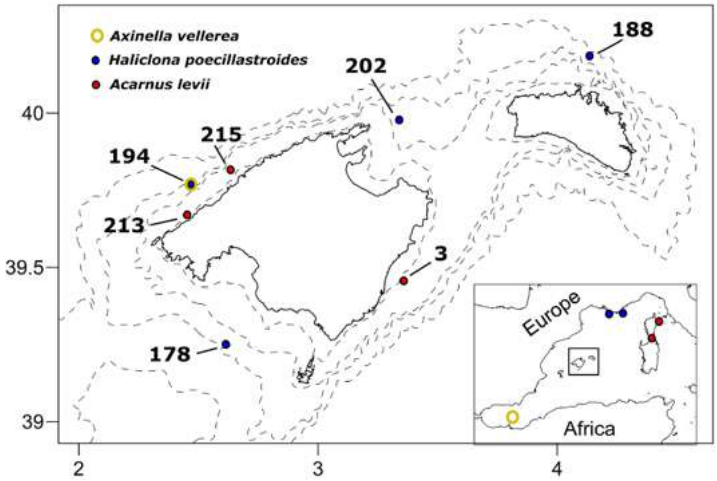

Fig. 4.1.1. Map of the studied area showing the stations (numbers) where sponges were collected. Coloured symbols represent the distribution of *Axinella vellerea*, *Haliclona poecillastroides* and *Acarnus levii*. The small map shows the previous records of the species in the Mediterranean for *A. vellerea* (*Sitjà & Maldonado, 2014; Sitjà et al. 2019*) and *A. levii* (*Vacelet, 1960, 1961*), and previous documented records for *H. poecillastroides* (*Vacelet, 1969*).

Morphological descriptions

External morphology, colour and texture were annotated prior to the sample conservation. Spicules preparations and histological sections were made according to the standard methods described by *Hooper (2003)*.

Spicules were observed with a Nikon S-Ke optical microscope and photographed with a CMOS digital camera. Images were processed with the Fiji software (*Schindelin et al. 2012*). For each sample, 30 spicules per spicule class or category were counted. Spicular sizes are provided as minimum-mean-maximum in chord length and minimum-mean-maximum in width and expressed in microns (µm). Thick sections of both tangential-surface and transversal-surface sections were made with a scalpel and, when necessary, dehydrated with alcohol and cleared with xylene. Cleared sections were re-hydrated with water, included in mounting media and observed with the microscope or a Leica M165C stereomicroscope. Aliquots of suspended spicules were transferred onto aluminium foil, air dried, sputter coated with gold and observed under a HITACHI S-3400N scanning electron microscope (SEM).

The terminology applied for the morphological description follows *Boury-Esnault & Rützler (1997)*. Identification was according to *Topsent (1904)*, *Sitjà & Maldonado (2014)* and *Vacelet (1960, 1969)*.

Table 4.1.1. Details of the sampling stations. GOC-73 (GOC), Beam trawl (BT).

Station	Year	Sampling device	Depth	Coordinates	Seabed characteristic
215	2016	GOC	68	39°49'6.6''N 2°38'22.19''E	Red algae bed
178	2017	GOC	152	39°14'57,12''N 2°37'3.42''E	Detritic
194	2017	GOC	148	39°46'25.68"N 2°27'59.22"E	Detritic
202	2017	GOC	135	39°58'40,26''N 3°20'11,56''E	Detritic
188	2018	GOC	245	40°11'6.72''N 4°7'57''E	Detritic
213	2018	GOC	66	39° 40' 10.92''N 2°26'58.92''E	Red algae bed
3	2018	BT	52	39°27'25.2''N 3°21'15.39''E	Red algae bed

Molecular analysis

DNA was extracted from a piece of choanosomal tissue (~2 cm^3) using the DNeasy Blood and Tissue Extraction kit (QIAGEN). Polymerase chain reaction (PCR) was used to amplify the Folmer fragment of the *Cytochrome C Oxidase subunit I* (*COI*; DNA barcoding), with the universal primers LCO1490 and HCO2198 (Folmer *et al*., 1994). PCR was performed in 25 µl volume reaction (17.2 µl ddH_20, 2.5 µl Mangobuffer, 1 µl DNTPs, 1.75 $MgCl_2$ 0.5 µl of each primer, 0.5 µl BSA, 0.05 µl TAQ and 1 µl DNA). The PCR thermal profile applied was: initial stage of 94°C for 5 min, then 37 cycles at 94°C for 15 s, 46°C for 15 s and 72°C for 15 s, followed by a final extension at 72°C for 7 min. PCR amplification of *A. vellerea* did not work, including another set of primers (LCO and Tetract-minibarR1) designed to amplify the *COI* minibarcode (the first 130 bp of the Folmer fragment) (Cárdenas & Moore, 2019). PCR products were purified using the QIAquickR PCR Purification Kit (QIAGEN). Both heavy and light strands were sequenced on an ABI 3130 sequencer using the ABI Prism Terminator BigDyeR Terminator Cycle Sequencing Reaction Kit (Applied Biosystems).

Sequences were imported into BioEdit 7.0.5.2. (*Hall, 1999*) and checked for quality and accuracy with nucleotide base assignment. Multiple sequence alignments (MSA) were obtained with ClustalW (Thompson *et al*., 1994). The DNA sequences obtained were deposited in the GenBank database (http://www.ncbi.nlm.nih.gov/genbank/) under the following accession numbers: MN508968, MN508969 and MN508967. Sequences were validated using the BLAST function from Genbank database (Altschul *et al*., 1990). The sequences were also used to reconstruct the phylogenetic relationships between species, through a phylogenetic tree based on Bayesian Inference (BI) and Maximum likelihood (ML). To build our alignments, we made a selection on the related sequences obtained after the BLAST search (Table S4.1.1). BI and ML trees containing *H. poecillastroides* (specimen CFM-IEOMA-6392) and proximal sequences of the order Haplosclerida (25 of which belong to Petrosiidae, 11 to Chalinidae, 5 to Callyspongiidae, 5 to

Phloeodictyidae and 6 to Niphatidae) were run. An additional sequence identified as Haplosclerida sp. was also used (GenBank ID MK833931). Sequences of *Axinella polyploides, Geodia barretti* and *Baikalospongia intermedia* were used as outgroups. For *A. levii* (specimens CFM-IEOMA-6397 and CFM-IEOMA-6398), BI and ML trees with sequences of the order Poecilosclerida (38 belong to the family Microcionidae, 9 Acarnidae, 7 Iotrochotidae, 4 Hymedesmiidae, 4 Myxillidae, 2 Coelosphaeridae and 1 Podospongiide), but also one sequence of Axinellida (*Acantheurypon pilosella*), were run. Sequences of *Axinella polyploides* and *Xestospongia muta*, were used as outgroups.

The Hasegawa-Kishino-Yano (*Hasegawa et al., 1985*) plus gamma distribution and proportion of invariable sites model (HKY+G+I) was assigned as the optimal substitution model of molecular evolution. This model was selected following Bayesian Criteria (BIC) and the Akaike Information Criterion corrected (AICc) using MEGA v.10.0.5 (Kumar *et al*., 2018). The codon position that were included were 1st+2nd+3rd. BI and ML analyses were performed with the CIPRES science gateway (http://www.phylo.org) (*Miller et al., 2010*): with Mr Bayes v 3.6.2. (*Ronquist et al., 2012*) conducting four independent MCMC runs (with four chains each) for 5 million generations, sampling every 1000 generations and discarding the first 25% of samples as burn-in. Convergence was assessed by effective sample size (ESS) calculation and was visualised using TRACER v.1.5. RAXML (*Stamatakis 2014*), was performed with 1000 bootstrap iterations. Genetic distance (p-distance) and number of base differences between pair of DNA sequences were estimated with MEGA v10.0.5 software (*Kumar et al., 2018*).

Results

Systematics

Class DEMOSPONGIAE Sollas, 1885

Subclass HETEROSCLEROMORPHA Cárdenas, Pérez and Boury-Esnault, 2012

Order AXINELLIDA Lévi, 1953

Family AXINELLIDAE Carter, 1875

Genus *Axinella* Schmidt, 1862

***Axinella vellerea* Topsent, 1904**

(Fig. 4.1.2, Table 4.1.1)

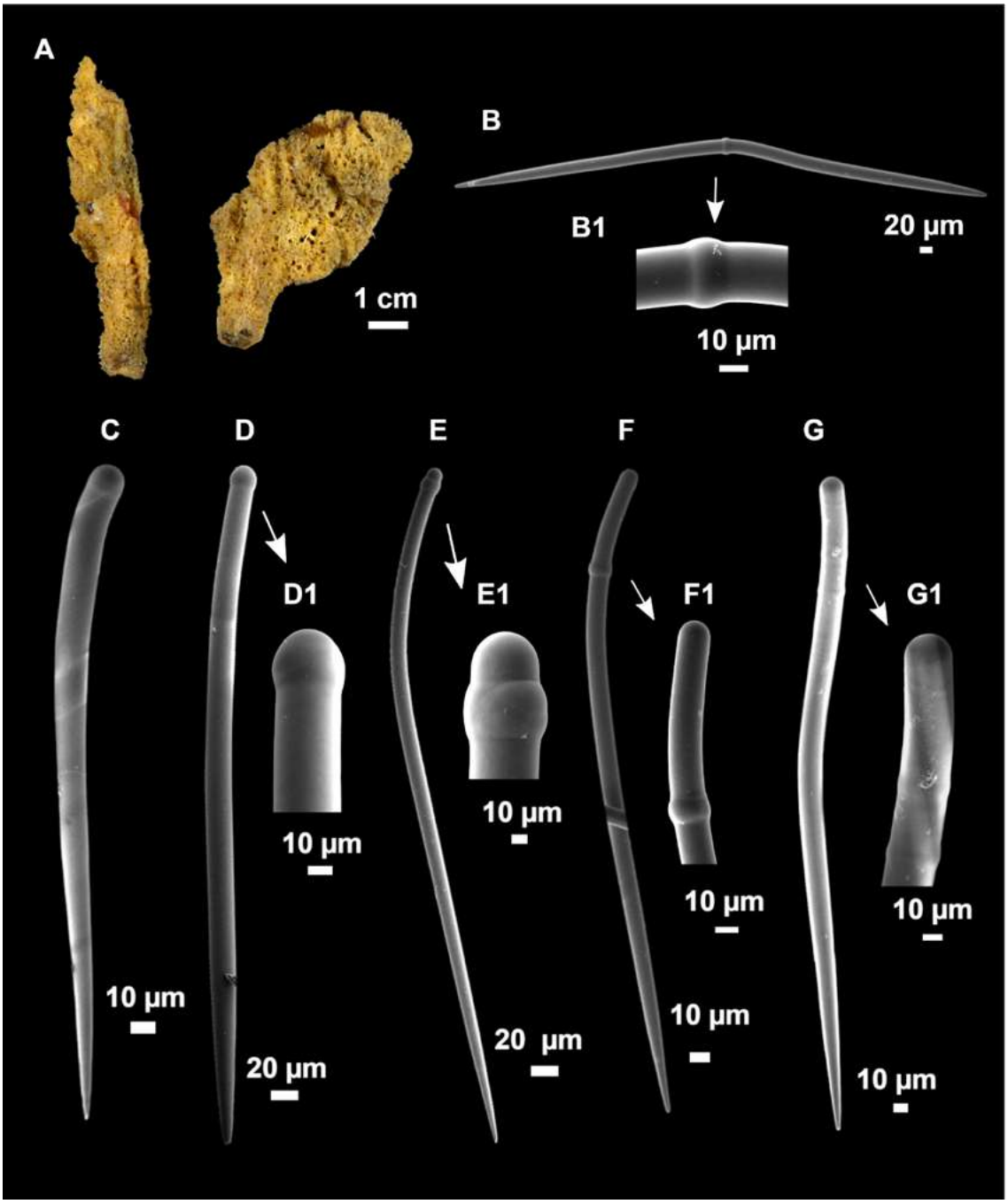

Fig. 4.1.2. *Axinella vellerea Topsent 1904*. (A) Habitus of CFM-IEOMA-6390 (right) and CFM-IEOMA-6391 (left). (B-G1) Spicules of CFM-IEOMA-6390. (B) Centrotylote oxea, with central swelling (B1). (C-G) Tylostyles occurring in a varying size and shape, with diversity of heads and terminal swellings (D1, E1, F1 and G1).

Material examined

CFM-IEOMA-6390 and CFM-IEOMA-6391, St. 194, 148 m, coll. P Ferriol and JA Diaz.

Outer morphology

Two individuals (Fig. 4.1.2A), 7x3 cm in 6390 and 5.5x1.5 cm in 6391, both supported by a tough peduncle of 1 cm in diameter. Color in life orange-yellow and ochre to light brown after preserved in EtOH. Consistency hard but slightly compressible, rough to the touch. Localized hispidation visible to the naked eye. Surface irregular and pores scattered through the body, up to 1 mm in diameter. There was a translucid dermal membrane, patent in some parts of the ectosome and inconspicuous in other zones.

Spicules

Oxeas (Fig. 4.1.2B), very rare and angulate, occasional marked swelling near the center of the shaft (Fig. 4.1.2B1), measuring 748-1065/21-26 μm (n=4) in 6390 and 623-1091/16-20 μm (n=4) in 6391.

Styles in a wide range of shapes and sizes (Fig. 4.1.2C-2G), with terminal, subterminal, single or multiple swellings (Fig. 4.1.2D1-2G1). They were slightly sinuous or curved in different grades, often resembling rhabdostyles. There was a large variation in size range, but no defined size categories. Measurements were 442-763-1345/13-22-31 μm in 6390 and 462-726-1309/13-19-25 μm in 6391.

Strongyles very rare and slightly curved, with symmetrical and roundish ends, same size range as styles.

Ecology notes

The species was found north-western Mallorca, an area under the seasonal influence of the so-called Balearic Current (*Garcia-Ladona et al., 1996*). This current appears in spring, flowing along the northern continental shelf edge off Mallorca and may have some influence on the communities of filter-feeding animals. The station was rich in filter-feeding or filter-feeding invertebrates like *Gryphus vitreus* (Born, 1778) and *Funiculina quadrangularis* (Pallas, 1766). There was also a high abundance of echinoderms and sponges.

Taxonomic remarks

The specimens matched the descriptions provided by *Topsent (1904)* and *Sitjà & Maldonado (2014)* in both spicular complement and abundance. Styles were the most abundant spicules, while diactines (mostly oxeas, some with strongylote modification) were rare, and their presence subjected to individual variation. The only difference is that in our specimens, styles are shorter (1345 μm) than specimens from the Atlantic (1800 μm) and Alboran Sea (1725 μm). The external morphology similarity with *Axinella centrotylota Pansini, 1982* should be noted. However, they differ in spicular complement and spicular sizes. In *A. centrotylota* oxeas are very abundant and measure 400-490/10-15 μm, while in *A. vellerea* they are notoriously rare and much larger (623-1091/16-26 μm). Moreover, styles of *A. centrotylota* are smaller (220-1270/8-15 μm) and can be divided in two categories, instead of a single category in *A. vellerea*.

Order HAPLOSCLERIDA

Family CHALINIDAE Gray, 1867

Genus *Haliclona* Grant, 1841

Haliclona poecillastroides (Vacelet, 1969)

Reniera poecillastroides Vacelet, 1969

Material examined

Samples CFM-IEOMA-6392, St. 178, 152 m, collectors P Ferriol and JA Diaz; CFM-IEOMA-6393, St. 194, 148 m, collectors P Ferriol and JA Díaz; CFM-IEOMA-6394, St. 202, 135 m, collectors P Ferriol and JA Diaz; CFM-IEOMA-6395 and CFM-IEOMA-6396, St. 188, 245 m, collector JA Diaz (Table 4.1.1).

Comparative material

Haliclona poecillastroides, paratype (Station Marine d'Endoume collection), Cassidaigne Canyon, off Marseille, France, Gulf of Lion, 150 m (Fig. 4.1.3C).

Outer morphology

Massive to lamellar, somehow irregular shape, up to 7 cm in diameter and 2 cm thick (Fig. 4.1.3A, Fig. 4.1.4A-C). Color on deck variable, 6394 and 6396 were whitish, while 6392 was dirty beige with pink shades (Fig. 4.1.3A) and 6395 and 6393 were dark gray. Once the specimens were fixed in EtOH, the color remained similar to the fresh state. It is remarkable that pinkish specimens colored the EtOH dark lilac, while the other specimens did not. Copious amounts of mucus were expelled when specimens were examined fresh on deck.

Consistency slightly hard to the touch and very friable. Surface slightly rough, but no hispidation visible to the naked eye. Inhalant and exhalant faces present, the former with a detachable crust, with small pores (Fig. 4.1.3A right, and Fig. 4.1.3A1 for close-up), while the latter without crust and with abundant rounded oscules of 1-5 mm diameter (Fig. 4.1.3A, left).

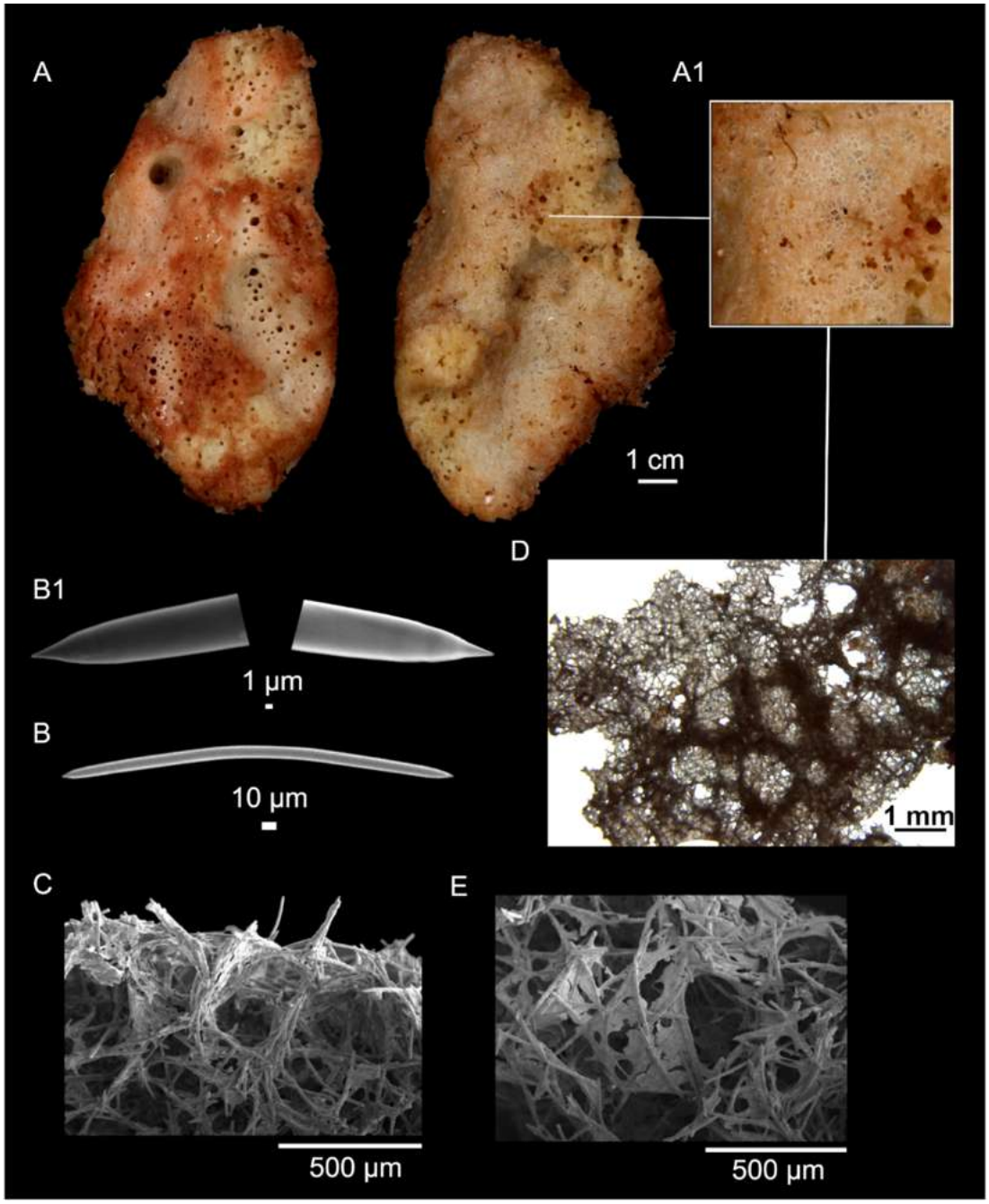

Fig. 4.1.3. *Haliclona poecillastroides* (Vacelet, 1969). (A) Habitus of CFM-IEOMA-6392 with detail of the ectosome (A1). (B-E) Spicules and skeletal arrangement of CFM-IEOMA-6392. (B) Oxea, with detail of heads (B1). (C) Transversal view of the choanosome, with the subectosomal condensation of spicule tracks. (D) Tangential view of the ectosome and the supporting subdermal tracks. (E) tangential view of the dermal membrane.

Spicules

Spicules were oxeas (Fig. 4.1.3B, B1), with some occasional stylote modifications. They were gently curved or straight, rarely sinuous, with tapered tips. Heterogeneous tips were found in some cases, with one tip more roundish, being probably intermediate forms of the stylote modifications. The oxeas sizes of each studied specimen are

presented in Table 4.1.2, overall measuring 232-295-380/6-12-16 µm, but spicules >350 µm were very rare. Some thinner juvenile oxeas of 150/4 µm were also present.

Skeletal structure

Choanosome composed by an isotropic and irregular net of spicule tracks, uni- to pauci-spicular, drawing heterogeneous meshes. These meshes were overlaid by oxeas in confusion, being only visible in some areas. The tracks condensed towards the surface and then ran in parallel to the surface, supporting the ectosome and generating rounded meshes (Fig. 4.1.3C and 4.1.3D).

Ectosome made of an isodictyal layer of single or occasionally double spicule mesh (Fig. 4.1.3E), forming a detachable crust that only persisted in some individuals. Under this crust, there were broad and characteristic subdermal spaces.

Fig. 4.1.4. (A) Holotype of *Haliclona poecillastroides* (https://science.mnhn.fr/institution/mnhn/collection/ip/item/2015-576). (B) Fresh image of the habitus of CFM-IEOMA-6393 (scale grid 1 cm). (C) Paratype of *Haliclona poecillastroides* (Station Marine d'Endoume collection). (D) Paratype of *Acanthacarnus levii* (Station Marine d'Endoume collection).

Ecology notes

The species was found at several stations western, northern and southern Mallorca and northern Menorca, from 135 to 245 m depth, at gravel and bathyal mud bottoms.

Remarks

Our material matched the description of *H. poecillastroides* in the external morphology, the shape of the spicules, the presence of styles of the same length as the oxeas and immature, smaller oxeas. However, the color appeared to be variable, with some individuals with pinkish shades. The spicules of our specimens are larger than those from the Gulf of Lion (*Vacelet, 1969; Griessinger, 1971*, Table 4.1.2), showing that the species may have a regional/seasonal variability in the spicule sizes, as indicated by these authors.

Table 4.1.2. Comparative table of the *Haliclona poecillastroides* individuals analyzed in this work. ID are the reference numbers of the CFM-IEOMA. Measures are given as minimum-mean-maximum for total length / minimum-mean-maximum for total width (as they appear in the cited texts). All measurements are expressed in μm.

Sample	Oxeas and styles	Colour
CFM-IEOMA-6392 West of Mallorca, 158 m	244-297-380/7-11-15	Cream with pink shades on deck, lilac in spirit.
CFM-IEOMA-6393 North-west of Mallorca, 148 m	232-281-313/6-11-14	Dark grey on deck and in spirit.
CFM-IEOMA-6394 North of Mallorca, 135 m	234-280-328/3-11-13	Cream on deck and in spirit.
CFM-IEOMA-6395 North of Menorca, 245 m	246-296-354/10-13-15	Dark grey on deck and in spirit
CFM-IEOMA-6396 North of Menorca, 245 m	265-304-339/9-13-16	Cream with pink shades on deck, dark lilac on spirit
Paratype remeasured (Station Marine d'Endoume) Gulf of Lion, 150 m	226-262-302/4-8-10	Whitish on spirit

Order POECILOSCLERIDA *Topsent 1928*

Family ACARNIDAE *Dendy, 1922*

Genus *Acarnus Gray, 1867*

Acarnus levii (*Vacelet, 1960*)

Acanthacarnus levii Vacelet, 1960

Material examined

CFM-IEOMA-6397, St. 215, 68 m, collector P Ferriol; CFM-IEOMA-6398, St. 3, 52 m, collector JA Diaz; and CFM-IEOMA-6399, St. 213, 66 m, collector JA Diaz.

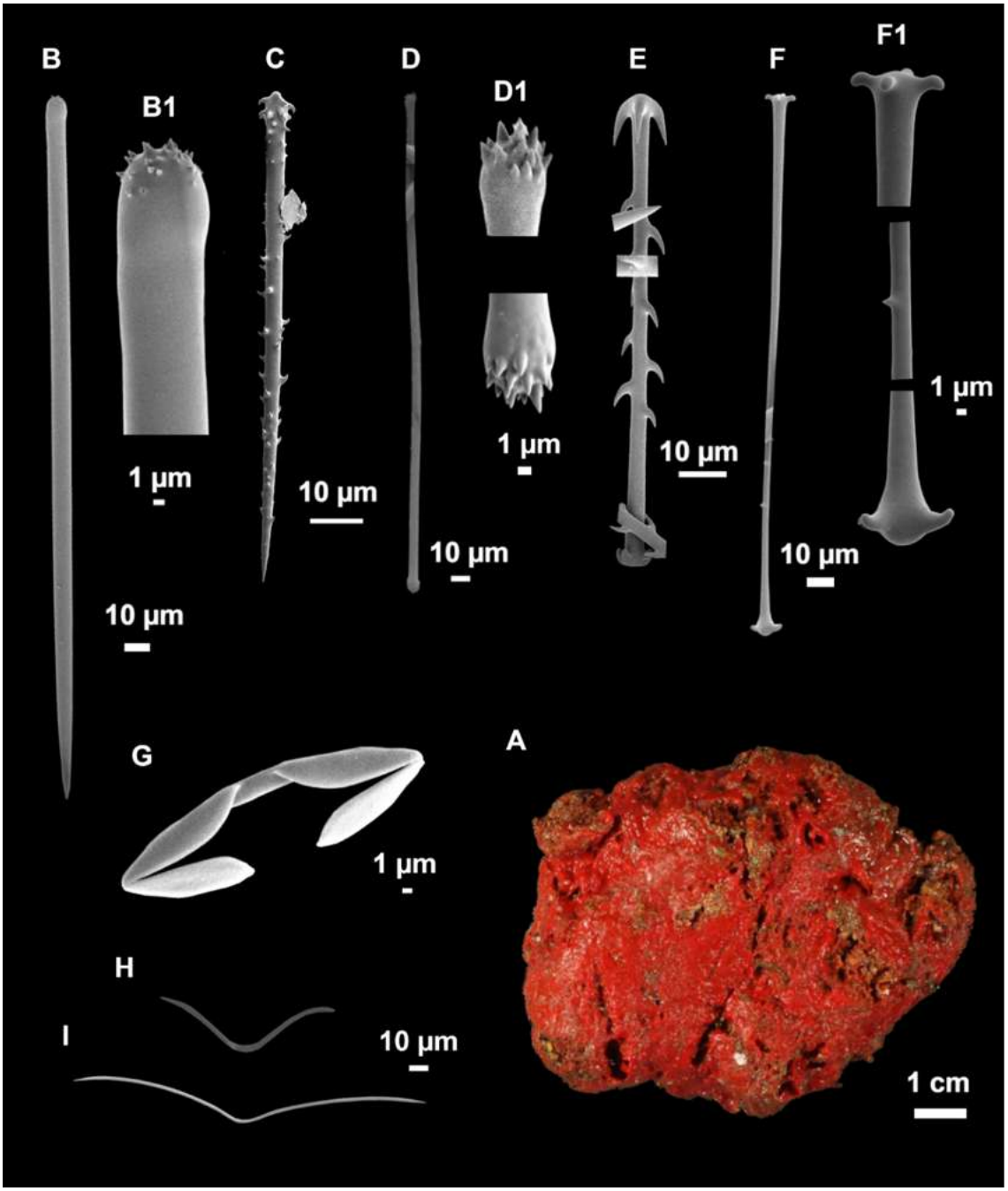

Fig. 4.1.5. *Acarnus levii (Vacelet, 1960)*. A: habitus of CFM-IEOMA-6397; B-I, spicules of CFM-IEOMA-6397; B: styles, with detail of the microspined head (B1); C: acanthostyle; D: tylote, with detail of the microspined heads (D1); E: cladotylote II; F: inmature Cladotylote, with details of the cladomes and the spination of the shaft (F1); G: palmate isochela; H: oxhorn toxas; I: accolada toxa.

Comparative material

Acarnus levii (Fig. 4.1.4D), paratype (Station Marine d'Endoume collection), R/V President Theodore Tissier, Corsica Channel, St. K. 204 (exogenous), 335-367 m.

Outer morphology

Individuals were massive, up to 5 cm diameter (Fig. 4.1.5A), with a tendency to become roundish. Some specimens were fleshy (6397 and 6399), while others incorporated large amounts of detritus in the choanosome (6398). Color in life bright red, brownish in EtOH, which became orange immediately after fixation of the sponge. Consistency compressible, a mark remains after pressed with the tweezers. Surface slightly rough to the touch. Ectosome consistent, not easily detachable. Openings were not visible.

Spicules

Styles straight or slightly curved (Fig. 4.1.5B), with microspined ends (Fig. 4.1.5B1), 279-373-481/3-7-11 μm.

Acanthostyles straight, with a marked head, finely and homogeneously spined (Fig. 4.1.5C), except just beneath the head, where spines were rare, 67-97-200/2-4-6 μm, although sizes >130 μm were very rare.

Tylotes straight or slightly contour, rarely tortuous (Fig. 4.1.5D), with spined heads (Fig. 4.1.5D1), 232-284-353/3-4-5 μm.

Cladotylote I, normal-shaped, abundant, stout and strongly hooked, with one cladome more developed than the other, measuring 156-191-231/4-6-10 μm.

Cladotylote II, (Fig. 4.1.5E) same morphology as Cladotylote I, measuring 83 - 105-140/3-4-7 μm.

Immature cladotylote, slightly spined (Fig. 4.1.5F), with similar sized cladomes (Fig. 4.1.5F1), 154-186-222/3-4-6 μm. These spicules, already described by *Vacelet (1960)*, were considered immature stages of cladotylotes I-II by *Van soest et al. (1991)*.

Palmate isochela (Fig. 4.1.5G), very common, 12-15-18/1-1-2 μm.

Oxhorn toxas (Fig. 4.1.5H), in a large size variation, but without distinguishable categories. The smaller ones tended to have a more pronounced curvature, 27-103-196/1-2-4 μm.

Accolada toxas (Fig. 4.1.5I), very rare, thin and straight, with a short and shallow curvature at the center, 185-195-264/2-2-3 μm.

Skeletal structure

A tangential ectosome composed of bundles of tylotes. Choanosomal structure composed by plumose spicule tracks, regularly connected by single large styles.

Ecology notes

The specimens were collected from red algae beds at 52-68 m depth, dominated by red algae, both calcareous and ‘soft’ species, the green algae *Codium bursa* (Olivi) C.

Agardh, 1817, the brown algae *Laminaria rodriguezii* Bornet, 1888 and fauna such as echinoderms and ascidians, including a high diversity and abundance of mesophotic sponges.

Table 4.1.3. Comparative table of the spicular set of the *Acarnus levii* individuals analyzed in this work (including a paratype from Corsica) and the Holotype. Numbers are the reference numbers of the CFM-IEOMA. Measures are given as minimum-mean-maximum for total length/minimum-mean-maximum for total width (or as they appear in the cited texts). All measurements are expressed in μm.

Sample	Styles	Acanthostyles	Tylotes	Cladotylote	Inmatyre Cladotylote	Oxhorn Toxa	Accolada Toxa	Chelae
CFM-IEOMA-6397	279-362-439/4-8-11	83-98-110/4-5-6	238-287-353/3-4-5	I. 58-185-215/5-7-10 II. 92-104-123/3-4-5	154-179-199/3-4-5	33-94-164/1-2-3	Very rare 185/2 (n=1)	15-16-18/1-1-1
CFM-IEOMA-6398	283-355-412/3-6-8	67-92-107/2-4-4	242-291-353/3 - 4-5	I. 168-197-222/5-6-7 II. 85-113-138/3-4-4	186-203-222/3-4-5	27-117-196/1-2-4	Rare 185-245/2-3 (n=7)	12-14-17/1-1-2
CFM-IEOMA-6399	349-404-481/4-8-10	79-95-126/3-4-5	232-273-313/3-4-5	I. 156-177-192/5-6-7 II. 83-97-128/3-4-4	173-181-189/4-5-6	27-91-163/1-2-4	Very rare 215-264/2 (n=3)	14-16-17/1-1-1
Holotype by *Van Soest et al. (1991)*	315-480/6-9	55-115/3-5	260-460/3-4.5	I. 180-210/5-6 II. 100-140/2-4	200/3	20-140/1-3	75-195/2 not found in the re-description	13-16
***Acanthoacarnus levii*, Paratype remeasured**	334-408-492/5-8-10	90-115-156/3-4-5	260-340-481/2-4-5	I. 184-205-231/4-6-7 II. 96-107-117/3-4-6	190-204/2-3 (n=4)	32-68-145/1-2-3	Very rare 218 / 3 (n=1)	14-16-17/1-1-2

Taxonomic remarks

There are currently 26 species of *Acarnus* in the world. In the Mediterranean and the northeast Atlantic, three species of this genus have been reported: *A. souriei (Levii, 1952)*, *A. tortilis (Topsent, 1892)* and *A. levii*. *A. levii* differs from *A. sourei* in the habitus (massive versus incrusting) and the possession of a single category of acanthostyles and three categories of cladotyles. It differs from *A. tortilis* by the presence of acanthostyles. Other similar species are the pacific *A. peruanus*, the Indo-Pacific *A. bicladotylota*, the southern Atlantic *A. nicoleae* and the Mexican *A. michoacanensis* (*Van Soest et al.,1991*; *Aguilar-Camacho et al., 2013*). The differences between *A. levii* and *A. peruanus* are minimal and reduced to spicular dimensions of the megascleres and toxas. However, due to the vast geographical distances between both species (western Mediterranean and eastern Central Pacific) they are unlikely to be the same species. *A. levii* differs with *A. bicladotylotus* in the reduced spination of cladotylote I, with *A. nicoleae* in the dimensions of the megascleres (*Van Soest et al., 1991*) and with *A. michoacanensis* in the possession of a single cladotylote category (versus two in *A. levii*) (*Aguilar-Camacho et al., 2013*).

The accolada toxas were reported in the original description of this species, but not found in the re-description by *Van Soest et al. (1991)*. We found them in all the studied specimens and in a paratype from the Corsica Channel, albeit in very low numbers. It is probable that they were overlooked by *Van Soest et al. (1991)*, who thought that Vacelet reported "thin growth stages of the choanosomal styles" instead of true toxas.

Genetics

Haliclona poecillastroides (specimen 6392) gave 613 bp COI Folmer fragment. For *A. levii*, sequences of two specimens (6397 and 6398) were obtained, resulting in edited fragments of 458 bp (POR246) and 617 bp, (POR615) respectively.

We generated, for each species (*H. poecillastroides* and *A. levii*) a BI and a ML tree. For *H. poecillastroides* (Fig. 4.1.6, large and small trees, respectively), both trees show similar topologies with all haplosclerid families being polyphyletic. The Bayesian reconstruction suggested that *H. poecillastroides* groups within a well-supported *Petrosia/Neopetrosia* clade, and not with the any *Haliclona* species (Fig. 4.1.6, large tree). The ML tree placed *H. poecillastroides* in a basal branch of a cluster that included both Chalinidae and Petrosiidae sequences, however, this allocation was poorly supported.

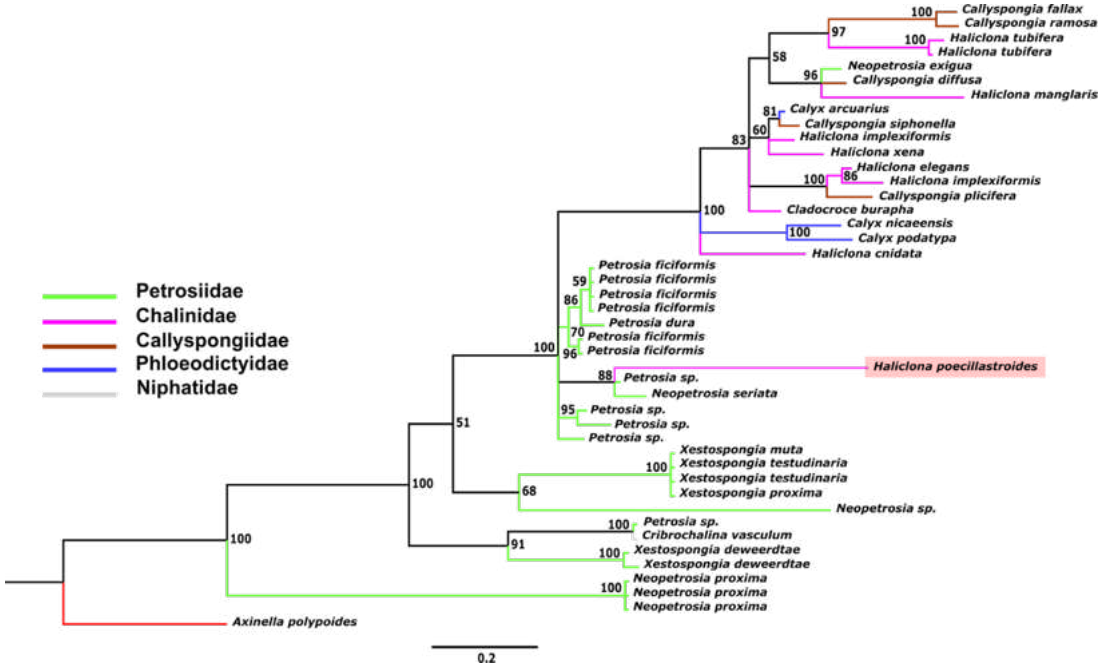

Fig. 4.1.6. Phylogenetic tree topology constructed with Maximum likelihood (small simplified tree) a Bayesian inference (large tree) for the *COI* sequences of *Haliclona poecillastroides* described in the present study and other related Haplosclerida. Branch colours represent different families. A sequence of *Axinella polypoides*, *Geodia barretti* and *Baikalospongia intermedia* are used as outgrups.

The BI and ML trees including *A. levii* were congruent (Fig. 4.1.7, large and small trees, respectively) and showed the family Acarnidae as polyphyletic. The Acarnidae are

distributed in three well-supported clades: 1) a clade contained *Iophon* spp. and *Acanthorhabdus fragilis*, 2) a clade contained *Paracornulum* spp. and finally, 3) a clade containing *A. levii*, nested in the Microcionidae and sister to *Clathria rugosa*.

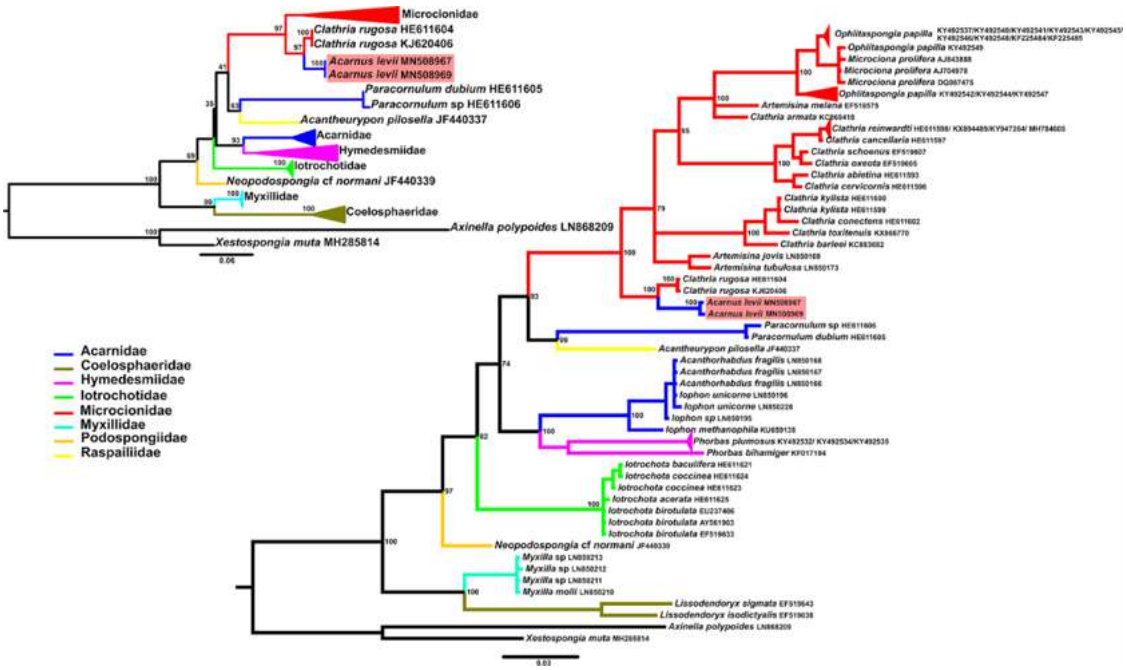

Fig. 4.1.7. Phylogenetic tree topology constructed with a Bayesian inference for the *COI* sequences of *Acarnus levii* described in the present study and other related sequences (large tree) and simplified tree topology obtained with RAXML (small tree). Branch colors represent different families. Sequences of *Xestospongia muta* and *Axinella polypoides* are used as outgroup.

For *H. poecillastroides*, lower *p*-values and bp differences were obtained when compared with *Petrosia* sp., *Petrosia* sp. E and *N. seriata* (7-8% *p*-distance and 41-43 bp differences). Otherwise, for *A. levii*, the lowest genetic distances were found when compared *A. levii* with *C. rugosa*, with a *p*-distance of 2% and 11 bp differences.

Discussion

Biogeography

The results obtained improve the knowledge of the sponge diversity in the western Mediterranean. We studied the sedimentary bottoms of the continental shelf and slope off Balearic Islands and reported the presence of three poorly-known species. For *Axinella vellerea* the presently work represents its second record in the Mediterranean, as it was recently reported from the Alboran Island (*Sitjà & Maldonado, 2014*). Moreover, this species had only been reported from other three localities: the type locality in the Azores Archipelago (Topsent, 1904), the Gulf of Cadiz (*Sitjà et al. 2019*) and the Folden fiord, in Norway (Burton, 1931). In its work, *Sitjà & Maldonado (2014)* considered this species as Atlantic, explaining its presence in the Alboran Island as a result of a penetration towards the Mediterranean. If the Atlantic origin is correct, a

Balearic presence must mean that *A. vellerea* populations expanded inwards the Mediterranean despite important oceanographic barriers, like the Almeria-Oran front and the Ibiza channel, which are efficient in retaining both larval and adult stages from many phyla (*Patarnello et al., 2007; Mokhtar-Jamaï et al. 2011; García-Merchán et al., 2012*). Although current knowledge on the genetic dynamics of sponge populations is scarce, in general terms, dispersive potential of the phylum is considered low (*Duran et al., 2004; Guardiola et al., 2012; Pérez-Portela et al., 2015*). Moreover, it is notorious that the number of recorded individuals in the Mediterranean and in the Atlantic is very similar. Considering the limited dispersive potential of the sponges, it is plausible to consider this species as Atlanto-Mediterranean instead of Atlantic.

The species *Haliclona poecillastroides* is documented for the first time in the Balearic Islands. Previously, this species was only known from two records in the Gulf of Lion and undocumented reports from the Menorca Channel *(Santin et al. 2018)*. Finally, *Acarnus levii* is reported for first time elsewhere than Corsica, representing the third records of the species and expanding its geographical range westwards (Fig. 4.1.1).

The present records highlight the singularity of the Balearic Islands ecosystems, whose oceanographic characteristics lead to conditions in which singular and poorly known sponge assemblages develop *(Bibiloni, 1990)*. Moreover, bottom trawl fishing pressure around the Archipelago is not as high as in adjacent waters off Iberian Peninsula, thus sedimentary insular bottoms present a better conservation state *(Quetglas et al., 2012)*. To this fact it must be added that in soft circalittoral bottoms around the Islands two widely distributed red algae facies (*Peyssonnelia* and maërl beds) provide substrate and increment the structural complexity, creating habitats with high biodiversity (*Ballesteros, 1992, 1994; Barbera et al., 2012; Ordines et al., 2017*).

All the sponge species here included were collected in the mesophotic zone, between 40 and 300 m depth, a transitional zone between shallow and deep communities that includes the circalittoral and the offshore circalittoral habitats (*Evans et al., 2016*). Here, the ecological factors (e.g. light, nutrients or temperature) are under a marked gradient that generates a biological mixture of shallow, deep and strictly mesophotic communities (*Soares et al., 2019*). In the Mediterranean and regarding sponges, much of the works published recently are focused on these transient communities (*Bertolino et al., 2015; Longo et al., 2018; Santin et al., 2018; Idan et al., 2018*). However, sampling on these depths is problematic and prone to logistic limitations. Currently, the objectives of MEDITS surveys include not only the assessment of the demersal resources but the entire benthic ecosystem exploited in the Mediterranean bottom trawl fishery. In this regard, the potential of MEDITS surveys to study deep-sea sponges is clear since the experimental bottom trawl used in the sampling is not only effective for the capture of fishes, decapods crustaceans and cephalopods, the target species for which it was designed (*Dremière et al., 1999; Fiorentini et al., 1999*), but other mega-benthic. In fact, MEDITS data is being used to model the distribution of sessile species (e.g. *Lauria et al., 2017*) and in the Balearic Islands it has been also used to study essential and

sensitive habitats and the influence of benthic communities on demersal resources (*Ordines & Massutí, 2009; Ordines et al., 2009, 2011*). Moreover, clear advances in biodiversity knowledge are being made from samples obtained during the MEDITS surveys, particularly in the case of small benthic fishes, like the Callionymidae and Gobidae fishes, but also other fishes and echinoderms (*Farias et al., 2016; Kovačić et al., 2017, 2018, 2019, Fricke and Ordines 2017a,b, Ordines et al. 2018, 2019a.b*).

Taxonomic incongruences

Our results show that *Acarnus levii* is, by both molecular analysis and morphology, more related to the family Microcionidae (genus *Clathria*) than to Acarnidae. Specifically, the species has a genetic proximity with *Clathria rugosa* (*Hooper & Lévi, 1993*), a New Caledonian microcionid species with singular "quasidiactinal subtylostyles" in the ectosome. These spicules resemble diactinal forms and are also spined in its basis and tips, a notorious fact since the presence of diactines in the ectosome is considered a diagnostical trait to separate Acarnidae and Microcionidae, (*Hooper & Van Soest., 2002*). In fact, the literature has other examples of *Clathria* spp. with dubious "quasidiactinal" spicules in the ectosome and other mixed features between *Clathria* and *Acarnus*: e.g. (*i*) *Clathria* (*Microciona*) *acarnoides* from the Caribbean has "cladotylote acanthostyles", which are very similar to the cladotylotes of *Acarnus*; and (*ii*) *Clathria* (*Clathria*) *nicoleae* has diactines in the ectosome, consisting on "tylostrongiles" strongly spined in the head and resembling the tylotes of some *Acarnus* spp. (*Aguilar-Camacho et al., 2013; Vieira de Barros, Santos & Pinheiro., 2013; Van Soest et al., 2014*). Moreover, other works have revealed the genetic proximity of the type species of the genus *Acarnus*, *A. innominatus* Gray 1867, to the family Microcionidae, through *16S*, *18S* and *28S* markers (*Redmond et al. 2013; Hajdu et al. 2013*).

The genus *Acarnus* is characterized by the presence of Cladotylotes, a strong synapomorphy that unites the group. For this reason, the relatedness of *A. levii* and *A. innominatus* with Microcionidae is potentially shared with all the Acarnids. If that is the case, the reallocation of the whole *Acarnus* to Microcionidae seems the right choice. In fact, *Lévi, 1973* already placed *Acarnus* in Clathriidae, a decision that was later refused by *Van Soest 1984*, who considered the genus to be more related to Myxillidae and Coelosphaeridae. However, since *Acarnus* is the type genus of Acarnidae, reassigning this genus to Microcionidae would requires assigning a new family to the rest of 12 remaining genera now in Acarnidae, and to expand the current definition of Microcionidae to include species with diactinal spicules in the ectosome, two actions that are far beyond the scope of the present work. For all exposed, we refrain from moving nor the species *A. levii* nor the genus *Acarnus* until a revision of both families is made, including sequences of other *Acarnus* spp. and *Clathria* spp. with *Acarnus*-like features.

On the other hand, and according to our COI phylogenetic analyses, *H. poecillastroides* is more related to the family Petrosiidae than to the Chalinidae. Both molecular and

morphological results support a Petrosiidae relationship: (*i*) choanosomal skeleton isotropic and confused, instead of composed by primary ascending tracks regularly interconnected by secondary tracks of Chalinidae; (*ii*) presence of a isodictyal ectosomal crust and a large subdermal space beyond; (*iii*) condensation of the choanosomal tracks near the surface to support the ectosome, from which draws parallel and circular meshes; and (*iv*) stony but friable consistency. Indeed, all these features are considered typical of Petrosiidae (*Van Soest, 1980; Desqueyroux-Faúndez & Valentine 2002*). It should be noted that the species *H. poecillastroides* was originally assigned to the family Renieridae *Schmidt, 1870* (now a synonym of Chalinidae) and the genus *Reniera Schmidt, 1862* (now a subgenus *Haliclona (Reniera)*). That classification was very broad and emphasized the organization of the skeleton and the amount of spongin/spicules as a character with systematic value. Thus, sponges with a disorganized skeleton and mostly composed by spicules were included in the family Renieridae, while those with a more organized, spongin-reinforced skeleton were considered as Haliclonidae (*de Laubenfels, 1932; Griessinger, 1971*). Later, *Wiedenmayer (1977)* used Nepheliospongiidae (*Clarke, 1900*) to group species "characterized by strong development of megascleres in relation to fleshy parts and spongin, hence by a stiff and hard, occasionally friable consistency. The spicules may be packed into stout, crowded fibers, or tracts, agglutinated by spongin, or they may be packed in confusion around canals and alveoles. The basic architecture is that of ascending tracts, diverging and becoming radial towards the surface, connected by tangential tracts arranged in layers parallel to the surface, i.e. accretive". This definition overlapped with that previously given to Renieridae. Nepheliospongiidae was latter split in two families by *Van Soest (1980)*, who erected the family Petrosiidae for those species "with an ectosomal skeleton consisting of an isotropic reticulation of single spicules or spicule tracts, and choanosomal skeleton verging towards an isotropic reticulation of spicule tracts, in which primary and secondary tracts are indistinct", and Oceanapiidae for species with an "ectosomal skeleton consisting of an often mutilayered isotropic reticulation of single spicules, […] and an irregular system of tangential thick spicule tracks". *H. poecillastroides skeleton* matches the definition of Petrosiidae, a family with four accepted genera: *Petrosia*, *Neopetrosia*, *Xestospongia* and *Acanthostrongylophora* (*Hooper, 1984*). It differs from both *Petrosia* and *Acanthostrongylophora* in not having a hispid ectosome, and with *Petrosia* also in lacking diverse spicule categories. It is, however, very similar to both *Xestospongia* and *Neopetrosia*, two genera with unclear relationship and overlapping diagnostical characters. These species are divided in basis of the size of the spicules and skeletal arrangement: those having spicules >200 μm belong to *Xestospongia* and if they are <200 μm to *Neopetrosia* (*Desqueyroux-Faúndez & Valentine, 2002*). However, this dichotomy is not always met such as in *Neopetrosia carbonaria* (*Lamarck, 1815*), *Neopetrosia dominicana* (Pulitzer-Finali, 1986), *Neopetrosia dutchi* (*van Soest et al., 2014*), *Neopetrosia ovata* (*Meesters & Becking, 2014*) and *Neopetrosia sigmatifera* (Vicente *et al*., 2019), all presenting oxeas >200 μm (see *Santos et al., 2016 and Vicente et al., 2019*). Conversely, in species like *Xestospongia dubia* (Ristau, 1978), *Xestospongia emphasis* (*de Laubenfels, 1954*), *Xestospongia mammillata* (*Pulitzer-*

Finali, 1982), *Xestospongia menzeli* (*Little, 1963*), *Xestospongia tuberosa* (*Pulitzer-Finali, 1993*) and *Xestospongia vansoesti* (*Bakus & Nishiyama, 2000*) oxeas may be <200 μm (revised in *Carvalho et al., 2016*). A possible cause that might explain differences in spicule size between the members of *Xestospongia* and *Neopetrosia* is the depth where they live, the availability of nutrients and the temperature (*Valisano et al. 2012*). In other demosponges, individuals inhabiting deeper habitats develop longer spicules than those inhabiting shallower ones (*Bavestrello et al., 1993; Uriz et al., 2003*). However, to this date this has not been tested in any *Neopetrosia* nor *Xestospongia* species. Another way to discern between both genera is the comparison of the skeletal arrangement, because the ectosome of *Neopetrosia* is "a simple tangential unispicular isodictyal network of small spicules", while in *Xestospongia* it consists of a "dense ectosomal brushes of large spicules". In addition, the choanosome of *Neopetrosia* is "more compact" than those of *Xestospongia* (*Desqueyroux-Faúndez & Valentine 2002*). In *H. poecillastroides*, spicules are >200 μm, but both ectosomal and choanosomal architectures are intermediate between *Neopetrosia* and *Xestospongia*. Moreover, the genetic results are not conclusive, and *H. poecillastroides* shows genetic similarities with both *N. seriata,* an Indo-Pacific shallow water species, and two *Petrosia* sp. A possible explanation for the somewhat ambiguous position of *H. poecillastroides* inside Petrosiidae is the lack of genetic works specifically dealing with this family. We foresee that *H. poecillastroides* may represent a potential new Petrosiidae genus with mixed characters between *Neopetrosia* and *Xestospongia,* gathering several chalinid species with Petrosiidae characters, such as: *Haliclona* (*Halichoclona*) *magna* (*Vacelet, 1969*), *H.* (*Halichoclona*) *fistulosa* (Bowerbank, 1866) or some *Haliclona* (*flagellia*) species (*Fourt et al, 2017; Van Soest, 2017; Dinn, 2020*). Those species are large, massive, massive-encrusting or tubular, with low spongin content, having a characteristic layer in the ectosome, large subectosomal spaces, and a low-organized choanosome with some ascending track of spicules (*de Weerdt, 2000*). Like the cases of *Xestospongia plana* and *Xestospongi friabilis*, two temperate species first included in *Haliclona* but later transferred to the genus *Xestospongia*, we propose to transfer *H. poecillastroides* to *Xestospongia* based on skeletal architecture morphology (*Costello et al., 2001*).

The phylogenetic tree shows the fairly known polyphyly of the order Haplosclerida (*Redmond et al., 2011*). The group is especially challenging because it has a very limited set of morphological traits, low number of synapomorphies and an elevated number of species (*Griessinger, 1971*). In this sense, the combined use of morphological characters and molecular markers has the potential to solve the relationship of its members because it allows to detect morphological homoplasies and phylogenetic relatedness. Contrary to Haplosclerida, poecilosclerids sponges emerge as a different case because they possess a very large and heterogeneous set of skeletal elements.

4.2. Sponges of Western Mediterranean seamounts: new genus, new species, and new records

Julio A. Díaz[1,2], Sergio Ramírez-Amaro[1,3] & Francesc Ordines[1],

Abstract

The seamounts Ses Olives (SO), Ausias March (AM) and Emile Baudot (EB) at the Mallorca Channel (Balearic Islands, western Mediterranean), are poorly explored areas containing rich and singular sponge communities. Previous works have shown a large heterogeneity of habitats, including rhodolith beds, rocky, gravel and sandy bottoms and steeped slopes. This diversity of habitats provides a great opportunity for improving the knowledge of the sponges from Mediterranean seamounts. Sponges were collected during several surveys carried out by the Balearic Center of the Spanish Institute of Oceanography at the Mallorca Channel Seamounts. Samples were obtained using a beam-trawl, rock dredge and remote operated vehicle. Additional samples were obtained from fishing grounds of the Balearic Islands continental shelf, using the sampling device GOC-73. Sponges were identified through the analysis of morphological and molecular characters. A total of 60 specimens were analyzed, from which we identified a total of 19 species. Three species and one genus are new to science: *Foraminospongia balearica* **gen. nov. sp. nov.**, *Foraminospongia minuta* **gen. nov. sp. nov**. and *Paratimea massutii* **sp. nov.** *Heteroxya* cf. *beauforti* represents the first record of the genus *Heteroxya* in the Mediterranean Sea. Additionally, this is the second report of *Axinella spatula* and *Haliclona* (*Soestella*) *fimbriata* since their description. Moreover, the species *Petrosia* (*Petrosia*) *raphida*, *Calyx* cf. *tufa* and *Lanuginella pupa* are reported for the first time in the Mediterranean Sea. *Petrosia* (*Strongylophora*) *vansoesti* is reported here for the first time in the western Mediterranean Sea. *Haliclona* (*S.*) *fimbriata* is reported here for the first time in the north-western Mediterranean Sea. *Hemiasterella elongata* is reported here for the second time in the Mediterranean Sea. The species *Melonanchora emphysema, Rhabdobaris implicata*, *Polymastia polytylota*, *Dragmatella aberrans*, *Phakellia ventilabrum* and *Pseudotrachya hystrix* are reported for the first time off Balearic Islands. Following the Sponge Barcoding project goals, we have sequenced the Cytochrome Oxidase subunit I (COI) and the 28S ribosomal fragment (C1-D2 domains) for *Foraminospongia balearica* **sp. nov.**, *Foraminospongia minuta* **sp. nov**., *H.* cf. *beauforti* and *C.* cf. *tufa,* and the COI for *Paratimea massuti* **sp. nov**. We also provide a phylogenetic analysis to discern the systematic location of *Foraminospongia* **gen. nov.**, which, in accordance with skeletal complement, is placed in the Hymerhabdiidae family. A brief biogeographical discussion is provided for all these species, with emphasis on the sponge singularity of SO, AM and the EB seamounts and the implications for their future protection.

Keywords: Biodiversity, Sponges, New genus, New species, New records, DNA barcoding, Seamounts, Mediterranean Sea.

Introduction

Seamounts are structures of high ecological and biological interest (*Rogers, 2018*), which provide excellent habitat for rich communities of filter-feeding animals, such as corals, crinoids and sponges (*Samadi et al., 2007*). These organisms are favored by enhanced currents, scarcity of fine sediment, accidented topography and predominance of hard substrata, features that characterize Seamounts (*White & Mohn, 2004*). Sponges are ubiquitous on seamounts, where they tend to form dense and diverse aggregations that provide habitat and refuge to other animals like crustaceans, mollusks and fishes (*Samadi et al., 2007*). Also, they are involved in benthic-pelagic coupling and recycling of nutrients, both processes of utmost importance in oligotrophic areas like the Mediterranean Sea, where they may contribute to the maintenance of higher trophic levels (*de Goeij et al., 2013*).

Despite their importance, very little is known about sponges of the Mediterranean seamounts, which is in contrast to the vast number of studies on sponge taxonomy available in other domains like the continental shelf or the submarine canyons (e.g. *Vacelet, 1961, 1969; Pulitzer-Finali, 1978, 1983; Boury-Esnault, Pansini & Uriz, 1994; Pansini, Manconi & Pronzato, 2011; Bertolino et al., 2015; Longo et al., 2018; Manconi et al., 2019; Enrichetti et al., 2020*). However, in recent years the increase in the use of Remote Operated Vehicles (ROV) has facilitated the access and study of Seamounts. Currently, information on sponges is available from the Erathostenes seamount in the Levantine Sea (*Galil & Zibrowius, 1998*), the Vercelli seamount in the northern Tyrrhenian Sea (*Bo et al., 2011*), the Ulisse and Penelope seamounts in the Ligurian Sea (*Bo et al., 2020*), the Avempace, Alboran Ridge, Seco de los Olivos and Cabliers seamounts in the Alboran Sea (*Boury-Esnault et al., 1994; Pardo et al., 2011; Sitjà & Maldonado, 2014; De la Torriente et al., 2018; Corbera et al., 2019*), and the Stone Sponge, Ses Olives, Ausias March and Emile Baudot seamounts in the Balearic Sea (*OCEANA, 2011; Aguilar et al., 2011; Maldonado et al., 2015*). However, most of these works adress the sponges at a community level, focusing on a general habitat characterization. Nonetheless, the studies adressing taxonomy have revealed that the Mediterranean seamounts are habitats for rare, poorly-known, or new species. For example, *Aguilar et al., (2011)* reported the carnivorous sponge *Lycopodina hypogea* (Vacelet & Boury-Esnault, 1996) at the Ausias March seamount, representing the first sighting of this species outside littoral caves. A singular reef formed by the Lithistid *Leiodermatium pfeifferae* (*Carter, 1873*) was recorded at the Stone Sponge seamount, being the first report of this species in the Mediterranean Sea (*Maldonado et al., 2015*).

Determining which species are present on a given seamount, and hence the seamount's biodiversity is a first step towards the development of management plans to protect these habitats. It is also crucial to understand seamounts' biocenosis, their structure and dynamics, how they can be affected by human disturbances, and to monitor potential biological invasions and long-term community changes (*Clark et al., 2012; Danovaro et al., 2020*).

Sponges are problematic as they are difficult to identify, which may lead to incorrect or underestimated biodiversity values. The use of molecular markers, a powerful tool to help in sponge identification, has shown that this group is much more specious than previously thought, and cryptic species are very common (*Cárdenas et al., 2012*). Thus, detailed morphological descriptions supported by a complete genetic database are crucial for future studies.

The objective of this work was to improve the taxonomic knowledge on the sponges at three seamounts of the Mallorca Channel in the Balearic Islands: Ses Olives, Ausias March and Emile Baudot. Currently, these seamounts are being assessed for inclusion in the Natura 2000 network, under the scope of the LIFE IP INTEMARES project. One of the goals of this project is to improve the scientific knowledge of areas of ecological interest that harbor rich, vulnerable and protected habitats and species, which is necessary knowledge for the development of management plans. High abundance and diversity of invertebrates were observed during several surveys carried out in 2018, 2019, and 2020 at these seamounts, highlighting sponges as the dominant group. In the present paper we provide detailed descriptions of 18 demosponges and one hexactinellida, including a new genus and four new species, together with new descriptions and records of poorly-known taxa. For the new and dubious species, the sequences of two most used barcoding genes, the mitochondrial Cytochrome Oxidase subunit I (COI) and the nuclear 28S ribosomal fragment (C1-D2 domains), are also provided.

Materials and Methods

Study area

The Mallorca Channel is located in the Balearic Promontory (western Mediterranean Sea), between the islands of Mallorca and Ibiza. The area harbors three seamounts: Ses Olives (SO; 1º 58' 58.8" N, 38º 57' 36" E) and Ausias March (AM; 1º 49' 4.8" N, 38º 44' 49.2" E) located east of Ibiza and Formentera islands, and Emile Baudot (EB; 2º 30' 0" N, 38º 43' 55.2" E) located south of Mallorca and east of Ibiza-Formentera (Fig. 4.2.1). The seamounts SO, AM and EB are 375, 264 and 600 m high, respectively and 10 to 17 km long, with tabular summits elongated in NE-SW trends and located at 225-290, 86-115 and 94-150 m depth, respectively. SO and AM are of orogenic origin, emerging from depths around 900 and 600 m in their eastern sides and being separated from Ibiza and Formentera islands by depths around 600 and 400 m. By contrast, EB is a guyot of volcanic origin, which in its western side emerges from a plain around 900 m deep, with numerous fields of pockmark type depressions, located between SO and AM. At the eastern side of EB there is the so-called Emile Baudot escarpment, which descend down to 2600 m deep and connects the EB to the abyssal plain of the Algerian sub-basin (between the Balearic Islands and the Algerian coast) (*Acosta et al., 2004*).

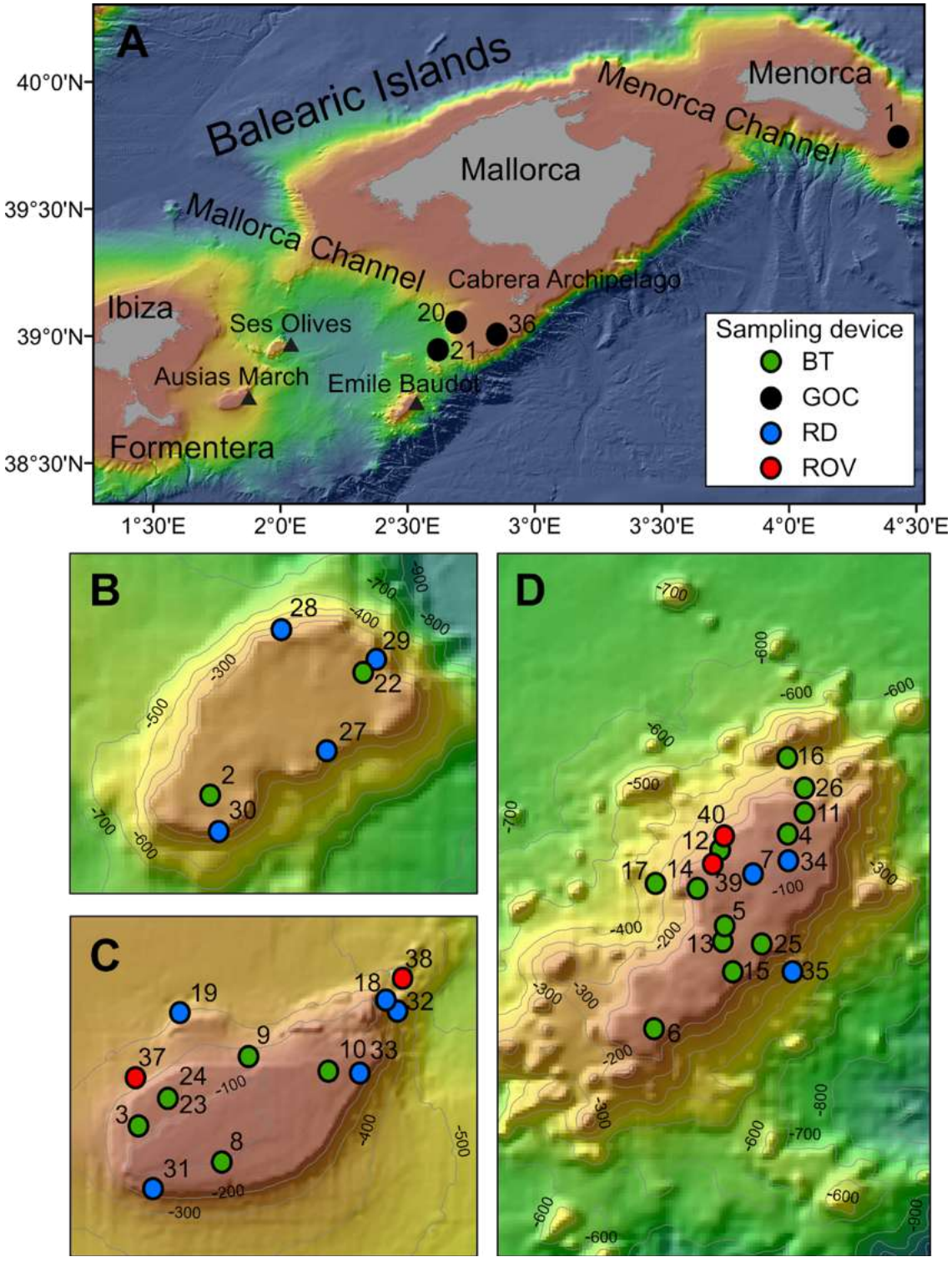

Fig. 4.2.1. Map of the studied area showing the location of the sampling stations of beam trawl (BT), bottom trawl type GOC73 (GOC), rock dredge (RD) and remote operated vehicle (ROV). The characteristics of these sampling stations are shown in Table 4.2.1. (A) general view of the Balearic Islands. (B) detail of Ses Olives. (C) detail of Ausias March. (D) detail of Emile Baudot.

The Algerian sub-basin hydrodynamics are mainly affected by density gradients, receiving warm and less saline Atlantic waters (*Pinot et al., 2002*). These surface waters

have high seasonal temperature variation, ranging from 13° C during winter to 26° C during summer, when a strong vertical temperature gradient is established between 50 and 100 m deep. The water column below this depth shows fewer variations than in other parts of the western Mediterranean Sea, being mainly influenced by the Levantine Intermediate Water (LIW). This water mass, originated in the eastern Mediterranean, has temperature and salinity around 13.3° C and 38.5 ppt, respectively, and is situated approximately between 200 and 700 m deep, just above the Western Mediterranean Deep Water, which is located in the lowest part of the water column (*Monserrat et al., 2008*). The western Mediterranean Intermediate Water, characterized by lower temperature (~12.5º C) because it is formed during winter in the Gulf of Lions by deep convection when sea-air heat flux losses are high enough, is found at 100-300 m deep, but does not reach the Mallorca Channel every year (*Monserrat et al., 2008*).

Within the general oligotrophy of the Mediterranean, the southern Balearic Islands waters in the Algerian sub-basin show more pronounced oligotrophy than waters of the Balearic sub-basin located north of the Archipelago, and above all than the adjacent waters off the Iberian Peninsula and the Gulf of Lions (*Estrada, 1996; Bosc et al., 2004*). The lack of supply of nutrients from land runoff and the lower influence of shelf/slope fronts flowing along the Iberian Peninsula and the northern insular shelf edge could explain these differences (*Massutí et al., 2014;* and references cited therein).

Sampling

Sponge samples were collected at SO, AM and EB seamounts with a Jennings type beam trawl (BT) of 2 and 0.5 m horizontal and vertical openings, respectively, and a 5 mm mesh size cod-end, a rock dredge (RD) and the Remote Operated Vehicle (ROV) Liropus 2000 with an extendable arm. Sampling was performed during INTEMARES research surveys carried out in 2018, 2019 and 2020 on board of the R/Vs *Angeles Alvariño* and *Sarmiento de Gamboa* (Fig. 4.2.1). Additional samples from trawl fishing grounds of the continental shelf off Mallorca and Menorca were collected during the MEDITS research surveys carried out in 2017, 2019 and 2020 using the bottom trawl net GOC-73 (GOC) of 2.5-3 m and 18-22 m vertical and horizontal openings, respectively and a 10 mm mesh size cod-end, on board the R/V *Miquel Oliver* (Fig. 4.2.1). The sampling strategy of the MEDITS surveys is detailed in *Bertrand et al. (2002)* and *Spedicato et al. (2019).* BT and GOC have been shown effective for sampling macro-benthic species of the epibenthic and nektobenthic communities of sedimentary bottoms, respectively (*Reiss et al., 2006; Fiorentini et al., 1999; Ordines & Massutí, 2009*). The SCANMAR and MARPORT systems were used to control the deployment and retrieval of both gears to the bottom. By contrast, RD and ROV were used for sampling rocky bottoms and steep slopes. A summary of sampling stations used in the present work can be found in Table 1.

Table 4.2.1. Details of sampling stations

R_{survey}	R_{study}	Year	Sampling device	Depth (m)	Coordinates	Area	Seabed characteristics
206	1	2017	GOC	135	39º47'37,2''N 4º26'15,4''E	E Me	Fishing ground, sedimentary bottom
20	2	2018	BT	275	38º56'6''N 1º57'58,3''E	SO	Detrital bed of muddy sand
22	3	2018	BT	105	38º44'30,5''N 1º46'5,9''E	AM	Rhodolith bed with invertebrates
51	4	2018	BT	128	38º44'53,9''N 2º30'41,4''E	EB	Coarse sand with dead rhodoliths
60	5	2018	BT	138	38º43'13,1''N 2º29'29,4''E	EB	Coastal detrital with sand
66	6	2018	BT	146	38º41'13,9''N 2º28'11,3''E	EB	Coastal detrital with sand and small dead rhodoliths
52	7	2018	RD	109	38º44'13,2''N 2º30'3,6''E	EB	Rhodolith bed
50	8	2019	BT	102	38º43'33,6''N 1º48'12,6''E	AM	Rhodolith bed with invertebrates
99	9	2019	BT	131	38º46'20''N 1º48'54,7''E	AM	Coastal detrital with sand and sponges
104	10	2019	BT	118	38º45'57,6''N 1º51'2,5''E	AM	Coastal detrital
124	11	2019	BT	152	38º45'19,1''N 2º31'0,5''E	EB	Detrital border
135	12	2019	BT	169	38º44'42,7''N 2º29'25,8''E	EB	Detrital border with sand
136	13	2019	BT	147	38º44'42,7''N 2º29'25,8''E	EB	Detrital border with gross black sand
166	14	2019	BT	433	38º44'3,1''N 2º28'12,7''E	EB	Detrital mud
167	15	2019	BT	151	38º42'21,6''N 2º29'37,3''E	EB	Detrital border with sand
175	16	2019	BT	410	38º46'21''N 2º30'44,3''E	EB	Detrital mud
177	17	2019	BT	156	38º43'57,7''N 2º28'54,1''E	EB	Detrital border with sand
95	18	2019	RD	275-220	38º47.8'0''N 1º52.6'0''E	AM	Rocky slope
103	19	2019	RD	302-231	38º47.4'0''N 1º47.2'0''E	AM	Rocky slope

224	20	2019	GOC	252	39º3’3,6’’N 2º42’2,9’’E	SW Ca	Fishing ground, sedimentary bottom
225	21	2019	GOC	754	38º57’11,5’’N 2º37’54,1’’E	SW Ca	Fishing ground, bathyal mud
1	22	2020	BT	289	38º58’0,5’’N 2º0’22,7’’E	SO	Detrital with encrusting sponges and small crustaceans
17	23	2020	BT	113	38º45’15,5’’N 1º46’53,4’’E	AM	Rhodolith bed with invertebrates
18	24	2020	BT	114	38º45’15,5’’N 1º46’53,4’’E	AM	Rhodolith bed with invertebrates
45	25	2020	BT	147	38º42’51,8’’N 2º30’13,7’’E	EB	Coarse sand and gravel with crustaceans and sponges
52	26	2020	BT	320	38º45’47,5’’N 2º31’0,5’’E	EB	Organogenic sediments, shells rests and gravel with sponges
3	27	2020	RD	288-318	38º56’4,7’’N 1º59’48,1’’E	SO	Rocks and rests of fossil Ostreids
7	28	2020	RD	325-255	38º58’41,9’’N 1º59’2,4’’E	SO	Rocks, rests of fossil Ostreids and fossil corals
8	29	2020	RD	315-295	38º58’11,3’’N 2º0’30,6’’E	SO	Rocks and rests of fossil Ostreids
14	30	2020	RD	325-270	38º55’33,6’’N 1º58’5,6’’E	SO	Mud, rocks and fossil Ostreids
20	31	2020	RD	104-138	38º42’51,1’’N 1º46’28,2’’E	AM	Rhodolith bed with sponges
27	32	2020	RD	222-195	38º47’31,2’’N 1º52’43,7’’E	AM	Carbonated rocks with encrusting sponges and gravels
28	33	2020	RD	135-140	38º45’56,5’’N 1º51’51,5’’E	AM	Rhodolith bed and rocks with sponges
43	34	2020	RD	118-116	38º44’25,1’’N 2º30’40,3’’E	EB	Rhodolith bed and rocks with sponges
46	35	2020	RD	280-306	38º42’21,6’’N 2º30’44,3’’E	EB	Basaltic rocks and fossil Ostreids with encrusting sponges
94	36	2020	GOC	142	39º1’13,8’’N 2º51’2,5’’E	SW Ca	Fishing ground, sedimentary bottom
07_1	37	2020	ROV	249-122	38º45’44,7’’N 1º46’0,8’’E	AM	Sedimentary slope and rhodolith bed with sponges
13	38	2020	ROV	465-352	38º48’22,3’’N 1º52’57’’E	AM	Rocky slope with large sponges
23	39	2020	ROV	133-169	38º44’27,6’’N 2º29’15’’E	EB	Rocky slope, rhodolith bed with sponges and corals
24	40	2020	ROV	150-134	38º44’46’’N 2º29’28,3’’E	EB	Rocky slope and summit, rhodolith bed with sponges and corals

On board, specimens were photographed and stored in absolute EtOH. External morphology, color and texture were annotated, prior to conservation. Spicule preparations and histological sections were made according to the standard methods described by *Hooper (2003)*. All the specimens were deposited in the Marine Fauna Collection (http://www.ma.ieo.es/cfm/) based at the Centro Oceanográfico de Málaga (Instituto Español de Oceanografía), with the numbers from CFM7356 to CFM7417 (*Table S4.2.1*).

The electronic version of this article in Portable Document Format (PDF) will represent a published work according to the International Commission on Zoological Nomenclature (ICZN), and hence the new names contained in the electronic version are effectively published under that Code from the electronic edition alone. This published work and the nomenclatural acts it contains have been registered in ZooBank, the online registration system for the ICZN. The ZooBank LSIDs (Life Science Identifiers) can be resolved and the associated information viewed through any standard web browser by appending the LSID to the prefix http://zoobank.org/. The LSID for this publication is: [urn:lsid:zoobank.org:pub:47EC2384-A88C-4654-8425-A7A46BC47AC5]. The online version of this work is archived and available from the following digital repositories: PeerJ, PubMed Central and CLOCKSS.

Morphological descriptions

Spicules were observed with a Nikon S-Ke optical microscope and photographed with a CMOS digital camera. Images were processed using the Fiji software (*Schindelin et al., 2012*). Whenever possible, at least 30 spicules per spicule type were measured. Spicules measures are written as length: min-average-max/thickness: min-average- max µm. Tangential and transversal thick sections were made with a scalpel and, if necessary, dehydrated with alcohol, mounted in DPX and observed under a compound microscope. Aliquots of suspended spicules were transferred onto foil, air dried, sputter coated with gold and observed under a HITACHI S-3400N scanning electron microscope (SEM).

Molecular analysis

DNA was extracted from a piece of choanosomal tissue (~2 cm^3) using the DNeasy Blood and Tissue Extraction kit (QIAGEN). Polymerase chain reaction (PCR) was used to amplify the Cytochrome C Oxidase subunit I (COI; DNA barcoding) and the C1-D2 domains of the 28S ribosomal gen, with the universal primers LCO1490/HCO2198 (*Folmer et al., 1994*) and C1' ASTR/D2 (*Vân Le et al., 1993; Chombard et al., 1998*), respectively. Sequences were aligned using Mafft (*Katoh et al., 2002*). The resulting sequences were deposited in the GenBank database (http://www.ncbi.nlm.nih.gov/genbank/) under the following accession numbers: MW858346-MW858351 for COI sequences and MW881149-MW881153 for 28S sequences; Table S4.2.1).

To assess the phylogeny of *Foraminospongia balearica* **sp nov.** and *Foraminospongia minuta* **sp. nov.,** two different approaches were used: Bayesian Inference (BI) and Maximum likelihood (ML). Here, we selected closely related sequences belonging to the orders Agelasida, Axinellida, Scopalinida and Biemnida, obtained after a BLAST search (*Altschul et al., 1990*). Additionally, two sequences belonging to the order Suberitida were used as outgroup. A complete list of the used sequences is available at Table S4.2.2. BI and ML analyses were performed with the CIPRES science gateway platform (http://www.phylo.org; *Miller et al., 2010*) using Mr Bayes version 3.6.2 (*Ronquist et al., 2012*) and RAxML (*Stamatakis, 2014*). For Mr Bayes, we conducted four independent Markov chain Monte Carlo runs of four chains each, with 5 million generations, sampling every 1000th tree and discarding the first 25% as burn-in, while RAXML was performed under the GTRCAT model with 1000 bootstrap iterations. Convergence was assessed by effective sample size (ESS) calculation and was visualised using TRACER version 1.5. Genetic distance (p-distance) and number of base differences between pair of DNA sequences were estimated with MEGA version 10.0.5 software (*Kumar et al., 2018*).

Results

A total of 60 specimens belonging to 2 classes, 9 orders, 13 families, 15 genera and 19 species were analyzed. All these species were collected at the Mallorca Channel seamounts, while three of them (*Phakellia robusta* Bowerbank, 1866, *Petrosia* (*Petrosia*) *raphida Boury-Esnault, Pansini & Uriz, 1994* and *Hemiasterella elongata* (*Topsent, 1928*) were also found at the continental shelf around Mallorca and Menorca. *In situ* images of some of these sponges, obtained with ROV from the seamounts of the Mallorca Channel, are shown in Fig. 4.2.2.

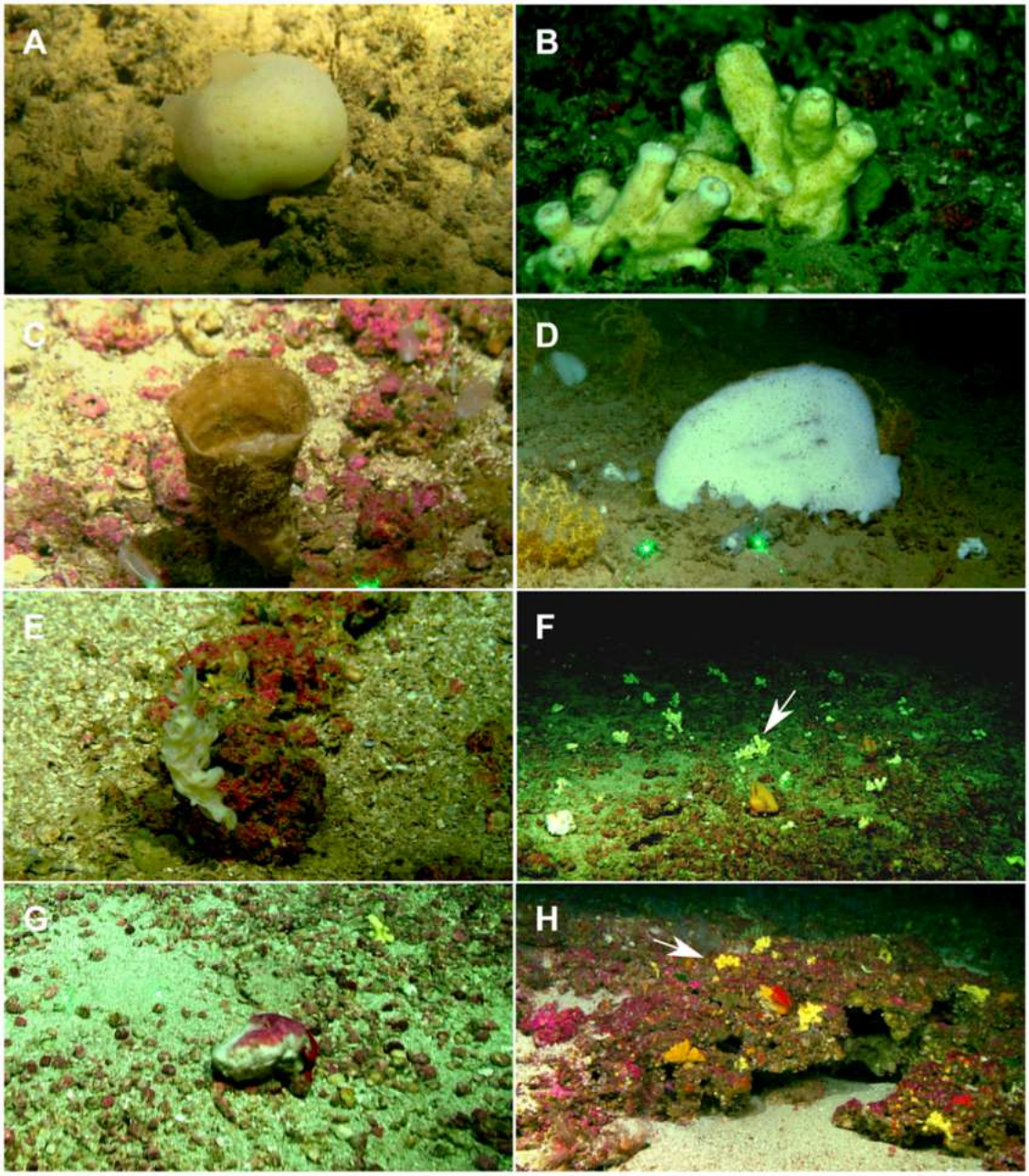

Fig. 4.2.2. Remote Operated Vehicle (ROV) images of the sponge fauna from the seamounts of the Mallorca Channel, Ses Olives (SO), Ausias March (AM) and Emile Baudot (EB). (A) specimen of *Polymastia polytylota* collected at 409 m depth in AM. (B) Holotype of *Foraminospongia balearica* **sp. nov.** collected at 129 m depth in the AM summit. (C) specimen of *Phakellia ventilabrum* collected at 132 m depth in the EB summit. (D) uncollected specimen of *Phakellia* sp. at 374 m depth in the north knoll of AM. (E) specimen of *Haliclona (soestella) fimbriata* collected at 131 m depth in the EB. (F) rhodolith bed at 110 m depth in the summit of AM, with different sponge species, including *F. balearica* **sp. nov.** (arrow), (G) uncollected specimen of *Calyx* cf. *tufa* at 106 m depth in the summit of AM, (H) coralligenous bottom at 97 m depth in the summit of AM, with several sponges, including *F. balearica* **sp. nov.** (arrow).

Systematics

Phylum PORIFERA Grant, 1836

Class DEMOSPONGIAE Sollas, 1885

Suborder HETEROSCLEROMORPHA Cárdenas, Pérez & Boury-Esnault, 2012

Order AGELASIDA Hartman, 1980

Family HYMERHABDIIDAE Morrow, Picton, Erpenbeck, Boury-Esnault, Maggs & Allcock, 2012

Genus *Foraminospongia* gen. nov.

(Figs. 4.2.2B, 4.2.2F, 4.2.2H; Fig. 4.2.3; Fig. 4.2.4, Fig. 4.2.5, Fig. 4.2.6; Table 4.2.2)

Type species

Foraminospongia balearica **sp. nov.**

Diagnosis

Hymerhabdiidae with massive, massive-tubular or bushy growth form, with styles, subtylostyles, tylostyles, and rhabdostyles. Besides, curved or angulated oxeas may be present. Ectosome with an aspicular dermal membrane supported by a plumoreticulated skeleton of styles, subtylostyles and tylostyles. Pores grouped into inhalant areas. Choanosome confusedly plumoreticulated.

Etymology

From the Latin *foramen* (pores) and *spongia* (sponge). The name refers to the fact that in both species, theira skin has areas where pores are grouped, giving a characteristic macroscopical appearance.

Foraminospongia balearica sp. nov.

(Figs. 4.2.2B, 4.2.2F, 4.2.2H; Fig. 4.2.3; Fig. 4.2.4; Fig. 4.2.5; Table 4.2.2)

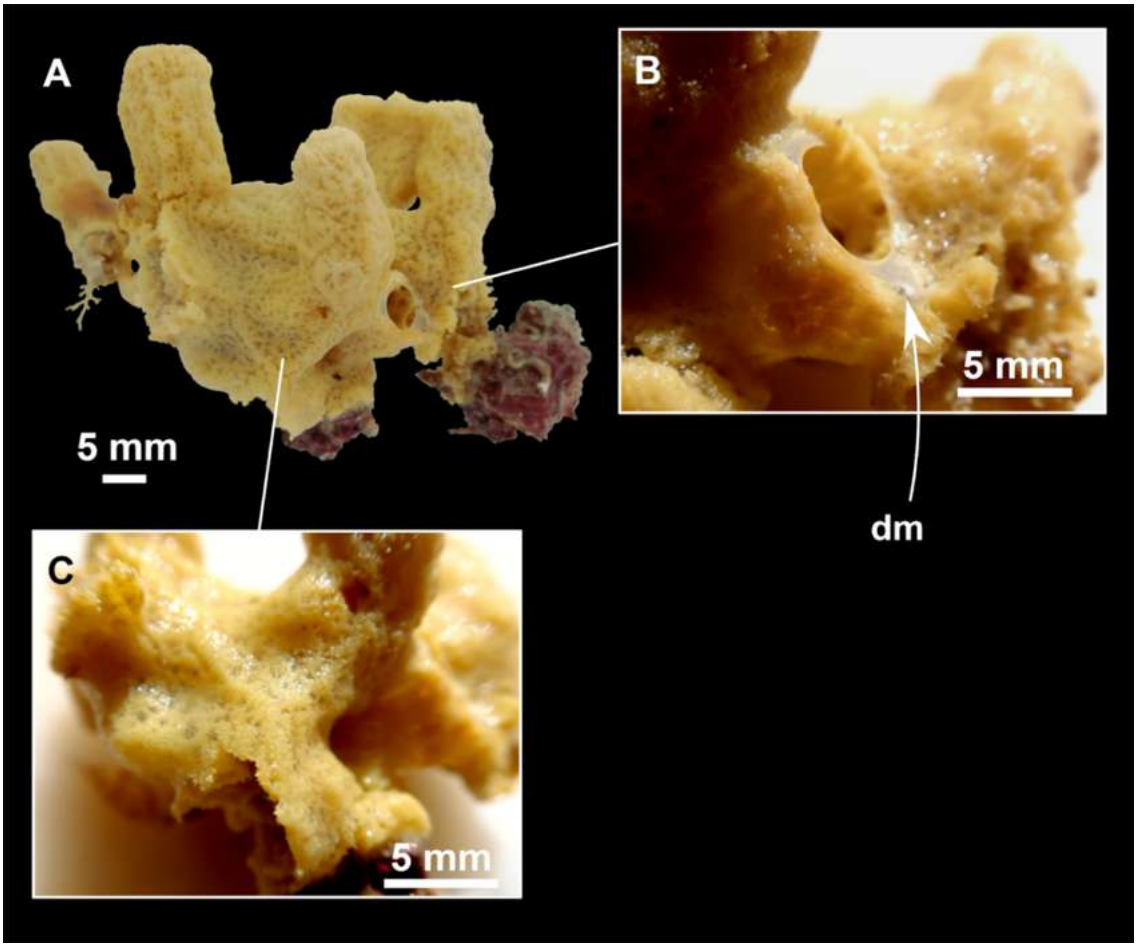

Fig. 4.2.3. *Foraminospongia balearica* **sp. nov.** (A) habitus of CFM-IEOMA-7356/i802 (holotype) in fresh state, with (B), detail of the oscula and the dermal membrane (dm) and (C), macroscopic view of the grooves at the skin.

Diagnosis

Massive-tubular to bushy *Foraminospongia*, with styles, rhabdostyles and oxeas.

Etymology

The name refers to the Balearic Islands, the area where the species has been collected.

Material examined

Holotype: CFM-IEOMA-7356/i802, St. 37, MaC (AM), ROV, coll. J.A. Díaz.

Paratypes: CFM-IEOMA-7357/i144, St. 4, MaC (EB), BT; CFM-IEOMA-7358/i293_1, St. 9, MaC (AM), BT; CFM-IEOMA-7359/i239 (not described), St. 8, MaC (AM), BT; CFM-IEOMA-7360/i745 (not described), St. 26, MaC (EB), BT; CFM-IEOMA-7361/i824_4, St. 39, MaC (EB), ROV, coll. J.A. Díaz.

Specimens observed but not sampled: St. 12, MaC (EB), BT; St. 14, MaC (EB), BT.

Comparative material

Foraminospongia minuta **sp. nov.**: CFM-IEOMA-7362/i439, St. 27, RD, SO; CFM-IEOMA-7363/i474, St. 29, MaC (SO), RD, coll. J.A. Díaz.

Rhabderemia sp.: CFM-IEOMA-7415/i729_1 (only a slide deposited at the CFM-IEOMA), St. 35, MaC (EB), RD, coll. J.A. Díaz.

Description

Massive-tubular or bushy sponges (Figs. 4.2.2B, 4.2.2F, 4.2.2H and Fig. 4.2.3A). Largest specimens up to 6 cm in diameter. When present, tubes are 2-3 cm in height and 1 cm in diameter. Sometimes several tubes are fused on another of its sides. Consistency slightly elastic, brittle, easily broken when manipulated. Surface smooth, rough to the touch. Color in life golden yellow, tan after preservation in EtOH. A translucid membrane is present, more evident near the oscula (Fig. 4.2.3B). Subdermal grooves forming a visible pattern (Fig. 4.2.3C). Circular oscula 0.3-0.6 cm. In most cases, oscula are placed at the end of tubes, however, the holotype also has a large osculum in the main body (Fig. 4.2.3B).

Skeleton

Ectosome characterized by a plumoreticulated tangential skeleton and a dermal membrane (Figs. 4.2.4A, 4.2.4B and 4.2.4C). In some areas of the dermal membrane there are small pores gathered. These porae areas correspond to the grooves that are perceptible to the eye. Choanosome, confusedly plumoreticulated with extensive spaces and ascending spicule tracts of 2-5 styles, sometimes protruding the surface. The tracts contain abundant spongin. In between the tracts transversal spicules are abundant (Figs. 4.2.4D-4.2.4E).

Spicules

Styles (Fig. 4.2.3A-3D): Fusiform, most gently curved, but sometimes abruptly curved once or twice. When the curvature is in the last portion of the spicule, they may resemble rhabdostyles. Roundish heads and sharp tips, sometimes telescoped, strongylote forms present. Swellings may happen at the head or below, sometimes barely visible, sometimes more patent, rarely tuberculated (Fig. 4.2.3D). Size range constant between specimens, not influenced by depth nor area (Table 4.2.2). They measure 177-375-634/3-9-14 µm.

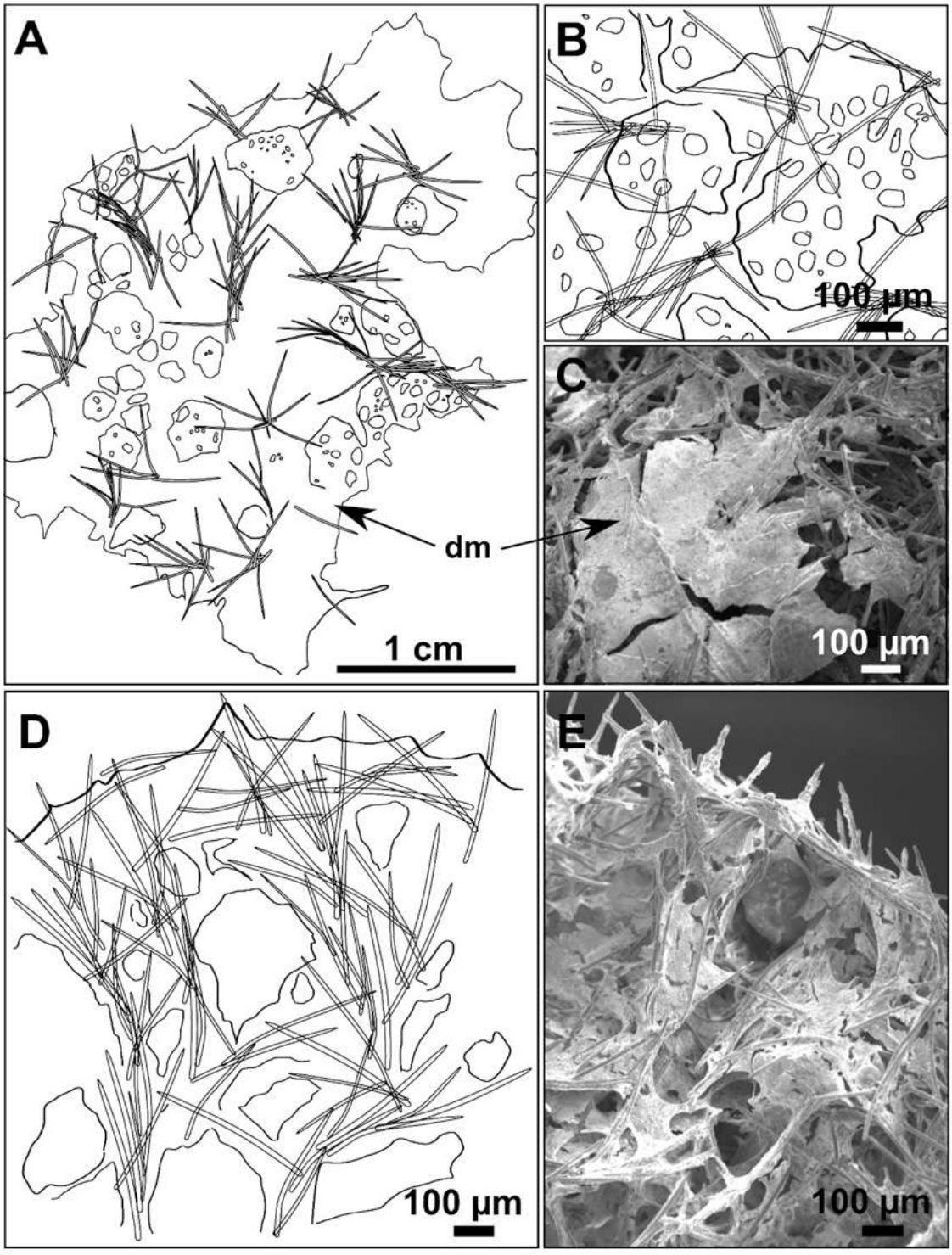

Fig. 4.2.4. Skeletal arrangement of *Foraminospongia balearica* **sp. nov.**, CFM-IEOMA-7356/i802 (holotype). (A-C) tangential images of the surface, showing the dermal membrane (dm). (D-E) transversal sections.

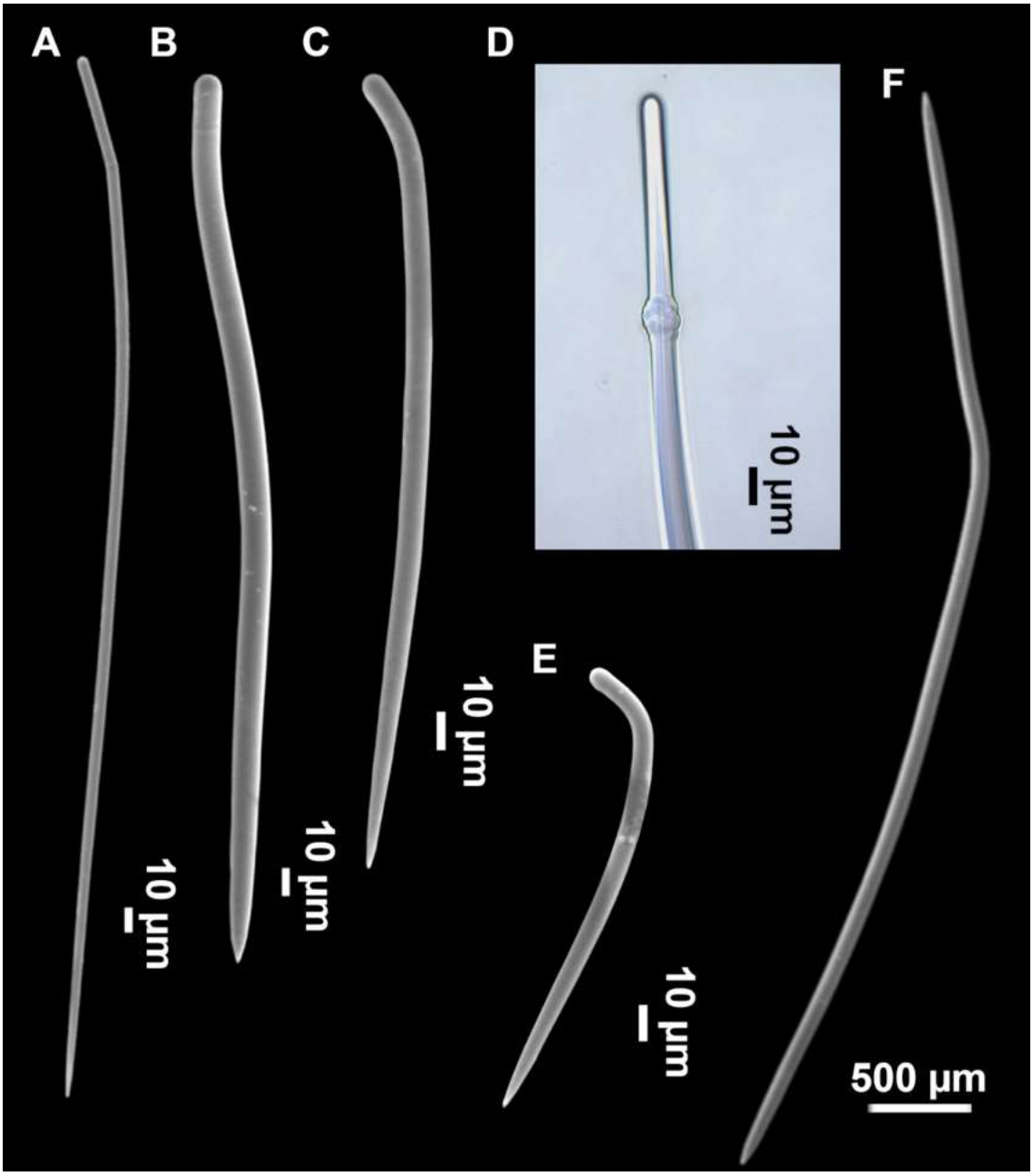

Fig. 4.2.5. SEM images of the spicules from *Foraminospongia balearica* **sp. nov.** CFM-IEOMA-7358/i293_1 (paratype). (A-D) styles. (E) rhabdostyles. (F) oxea.

Rhabdostyles (Fig. 4.2.3E): Uncommon. Abruptly curved below the head. Stylote, subtylote and tylote modifications present. Round head and acerated tips. They measure 90-143-179/3-5-7 µm. specimens

Oxeas (Fig. 4.2.3F): specimensCurved or bent, with one, two or several curvatures, sometimes slightly sinuous. Tips acerated or telescoped. They measure 249-520-763/3-8-13 µm. Their abundance varies between specimens.

Table 4.2.2. Comparative characters of *Foraminospongia balearica* **sp. nov.** and *Foraminospongia minuta* **sp. nov.** Depth (m), area (SO: Ses Olives; AM: Ausias March; EB: Emile Baudot) and sampling station (St; see R*study* in Table 1) where these specimens were collected are also shown. Spicule measures are given as minimum-mean-maximum for total length/minimum-mean-maximum for total width. A minimum of 30 spicules per spicule kind are measured, otherwise it is stated. All measurements are expressed in µm. Specimen codes are the reference numbers of the CFM-IEOMA/and author collection. np: not present.

Specimen	Style	Rhabdostyle	Oxea
F. balearica **sp. nov.** CFM-IEOMA-7356/i802 Holotype AM (St. 13), 249-122 m	188-378-492 /6-11-14	90-179/4-7 (n= 9)	456-609/9-11 (n= 3)
F. balearica **sp. nov.** CFM-IEOMA-7357/i144 Paratype EB (St. 4), 128 m	197-378-501 /4-9-12	108-164/3-5 (n= 5)	249-493-656/4-8-12 (n= 15)
F. balearica **sp. nov.** CFM-IEOMA-7358/i293_1 Paratype AM (St. 9), 127 m	179-356-516/3-8-14	138-179/3-6 (n= 5)	328-527-763/3-8-13
F. balearica **sp. nov.** CFM-IEOMA-7361/i824_4 Paratype EB (St. 39), 133-169 m	177-403-634 /5-9-13	92-165/3-6 (n= 9)	600/9 (n= 1)
F. minuta **sp. nov.** CFM-IEOMA-7362/i439 Holotype SO (St. 26), 318-288 m	283-509-658/9-14-21	175-262/7-9 (n= 7)	np
F. minuta **sp. nov.** CFM-IEOMA-7363/i474 Paratype SO (St. 28), 295-315 m	244-416-555/10-14-20	147-232/7-9 (n= 4)	np

Genetics

Two *COI* Folmer fragment sequences were obtained for the Holotype (CFM-IEOMA-7356/i802) and for one paratype (CFM-IEOMA-7358/i293_1) (Genbank id's MW858346 and MW858347, respectively). Besides, we obtained a *28S* sequence (C1-D2 domains) for the Holotype (Genbank id MW881153).

Ecology

The species is very abundant on the EB and AM, between 100 and 169 m (Table 2). It can be mainly found on rhodolith beds and sedimentary bottoms with gravel, together with other sponges like *Poecillastra compressa* (Bowerbank, 1866), *Axinella* spp., *Halichondria* spp. or some Haplosclerids, as well as with a very broad number of crustaceans and echinoderms. It was also collected down to 433 m (St. 14).

Foraminospongia minuta **sp. nov.**

(Fig. 4.2.6; Table 4.2.2)

Diagnosis

Small, massive-encrusting and grayish in color *Foraminospongia*, with only styles and rhabdostyles as spicules.

Etymology

The name refers to the small size of the two collected specimens.

Material examined

Holotype: CFM-IEOMA-7362/i439, St. 27 (INTEMARES0720), MaC (SO), RD.

Paratype: CFM-IEOMA-7363/i474, St. 29 (INTEMARES0720), MaC (SO), RD**.**

Comparative material

Foraminospongia balearica **sp. nov.**: CFM-IEOMA-7357/i144, St. 4 (INTEMARES0718), MaC (EB), BT; CFM-IEOMA-7358/i293_1, St. 9 (INTEMARES1019), MaC (AM), BT; CFM-IEOMA-7356/i802, St. 37 (INTEMARES0820), MaC (AM), ROV; CFM-IEOMA-7361/i824_4, St. 39 (INTEMARES0820), MaC (EB), ROV.

Rhabderemia sp.: CFM-IEOMA-7415/ i729_1, St. 35 (INTEMARES0720), MaC (EB), RD.

Description

Small massive-encrusting sponge (Figs. 4.2.6A and 4.2.6B), about 1.5 cm in diameter and 0.5 cm in height. Consistency: compressible and slightly crumby. Velvety surface. The holotype was brownish due to mud, the paratype was grayish, both in life and after preservation in EtOH. Translucent membrane that can be peeled off is present, with grooves forming a distinguishable pattern (Fig. 4.2.6B). A single, circular oscule is present on the holotype.

Skeleton

The ectosome consists of a tangential reticulation of styles (Fig. 4.2.6C), and some loose rhabdostyles.

The choanosome is a plumoreticulated net of styles, with some loose rhabdostyles (Fig. 4.2.6D).

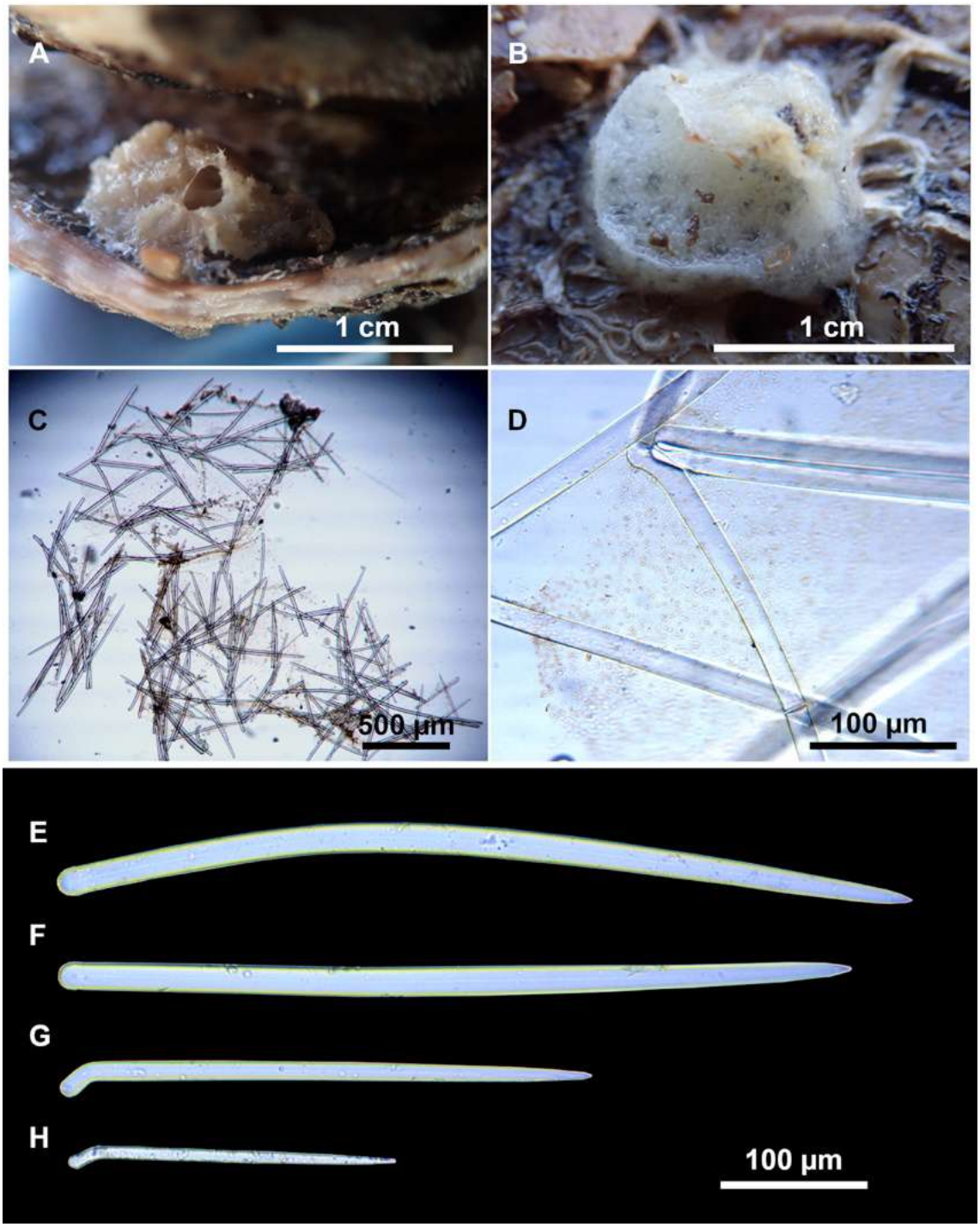

Fig. 4.2.6. *Foraminospongia minuta* **sp. nov**. (A) habitus of CFM-IEOMA-7362/i439 (holotype) in fresh state. (B) on deck image of CFM-IEOMA-7363/i474 (paratype). (C) optic microscope image of the tangential skeleton of the holotype. (D) schematic illustration of the choanosome of the holotype. (E-F) styles. (G-H) rhabdostyles.

Spicules

Styles (Figs. 4.2.6E and 4.2.6F): Fusiform, gently curved or straight. Heads roundish and swelled in most cases. Sharp tips. Most are tylota. Size range variable between the holotype and the paratype (Table 2). They measure 244-465-658/9-14-21 µm.

Rhabdostyles (Fig. 4.2.6G and 4.2.6H): Uncommon. Abruptly curved below the head, most with roundish, tylota modifications at the head and sharp tips. They measure 147-209-262/7-8-9 μm.

Genetics

Sequences of *COI* Folmer fragment and *28S* C1-D2 domains were obtained for the holotype and deposited in Genbank under accession numbers MW858348 and MW881151, respectively.

Ecology

Both specimens were found at SO, between 288 and 318 m deep, associated to hard bottoms with fossil ostreids reefs.

Remarks on *F. balearica* sp. nov. and *F. minuta* sp. nov.

Regarding the interspecific variability of *F. balearica* **sp. nov.**, the spicules of the studied specimens are in the same size range, except for the styles of the specimen from AM (CFM-IEOMA-7358/i293_1), which are shorter and thinner than those of the specimens from EB. Also, specimen CFM-IEOMA-7358/i293_1 has much more abundant oxeas than the others.

Regarding *F. minuta* **sp. nov.**, the features of this species support the differential diagnostic characters of the genus *Foraminospongia* (plumoreticulated choanosomal skeleton, ectosome formed by a reticulation of spicules, dermal aspicular membrane with poral areas, presence of large styles and small rhabdostyles), but differs from *F. balearica* **sp. nov.** in its external morphology, being much smaller and massive-encrusting compared to massive-tubular or bushy and of a greyish color instead of golden yellow in the latter. Also, the spicular complement is different: *F. minuta* **sp. nov.** lacks oxeas and has longer and thicker styles and rhabdostyles. The differences in the size of the styles between the holotype and the paratype are notable, considering that both were collected at similar depths and habitats. These differences could suggest intraspecific variability for the spicule size within the species; however, more specimens are needed to corroborate this statement.

The morphological differences between the two species are backed by genetic results. The phylogenetic reconstructions for *COI* and *28S* fragments show well-supported separation between the two *F. balearica* **sp. nov.** sequences and the *F. minuta* **sp. nov.** sequence. Between the two species, the differences in bp and p-distance (in percentage) for *COI* Folmer and the *28S* fragments were 1 bp/0.2% and 1bp/0.1%, respectively.

Remarks on the genus *Foraminospongia*

The family Hymerhabdiidae was recently erected to include the genera *Hymerhabdia*, *Prosuberites* and some species of the polyphyletic genus *Axinella* and *Stylissa* (*Morrow*

et al., 2019). Here, we propose *Foraminospongia* as a new hymerhabdiid genus. The main differences between *Foraminospongia* **gen. nov.** and both *Hymerhabdia* and *Prosuberites* are the growing habit, with *Foraminospongia* **gen. nov.** being massive, massive-tubular or bushy against encrusting. Also, it differs from *Prosuberites* in the presence of rhabdostyles and oxeas. However, the presence of rhabdostyles and oxeas is shared with *Hymerhabdia*, but the genetic differentiation between *Foraminospongia* and *H. typica* (type species of *Hymerhabdia*) is clear (Fig. 4.2.7). In addition, the ectosome with a dermal membrane and grouped pore areas of *Foraminospongia* is not present in any *Hymerhabdia* apart *Hymerhabdia oxeata* (*Dendy, 1924*) that has a dermal membrane, although neither Dendy nor the re-examination done by *Hooper & Van Soest (1993)* described pore areas. Therefore, *H. oxeata* could represent an intermediate stage between genuine *Hymerhabdia* and *Foraminospongia* species. However, the last statement is only speculative and must be checked in future works.

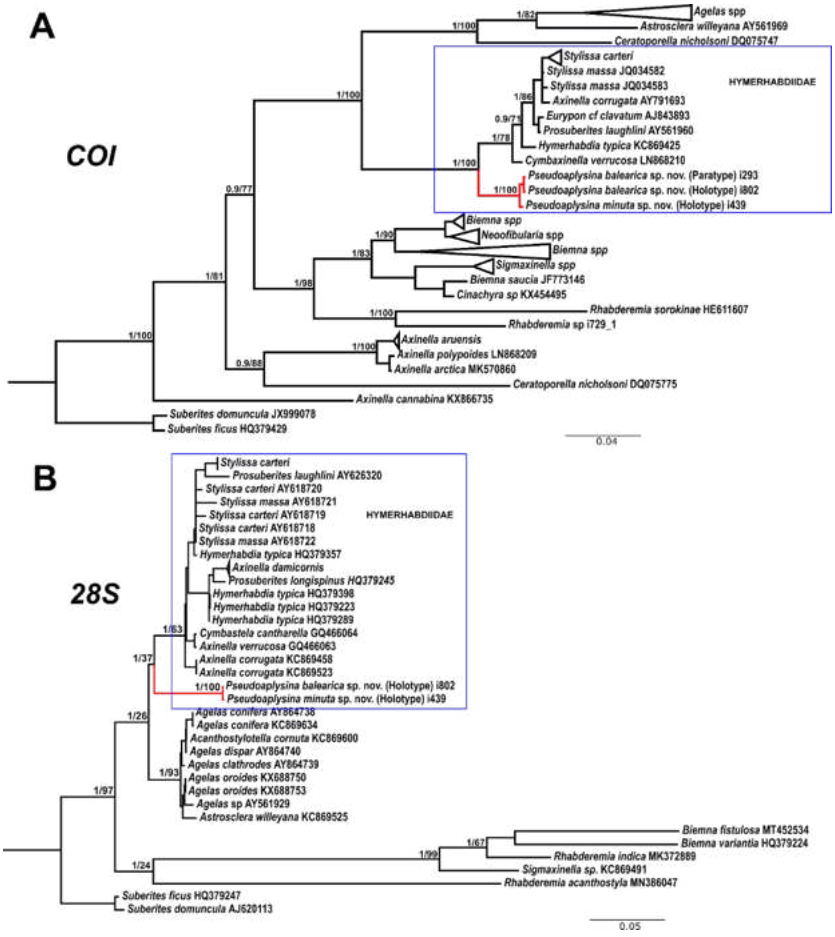

Fig. 4.2.7. Phylogenetic tree topology for specimens of *Foraminospongia balearica* **sp. nov**., *Foraminospongia minuta* **sp. nov**. described in the present study and other related Agelasids. The tree was constructed with Maximum likelihood and Bayesian inference, based on COI (A) and 28S (B) fragments. Posterior probabilities and bootstrap support values are shown at the nodes. A sequence of Suberites domuncula and Suberites ficus are used as outgroups in both trees.

As stated before, there are species of *Axinella* and *Stylissa* that are grouped inside Hymerhabdiidae. Although currently all these species are kept in Axinellida and Suberitida, respectively (*Van Soest et al., 2021*), they are phylogenetically related to *Foraminospongia* (see Fig. 4.2.7). To resolve this relatedness, we have included in the phylogenetic analysis sequences of *A. damicornis* (Esper, 1794), *A. verrucosa* (Esper, 1794), *A. corrugata* (George & Wilson, 1919), *S. carteri* (Dendy, 1889) and *S. massa* (Carter, 1887) used by *Morrow et al. (2012)* to define Hymerhabdiidae. The resulting trees show that those species are clearly different from *Foraminospongia,* which is corroborated by their morphology (*Pansini, 1984; Hooper & Van Soest, 2002*).

The genus *Rhabderemia* (Order Biemnida, family Rhabderemiidae) resembles *Foraminospongia* in having rhabdostyles and possessing a plumoreticulated choanosomal skeleton. However, most Rhabderemia also have peculiar rugose microscleres (thraustoxeas, spirosigmata, thraustosigmata, microstyles). To clarify the potential relatedness of *Rhabderemia* and *Foraminospongia*, we have included in the phylogenetic analyses the species *Rhabderemia sorokinae* Hooper, 1990, *R. indica* Dendy, 1905 and *R. destituta* Van Soest & Hooper, 1993. Moreover, we included in the *COI* tree one sequence of an encrusting *Rhabderemia* sp. (CFM-IEOMA-7415/ i729_1; Genbank ID MW881152) collected at the EB, with spined rhabdostyles, toxas and spirosigmata (Fig. 4.2.7B). Other sequences of Biemnida available at the genbank have also been included (see Table S4.2.2).

The sequence of *Rhabderemia* sp. (CFM-IEOMA-7415/ i729_1; Genbank ID MW881152) clustered together with *R. sorokinae,* a Great Barrier Reef sponge which also has spined rhabdostyles, toxas and spirosigmata, in addition to microspined microstyles, a fact that confirms that archetypical rhabderemids are not related to *Foraminospongia*. However, microscleres are lacking in *R. mona* (*de Laubenfels, 1934*) and *R. destituta,* so they resemble *Foraminospongia*. *Rhabderemia mona* is a Caribbean sponge described from bathyal depths off Puerto Rico, used to erect the genus *Stylospira* for "sponges having no spicules other than peculiar spirally twisted styles" (*de Laubenfels, 1934*). This single specimen was later studied by *Van Soest & Hooper (1993)* on a revision of the genus, who concluded that *Stylospira* should be considered a subgenus of *Rhabderemia*. *Van Soest & Hooper (1993)* also described *R. destituta* from the Galapagos Islands, a second species matching de Laubenfels' diagnosis. Interestingly, apart from the lack of any kind of microscleres (even though de Laubenfels reported raphides for *R. mona*, not found by *Van Soest & Hooper, 1993*), both species had smooth rhabdostyles, just as *Foraminospongia*, which is in contrast to most of the other *Rhabderemia* spp. Among the 30 known species of the genus, only *R. stellata* (Bergquist, 1961), *R. spirophora* (Burton, 1931), *R. gallica* (Van Soest & Hooper, 1993), *R. profunda* (Boury-Esnault, Pansini & Uriz, 1994), *R. africana* Van Soest & Hooper, 1993, *R. prolifera* Annandale, 1915 and *R. meirimensis* Cedro, Hajdu & Correira, 2013 have smooth rhabdostyles.

Unfortunately, there are no sequences available for *R. mona* nor *R. destituta*, so their potential relatedness with *Foraminospongia* cannot be addressed. However, it should be noted that both species have only rhabstosytles as megascleres, wich is in contrast to the heterogenous set of megascleres shown by *Foraminospongia* (styles, tylostyles, subtylostyles, rhabdostyles and oxeas). This seems a strong argument against congeneric relatedness with *Foraminospongia*. However, this issue should be properly addressed in the future when sequences of *R. mona* and *R. destituta* become available.

Order AXINELLIDA Lévi, 1953

Family AXINELLIDAE Carter, 1875

Genus *Axinella* Schmidt, 1862

Axinella spatula Sitjà & Maldonado, 2014

(Fig. 4.2.8; Table 4.2.3)

Material examined

CFM-IEOMA-7364/i338_1A, CFM-IEOMA-7365/i338_1B and CFM-IEOMA-7366/i338_1C, St. 11 (INTEMARES1019), MaC (EB), BT, coll. J.A. Díaz.

Description

Small, erect, cylindrical, and slightly flattened sponges, up to 3 cm height and 2-3 mm width (Figs. 4.2.8A-4.2.8C). Very hispid all along the body. Orange in life (Fig. 4.2.8A) and orange beige after preservation in EtOH (Fig. 4.2.8B).

Skeleton

As in *Sitjà & Maldonado (2014)*.

Spicules

Styles (Figs. 4.2.8D-4.2.8F): with a wide size range, rounded ends and sharp tips. Straight or slightly curved. The largest ones may be slightly sinuous, sometimes with subterminal swellings (Fig. 4.2.8D1). Rhabdostyle modifications are present in small and intermediateintermediate stages (Fig. 4.2.8F). They measure 248-722-1304/4-14-17 μm.

Oxeas: curved or bent, sometimes centrotylote (Figs. 4.2.8G-4.2.8K), with the curvature point at the center or displaced towards one of the extremities. Tips acerated. They measure 187-357-507/5-11-16 μm.

Raphides in trichodragmata (Fig. 4.2.8C, detail), abundant and of the same morphology in all specimens. They measure 32-40-56/5-7-11 μm.

Ecology and distribution

Found only on the north-eastern part of EB, at 152 m deep, on gravel bottoms with dead rhodoliths and with a large abundance of sponges such as *P.* (*Petrosia*) *ficiformis* (Poiret, 1789), *P.* (*Petrosia*) *raphida* Boury-Esnault, Pansini & Uriz, 1994, *P.* (*Strongylophora*) *vansoesti* Boury-Esnault, Pansini & Uriz, 1994 and several Tetractinellida.

With the present record, the species distribution widens towards the north-western Mediterranean Sea, since previously it was known only for the type's location, at the Alboran Island (*Sitjà & Maldonado, 2014*).

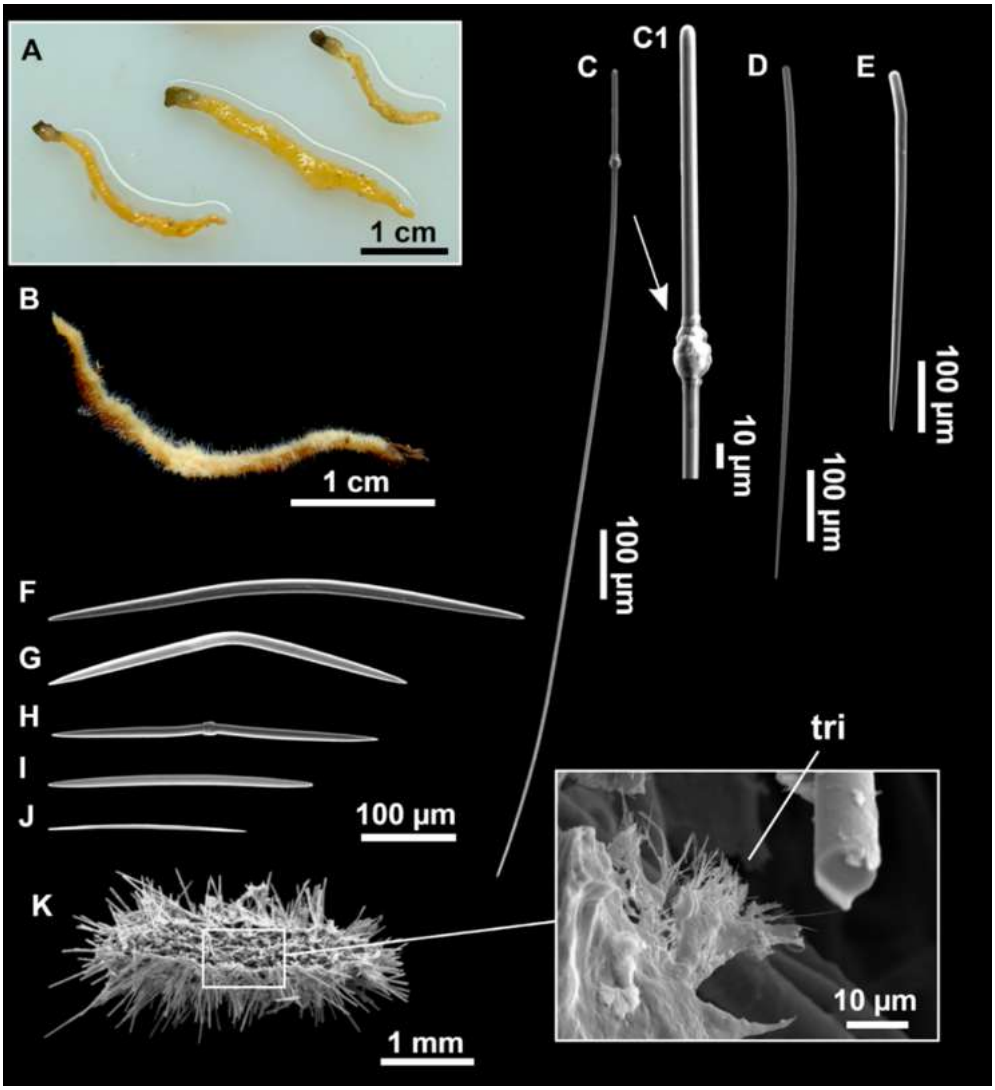

Fig. 4.2.8. *Axinella spatula Sitjà & Maldonado, 2014*. (A) photograph of fresh material deposited under CFM-IEOMA-7364-7366/i338_1A-1C. (B) habitus of CFM-IEOMA-7366/i338_1C preserved in EtOH. (C) SEM images of the skeletal structure of CFM-IEOMA-7366/i338_1C with detail of the inner ectosomal layer, with trichodragmata (tri). (D) long styles with (D1) subterminal swelling. (E) regular shaped style. (F) style with rhabdose modification. (G) oxea asymmetrically curved. (H) oxea centrocurved. (I) oxea centrotylota. (J-K) small oxeas.

Table 4.2.3. Comparative characters of the collected specimens of *Axinella spatula* Sitjà & Maldonado, 2014, and those reported for the type material (*Sitjà & Maldonado, 2014*). Depth (m), area (EB, Emile Baudot) and sampling station (St; see Rstudy in Table 4.2.1) where these specimens were collected are also shown. Spicule measures are given as minimum-mean-maximum for total length/minimum-mean-maximum for total width (or as they appear in the cited texts). A minimum of 30 spicules per spicule kind are measured, otherwise it is stated. All measurements are expressed in mm. Specimen codes are the reference numbers of the CFM-IEOMA/and author collection for the Balearic specimens and the reference numbers of Invertebrate Collection of the National Museum of Natural Sciences (MNCN) of Madrid for *Sitjà & Maldonado (2014)* specimens.

Specimen	Styles	Oxeas	Trichodragmata	Color
MNCN-Sp145-BV33A *Sitjà & Maldonado, (2014)* Holotype Alboran Island, 134-173 m	165-1050/3-15	180-520/3-15	25-30/5-8	Beige after EtOH
MNCN-Sp188-BV41A *Sitjà & Maldonado, (2014)* Paratype Alboran Island, 102-112 m	119-1400/4-15	190-750/5-20	25-35/5-8	Beige after EtOH
MNCN-Sp57-BV21B *Sitjà & Maldonado, (2014)* Paratype Alboran Island, 93-101 m	245-1225/8-18	120-432/9-12	25-30/6-10	Black after EtOH
CFM-IEOMA-7364/i338_1A EB (St. 11), 152 m	349-613-1161/7-13-16 (n=20)	187-374-507/5-11-16	32-39-47/5-7-10	Orange in life orange beige after EtOH
CFM-IEOMA-7365/i338_1B EB (St. 11), 152 m	248-900-1304/11-17-26 (n=17)	219-377-485/7-11-16	36-45-56/5-7-8 (n=9)	Orange in life orange beige after EtOH
CFM-IEOMA-7366/i338_1C EB (St. 11), 152 m	332-638-1265/4-12-17 (n=23)	247-332-493/7-10-16	32-39-52/5-7-11	Orange in life orange beige after EtOH

Remarks

The specimens match well with those originally described from the Alboran Sea. Balearic specimens are smaller (maximum height of 3 cm against maximum height of 10 cm in alboran specimens). Also, the size range of their styles and oxeas are not as wide as in Alboran specimens and trichodragmata of our specimens were always longer (Table 3).

Sitjà & Maldonado (2014) described two phenotypes, according to the color acquired after preservation in EtOH (black or beige). Also, they found skeletal variations linked to each group, corresponding to a higher or lower presence of short styles, the morphology of the trichodragmata or the skeletal arrangement. The specimens collected here correspond only to the beige phenotype.

Phakellia robusta Bowerbank, 1866

Synonymised names.

Phacellia robusta (Bowerbank, 1866) (misspelling of genus name)

Material examined

CFM-IEOMA-7367/i347_2, St. 12 (INTEMARES1019), MaC (EB), BT; CFM-IEOMA-7368/i405 and CFM-IEOMA-7369/i409, St. 15 (INTEMARES1019), MaC (EB), BT; CFM-IEOMA-7370/i414_2, St. 16 (INTEMARES1019), MaC (EB), BT; CFM-IEOMA-7371/i417, St. 17 (INTEMARES1019), MaC (EB), BT; CFM-IEOMA-7372/i712 (INTEMARES0720), St. 25, MaC (EB), BT; CFM-IEOMA-7373/i731, St. 35 (INTEMARES0720), MaC (EB), RD; CFM-IEOMA-7374/POR760, St. 20 (MEDITSGSA519), south-western Cabrera archipelago, GOC and CFM-IEOMA-7375/POR762, St. 21 (MEDITSGSA519), south-western Cabrera archipelago, GOC.

Ecology and distribution

The species was frequent at the studied area, being found in a broad depth range (150-750 m) on both rocky and sedimentary bottoms. In the trawl fishing grounds of the continental shelf around Mallorca and Menorca it was mostly found below 300 m deep, where most of the collected specimens were larger. In the seamounts of the Mallorca Channel, the species was common on gravel bottoms 150-170 m deep, where specimens tended to be very small (1.5-3 cm in height) and in rocky outcrops and vertical walls, where sizes were intermediate (4-12 cm in height) and large (20-35 cm in height).

The species is reported for the first time in the Mallorca Channel, being its second record at the Balearic Islands, where it was previously recorded by *Santin et al. (2018)* from the Menorca Channel. In the Mediterranean, it is also known from the Gulf of Lions (*Vacelet, 1969*), the Tyrrhenian Sea (*Topsent, 1925*), the Alboran Sea (*Maldonado, 1992*), the Strait of Sicily (*Calcinai et al., 2013*) and the Adriatic Sea (*D'Onghia et al., 2015*). Besides, the species has been reported from several localities of the North Atlantic including the Gulf of Cadiz (*Sitjàà et al., 2019*), the Azores Islands (*Topsent, 1904*), the Cantabrian Sea (*Ferrer-Hernández, 1914*) and the North Sea (*Bowerbank, 1866*).

Phakellia ventilabrum **(Linnaeus, 1767)**

Synonymised names

Halichondria ventilabrum (Linnaeus, 1767)

Phacellia ventilabrum (misspelling of genus name)

Phakellia ventilabra (ruling of ICZN)

Spongia strigose Pallas, 1766 (genus transfer & junior synonym)

Spongia venosa Lamarck, 1814 (genus transfer & junior synonym)

Spongia ventilabra Linnaeus, 1767 (genus transfer & incorrect spelling)

Spongia ventilabrum Linnaeus, 1767 (genus transfer)

Material examined

CFM-IEOMA-7376/i822_1, St. 39 (INTEMARES0820), MaC (EB), ROV.

Ecology and distribution

The single specimen was collected on a rhodolith bed in the summit of the EB at 132 m deep (Fig. 4.2.2C) where, according to preliminary analysis of ROV videos, it seems to be a rare species.

This is the first report of the species at the Balearic Islands. The species has been widely reported in the North Atlantic (e.g. *Alvarez & Hooper, 2002*), to Greenland (*Lundbeck, 1909; Hentschel, 1929*) and Canada (*Lambe, 1900*). In the Mediterranean, it has been reported northern of the Iberian Peninsula (*Uriz, 1984*), in the Alboran Sea (*Maldonado, 1992*) and Corsica (*Vacelet, 1961*).

***Phakellia hirondellei* Topsent, 1890**

Synonymised names

Axinella hirondellei Topsent, 1890 (reverted genus transfer)

Phakellia robusta var. Hirondellei (Topsent, 1890) (status change)

Tragosia hirondellei (Topsent, 1890) (reverted genus transfer)

Material examined

CFM-IEOMA-7377/i353, St. 13 (INTEMARES1019), MaC (EB), BT; CFM-IEOMA-7378/i623, St. 33 (INTEMARES0720), MaC (AM), RD.

Ecology and distribution

The species was found at two stations of similar depth (135-147 m) in AM and EB. Both stations are located at the border of the summit, an area that may be affected by enhanced water current and an increase in nutrient and food supply (*Samadi et al., 2007; Rogers, 2018*). This could explain the common presence of large erect sponges such as *Poecillastra compressa* (Bowerbank, 1866) on stations located at these areas (personal observations).

The species is reported for the first time in the Mallorca Channel, being its second record at the Balearic Islands, where it was previously recorded by *Santin et al. (2018)*

from the Menorca Channel. In the Mediterranean Sea, it is also known in the north of the Balearic Sea (*Uriz,* 1984) and in the Gulf of Lions, the Ligurian Sea and Corsica (*Fourt et al., 2017*) and the Alboran Sea (*Boury-Esnault, Pansini & Uriz, 1994*).

Family HETEROXYIDAE Dendy, 1905

Genus *Heteroxya* Topsent, 1898

Heteroxya* cf. *beauforti

(Figs. 4.2.9, 4.2.10 and 4.2.11; Table 4.2.4)

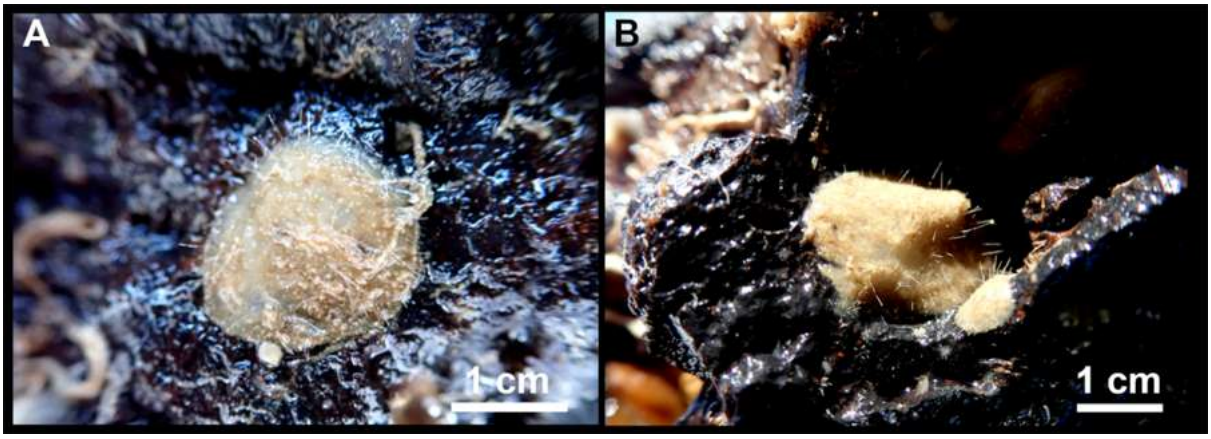

Fig. 4.2.9. *Heteroxya* cf. *beauforti.* (A) habitus of CFM-IEOMA-7380/i726 in fresh state. (B) habitus of CFM-IEOMA-7382/i461 in fresh state (large patch).

Material examined

CFM-IEOMA-7381/i444, St. 27 (INTEMARES1019), MaC (SO), RD; CFM-IEOMA-7382/i461, St. 28 (INTEMARES0720), MaC (SO), RD; CFM-IEOMA-7350/i487, St. 30 (INTEMARES0720), MaC (SO), RD; CFM-IEOMA-7380/i726 and CFM-IEOMA-7379/i727, St. 35, MaC (EB), RD. All specimens collected by J.A. Díaz.

Description

Small encrusting patches, circular or irregular, up to 2 cm in diameter (Figs. 4.2.9A and 4.2.9B). Body less than 1 mm thick. Consistency hard and slightly flexible. Hispidation visible to the naked eye. Greyish in life and after preservation in EtOH. No pores observed.

Skeleton

A basal spongin layer adheres to the substrate and allows the whole body to be peeled-off with a scalpel. Just upon this layer there are Oxea II running parallel to the substrate. The choanosome has low spicule content. Choanosomal chambers are relatively well developed in the thicker parts of the sponge (Figs. 4.2.10A and 4.2.10B). Thick areas also have ascending tracts of Oxea II, with Oxea II placed in between. The choanosomal

tracts are not present in the thinner areas (Fig. 4.2.10C). The basal layer and the choanosome have abundant circular bodies 3-9 µm in diameter, dark or transparent (Fig. 4.2.10B). The ectosome is constructed by a dense palisade of Oxea II, perpendicular to the surface, with Oxea I placed in the same perpendicular position, emerging towards the exterior. Long styles are found here and there outcrossing the ectosome and causing the hispidation.

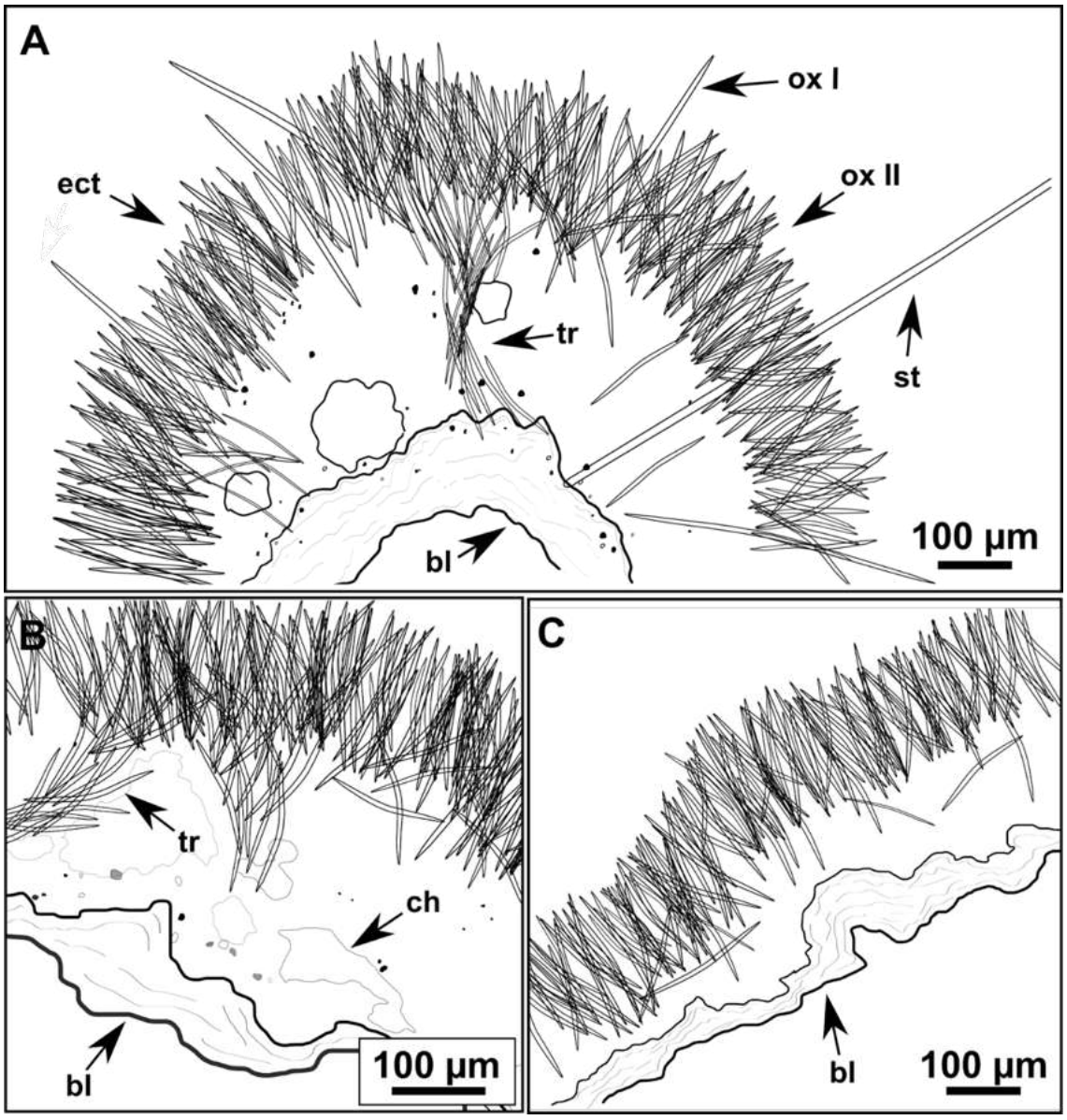

Fig. 4.2.10. Schematic illustration of *Heteroxya* cf. *beauforti* skeleton in transversal section. (A) general view. (B) body arrangement on a thick area. (C) body arrangement on a thin area. (ox I) oxea I. (ox II) oxea II. (bl) basal lamina. (ect) ectosome. (ch) choanosome. (tr) spicule tracks.

Spicules

Oxeas I (Fig. 4.2.11A): may be gently curved or bent in the middle, with sharp tips. They measure 319-482-623/7-10-15 µm.

Oxeas II (Figs. 4.2.11B): gently curved, curved or bent in the middle. Some stylote modifications present. Many with teratogenic parts like bifid tips, swellings or poliaxonal modifications (Figs. 4.2.11C and 4.2.11D). They measure 104-198-293/3-7-10 µm.

Hispidating styles (Fig. 4.2.11E-E2): very long and thin, curved, with round ends and sharp tips. Most broken, only three complete from specimen CFM-IEOMA-7381/i444, measuring 1151-3502/8-14 µm (n= 3).

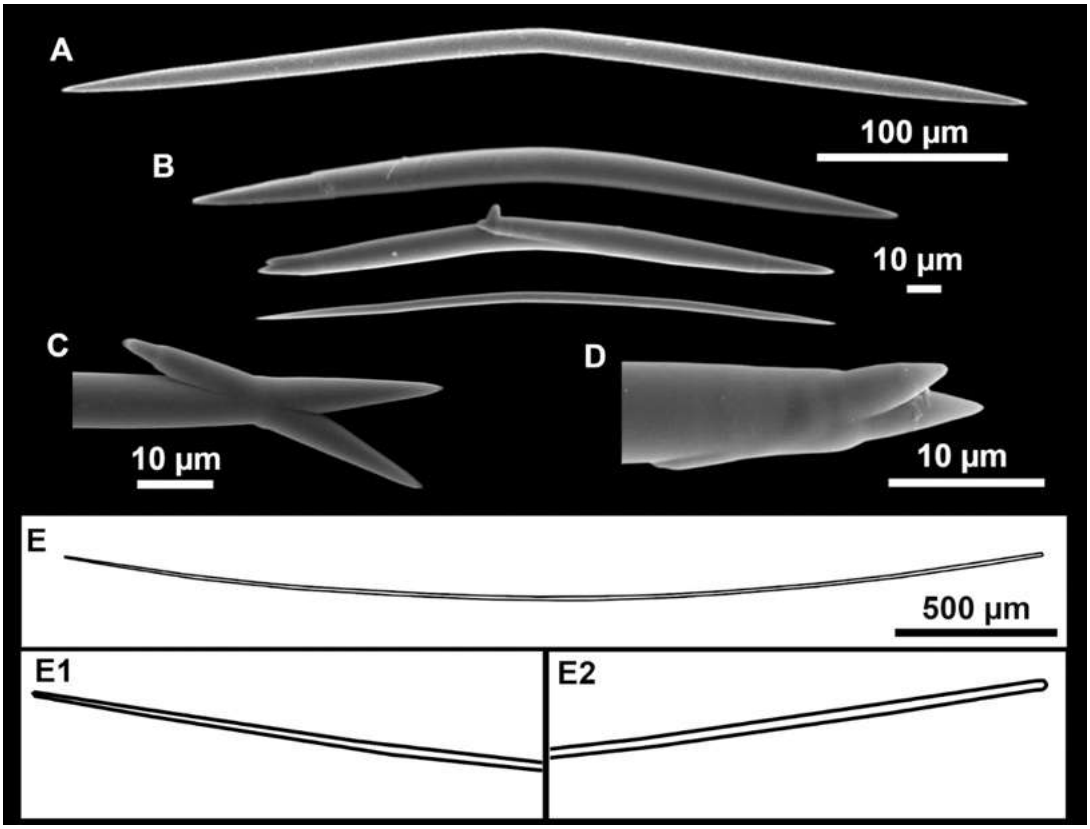

Fig. 4.2.11. Spicules of *Heteroxya* cf. *beauforti*. (A) Large oxeas I. (B) Small oxeas II. (C-D) Detail of polyactinal teratogenic modifications of oxeas II. (E) Drawing of a style with details of the tip (E1) and the head (E2).

Ecology and distribution

The species has been collected on smooth basaltic rocks between 270 and 325 m deep at SO and EB, where it seems to be rather common. Mostly associated with other minute encrusting sponges like *Hamacantha* spp. or *Bubaris* spp.

Heteroxya cf. *beauforti* represents the first record of a species belonging to the genus *Heteroxya* in the Mediterranean Sea.

Genetics

Sequences of *COI* Folmer fragment and the *28S* C1-D2 domains were obtained from the specimen CFM-IEOMA-7380/i726. Both sequences were deposited at the Genbank, under the accession numbers MW858350 and MW881150, respectively.

Table 4.2.4. Comparative characters of species of the genus *Heteroxya*. Depth (m), area (SO, Ses Olives; EB, Emile Baudot) and sampling station (St; see Rstudy in Table 1) where these specimens were collected are also shown. Spicule measures are given as minimum-mean-maximum for total length/minimum-mean-maximum for total width. A minimum of 30 spicules per spicule kind are measured, otherwise it is stated. All measurements are expressed in mm. Specimen codes are the reference numbers of the CFM-IEOMA/author collection. np, not present; nm, not measured.

Specimen	Oxea I	Oxea II	Style
H. corticata Syntypes by *Morrow et al., (2019)* (Azores), 1165-1240 m	1600-1700-2000/26-32-37, Microspined ends	235-310-420/12-23 Spined	np
H. beauforti *Morrow et al., (2019)* Holotype (Celtic Seas), 629-1469 m	622-1030-1385/10-16-21 Smooth	207-280-370/11-14-16 Smooth	5000-5650-6300/23-25-27
H.* cf. *beauforti **CFM-IEOMA-7380/i726** **EB (St. 35), 280-306 m**	434-569/7-13 (n=7) Smooth	107-180-287/4-6-9 Smooth	broken
H.* cf. *beauforti **CFM-IEOMA-7381/i444** **SO (St. 27), 288-318 m**	319-467-580/6-10-14 (n=23) Smooth	104-171-257/4-6-8 Smooth (n=23)	1151-3502/8-14 (n=3)
H.* cf. *beauforti **CFM-IEOMA-7382/i461** **SO (St. 28), 255-325 m**	327-460-586/6-10-15 Smooth	167-233-286/3-7-9 Smooth	broken
H.* cf. *beauforti **CFM-IEOMA-7379/i727** **EB (St. 35), 280-306 m**	420-530-623/9-12-15 (n=18) Smooth	142-192-293/6-8-10 Smooth	broken
H.* cf. *beauforti **CFM-IEOMA-7450 /i487** **SO (St. 30), 270-325 m**	nm	nm	nm

Remarks

The genus *Heteroxya* contains two species, *H. corticata* Topsent, 1898 and *H. beauforti* Morrow, 2019. *Heteroxya corticata* is the type of the genus, known only from deep waters (1200-1600 m) of the Azores Archipelago. The species has two categories of oxeas, both microspined, and lacks styles. Conversely, *H. beauforti* is known from slightly shallower waters of Ireland (630-1470 m), has smooth oxeas and posses long hispidation styles (Table 4). The genus was reviewed by *Morrow et al. (2019)*, that sequence the COI of both holotypes. They found no differences between the COI of *H. corticata* and *H. beauforti* but conclude that morphological differences were enougth to consider both as different species.

Morphologically, our material is more related to *H. beauforti* due to the abscense of microspined oxeas and the presence of hispidation styles. We have found circular

bodies embedded in the choanosome and the basal layer, which can be equivalent to the spherulous cells found in *H. beauforti* (*Morrow et al., 2019*). However, oxea I, oxea II and styles are markedly shorter and thinner in our material than those of *H. beauforti.* Those differences may be a result of depth, nutrient, or temperature differences. On the other hand, the COI sequence of our material is identical to the sequences of *H. corticata* and *H. beauforti*. We have sequenced the *28S* C1-D2 domains, but there are no published sequences to compare. Considering the lack of genetic differences and the affinity of our material to *H. beauforti*, here we believe that erecting a new species is not justified. Future works using other markers will clarify if *H*. cf. *beauforti* and *H. beauforti* are conspecific, or if *H.* cf. *beauforti* is a different species.

Family STELLIGERIDAE Lendenfeld, 1898

Genus *Paratimea* Hallmann, 1917

***Paratimea massutii* sp. nov.**

(Fig. 4.2.12; Table 4.2.5)

Diagnosis

Massive ovoid sponge with oxeas as megascleres and oxeas as auxiliary spicules. Centrotylotism occasionally present in both. Oxyasters smooth.

Etymology

Dedicated to Professor Enric Massuti, for his contribution to the knowledge of the benthic communities of the Balearic Islands.

Material examined

Holotyope: CFM-IEOMA-7383/i403, St. 15 (INTEMARES1019), MaC (EB), BT, coll. J.A. Díaz.

Paratype: CFM-IEOMA-7384/i420, St. 17 (INTEMARES1019), MaC (EB), BT, coll. J.A. Díaz.

Description

Both specimens are massive, subspherical, the largest (holotype, CFM-IEOMA-7383/i403; Fig. 4.2.12A) measuring about 5 cm in diameter, having a lobose surface with grooves and humps. Skin of a leathery touch, hispid only in the grooves. Color in life differing between the upper and the lower faces, the former having the first a brownish tinge while the latter a whitish to beige shade (Fig. 4.2.12A and 12B). After preservation in EtOH the whole body turns homogeneous vanilla cream (Fig. 4.2.12C). Both specimens have 4-6 circular oscula, 1-2 mm in diameter, scattered throughout the body. However, the holotype also has a main

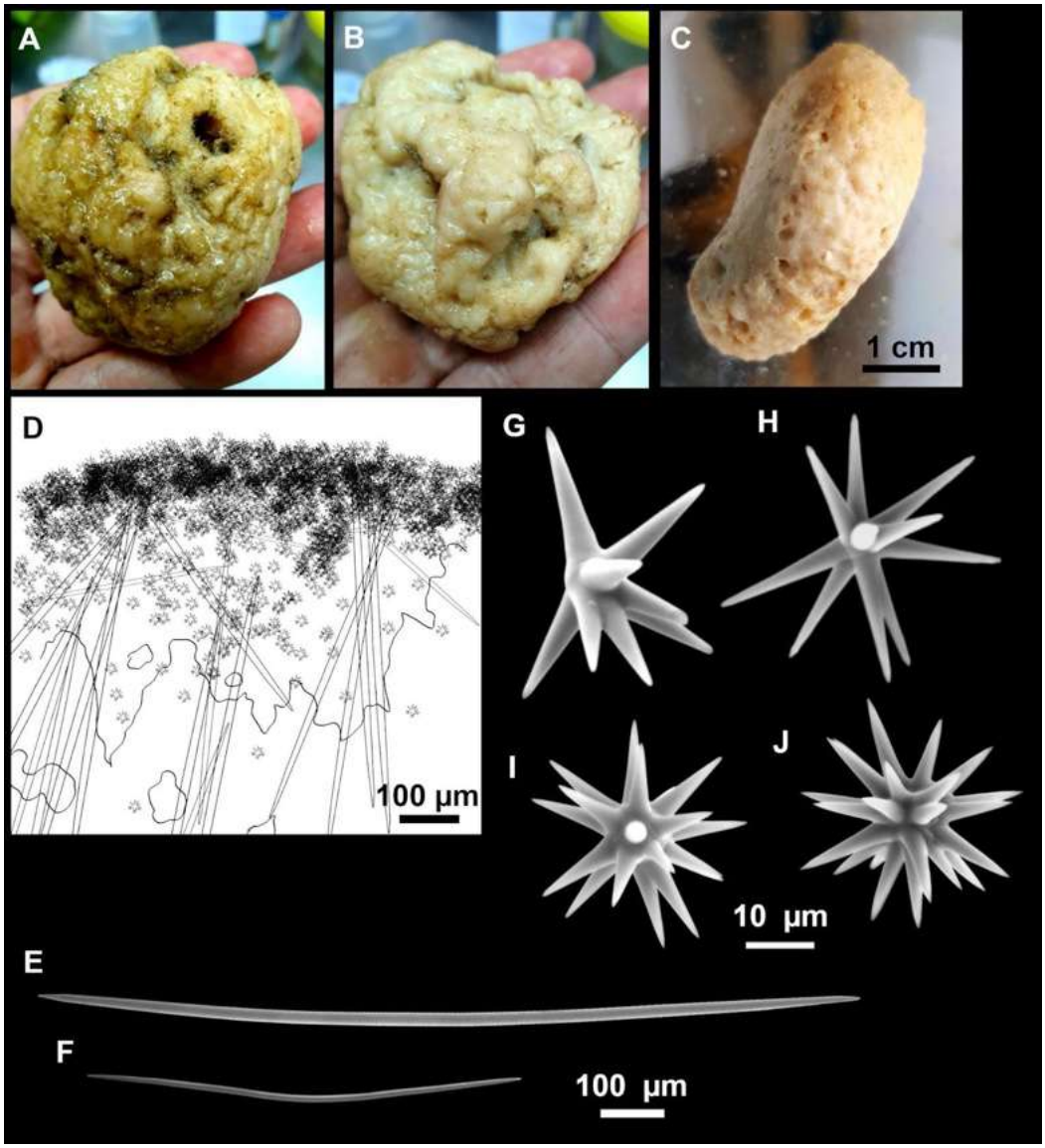

Fig. 4.2.12. *Paratimea massutii* **sp. nov.** (A-B) habitus of the holotype CFM-IEOMA-7383/i403 in fresh state, on its upper (A) and lower (B) sides. (C) habitus of the paratype CFM-IEOMA-7384/i420 preserved in EtOH. (D) schematic illustration of a transversal section of the holotype. (E-J) SEM images of the Holotype. (E) oxea I, (F) oxea I (auxiliar spicule). (G-J) oxyasters (all with same bar scale).

large and circular osculum, about 1 cm in diameter, on the upper side. Both specimens expelled a considerable amount of mucus when collected.

Skeleton

Ectosome not separable from the choanosome, formed by a dense crust of oxyasters and tangential principal and auxiliary oxeas. Choanosome composed of irregularly arranged oxeas and oxyasters, although radial bundles of large oxeas are present in the periphery, supporting the ectosome (Fig. 4.2.12D).

Spicules

Oxea I (Fig. 4.2.12E): robust and fusiform, some double bent, sometimes slightly centrotylote. They measure 910-1390-1711/11-21-33 μm.

Oxea II (Fig. 4.2.12F): uncommon. Bent or slightly sinuous, sometimes centrotylote. They measure 469-746-1088/3-7-10 μm.

Oxyasters (Figs. 4.2.12G-4.2.12J): with long, smooth and sharp rays. About 7-25 rays, occasionally less. Smaller ones tend to have more rays than larger ones, measuring 25-38-57 μm. Occasionally, some two-rayed oxyaster present.

Ecology and distribution

Found at two stations on calcareous gravel bottoms on the summit of EB (155 and 167 m deep), which was dominated by sponges such as *Hexadella* sp., *Phakellia robusta* and different species of the order Tetractinellida. A large number of the brachiopod *Gryphus vitreus* (*Born,* 1778) and echinoderms were also recorded.

This is the first report of the genus *Paratimea* in the Balearic Islands, and the deepest record in the Mediterranean Sea.

Genetics

Sequences of *COI* Folmer fragment were obtained from the Holotype (CFM-IEOMA-7383/i403) and deposited at Genbank under the accession number MW858351.

Remarks (see Table 4.2.5 for a detailed comparison with other *Paratimea* spp.)

Morphologically, the species resembles *Paratimea oxeata* Pulitzer-Finali, 1978, a Mediterranean species reported at rocky and muddy bottoms, at 35-60 and 110 m deep, respectively (*Pulitzer-Finali, 1978; Bertolino et al., 2013*), and at submarine caves at 15-20 m deep (*Morrow et al., 2019*). However, *P. massutii* **sp. nov.** is massive, a feature only shared with the cave specimen (S153) reported by *Morrow et al. (2019).* Notwithstanding, in *P. massutii* **sp. nov.** oxeas I are thicker, oxeas II longer and oxyasters slightly larger and with more actines (2-25 versus 4-12). A comparison of the *COI* sequences between the holotype of *P. massutii* **sp. nov.** and the cave specimen confirms those morphological differences, with 15 bp differences and a *p*-distance of 2%. On the other side, both the holotype and the specimens studied by *Bertolino et al. (2013)* differ from *P. massutii* **sp. nov.** in being cushion shaped or encrusting and having smaller oxeas. Unfortunately, no sequences of *Bertolino et al. (2013)* specimens

Table 4.2.5. Comparative characters of *Paratimea* spp. from the Mediterranean and the north-eastern Atlantic, including *Paratimea massutii* **sp. nov.** Depth, area (EB, Emile Baudot) and sampling station (St; see Rstudy in Table 1) where these specimens were collected are also shown. Spicule measures are given as minimum-mean-maximum for total length/minimum-mean-maximum for total width. A minimum of 30 spicules per spicule kind are measured, otherwise it is stated. All measurements are expressed in mm. Specimen codes are the reference numbers of the CFM-IEOMA/author collection. np, not present; nr, not reported.

Specimen	Megascleres	Accessory Oxeas	Oxyaster	Other spicules	External morphology
P. massutii **sp. nov.** CFM-IEOMA-7383/i403 Holotype EB (St. 15), 151 m	Oxeas 910-1419-1711/16-24-33 (n=17)	469-681-827/3-8-10 (n=7)	Smooth, 25-36-45 9-25 rays	np	Massive, lobate surface, whitish with brownish ink apex
P. massutii **sp. nov.** CFM-IEOMA-7384/i420 Paratype EB (St. 17), 156 m	Oxeas 1130-1374-1561/11-20-28	556-755-862/3-6-8	Smooth, 27-39-57 7-20 rays (occasionally 2 rays)	np	as i403
P. oxeata Pulitzer-Finally, (1978) Holotype Bay of Naples, 60 and 100-110 m	1000-1450/14-24	250-650/3-7	40-60	np	Encrusting, up to 4x5x0,4 cm, drab color in life, white after formalin and EtOH
P. oxeata *Beertolino et al., (2013)* Ligurian Sea, 35 m	810-961-1200/15-18-25	300-547-700/3-5-5	25-42-60	np	Small (0.5 cm^2) insinuating sponge, gray colored in dry state.
Paratimea oxeata *Morrow et al., (2019)* Gulf of Lion, Caves, 15-20 m	1000-1500/14-24	250-650/3-7	20-40 but up to 60 when reduced rays 4-12 rays	np	Massive lobose, surface conulose, oscules arranged on top of raised humps, Pale yellow-cream
P. loricata (*Sarà, 1958a*) Holotype Ligurian Sea *infralittoral*	Oxeas, aberrant terminations, 320-420/5-7 (most common) and 600/15 (n=1)	Centrotylote 105-180/2-3	Large: 40-50 Small: 12-20 (rare)	Tylostylestrilobated head 130-170/4-7	Encrusting, elastic but friable, whitish-yellow after EtOH

P. pierantonii (*Sarà, 1958b*) Holotype and paratypes Tyrrhenian Sea 30 cm, tidal cave	Styles and Subtylostyles: 1530-2550/12-18	650-1175/4-10, centrocurved, non-centrotylote	15-25	np	Cushion shaped with papillae. Hispid, smooth to the touch. Orange yellow at the surface, brownish inside.
P. arbuscula (*Topsent, 1928*) Holotype Azores, 650-914 m	Curved or flexuous, centrotylote. Some modified to styles. 560-1000/5-12	nr	Without centrum, conical, acanthose actines, 15-60 most with 12 rays	np	Small arbuscular sponge, up to 1 cm in heigth 1 mm in width, hispid. Whitish. Asters concentrated at the periphery
P. duplex (*Topsent, 1927*) Reproduced from *Morrow et al., (2019)* North Atlantic Ocean, 240-2165 m	Centrotylote oxeas 2000-2600/20-40, styles to subtylostyles 1600-1800/25-35	Weakly centrotylote 360-770/7-9	Without centrum, smooth rayed, 50-100 10-15 rays	np	cushion shaped, 3 mm thick, with a conulose surface
P. constellata (*Topsent, 1904*) Holotype, reproduced from *Morrow et al., (2019)* Roscoff (Celtic seas) 40 m	Long, slender tylostyles 2500-3000/13-14	Centrotylote oxeas 379-670-900/8-10	Smooth-rayed euasters 14-30-46	np	Cushion shaped, 2-3 mm thick, yellow gold
P. loenbergi (*Alander, 1942*) Holotype Reproduced from *Morrow et al., (2019)* Väderöfjord (Sweden), 60 m	1350-3000/10-13-15 (n=4); head, 16-20-27	Slightly bent, 530-712-930/5-5-6 (n=7)	Smooth 22-28-36	Small category of tylostyles 180-225/12-15 not found by *Morrow et al. (2019)*	Thin, hispid crust, pale yellow.
P. hoffmannae Morrow & Cárdenas, 2019 Norway (Holotype) Ireland (Paratype) 328 m (Holotype) 1500 m (Paratype)	Large, curved oxeas, occasionally centrotylote 2056-2187-2250/25-26-28	Rare, bent, occasionally centrotyle 353-446-520/3-4-5	Asymmetic 42-60-81 µm 7-18 smooth, tapering rays	np	Massive, subspherical. Holotype is ~7 in diameter. Surface covered in large conules, 1-4 mm in height. Creamish white.

are available to compare. *Paratimea massutii* **sp. nov.** is also similar to *P. hoffmannae* Morrow & Cárdenas, (2019), a North Atlantic species found in Norway and Ireland that is also massive and subspherical and has oxeas as both megascleres and auxiliary spicules. However, the large oxeas are much larger and thicker than in *P. massutii* **sp. nov.**, in contrast to the auxiliary spicules, which are shorther and thinner. Also, the oxyasters of *P. hoffmannae* are larger and with less actines. As for *P. oxeata*, COI sequences between *P. hoffmannae* and *P. massutii* **sp. nov.** are notably distant, with 13 bp differences and a *p*-distance of 2%. A similar case happens with *P. lalori* Morrow, 2019 from Ireland. This species is also massive-subspherical with oxeas as main megascleres and auxiliary spicules. Just as in *P. hoffmannae*, megascleres of *P. lalori* are longer and thicker than those of *P. massutii* **sp. nov.**, auxiliary spicules are shorter and thinner and oxyasters slightly larger and with fewer actines.

Paratimea massutii **sp. nov.** also differs from the other Mediterranean *Paratimea* spp. as follows: *P. loricata* (Sarà, 1958a) is encrusting, has much smaller oxeas I and oxeas II and two categories of oyasters, and bears tylostyles; *P. pierantonii* (Sarà, 1958b) is cushion-shaped, has styles and subtylotyles as megascleres, longer, thicker, and never centrotylote oxeas II and smaller oxyasters.

Also, *P. massutii* **sp. nov.** differs from the North-eastern Atlantic *Paratimea* spp. as follows: *P. constellata* is cushion shaped, has tylostyles and smaller oxyasters*; P. arbuscula* (Topsent, 1928), is arbustive, lacks auxiliary spicules and has smaller, acanthose oxyasters; *Paratimea duplex* (Topsent, 1927) is cushion shaped, has much larger oxeas I, have styles, subtylostyles, and two categories of oxyasters; *P. loennbergi* (Alander, 1942) is thinly encrusting, has tylostyles and smaller oxyasters.

Order BUBARIDA Morrow & Cárdenas, 2015

Family BUBARIDAE Topsent, 1894

Genus *Rhabdobaris* Pulitzer-Finali, 1983

Rhabdobaris implicata Pulitzer-Finali, 1983

Synonymised names

Cerbaris implicatus (Pulitzer-Finali, 1983)

Material examined

CFM-IEOMA-7385/i338_2_1, St. 11 (INTEMARES1019), MaC (EB), BT, coll. J.A. Díaz; CFM-IEOMA-7386/i698, St. 34 (INTEMARES0720), MaC (EB), RD, coll. J.A. Díaz

Ecology and distribution

Uncommon sponge found at two stations on the EB summit at 117 and 152 m deep, growing on living rhodoliths. Both stations were rich in massive demosponges, including large Tetractinellids, *Petrosia* (*Petrosia*) *ficiformis* and *P.* (*Strongylophora*) *vansoesti*.

This is the third time that the species is recorded, previously only known from the holotype collected in Corsica (*Pulitzer-Finali, 1983*) and the neotype collected at the Alboran Island (*Sitjà & Maldonado, 2014*).

Order DESMACELLIDA Morrow & Cárdenas, 2015

Family DESMACELLIDAE Ridley & Dendy, 1886

Genus *Dragmatella* Hallman, 1917

Dragmatella aberrans (Topsent, 1890)

(Fig. 4.2.13; Table 4.2.6)

Material examined

CFM-IEOMA-7387/i52_b1, St. 2 (INTEMARES0718), MaC (SO), BT, coll. F. Ordines; CFM-IEOMA-7388/i175, St. 5 (INTEMARES0718), MaC (EB), BT, coll. J.A. Díaz.

Description (modified from *Hooper & Van Soest, 2002*)

Small hollow sponge encrusting on stones or corals. Up to 2 cm in diameter. Whitish gray in life and after preservation in EtOH. Surface smooth, but provided with long thin, pointed fistules (Fig. 4.2.13A and 4.2.13B).

Skeleton

Ectosome composed of parallel tight tracts of styles, disposed in 4-5 layers of 30-50 µm in thickness (Fig. 4.2.13C). The raphides, sometimes grouped in trichodragmata, are scattered in the ectosomal and choanosomal tracts. Choanosome is cavernous (Fig. 4.2.13D), with tracts of styles, about 200 µm long, verging from a basal layer towards the ectosome.

Spicules

Styles (Figs. 4.2.13E and 4.2.13E1) fusiform, tapering towards the head, slightly or abruptly bent. They measure 349-546-676/6-10-15 µm.

Raphides (Figs. 4.2.13F and 4.2.13F1) abundant, straight, with an irregular shaft and one end hook-shaped, occasionally with central swellings. They measure 162-195-222/1-2-3 µm.

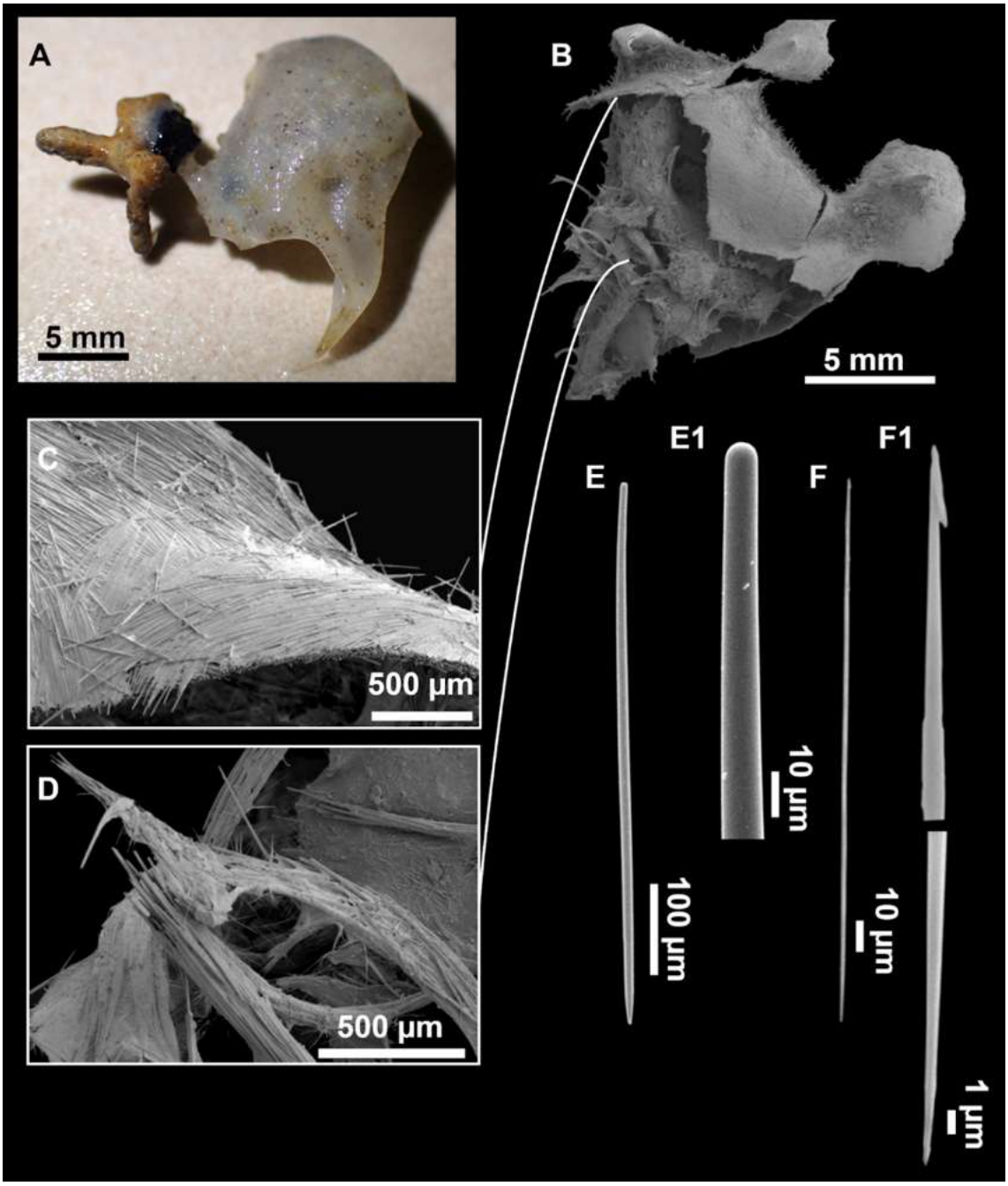

Fig. 4.2.13. *Dragmatella aberrans* (Topsent, 1890). (A) habitus of CFM-IEOMA-7388/i175 preserved in EtOH. (B-D) SEM images of the skeletal structure of CFM-IEOMA-7388/i175. (B) general view of the skeletal arrangement. (C) detail of the ectosome. (D) view of the ascending choanosomal tylostyle tracks. (E-E1) mycalostyles. (F) raphides with (F1) detail of the hook-shaped ends and central irregularities.

Ecology and distribution

Abundant species on sedimentary bottoms, with rests of calcareous shells and corals, found in SO, AM and EB and, to a lesser extent, on trawl fishing grounds of the continental shelf off Mallorca (between 138 and 362 m deep). On the same bottoms other small encrusting sponges such as *Hamacantha* spp. or *Bubaris* spp., the pedunculated *Rhizaxinella pyrifera* (Delle Chiaje, 1828) and *Thenea muricata*

(Bowerbank, 1858), the brachiopod *Gryphus vitreus* (Born, 1778) and small crustaceans are to be found.

This is the first report of the species in the Balearic Islands. In the Mediterranean Sea it has been recorded at the Gulf of Lions (*Vacelet, 1969*), Corsica (*Pulitzer-Finali, 1983*) and the Alboran Sea (*Boury-Esnault, Pansini & Uriz, 1994; Sitjà & Maldonado, 2014*). In the North Atlantic Ocean, this species has been recorded at several locations, including the coast of Portugal (*Topsent, 1895*), the Josephine Bank (*Topsent, 1928*) and the Cantabric Sea (*Topsent, 1890*).

Remarks

The species is easily distinguished by its hollow body and the possession of both styles and raphides. The latter have singular hook-shaped ends, a feature that had not been recorded before, and that is similar to the raphides found in some species of the genus *Dragmaxia* (Order Axinellida) (*Hooper & Van Soest, 2002*). No molecular data are

Table 4.2.6. Comparative characters of representative reports of *Dragmatella aberrans.* Depth (m), area (SO, Ses Olives; EB, Emile Baudot) and sampling station (St; see Rstudy in Table 1) where these specimens were collected are also shown. Spicule measures are given as minimum-mean-maximum for total length/minimum-mean-maximum for total width. A minimum of 30 spicules per spicule kind are measured, otherwise it is stated. All measurements are expressed in mm. Specimen codes are the reference numbers of the CFM-IEOMA/author collection.

Specimen	Styles	Raphides
Topsent, (1892) Cantabric Sea	600	180
Topsent, (1928) Cap Sines (Portugal)	600-800/9-11.5	70-200/12-20
Vacelet, (1969) Cassidaigne (Gulf of Lion)	350-600/6-13	150-210
Pulitzer-Finali, (1983) Calvi (Corsica) 128-150 m	400-600/6-14	200
Boury-esnault et al. (1994) Atlantic (485 m) and Alboran Sea (195 m)	315-571-631/5-11-16	95-207-260/0.4-2-3
CFM-IEOMA-7387/i52_b1 **SO (St. 2) 275 m**	349-555-676/6-9-13	162-197-222/1-2-3
CFM-IEOMA-7388/i175 **EB (St. 5) 138 m**	351-539-651/8-11-15	163-193-214/1-2-3

available for *Dragmatella*, but a phylogenetic relationship with *Dragmaxia* is unlikely, given the possession of styles and the skeletal arrangement of both genera. Therefore, hook-shaped raphide are probably homoplasic.

Order HAPLOSCLERIDA *Topsent, 1928*

Family CHALINIDAE Gray, 1867

Genus *Haliclona* Grant, 1841

Subgenus *Soestella De Weerdt, 2000*

Haliclona (*Soestella*) *fimbriata Bertolino & Pansini, 2015*

Material examined

CFM-IEOMA-7389/i825_1, St. 40 (INTEMARES0820), MaC (EB), ROV, coll. J.A. Díaz.

Ecology and distribution

The species was spotted regularly at the rhodolith beds of the EB summit, between 134 and 150 m deep. However, it was less abundant and not forming patches, as occurs in some areas of the Gulf of St. Eufemia in the Tyrrhenian Sea, where *Bertolino et al. (2015)* reported densities of 7.4±0.7 specimens/m^2.

This is the second report of the species, previously recorded only at the Gulf of St. Eufemia (southern Tyrrhenian Sea; *Bertolino et al., 2015*), expanding its distribution range towards the westernmost part of the Mediterranean Sea.

Family PETROSIIDAE Van Soest, 1980

Genus *Petrosia* Vosmaer, 1885

Subgenus *Strongylophora* Dendy, 1905

Petrosia (*Strongylophora*) *vansoesti* Boury-Esnault, Pansini & Uriz, 1994

Material examined

CFM-IEOMA-7390/i192_A and CFM-IEOMA-7391/i192_B, St. 6, MaC (EB), BT, coll. F. Ordines; CFM-IEOMA-7392/i313_P and CFM-IEOMA-7393/i313_G, St. 11, MaC (EB), BT, coll. J.A. Díaz; CFM-IEOMA-7394/i351, St. 13, MaC (EB), BT, coll. J.A. Díaz; CFM-IEOMA-7395/i694, St. 34, MaC (EB), RD, coll. J.A. Díaz.

Ecology and distribution

Large amounts of *P.* (*S*) *vansoesti* were collected from various stations in the summit of the EB, suggesting that it is an important species inhabiting Mediterranean seamounts and probably a habitat builder that confers three-dimensionality to the seafloor. The species was found from 116 to 152 m deep, on stations with living and dead rhodoliths and gravels, associated with large sponges such as *P.* (*P.*) *ficiformis* and some tetractinellids and halichondrids. Many groups of invertebrates, such as small crustaceans and echinoderms, were also observed at these stations.

This is the first record of the species in the western Mediterranean. The type locality is the Gulf of Cadiz, in the north-eastern Atlantic. In the Mediterranean it has been recorded in marine caves at both the Ionian Sea (*Costa et al., 2019*) and the Aegean Sea (*Gerovasileiou & Voultsiadou, 2019*). It has also been recorded at the Levantine Sea, living on rocks at depths shallower than 3 m (*Evcen & Çinar, 2018*). On the Balearic Islands, the species has only been collected in EB.

Subgenus *Petrosia* Vosmaer, 1885

***Petrosia* (*Petrosia*) *raphida* Boury-Esnault, Pansini & Uriz, 1994**

(Fig. 4.2.14; Table 4.2.7)

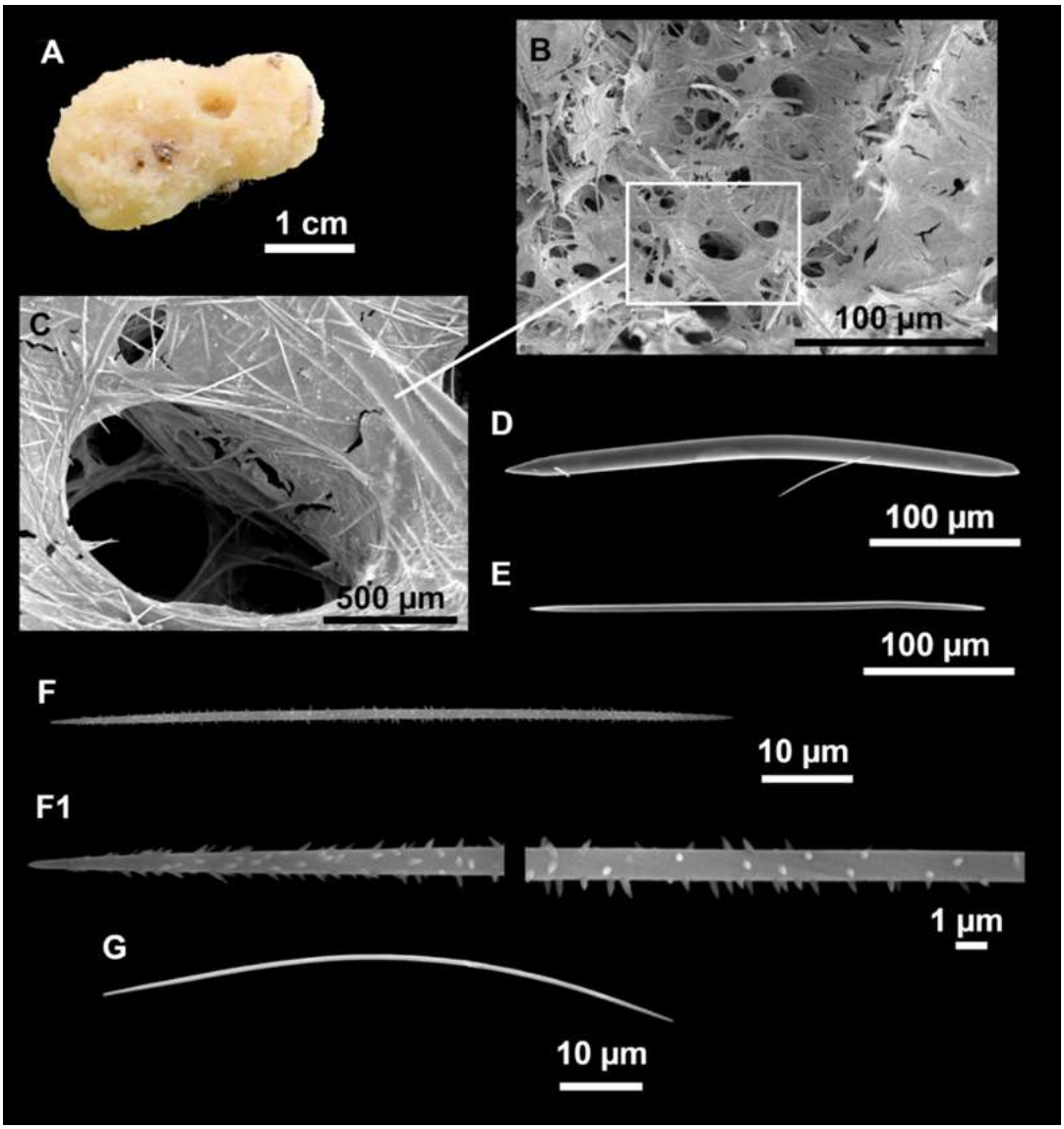

Fig. 4.2.14. *Petrosia (petrosia) raphida Boury-Esnault, Pansini & Uriz, 1994*. (A) habitus of CFM-IEOMA-7451/i242, preserved in EtOH. (B) SEM image of the choanosome. (C) detail of a choanosomal chamber. (D) oxeas. (E) young stages of oxeas. (F-F1) acanthoses raphides. (G) smooth raphides.

Material examined

CFM-IEOMA-7396/POR406, St. 1 (MEDITSGSA517), south-east of Menorca, GOC, coll. J.A. Díaz; CFM-IEOMA-7397/i178_3, St.5 (INTEMARES0718), MaC (EB), BT, coll. F. Orines; CFM-IEOMA-7451/i242 and CFM-IEOMA-7398/i254_2, St.8 (INTEMARES1019), MaC (AM), BT; CFM-IEOMA-7399/i305, St.10 (INTEMARES1019), MaC (AM), BT, coll. J.A. Díaz; CFM-IEOMA-7400/i312, St.11 (INTEMARES1019), MaC (EB), BT, coll. J.A. Díaz.

Description

Massive sponges, the largest collected specimen measuring about 4.5 cm in diameter and 2.5 cm in height (Fig. 4.2.14A). Whitish in life, beige after preservation in EtOH. Consistency hard, slightly crumbly. Surface rough due to minute conules, although in some specimens this is less obvious. There are 1 to 6 circular oscules of 2-5 mm diameter.

Table 4.2.7. Comparative characters from published records of *Petrosia (Petrosia) raphida Boury-Esnault, Pansini & Uriz, 1994* and present work. Depth (m), area (SO, Ses Olives; AM, Ausias March; EB, Emile Baudot) and sampling station (St; see Rstudy in Table 1) where these specimens were collected are also shown. Spicule measures are given as minimum-mean-maximum for total length/minimum-mean-maximum for total width. A minimum of 30 spicules per spicule kind are measured, otherwise it is stated. All measurements are expressed in mm. Specimen codes are the reference numbers of the CFM-IEOMA/author collection.

Specimen	Oxeas	Raphides
Boury-Esnault, Pansini & Uriz, (1994) Holotype, Gibraltar, 580 m	354-449- 499/26-32-36 (strongyles)	81-95-108/1
Sitjà et al., (2019) Volcano of Gulf of Cadiz (Pipoca), 530-573	290-500/20-25 (rarely as short as 7.5)	75-100/1 (some without spines)
CFM-IEOMA-7396/POR406 **South-east of Menorca (St. 1), 134 m**	271-369-432/9-13-16	62-78-91/1-1-2
CFM-IEOMA-7397/i178_3 **EB (St. 5) 138 m**	242-378-450/10-16-19	72-80-89/2-3-4
CFM-IEOMA-7451/i242 **AM (St. 8) 101 m**	268-333-380/11-14-17	70-80-91/1-2-2
CFM-IEOMA-7398/i254_2 **AM (St. 8) 101 m**	300-378-426/9-15-19	66-75-86/1-2-2
CFM-IEOMA-7399/i305 **AM (St. 10) 118 m**	242-346-394/9-15-19	65-75-88/1-2-2
CFM-IEOMA-7400/i312_1 **EB (St. 11) 152 m**	349-403-453/8-15-19	70-79-95/1-2-2

Skeleton

Ectosome form a detachable crust not evident to the naked eye, tightly adhering to the choanosome, and made of irregular net of polygonal to triangular meshes. Meshes are

constituted by one or two spicules. Spongin is present and fully embedded with raphides.

Choanosome (Figs. 4.2.14B and 4.2.14C) with an isotropic net of pauci-spicular spicule tracts covered by spongin, forming roundish meshes. These meshes are abundantly embedded by raphides. The tracts tend to condense towards the surface, supporting the ectosome.

Spicules

Oxeas (Figs. 4.2.14D and 4.2.14E): curved, with mucronated ends. Some polyaxonal modification in the shaft and ends may be present. They measure 242-372-450/9-15-19 µm, although underdeveloped stages (196-368/3-8 µm) are present. Styles and strongyles of the same length and width as the oxeas, present but scarce.

Raphides (Figs. 4.2.14F and 4.2.14F1): slightly curved, most minutely spined, although smooth ones are also present (Fig. 4.2.14G). They measure 62-77-95/1-2-2 µm.

Ecology and distribution

This species is very common in both AM and EB at the 101-152 m bathymetric range, and has been also found at the same depths off the southern coast of Menorca (Table 4.2.7). It can be found as a free-living sponge or growing attached to small fragments of calcareous sediments. However, it is also commonly found as an epibiont of other sponges and rhodoliths. The species seems to prefer massive specimens of *Hexadella* sp. and *Halichondria* sp. as substrate.

This is the first record of the species in the Mediterranean, but at a considerably shallower depth (101-152 m) than in the north-eastern Atlantic, where the species was reported at 580 m deep in the Strait of Gibraltar (*Boury-Esnault, Pansini & Uriz, 1994*) and at 530-575 m deep in the Gulf of Cadiz (*Sitjà et al., 2019*) (Table 4.2.7).

Remarks

The species is easily recognized due to the presence of characteristic spined raphides, added to other Petrosid features such as the skeletal architecture and the morphology of the oxeas. Remarkably, the specimens described in this study differ from the two previous reports in having much smaller oxeas (see below in brackets). This could be explained by the scarcity of nutrients in waters around the Balearic Islands, the bathymetric range in which the specimens were collected and/or differences in water temperature, seasonal variability and population phenotypes (*Simpson, 1978; Valisano et al., 2012*). These variables could also be the cause of differences in the morphology of the megascleres already noted by *Sitjà et al., (2019)* when comparing their material with the holotype. In the specimens from the Gulf of Cadiz (north-eastern Atlantic), strongyles were rare. Instead, megascleres consisted mostly of oxeas with stepped tips and some occasional stylote or strongylote modifications. This last feature is shared

with specimens of the Balearic Islands but not with the holotype, whose spicules have mostly strongylote extremities. These differences may be related to variations in nutrient regimes between the Balearic Islands and these areas (*Santinelli, 2015*).

Family PHLOEODICTYIDAE Carter, 1882

Genus *Calyx* Vosmaer, 1885

Calyx cf. *tufa*

(Fig. 4.2.15; Table 4.2.8)

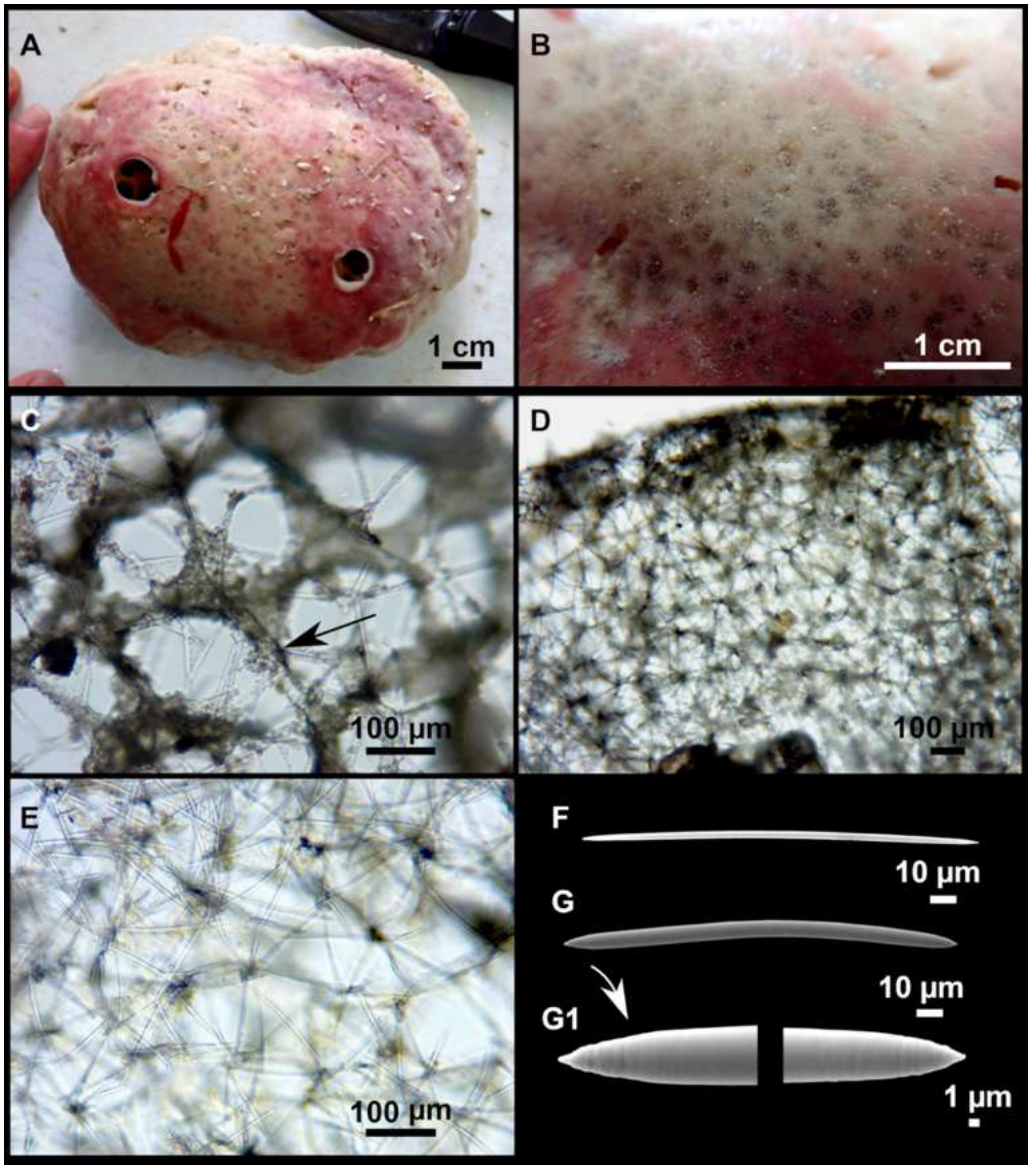

Fig. 4.2.15. *Calyx* cf. *tufa*. (A) Habitus of CFM-IEOMA-7403/i525 in fresh state. (B) Detail of the ectosome with poral areas. (C) View of a poral area of the ectosome with spherulous cells (arrow). (D) Transversal section of the choanosome. (E) Detail of the reticulation of the choanosome. (F-G) Immature and mature oxeas, with (G1) detail of the tips of (G).

Material examined

CFM-IEOMA-7403/i525, St. 24 (INTEMARES0720), MaC (AM), BT, coll. J.A. Díaz;
CFM-IEOMA-7401/i75, St. 3 (INTEMARES0718), MaC (AM), BT, coll. F. Ordines;
CFM-IEOMA-7402/i515, St. 23 (INTEMARES0720), MaC (AM), BT, coll. J.A. Díaz.

Description

Large, massive and semicircular sponges, up to 15 cm in diameter and 5 cm in height (Fig. 4.2.15A). Surface smooth to the touch; consistency stony hard and uncompressible. Choanosome slightly friable and cavernous. Color in life beige, with pink tints in the upper side of the body and whitish beige in the lower. It became homogeneous brownish beige after preservation in EtOH. Two to three large and circular oscula are located in the upper side of the body, measuring 1.3 cm in diameter. Ostia grouped in poral areas of the ectosome (Fig. 4.2.15B).

Table 4.2.8. Comparative characters from *Calyx* cf. *tufa* and *Calyx tufa* Ridley & Dendy, 1886. Depth (m), area (AM, Ausias March) and sampling station (St; see Rstudy in Table 1) where these specimens were collected are also shown. Spicule measures are given as minimum-mean-maximum for total length × minimum-mean-maximum for total width. A minimum of 30 spicules per spicule kind are measured, otherwise it is stated. All measurements are expressed in mm. Specimen codes are the reference numbers of the CFM-IEOMA/and author collection. nr, not reported.

Specimen	Oxeas	External morphology
Calyx* cf. *tufa **CFM-IEOMA-7403/i525 AM (St. 24), 114 m**	146-170-189/6-7-8	Large, massive, roundish. Surface smooth. Stony hard and incompressible. Ectosomal crust present. Beige with pink tints at the upper side. Whitish beige after EtOH
Calyx* cf. *tufa **CFM-IEOMA-7402/i515 AM (St. 23), 113 m**	140-171-205/4-7-9	As the Holotype
Calyx* cf. *tufa **CFM-IEOMA-7401/i75 AM (St. 3), 105 m**	132-178-206/4-6-9	As the Holotype
Calyx tufa *Ridley & Dendy, (1886)* Holotype St Lago (Cape Verde) 219 m	200/10	Massive, cake-like. Firm, almost stony, but brittle. Surface smooth but uneven. Dermal membrane (=ectosomal crust) readily peeling off. Vents rather small, circular, flush. Greyish yellow.
Calyx tufa *Topsent (1892)* Cantabrian Sea 300 m	nr	Firm but crumbly. Without ectosomal crust due to damaging. Light brown.

Skeleton

The ectosome (Fig. 4.2.15C) is formed by a crust of tangential spicules, forming triangular paucispicular meshes that become less dense at the poral areas. Spongin present but not abundant, with a granular appearance due to the presence of spherulous cells filled with granules (Fig 4.2.15C, arrow).

The choanosome (Figs. 4.2.15D and 4.2.15E) is mostly composed of a rather isotropic, unispicular net of spicules.

Spicules

Oxeas (Figs. 4.2.15F and 4.2.15G): slightly curved, with stepped or slightly mucronate points (Fig. 4.2.15G1) and rarely bent in the middle. They measure 132-173-206/4-7-9 µm.

Genetics

Sequences of *COI* Folmer and *28S* C1-D2 domains were obtained from the specimen CFM-IEOMA-7403/i525 and deposited in Genbank under the accession numbers MW858349 and MW881149, respectively.

Ecology

The species was found only at the summit of AM between 105 and 114 m deep, associated with rhodolith beds. It has also been found amongst with diverse set of sponges, including large Tetractinellids and other sponges such as *Hexadella* sp., *Axinella* spp. or *P. (P.) raphida*, as well as among many other invertebrates typically inhabiting the rhodolith beds, like small crustaceans and echinoderms. The pink coloration of its upper skin is probably caused by symbiotic cyanobacteria, as commonly happens in other Haplosclerids (*Rützler, 1990*).

Remarks

There are only two reported species of *Calyx* from the north-eastern Atlantic and the Mediterranean: *Calyx nicaeensis* (Risso, 1827) and *C. tufa* (Ridley & Dendy, 1886). The first is the type species of the genus, which is a well-known species characterized by its growing habit (vasiform), blackish color and large size. This species has been widely reported at both the western and eastern Mediterranean in infralittoral and circalittoral bottoms at 3-50 m deep (*Trainito et al., 2020*). *Calyx* cf. *tufa* clearly differs from *C. nicaeensis* in morphology (massive *vs.* vasiform, respectively), genetics (COI: 11 bp difference; 28S: 43 bp difference) and bathymetry (105-114 vs. 3-50 m, respectively). *Calyx tufa* is only known from its type locality at Cape Verde (*Dendy, 1886*) and from the Cantabrian Sea (*Topsent, 1892*). The species that we studied shares many characteristics with *C.* cf. *tufa*, including external morphology, consistency, and skeletal architecture. Unfortunately, the only description available is the one provided by *Dendy (1886)*, which is too general and matches with the characters of many other *Calyx* spp. (e.g., *Calyx podatypa* de Laubenfels 1934; *Calyx magnoculata* Van Soest,

Meesters & Becking, 2014; *Calyx nyaliensis* Pulitzer-Finali, 1993). The large distances between the reports of *C. tufa* and *C.* cf. *tufa*, the strong genetic barriers that separate the two records (the Strait of Gibraltar and the Almeria-Oran front), the generalized low dispersive potential of some sponge species (*Riesgo et al., 2019; Griffiths et al., 2021*) and the difference of habitats, are reasons that may suggest that the species that we report here is different from *C. tufa*. Moreover, no intermediate geographical findings have been reported, which would be expected if there was conspecificity (*Topsent, 1928*; *Maldonado, 1992*; *Boury-Esnault, Pansini & Uriz, 1994*; *Sitjà & Maldonado, 2014*; *Sitjà et al., 2019*). It should be noted that *C.* cf. *tufa* is a very large, massive, and easily recognizable sponge, which cannot be easily go unnoticed. However, considering that we did not study the holotype and that no genetic sequences of *C. tufa* are available, the possible conspecificity of *C.* cf. *tufa* with *C. tufa* cannot be completely assessed. Therefore, future work comparing the holotype of *C. tufa* may be needed to determinate if both species are different or conspecific. Considering the mentioned lack of data, here we use the more conservative choice by assigning the present record to *C.* cf. *tufa*.

Order POECILOSCLERIDA Topsent, 1928

Family MYXILLIDAE Dendy, 1922

Genus *Melonanchora* Carter, 1874

Melonanchora emphysema (Schmidt, 1875)

(Fig. 4.2.16)

Synonymised names

Desmacidon emphysema Schmidt, 1875 (genus transfer)

Material examined

CFM-IEOMA-7404/i573, St. 31 (INTEMARES0720), MaC (AM), RD, coll. J.A. Díaz.

Description

Hollow sponge with a detachable, smooth and paper-like ectosome provided with fistulas (Fig. 4.2.16A). About 2 cm in diameter. The choanosome is loose and includes sediment. Greyish white in life and after preservation in EtOH.

Skeleton

As in the previous records of the species (*Schmidt, 1785; Vacelet, 1969; Pulitzer-Finalli, 1983*).

Spicules

Tylotes (Figs. 4.2.16B and 4.2.16C) slightly curved, with roundish ends. Their length tends to be inversely related to their thickness. They measure 359-446-556/5-8-11 µm.

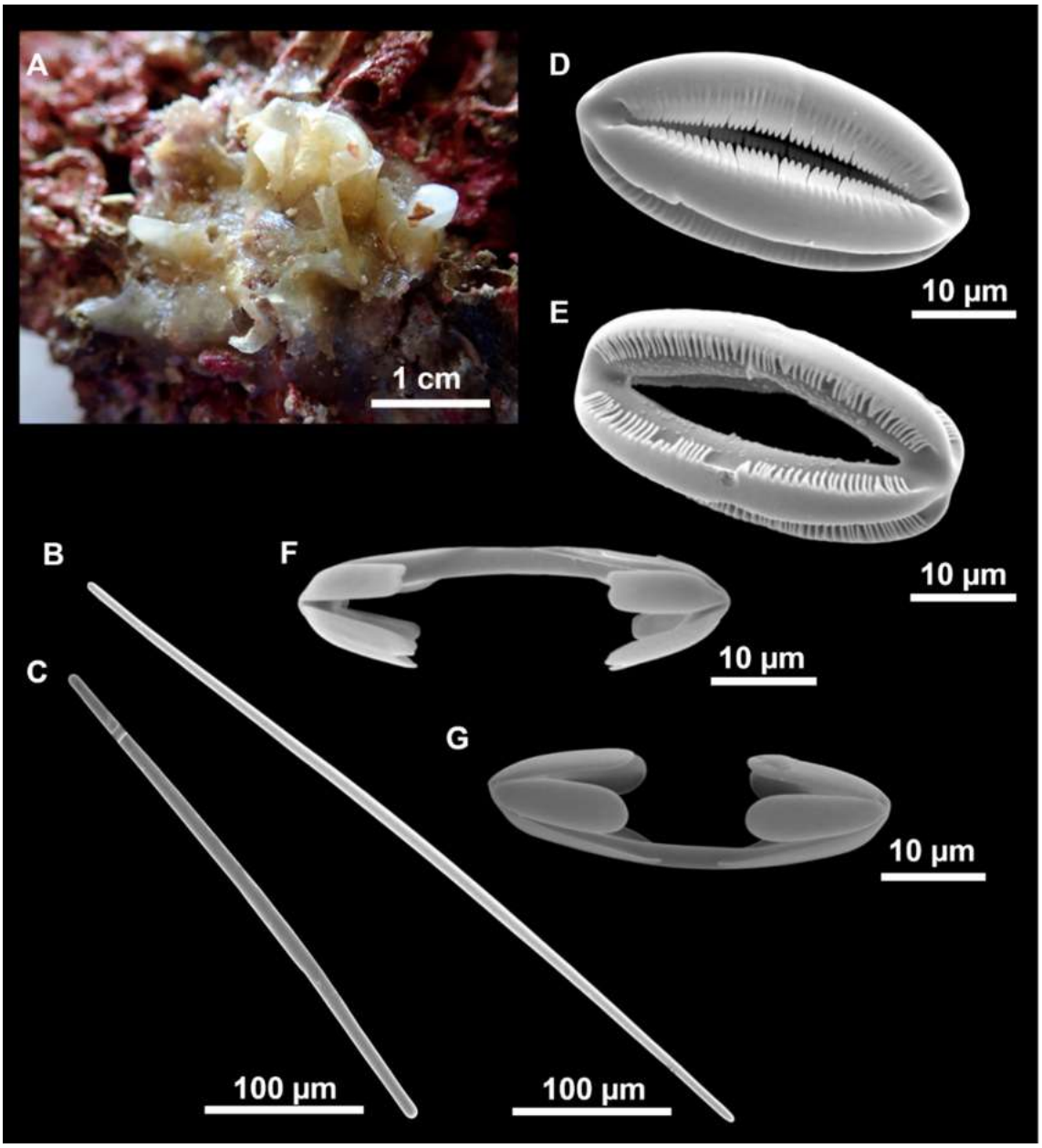

Fig. 4.2.16. *Melonanchora emphysema* (Schmidt, 1875). (A) Habitus of CFM-IEOMA-7404/i573 in a fresh state, attached to a rhodolith. (B-C) tylotes. (D-E) Spheranchoras. (F) Anchorate isochela I. (G) Anchorate isochela II.

Spheranchoras (Fig. 4.2.16D and 4.2.16E) of usual morphology, but uncommon. They measure 36-40-46/14-19-23 µm (n= 11).

Arcuate isochela I (Fig. 4.2.16F) with well-developed fimbriae and spatulated and bifid alae. They measure 29-42-47 µm.

Arcuate isochela II (Fig. 4.2.16G) similar to isochela I, but with rounded alae. They measure 14-18-21 µm.

Ecology

The single specimen was found in AM, on a rhodolith bed between 104 and 138 m deep. It was growing upon a large rhodolith, which was extensively epiphyted by encrusting, massive-encrusting or pedunculated sponges (like *Hamacantha* sp. or *Jaspis* sp.) or pedunculated Axinellids.

Remarks

The specimen matches well with the previous records of the species, both in external morphology, spicules and skeletal arrangement. This is the third record of this species in the Mediterranean, where it was recorded in the canyon de Cassidaigne in the Gulf of Lions (*Vacelet, 1969*) and Corsica (*Pulitzer-Finali, 1983*). In the North-Atlantic, it has been reported at several localitions: the type locality at Norway (*Schmidt, 1875*), the east Greenland shelf (*Lundbeck, 1905*), the Faroe Plateau (*Hentschel, 1929*) and the north coast of the Iberian Peninsula (*Solorzano,1990*). The vast distances between the Mediterranean and the North Atlantic reports (being the closest off northern Iberian Peninsula), and the lack of intermediate reports in well-studied areas such as the Alboran Sea, may indicate that Mediterranean and North Atlantic *M. emphysema* are different species, as already discussed by *Vacelet (1969)*.

Order POLYMASTIIDA *(Morrow & Cárdenas, 2015)*

Family POLYMASTIIDAE *(Gray, 1867)*

Genus *Polymastia* (Lammarck, 1815)

Polymastia polytylota Vacelet, 1969

(Fig. 4.2.17; Table 4.2.9)

Material examined

CFM-IEOMA-7405/i810, St. 39 (INTEMARES0820), MaC (AM), ROV, coll. J.A. Díaz.

Description

Rounded sponge, 2 cm high and wide, with two conical papillae (0.5 cm high and 3 mm wide) placed on the upper side of the body (Figs. 4.2.17A and 4.2.17B). Consistency hard and slightly compressible. Surface smooth to the touch, but microhispid under the stereomicroscope. Cream color before and after preservation in EtOH, with a darker choanosome. The specimen suffered a contraction after collection. In situ the sponge was 4.5 cm in height and 4 cm in width, being looser and with its surface full of visible ostia (Fig. 4.2.2A).

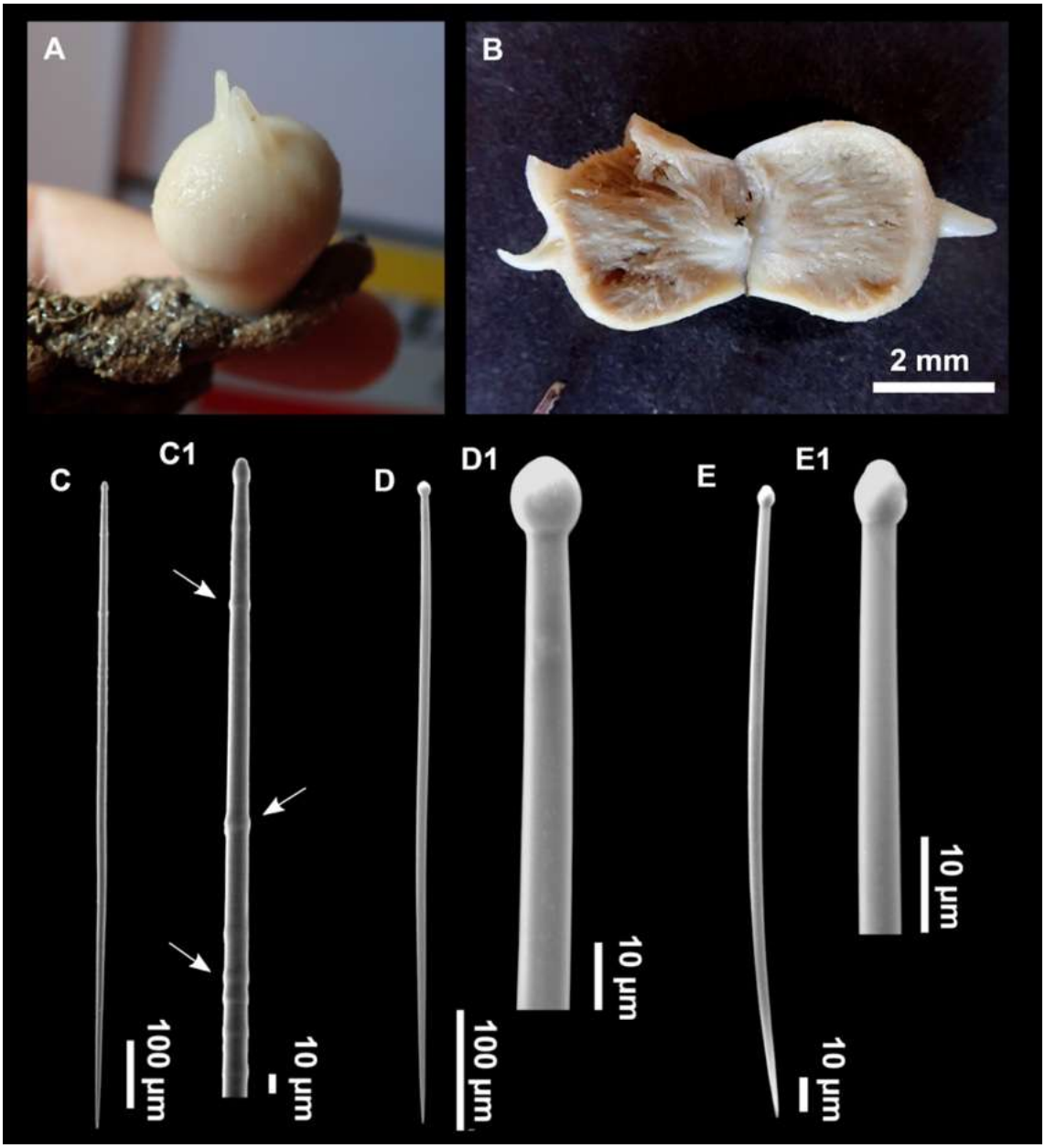

Fig. 4.2.17. *Polymastia polytylota Vacelet, 1969*. (A-B) Habitus of CFM-IEOMA-7405/i810, on fresh state (A), and preserved in EtOH (B). (C-C1) Principal subtylostyles with detail of the tyles in the shaft (arrows). (D) Intermediary tylostyles with (D1) detail of the head. (E) Ectosomal tylostyles with (E1) detail of the head.

Skeleton

As in the previous reports of the species (*Vacelet,1969; Pulitzer-Finali, 1983; Boury-Esnault, 1987; Boury-Esnault, Pansini & Uriz, 1994*).

Spicules

Principal tylostyles (Figs. 4.2.17C and 4.2.17C1): straight and fusiform, with several tyles in the proximal half part of the shaft. They measure 438-909-1154/8-11-15 µm.

Intermediary tylostyles (Figs. 4.2.17D and 4.2.17D1): fusiform, with a rounded head, often showing a vesicle. They measure 308-443-586/6-7-9 µm.

Ectosomal tylostyles (Fig. 4.2.17E and 4.2.17E1): slightly curved. They measure 121-166-200/2-3-5 µm.

Table 4.2.9. Comparative characters from *Polymastia polytylota* Vacelet, 1969. Depth (m), area (AM, Ausias March) and sampling station (St; see Rstudy in Table 1) where these specimens were collected are also shown. Spicule measures are given as minimum-mean-maximum for total length/minimum-mean-maximum for total width. A minimum of 30 spicules per spicule kind are measured, otherwise it is stated. All measurements are expressed in mm. Specimen codes are the reference numbers of the CFM-IEOMA/and author collection.

Specimen	Principal tylostyles	Intermedium tylostyles	Ectosomal tylostyles
Boury-Esnault, (1987) Redescription of the Holotype Toulon, but also in Corsica 165-270 m	650-990/10-13	210-490/7-10	70-180/2-5
Boury-Esnault, Pansini & Uriz, (1994) Alboran Sea (480 m) and North Atlantic (362-485 m)	668-854-1108/5-13-16	276-403-509/5-11-13	94-115-143/3-3-4
Pulitzer-Finali, (1983) North of Corsica (117 m)	650-810/10-13	210-490/7-10	80-120/2-3
CFM-IEOMA-7405/i810 AM (St. 3) (352-465 m)	438-909-1154/8-11-15	308-443-586/6-7-9	121-166-200/2-3-5

Ecology and distribution

Only one specimen collected in the northern part of the AM, between 352 and 465 m deep, on a rocky bottom characterized by enhanced water movement, with several large *Phakellia* spp, *Pachastrella* spp and *Poecillastra compressa*, as well as other *Polymastia* cf. *polytylota*. Although the present specimen was the only collected, it's easy identification and the other sightings during ROV transects may suggest that this sponge is quite common in some areas of the Mallorca Channel.

This is the first documented record of the species at the Balearic Islands. In the Mediterranean it is known from the type locality at the Gulf of Lions (*Vacelet, 1969*), the Ligurian Sea (*Vacelet, 1969; Pulitzer-Finali, 1983*) and the Alboran Sea, while it has been also reported at the Gulf of Cadiz in the north-eastern Atlantic (*Boury-Esnault, Pansini & Uriz, 1994*).

Remarks

The present specimen matches with the previous descriptions of the species in external morphology, skeletal architecture and spicule morphometrics. The only difference is

that our specimen has two papillae instead of one. The Fig. 4.2.2A shows the first in-situ image of this species.

Genus *Pseudotrachya* Hallmann, 1914

Pseudotrachya hystrix (Topsent, 1890)

(Fig. 4.2.18; Table 4.2.10)

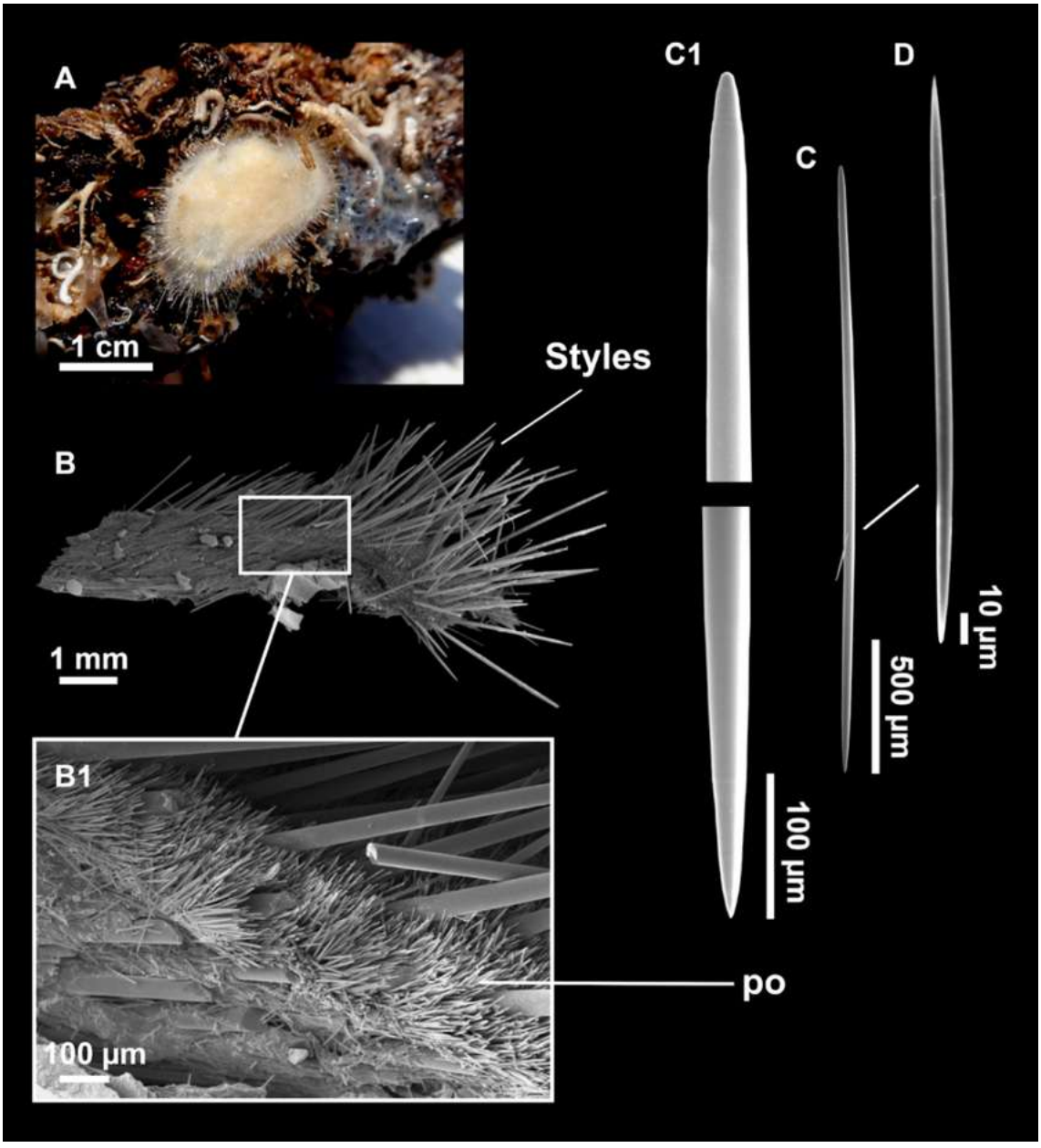

Fig. 4.2.18. *Pseudotrachya hystrix* (*Topsent, 1980*). (A) habitus of CFM-IEOMA-7407/i613 on fresh state. (B-B1) SEM images of the skeletal structure. (po) palisade of oxeas. (C-C1) anisoxeas. (D) microxeas.

Material examined

CFM-IEOMA-7406/i303_A, St. 19 (INTEMARES1019), MaC (AM), RD, coll. J.A. Díaz; CFM-IEOMA-7407/i613, St. 32 (INTEMARES0720), MaC (AM), RD, coll. J.A. Díaz.

Table 4.2.10. Comparative characters from *Pseudotrachya hystrix* (Topsent, 1890). Depth (m), area (AM, Ausias March) and sampling station (St; see Rstudy in Table 1) where these specimens were collected are also shown. Spicule measures are given as minimum-mean-maximum for total length/minimum-mean-maximum for total width. A minimum of 30 spicules per spicule kind are measured, otherwise it is stated. All measurements are expressed in mm. Specimen codes are the reference numbers of the CFM-IEOMA/and author collection. nr, not reported.

Specimen	Anisoxeas	Microxeas
Topsent, (1892) Holotype Azores, 318-454 m	up to 7000/70	185/6
Topsent, (1928) Azores, 650-914 m	nr	nr
Sarà, (1959) Tyrrenhian sea, 100 m	4000-5000/35-45	150-240/3-5
Boury-Esnault, Pansini & Uriz, (1994) Alboran Sea, 153-568 m	2000-3400-4300/18-44-63	200-235-330/5-6-7
Vacelet, (1969) St. 15: Cassidaigne (150 m) St. 23: Corse (210-240 m) St. 34: Cassidaigne (270 m) St. 46: Cassidaigne (450-550 m)	St15: 1000-1250/22-30 St23:>2000/30-35 St34: 1600-6600/18-40 St46:1100-4500/20-60	110-320/3-5 Stylote modifications
CFM-IEOMA-7406/i303_A **AM (St. 19), 231-302 m**	834-1689-3358/10-25-42	156-185-217/4-5-6
CFM-IEOMA-7407/i613 **AM (St. 32), 195-222 m**	768-2088-3402/18-32-45	152-203-270/3-5-6

Description

Roundish and pad-like encrusting sponge, up to 2 cm diameter and 3 mm in height (Fig. 4.2.18A). Coloration beige in life and whitish after preservation in EtOH. Very hispid surface. Consistency hard and only slightly compressible. No papillae, oscula and ostia inconspicuous.

Skeleton (modified from *Plotkin et al., 2013*)

Single layered cortex (palisade of microxeas). Main choanosomal skeleton of principal anisoxeas radially arranged, echinating the surface and auxiliary choanosomal skeleton of microxeas (Figs. 4.2.18B and 4.2.18B1).

Spicules

Anisoxeas (Figs. 4.2.18C and 4.2.18C1): straight and robust, with stepped ends. Intermediary stages between oxeas and styles present. Anisoxea size differs between specimens, measuring 834-1689-3358/10-25-42 µm in specimen i303 and 768-2088-3402/18-32-45 µm in specimen i613. Small and immature anisoxeas also present, but very scarce, about 500/10 µm.

Microxeas (Fig. 4.2.18D): fusiform and measuring 156-185-217/4-5-6 µm in specimen i303 and 152-203-270/3-5-6 in specimen i613.

Ecology and distribution

In addition to the two specimens described above, several other *P. hystrix* were collected from rocky slopes of AM and EB, between 195 and 302 m deep, suggesting that this species could be quite common in the Mallorca Channel seamounts. The species is found at rocky slopes, together with other small encrusting sponges such as *Hamacantha* spp., *Bubaris* spp. and the Hexactinellid *Tretodyctium* sp.

This is the first record of the species in the Balearic Islands, expanding its geographical distribution in the Mediterranean, where it was previously reported at the Tyrrhenian Sea (*Sarà, 1959*), the Ligurian Sea (*Pulitzer-Finali, 1983*), the Gulf of Lions (*Vacelet, 1969*) and the Alboran Sea (*Booury-Esnault, Pansini & Uriz, 1994*).

Remarks

This is a well-known species, characterized by their enormous megascleres with unequal tips (oxeote to stylote), and their small microxeas. Variations in the size of megascleres have been previously documented and may be related to ecological factors such as depth, nutrient availability, or temperature (*Maldonado et al., 1999*). However, due to their size, the largest megascleres were mostly broken, which could be a reason for the lack of reports on sizes 5000-7000 µm (Table 10).

Order TETHYIDA *Morrow & Cardenas, 2015*

Family HEMIASTERELLIDAE Lendenfeld, 1889

Genus *Hemiasterella* Carter, 1879

***Hemiasterella elongata* Topsent, 1928**

Material examined

CFM-IEOMA-7408/i149_4, St. 7 (INTEMARES0718), MaC (EB), RD, coll. J.A. Díaz;
CFM-IEOMA-7409/i337, St. 11 (INTEMARES1019), MaC (EB), BT, coll. J.A. Díaz;
CFM-IEOMA-7410/i531, St. 24 (INTEMARES0720), MaC (AM), BT, coll. J.A. Díaz;
CFM-IEOMA-7411/POR1066, St. 36 (MEDITSGSA0520), south-western Cabrera Archipelago, GOC, coll. J.A. Díaz.

Ecology and distribution

This species was found at mesophotic bottoms, between 109 and 152 m deep, generally associated with rhodolith beds, or areas with dead rhodoliths on the summits of EB and AM, but also sporadically at the same depths on trawl fishing grounds of the continental shelf of Mallorca.

This is the third record of the species and the third for the Mediterranean, where it was only known from the Alboran Sea (*Sitjà & Maldonado, 2014*). It is also the third report worldwide, considering the type locality at Cabo Verde in the eastern Atlantic (*Topsent, 1928*).

Class HEXACTINELLIDA Schmidt, 1870

Subclass HEXASTEROPHORA Schulze, 1886

Order LYSSACINOSIDA Zittel, 1877

Family ROSSELLIDAE Schulze, 1885

Subfamily LANUGINELLIDAE Gray, 1872

Genus *Lanuginella* Schmidt, 1870

***Lanuginella pupa* Schmidt, 1870**

(Fig. 4.2.19)

Material examined

CFM-IEOMA-7412/i286_1, CFM-IEOMA-7413/i286_2 and CFM-IEOMA-7414/i286_3, St. 18 (INTEMARES1019), MaC (AM), RD, coll. J.A. Díaz

Description

Tubular (CFM-IEOMA-7412/i286_1) to calyx-like (CFM-IEOMA-7413/i286_2 and CFM-IEOMA-7414/i286_3) sponges (Fig. 4.2.19A), up to 4 cm high and 2 cm in diameter. Surface smooth, but slightly hispid at localized areas. Fragile consistency and soft touch. Dirty white color in life and white after preservation in EtOH. All the three specimens present a single, circular oscule at the upper part of the body. One of the calyx-like specimens (CFM-IEOMA-7413/i286_2) has a minute and short peduncle.

Skeleton

As usual for the species (see *Ijima, 1904*; *Tabachnick, 2002* and *Sitjà et al., 2019* for detailed descriptions)

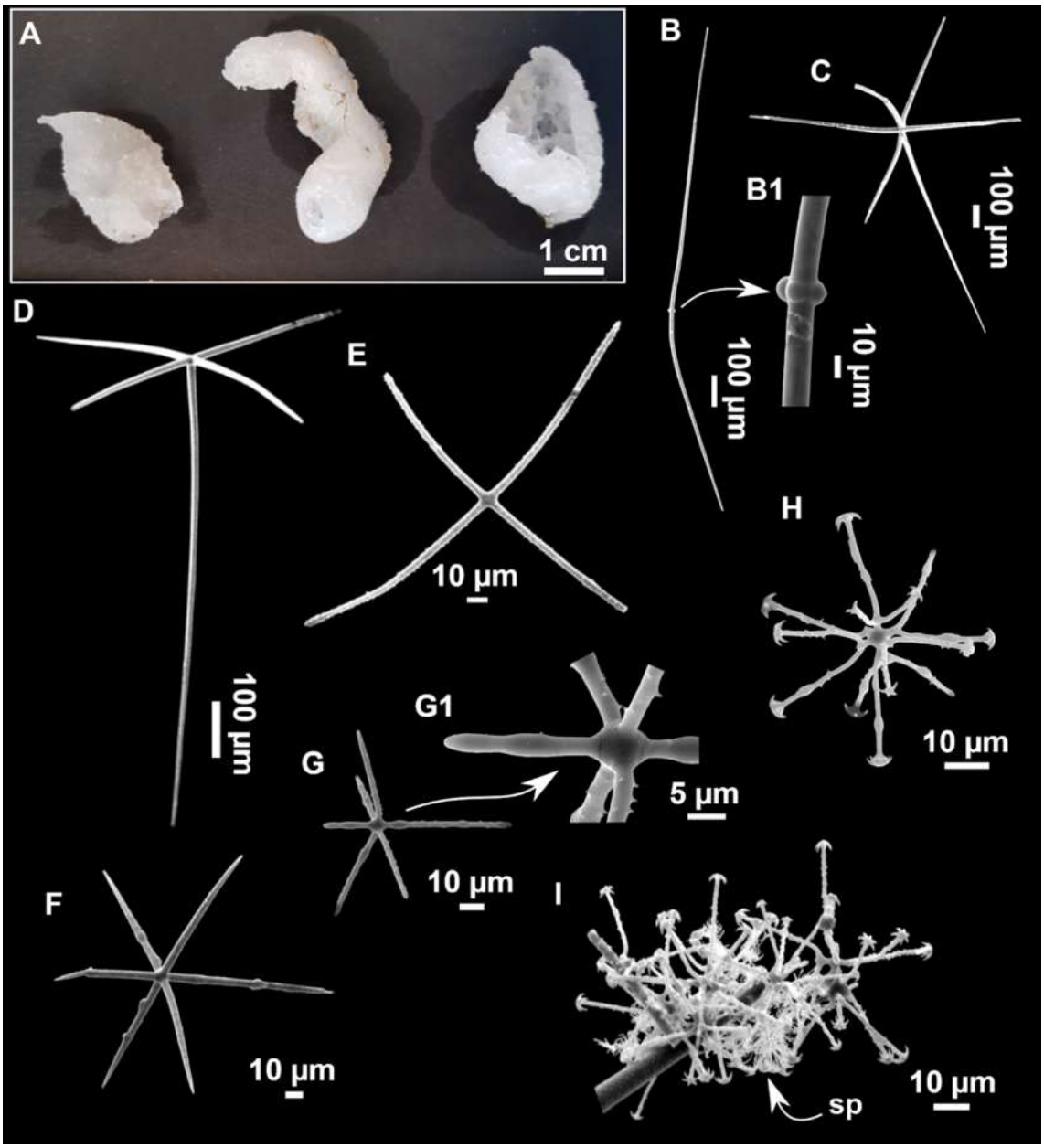

Fig. 4.2.19. *Lanuginella pupa Schmidt, 1870*. (A) Habitus of CFM-IEOMA-7413/i286_2 (left), CFM-IEOMA-7412/i286_1 (middle), i286_3/CFM-IEOMA-7414 (right) preserved in EtOH. (B-I) SEM images of spicules from CFM-IEOMA-7412/i286_1. (B) Choanosomal diactine with (B1) detail of the four central tubercles. (C) Choanosomal hexactine. (D) Hypodermal pentactine. (E) Stauractine. (F-G) Atrial hexactines with (G1) detail of the spines of (G). (H) Discohexaster. (I) Agglomeration of discohexasters, with a strombiloplumicome (sp) beneath.

Spicules

Choanosomal diactines (Fig. 4.2.19B): long and slim, slightly sinuous, with four vestigial tubercles in the center (Fig. 4.2.19B1), which may have swellings all over the shaft and spines on their tips. They measure 245-1611/3-15 µm.

Choanosomal hexactines (Fig. 4.2.19C): with actines of different lengths, sometimes sinuous. They measure 349-983/10-25 µm (n= 12).

Hypodermal pentactines (Fig. 4.2.19D): with a ray reduced to a stump or absent. Proximal rays are much larger than the others and perpendicularly arranged. Rays are smooth or slightly rugose. Proximal ray measuring 242-950/7-19 µm (n= 8) and perpendicular rays measuring 137-850/4-20 µm (n= 28).

Stauractines (Fig. 4.2.19E): with four actines perpendicularly arranged one another in the same plane. They are straight or slightly curved, strongly spined, with roundish tips. They measure 61-111/3-5 µm (n= 23).

Dermal hexactines (not shown): uncommon. Rugose, with the proximal ray slightly longer than the distal one. Overall measures: proximal rays 151/7 µm (n= 1), distal rays 105/6 µm (n= 1) and perpendicular rays 68-110/2-6 µm (n= 3).

Paratetractin: only a single spicule observed, measuring 77/4 (n= 1).

Atrialia hexactines (Fig. 4.2.19F and 4.2.19G): common. Slightly rough to smooth. Overall measures: proximal rays 107-159/4-6 µm (n= 8), distal rays 70-102/4-7 µm (n= 8) and perpendicular rays 70-150/3-7 µm (n= 22).

Discohexasters (Fig. 4.2.19H): rather uncommon. Some with underdeveloped, twisted rays. They measure 43-76 µm (n= 29).

Strobiloplumicomes (Fig. 4.2.19I): very rare and not found in specimen CFM-IEOMA-7413/i286_2. They measure: 20-38 µm (n= 6).

Ecology and distribution

Species found only at one station located in a rocky slope at SO, between 220 and 275 m deep. It was associated with fossil ostreid reefs and carbonate rocks, together with other encrusting sponges like *Hamacantha* sp., *Bubaris* sp., and *Jaspis* sp.

This poorly-known species is the single representative of the genus *Lanuginella*, reported at several distant locations around the world: Kagoshima Gulf at the Sea of China (*Okada, 1932*), Ki Island at the Sea of Banda (*Schulze, 1887*). In the northern Atlantic it was recorded at Cabo Verde (*Schmidt, 1870*), the Gulf of Cadiz (*Sitjà et al., 2019*) and the Strait of Gibraltar (*Topsent, 1895*). This is the first record of the species in the Mediterranean Sea, increasing its already wide distribution. However, a revision of the species is needed, and it is likely that such a cosmopolitan distribution may indicate that *L. pupa* represents a species complex. However, deep-sea species tend to be more widely distributed than shallow ones, probably because of the uniformity of the environmental conditions (*McClain & Hardy, 2010*). A detailed examination of worldwide specimens, combined with molecular methods, may shed more light on it.

Discussion

Biogeography and seamount singularity

The present study increases the knowledge of the sponge diversity of the Mediterranean seamounts. We describe a new genus, 4 new species, and 15 new geographical reports, including two new reports for the Mediterranean Sea. This study also highlights *Foraminospongia balearica* **sp. nov.** as one of the most common sponges at AM and EB, being large and easily distinguishable. This species was never recorded at other previously explored Mediterranean seamounts or ridges of a similar depth range, such as the Seco de los Olivos or the Alboran Ridge, whose sponge fauna has been already studied (*Sitjà & Maldonado, 2014; Würtz & Rovere, 2015; De la Torriente et al., 2018*). Therefore, the Mallorca Channel seamounts may be considered unique faunal refuges, appealing to what is called the "Seamount endemism hypothesis" (*de Forges et al., 2000*), which suggests that geographical separation of seamounts is reflected by genetic isolation of their fauna, which promotes speciation by vicariance. This hypothesis has been questioned, as some works have shown that benthic fauna (including sponges) is well connected among isolated seamounts (*Samadi et al., 2006; Ekins et al., 2016*). However, others have shown structured populations between seamounts (*Castelin et al., 2010*), or between seamounts and the continental shore populations (*Crochelet, 2020*). Other authors suggest that there is a mixture of panmictic and structured populations, largely dependent on the characteristics of the single species nature (*Rogers, 2018*). If we consider that the dispersal of sponges tends to be very limited (*Maldonado, 2006; Riesgo et al., 2019; Shaffer et al., 2020; Griffiths et al., 2021*), it is plausible that certain seamount sponge populations are highly structured. This limitation in the dispersal may be enhanced in isolated seamounts or in those with peculiar or unique ecological characteristics. In this sense, both AM and EB have very shallow summits and are placed in an area of special oligotrophy (e.g. *Bosc et al., 2004; Uitz et al., 2012*). The nearest habitat with similar features is the continental shelf of the Balearic promontory, although these areas tend to be under the impact of bottom-trawling (*Farriols et al. 2017; Ordines et al., 2017*), with the consequent impoverishment of benthic communities (*Jennings & Kaiser, 1998*). In fact, most of the species of SO, AM and the EB had not been found at the continental shelf of the Balearic Islands (*Bibiloni, 1990; 1993; Grinyo et al., 2018; Santin et al., 2018*), except for *Phakellia robusta, P. hirondellei* (*Santin et al., 2018*)*, Petrosia* (*Petrosia*) *raphida,* and *Hemiasterella elongata* (this work).

The particular conditions of the Balearic Islands, extreme oligotrophy, geographical isolation, low fishing pressure and heterogeneity of habitats (*Quetglas et al., 2012*; *Massutí et al., 2014*) suggest this area is a hotspot of sponge diversity, with much of its fauna still unknown, especially at depth below 90 m (*Bibiloni, 1990; Santin et al., 2018; Díaz et al., 2020*). In recent years, this high diversity has been evidenced by the presence of rich benthic assemblages (*Ordines & Massutí, 2009*; *Barberá et al., 2012*; *Ordines et al., 2017*), as well as by a high number of new species and new geographical reports (e.g. *Kovačić et al., 2017, 2019; Ordines et al., 2019a,b,c; Díaz et al., 2020*). Thus, there is a need to find out which sponge species inhabit those waters and how much do they contribute to the benthic biomass. Sponges are key components of the benthic ecosystems, playing important biogeochemical roles (*de Goeij et al., 2013*) and

serving as food or refugee to many other animals (*Maldonado et al., 2017*). Future works should characterize those benthic habitats of the continental shelf and slope around the Balearic Islands that are potentially similar to those of the Mallorca Channel seamounts (e.g. non-impacted sedimentary and rocky bottoms with rhodoliths and gravels located between 90 and 150 m deep and rocky slopes down to 400-500 m deep). Then, both biocenosis should be compared to confirm the singularity of the habitats of the Mallorca Channel seamounts.

Integrative taxonomy

The generalized lack of distinctive characters has caused sponges to be one of the most difficult groups to classify. This difficulty is also reflected by sponge phylogenetic relationships, with polyphyletic taxa present in all the levels of the Linnean classification (e.g. *Cardenas, 2012; Diaz et al., 2020*). Thus, the use of both morphology and molecular markers is central to the improvement of the knowledge of this group of organisms. Following this approach, here we have proposed the new genus *Foraminospongia* to be erected in the family Hymerhabdiidae, supported by the two new species *Foraminospongia balearica* **sp. nov.** and *Foraminospongia minuta* **sp. nov.**, confirmed by morphological traits and both COI and 28S markers. On the other hand, the species *Heteroxya* cf. *beauforti* has shown no variability in its COI sequence relative to its North Atlantic congenerics, which highlights the importance of morphology and the need to combine both approaches. The COI is known to be a low-resolution marker to discriminate species of sponges, so we also sequenced the more variable 28S marker. However, no 28S sequences are currently available in any database for comparison with the other *Heteroxya* spp.: this issue should thus be addressed in the future.

A key subject in sponge taxonomy is the robustness of the skeletal characters as a species diagnostic tool, and how reliable they are for discriminating species and populations. Reliable discrimination is further complicated by the fact that skeletal elements may change depending on environmental conditions such as temperature, depth, or nutrient concentration; skeletal elements may also change due to intraspecific plasticity, overall modifying length, width, morphology, and even their presence or absence (*Cárdenas et al., 2012; Abdul Wahab et al., 2020*). No consensus has ever been reached to consider a given morphological deviation as enough evidence to erect a new species, a fact that remains arbitrary. We have found differences in the spicular morphometry between the specimens of the Balearic Islands and specimens of other areas of the Mediterranean and the North Atlantic Ocean; these differences have been described here for most of the species to some extent. Since the dispersive potential, long-distance connectivity, and speciation of sponges are poorly understood, most of the diagnosis in the present work were performed under a conservative approach, only proposing new species when we found solid morphological evidence. Taking this into account, factors like vast geographical distances, presence of oceanographic barriers or minor morphometric differences were not considered enough evidence for species

delimitation. In the case of *Calyx* cf. *tufa*, its potential conspecificity with the North Atlantic species *C. tufa* cannot be discarded. We did not get access to any material of *C. tufa,* and no sequences are available for comparison; moreover, the original description is too vague and general. However, as stated above, the absence of any intermediate records of such a big, conspicuous, and easily recognizable sponge is noteworthy. Also, the recorded depths of *C. tufa* for the Atlantic are much deeper than those for *C.* cf. *tufa* (219 and 300 m versus 105-114 m). Future work is need to clarify if both species are synonyms, or if *C.* cf. *tufa* is a new species for science.

626

627

From caves to seamounts: the hidden diversity of tetractinellid sponges from the Balearic Islands, with the description of eight new species

Julio A. Díaz[1,2], Francesc Ordines[1], Enric Massutí[1] & Paco Cárdenas[3,4]

[1]Centre Oceanogràfic de les Balears, Instituto Español de Oceanografía (CSIC), Moll de Ponent s/n, 07015 Palma (Spain).

[2]Laboratori de Genètica, Biology Department, University of the Balearic Islands, Carretera de Valldemossa km 7.5, 07122 Palma (Spain).

[3]Pharmacognosy, Department of Pharmaceutical Biosciences, Uppsala University, Husargatan 3, 751 23 Uppsala, Sweden.

[4]Museum of Evolution, Uppsala University, Norbyvägen 16, 752 36 Uppsala, Sweden.

Corresponding authors: Julio A. Díaz, Paco Cárdenas

E-mails: julio.diaz@ieo.csic.es, paco.cardenas@em.uu.se

Abstract

The sponge fauna of the Western Mediterranean is one of the most studied in the world. Yet sampling new habitats and a poorly studied region like the Balearic Islands highlights once again our limited knowledge of this group of animals. This work focused on demosponges of the order Tetractinellida collected in several research surveys (2016-2021) on a variety of ecosystems of the Balearic Islands, including shallow caves, seamounts and trawl fishing grounds, in a broad depth range (0-725 m). Tetractinellid material from the North Atlantic and more than twenty type specimens were also examined and, for some, re-described in this work. All species were barcoded with the traditional molecular markers COI (Folmer fragment) and 28S (C1-C2 or C1-D2 fragment). A total of 36 species were identified, mostly belonging to the family Geodiidae (15 species), thereby bringing the number of tetractinellids recorded in the Balearic Islands from 15 to 39. Eight species from this study are new: *Stelletta mortarium* **sp. nov.**, *Penares cavernensis* **sp. nov.**, *Penares isabellae* **sp. nov.**, *Geodia bibilonae* **sp. nov.**, *Geodia microsphaera* **sp. nov.** and *Geodia matrix* **sp. nov.** from the Balearic Islands; *Geodia phlegraeioides* **sp. nov.** and *Caminus xavierae* **sp. nov.** from the North East Atlantic. *Stelletta dichoclada* and *Erylus corsicus* are reported for the first time since their description in Corsica in 1983. Finally, after comparisons of type material, we propose new synonymies: *Geodia anceps* as a junior synonym of *Geodia geodina, Erylus cantabricus* as a junior synonym of *Erylus discophorus* and *Spongosorites maximus* as a junior synonym of *Characella pachastrelloides*.

Introduction

Tetractinellida is the second most diverse demosponge order, with currently ~1180 described species belonging to 98 genera and 23 families (*de Voogd et al., 2024*). They are found in all oceans and latitudes, but usually more present in the deep sea and cryptic habitats such as caves, and less frequently in light-exposed areas (e.g. *Maldonado & Young, 1996; Grenier et al. 2018*). The astrophorin tetractinellids are

known to constitute boreo-arctic North Atlantic and Western Mediterranean sponge grounds, structural habitats that increase the biodiversity and provide refuge for many demersal species of commercial interest (*Klitgaard, 1995; Klitgaard & Tendal, 2004; Maldonado et al., 2015*).

The spicular set of tetractinellids is characterized by four-branched megascleres, called triaenes, in combination with either i) star-shaped microscleres, called asters, in the suborder Astrophorina or ii) c/s-shaped microscleres, called sigmaspires, in the suborder Spirophorina. Some genera have developed hypersilicified spicules called desmas and have been traditionally grouped in the lithistids. These genera are now realocated to the tetractinellids (*Cárdenas et al., 2012*; *Schuster et al., 2015*). Both triaenes and microscleres can be secondary lost in some groups or species (*Cárdenas et al., 2011; Schuster et al., 2015*). The triaenes and asters diversified in a wide range of sizes and morphologies are occasionally found together with other microscleres such as microxeas, microrhabds, amphisanidasters, spherules or raphides. This spicular richness and heterogeneity makes the identification of tetractinellids based on spicules easier than in other demosponge groups and has attracted the attention of systematists to investigate the evolution of demosponge spicules (*Chombard et al., 1998; Cárdenas et al., 2010; Cárdenas et al., 2011; Cárdenas & Rapp, 2013; Schuster et al., 2015*). However, despite being a well-studied sponge order, several pending systematic questions remain. For instance, some groups such as Pachastrellidae, Ancorinidae or the genera *Erylus* and *Penares* are clearly polyphyletic (*Cárdenas et al., 2012*), which is often linked to the unresolved phylogenetic position of other taxa such as Calthropellidae, *Characella*, *Jaspis* and *Ecionemia*.

The Mediterranean Sea currently holds 83 species of Tetractinellida: 62 Astrophorina (including 6 lithistids), eight Spirophorina (including three lithistids) and nine Thoosina (*de Voogd et al., 2024*). Only 16 are currently recorded from the Balearic Islands, in contrast with the 26 species reported from the Alboran island, also in the Western Mediterranean (*Sitjà & Maldonado, 2014*). Indeed, taxonomic studies on sponges in the Balearic Islands are few and fragmentary compared to other areas of the Western Mediterranean (*Bibiloni & Gili, 1982; Bibiloni, 1990, 1993; Uriz et al., 1992; Díaz et al., 2019, 2020, 2021*). The first tetractinellid sponges reported from the Balearic Islands are *Penares helleri* (Schmidt, 1864) and *Penares euastrum* (Schmidt, 1868), found in Bibiloni & Gili (1982), a faunistic work on an infralittoral cave in the island of Mallorca. This work was followed by the publication of a thesis on sponge taxonomy encompassing samples from different depths, areas and biocenosis of the Islands (*Bibiloni, 1990*) which enriched the list of tetractinellids with seven new additions: *Geodia cydonium* (Linnaeus, 1767), *Stryphnus mucronatus* (Schmidt, 1868), *Pachastrella monilifera* Schmidt, 1868, *Poecillastra compressa* (Bowerbank, 1866), *Calthropella (Calthropella) pathologica* (Schmidt, 1868), *Dercitus (Stoeba) plicatus* (Schmidt, 1868) and *Jaspis johnstoni* (Schmidt, 1862). Later, *Uriz (1992)* found the species *Erylus discophorus* (Schmidt, 1862) and *Stryphnus ponderosus* (Bowerbank, 1866) at the National Park of Cabrera; *Massuti & Reñones (2005)* reported the species *Thenea muricata* (Bowerbank, 1858) on fishing grounds; *Maldonado et al. (2015)* reported *Nethea amygdaloides* (Carter, 1876) and the lithistid *Leiodermatium pfeifferae* (Carter, 1873) near the Emile Baudot seamount; *Santin et al. (2018)* reported *Craniella*

cranium (Müller, 1776) and *Neophrissospongia nolitangere* (Schmidt, 1870) from the Menorca Channel.

The Balearic Islands are a Western Mediterranean archipelago of four main islands and several islets. Its marine habitats are very heterogeneous and harbor rich and diverse biocenosis, developing in habitats like karstic caves, *Posidonia oceanica* (Linnaeus) Delile, 1813 meadows, rhodoliths and soft red algae beds, coralligenous outcrops, mud and detrital bottoms, slopes, canyons and seamounts (*Canals & Ballesteros, 1997; Acosta et al., 2003*). These ecosystems are in a context of elevated oligotrophy, as a consequence of the scarcity of rain and the absence of rivers, which reduces the terrigenous inputs and nutrient supply. These facts contribute to the singularity of some communities, and, for instance, photosynthetic biocenosis tend to develop deeper than in adjacent areas of the Iberia Peninsula (*Ballesteros, 1994*), a fact that dilates the biological range of the species found on these habitats, enhancing mesophotic zones where suspension feeders dominate (*Zabala & Ballesteros, 1989*). The diversity of the habitats coupled with the well-preserved seamounts of the Mallorca Channel, which show a high sponge diversity (*Díaz et al., 2021; Massutí et al., 2022*) suggest that a higher number of tetractinellid species should be present. The aim of this study was to improve our knowledge on the tetractinellid fauna of the Balearic Islands using an integrative approach on newly collected samples, combining morphology and molecular markers. This study also included the revision of poorly-known type material, as well as the study of some comparable species from the North Atlantic, some of which turned out to be new.

Material and Methods

Study area

The Balearic Promontory (Fig. 4.3.1) is a seafloor elevation in the Western Mediterranean, of approximately 400 km length and 105 km wide, containing the Mallorca-Menorca shelf to the east and the Ibiza-Formentera shelf to the west. The continental shelf is narrow and shallow, with a mean depth of 87 m, characterized by the presence of calcareous sediment and by the scarcity of terrigenous input. It harbors rich photophilic habitats of soft and calcareous red algae that develop until depths of 100-150 m, leading to detrital muds of the shelf border. The slopes are very steep and descend until the surrounding abyssal plains of the Valencia Trough and the Algerian Basin (*Acosta et al., 2003*). As other areas of the Western Mediterranean, most sedimentary bottoms of the continental shelf and the upper and middle slope around the Balearic Islands, between 50 and 800 m depth, have been exploited by the trawling fleet for several decades (*Farriols et al., 2017*).

Two channels are present in the Balearic Promontory, the Menorca Channel (MeC), between Menorca and Mallorca, and the Mallorca Channel (MaC), between Mallorca and Ibiza. The first channel is narrow and shallow, and it is influenced by the strong northern winds originating in the Gulf of Lion and the hydrodynamic conditions of the Balearic sub-basin, mainly shaped by Mediterranean waters and under the influence of the Balearic Current, flowing along the northern shelf edge of the Balearic Promontory (*Massutí et al., 2014*). In 2014, the MeC was included in the Natura 2000 Network, in the light of the singularity of its habitats and its high diversity of benthos (*Barberá et*

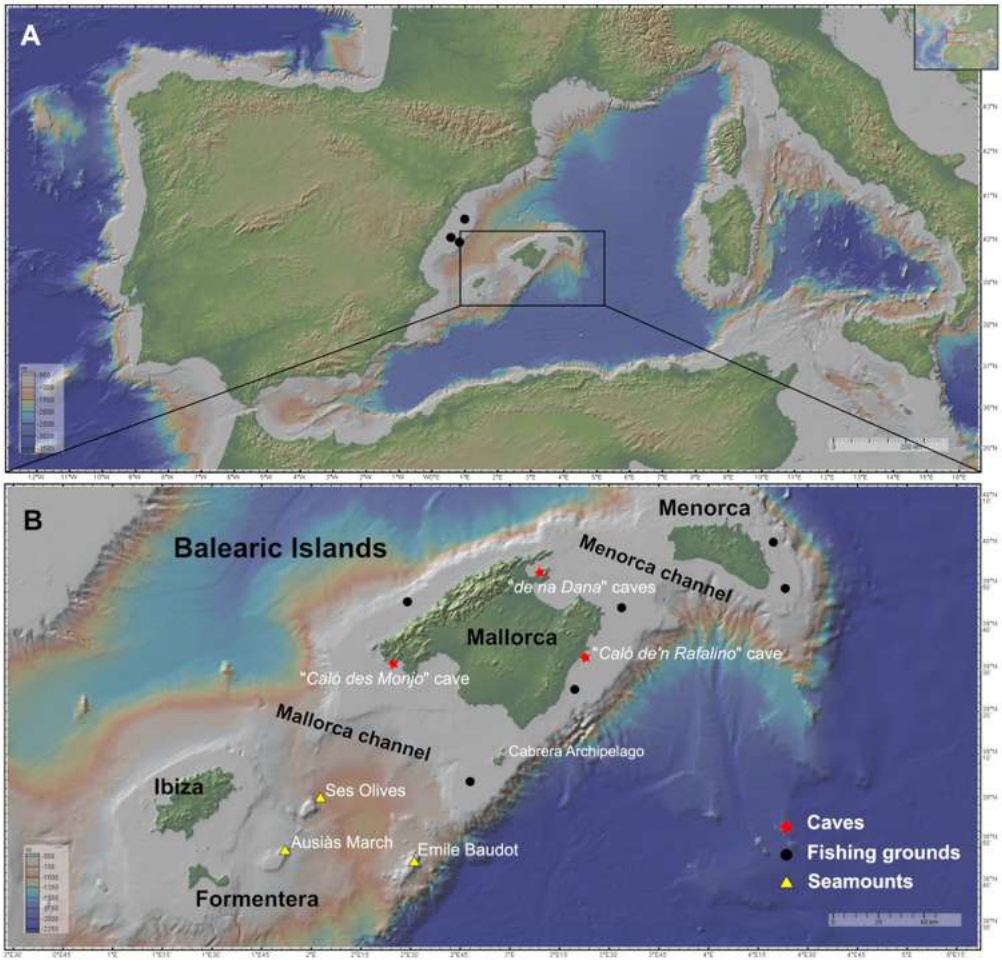

Figure 4.3.1. Maps of the studied area showing the location of the sampling stations of caves (red star), fishing grounds (black circle), and the seamounts SO, AM and Emile Baudot (yellow triangle). The characteristics of the sampling stations are shown in Table 4.3.1. (A) Map of the Western Mediterranean. Black dots show the fishing grounds sampled on the Catalan shelf (next to Columbretes islands). (B) Map of the Balearic Islands. Maps made with GeoMapApp v.3.6.15 (http://www.geomapapp.org).

al., 2012). Conversely, the MaC separating the two shelves (Mallorca-Menorca and Ibiza-Formentera) is wider, deeper and more heterogeneous than the MeC, containing not only continental shelf and slope bottoms but also abyssal plain. The MaC, being located in the Algerian sub-basin, is more influenced by the Atlantic waters (*Massutí et al., 2014*); the MaC also contains several seamounts, among which stand out Ses Olives (SO), Ausias March (AM), and Emile Baudot (EB).

SO rises from 650-900 to 250 m depth at its shallowest part; it has a flat summit composed of fine sediments. AM has a minimum depth of 86 m and a height 264 m, with a summit in the mesophotic zone, where sediments are coarser, mainly composed of gravel and sand. Finally, EB represents a strongly irregular and uneven elevation, that rises from 900 to 94 m, with numerous mounds, depressions and rocky outcrops. Both SO and AM are of tectonic origin, while EB is of volcanic origin (*Acosta et al., 2004*).

776 **Table 4.3.1.** Details of the sampling stations. BT: beam trawl, DR: rock dredge, SO: Ses Olives, Ausias March: AM, Emile Baudot: Emile Baudot.

Survey	Station	Date	Depth range	Sampling device	Latitude start	Longitude start	Latitude end	Longitude end	Area
INTEMARES_A22B_0820	11	26/08/2020	200-307	ROV	38º 46' 57.6" N	1º 46' 40.8" E	38º 46' 51" N	1º 47' 0" E	Ausias March (Mallorca Channel)
INTEMARES_A22B_0820	20	28/08/2020	523-912	ROV	38º 42' 44.4" N	2º 37' 8.4" E	38º 42' 39.6" N	2º 36' 30" E	Emile Baudot (Mallorca Channel)
INTEMARES_A22B_0820	21	28/08/2020	425-733	ROV	38º 47' 36.6" N	2º 32' 49.8" E	38º 47' 15" N	2º 32' 56.4" E	Emile Baudot (Mallorca Channel)
INTEMARES_A22B_0820	24	29/08/2020	134-150	ROV	38º 44' 27.6" N	2º 29' 16.8" E	38º 44' 34.2" N	2º 29' 32.4" E	Emile Baudot (Mallorca Channel)
INTEMARES_A22B_0820	25	29/08/2020	100-124	ROV	38º 43' 54.6" N	2º 30' 9.6" E	38º 44' 8.4" N	2º 30' 36" E	Emile Baudot (Mallorca Channel)
INTEMARES_A22_0718	68	30/07/2018	135	Rock Dredge	38º 41' 54.6" N	2º 28' 45.6" E	38º4' 0.06" N	2º28'35.4"E	Emile Baudot (Mallorca Channel)
INTEMARES_A22_0718	51	03/08/2018	127	Beam trawl	38º44’53.9’’N	2º30’41.4’’E	38º44’58.9’’N	2º30’54.7’’E	Emile Baudot (Mallorca Channel)
INTEMARES_A22_0718	52	03/08/2018	108	Rock Dredge	38º44’13.2’’N	2º30’3.6’’E	38º44’12.5’’N	2º30’12’’E	Emile Baudot (Mallorca Channel)
INTEMARES_A22_0718	60	03/08/2018	137	Beam trawl	38º43’13.1’’N	2º29’29.4’’E	38º43’5.5’’N	2º29’20.4’’E	Emile Baudot (Mallorca Channel)
INTEMARES_A22B_0720	8	21/07/2020	315-295	Rock Dredge	38º58’11.3’’N	2º0’30.6’’E	38º58’12’’N	2º0’25.2’’E	Ses Olives (Mallorca Channel)

INTEMARES_A22B_0720	18	23/07/2020	112	Beam trawl	38º45’15.5’’N	1º46’53.4’’E	38º45’16.2’’N	1º46’54.1’’E	Ausias March (Mallorca Channel)
INTEMARES_A22B_0720	19	23/07/2020	111-94	Rock Dredge	38º 43' 49.8" N	1º 45' 34.2" E	38º 43' 46.2" N	1º 45' 43.2" E	Ausias March (Mallorca Channel)
INTEMARES_A22B_0720	21	23/07/2020	105	Beam trawl	38º 44' 55.2" N	1º 50' 9.6" E	38º 45' 19.2" N	1º 50' 29.4" E	Ausias March (Mallorca Channel)
INTEMARES_A22B_0720	26	24/07/2020	127	Beam trawl	38º 26' 0.72" N	1º 26' 20.52" E	38º 26' 0.36" N	1º 26' 26.28" E	Ausias March (Mallorca Channel)
INTEMARES_A22B_0720	30	24/07/2020	265-204	Rock Dredge	38º 47' 18.6" N	1º 47' 0.6" E	38º 46' 58.2" N	1º 47' 7.8" E	Ausias March (Mallorca Channel)
INTEMARES_A22B_0720	34	25/07/2020	111-105	Rock Dredge	38º 46' 1.8" N	1º 49' 5.4" E	38º 45' 55.2" N	1º 49' 14.4" E	Ausias March (Mallorca Channel)
INTEMARES_A22B_0720	42	26/07/2020	143-139	Rock Dredge	38º 43' 32.4" N	2º 29' 16.8" E	38º 43' 37.8" N	2º 29' 6" E	Emile Baudot (Mallorca Channel)
INTEMARES_A22B_0720	43	26/07/2020	118-116	Rock Dredge	38º44’25.1’’N	2º30’40.3’’E	38º44’26.9’’N	2º30’33.5’’E	Emile Baudot (Mallorca Channel)
INTEMARES_A22B_0720	45	26/07/2020	149-151	Beam trawl	38º42’51.8’’N	2º30’13.7’’E	38º42’28.1’’N	2º29’24’’E	Emile Baudot (Mallorca Channel)
INTEMARES_A22B_0720	52	27/07/2020	297	Beam trawl	38º45’47.5’’N	2º31’0.5’’E	38º45’56.9’’N	2º30’37.1’’E	Emile Baudot (Mallorca Channel)
INTEMARES_A22B_0720	53	27/07/2020	108-102	Rock Dredge	38º 44' 0.6" N	2º 30' 43.2" E	38º 44' 8.4" N	2º 30' 24.6" E	Emile Baudot (Mallorca Channel)
INTEMARES_A22B_0720	54	27/07/2020	207-124	Rock Dredge	38º 43' 19.8" N	2º 30' 54" E	38º 43' 31.2" N	2º 30' 43.8" E	Emile Baudot (Mallorca Channel)

INTEMARES_A22B_0720	59	28/07/2020	526-550	Rock Dredge	38º 26' 3.96" N	2º 26' 25.56" E	38º 26' 3.12" N	2º 26' 29.16" E	Emile Baudot (Mallorca Channel)
INTEMARES_A22B_1019	3	11/10/2019	293-255	Rock Dredge	38º 58' 41.4" N	1º 59' 13.2" E	38º 58' 33" N	1º 59' 13.2" E	Ses Olives (Mallorca Channel)
INTEMARES_A22B_1019	8	11/10/2019	241	Rock Dredge	38º 57' 35.4" N	2º 79' 54.6" E	38º 57' 42" N	2º 97' 44.4" E	Ses Olives (Mallorca Channel)
INTEMARES_A22B_1019	36	13/10/2019	609	Beam trawl	38º 57' 51" N	1º 56' 34.2" E	38º 57' 59.4" N	1º 56' 40.2" E	Ses Olives (Mallorca Channel)
INTEMARES_A22B_1019	48	15/10/2019	124	Beam trawl	38º 43' 30.6" N	1º 49' 41.4" E	38º 43' 39" N	1º 49' 51" E	Ausias March (Mallorca Channel)
INTEMARES_A22B_1019	50	15/10/2019	98	Beam trawl	38º43’33.6’’N	1º48’12.6’’E	38º43’34.7’’N	1º48’23.4’’E	Ausias March (Mallorca Channel)
INTEMARES_A22B_1019	58	15/10/2019	135	Beam trawl	38º 46' 55.2" N	1º 52' 16.8" E	38º 47' 5.4" N	1º 52' 19.8" E	Ausias March (Mallorca Channel)
INTEMARES_A22B_1019	103	21/10/2019	231-302	Rock Dredge	38º47.4’0’’N	1º47.2’0’’E	38º47.3’’0’’N	1º47.2’0’’E	Ausias March (Mallorca Channel)
INTEMARES_A22B_1019	124	24/10/2019	145-147	Beam trawl	38º45’19.1’’N	2º31’0.5’’E	38º45’20.9’’N	2º31’8.4’’E	Emile Baudot (Mallorca Channel)
INTEMARES_A22B_1019	136	25/10/2019	141-145	Beam trawl	38º44’42.7’’N	2º29’25.8’’E	38º43’13.1’’N	2º29’21.5’’E	Emile Baudot (Mallorca Channel)
INTEMARES_A22B_1019	158	27/10/2019	141-145	Beam trawl	38º 42' 57.6" N	2º 29' 17.4" E	38º 42' 55.8" N	2º 29' 6" E	Emile Baudot (Mallorca Channel)
INTEMARES_A22B_1019	167	28/10/2019	147	Beam trawl	38º42’21.6’’N	2º29’37.3’’E	38º42’12.6’’N	2º29’29.4’’E	Emile Baudot (Mallorca Channel)

INTEMARES_A22B_1019	165	28/10/2019	312	Rock Dredge	38º 46' 58.2" N	2º 31' 6" E	38º 46' 52.8" N	2º 31' 7.8" E	Emile Baudot (Mallorca Channel)
INTEMARES_A22B_1019	177	29/10/2019	150	Beam trawl	38º43’57.7’’N	2º28’54.1’’E	38º43’47’’N	2º28’53.4’’E	Emile Baudot (Mallorca Channel)
MEDITS_ES05_16	181	08/06/2016	142	GOC73	39º 1’ 9.48’’ N	2º 51’ 1.8’’ E	39º 2’ 15.72’’ N	2º 49’ 44.4’’ E	Fishing ground (Cabrera Archipelago)
MEDITS_ES05_17	194	12/06/2017	148	GOC73	39º 46’ 25.68’’N	2º 27’ 59.22’’E	39º 46’ 25.41’’N	2º 27’ 59.33’’E	Fishing ground (Sóller)
MEDITS_ES05_17	206	15/06/2017	134	GOC73	39º47’37.2’’N	4º26’15.4’’E	39º47’37.2’’N	4º26’15.4’’E	Fishing grounds (Maó)
MEDITS_ES05_19	184	14/06/2019	50	GOC73	39º 27' 0" N	3º 20' 15.6" E	39º 27' 0.42" N	3º 21' 6.6" E	Fishing ground (Portocolom)
MEDITS_ES05_20	74	16/06/2020	72	GOC73	40º 0' 30.6" N	4º 18' 54.6" E	40º 0' 0.6" N	4º 18' 13.8" E	Fishing ground (Maó)
MEDITS_ES05_20	76	16/06/2020	132	GOC73	39º 47' 52.2" N	4º 26' 22.8" E	39º 46' 36.6" N	4º 25' 22.8" E	Fishing ground (Maó)
MEDITS_ES05_21	212	17/06/2021	63	GOC73	39º 44' 52.2" N	3º 35' 20.4" E	39º 4' 0" N	3º 34' 33.6" E	Fishing ground (Menorca channel)
MEDITS0521_PITIUSSES	2	18/08/2021	54	GOC73	38º 35’ 15.72’’N	1º 26’ 35.52’’ E	38º 35’ 45.6’’N	1º 27’ 40.32’’E	Fishing ground (South of Formentera)
MEDITS_ES06N_20	3	30/05/2020	74	GOC73	40º 01' 57.6" N	0º 34' 9.6" E	40º 0' 40.8" N	0º 33' 18.6" E	Fishing ground (Columbrets)
MEDITS_ES06N_20	6	31/05/2020	144	GOC73	39º 53' 31.2" N	0º 53' 9" E	39º 54' 38.4" N	0º 54' 34.8" E	Fishing ground (Columbrets)

MEDITS_ES06N_20	14	01/06/2020	96	GOC73	40º 18' 39" N	1º 7' 28.2" E	40º 1' 0.12" N	1º 6' 37.8" E	Fishing ground (Sant Carles de la Ràpita)
MEDITS_ES05_17	219	18/06/2017	65	GOC73	39º 51' 4.2" N	4º 05' 37.8" E	39º 50' 24" N	4º 06' 45" E	Fishing ground (Son Bou)
LITORAL CAVES	-	06/05/2020	0-0.5	Scuba diving	39°33' 23.49''N	3°22´7.35" E	39°33' 23.49"N	3°22´7.35" E	Cova de Sa Figuera (Manacor)
LITORAL CAVES	-	23/05/2020	0-0.5	Scuba diving	39°33' 20.9''N	3°22´2.39'' E	39°33' 20.9"N	3°22´2.39" E	Cova Caló den Rafalino (Manacor)
LITORAL CAVES	-	17/01/2021	3-4	Scuba diving	39°23' 31.12''N	3°14´58.07'' E	39°23' 31.12"N	3°14´58.07" E	Cova cala Sa Nau (Felanitx)
LITORAL CAVES	-	06/05/2021	6	Scuba diving	39°31' 39.38''N	2°25´50.63" E	39°31' 39.38"N	2°25´50.63" E	Cova Caló des Monjo (Calvià)
LITORAL CAVES	-	14/08/2021	0-0.5	Scuba diving	39°52' 19.86''N	3°9´8.50"E	39°52' 19.86"N	3°9´8.50" E	Coves De Na Dana (Alcúdia)

777

Patches of bio-constructions have been found in the summits of AM and EB, where rhodolith beds and coralligenous outcrops predominate, while rocky bottoms predominate in the flanks of SO, AM and EB, mainly colonized by filtering species, such as sponges and corals. According to these authors, in the less steep flanks and bathyal terraces of the upper and middle slope of these seamounts, muddy soft sediments are found, accumulating facies of the brachiopod *Gryphus vitreus* (Born, 1778), burrowing megafauna, small sponges and/or dead coral debris. The deepest areas of the middle slope at the base of seamounts are dominated by the finest muddy sediments and the presence of pockmarks fields (*Massutí et al., 2022*).

Sampling

Specimens were collected during i) seven MEDITS research surveys on board the R/V *Miguel Oliver*, carried out annually from 2016 to 2021 on fishing grounds of the Balearic Islands shelf and slopes, between 50 and 800 m depth; ii) one MEDITS survey carried out in 2020 on board the R/V *Miguel Oliver* along the northeastern Iberian Peninsula within the same bathymetric range; and iii) four research surveys carried out on board R/V *Ángeles Alvariño* and R/V *Sarmiento de Gamboa*, within the framework of the LIFE IP INTEMARES project at the SO, AM and EB seamounts of the MaC, in August 2018, October 2019 and July-August 2020 (Fig. 4.3.1A-B). The MEDITS program is carried out in most of the northern coast of the Mediterranean and aims to assess the state of the demersal resources and nekton-benthic ecosystems (*Spedicato et al., 2019*). The objective of the LIFE IP INTEMARES project at the MaC is to improve the scientific knowledge on biodiversity, benthic habitats and human activities, to include SO, AM and EB seamounts in the Natura 2000 network (*Massutí et al., 2022*). Several sampling devices were used in mesophotic and bathyal bottoms for both MEDITS and INTEMARES surveys: the experimental bottom trawl gear GOC-73 *(Bertrand et al., 2002; Spedicato et al., 2019*), a Beam Trawl (BT), Rock Dredges (RD) and the Remote Operated Vehicle (ROV) *Liropus 2000* which was also used to film underwater. Screenshots of the film were used to study the in situ morphology of the specimens (Fig. 4.3.2).

Shallow water caves were explored by scuba diving or free apnea in May and November 2020 and in January, May and August 2021. Most of them can be classified as littoral marine caves created by sea erosion. They have salty water and marine fauna, being shallow (0-10 m depth) and located eastern (“Cova de sa Figuera”, “Cova de ca’n Rafalino”, “Cova de Cala Sa Nau”), northern (“Coves de Na Dana”), and western (“Cova Caló des Monjo”) off Mallorca island (Fig. 4.3.1B). Their sizes are quite variable, “Cova de Cala Sa Nau” being the largest and the most important in terms of benthic organisms, with a spacious entrance and a main chamber having 76/36/8 m in maximum length/width/depth (*Gràcia et al., 1998*). This cave is commonly frequented by scuba divers, especially in summertime, potentially having a negative impact on the sponge community. In contrast, the “Cova de ca’n Rafalino” is the smallest, being a short tunnel only several meters long, with a depth of 1-2 m and between 0.5 and 3 m wide. Inland freshwater infiltration has been observed in “Cova de ca’n Rafalino” and “Coves de na Dana”. Due to the cave architecture, benthic organisms inhabiting the caves are relatively well protected from the action of waves. Details of sampling stations are

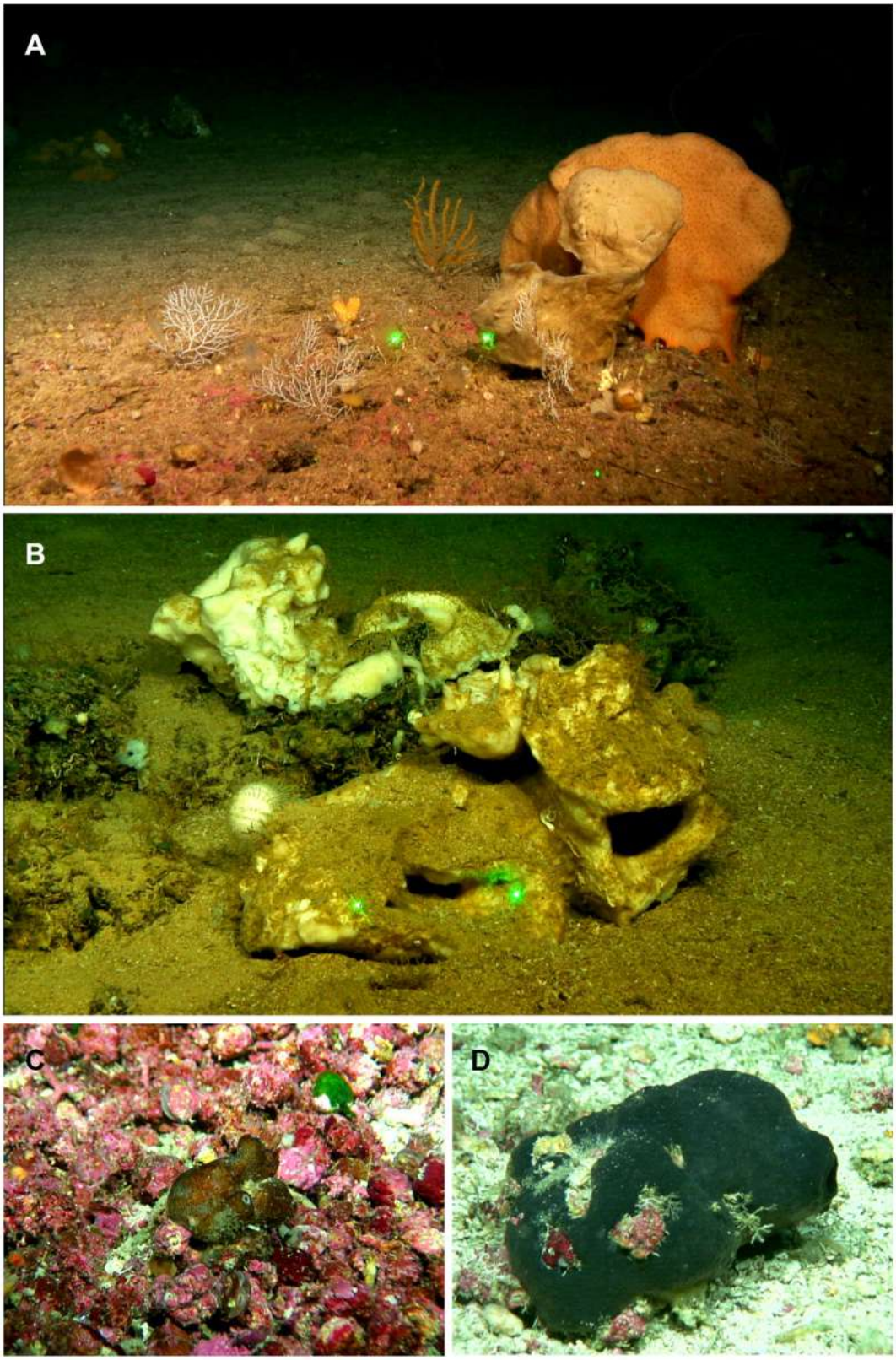

Figure 2. Remote Operated Vehicle (ROV) images of the tetractinellid fauna from the seamounts of the Mallorca Channel, Ses Olives (SO), Ausias March (AM) and Emile Baudot (EB). (A) *Poecillastra compressa* (orange) specimen at 149 m depth in EB. (B) *Pachastrella ovisternata* specimen field #i808 collected at 263 m depth in the AM. (C) *Penares euastrum* (dark gray) at 90 m depth in the AM summit. (D) *Stryphnus mucronatus* specimen i827_1 collected at 100 m depth at the EB summit.

summarized in Table 4.3.1. In situ images of the specimens were taken with an Olympus Tg5 digital camera (Fig. 3).

For oceanographic surveys, once the sampling gear was on board, sponges were separated from the rest of the catch and photographed, then macroscopic characters like morphology, color and texture were annotated prior to sample fixation. Samples for both morphological and molecular analysis were preserved in absolute ethanol (EtOH).

Specimens from this study were all deposited in the zoological collection at the Museum of Evolution, Uppsala University (Uppsala, Sweden) with UPSZMC# for non-type specimens and UPSZTY# for type material (Table S4.3.1), under Material Transfer Agreement 2023:074. Two exceptions: the holotype of *Geodia phlegraeioides* **sp. nov.** was deposited at the MNCN in Madrid (Spain), and the holotype of *Caminus xavierae* **sp. nov.** was already deposited at Naturalis in Leiden (The Netherlands). DNA extractions from the Balearic islands new species were deposited at the Museum of Evolution (holotypes) and at the Balearic Biodiversity Center (https://centrebaleardebiodiversitat.uib.eu/; paratypes), with same deposit numbers as the UPSZTY museum numbers.

The electronic version of this article in Portable Document Format (PDF) will represent a published work according to the International Commission on Zoological Nomenclature (ICZN), and hence the new names contained in the electronic version are effectively published under that Code from the electronic edition alone. This published work and the nomenclatural acts it contains have been registered in ZooBank, the online registration system for the ICZN. The ZooBank LSIDs (Life Science Identifiers) can be resolved and the associated information viewed through any standard web browser by appending the LSID to the prefix http://zoobank.org/. The LSID for this publication is: [urn:lsid:zoobank.org:pub:A88AE49E-B422-4F9A-A5E0-BB6C6B8FC185]. The online version of this work is archived and available from the following digital repositories: PeerJ, PubMed Central SCIE and CLOCKSS.

Morphological descriptions

To obtain dissociated spicules preparations, a fragment of tissue was digested with bleach, the remaining spicules washed with pure water first, then with 50% EtOH and finally with 96% EtOH. Spicules were observed and measured with an optical microscope. For each sample, unless otherwise indicated, 25 spicules per spicule category were counted. Spicule measurements given in the text are always the range observed from all measured specimens, unless otherwise stated. Handmade thick sections with a scalpel were made to study the skeleton oganization of every species. For precious type material, such as the *Schmidt (1868)* collection, regular thick sections (100–800 µm) were made by embedding small pieces of the specimens using an Agar Low Viscosity Resin kit (Agar Scientific). Embedded pieces were sectioned with a diamond wafering blade on a Buehler IsoMet™ Low Speed cutting machine. For SEM images, aliquots of suspended spicules were transferred onto aluminum foil, air dried, sputter coated with gold and observed under a HITACHI S-3400N scanning electron microscope (SEM) at the *Serveis Científico-tècnics* of the University of the Balearic Islands (UIB). The terminology applied for the morphological description of the spicules follows *Boury-Esnault & Rützler (1997)* and *Hooper & Van Soest (2002)*.

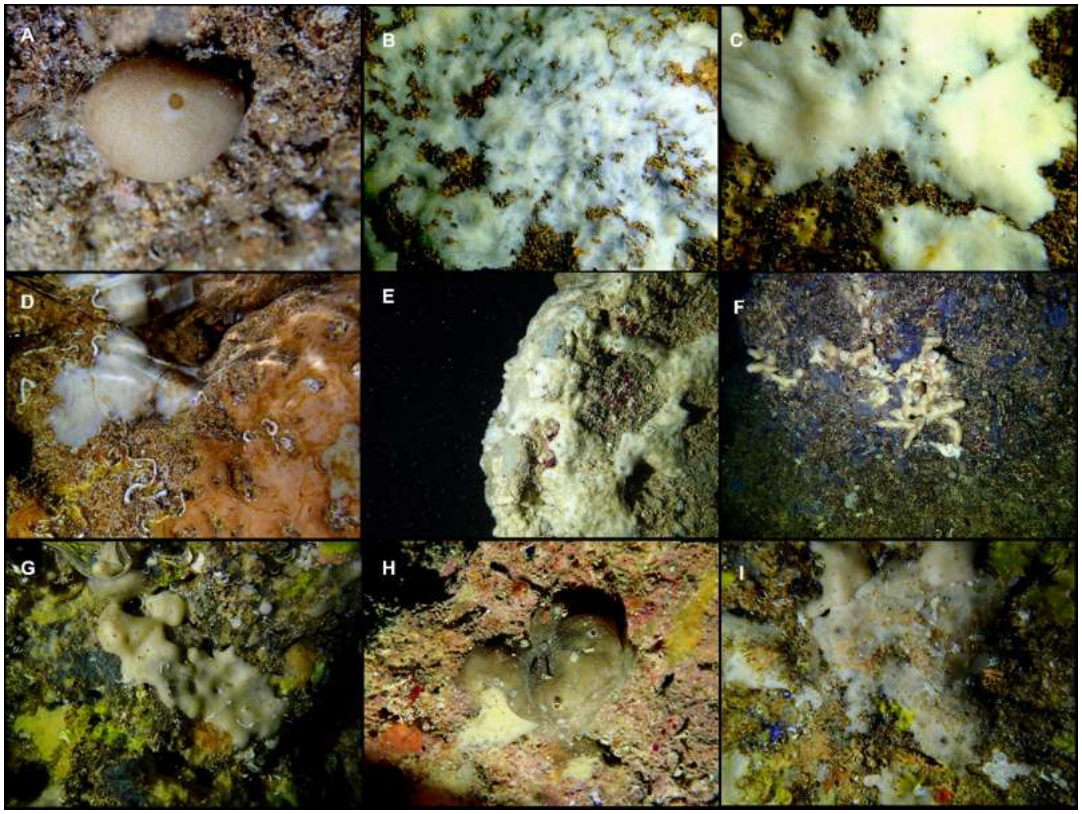

Figure 3. Tetractinellids from Mallorca caves. (A) *Caminella intuta* (specimen LIT05) in ‘‘Sa cova de sa Figuera’’ cave, 0–0.5 m. (B–C) *Erylus discophorus* specimens LIT72 and LIT71 collected at 0–1 m at ‘‘Coves de na Dana’’ caves. (D) *Erylus* cf. *deficiens* (white), specimen LIT10 collected at 0–0.5 m at ‘‘Cova des Caló den Rafalino’’ cave. (E) Community dominated by *Penares bibilonae* **sp. nov.** and *Penares cavernensis* **sp. nov.** (uncollected specimens) at 4–5 m at ‘‘Cala sa Nau’’ cave. (F) *Penares cavernensis* **sp. nov.** (uncollected specimen) at 4–5 m depth, at ‘‘Cala sa Nau’’ cave. (G) *Penares cavernensis* **sp. nov.** (paratype) LIT65, col-lected at 6 m depth at ‘‘es Caló des Monjo’’ cave. (H) *Penares cavernensis* **sp. nov.** (paratype) LIT45, col-lected at 3–4 m ‘‘Cala sa Nau’’ cave. (I) *Penares isabellae* **sp. nov.** (paratype) LIT66 collected at 6 m depth at ‘‘es Caló des Monjo’’ cave.

Molecular analysis

DNA was extracted from a piece of choanosomal tissue (~2 cm^3) using the DNeasy Blood and Tissue Extraction kit (QIAGEN). Polymerase chain reaction (PCR) was used to amplify the Folmer fragment (658 bp) of the mitochondrial cytochrome c oxidase subunit I (COI) and the C1-C2 (~369 bp) or C1-D2 (~800 bp.) fragments of the nuclear rDNA 28S gene.

For COI, the universal Folmer primers LCO1490/HCO2198 were used (*Folmer et al., 1994*), except for the *Craniella* species for which we used primers LCO1490/COX1R1 (Rot et al., 2006); this primer set amplifies a longer fragment ca. 1180 bp (Folmer + Erpenbeck fragments). When LCO1490/HCO2198 failed to amplify COI (especially for some *Erylus* and *Penares* species), the primers LCO/TetractminibarR1 were used to amplify the first 130 bp of the Folmer marker, also called the Folmer COI minibarcode (*Cárdenas & Moore, 2019*). The primers jgHCO (*Geller et al., 2013*) and ErylusCOIF2 (5’-CTCCYGGATCAATGTTGGG-3’) were then used to amplify the rest of the Folmer fragment (*Cárdenas et al., 2018*). For 28S, the primer set C1’ASTR/D2 (*Vân Le et al.,*

1993; Cárdenas et al., 2011) was used to get the C1-D2 domains. When the C1'ASTR/D2 primers failed to amplify 28S, we used the primers C1'/Ep3 to get the shorter C1-C2 fragment. PCR was performed in 50 µl volume reaction (34.4 µl ddH20, 5 µl Mangobuffer, 2 µl DNTPs, 3.5 $MgCl_2$, 1 µl of each primer, 1 µl BSA, 0.1 µl TAQ and 2 µl DNA). PCR thermal profile used for amplification was [94°C / 5 min; 37 cycles (94°C / 15 s, 46°C / 15 s, 72°C / 15 s); 72°C / 7 min]. PCR products were visualized with 1% agarose gel and purified using the QIAquickR PCR Purification Kit (QIAGEN) and sequenced at Macrogen Inc. (South Korea).

Sequences were imported into BioEdit 7.0.5.2. (*Hall, 1999*) and checked for quality and accuracy with nucleotide base assignment. Sequences were aligned using Mafft (*Katoh et al., 2002*). The resulting sequences were deposited in GenBank (http://www.ncbi.nlm.nih.gov/genbank/) with the following accession numbers: ON130519-ON130569, OR045842-OR045844 and OR045913-OR045914 for COI and ON133879-ON133850 and OR044718 for 28S (Table S4.3.2). Eight COI minibarcodes (111-130 bp), too small to be submitted to GenBank, were deposited on the Sponge Barcoding Project instead (https://www.spongebarcoding.org) with sequence numbers 2683 to 2690. The final COI and 28S alignment fasta files were deposited as *Data S1*.

Phylogenetic analysis were conducted using two different approaches: Bayesian Inference (BI) and Maximum likelihood (ML), performed with the CIPRES science gateway platform (http://www.phylo.org; *Miller et al., 2010*) using MrBayes version 3.6.2 (*Ronquist et al., 2012*) and RAxML (*Stamatakis, 2014*). For MrBayes, we conducted four independent Markov chain Monte Carlo runs of four chains each, with 5 million generations, sampling every 1000th tree and discarding the first 25% as burn-in, while RAxML was performed under the GTRCAT model with 1000 bootstrap iterations. Convergence was assessed by effective sample size (ESS) calculation and was visualized using TRACER version 1.5. Genetic distance (p-distance) and number of base differences between pairs of DNA sequences were estimated with MEGA version 10.0.5 software (*Kumar et al., 2018*).

Comparative material and abbreviations

To help with our specimen identifications and descriptions, comparative material was used from the following institutions, for which we provide their abbreviations: BELUM Mc, Ulster Museum Belfast (Northern Ireland, UK); CEAB.POR.BIO, Porifera Collection at the 'Centro de Estudios Avanzados de Blanes' (Blanes, Spain); COLETA, 'Coleção de Referência Biológica Marinha dos Açores', reference collection of the Department of Oceanography and Fisheries, University of the Azores (Portugal); CPORCANT, Colección PORíferos del CANTábrico, IEO-CSIC (Gijón, Spain); HBOI, Harbor Branch Oceanographic Institute, Florida Atlantic University (Fort Pierce, FL, USA); MNCN, Museo Nacional de Ciencias Naturales (Madrid, Spain); MNHN, Muséum National d'Histoire Naturelle (Paris, France); MSNG, Museo Civico di Storia Naturale "G. Doria" (Genoa, Italy); NHM, Natural History Museum (London, UK); PC, personal collection of P. Cárdenas, Uppsala University (Sweden); RMNH, Rijksmuseum van Natuurlijke Historie, Naturalis Biodiversity Center (Leiden, The Netherlands); SME, Station Marine d'Endoume (Marseille, France); UPSZMC/UPSZTY, zoological collection at the Museum of Evolution (Uppsala,

Sweden); ZMBN, zoological collection at the Bergen Museum (Bergen, Norway); ZMUC, Zoological Museum, University of Copenhagen (Denmark).

Type material from different museums were revised or re-examined for comparison with our specimens, especially from the natural history museums collections in London (UK), Paris (France) and Genoa (Italy). Notably, tetractinellids described by *Schmidt (1868)* from Algeria, currently stored at the MNHN Paris, were all examined. This historical collection gathers samples from the French 'Exploration Scientifique de l'Algérie' in 1842 and those collected by French zoologist Henri Lacaze-Duthiers in La Calle (El Kala) in 1860-1862, while he was studying the red coral.

Results

In total, we have analyzed 174 samples, belonging to nine families, 17 genera and 36 species of tetractinellids. For a given specimen, different field codes were provided depending on the collection survey. Author field collection numbers follows the nomenclature "Lit###" for cave samples collected with free apnea or scuba diving, "POR###" for samples collected during the MEDITS surveys and "i###" for samples collected during INTEMARES surveys. Spicule measurements given in the text are always the range observed from several specimens, unless otherwise stated. Spicule measurements for specific specimens can be found in the Tables dedicated to the different species. Two large phylogenetic trees have been obtained with COI and 28S markers (Fig. S1 and Fig. S2) and subparts of these trees will be presented next to the descriptions of the species. Taxonomic authority of new species is restricted to Díaz & Cárdenas.

Systematics

Class Demospongiae Sollas, 1885

Subclass Heteroscleromorpha Cárdenas, Pérez & Boury-Esnault, 2012

Order Tetractinellida Marshal, 1876

Suborder Astrophorina Sollas, 1887

Family Ancorinidae Schmidt, 1870

Genus *Stelletta* Schmidt, 1862

Stelletta dichoclada Pulitzer-Finali, 1983

(Figs. 4.3.4-6; Table 4.3.2)

Material examined

UPSZMC 190946, field#i416_A, MaC (EB), St. 177 (INTEMARES1019), 151 m, beam trawl, coll. J. A. Díaz; UPSZMC 190944, field#i589_1, MaC (AM), St. 21, (INTEMARES0720), 112 m, beam trawl, coll. J. A. Díaz; UPSZMC 190945, field#i715_2, MaC (EB), St. 45, (INTEMARES0720), 147 m, beam trawl, coll. J. A. Díaz.

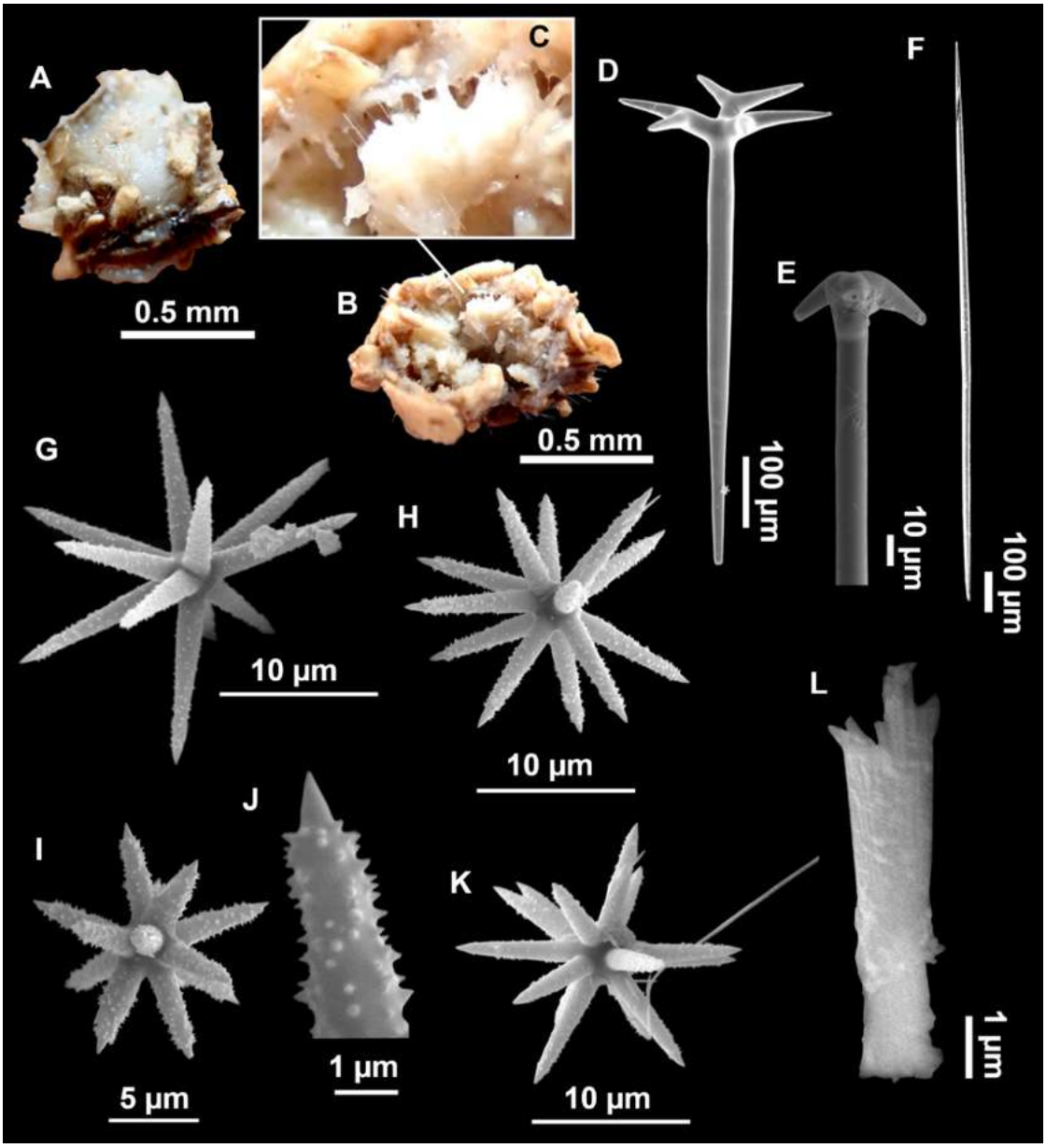

Figure 4. *Stelletta dichoclada* (*Pulitzer-Finali, 1983*), specimens from the Balearic Islands. (A) Habitus of field i715_2 on deck. (B) Habitus of field i589_1 after fixation, with (C) detail of the cortex. (D–L) SEM images of spicules from field i589_1. (D) Dichotriaene. (E) Detail of the head of an anatriaene. (F) Oxea. (G–K) Oxyasters. (L) Raphides in trichodragmata.

Comparative material

Stelletta dichoclada, holotype, MSNG 47152, NIS.83.34a, off Calvi (Corsica) 123-147 m, detrital bottom, July 1969, dredge (Fig. 4.3.5).

Stelletta lactea Carter, 1871, UPSZMC 190949, Strangford Lough (Northern Ireland), 0 m, October 2021, collected by hand at low tide, coll. C. Morrow, id. C. Morrow.

Outer morphology (Fig. 4.3.4A-C and Fig. 4.3.5A)

Small subspherical, up to 1 cm in diameter, completely encrusted by calcareous sediment (Fig. 4.3.4A-C), cortex and choanosome grayish in life and in EtOH. Sponges are

995 **Table 4.3.2.** Spicule measurements of *Stelletta dichoclada* and *Stelletta lactea*. Measurements are given as minimum-mean-maximum for total
996 length/minimum-mean-maximum for total width. All measurements are expressed in µm. Specimens here measured are in bold. Balearic specimen
997 codes are the field#. Rh: rhabdome; pc: protoclad; dc: deuteroclad; -:not found/not reported. EB: Emile Baudot; AM: Ausias March; SO: Ses Olives.

Material	**Depth** (m)	**Oxeas** (length/width)	**Anatriaene** Rhabdome (length/width) Clad (length/width)	**Plagiotriaenes** Rhabdome (length/width) Clad (length/width)	**Dichotriaenes** Rhabdome (length/width) Protoclad (length/width) Deuteroclad (length/width)	**Oxyasters** (length)	**Trichodragma** (length/width)
S. dichoclada **holotype** **MSNG 47152** **Corsica**	123-147	1134-1463-2555/13-19-32	-	Rh: 167-391/6-15 (N=2) Cl: 34-56/6-14 (N=2)	Rh: 305-854-1130/12-40-52 (N=23) Pt: 33-55-71/12-33-43 Dt: 17-114-181/6-24-33	10-16-28	21-28-38/ 6-8-13 (N=13)
S. dichoclada **i416_A** **EB**	151	829-1863-3100/ 9-16-25 (N=19)	-	Rh: 297-410-529/10-13-19 (N=8) Cld: 26-59-85/9-11-15 (N=8)	Rh: 585-1059-1398/20-32-45 (N=25) Pt: 40-62-102/20-27-33 (N=25) Dt: 27-88-123/15-20-31 (N=25)	7-13-25 (N=100)	22-27-34/ 4-7-12 (N=36)
S. dichoclada **i589_1** **AM**	110	839-1602-2520/ 7-16-24 (N=21)	Rh: 1659-1841/8-11 (N=2) Cld: 15-23/6-9 (N=2)	Rh: 412/17 Cld: 69/16 (N=1)	Rh: 383-741-982/16-27-36 (N=20) Pt: 41-57-77/15-23-33 Dt: 14-70-109/6-16-24 (N=20)	7-13-24 (N=63)	19-29-34/ 6-9-10 (N=18)
S. dichoclada **i715_2** **EB**	150	1130-1762-2067/8-20-30 (N=14)	Rh: 2799 (N=1)/9-14 (N=3) Cld: 33-38-41/9-10 (N=4)	Rh: 276-650/10-18 (N=4) Cld: 45-96/8-16 (N=4)	Rh: 540-1170-1515/18-34-44 (N=7) Pt: 39-74-101/16-30-36 (N=7) Dt: 32-84-117/11-21-28 (N=7)	9-16-31 (N=58)	18-25-32/ 6-9-18 (N=20)
S. lactea **UPSZMC 190949** **N. Ireland**	0	480-817-1361/ 6-19-42 (N=16)	-	Rh: 286-421-686/10-16-29 Cl: 58-94-181/10-15-26 (N=19)	Rh: 262-477-725/11-19-26 (N=5) Pt: 30-61-109/12-17-25 Dt: 22-35-62/8-13-18 (N=6)	6-10-13	28-36-45/ 6-12-19 (N=8)
S. lactea Holotype Devon (North Atlantic) (*Sollas, 1888*)	Littoral	1250/ -	-	Rh: 825/- Cl: -	Rh: 825/- Cl:-/-	12.5	25/ -
S. lactea Ionian Sea (*Pulitzer-Finalli, 1983*)	2-3	630-850/ -	-	Rh: 350-550/- Cl: 350/- (reduced clads and rhabdome)	Very rare	5-11 (spherasters to oxyasters)	25/ -

998

slightly compressible, hispid to the naked eye. Cortex patent (Fig. 4.3.4C), about 1 mm in width.

Spicules (Fig. 4.3.4D-L Table 4.3.2)

Plagiotriaenes (as the ones observed in the holotype: Fig. 4.3.5C) small, fusiform, slightly curved rhabdome, with a slight swelling just below the cladome. Clads are pointed upwards. Rhabdome: 167-650 x 6-19 µm, clads: 26-96x6-16 µm. Plagiotriaenes are very scarce, and may represent immature stages of the dichotriaenes because it is common to find small and incipient bifurcated clads in the plagiotriaenes; also, the dichotriaenes are always larger.

Dichotriaenes (Fig. 4.3.4D), rhabdome robust, straight or slightly curved, fusiform. The short-sized dichotriaenes have protoclads longer or the same length as deuteroclads while in large-sized dichotriaenes, protoclads are shorter than deuteroclads. Occasionally, 1-2 clads may not be bifurcated. Rhabdome: 305-1515/12-52 µm, protoclad 33-102/12-43 µm and deuteroclad 14-181/6-33 µm.

Anatriaenes (Fig. 4.3.4E), very scarce, most are broken, with slightly curved rhabds. Rhabdome: 1659-2799/8-14 µm, cladi 14-41/6-10 µm.

Oxea (Fig. 4.3.4F), thin, slightly curved, and fusiform, 829-3100/7-32 µm.

Oxyasters (Fig. 4.3.4G-K), spherical, with short centrum and large actines, spiny along the whole actine with a clear pointy end. Only one size category, 7-31 µm in diameter.

Raphides in trichodragma (Fig. 4.3.4L), trichodragma length/width: 18-38/4-18 µm.

Ecology notes

Always found on sedimentary bottoms with sand and gravels, at mesophotic depths between 112 m and 151 m.

Genetics

We have sequenced the Folmer fragment in two pieces for specimens i589_1 and i715_2 (ON130566 and ON130567) and 28S (C1-D2) for all three specimens (ON133865, ON133864 and ON133866). The Folmer fragments of i589_1 (AM Seamount) and i715_2 (EB Seamount) have 1 bp difference. The 28S (C1-D2) of i589_1 (AM) and i416_A/#i715_2 (EB) have 1 bp. difference.

Remarks

Specimens were found on the EB and AM Seamounts at 112-151 m. This is the second record of *S. dichoclada* in the literature since its original description by *Pulitzer-Finali (1983)* from a specimen collected off Corsica at similar depths (123-147 m). The holotype is a small hemispherical sponge (Fig. 4.3.5A), 0.7 cm in diameter x 0.7 cm in height; openings not visible. Cortex is conspicuous, about 1 mm in width, beige in color, crusty to the touch, resilient, and incorporates sediment. Choanosome dirty orange, softer than the cortex (fleshier). Spicules of the holotype have been re-measured (Table 4.3.2) and examined with SEM (Fig. 4.3.5B-H). Our material differed from the holotype by the presence of a few anatriaenes in specimens i589_1 and i715_2, but not

in the holotype, nor i416_A. However, anatriaenes were very uncommon, which may explain

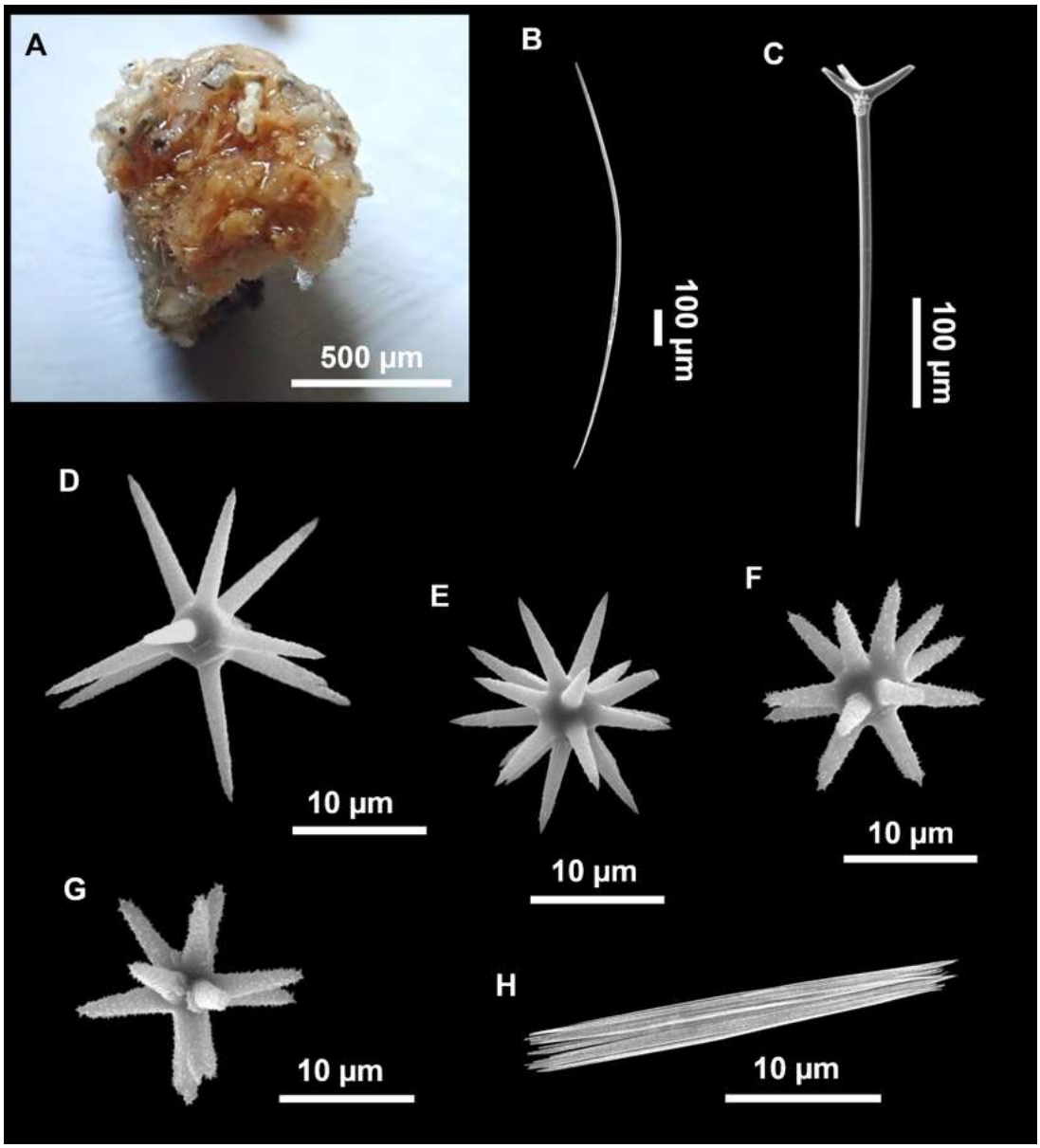

Figure 4.3.5. Holotype of *Stelletta dichoclada* MSNG 47152 (Pulitzer-Finali, 1983), from Corsica. (B) Oxea. (C) Plagiotriaene. (D–G) Oxyasters to strongylasters. (H) Raphides in trichodragmata.

their absence in the holotype and i416_A slides. Importantly, trichodragmas were not mentioned in the original description but they are definitely present in the holotype and our specimens (Fig. 4.3.4 and Fig. 4.3.5). To ensure that those are not foreign material, we have made digestions from two different parts of the holotype body: both contained trichodragmas. The holotype contains several foreign spicules, notably microtriods to microcalthrops with annulated rugose surface, identical to those described in the same work for *Annulastrella verrucolosa* (Pulitzer-Finali, 1983), collected at the same station. Also, there are foreign spirasters similar to those from the order Clionaida Grant, 1826.

We have not tried to amplify the DNA from the holotype because it had been conserved in formalin. Surprisingly, in the Balearic specimens we detected two haplotypes for both

markers, each time with 1 bp difference. One haplotype corresponded to i589_1, collected at the AM, while the other haplotype was shared with i416_A and i715_2, from the EB. This may suggest that each seamount harbors isolated populations, or perhaps that *S. dichoclada* represents a species complex with two cryptic species. This should be assessed in further studies, by using more variable markers and sequencing more individuals.

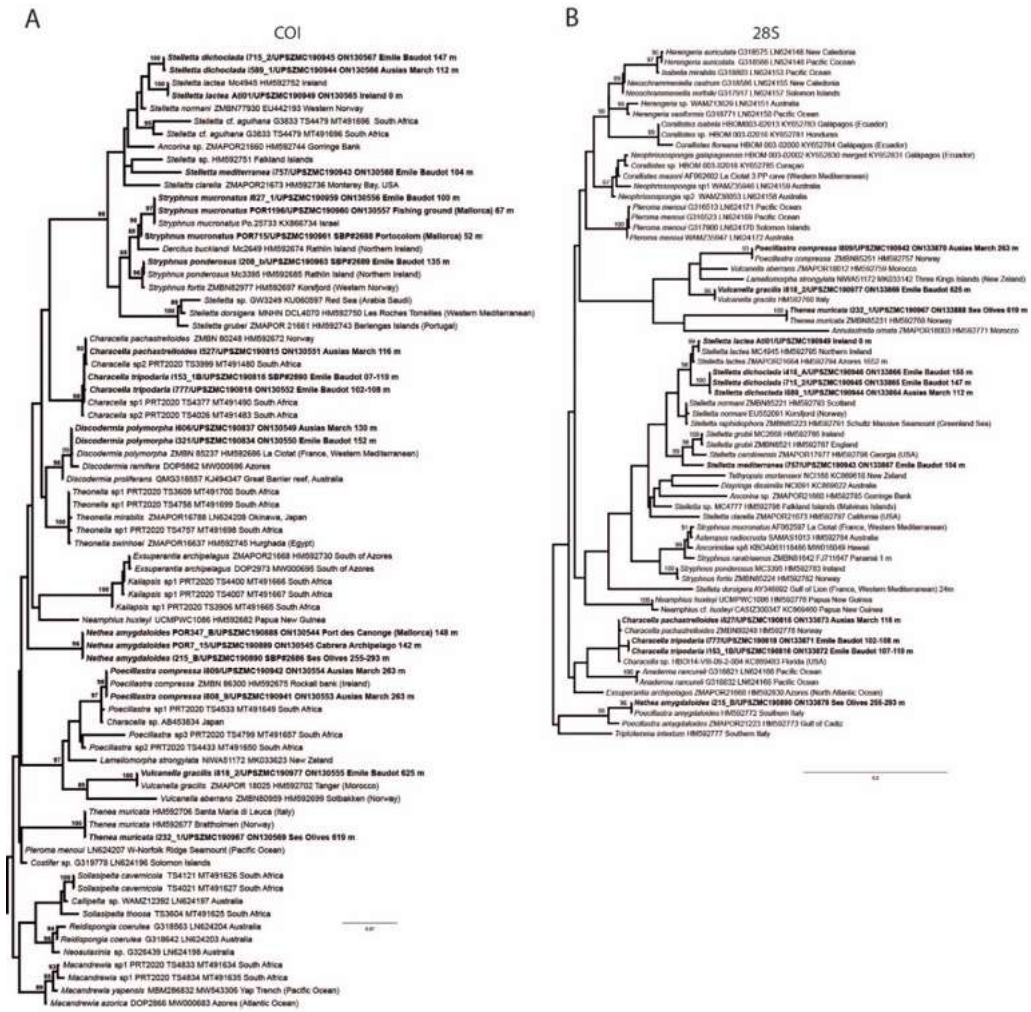

Figure 4.3.6. Detail of COI (A) and 28S (B) phylogenetic trees showing the Ancorinidae family. In bold are new sequences from this study. Specimen codes are written as ''field number/museum number'' followed by Genbank accession number. The original trees can be seen as Figs. S1–S2.

Stelletta dichoclada appears to belong to a clade with North Atlantic species (*S. lactea*, *Stelletta normani* Sollas, 1880 and *Stelletta rhaphidiophora* Hentschel, 1929*)* (Fig. 4.3.6 and Figs. S1-S2). In this clade all species share dichotriaenes, trichodragmas and one category of oxyasters. For both markers, the closest sister-species is the shallow-water to intertidal North Atlantic *S. lactea*. We sequenced a specimen of *S. lactea* from the intertidal area off Northern Ireland (UPSZMC 190949, ON130565 (COI), OR044718 (28S)). *Stelletta dichochlada* and *S. lactea* UPSZMC 190949 have respectively 17-18 pb difference in COI and 19-20 bp difference in 28S so they are significantly different genetically, despite their morphological strong similarities. A SEM plate for *S. lactea* has also been made to compare the microscleres (Fig. S4). In fact, both *S. lactea* and *S.*

dichoclada share similar spicular types, with similar morphologies: there is no clear spicule or external morphological difference between these species. Our *S. lactea* comparative specimen did have shorter/thicker oxeas, dichotriaenes with shorter rhabds, smaller oxyasters and longer trichodragmas (Table 4.3.2) but this would need to be confirmed with the measurements of several more *S. lactea* specimens.

However, there are also several Mediterranean records of *S. lactea*: Gulf of Lion (*Boury-Esnault, 1971; Pouliquen, 1972*), the Tyrrhenian Sea (*Sarà, 1958b, 1960*) and the Ionian Sea (*Pulitzer-Finalli, 1983*), all from shallow waters, in agreement with most North Atlantic specimens but unlike *S. dichoclada*, which seems to be a mesophotic species. There are no sequences of Mediterranean *S. lactea* specimens, so its presence in the Mediterranean Sea cannot be confirmed, and relatedness with *S. dichoclada* cannot be currently assessed.

***Stelletta mediterranea* (Topsent, 1893)**

(Figs. 4.3.6-4.3.7, Table 4.3.3)

Material examined

UPSZMC 190943, field#i757, MaC (EB), St. 53, (INTEMARES0720), 97-102 m, rock dredge, coll. J. A. Díaz.

Comparative material

Stelletta mediterranea, holotype, MNHN DT2305 (two spicule slides), Cap l'Abeille, Banyuls, France, 30-40 m.

Outer morphology

Small, about 1.3 cm in diameter (Fig. 4.3.7A). Hemispherical body polarized in upper (rounded) and basal (flattened) parts; hispid surface. Externally pink when alive, grayish after preservation. Choanosome color not recorded on deck, grayish after preservation. Free of agglutinated sand. Cortex 1 mm thick. Hard consistency, barely compressible. Openings inconspicuous.

Spicules

Plagiotriaenes (Fig. 4.3.7B), very scarce, rhabdome slightly curved, fusiform, measuring 240-1070 (N=3) /13-27 (N=6) µm. Cladome, with clads measuring 73-132/13-24 (N=6) µm. A single plagiotriaene with two bifurcated clads was observed (Fig. 4.3.7C), of the same length as the regular plagiotriaenes.

Anatriaene (Fig. 4.3.7D), rare, with teratogenic clads in form of aborted hooks just beneath the cladome.

Oxea I (Fig. 4.3.7E-F), large, robust, fusiform, most are bent at the middle, 1528-2189-2699/24-47-74 µm

Oxea II (Fig. 4.3.7G), small, thin, fusiform, bent at the middle, some slightly flexuous, 694-1151-1418/5-11-17 (N=23) µm.

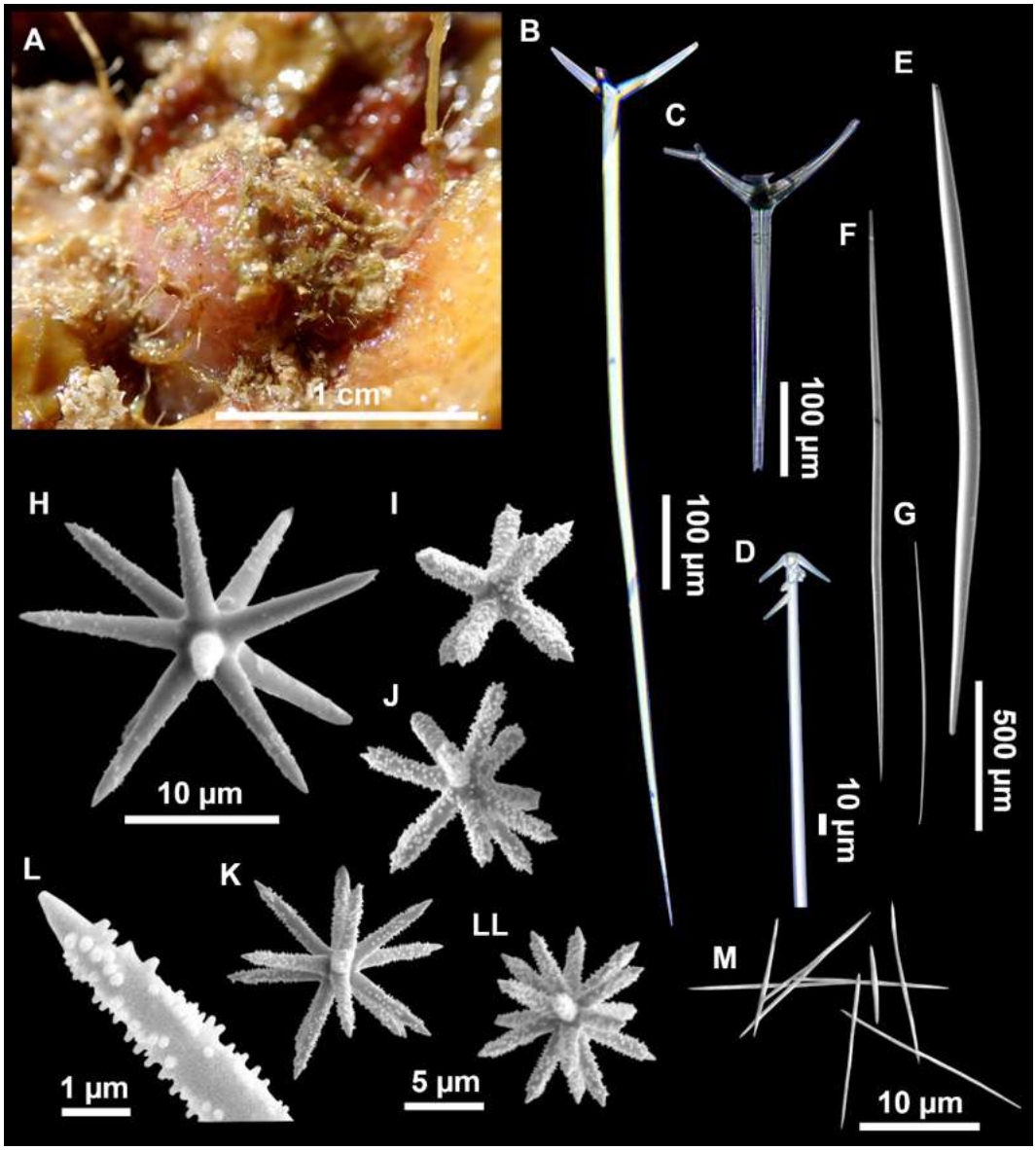

Figure 4.3.7. *Stelletta mediterranea* (Topsent, 1893), specimen #i757. (A) Habitus on deck, before fixation. (B–D) Optical microscope images. (B) Plagiotriaene. (C) Plagiotriaene with bifurcated clads. (D) Anatri-aene. (E–M) SEM images (E–F) Oxea I. (G) Oxea II. (H–LL) Oxyasters. (M) Raphides.

Oxyasters (Fig. 4.3.7H-LL), abundant, only one size category (9-14-24 µm) but small ones are strongylaster-like, while larger ones are more like oxyasters; 5-18 actines, less actines in larger oxyasters. Spines are distributed all along the actine in small oxyasters, and absent near the centrum in large ones.

Raphides in trichodragma (Fig. 4.3.7M), length/width measuring 13-16-20/3-6-10 (N=14).

Ecology notes

Found at the shallowest part of the EB summit (104 m). The area was rich in sponges and in coralligenous red algae. Epibiont on a large Irciniidae.

Table 4.3.3. Spicule measurements of *Stelletta mediterranea.* Measurements are given as minimum-mean-maximum for total length/minimum-mean-maximum for total width. All measurements are expressed in µm. Specimens here measured are in bold. The Balearic specimen code is the field#. Rh: rhabdome; cl: cladome; -:not found/not reported. EB: Emile Baudot.

Material	**Depth**	**Macroscopic features**	**Oxeas** (length/width)	**Anatriaene** Rhabdome (length/width) Clad (length/width)	**Plagiotriaenes** Rhabdome (length/width) Clad (length/width)	**Oxyasters** (length)	**Trichodragma** (length/width)
Holotype, Banyuls, France MNHN DT 2305 *(*Topsent, 1894*)	30-40	Encrusting, hispid, 4-8 mm thick	I. 866-1618-2048/ 10-45-57 II.* 650-1300/ 3-4	Rh: -/8 Cl: 37/- (N=1)	Rh: 765-1030-1244/ 13-39-50 Cl: 38-122-175/ -	8-12-16 (N=3) (abundant)	17*/-
i757 EB	105	Hemispherical, hispid, 1.3 cm	I. 1528-2189-2699/ 24-47-74 (N=45) II. 694-1151-1418/ 5-11-17 (N=23)	Rh: 1652-1761/4-7 (N=2) Cl: 12-18/3-4 (N=2)	Rh: 240-1070 (N=3)/ 13-27 (N=6) Cl: 73-132/ 13-24 (N=6)	9-14-24 (N=48)	13-16-20/ 3-6-10 (N=14)
Alboran Sea (*Pansini, 1987*)	70-80	Massive, cylindrical, hispid, 8-2.5 cm	I. 2750/ 66 II. 700-800/ 4-6	Rh: 1600/14 Cl: -/-	Rh: 950 / 30 Cl: 115/ 35	8-17	-

Genetics

Only the second part of the Folmer COI fragment (ON130568) was obtained; 28S (C1-D2) was also sequenced (ON133867).

Taxonomic remarks

This specimen is assigned to *S. mediterranea*, a poorly known species described by *Topsent (1893)* in Banyuls (France), and later recorded in the Alboran and Aegean seas (*Pansini, 1987; Vamvakas, 1971*). The spicules from the type slides were re-measured for the present study (Table 4.3.3). Similarities between our material and *S. mediterranea* are: i) presence of two categories of oxeas, ii) presence of plagiotriaenes (although Topsent called those spicules orthotriaenes, they are clearly pointing forward, (see *Topsent, 1984*, Plate XIV, Figure 3)) and especially iii) characteristic anatriaenes with teratogenic clads (Fig. 4.3.7D). Also, spicular sizes of both megascleres and microscleres fit with those of the holotype and *Pansini (1987)* (Table 4.3.3): the plagiotriaenes in the type are slightly more robust and its oxeas II are slightly thinner. Our specimen and the one from *Pansini (1987)* share a similar pink color when alive. Trichodragmas were not reported by *Pansini (1987),* but they could have been missed since they are not abundant in our specimen. The 28S tree (Fig. 4.3.6B) clearly suggests that this species groups with *Stelletta grubii* Schmidt, 1862 and *Stelletta carolinensis* (Wells, Wells & Gray, 1960) (well supported) while its position with COI (Fig. 4.3.6A) is more ambiguous (not supported) and could be explained by the fact that we only have a small sequence.

***Stelletta mortarium* sp. nov. Díaz & Cárdenas**

(Figs. 4.3.8-10, Table 4.3.4)

Etymology

Due to its resemblance to a “morter”, a type of ancient pottery kitchen bowl commonly used in Mallorcan cuisine.

Material examined

Holotype: UPSZTY 190957, field#i714_1, St. 45 (INTEMARES0720), MaC (EB), beam trawl, 150 m, coll. J. A. Díaz (Fig. 4.3.8).

Paratypes: UPSZTY 190950-51, field#i352_1 and field#i352_2, St. 136, MaC (EB), beam trawl, 146 m, coll. J. A. Díaz; UPSZTY 190952, field#i401_2, St. 167, MaC (EB), beam trawl, 151 m, coll. J. A. Díaz; UPSZTY 190953-54, field#i406-A and field#i406-B, St. 167, MaC (EB), beam trawl, 151 m, coll. J. A. Díaz.

Other specimens: UPSZMC 190955-190956, field#i582 and field#i594 (Fig. 4.3.9), St. 21 (INTEMARES0720), MaC (AM), beam trawl, 109 m, coll. J. A. Díaz.

Comparative material

Stelletta defensa Pulitzer-Finali, 1983, holotype, MSNG 47153, NIS.83.36, Calvi, Corsica, Ligurian Sea, July 1969, dredge, 121-149 m, detrital bottom (Fig. S3); paratype, MSNG 47154, NIS.85.3, July 1969, dredge, 121-149 m, detrital bottom.

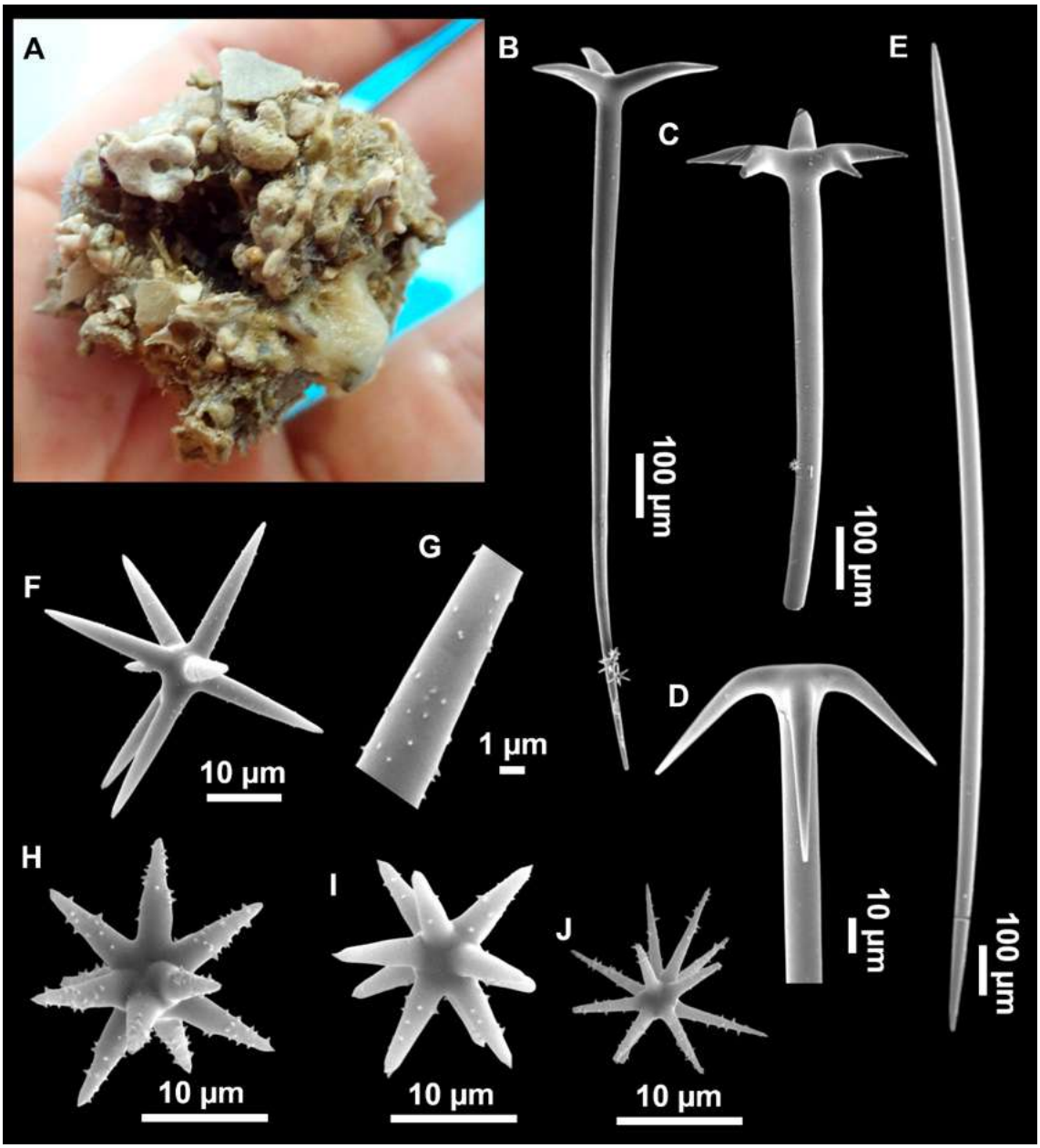

Figure 4.3.8. Holotype (UPSZTY 190957) of *Stelletta mortarium* **sp. nov.** (A) Habitus on deck before fix-ation. (B–J) SEM images of the holotype spicules. (B) Orthotriaenes. (C) Dichotriaenes. (D) Detail of the cladome of an anatriaene. (E) Oxea I. (F) Oxyaster I, with detail of the spines (G). (H–J) Oxyasters II at different development stages.

Stelletta dorsigera Schmidt, 1864, MNHN DCL4070, Roches Toreilles, France, 25 m, Oct. 1994, id. J. Vacelet and N. Boury-Esnault, COI: HM592750; 28S: AY348892.

Stelletta grubii Schmidt, 1862, BELUM Mc2668, Rathlin Ireland, Northern Ireland, summer 2005, id. B. Picton, 28S: HM592786 (*Cárdenas et al., 2011*).

Stelletta hispida (Bucchich, 1886), ZMBN 25636, Gulf of Cadiz, 1215 m, id. E. *Arnesen (1932)*.

Stelletta tuberosa (Topsent, 1892), MNHN DCL4066, Bay of Biscay, 4400 m, BIOGAS V expedition (Centob), id. P. Cárdenas.

Stelletta simplicissima (Schmidt, 1868), holotype, MNHN Schmidt collection#62, Algiers.

Stelletta stellata Topsent, 1893, UPSZMC 190958, South of Porto Cesareo lagoon, Apulia, SE Italy, 0.5 m, 27 July 2017. coll. P. Cárdenas and F. Cardone, id. P. Cárdenas and F. Cardone.

Outer morphology

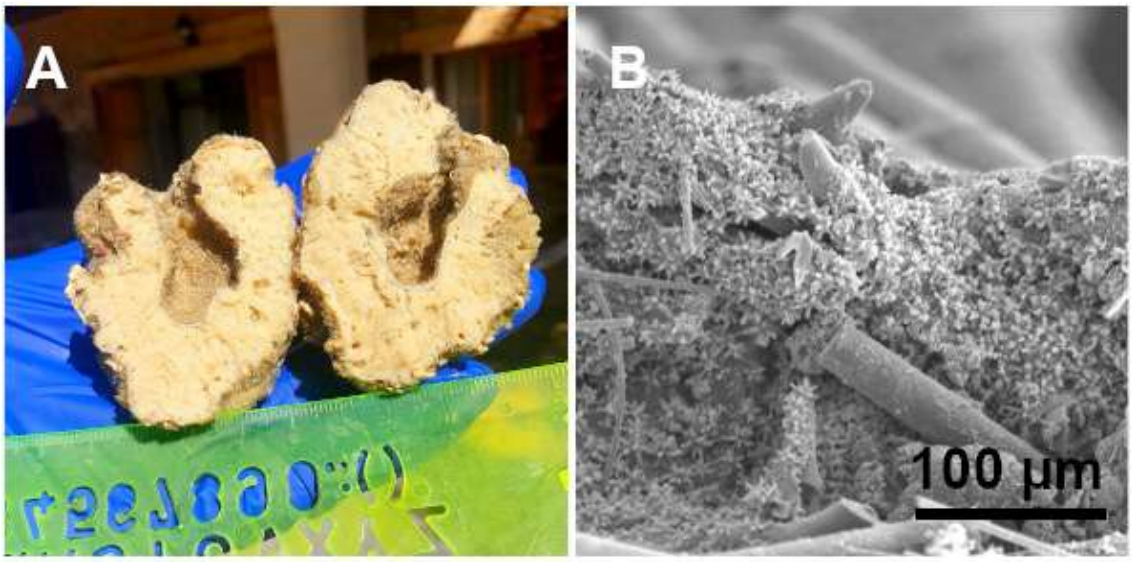

Figure 4.3.9. *Stelletta mortarium* **sp. nov.**, paratype #i594. (A) Transversal view after ethanol. (B) Detail of the cortex made up by oxyasters II.

Massive, circular to ellipsoid sponges, 3-6.5 cm in diameter, 2.5-6.5 cm in height with an atrium on its upper side (Fig. 4.3.8A; Fig. 4.3.9A). The atrium also has an ellipsoid shape, the opening 1.5-3 cm in diameter, and subsequent hole 1.5-3 cm deep (Fig. 4.3.9A). In specimen i582, the atrium does not generate a hole, but a concave depression at the surface. Color alive grayish (Fig. 4.3.8A). In EtOH, surface color dark gray and choanosome cream (Fig. 4.3.9A). Hard consistency, slightly compressible. Hispidation visible to the naked eye, present all over the surface, including the atrium. The atrium contains many small uniporal oscules, each with its own sphincter. Minute cribriporal pores are distributed on the sides of the specimens. Cortex ~0.5 mm thick. Abundant sediments or pebbles are incorporated into the surface, but not in the choanosome, which is fleshy.

Spicules

Orthotriaenes (Fig. 4.3.8B), stout rhabdome, slightly curved, fusiform, with a sharp tip, measuring 482-1865/12-65 µm. Cladome also stout and with a sharp tip, 43-287/11-50 µm. The smallest triaene showed a marked swelling beneath the cladome, and its clads were more triangular.

Dichotriaenes (Fig. 4.3.8C), rare, only in specimens i714_1 and i401_2. Same size and morphology as orthotriaenes, rhabdome measuring 1159-1498/39-52 µm, while cladome measuring 29-71/33-44 µm (protoclad) and 86-133/24-36 µm (deuteroclad).

Table 4.3.4. Spicule measurements of *Stelletta mortarium* **sp. nov.**, given as minimum-mean-maximum for total length/minimum-mean-maximum for total width; all measurements are expressed in µm. Specimen codes are the field#. Rh: rhabdome; Cl: clad; pc: protoclad; dc: deuteroclad; -:not found/not reported. EB: Emile Baudot; AM: Ausias March.

Material	**Depth** (m)	**Oxeas** (length/width)	**Anatriaenes** Rhabdome (length/width) Clad (length/width)	**Protriaenes** Rhabdome (length/width) Clad (length/width)	**Orthotriaenes** Rhabdome (length/width) Clad (length/width)	**Dichotriaenes** Rhabdome (length/width) Protoclad (length/width) Deuteroclad (length/width)	**Oxyasters** (length)
i714_1 (UPSZTY 190957) holotype EB	152	I. 1300-1913-2548/13-33-58 (N=25) II. 1531/8 (N=1)	Rb: -/5-13 (N=3) Cl: 18-55/3-12 (N=3)	Rb: 1156/6 (N=1) Cl: 69/5 (N=1)	Rh:720-1093-1499/26-48-65	Rh: -/52 (N=1) Pt: 42/44 (N=1) Dt: 107/32 (N=1)	I. 16-34-47 II. 16-19-24 (N=15)
i352_1 paratype EB	146	I. 791-1480-2262/8-19-38 (N=13) II. 753-967-1611/5-8-10 (N=12)	Rh: 2007-2295/10-12 (N=5) Cl: 26-53/8-11 (N=5)	Rh: 1194-1216/5-8 (N=2) Cl: 38-82/3-6 (N=2)	Rh: 705-1213-1579/14-44-55 (n=15) Cl: 48-147-221/13-36-46 (n=15)	-	I. 14-27-37 II. 11-15-23
i401_2 paratype EB	150	I 2025-2374-2762/16-27-36 (N=16) II. 985-1134/8-11 (N=3)	Rb: 1760-2605-3055/10-15-20 (N=8) Cl: 32-61-87/10-13-18 (N=8)	-	Rh: 800-1396-1865/24-39-51 (N=12) Cl: 76-138-201/19-33-50 (N=12)	Rh: 1159-1498/39-48 (N=2) Pt: 29-71/33-42 (N=2) Dt: 86-133/24-36 (N=2)	I. 11-25-38 II. 8-13-17
i582 AM	112	I. 1599-2469/15-51 (N=7) II. 1627/7 (N=1) (flexuous)	Rb: 1626-2214 (N=2)/7-13 (N=4) Cl: 22-74 (N=4)/5-11 (N=4)	-	Rb: 482-1030-1713/12-30-53 Cl: 43-132-287/12-26-49	-	I. 12-26-38 II. 14-15-19 (N=18)
i594 AM	112	I.1437-2019-2592/15-28-43 II. -	Rb: 2516/14 Cl: 71/10	Rb: 1267 (N=1)/9 (N=2) Cl: 69-84/7 (N=2)	Rb: 513-1129-1763/14-36-64 Cl: 45-141-270/11-29-47	-	I. 15-26-38 II. 8-15-21

Anatriaenes (Fig. 4.3.8D), uncommon, rhabdome straight and stout, 1626-3055/5-20 µm. Cladome with tips of the cladi sharp, curved inwards, 18-87/3-18 µm. Some with underdeveloped cladome, resembling oxeas.

Protriaenes, very rare, rhabdome thin and slightly curved, measuring 1156-1267/5-9 µm. Cladi measuring 38-82/3-7 µm. Not found in i402_1 and i582.

Oxea I (Fig. 4.3.8E), robust, slightly curved, fusiform, 791-2762/8-58 µm.

Oxea II, slender, slightly curved or flexuous, 753-1627/5-11 µm. Common in specimen i352_1, very rare in i401_2, i582 and i714_1, and not observed in i594. Some have at their tip structures that remind of an aborted cladome so they may be anatriaenes with underdeveloped clads: this was pointed out by Topsent (1893) when describing similar oxeas II in *S. mediterranea.*which has similar oxeas II.

Oxyasters I (Fig. 4.3.8F), choanosomal, having 6-11 long actines, faintly spined (Fig. 4.3.8G), small centrum, 11-47 µm in diameter.

Oxyasters II (Fig. 4.3.8H-J and Fig. 4.3.9B), ectosomal, having 9-15 short actines with more robust spines than oxyasters I and a centrum that is about 1/3 of the total diameter. The centrum is devoid of spines; overall measuring 11-24 µm.

Ecology notes

The species was found in the AM and the EB, on detrital bottoms with gross sand and gravels, from 111-152 m depth.

Genetics

COI (ON130562, ON130563, ON130564) and 28S (C1-C2) (ON133861, ON133862, ON133863) markers were obtained from i352_1 (paratype), i594 and i714_1 (holotype).

Taxonomic remarks

There are 10 species of *Stelletta* without raphides in the Northeast Atlantic/Mediterranean region: *S. dorsigera, S. grubii, S. hispida, S. addita* (Topsent, 1938)*, S. simplicissima, Stelletta pumex* (Nardo, 1847)*, S. defensa, S. stellata, S. tuberosa* and *Stelletta ventricosa* (Topsent, 1904). *S. dorsigera* has a conspicuous dark cortex with characteristic conules, unlike the cortex of *S. mortarium* **sp. nov.** Also, *S. dorsigera* is subspherical and not bowl shaped like our specimens. *S. dorsigera* has smaller oxyasters than *S. mortarium* **sp. nov.**, measuring 8-12 µm (Uriz, 1981) versus 11-47 µm. *S. grubii* lacks anatriaenes and protriaenes and its orthotriaenes have much shorter and downwards curved clads. Besides, COI/28S of *S. dorsigera* and *S. grubii* are far apart from our COI/28S sequences in our phylogenetic analyses (Fig. 4.3.10).

S. hispida has large plagiotriaenes instead of ortho/dichotriaenes, anatriaenes and protriaenes. Besides, it has styles instead of oxeas and a small (2,5 cm) spherical body shape (*Bucchich, 1886*). The size of the ortho/dichotriaenes in *S. mortarium* **sp. nov.** are four times longer and nearly two times thicker than in *S. addita*: dichotriaenes of *S. addita* have a rhabdome 225-350/25 µm (vs. 1159-1498/39-48 µm in *S. mortarium* **sp. nov.)**. Also, the triaenes of *S. addita* are mostly dichotriaenes, while *S. mortarium* **sp. nov.**, has mostly orthotriaenes. Moreover, no anatriaenes nor protriaenes were described

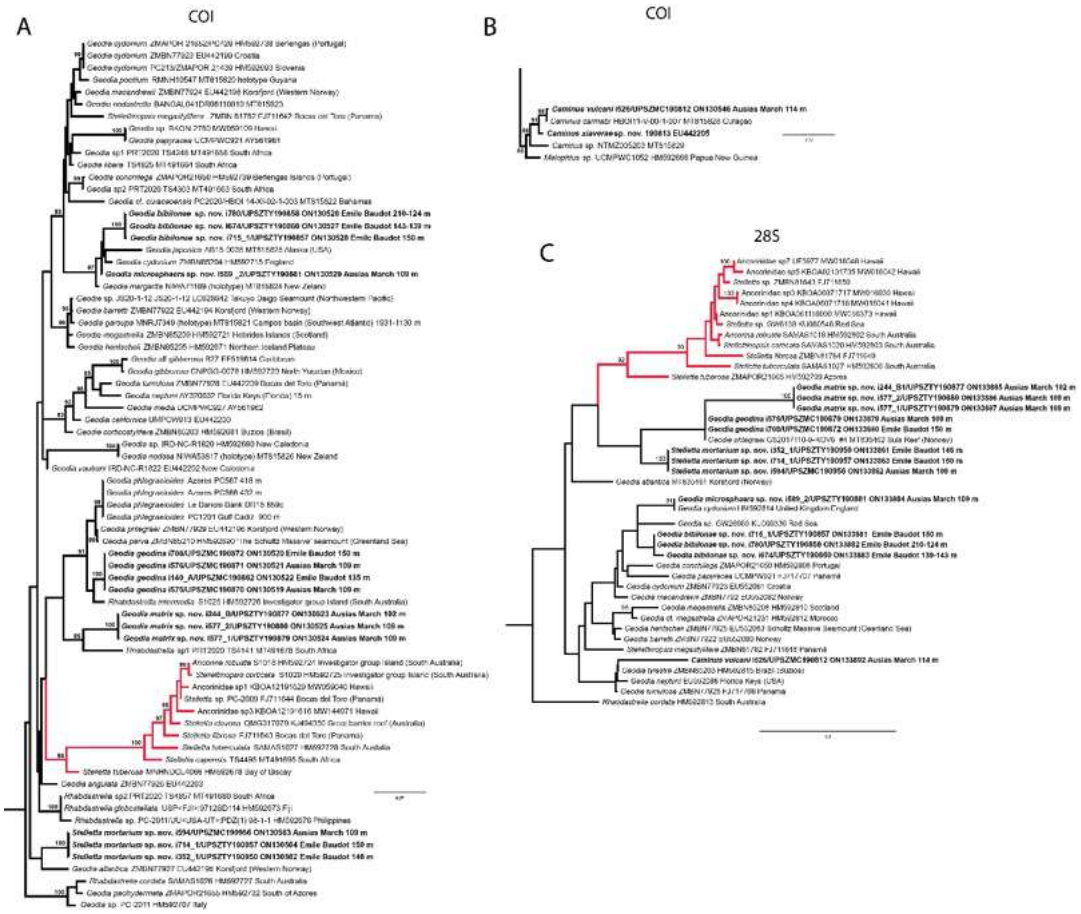

Figure 4.3.10. Details of the COI (A–B) and 28S (C) trees of Geodiidae including the 'Geostelletta' clade (in red). Specimen codes are written as ''field number/museum number'' followed by Genbank accession number. The original trees can be seen as Figs. S1–S2.

for *S. addita*. Descriptions of the type of *S. pumex* are very poor (*Nardo, 1847; Schmidt, 1864*) but if we follow the short redescription made by *Sollas (1888)* it appears *S. pumex* has only one type of aster which can be quite variable (vs. two types of aster in *S. mortarium* **sp. nov.**) and only plagiotriaenes (versus essentially orthotriaenes in our species, along with some dicho-, ana- and protriaenes).

We found that in the MNHN *Schmidt (1868)* collection the holotypes of *S. mucronatus* (found in jar#63 labeled '*Myriastra simplicissima*' and '*Myriastra addita*') and *Stelletta simplicissima* (found in jar#62 labeled '*Stelletta mucronata*') had been exchanged. Furthermore, according to the labels of jar#63 (MNHN DT 758), the holotypes of *S. simplicissima and S. addita* should have been stored together, since originally, they were both identified as *S. simplicissima* by *Schmidt (1868)*. However, the holotype of *S. addita* was missing from either jar (#62 or #63). This may have happened when *Topsent (1938)* revised the Schmidt collection and described *S. addita*, the types were not placed back properly and the holotype of *S. addita* was misplaced and is presumably lost. The holotype of *S. simplicissima* is a brown subglobular specimen 2 x 3.5 cm. It has only stout plagiotriaenes with short clads (70-153 µm, our measurements) and very robust oxeas (2300-2700/80 µm, our measurements), while the largest oxeas of *S. mortarium* **sp. nov.** are 8-58 µm thick. Also, newly made thick sections of the holotype showed that *Schmidt (1868)* and *Sollas (1888)* overlooked short trichodragmas ~12-15/5 µm

long, which are not very abundant but clearly present close to the cortex. As for *S. addita,* it has essentially dichotriaenes (and some rare orthotriaenes) and two sizes of strongylasters (*Topsent, 1938*) while *S. mortarium* **sp. nov.** has essentially orthotriaenes and two sizes of oxyasters. *S. tuberosa* is a deep-sea species from the North Atlantic found deeper (454-4400 m) than our specimens, they have a subspherical shape, much bigger megascleres and oxyasters (*Cárdenas & Rapp, 2015*). Their COI/28S is also quite different from those of our new species (Fig. 4.3.10).

The secondary loss of sterrasters in some *Geodia* (Geodiidae family) results in the same spicule repertoire as *Stelletta* species (Ancorinidae family), with triaenes, oxeas and asters (*Cárdenas et al., 2011*). *Stelletta* is therefore currently polyphyletic, with several of its representatives (e.g. *S. tuberosa*) grouping in a temporarily named 'Geostelletta' clade while others are true ancorinids (*Stelletta* sensu stricto) (*Cárdenas et al., 2011*). Both COI and 28S suggest that *S. mortarium* **sp. nov.** groups with *Geodia*, but not in the 'Geostelletta' clade, thereby suggesting there are several *Stelletta*-like *Geodia* clades amongst the *Geodia*. Actually, the position of *S. mortarium* **sp. nov.** is somewhat uncertain and poorly supported even within *Geodia* (Fig. 4.3.10). We refrain from allocating this species in the genus *Geodia*, until more species of *Stelletta* are sequenced so that new genera or subgenera can be formally created and defined based on shared morphological characters. We further note that so far none of the *Stelletta*-like *Geodia* possess raphides/trichodragmas, a spicule absent in the Geodiidae in general, so the presence of this spicule could be a good character to discriminate more efficiently some of the *Stelletta* sensu stricto species.

Genus *Stryphnus* Sollas, 1886

Stryphnus mucronatus (Schmidt, 1868)

(Figs. 4.3.2D, 4.3.6A and 4.3.11, Table 4.3.5)

Material examined

UPSZMC 190959, field#i827_1, St. 25 (INTEMARES0820), MaC (EB), ROV, 100 m; UPSZMC 190960, field#POR1196, St. 212 (MEDITSGSA521), east of Mallorca (Cala Ratjada), 63 m, GOC-73, coll. J. A. Díaz; UPSZMC 190961, field#POR715, St. 184 (MEDITSGSA519), east of Mallorca (Portocolom), 52 m, GOC-73, coll. J. A. Díaz.

Comparative material

Stryphnus mucronatus, holotype, MNHN DT758, Schmidt collection#63, Algeria, 'Exploration Scientifique de l'Algérie', 1842; PC440, field#GOR 06.80, Gettysburg Peak, Gorringe Bank, scuba diving, 36-42 m, LusoExpedição 2006, coll. J. R. Xavier, specimen mentioned in *Xavier & van Soest (2007)*.

Outer morphology

Massive sponges, 5-12 cm in diameter (Fig. 4.3.11A). All three specimens grow on several calcareous red algae, which are included in the sponge body. Specimen i827_1 serves as a substrate for *Haliclona (Flagellia)* sp., *P. monilifera* and a calcareous sponge. Oscula cribiporal, with several orifices surrounded by a sphincter. On the video recording we

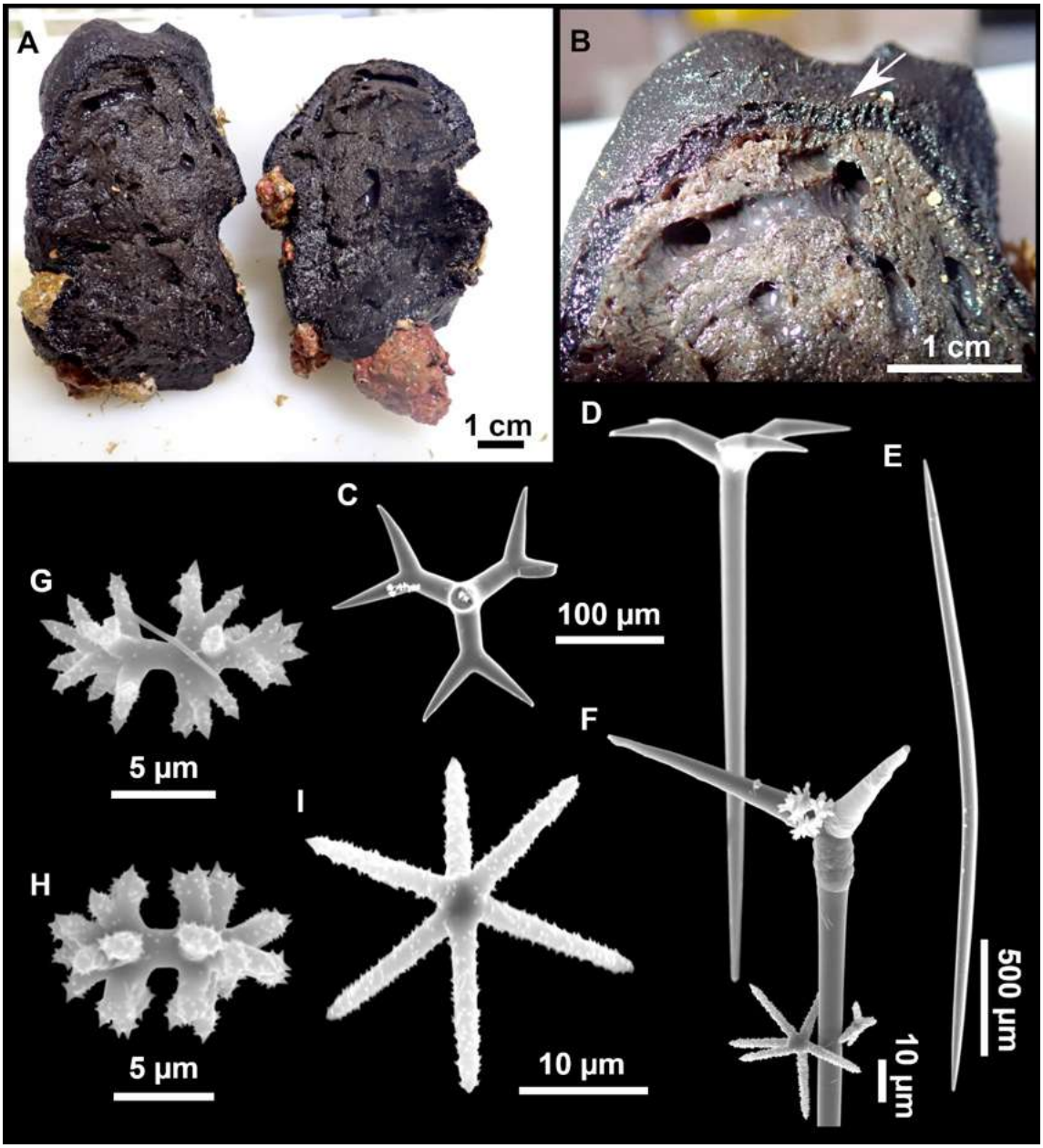

Figure 4.3.11. *Stryphnus mucronatus* (*Schmidt, 1868*), specimen i827_1. (A) Habitus on deck before fixa-tion. (B) Detail of a transversal cut, showing the cortex (arrow). (C–D) Dichotriaenes. (E) Oxea. (F) Pla-giotriaene. (G–H) Amphisanidasters. (I) Oxyasters.

observe an oscule, 1 cm in diameter (Fig. 4.3.2D). However, on deck we observe 2-4 contracted orifices, measuring 2-4 mm in diameter. Pores inconspicuous. Same color on deck and in EtOH: dark black cortex and a slightly paler choanosome (Fig. 4.3.11B). EtOH strongly colored dark by the specimens. Hard but slightly flexible consistency. Surface visually smooth but rough to the touch. Cortex patent, 3 mm in thickness (Fig. 4.3.11B, arrow).

Spicules

Dichotriaenes (Fig. 4.3.11C-D), scarce, only found in i827_1. Rhabdome: 333-420-498/15-22-29 (N=7), the protoclad: 40-49-62/13-20-25 µm and the deuteroclad: 21-49-73/8-13-17 µm (N=11).

Plagiotriaenes (Fig. 4.3.11F), only two found, one in specimen POR715 and one in i827_1. This spicule showed tuberculous processes below the cladome. Plagiotriaenes probably represent immature stages of the dichotriaenes. Rhabdomes measure 209-302/9-12 µm (N=2), while clads measure 54-79/9-10 µm (N=2)

Oxeas (Fig. 4.3.11E), Fusiform, large, bent at the middle, rarely modified to styles: 400-2471/6-59 µm.

Oxyasters (Fig. 4.3.11I), small centrum and long actines, spined all over its shaft: 14-38 µm with 5-11 actines.

Amphisanidasters (Fig. 4.3.11G-H), actines radiating from both ends of the shaft, spined: 7-15 µm long. In POR715 most are underdeveloped and have extra actines on its shaft.

Ecology notes

The species is not common in the Balearic Islands. It was found at the summit of the EB and in the fishing grounds east of Mallorca. Fishing ground stations were shallower (52 and 63 m) than the EB station (100 m). In both cases, sponges were growing on red algae bottoms.

Genetics

The COI Folmer region from specimen i827_1 (Fig. 4.3.2D and Fig. 4.3.11A) from the EB seamount was sequenced in two parts (ON130556). The miniCOI was sequenced for POR715 and the second part of COI for POR1196, both from fishing grounds east of Mallorca (SBP#2688 and ON130557). The COI of individual i827_1 and the COI fragments of POR715 and POR1196 match, and are identical to the sequence from specimen Po.25733 from the Eastern Mediterranean (Israel) (*Idan et al., 2018*).

Taxonomic remarks

Easily recognizable species, macroscopically characterized by its massive shape, black color, and thick cortex. The spicular set is quite homogeneous between the individuals of the Balearic Islands, as well as with individuals from other localities of the Mediterranean (Table 4.3.5). Triaenes are very rare, to the point that we did not find them in one specimen. As far as we know, this rarity of triaenes has not been reported before in this species (*Topsent, 1894, 1925; Vacelet, 1961, 1969; Pansini, 1987*). The scarcity of triaenes is shared with *Stryphnus raratriaenus* Cárdenas et al., 2009, from the Caribbean. As already stated (*Cárdenas et al., 2009*), scarcity (or lack) of triaenes support the phylogenetic closeness to the genus *Asteropus* Sollas, 1888, which is essentially a *Stryphnus* without triaenes. Our findings (morphology and phylogenetic tree) suggest once again that both genera are probably synonymous, a fact that requires further revision of Atlantic species and sequencing of more species of *Asteropus* in particular.

Stryphnus ponderosus (Bowerbank, 1866)

(Figs. 4.3.6A and 4.3.12, Table 4.3.5)

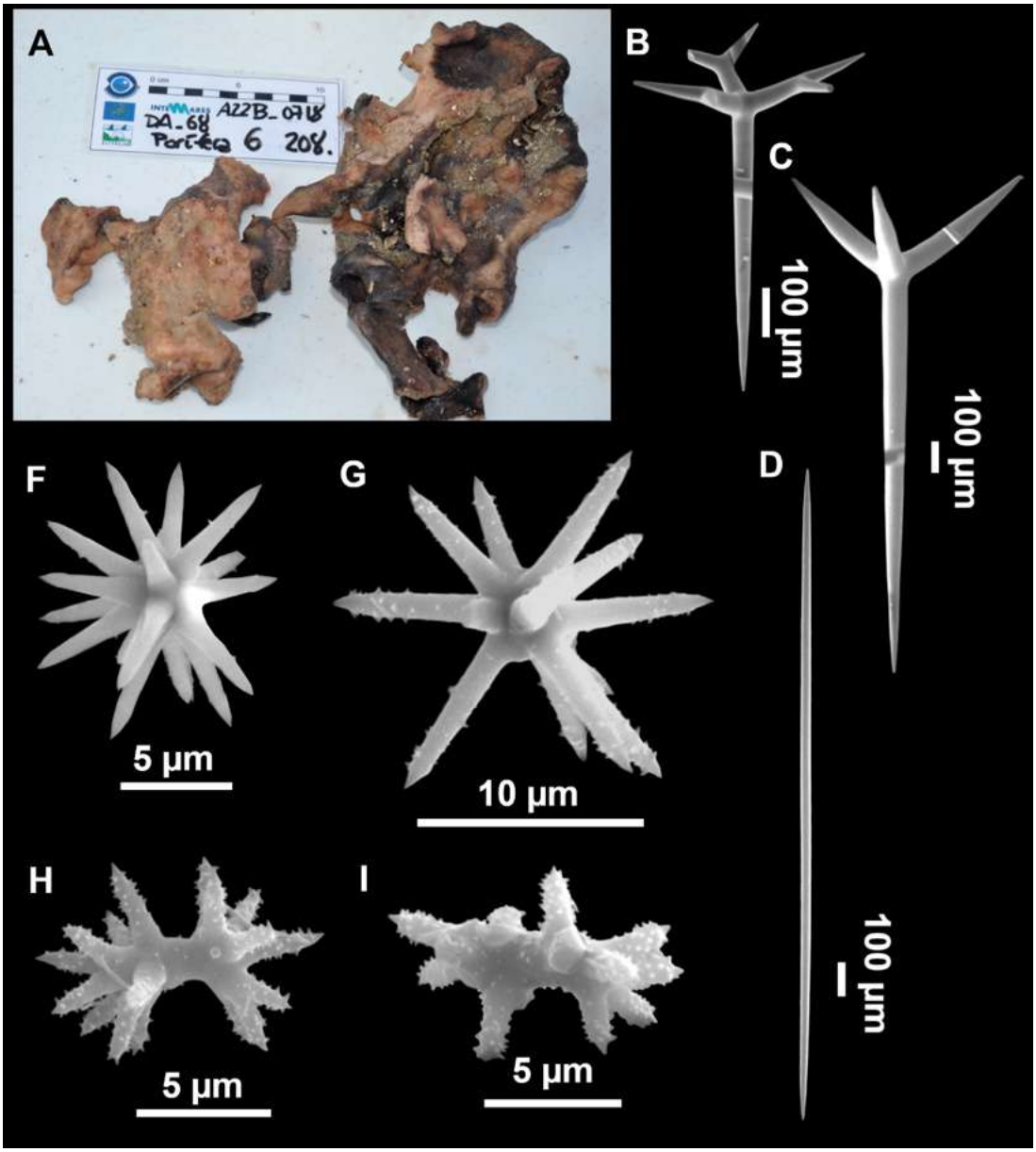

Figure 4.3.12. *Stryphnus ponderosus* (*Bowerbank, 1866*) specimen field i208_b. (A) Habitus on deck before fixation. (B) Dichotriaene. (C) Plagiotriaene. (D) Oxeas. (E–F) Oxyasters. (G–H) Amphisanidasters.

Material examined

UPSZMC 190963, field#i208_b, St. 68 (INTEMARES0718), MaC (EB), rock dredge, 135 m, coll. F. Ordines & H. Marco; UPSZMC 190964, field#POR778_1, (MEDITSGSA06N), St. 3 (2020), GOC-73, 76 m (Benicassim), coll. J. A. Díaz; UPSZMC 190966, field#POR798, (MEDITSGSA06N), St. 14 (2020), GOC-73, 96 m (St Carles de la Rápita), coll. J. A. Díaz.

Outer morphology

Large specimens, up to 25 cm in diameter, 1.5-3 cm in width (Fig. 4.3.12A). Flattened, concave or irregular and slightly lobulated. With large holes and depressions that increase its exposed surface. Color in life of a dark tint on the upper side, with some whitish areas on its lower side. Color remains after EtOH preservation, yet the EtOH

gets colored in black. Openings up to 1 mm in diameter, essentially located on the upper side of the body, surrounded by circular areas without pigment. Hard consistency. Hispidation localized. Poorly-delimited cortex, less than 0.5 mm thick.

Spicules

Dichotriaenes (Fig. 4.3.12B). Rhabdome short, straight, and fusiform, 310-732/17-58 µm. Cladome with protoclads projected outwards in a 120° angle with respect to the rhabdome 39-158/14-48 µm. Deuteroclads in a 90° angle, 31-170/8-35 µm. Rarely some of the clads may not be bifurcated.

Plagiotriaenes (Fig. 4.3.12C). Rabdome straight, most with a swelling just below the cladome. Scarce to absent in some specimens. Rhabdome 146-757/9-51 µm, cladi: 46-344/8-50 µm.

Oxeas (Fig. 4.3.12D). Stout, fusiform, slightly curved, 1058-2850/11-62 µm.

Oxyasters (Fig. 4.3.12E-F). with numerous and sharp actines, more or less spined, 11-23 µm.

Amphisanidasters (Fig. 4.3.12G-H). Strongly spined, 8-15 µm long.

Ecology notes

In the MaC, only found at the summit of the EB, an area with gross sand and both death and live rhodoliths. Other large sponges were also collected in the same dredge, including *Jaspis* sp., *P. compressa* or *P. monilifera*. Also found at two stations of the fishing grounds in front of the Ebro delta, at 76 and 95 m depth. Individual i208_b from EB was free of epibionts but specimens from the fishing grounds were almost entirely overgrown by other sponges (e.g. *Desmacella annexa* Schmidt, 1870, *Haliclona* cf. *fulva* (Topsent, 1893)). The specific association with *D. annexa* has been reported before in the Northeast Atlantic (*Cárdenas & Rapp, 2015*).

Genetics

Only the miniCOI was obtained for i208_b from the EB seamount (SBP#2689).

Remarks

This species occurs in the Northeast Atlantic and the Western Mediterranean, from the intertidal to mesophotic depths (0-200 m, this study). For most of the records, only dichotriaenes were found, and no plagiotriaenes reported. Subsequently, a variety of *S. ponderosus* with plagiotriaenes was reported under the name *S. ponderosus var. rudis*, because *Stryphnus rudis* Sollas, 1888, a junior synonym of *S. fortis*, was known to have both dichotriaenes and plagiotriaenes. Latter, *Cárdenas & Rapp (2015)* synonymized *S. ponderosus var rudis* as *S. ponderosus*, also establishing the morphological and ecological distinctions between *S. ponderosus* (shallow temperate North Atlantic and Mediterranean species) and *S. fortis* (deep-sea boreo-arctic species). The presence, absence or abundance ratio between the plagiotriaenes and dichotriaenes seems to have a specific, although highly variable, value: *S. ponderosus* has a prevalence of dichotriaenes while *S. fortis* has a prevalence of plagiotriaenes.

Table 4.3.5. Spicule measurements of *Stryphnus mucronatus* and *Stryphnus ponderosus*, given as minimum-mean-maximum for total length/minimum-mean-maximum for total width; all measurements are expressed in µm. Specimen codes are the field#. Rh: rhabdome; Cl: clad; pc: protoclad; dc: deuteroclad. -:not found/not reported. EB: Emile Baudot.

Material	**Depth** (m)	**Oxeas** (length/width)	**Plagiotriaenes** Rhabdome (length/width) Clad (length/width)	**Dichotriaenes** Rhabdome (length/width) Protoclad (length/width) Deuteroclad (length/width)	**Amphisanidasters** (length)	**Oxyasters** (length)
S. mucronatus **POR715** **Mallorca**	52	400-1247-2036/ 6-23-42	Rh: 302/12 Cl: 79/10 (N=1)	-	7-10-14	17-22-36
S. mucronatus **i827_1** **EB**	100	1137-1889-2356/ 15-37-59 (N=20)	Rh: 209/9 Cl: 54/9 (N=1)	Rh: 333-420-498/15-22-29 (N=7) Pt: 40-49-62/13-20-25 Dt: 21-49-73/8-13-17 (N=11)	7-11-15	21-29-38
S. mucronatus **POR1196** **Menorca**	63	962-1857-2471/ 9-33-49 (N=29)	-	-	9-11-14 (N=23)	14-25-36 (N=16)
S. mucronatus **PC440** **Gorringes Bank**	36-42	807-1224-1571/ 7-14-18	-	-	9-12-16	19-29-44
S. ponderosus **i208** **EB**	135	1211-1850-2419/ 15-31-44 (N=11)	Rh: 650/45 Cld: 213/43 (N=1)	Rh: 367-519-732/17-27-44 Pt: 39-71-103/14-26-42 Dt: 37-72-145/10-18-31 (N=9)	8-11-14	13-15-17
S. ponderosus **POR778_1** **Benicassim** **Iberian Península**	76	1176-1812-2315/ 20-41-53	Rh: 146-337-597/9-23-31 Cld: 46-121-188/8-23-36 (N=17)	Rh: 368-441-555/24-33-48 Pt: 63-95-119/22-30-42 Dt: 31-68-153/11-17-30 (N=9)	8-10-13	11-15-18
S. ponderosus **POR798** **St Carles de la rápita** **Iberian Península**	95	1058-1759-2850/ 11-31-62	Rh: 306-514-757/16-29-51 Cld: 80-170-344/14-25-50 (N=6)	Rh: 310-481-681/18-32-58 Pt: 62-99-158/15-29-48 Dt: 42-75-170/8-18-35	9-12-15	14-18-23

We have found both plagiotriaenes and dichotriaenes in all the specimens. However, plagiotriaenes were abundant in the shallowest specimen (POR778_1, N=17, 76 m), as opposed to very rare in the two deepest specimens (POR798, N=6, 95 m; i208_b, N=1, 135 m). It may suggest that plagiotriaenes are early dichotriaenes stages, and that specimens living in deeper waters having more silica at their disposal, their spicules are more easily fully developed and mature. *Cardenas & Rapp (2015)* suggested that population differences could explain the different ratios between plagiotriaenes and dichotriaenes found in the different specimens of *S. fortis*. Future laboratory experiments with different silica levels could help understand the relationship between plagiotriaenes and dichotrianees in these species.

We only managed to sequence a Folmer minibarcode (130 bp) from specimen i208_b. The sequence is identical to a sequence of *S. ponderosus* from Northern Ireland (HM592685), a fact that confirms the Mediterrano-Atlantic distribution of the species. It has a 2 bp difference with *S. fortis* from Norway (HM592697) and a 4 bp difference with *S. mucronatus*.

In the Mediterranean, *S. ponderosus* has been widely reported. It is known from the Gulf of Lion (*Vacelet, 1969*), the Alboran Sea (*Maldonado, 1992*), the Catalan Coast (*Uriz, 1981*), the Adriatic Sea (*Babiç, 1922*) and the Aegean Sea (*Voultsiadou, 2005*). In the Balearic Islands, it is only known by an undocumented report at the Cabrera archipelago littoral (*Uriz et al., 1992*). The present record is the second in the Balearic Islands, and the first on a Mediterranean Seamount.

Family Calthropellidae Lendenfeld, 1907

Genus *Calthropella* Sollas, 1888

Subgenus *Calthropella* Sollas, 1888

***Calthropella (Calthropella) pathologica* (Schmidt, 1868)**

(Figs. 4.3.13 and 4.3.14, Table 4.3.6)

Material examined

UPSZMC 190806-07, field#i693-i682, St. 43 (INTEMARES0720), 116-118 m, rock dredge, MaC (EB), coll. J. A. Díaz.

Comparative material

Calthropella (C.) pathologica, lectotype, MNHN DT753, Schmidt collection#66, Algeria, 'Exploration Scientifique de l'Algérie', 1842; paralectotype, MNHN DT754, Schmidt collection#87, Algeria, 'Exploration Scientifique de l'Algérie', 1842; PC324, La Ciotat, 3PP cave, 28S: AF062596; MNHN DCL4076, field#ASC6/327-6, Apulian Platform, off Cape Santa Maria di Leuca, Southern Italy, 39.56, 18.43, 560-580 m, ROV dive 327-6, Ifremer MEDECO leg1 (ifremer), 17 Oct. 2007, coll. J. Reveillaud, erroneously assigned to *C. (C.) geodioides* (Carter, 1876) in *Cárdenas et al. (2011)*, COI: HM592705, 28S: HM592826.

Calthropella (C.) geodioides, holotype, NHM 82.7.28.16, Cape St. Vincent, Portugal, 534 m; ZMAPOR 21667, EMEPC/G3-D4-Ma11a, SE of Terceira Island, Azores,

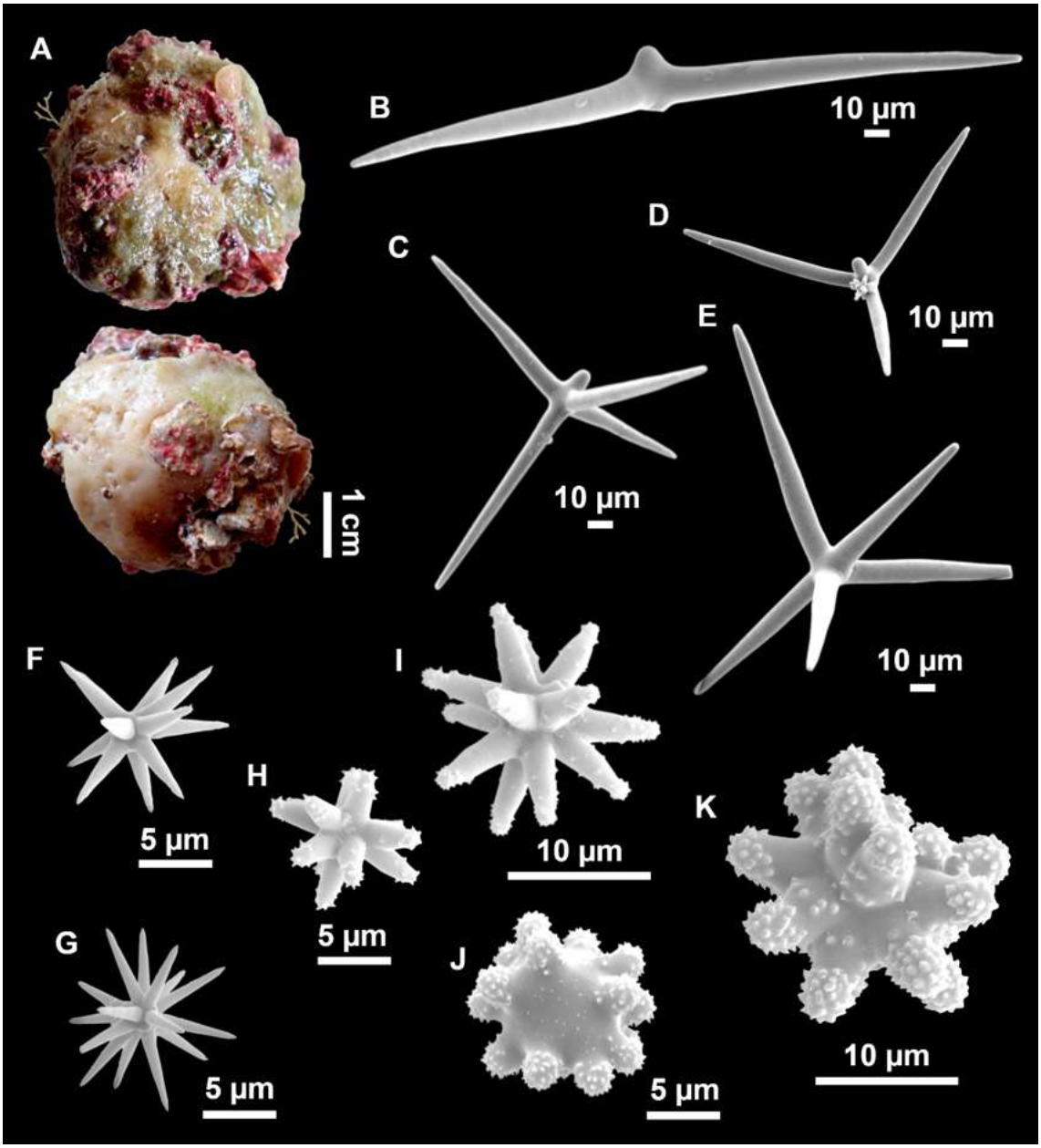

Figure 4.3.13. *Calthropella (Calthropella) pathologica* (*Schmidt, 1868*), specimen i693. (A) Habitus on deck before fixation. (B–E) Different calthrop modifications. (F–G) Oxyasters. (H–K) Tuberculated strongylasters.

38.4265°N, 26.8206°W, 1201 m, 18 May 2007, COI: HM592734, 28S: HM592825 (*Cárdenas et al., 2011*), SEM images presented in *van Soest et al. (2010*, Fig. 24).

Outer morphology

Massively irregular. Specimen i682 measures 7x9x4 cm and specimen i693 measures 5x4x3.5 cm, both overgrowing coralligenous red algae. Color in life beige with areas of dirty green, more localized in one of the body sides. On a transversal section, the green color persists in the first mm and then fades away turning into a beige choanosome. This first mm corresponds to a well-delimited cortex, which can be distinguished with the naked eye. Stony hard consistency, surface optically smooth, slightly rugose to the touch, overgrown by encrusting sponges (e.g. *Jaspis* sp.); pores inconspicuous.

Spicules

Calthrops (Fig. 4.3.13B-E), with 2-5 cladi and large variability, including aborted actines, teratogenic modifications and stylote ends. On a wide but continuous size range, overall measuring 54-879/6-94 μm. Potentially divisible in two categories (54-278/6-37 μm and 318-879/31-94 μm) but with intermediate sizes. Mesocalthrop modifications present in both large and small sizes but more common in small ones.

Oxeas (not shown), thin, invariably broken, scarce, up to 2839/17 μm.

Oxyasters (Fig. 4.3.13F-G), scarce, with many rays and sometimes a few small spines(only detectable by SEM), 9-18 μm.

Strongylasters to spherasters (Fig. 4.3.13H-K) with more or less spiny actines, variations with large centrum/short actines to small centrum/longer actines. Sizes of both kinds overlap so they probably belong to the same category, 6-23 μm.

Ecology notes

Both specimens were found at the same station; rhodolith bed at the summit of the EB, and both included rhodoliths to their bodies, which probably served as substrate. The station was rich in massive sponges like *P. monilifera*, *Jaspis* sp. or *Spongosorites* spp.

Genetics

We obtained the Folmer COI of i693 (ON130548) but only the miniCOI from i682 (SBP#2687). 28S (C1-C2) was obtained from i693 (ON133856).

Remarks

We assign with hesitation the Balearic material to *C. (C.) pathologica.* As stated by *van Soest et al. (2010)*, *C. (C.) pathologica* and *C. (C.) geodioides* are morphologically similar, and may be differentiated by i) the shape of the asters (longer actines in *C. (C.) pathologica*), ii) occasional calthrops with dichotomous clads in *C. (C.) geodioides* (absent in *C. (C.) pathologica*) and iii) mesocalthrops and dimesocalthrops in *C. (C.) pathologica* (absent in *C. (C.) geodioides*).

New spicules preparations were made from the holotype of *C. (C.) geodioides* and thick sections were made of the lecto- and paralectotype of *C. (C.) pathologica*; SEM images of the spicules of the lectotype of *C. (C.) pathologica* were previously presented by *van Soest et al. (2010*, Fig. 26). Based on re-examination of the types, MNHN DCL4076 from Santa Maria di Leuca was re-identified as *C. (C.) pathologica* and not *C. (C.) geodioides* as originally identified by *Cárdenas et al. (2011)*. *C. (C.) pathologica* possesses long thin oxeas that form occasional large bundles, visible on the thick sections of the lectotype. We also found fragments of long oxeas in *C. (C.) geodioides.*

We confirm that asters usually have longer actines in *C. (C.) pathologica* than in *C. (C.) geodioides*. Dichocalthrops have not been found in any of the *C. (C.) pathologica* examined, including the holotype, which is in accordance with the literature. On the other hand, dichocalthrops of all sizes are more or less abundant in *C. (C.) geodioides,* including the type, where they are particularly numerous. Given the extreme variability in calthrop morphology (including cladi size, number and aberrant forms), this character

Table 4.3.6. Spicule measurements of *Calthropella (Calthropella) pathologica* and *Calthropella (Calthropella) geodioides*, given as minimum-mean-maximum for total length/minimum-mean-maximum for total width; all measurements are expressed in µm. Specimen codes are the field#. Rh: rhabdome; Cl: clad; pc: protoclad; dc: deuteroclad; -:not found/not reported; EB: Emile Baudot.

Material	**Depth** (m)	**Oxeas** (length/width)	**Calthrops I** (length/width of actine)	**Calthrops II** (length/width of actine)	**Oxyasters** (length)	**Spherasters or strongylasters** (length)
C. (C.) pathologica **i682** **EB**	117	Always broken (fragments up to 1652/12)	54-124-262/6-16-37 4+1 (aborted) and 5 actines	318-512-879/46-66-94 2, 3, 4+ 1 (aborted) and 5 actines	9-11-18 (N=12)	6-12-20
C. (C.) pathologica **i693** **EB**	117	Always broken (fragments up to 2839/17)	68-138-278/9-14-26 4+1 (aborted) and 5 actines	335-452-608/31-46-59 (N=14) 2, 3, 4+ 1 (aborted) and 5 actines	8-12-16 (N=13)	8-15-23
C. (C.) pathologica lectotype, paralectotype MNHN DT 753 MNHN DT754 Algeria (*van Soest et al., 2010*)	-	Always broken (fragments up to 2000/12)	-	32-366/5-72 short-shafted triaenes and mesotriaene modifications Curved and stunted cladi. No dichocalthrops	smooth: 9-10-12 lightly spined: 23-25-27	9-18-24
C. (C.) geodioides holotype, Near Cape St. Vincent (Portugal) (*Sollas, 1888*)	534	736/93	3+ 1 (aborted) actine Dichocalthrop modification present	785/85 3+ 1 (aborted) actine	-	spheraster 25
C. (C.) geodioides Terceira (Azores) (*Topsent, 1904*)	599 and 845	-	3+1 (aborted) and 4 actines Dichocalthrop modification present	2, 3 and 4 actines Dichocalthrop modification present	12-15	20
C. (C.) geodioides ZMAPOR 21667 Terceira (Azores) (*van Soest et al., 2010*)	1201	Invariably broken, at least 500/5. Absent in some specimens	Dichocalthrops (few, absent in some specimens) Pc: 75-92 /12 Dc: 28-31 Rh: 92-120	102-351-705/11-52-128 possibly divisible in two categories: 102-180 and 434-705 3 actines	13-18	7-28

may depend on ecological factors and is potentially misleading so it needs to be further tested in the future. After examining our comparative material, the presence of one or two (mesocalthrop) actines appears to be a solid character: in *C. (C.) pathologica*, small calthrops show 'meso' modifications, both in the form of 4 (fully developed) + 1 underdeveloped actine (Fig. 4.3.13C) and in the form of 5 (fully developed) actines (Fig. 4.3.13E) while in *C. (C.) geodioides* they always have 4 (fully developed) + 1 (underdeveloped) actine. Regarding the large calthrops, in *C. (C.) pathologica* those can have 4+1 and 5 actines while in *C. (C.) geodioides* they always show 3, 4 or 4+1 actine. Analysis of COI/28S sequences revealed 2 bp. differences between the Azores specimen ZMAPOR 21667 (HM592734), and Mediterranean ones (including those from the EB seamount (i682 and i693), and specimen MNHN DCL4076 (HM592705) from Santa Maria di Leuca, Italy). To conclude, both species appear valid for now, based on three morphological differences and COI/28S.

Note: we noticed a typo in the *C. (C.) geodioides* material described by *van Soest et al. (2010,* p. 59 and Fig. 22): it should not be 'ZMAPOR 21666' (EMEPC/G3-D03A-Ma012) which is a *C. (C.) durissima* (IDed and sequenced by *Cárdenas et al. (2011)*. *Van Soest et al. (2010)* meant 'ZMAPOR 21667' (EMEPC/G3-D4-Ma11a). However, the collecting information is correct.

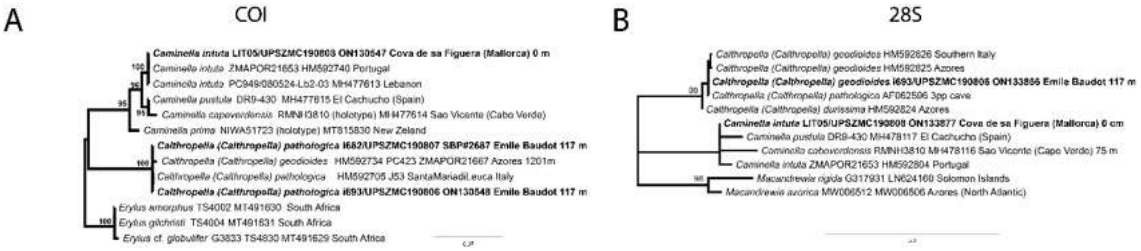

Figure 4.3.14. Detail of the COI (A) and 28S (B) trees for Calthropellidae and *Caminella*. Specimen codes are written as ''field number/museum number'' followed by Genbank accession number. The original trees can be seen as Figs. S1–S2.

Family Geodiidae Gray, 1867

Subfamily Erylinae Sollas, 1888

Genus *Caminella* Lendenfeld, 1894

Caminella intuta (Topsent, 1892)

(Figs. 4.3.14 and 4.3.15)

Material examined

UPSZMC 190808, field#LIT05, "Cova de sa Figuera" (cave), east of Mallorca, free apnea, 0-0.5 m, coll. J. A. Díaz.

Outer morphology

Hemispherical, 1.5 cm in maximum diameter (Fig. 4.3.15A). Ectosome light brown on live specimen, and after fixation in EtOH. Choanosome color not recorded on live specimen, whitish after fixation. Cortex has a stony hard consistency and is slightly

rough to the touch, choanosome is hard but compressible. The cortex can be separated from the rest

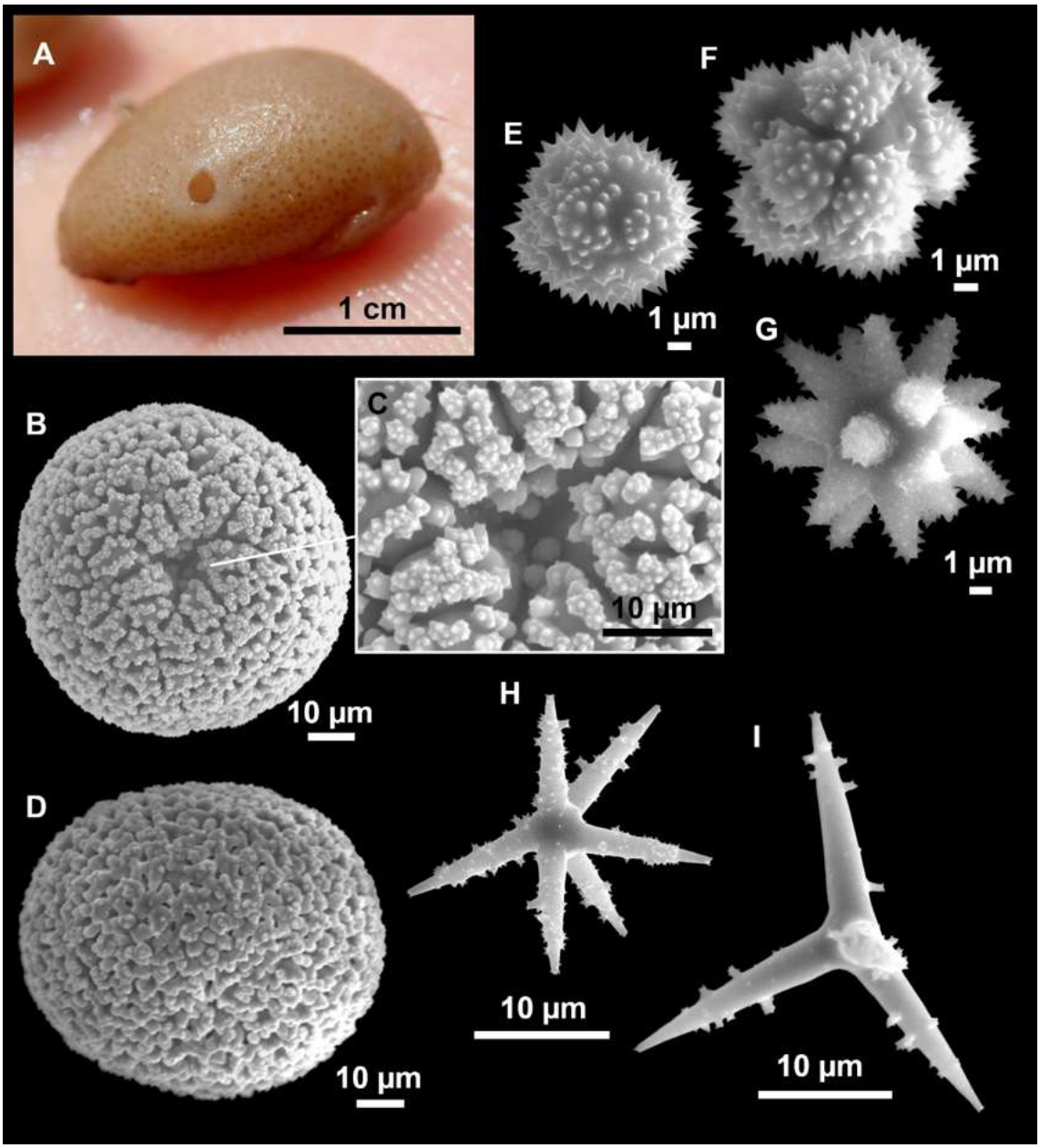

Figure 4.3.15. *Caminella intuta* (Topsent, 1892), specimen LIT05. (A) Habitus in fresh state, just after col-lection. (B–D) Sterrasters with (C) surface details. (E–G) Spherules to spherasters. (H–I) Oxyasters.

of the body, ~0.5 mm thick. Surface covered with circular pores, which have a ring-shape in life (open), and a dot-shape after fixation (contracted). Three circular oscula, 1-2 mm in diameter in live specimen, slightly smaller due to contraction after fixation.

Spicules

Dichotriaenes, robust, with short conical rhabdome, 398-399 (N=2)/65-72 (N=3), long protoclads and short deuteroclads, 60-95/67-150 (N=5) and 248-360/49-68 (N=5), respectively.

Oxeas, fusiform, scarce, 1313-1860/15-34 (N=3).

Sterrasters (Fig. 4.3.15B-D), spherical to oval; no clear rosettes but intricate brain-like surface covered with small warts (Fig. 4.3.15BC)

Spiny spherasters to spherules (Fig. 4.3.15E-G), 5-9-12 μm in diameter.

Oxyasters (Fig. 4.3.15H-I), 4-15 actines, 13-19-27 μm in diameter. Actins are acanthose with robust and triangular spines that are also microspined. Large oxyasters tend to have less actines than smaller ones.

Ecology and distribution

A single specimen found in the dark area of a littoral cave, firmly attached to a vertical wall, no more than 30 cm deep. Our specimen was living in an area that emerges with high waves, a fact suggesting that the species can survive short periods of air exposure. No epibionts.

Genetics

Folmer COI (ON130547) and 28S (C1-C2) (ON133877) were obtained. COI was identical to previously sequenced *C. intuta* from Lebanon, and Portugal. The 28S was also identical to specimen ZMAPOR 21653 (Portugal), but differs in 1 bp with specimen SME PL617PC-7 from Cosquer Cave, Marseille, France.

Taxonomic remarks

The external morphology, spicular set/sizes matches well with a revision of the species, including a redescription of type material (*Cárdenas et al., 2018*). Genetically, the only discrepancy with the published sequences is the 1 bp difference in the 28S sequence when compared to a specimen from Marseille (PL617PC-7). Unfortunately, no COI is available for that same specimen. This is the first record of the species in the Balearic Islands, and the shallowest for the species.

Genus *Caminus* Schmidt, 1862

Caminus vulcani Schmidt, 1862

(Figs. 4.3.10 and 4.3.16, Table 4.3.7)

Material examined

UPSZMC 190809, field#i142_C, St. 51 (INTEMARES0718), MaC (EB), beam trawl, 135 m, coll. J. A. Díaz; UPSZMC 190810, field#i254_4, St. 50 (INTEMARES1019), MaC (AM), beam trawl, 102 m, coll. J. A. Díaz; UPSZMC 190811, field#i391_2, St. 158 (INTEMARES1019), MaC (EB), beam trawl, 146 m, coll. J. A. Díaz; UPSZMC 190812, field#i526, St. 18 (INTEMARES0720), MaC (AM), beam trawl, 114 m, coll. J. A. Díaz.

Comparative material

Caminus vulcani, MNHN DT2288, slide, Banyuls, France, 30-40 m, specimen studied by *Topsent (1894)*; SME, wet specimen, Cassidaigne canyon, off Marseille, France, 100-150 m, trawl, 16 June 1961, specimen studied by *Vacelet (1969)*.

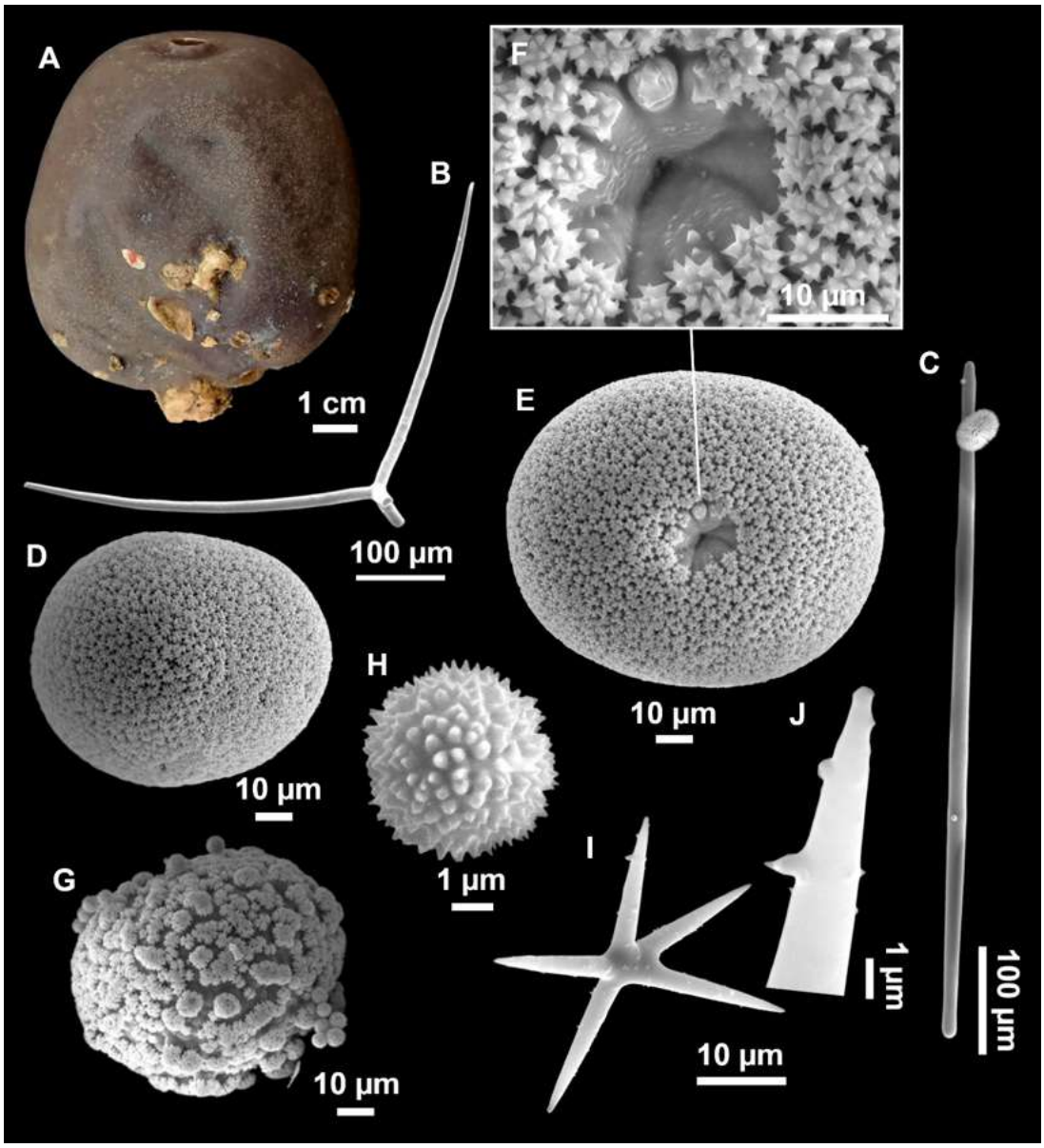

Figure 4.3.16. *Caminus vulcani Schmidt, 1862*, specimen i254_4. (A) Habitus after ethanol. (B) Orthotri-aene. (C) Strongyle. (D–G) Sterrasters with (F) detail of the rosettes. (H) Spherules. (I) Oxyaster with (J) detail of the spines.

Caminus xavierae **sp. nov.**, ZMAPOR 20422, holotype, Cueva Agua Dulce, Tenerife, Canary Islands, 5-10 m, scuba diving, field#CAN.07.05, 15 Jan 2007, coll. J. R. Xavier.

Outer morphology

Subspherical sponges (Fig. 4.3.16A) 3-8 cm in diameter, with an apical rounded oscula (2-4 mm in diameter), with a raised rim. Larger specimens (i254_4, i526) tend to acquire an ellipsoid, constricted shape. Same color in life and after preservation in EtOH: dark grayish ectosome and brownish choanosome. Hard (1 mm thick) but breakable cortex, pulpy choanosome. Smooth surface, with a mosaic visible to the naked eye, consisting of whitish polygonal patterns, which reflect the distribution of the pores; these patterns are even more obvious on dried cortex.

Table 4.3.7. Spicule measurements of *Caminus vulcani* Schmidt, 1862 and *Caminus xavierae* **sp. nov.**, given as minimum-mean-maximum for total length/minimum-mean-maximum for total width; all measurements are expressed in µm. Specimen codes are field#. Rh: rhabdome; Cl: clad; pc: protoclad; dc: deuteroclad; -:not found/not reported; EB: Emile Baudot, AM: Ausias March.

Material	**Depth** (m)	**Cortex thickness** (mm)	**Oxeas** (length/width)	**Strongyles** (length/width)	**Orthotriaenes** Rhabdome (length/width) Clad (length/width)	**Sterrasters** (diameter)	**Oxyasters** (length)	**Spherules** (length)
C. vulcani **i526 AM**	114	-	774/ 18 (N=1)	521-700-856/ 8-15-20	Rh: 606 (N=1)/15-20 (N=2) Cl: 355-378/11-16 (N=2)	79-96-113	35-59-99 (2-6 actines)	3-5-7
C. vulcani **i391_2 EB**	146	-	672-787/ 8-18 (N=4)	510-697-836/ 14-19-22 (N=17)	Rh: -/19-28 (N=5) Cl: 465-537/16-25 (N=5)	83-104-133	34-47-95 2-7 actines	3-4-6
C. vulcani **i254_4 AM**	102	1.5-2	424-562/ 3-9 (N=3)	511-745-962/ 10-15-20 (N=22)	Rh: 668 (N=1)/15-24 (N=4) Cl: 253-495/12-21 (N=4)	72-93-112	36-50-65 4-8 actines	3-4-5
C. vulcani **Cassidaigne, France (*Vacelet, 1969*)**	100-150	-	378-637-861/ 5-7-10 (N=14)	449-658-806/ 10-16-21	Rh: 376-597 (N=3)/15-22 (N=4) Cl: 266-487/11-24 (N=4)	71-92-106	36-50-72 2-6 actines (2 actines= large)	3-4-5
C. vulcani South Gulf of Lion, Banyuls (*Topsent, 1894*)	30-40	-	-	850/ 15-17	Rh: 480-570/15-17 Cl: 350-380	105-115/ 85-88	40 (mean) 2-5 actines	4
C. vulcani several specimens including neotype (*Uriz, 2002*)	-	1.5-2	-	850-880/ 15-17	Rh: 480-572/15-17 Cl: 320-360/- (in chord length, with long and straight clads)	100-115/ 87-90	35-42	3-4
***C. xavierae* sp. nov. Holotype (ZMAPOR 20422) Canary Islands**	5-10	0.5	broken	232-405-520/ 4-12-17	Rh: 326-458/ 5-14-20 (N=9) Cl: 77-225-326/-	70-81-92	13-25-37 (2-5 actines)	3-5
***C. xavierae* sp. nov. paratype UPSZMC 190814 Canary Islands**	5-10	0.5	379-450-531/ 7-9-11	476-541-639/ 11-15-18	Rh: broken Cl: 228-241/14-23 (N=2)	50-73-86	25 (N=1)	2-4-5
C. cf. *xavierae* **sp. nov.** Canary Islands (*Cruz, 2002*)	5-10	-	-	250-440/ -	-	80-120	16-24 (3-5 actines)	3-5
Caminus carmabi Bonaire, Caribbean (*van Soest et al., 2014*)	120-137 and 198	-	-	600-860-936/ 14-21-25	Rh: - Cl: 250-650-1020/18-24-30	140-190-210/125-144-162	51-65-81 (4-8 actines)	4-5-7

Spicules

Orthotriaenes (Fig. 4.3.16B), few, with clads curved forward, sometimes sinuous, short straight rhabdomes, only slightly longer than the cladi. Malformations like stylote termination or aberrant actines present in both rhabdome and cladome. Rhabdome: 606-668/15-28 µm, clads: 253-537/11-25 µm.

Strongyles (Fig. 4.3.16C), straight or curved, with round tips, 510-962/10-22 µm. Immature stages with oxeota ends are also present, 424-787/8-22 µm.

Sterrasters (Fig. 4.3.16D-G), spherical, with a very pronounced hilum (Fig. 4.3.16E, F), 72-133 µm in diameter.

Spherules (Fig. 4.3.16H), rugose, 3-6 µm in diameter.

Oxyasters (Fig. 4.3.16I-J), with small spines, 34-99 µm in diameter and having 2-8 actines, oxyasters with 2 actines tend to be larger.

Ecology notes

Only found at the summit of the EB and the AM, inhabiting the mesophotic zone (depth range 102-146 m).

Genetics

COI (ON130546) and 28S (C1-C2) (ON133892) were obtained from specimen i526. This is the first 28S fragment published for the genus *Caminus*. COI sequence was 8 bp different with *C. xavierae* **sp. nov.** from Tenerife (EU442205), and only 1 bp different with *Caminus carmabi* van Soest, Meesters & Beckings, 2014 from the Caribbean (MT815828).

Taxonomic remarks. See remarks below for *C. xavierae* **sp. nov.**

***Caminus xavierae* sp. nov. Díaz & Cárdenas**

(Figs. 4.3.10 and 4.3.17; Table 4.3.7)

As *Caminus vulcani*: Cárdenas et al., 2011; Cárdenas, 2020 (Figs. 5F, G).

Etymology

Named after sponge biologist Joana R. Xavier for collecting this species in the Canary Islands, and for her continuous efforts and leadership to support deep-sea sponge research.

Material examined

Holotype: ZMAPOR 20422 (wet specimen), UPSZTY 190813 (thick section and spicule slide), field#CAN.07.05, Cueva Agua Dulce, Tenerife, Canary Islands, 5-10 m, scuba diving, 15 Jan. 2007, coll. J. R. Xavier.

Paratype: UPSZTY 190814, spicule slide preparation, same locality as holotype, field#CAN.07.06, 15 Jan. 2007, coll. J. R. Xavier.

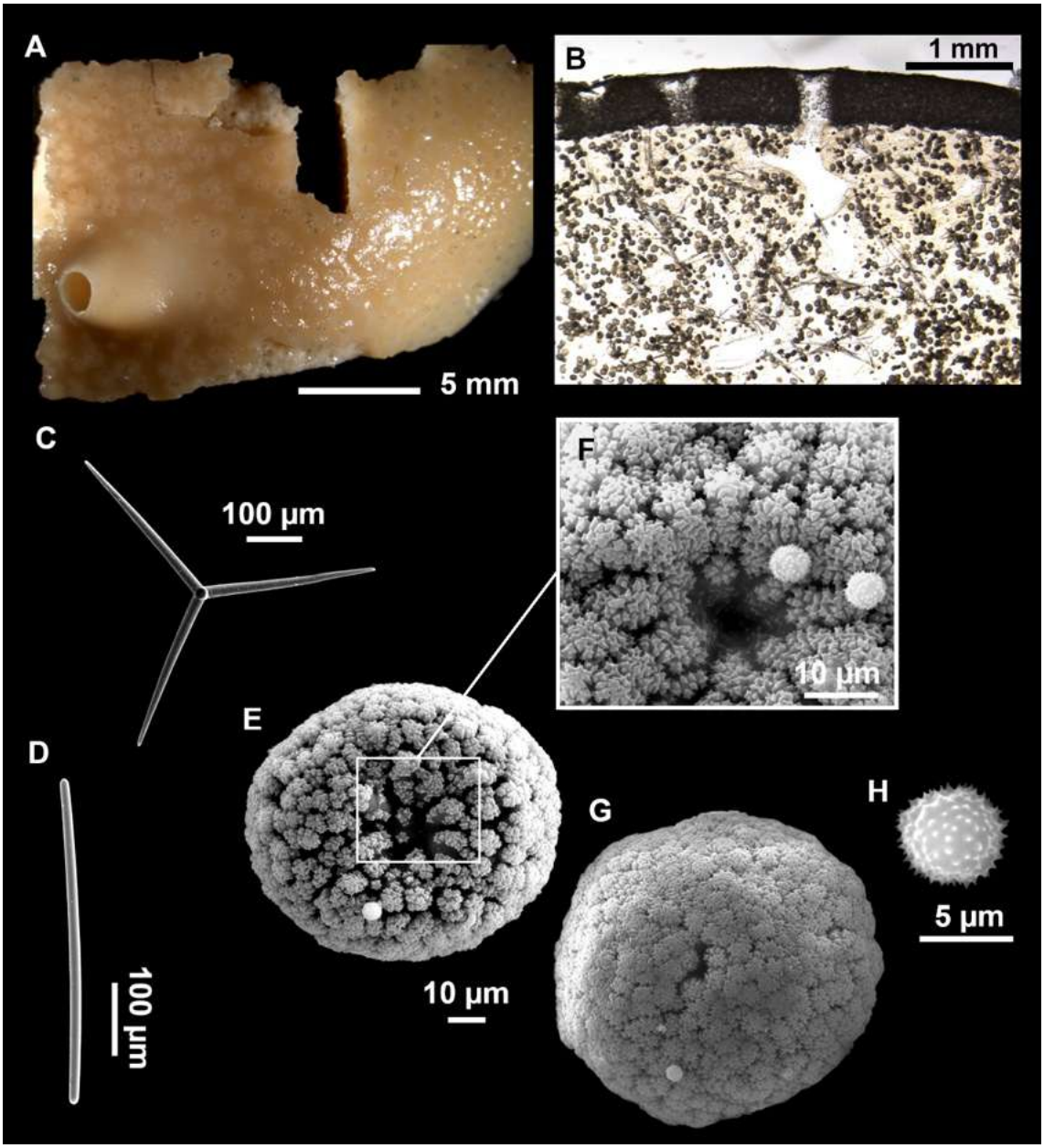

Figure 4.3.17. Holotype of *Caminus xavierae* sp. nov. (ZMAPOR 20422), Tenerife, Canary Islands. (A) Habitus after ethanol fixation. (B) Optical microscope image of a thick transversal section; three cribripo-ral pores visible across the cortex. (C) Orthotriaene. (D) Strongyle. (E–G) Sterrasters with (F) detail of the rosettes with spherules; picture E was already used in *Cárdenas* (*2020*, Fig. 5F). (H) Spherules. Oxyasters not shown. Figure source credit: Paco Cárdenas.

Comparative material

Caminus vulcani (this study).

Caminus carmabi, HBOI 11-V-00-1-007, specimen code 200005111007, Kaap Sint Marie, South coast, Curacao, 12.180550, -69.083980, 282 m, Johnson Link II-3209, 11 May 2000, id: P. Cárdenas, COI: MT815828.

Outer morphology

Holotype is 2.5 x 1 cm, massive encrusting with a unique oscule opening with raised margins (2-5 mm high) (Fig. 4.3.17A). Pores are distributed on the body of the sponge with the typical *Caminus* star-shaped pattern. Color in EtOH is light yellow to light brown; the raised oscule is lighter. Choanosome is beige.

Skeleton

Typical *Caminus* skeleton (Fig. 4.3.17B) with a distinct cortex (0.5 mm thick) essentially made of sterrasters, and covered with a thin layer of spherules. Below, a subcortical fibrous layer and a few triaenes supporting the cortex with their clades. In the choanosome, bundles of strongyles with no particular orientation, and numerous sterrasters, spherules and oxyasters.

Spicules (holotype and paratype)

Orthotriaenes (Fig. 4.3.17C), not abundant. sometimes ectopic clades on the rhabdome, rhabdome: 326-458/5-20 µm, clads: 77-326/14-23 µm.

Strongyles (Fig. 4.3.17D), straight or curved, 232-639/4-18 µm.

Sterrasters (Fig. 4.3.17E-G), spherical to elongated, common unequal length of the actines giving a cauliflower-like aspect, 50-92 µm in diameter.

Spherules (Fig. 4.3.17H), 2-5 µm in diameter.

Oxyasters, sometimes looking like strongylasters (with thicker actines), 2-5 actines, many irregular, 13-37 µm in diameter.

Ecology notes

Until now only found in underwater caves (Agua Dulce and San Juan) in Tenerife, Canary Islands.

Genetics

COI from the holotype (EU442205) and the paratype (COI unpublished) are identical and differ in 8 bp with the COI of *C. vulcani* and 7 bp with the COI of *C. carmabi.*

Taxonomic remarks on *Caminus vulcani* and *Caminus xavieriae* sp. nov.

Caminus vulcani is a well-known species, easily recognizable due to its macroscopical habit and its spicular set. In the Mediterranean, the species is recorded from shallow waters including caves (*Topsent, 1894*, 30-40 m; *Pulitzer-Finalli, 1983*, 15 m; *Grenier et al., 2018*) to mesophotic depths (*Vosmaer, 1894, 1*50-200 m; *Vacelet, 1969*, 100-150 m; *Maldonado, 1992*, 70-120 m). In general terms our material matches with the revision by *Uriz (2002)* only differing in that MaC specimens have strongyles in a wider size range (510-962/10-22 µm vs 850 vs 880/15-17 µm) and larger oxyasters (36-95 vs 35-42 µm). Besides, type material of *C. vulcani* comes from the Adriatic Sea (*Schmidt, 1862*), so we consider that our material is conspecific with the type because of geographical proximity and morphological similarities. It is reported here for the first-time in the Balearic Islands.

The only published Atlantic records of *C. vulcani* came from shallow caves in Tenerife, Canary Islands (*Cruz, 2002; Cárdenas et al., 2010*). Interestingly, COI from those

Canary Island specimens differs by 8 bp with COI of our specimens from the MaC Seamounts, which clearly indicates that they are two separate species. A new species is proposed for Canary Island specimens, *Caminus xavierae* **sp. nov.**, characterized by three main spicule differences with *C. vulcani*: i) shorter strongyles (232-639/4-18 µm vs. 510-962/8-22 µm in *C. vulcani*), ii) smaller sterrasters on average (average sizes of 73-80 µm vs. average sizes of 92-104 µm) and iii) shorter oxyasters (13-37 µm vs. 36-99 µm) (Table 4.3.7). The "cauliflower" morphology of the sterrasters (vs. regular subspherical shape in the other *Caminus* species) may be another specific character but SEM examination of more specimens is required to confirm this.

Caminus xavierae is the fourth species of *Caminus* in the Atlantic after the Caribbean *C. carmabi*, the Caribbean/Brazilian *Caminus sphaeroconia* Sollas, 1886 and the Mediterranean *C. vulcani*. *C. sphaeroconia* differs from all with the absence of oxyasters while the sterrasters (average of 190/144 µm) and oxyasters (average of 65 µm) of *C. carmabi* are much larger than in *C. xavierae*.

Interestingly, the COI sequence of *C. vulcani* (i526) and *C. carmabi* showed they are genetically closer to each other (1 bp. difference) than to *C. xavierae* **sp. nov. (**7-8 bp). This confirms the morphological similarities observed between them, highlighted in the original description of *C. carmabi*: "*Our material is most similar to Mediterranean* Caminus vulcani *Schmidt, 1862, but in that species sterrasters are smaller (105-115/85-88) and calthrops have also shorter and thinner cladi"* (*van Soest et al., 2014*)". *C. vulcani* and *C. carmabi* are therefore mesophotic sister species. Such small genetic differences in COI on either side of the Atlantic is in accordance with what is observed in other tetractinellid sister-species (P. Cárdenas, unpublished data). In the 28S tree, *C. vulcani* groups with *Geodia* and not with the Erylinae (Fig. 4.3.10). This unexpected result implies a long branch and no bootstrap support so it may be explained by the short length of our fragment and low polymorphism of the sequence obtained.

Genus *Erylus* Gray, 1867

Erylus cf. *deficiens* Topsent, 1927

(Figs. 4.3.18-4.3.19, Table 4.3.8)

Material examined

UPSZMC 190838, field #LIT10, Calo d'en Rafalino (Cala Morlanda), Mallorca, semi-submerged cave, 0-0.5 m, free apnea, coll. J. A. Díaz.

Comparative material

Erylus deficiens, holotype, MNHN DT1111 (slide), Porto Santo Bay, Madeira, 33 02'N, 16 19' 45'' W, 100 m, St. 801, 2 July 1897, trawl; ZMAPOR 21693, Gettysburg Peak, Gorringe Seamount, 32 m, 3 June 2006, coll: J. Xavier, field# GOR 06.01, COI: HM592687, 28S: HM592823, specimen identified as *Erylus* sp. in *Xavier & van Soest (2007)* and *Cárdenas et al. (2011)*; ZMAPOR 20419, Reserva do Garajau, Madeira, 7 m, 17 Feb. 2005, coll: J. Xavier, field#MAD.05.02.31, COI: EU442204, 28S: EU552088.

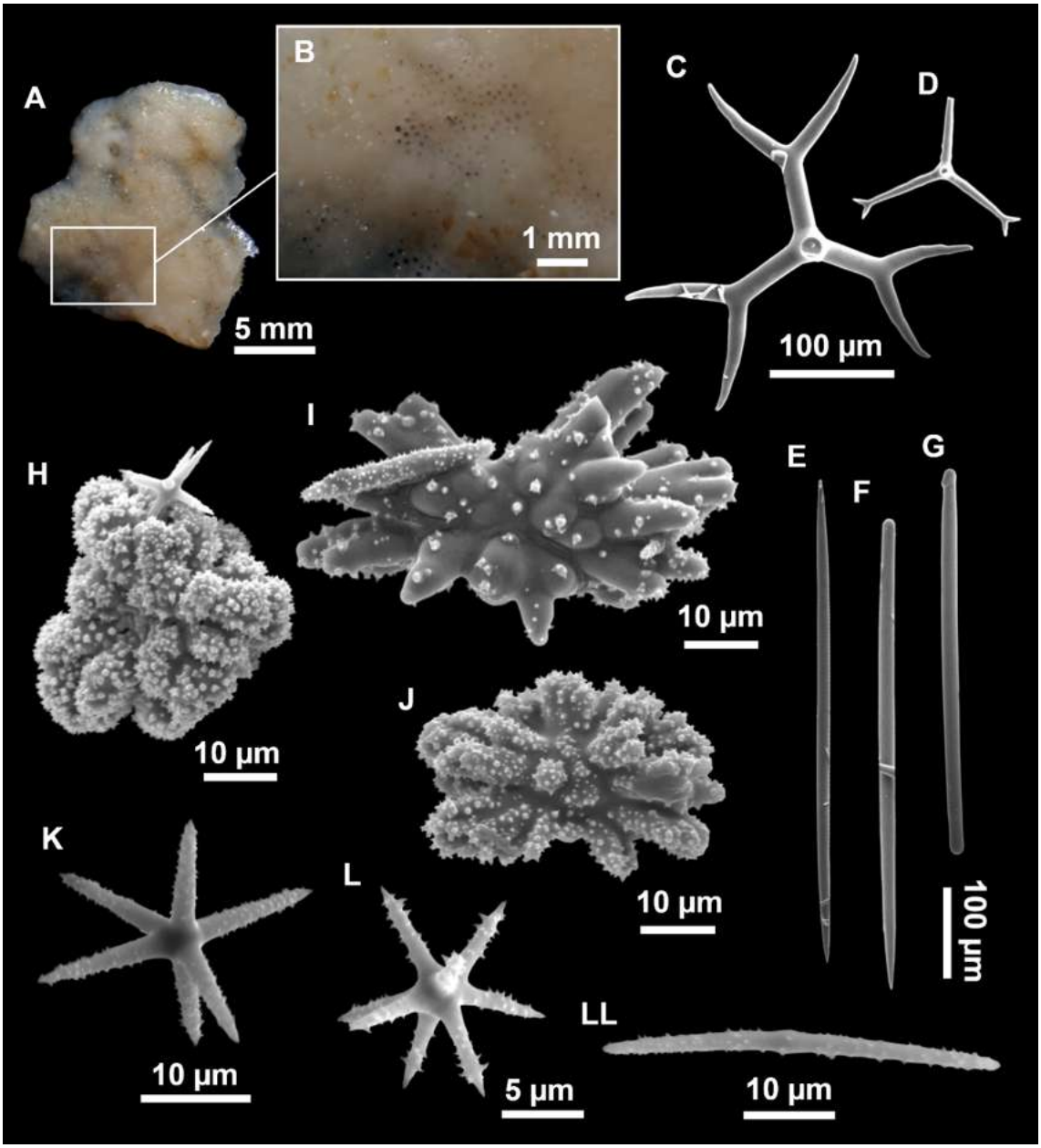

Figure 4.3.18. *Erylus* cf. *deficiens* (*Topsent, 1927*), specimen LIT10. (A) Habitus after ethanol fixation with (B) details of the pores. (C) Dichotriaene. (D) Juvenile dichotriaene. (E–G) Oxea, style and strongyle. (H– J) Aspidasters. (K–L) Oxyasters. (LL) Microrhabd.

Outer morphology

Small crust (Fig. 4.3.18A), 4-5 cm in maximum diameter, 0.2-0.4 cm in width. Whitish in life, dark brown after EtOH fixation. Skin smooth and hard to the touch, choanosome crumbly. Minute pores, <0.1 mm in diameter (visible to the naked eye), gathered (Fig. 4.3.18B). Oscules not observed.

Spicules

Dichotriaenes (Fig. 4.3.18C-D), uncommon malformations like aborted actines and stylote terminations. Juvenile stages with protoclads much longer than deuteroclads, which are very small, sometimes barely visible. Rhabdome:145-182 (N=4)/8-17-26, the protoclad: 47-67-86/8-14-25 µm and the deuteroclad: 11-79-135/4-11-18 µm.

Orthotriaenes, rare, rhabdome 76 (N=1)/8-11 µm (N=4), cladi 61-133/6-10 µm (N=4).

Oxeas (Fig. 4.3.18E), robust, straight to slightly curved, and fusiform, 280-503-647/4-11-17 µm.

Styles to strongyles (Fig. 4.3.18F-G) look like oxea modifications, tend to be shorter and thicker, especially the strongyles. Styles measure 193-520/14-15 µm (N=2), while strongyles measure 248-412-504/11-17-27 µm (N=14).

Aspidasters (Fig. 4.3.18H-J), very scarce, always with an irregular shape due to unequal actine lengths, 31-42-56 µm (N=13).

Oxyasters (Fig. 4.3.18K-L), with 4-9 spined actines, 12-21-36 µm.

Microrhabds (Fig. 4.3.18LL), very spiny, with less spines at the center, some being centrotylote, 22-36-55/2-3-6 µm.

Ecology and distribution

Single specimen found in a littoral, semi-submerged cave in the intertidal zone, periodically exposed to the air. The cave receives freshwater inputs that may increase silicon levels.

Genetics

Folmer COI (ON130535) and 28S C1-C2 (ON133853) were obtained.

Taxonomic remarks. See general discussion on *E. discophorus, E. mamillaris* and *E. deficiens* below, after the description of *E. mamillaris*.

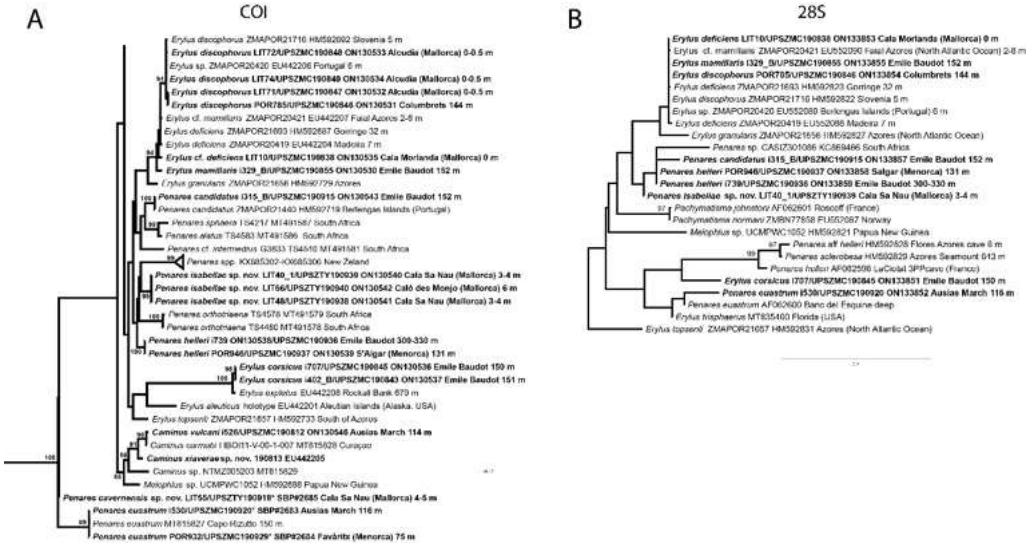

Figure 4.3.19. Detail of the COI (A) and 28S (B) trees of Erylinae (*Erylus, Penares, Pachymatisma, Cami-nus, Melophlus*). Specimen codes are written as ‘‘field number/museum number’’ followed by Genbank accession number. The original trees can be seen as Supplementary.

Erylus discophorus (Schmidt, 1862)

(Figs. 4.3.19-4.3.20, Table 4.3.8)

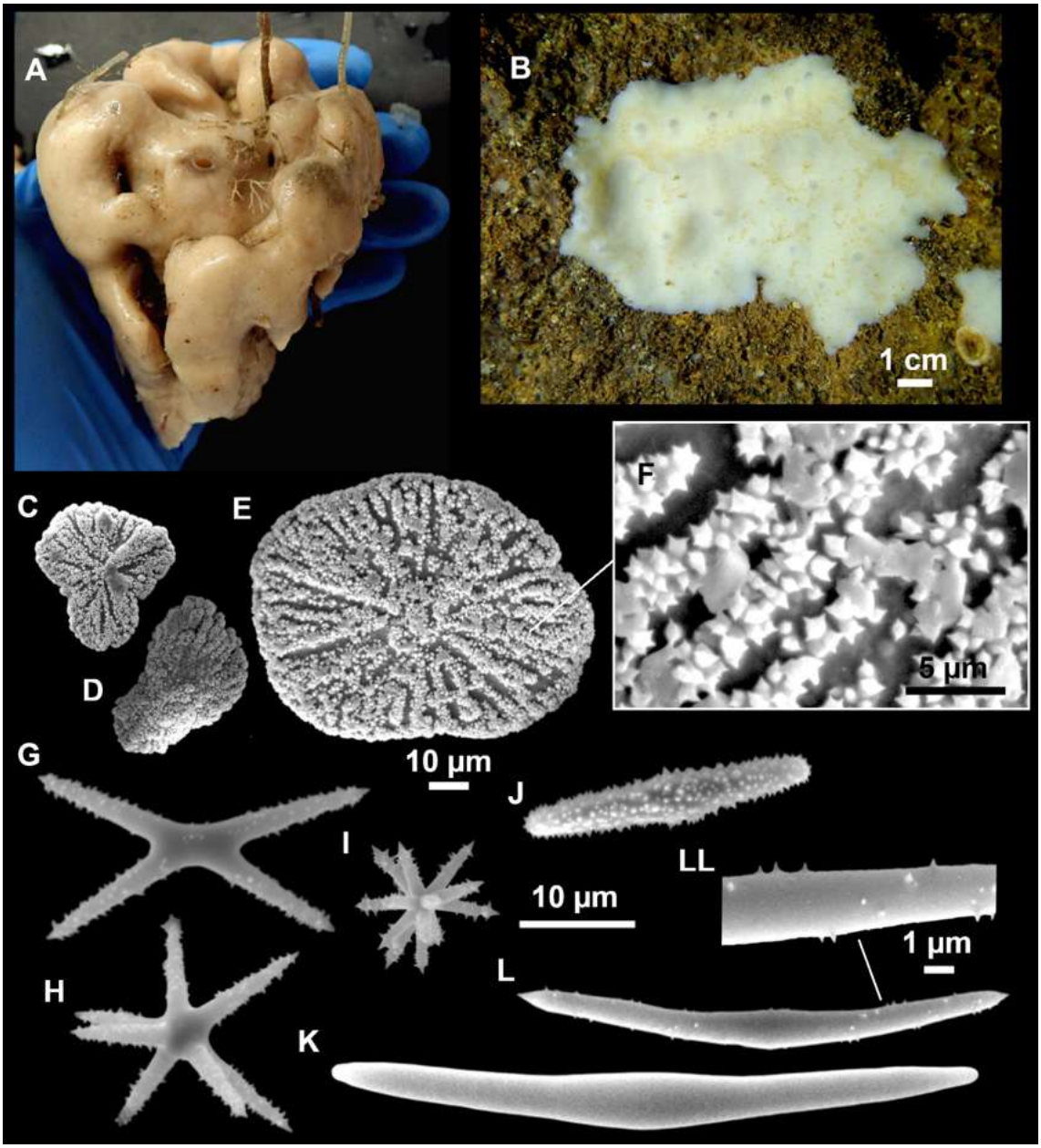

Figure 4.3.20. *Erylus discophorus* (Schmidt, 1862). (A) Habitus of POR785 on deck. (B) Cave specimen LIT74 in situ. (C–F) Aspidasters of LIT74 with (F) detail of the rosettes. (G–I) Oxyasters from POR785. (J) Microrhabds I from POR785. (K) Smooth microrhabd II from LIT74. (L) Microspined microrhabd II from LIT74 with (LL) detail of the spines.

Material examined

UPSZMC 190846, field#POR785, St. 6 (MEDITS06N20), fishing ground off Columbretes Islands, GOC-73, 144 m, coll. J. A. Díaz.

UPSZMC 190847-49, field#LIT71, field#LIT72 and field#LIT74, Coves de na Dana (Alcudia), Mallorca, semi-submerged cave, scuba diving, 0-1 m, coll. J. A. Díaz and A. Frank.

Comparative material

Scutastra cantabrica Ferrer-Hernández, 1912, paratype, NHM 30.1.21.5, wet specimen, Santander, Spain; *Erylus discophorus*, ZMUC, off São Pedra Bay, São Vincente, Madeira, 40 m, St. 40, originally identified as *S. cantabrica* by *Burton (1956)*, here re-identified.

Outer morphology

Fishing ground specimen POR785 is massive (Fig. 4.3.20A), lobulate, measuring 10 cm in height and 7 cm in diameter. Color beige with dark shades in life, and after fixation in EtOH. Dark shades more present on the upper part and around the oscula. Choanosome beige. Surface smooth. Consistency hard but slightly flexible. Circular oscula, 2-3 mm in diameter, placed at the top of the lobules. Inhalant pores not observed.

Cave specimens are encrusting (Fig. 4.3.20B), 0.3-0.5 cm width, spreading 7-8 cm on the vertical walls. Color in life whitish to beige with some brownish areas, probably caused by diatoms. Same color for the ectosome and the choanosome. Color slightly paler after fixation in EtOH. Inner channels visible only in areas where the body was thinner. Surface smooth, but wrinkled after collection due to contraction. Hard consistency. When alive, many small and circular oscula visible, 1-2 mm in diameter, aligned on the top of small ridges (Fig. 4.3.20B). Pore groupings visible to the naked eye, in depressed parts of the specimen.

Spicules

Dichotriaenes, robust, with short and fusiform rhab. Rhabdome: 123-557/8-62 µm, protoclad: 46-111/7-52 µm and deuteroclad: 10-262/3-44 µm.

Orthotriaenes, very scarce, only found in POR785 (N=3) and LIT72 (N=1), rhabdome 135-464/9-18 µm, clad 96-164/7-17µm.

Oxeas, slightly curved and fusiform, 388-978/5-29 µm, sometimes modified to styles (384-650/10-25 µm) and strongyles (183-796/11-22 µm).

Aspidasters (Fig. 4.3.20C-F), circular to slightly elongated, 33-95 µm (max. diameter).

Oxyasters (Fig. 4.3.20G-I), with 4-12 spined actines, 6-30 µm.

Microrhabds I (Fig. 4.3.20J), densely recovered with robust spines, centrotylote, 14-68/1-5 µm.

Microrhabds II (Fig. 4.3.20K-LL) uncommon, smooth to microspined, curved and centrotylote, 41-89/3-6 µm.

Ecology and distribution

Species found in a fishing ground close to Columbrets (POR785) and in a shallow water cave with freshwater inflow (LIT71, LIT72 and LIT74). Cave specimens were very abundant, and found just below the water surface. The only previous mention of *E. discophorus* in the Balearic Islands was from shallow caves off Cabrera Archipelago *(Uriz et al., 1992*).

Genetics

Folmer COI was obtained from all specimens (POR785, ON130531; LIT71, ON130532; LIT72, ON130533; LIT74, ON130534) whereas 28S (C1-C2) was obtained only from POR785 (ON133854).

Taxonomic remarks. See general discussion after the description of *E. mamillaris*.

Erylus cf. *mamillaris* (Schmidt, 1862)

(Figs. 4.3.19 and 4.3.21; Table 4.3.8)

Material examined

UPSZMC 190850, field#i142_B, St. 51 (INTEMARES0718), MaC (EB), 128 m, beam trawl, coll. F. Ordines; UPSZMC 190851-52, field#i179_A-179_B, St. 60 (INTEMARES0718), MaC (EB), 138 m, beam trawl, coll. F. Ordines; UPSZMC 190853-56, field#i314, field#i329_A, field#i329_B, field#i329_C, St. 124 (INTEMARES1019), MaC (EB), 152 m, beam trawl, coll. J. A. Díaz.

Comparative material

Erylus cf. *mamillaris*, ZMAPOR 20421, Ponta Furada, Faial Island, Azores, 2-8 m, 6 Sept. 2005, field#FUR05.09.14, coll: J. R. Xavier, COI: EU442207, 28S: EU552090.

Outer morphology

Massive, ovoid and lobated sponges (Fig. 4.3.21A), which often agglomerate foreign sediments, pebbles, worm tubes. The largest specimen (i314) is 9.5x5 cm. Single apical oscule on each lobe. Dark brown on its upper side, progressively fading to light brown or whitish at its basal area; choanosome lighter, cream colored. Surface visually smooth but rough to the touch, texture is quite firm, only very slightly compressible. Cortex less than 1 mm thick, clearly distinguishable. Choanosome fleshy, light brown and showing a well-developed aquiferous system.

Spicules

Dichotriaenes (Fig. 4.3.21B), scarce, may be significatively thick. Rhabdome: 335 (N=1)/27-40-57 (N=5) µm, protoclad: 115-133-151/27-34-52 (N=5) µm and the deuteroclad: 119-139-161/19-27-39 (N=5) µm.

Oxeas (Fig. 4.3.21C) robust and fusiform, slightly curved 429-1037/5-28 µm. One single stylote modification was observed in specimen i179_B (not measured).

Aspidasters (Fig. 4.3.21D-H), slightly elongated, 64-121/33-91 µm (length/width).

Oxyasters (Fig. 4.3.21I-J), 4-13 spined actines, 14-56 µm in diameter.

Microrhabds (Fig. 4.3.21K), spined and centrotylote, 15-31/1-4 µm.

Ecology and distribution

Species found at several stations on the EB summit, always on sedimentary bottoms at mesophotic depths, just below the photic zone.

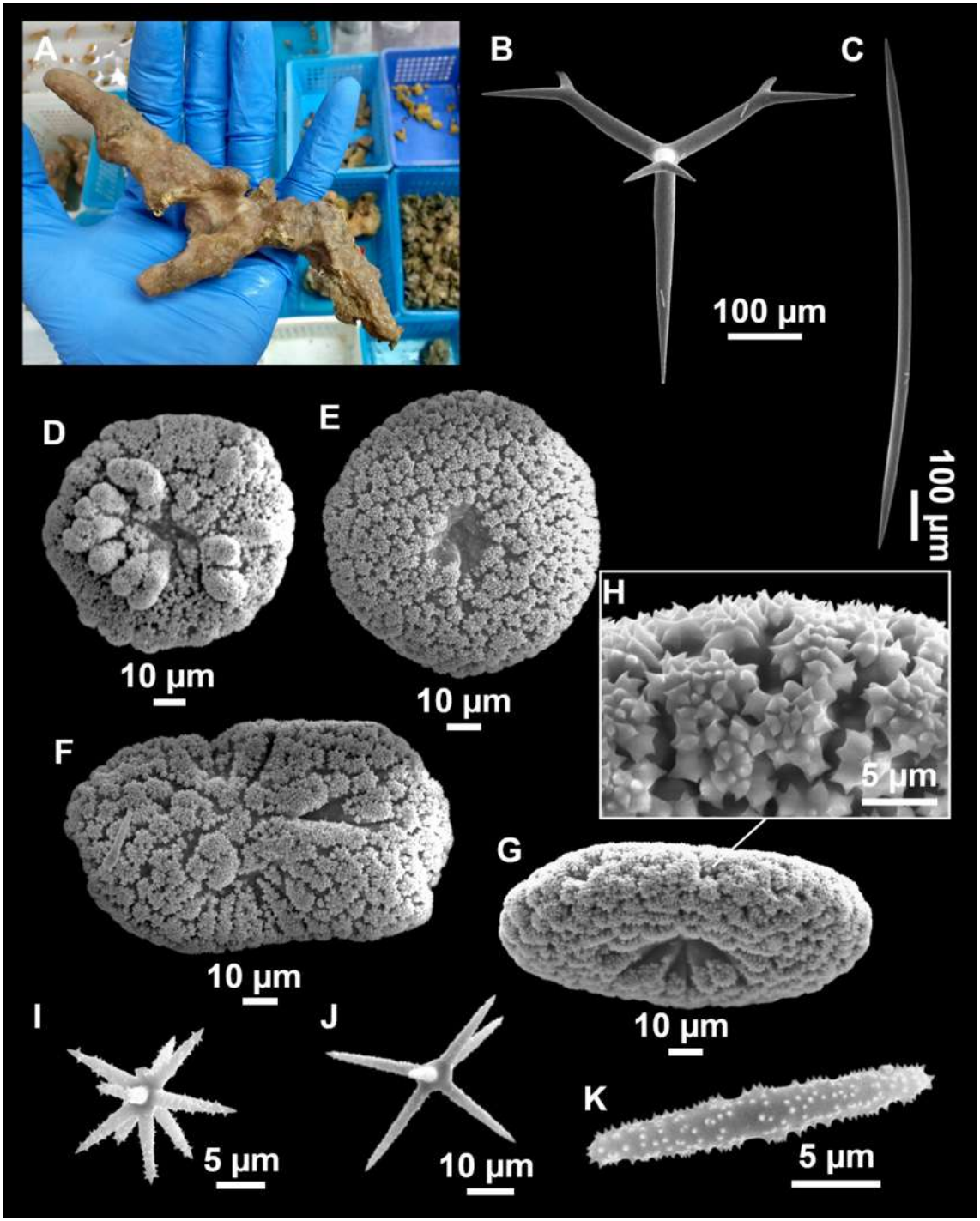

Figure 4.3.21. *Erylus* cf. *mamillaris* (*Schmidt, 1862*). (A) Habitus of i314 on deck. (B–K) SEM images of i179_1. (B) Dichotriaene. (C) Oxea. (D–H) Aspidasters with (H) detail of rosettes. (I–J) Oxyasters. (K) Microrhabd.

Genetics

Folmer COI (ON130529) and 28S C1-C2 (ON133884) obtained from specimen i329_B.

Taxonomic remarks on *Erylus discophorus, E. mamillaris* and *E. deficiens*

E. mamillaris, *E. discophorus* and *E. deficiens* form a poorly understood complex of Mediterranean and Northeast Atlantic species with similar spicule sets: dichotriaenes,

spiny microrhabds, spiny oxyasters and aspidasters (*Sollas, 1888; Topsent, 1927, 1928; Cárdenas et al., 2011; Cárdenas, 2020*). The conspecificity of specimens assigned to one or the other species have been extensively debated in the literature (*Sollas, 1888; Lendenfeld, 1894; Marenzeller, 1889; Topsent, 1901, 1928; Pulitzer-Finalli, 1972*). A character proposed to differentiate these three species are aspidasters size, morphology and abundance: larger and more elongated in *E. mamillaris* vs. small and more rounded in *E. discophorus* and extremely scarce to absent in *E. deficiens* (*Topsent, 1928*). We note that this has some consequences on the rosette arrangement of aspidasters in the three species, giving more of a radial pattern in *E. discophorus*, a more regular pattern in *E. mamillaris* and a more irregular/disorganized pattern in *E.* cf. *deficiens*. Also, the size and abundance of microrhabds seem to differ between species, being smaller and less common in *E. mamillaris* and larger and more common in *E. discophorus* (*Sollas, 1888; Lendenfeld, 1894*) and *E. deficiens* (*Topsent, 1928; Vacelet, 1976*; cf. holotype redescription in Table 4.3.8). *Lendenfeld (1894)* also mentioned microrhabd morphology as a significant character, being more heterogeneous in *E. discophorus* than in *E. mamillaris* (with pointed and rounded variations). In the same work, the presence of differently spined to smooth microrhabds in *E. discophorus* is also mentioned (see Table 4.3.8 for details). The Balearic specimens were identified primarily according to aspidaster characters, then the microrhabds were carefully compared (Table 4.3.8). Microrhabds are indeed shorter in *E. mamillaris* (15-31 vs. 14-68 µm). A second rare category of microrhabds (microrhabds II) was found in *E. discophorus*: larger, smooth to minutely spined. These microrhabds II tend to have pointed tips, close to those drawn by *Lendenfeld* (*1894*, Taf III fig 41a). This rare spicule type is not singled out in previous descriptions (Table 4.3.8) maybe because they are too rare and not easily spotted; for instance, we could not find them in the paratype of *Scutastra cantabrica*. So we are hesitant to consider them as a specific character of *E. discophorus*. However, microrhabds II were absent in all *E. mamillaris* and *E. deficiens* specimens examined, and must be taken into account for a future revision of the types and this species complex.

Regarding spicule size variation in *E. discophorus*, the deeper specimen POR785 had wider oxeas, triaenes and microrhabds and larger oxyasters than the cave specimens (LIT71, LIT72, LIT74). This may be explained by ecophysiological differences, deeper specimens are usually subjected to higher silica concentrations and therefore larger spicules, a phenomenon well described in the Geodiidae (*Cárdenas & Rapp, 2013*). There may be other parameters at play: fishing grounds near Columbrets are a more eutrophic habitat than shallow caves of Mallorca, mainly because of the influence of the river inflows from the Iberian Peninsula.

Macroscopically, *E. deficiens* tends to be described as having a massive lobated external morphology with one single large oscule at the summit of each lobe, and a dark smooth cortex (*Topsent, 1928*). The species was first considered a variety of *E. discophorus* by Topsent, but later erected as a valid species. It was described in Madeira (at 100 m depth), and later collected in the Gorringe Bank (*Xavier & van Soest, 2007*) and the Ligurian Sea (*Topsent, 1927; Vacelet, 1976*). The most remarkable character of *E. deficiens* is the rarity to complete absence of aspidasters. Moreover, *Topsent (1928)* mentions the higher abundance of microrhabds in *E. deficiens* than in *E. discophorus*, to

Table 4.3.8. Spicule measurements of *Erylus discophorus* (Schmidt, 1862)*, E. mamillaris* (Schmidt, 1862) and *E. deficiens*, given as minimum-mean-maximum for total length/minimum-mean-maximum for total width; all measurements are expressed in µm. Specimen codes are field#. Rh: rhabdome; Cl: clad; pc: protoclad; dc: deuteroclad; -=not found/not reported; EB: Emile Baudot.

Material	**Depth** (m)	**Macroscopical morphology**	**Oxeas** (length/width)	**Orthotriaenes** Rhabdome (length/width) Clad (length/width)	**Dichotriaenes** Rhabdome (length/width) Protoclad (length/width) Deuteroclad (length/width)	**Aspidasters** (diameter)	**Spined microrhabds (I)** (length/width)	**Smooth microrhabds (II)** (length/width)	**Oxyasters** (length)
E. discophorus holotype Lesina (Adriatic) (*Sollas, 1888; Topsent, 1928**)	-	Irregular, flattened, tuberose mass. Cortex 0.2-0,25 mm thick. Black internally because of pigment-cells in the cortex	1060-1240/35	-	Rh: 556/52 Pc: 127-143/- Dc: 175-368/-	84-106/77 15 thick (thin, circular or elliptical) 65 (all circular)*	28/3.5 13-45/2-5*	-	46 3-12 actines
E. discophorus Adriatic (*Pulitzer-Finalli, 1983*)	0-30	Small, encrusting or insinuating. Color in life white, cream, brownish.	500-1600/-	-	Rh: 250-750/- Pc: - Dc: -	40-110	12-60	-	12-40
***E. discophorus* POR785 Columbrets**	144	Massive, large, fleshy, rounded body with bulbous processes. Beige color. Dark ring surrounding the oscula	600-777-978/6-21-29 Styles: 650/25 (N=1)	Rh: 135-464/9-18 Cl: 96-164/7-17 (N=3)	Rb: 217-390-557 (N=5)/13-34-62 Pc: 57-80-95/12-32-52 Dc: 49-162-262/8-27-44	64-76-95/ 45-60-71 (most circular, some subcircular)	14-22-50/1-3-5 (abundant)	46-54-68/4-5-6 (N=10)	10-23-29 (4-11 actines)
***E. discophorus* LIT71 Coves de na Dana (Cave)**	0-1	Encrusting, whitish	458-624-734/5-11-16 Styles: 384-541/10-12 (N=3) Strongyles: 402-466/11-13 (N=3)	-	Rb: -/8-20 Pc: 46-82/7-15 Dc: 10-109/3-12 (N=5)	40-47-54 (N=14) (most circular, some subcircular)	19-33-55/1-2-3 (abundant)	61-70-89/3-3-3 (N=6)	7-15-30
***E. discophorus* LIT72 Coves de na Dana (Cave)**	0-1	Encrusting, whitish	388-480-652/5-9-11 (N=15) Styles: 439/12 (N=1) Strongyles: 183-351/16-17 (N=2)	Rb: -/10 Cld: 105/8 (N=1)	Rb: 123-273 (N=3)/8-21 (N=8) Pc: 48-70-111/8-12-17 (N=11) Dc: 19-57-91/6-10-14 (N=11)	33-48-71	16-26-46/1-2-3 (abundant)	45-58-76/2-3-5 (N=21)	6-14-21
***E. discophorus* LIT74 Coves de na Dana (Cave)**	0-1	Encrusting, whitish	580-764-956/8-14-22 Styles: 647/25 (N=1) Strongyles:	-	Rb: 221-360-508/17-21-26 (N=5) Pc: 52-80-100/9-18-31 (N=15) Dc: 46-95-172/8-14-23 (N=15)	44-73-92	17-38-68/2-3-5 (abundant)	41-63-86/4-4-5 (N=9)	8-19-30 (5-12 actines)

			385-796/11-22 (N=4)						
E. discophorus Bay of Naples (cave) (*Pulitzer-Finalli, 1972*)	2	Very small, cushion-shaped, white with brown shades	480-915/10-17 Styles: 400-710/12-18.5 Strongyles: 355-515/14-20	-	Rh: 150 pm, Cladome: 400	37-57/ 37-49	24-62	-	8-24 (5-12 actines)
***Scutastra cantabrica* paratype NHM 30.1.21.5 Santander Spain**	-	Massive	449-677-938/ 4-10-14	-	Rb: 137-205-260 (N=5)/7-10-13 (N=11) Pc: 85/- (N=1) Dc: 52/- (N=1)	32-41-50 (ellipsoidal, underdeveloped)	21-38-70/1.5-4 (most are centrotylote)	-	18-26-40
E. mamillaris holotype Adriatic NHM slide by Sollas (1888) Strasbourg slide by *Topsent (1928)** NHM slide by *Uriz (2002)***	-	Massive lobes, each with a single large oscule at the extremity. External color is black	1500/32 750-1500/ 18-32**	-	Rh: 716/44 Pc: 90/36 Dc: 90 Rh: 532-717/25-44 Pc: 90/32-35 Dc: 60-90/-**	77.5-106/43-51.6 (ellipsoidal) 70-80/38-42 (circular to elongated)* 62-106/29-52 (ellipsoidal to more elongated)**	23.7/4 11-18/2 13-24/2-4 (occasionally centrotylote)**	-	19 14-28^**
E. mamillaris Bay of Naples (cave) (*Pulitzer-Finalli, 1972*)	1	Fragment, brown	610-(700-900)-1420/ 16-20-32	-	Rh: 280-700/20-40 Pc: 70-110 Dc: 25-260	70-89-105/ 35-47-60 20-30 thick	16-22-29/2-2.5	-	13-23 (6-12 actines)
***E.* cf. *mamillaris* ZMAPOR 20421 Faial, Azores**	2-8	Massive, dark color	465-833-1126/ 7-20-30	Rh: - Cl: 92-225 (N=3)	Rb: 182-415-612/13-30-45 (N=21) Pc: 62-90-127/- Dc: 23-131-200/-	77-85-102/ 32-50-42 (all elongated)	11-16-24/<2.5	-	11-16-24
E. cf. *mamillaris* Faial, Azores (*Boury-Esnault & Lopes, 1985*)	6-10	Massive, lobated	spA: 320-642-1166/ 6-16-26 spB: 288-506-736/ 5-10-13	-	Rb: 253-275-281/ 4-5-6 Pc: 77-83-96/3-5-6 Dc: 32-67-83/3-4-6	spA 68-90-94/ 36-43-55 spB 30-42-50/ 25-32-38	spA 16-20-26/ 3-3-5 spB 16-20-23/ 3-3-3	-	spA 13-17-23 spB 8-12-13
***E.* cf. *mamillaris* i329_B EB**	152	Massive	429-817-1037/ 5-19-28 (N=5)	-	not measured	64-85-109/ 33-67-91	15-20-24/1-2-3 (few)	-	14-29-56 (6-13 actines)
***E.* cf. *mamillaris* i179_A EB**	138	Small massive	699-843-949/ 7-17-24 (N=6)	-	Rb: 335 (N=1)/27-40-57 (N=5) Pc: 115-133-151/27-34-52 (N=5)	69-97-121/ 43-68-86	18-24-31/2-3-4 (few)	-	17-35-50 (4-13 actines)

					Dc: 119-139-161/19-27-39 (N=5)				
E. deficiens **holotype MNHN DT1111 Madeira**	100	Massive, very large, lobated, large, upper part black	510-726-969/ 3-6-10	-	Rb: 175-229-360 (N=9)/7-9-15 (N=14) Pc: 25-52-72/- (N=7) Dc: 25-54-132/- (N=7)	20-31-55 (mostly discoidal, underdeveloped)	17-37-80/>2.5 (very abundant)	-	8-15-22
E. deficiens **ZMAPOR 21693 Gorringe Bank**	32	Massive, large	316-513-643/ 2-6-9	-	Rb: 84-208-303/3-5-8 (N=16) Pc: 157/- (N=1) Dc: 121/- (N=1)	-	22-35-52/thin	-	8-14-30
E. deficiens **ZMAPOR 20419 Madeira**	7	Massive, black	400-749-918/ 2-7-10	Cld: 75-88-125 (N=7)	Rh: 107-211-275 (N=4)/ 4-7.6-12 (N=12) Pc: 50-55-62 (N=5) Dc: 45-54-65 (N=5)	27-37-49 (N=3) (very rare)	17-32-80/<2.5 (thin, not centrotylote)		9-14-29
E.* cf. *deficiens **LIT10 Caló den Rafelino (Cave)**	0	Small encrusting	280-503-647/ 4-11-17	Rb: 76 (N=1)/8-11 (N=4) Cld: 61-133/6-10 (N=4)	Rb: 145-182 (N=4)/8-17-26 Pc: 47-67-86/8-14-25 Dc: 11-79-135/4-11-18	31-42-56 (N=13)	22-36-55/2-3-6	-	12-21-36
E. cf. *deficiens* Port-Cros, France (*Vacelet, 1976*)	10-42	Massive, large	450-850/ 5-10	-	Rh: 160-320/5-10 Pc: 40-120/5 Dc: 70-110	25-30 or 25-30/30-40 (discoidal to ellipsoidal) (very rare or absent)	15-32 (up to 50) (abundant)	-	7-17

1946

1947

compensate the deficit of aspidasters (the more aspidasters the less microrhabds and vice versa). *Topsent (1928)* also proposed growth habit as a character to separate both species: *E. deficiens* being much larger with lobate processes and *E. discophorus* encrusting and smaller. A spicule slide (MNHN DT 1111) of the holotype of *E. deficiens* from Madeira was compared with specimens morphologically identified as *E. deficiens* from Gorringe Bank (ZMAPOR 21693) (*Xavier & van Soest, 2007*), Madeira (ZMAPOR 20419) and our cave specimen (LIT10). All specimens were massive except for the encrusting Mallorcan specimen; spicule sizes were all quite similar (Table 4.3.8). Microrhabds were similar as in *E. discophorus* but comparatively slightly shorter and thinner.

Type material of *S. cantabrica* from the Northern coast of Spain (Santander, Cantabria) is reexamined here for the first time: a new spicule slide was made and spicules measured (Table 4.3.8). Shape and size of the spicules conform to those of *E. discophorus*, except for irregular megascleres and the discoid aspidasters which are common but slightly smaller (32-41-50 µm in diameter) and underdeveloped (actines not fused). Such underdeveloped aspidasters and irregular megascleres are actually not uncommon in several *E. discophorus* specimens from Banyuls, France (*Boury-Esnault & Lopes, 1985*) or Portugal (*Cárdenas & Rapp, 2013*, Fig. 4.3.12A) and could be linked to low silica concentrations (*Cárdenas & Rapp, 2013*). We therefore confirm the suggestion of *Boury-Esnault & Lopes (1985)* in considering *S. cantabrica* a junior synonym of *E. discophorus*. Another specimen from Madeira identified as *S. cantabrica* by *Burton (1956)* was also re-examined: it has abundant aspidasters (discoidal to elongated, some underdeveloped, 30-55 µm), oxyasters (8-22 µm), mostly straight non-centrotylote spiny microrhabds and regular megascleres: it is therefore re-identified as a typical *E. discophorus*.

Cárdenas et al. (2011) had shown that these three *Erylus* species were genetically very close. The present study enriches the sequence sampling to further test the validity of these species. The COI tree (Fig. 4.3.19A) is more informative than the 28S tree because we only obtained the more conserved 28S (C1-C2) region which showed no bp differences between the species (Fig. 4.3.19B), so in this case we will only discuss the COI tree. In the COI tree, *E. discophorus* specimens POR785, LIT71, LIT72 and LIT74 strongly group together in a cluster that also includes *Erylus* sp. (EU442206) from Portugal (6 m depth), and *E. discophorus* (HM592692) from Slovenia (5 m). The cluster includes several haplotypes differentiated by 0-2 bp differences. This number of bp differences in COI may indicate the presence of two cryptic species, but also be caused by intraspecific variability. It is far beyond the scope of the present work to elucidate this, and future works with a more extensive sampling shall be conducted. Identical COI sequences were obtained for the encrusting LIT71 and the massive deeper POR785 suggesting that shape is not a diagnostic character. More variable genetic markers would be needed to see if they could be ecotypes. A second paraphyletic group is represented by Atlantic specimens *E.* cf. *mamillaris* (Azores, 7 m) and two *E. deficiens* (Gorringe Bank, 32 m and Madeira, 7 m) with 1 bp. difference. *E.* cf. *mamillaris* has 2 bp differences with both *E. deficiens* sequences. A third group is only represented by the cave Mallorca specimen LIT10 identified as *E.* cf. *deficiens*, which is 6-8 bp different from the other sequences. Since the type locality of *E. deficiens* is Madeira, we can be more or less confident that our specimens sequenced from Gorringe and Madeira are

closer to the type locality. This suggests that LIT10 most probably represents a new species from the Mediterranean Sea. However, the difficulty to find clear diagnostic morphological characters and the presence of only one specimen pushes us to delay a new species description. This result also suggests that the character of rare aspidasters may have appeared in different lineages of *Erylus* independently. Finally, the COI sequence of specimen *E.* cf. *mamillaris* i329_B diverges alone, clearly apart from another *E* cf. *mamillaris* from the shallow Azores. This suggests that slightly elongated aspidasters and small microrhabds may not be good specific characters either. All the deep specimens collected from the EB seamount (i179_1, i179_2, i314, i329_A and i329_C) shared the same spicular characters so they must all belong to the same species, which may be conspecific with *E. mamillaris* from the Adriatic Sea. However, comparison with type material would be necessary to address this matter in future works.

Altogether, these phylogenetic results cast doubt on the current spicule characters (aspidaster morphology mainly) used to discriminate these species. To our knowledge, this is the first time such a sponge species complex is revealed in the Mediterranean Sea with many COI haplotypes from populations from different depths and habitats. Additional genetic markers and specimens from these different populations will be necessary to resolve the *Erylus discophorus/mamillaris/deficiens* complex.

Erylus corsicus **Pulitzer-Finali, 1983**

(Figs. 4.3.19 and 4.3.22; Table 4.3.9)

Material examined

UPSZMC 190845, field#i707, St. 45 (INTEMARES0720), MaC (EB), 150 m, beam trawl, coll. J. A. Díaz; UPSZMC 190841, field#i389_1, MaC (EB), St. 158 (INTEMARES1019), beam trawl, coll. J. A. Díaz; UPSZMC 190840, field#i356_A, MaC (EB), St. 136 (INTEMARES1019), beam trawl, coll. J. A. Díaz; UPSZMC 190843, field#i402_B, MaC (EB), St. 167 (INTEMARES1019), 151 m, beam trawl, coll. J. A. Díaz.

Comparative material

Erylus corsicus, holotype (slide), MSNG 47157 (NIS.85.14), off Calvi (Corsica), 121-149 m, 14 July 1969.

Erylus papulifer Pulitzer-Finali, 1983, holotype, MSNG 47155 (NIS.19.4a), wet specimen, off Calvi Corsica, 135 m, 18 July 1975; paratype, MSNG 47156 (NIS.19.4c), same locality as holotype.

Erylus expletus Topsent, 1927, holotype, MNHN DT837 and DT1326, two slides, off Säo Jorge, Azores, 1 Aug. 1895, St. 616, 1022 m; ZMAPOR 18142, SE of Rockall Bank, West coast of Ireland, 55º30’13.93’’N, 15º47’6.18’’W, 679 m, 2 Sept. 2004, coll: R. van Soest, field# M2004/33-05, id. P. Cárdenas, COI: EU442208.

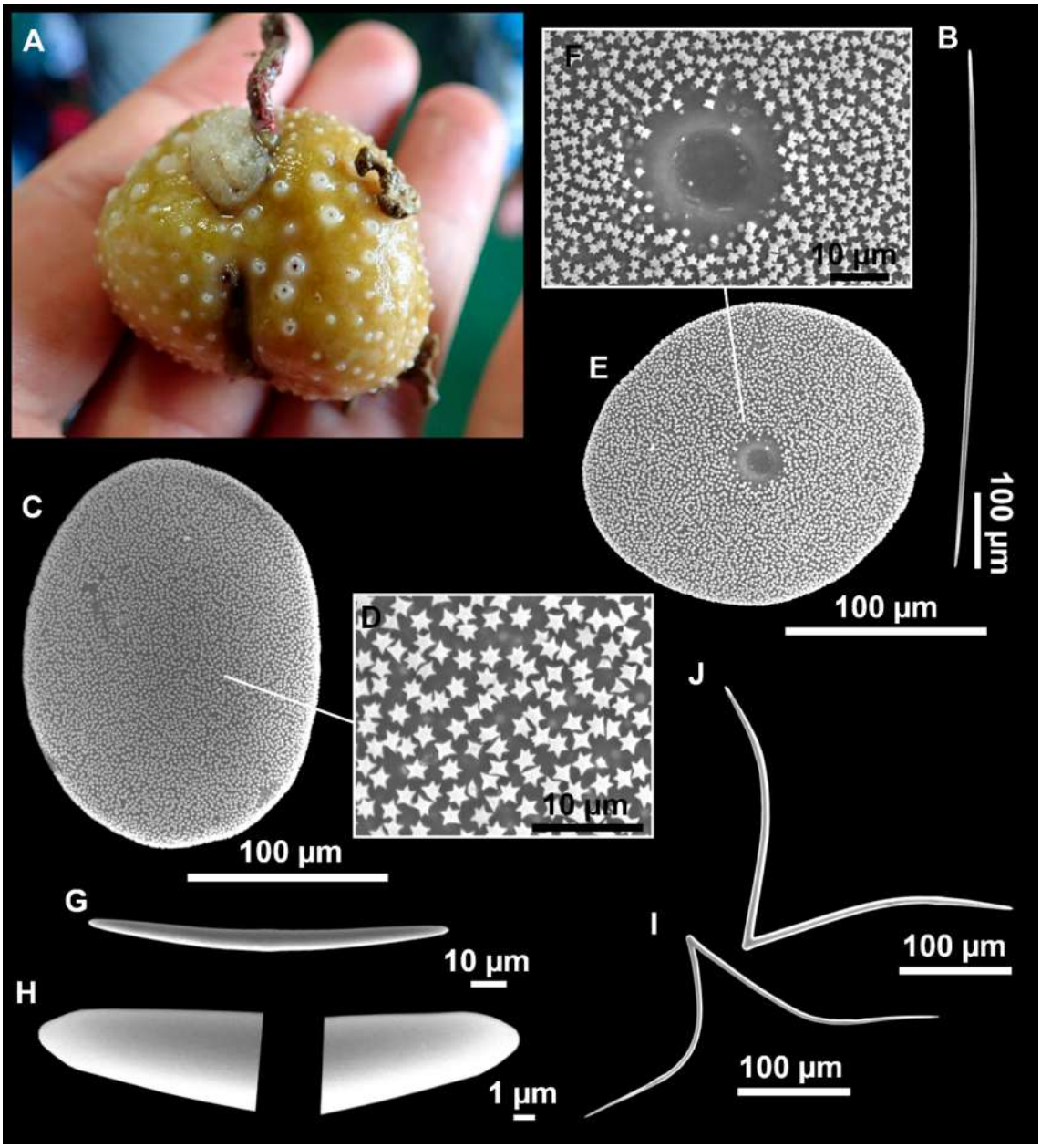

Figure 4.3.22. *Erylus corsicus* Pulitzer-Finali, 1983, specimen i707. (A) Habitus on deck. (B–J) SEM images. (B) Oxea. (C–F) Aspidasters with (D–F) detail of the rosettes and hilum. (G) Microrhabd with (H) detail of microrhabd tips. (I–J) Toxas.

Outer morphology

Massive globular sponges, 1 to 3.5 cm in diameter (Fig. 4.3.22A). Hard, slightly compressible cortex, fleshy choanosome. After fixation in EtOH, the choanosome contracts and tends to get separated from the cortex, which remains resilient. Beige color in life, some individuals have a brownish tinge in localized areas, product of diatom colonization. The brownish stains disappear after EtOH fixation, and then both cortex and choanosome are beige. Small abundant openings, often with a lighter colored ring, scattered all over the surface, 0.1-1 mm in diameter.

Table 4.3.9. Spicule measurements of *Erylus expletus*, *E. corsicus* and *E. papulifer*, given as minimum-mean-maximum for total length/minimum-mean-maximum for total width; all measurements are expressed in µm. Specimen codes are field#. Rh: rhabdome; Cl: clad; pc: protoclad; dc: deuteroclad; -:not found/not reported; EB: Emile Baudot.

Material	**Depth** (m)	**Oxeas** (length/width)	**Triaenes** Rhabdome (length/width) Protoclad (length/width) Deuteroclad (length/width) Clad (lenght/width)	**Aspidasters** (length/width)	**Toxas** (length/middle width)	**Microrhabds** (length/width)
E. corsicus **holotype** **MSNG 47157** **Corsica**	121-149	448-782-1132/ 6-11-20	Rh: 176/6 Cl: 109/5 (N=1) (orthotriaenes)	146-185-249/84-127-155 Ratio 1.2-2.0 (many irregular)	122-195-279/3-6-9 (2 actined, N=18) 136/3 (3 actined, N=1)	39-103-143/2-5-9
E. corsicus **i707** **EB**	147	571-943-1203/9-15-19	Rh: 654/18 Cl: 323/20 (N=1)	172-215-250/139-164-202 Ratio 1.1-1.5 (mostly regular)	296-425/7-10 (2-actined, N=7)	42-91-171/ 4-6-10
E. corsicus **i356_A** **EB**	146	534-1055-1342/ 6-17-25	-	133-183-230/106-145-181 Ratio 0.9-2.1 (many irregular)	204-346/6-8 (2-actined, N=6) (rare)	35-73-136/ 3-5-8
E. corsicus **i402_B** **EB**	151	616-1152-1371/ 6-16-21	Rh: 340-578/12-31 (N=3) Cl: 172-387/11-31 (N=4) One stylote end modification	144-200-227/120-158-185 Ratio 1.1-1.5 (mostly regular)	270/8 (1-actined N=1) (rare)	44-99-165/ 2-5-9
E. papulifer **holotype** **MSNG 47155** **Corsica**	135	633-1034-1355/ 13-16-22	Rh: -/28-43 Pc: 152-238/24-33 Dc: 178-318/19-28 (N=8) (mostly dichotriaenes)	150-175-192/114-150-173 Ratio 1.0-1.5 20-30 thick (subspherical)	117-167/7-9 (1 actined, N=4) 68-135-201/4-7-11 (2 actined) 96-149/3-7 (3 actined, N=8) 66/4 (4 actined, N=1)	46-60-70/ 3-4-5
E. papulifer **paratype** **MSNG 47156 (Nis19.4c)** **Corsica**	135	1033-1235-1462/ 12-17-24 (N=18)	Rh: 541-606 (N=2)/20-43 (N=9) Pc: 151-236/11-32 Dc: 126-353/12-28 (N=9) (mostly dichotriaenes)	136-178-195/114-139-157 Ratio 1.1-1.5 (oval to lemon shaped)	67-133-184/3-6-11 (2 actined, N=20) 112-140/4-7 (3 actined, N=2)	52-67-86/ 2-4-6
E. papulifer **paratype** **MSNG 47156 (Nis19.4b)** **Corsica**	135	548-1090-1451/ 9-15-19 (N=19)	Rh: -/18-u-31 Pc: 205-221-238/16-21-29 Dc: 91-152-236/12-15-20 (N=4) (mostly dichotriaenes) Rh: 186/27 Cl: 281/22 (N=1; orthotriaene)	150-172-199/116-135-149 Ratio 1.2-1.4	74-103-155/2-5-8 (2 actined, N=13) 72-99-121/2-3-6 (3 actined, N=6)	49-59-74/ 3-4-6
E. papulifer Marseille caves, France (*Pouliquen, 1972*)	2-10	350-900/ 10-12	Rh: (short) Cl: 320 Pc: 100-120 Dc: 130-150 (ortho- and dichotriaenes)	90-160/-	120-180/-	30-80/3-5

Spicules

Orthotriaenes, very scarce, cladi curved outwards and rhabdome straight. Rhabdome: 340-654/12-31 µm. Cladi: 172-387/11-31 µm.

Oxeas (Fig. 4.3.22B), slightly curved and fusiform, 534-1371/6-25 µm.

Aspidasters (Fig. 4.3.22C-F), discoid to elongated but most are oval, being up to two times longer than wider. Underdeveloped or aberrant forms are present, more or less common depending on the specimen. Rosettes of type 3 (Fig. 4.3.22D) *sensu Cárdenas (2020)*; well defined hilum (Fig. 4.3.22F). On average, length: 133-250 µm, width: 106-202 µm.

Microrhabds (Fig. 4.3.22G-H), on a wide size range, smooth, slightly curved and faintly centrotylote, 35-171/2-10 µm.

Toxas (Fig. 4.3.22I-J), scarce, most 2-actined, rarely 3-actined. With a central swelling, overall measuring 204-425/6-10 µm.

Ecology notes

Species found at the summit of the EB, between 146-151 m, on sandy sedimentary bottoms. The species is always covered by a brownish coating produced by diatom aggregations (observation with microscope). The diatoms seem to be favored by the smooth surface that offers the aspidasters on its external side, acting as substrate.

Genetics

COI was obtained from specimens i707 (ON130536) and i402_B (ON130537) while the 28S (C1-C2) fragment has only been obtained from specimen i707 (ON133851).

Taxonomic remarks

Thought to be divergent reduced oxyasters (*Topsent, 1928*), toxas are a rare spicule type in *Erylus* species. And yet, three very similar *Erylus* with toxas are recorded from the Mediterranean Sea: *E. corsicus, E. papulifer* and *E. expletus* (this last one is also reported from the Northeast Atlantic). The type material of these three species was compared here for the first time to test their validity and to compare with our material (Table 4.3.9). *E. expletus* is the first one to be described, from the deep waters of the Azores, 1022 meter depth (*Topsent, 1927, 1928*) and subsequently from Rockall Bank (*van Soest et al. 2007*), shallow waters of the Canary Islands (*Cruz, 2002*) and underwater caves around Marseille, France (*Pouliquen, 1972*). *E. papulifer* is based on six specimens collected from mesophotic depths in Corsica (*Pultizer-Finali, 1983*). The type material has been re-examined here (Fig. 4.3.23A-K): they are subglobular sponges, the holotype measures 2.5 cm in diameter (Fig. 4.3.23A) while paratypes measure about 1 cm in diameter. They have a hard but breakable consistency, slightly compressible. Color after formalin fixation is dirty beige with orangish pink (peach) areas. Small abundant openings are scattered all over the surface, 0.1-1 mm in diameter. In terms of external morphology, *E. expletus* (*Topsent 1928*, Pl. I, fig 20), *E. papulifer* (Fig. 4.3.23A) and our material (Fig. 4.3.22A) are very similar. Actual differences between *E. papulifer* and *E. expletus* were not clearly stated by *Pultizer-Finali (1983)* except for "*the shape and size of aspidasters*". *E. corsicus* is also described by *Pulitzer-*

Finali (1983), based on a single tiny specimen, which was completely digested to make a single spicule

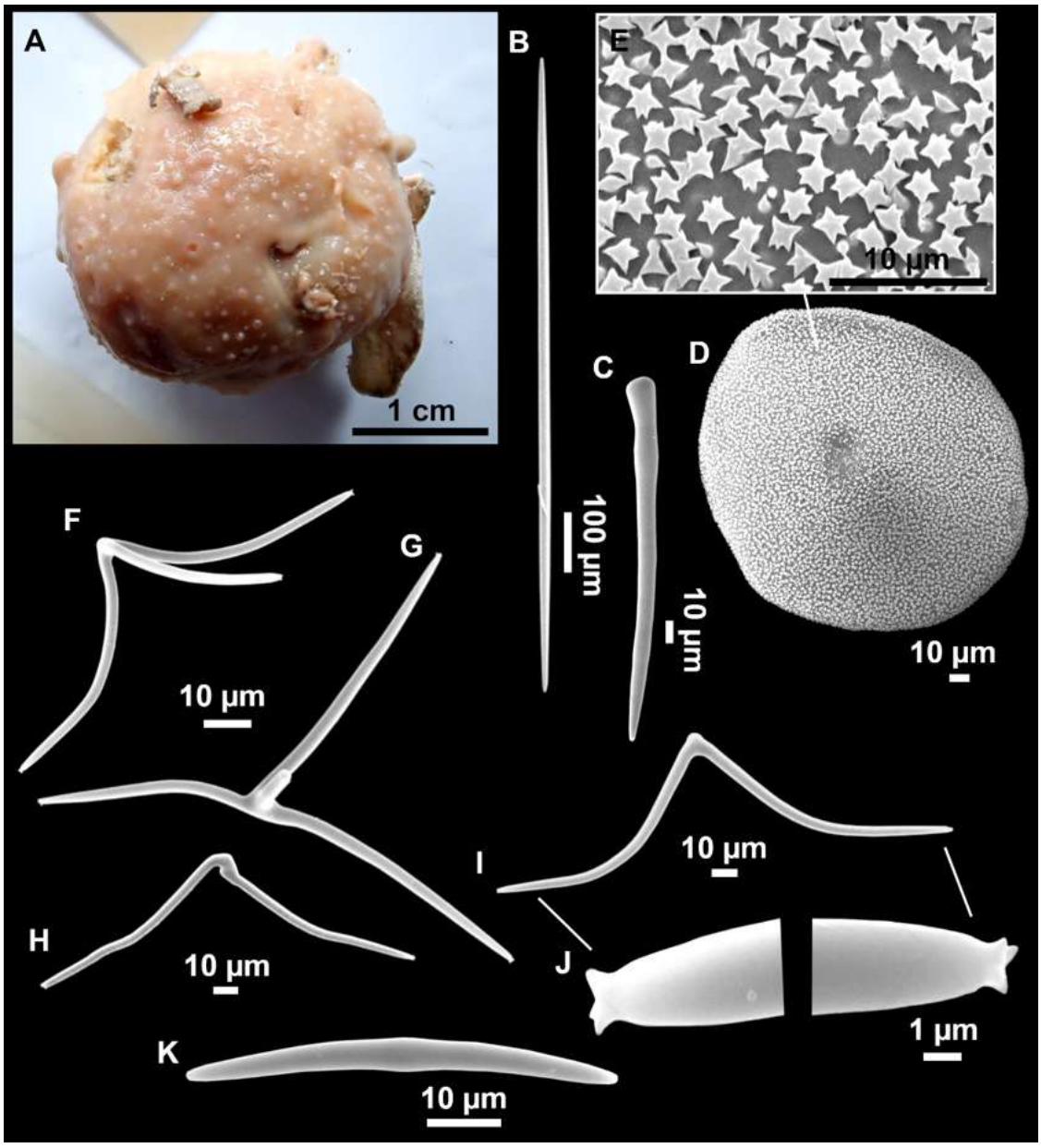

Figure 4.3.23. Holotype of *Erylus papulifer Pulitzer-Finali, 1983*, MSNG 47155, Corsica. (A) Habitus, for-malin preservation. (B) Oxea. (C) Style. (D) Aspidaster with (E) detail of the rosettes. (F–J) Oxyasters with (J) detail of the spurs at oxyasters tips. (K) Microrhabd.

preparation, which was examined here. The *E. corsicus* specimen was collected in the same dredge as several *E. papulifer* specimens. *Pulitzer-Finali (1983)* based *E. corsicus* on having larger and more irregular aspidasters than *E. papulifer*, and a wider length range of microrhabds (48-160 µm vs. 50-80 µm in *E. papulifer*).

After careful observation and measurements of spicules (Table 4.3.9), we first note that *E. papulifer* is the only species with dichotriaenes while *E. expletus* and *E. corsicus* have very few orthotriaenes. *E. expletus* seems to be discriminated by i) a majority of aspidasters with a characteristic lemon-shape (*Topsent, 1928*, pl. V, fig. 10), while *E. corsicus/papulifer* have oval to lemon-shape or irregular aspidasters (Fig. 4.3.22C-E and

Fig. 4.3.23D), ii) two separate sizes of microrhabds vs. only one in *E. corsicus/papulifer* (Fig. 4.3.22G and Fig. 4.3.23K) and iii) absence of 3-actin toxas (in the holotype), which are present in *E. corsicus/papulifer,* but quite rare (Fig. 4.3.23F), which makes this third character difficult to use. Following the two first characters mentioned, our material is not *E. expletus*. No 3-actin toxas were found in our material but since they can be quite rare, we may have missed them. Then our material shares some characters with *E. corsicus* and some with *E. papulifer*. As in *E. corsicus*, our material has rare orthotriaenes, irregular aspidasters (not in all our specimens), and larger aspidasters, toxas and microrhabds. As in *E. papulifer,* some of our specimens have mostly regular aspidasters and have 1-actin toxas. This suggests that the irregular aspidasters may be due to the environment and therefore would not be a reliable specific character. SEM observations of toxas in the holotype of *E. papulifer* revealed spines at the tips of the actines (Fig. 4.3.23I-J), which were not present in our material (Fig. 4.3.22I-J) or in *E. expletus* from Rockall Bank (data not shown). This new character needs further confirmation in order to consider it as diagnostic. All things considered, our specimens were identified as *E. corsicus*, the second report of *E. corsicus* after its original description. However, the validity of *E. corsicus* originally based on a single tiny specimen from the same locality as *E. papulifer* remains dubious and would need to be further tested with additional material, and more importantly genetic sequences from other Mediterranean populations. In the Mediterranean Sea, *E. expletus* has been reported from shallow water caves off Marseille, France (*Pouliquen, 1972*). Since the Marseille specimens have smaller aspidasters, toxas and oxeas than *E. expletus* and only one size of microrhabds, we propose that they are instead *E. papulifer*, thus restricting *E. expletus* to the North Atlantic. More specimens and sequences of *E. expletus, E. papulifer* and *E. corsicus* are now necessary to test the robustness of these spicular characters. The COI tree currently confirms that our *E. corsicus* and *E. expletus* are different but very close species with only a 3 bp difference (Fig. 4.3.19A). The phylogenetic position of *E. corsicus/E. expletus* within the Erylinae is still ambiguous and not supported (Fig. 4.3.19).

Genus *Penares* Gray, 1867

Penares euastrum (Schmidt, 1868)

(Figs. 4.3.19 and 4.3.24; Table 4.3.10)

Material examined

UPSZMC 190921-190922, field#i142_A-i146_4, St. 51 (INTEMARES0718), MaC (EB), 128 m, beam trawl, coll. J. A. Díaz; UPSZMC 190924, field#i524_b, St. 17 (INTEMARES0720), MaC (AM), 113 m, beam trawl, coll. J. A. Díaz; UPSZMC 190926-190927 and UPSZMC 190920, field#i528-529 and field#i530, St. 18 (INTEMARES0720), MaC (AM), 112 m, coll. J. A. Díaz, beam trawl; UPSZMC 190928, field#POR469, St. 219 (MEDITSES052017), Son Bou (South-west of Menorca), 65 m, GOC-73, coll. J. A. Díaz; UPSZMC 190929, field#POR932_1, St. 74 (MEDITSES052020), Favàritx (Northeast off Menorca), 75 m, GOC-73, coll. J. A. Díaz; UPSZMC 190930, field#POR975, St. 78 (MEDITS052020), Ciutadella (West off Menorca), 56 m, GOC-73, coll. J. A. Díaz; UPSZMC 190931, field#POR1141, St. 185 (MEDITS052021), Sa Costera (North of Mallorca), 61 m, GOC-73, coll. J. A. Díaz;

UPSZMC 190932, field#POR1253, St. 02 (MEDITS0521_PITIUSSES), South of Formentera, 54 m, GOC-73, coll. J. A. Díaz.

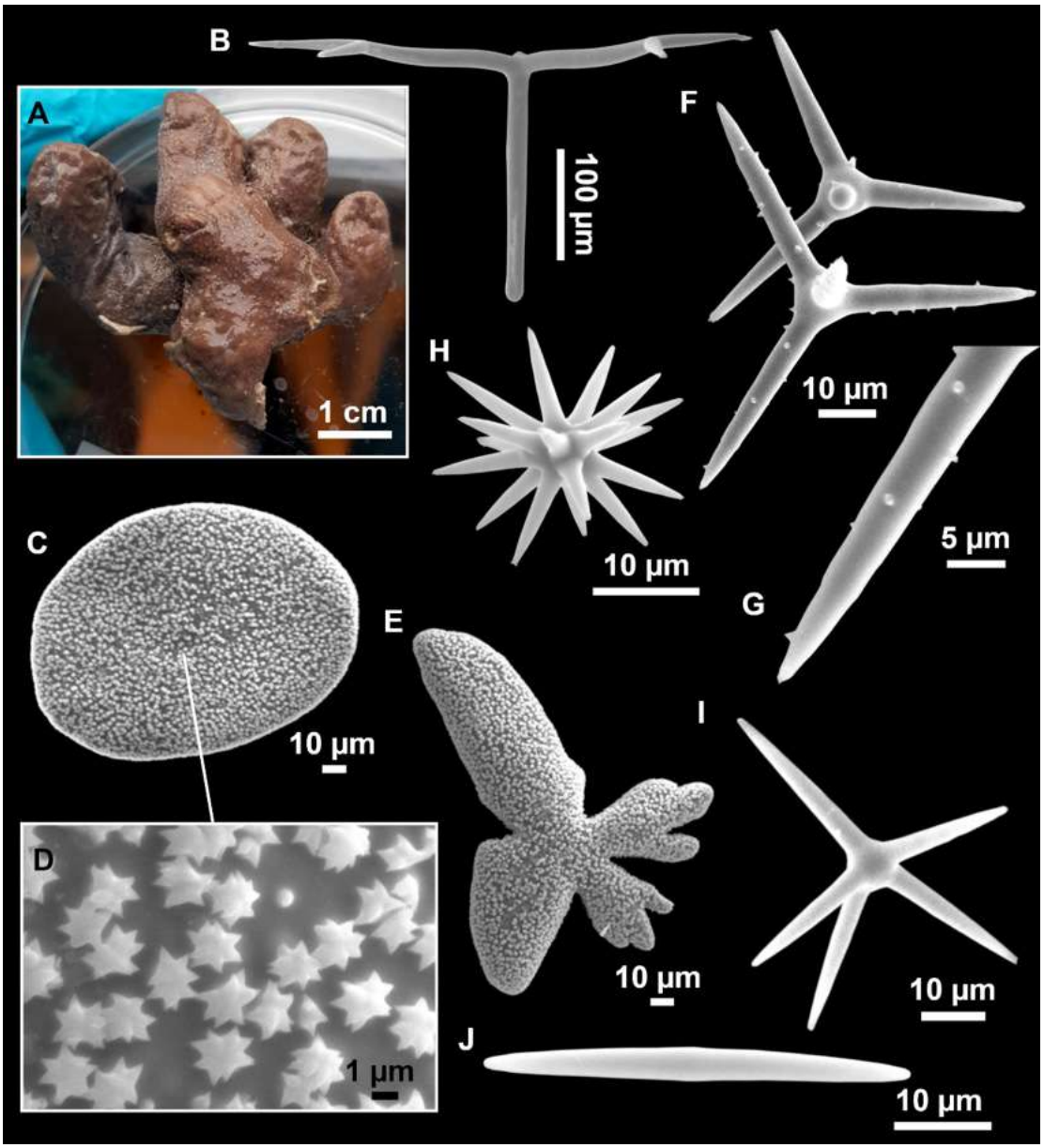

Figure 4.3.24. *Penares euastrum* (*Schmidt, 1868*), specimen i142_A. (A) Habitus after EtOH fixation. (B) Dichotriaene. (C–E) Aspidasters with (D) detail of the rosettes. (F) Oxyasters I with (G) detail of the spines. (H–I) Oxyasters II. (J) Microrhabd.

Comparative material

Penares euastrum, holotype, MNHN Schmidt collection#76, wet specimen, La Calle, Algeria, coll: H. de Lacaze-Duthiers.

Outer morphology

Massive, irregular lobose sponge, reaching about 12 cm in maximum diameter (Fig. 4.3.24A). Surface dark brown except at the basal area, where it is whitish. Pores are located on white circular areas throughout the body, giving a characteristic appearance. Circular oscula placed apically. Cortex <1 mm.

Table 4.3.10. Spicule measurements of *Penares euastrum, Penares cavernensis* **sp. nov.** and *Penares aspidodiscus*, given as minimum-mean-maximum for total length/minimum-mean-maximum for total width; all measurements are expressed in µm. Specimen codes are the field#. Rh: rhabdome; Cl: clad; pc: protoclad; dc: deuteroclad; -=not found/not reported; n.m.= not measured; EB: Emile Baudot, AM: Ausias March.

Material	**Depth** (m)	**Oxeas** (length/width)	**Orthotriaenes** Rhabdome (length/width) Clad (length/width)	**Dichotriaenes** Rhabdome (length/width) Protoclade (length/width) Deuteroclade (length/width)	**Aspidasters** (Maximum diameter/minumum diamater)	**Microrhabds** (length/width)	**Oxyasters I** (length)	**Oxyasters II** (length)
P. euastrum **holotype MNHN#76 La Calle, Algeria**	-	872-1043-1348/ 13-18-21 (N=5)	Rh: 526/29 Cl: 364/21 (N=1)	Rh: -/29-34 Pt: 155-224/21-26 Dt: 89-164/17-20 (N=3)	100-131-165/ 60-91-107 (oval)	37-48-56/ 2-3-4 (N=14) (abundant)	32-49-62 (2-6 actines)	8-11-16
P. euastrum **POR932_1 Menorca**	75	465-895-1178/ 4-12-17 (N=19) (strongyle modifications)	always with one or two bifurcated clads	Rh:-/33-36 Pt: 154-180/23-28 Dt: 59-71/14-21 (N=2)	97-121-142/8 5-103-118 (discoid to oval) (bulbous stumps in the hilum)	43-55-74/ 2-3-4 (abundant)	25-49-59 (2-6 actines)	8-15-28
P. euastrum **POR975 Menorca**	56	638-868-1302/ 6-16-25 (N=12) (strongyle and style modifications)	n.m.	n.m.	116-138-154/88-102-116 (N=16) (discoid to oval)	37-46-55/2-3-4 (N=11) (scarce)	25-53-74 (N=19) (2-6 actines)	9-13-19 (N=19)
P. euastrum **POR1253 Formentera**	53	661-1013-1271/ 15-24-38 (N=11)	n.m.	n.m.	118-143-172/74-89-98 (mostly oval)	27-42-59/2-3-3 (scarce)	43-60-77 (N=21) (2-5 actines)	8-13-15
P. euastrum **i142_A EB**	128	n.m.	n.m.	n.m.	128-151-182/94-109-142 (N=11)	39-58-71/3-5-5 (N=13) (abundant)	29-48-63 (3-9 actines) (N=14)	15-20-22 (N=7)
P. euastrum **i524_b AM**	113	587-849-1172/ 13-19-26 (N=9)	n.m.	n.m.	111-145-171/77-107-125 (discoid to oval)	43-54-69/3-4-6 (abundant)	39-49-57 (4-10 actines)	12-17-21
P. euastrum **i530 AM**	112	756-1045-1390/ 15-24-33	n.m.	Rh: 344-387/19-31 (N=3) Pt: 148-185-206/20-31-45 Dt: 46-138-220/11-23-36 (N=8)	121-144-168/87-98-109 (oval)	36-49-67/3-4-5 (abundant)	34-53-66 (3-7 actines)	11-17-24
P. euastrum Banyuls, France as *E. stellifer* (Topsent, 1894)	25-30	1000/ 20-25	Rh: - Cl: 250/27	Rh: - Pt: 220-270/28-30 Dt:50-100/-	135/ 95 (oval)	55-65	actines 23 long (3-5 actines)	actines 5 long

P. euastrum Ibero-Moroccan Gulf, North Atlantic (*Boury-Esnault, et al., 1994*)	1378	910-1015-1150/ 16-20-20 (oxeas to styles and strongyles)	-	Rh: short Pt: 160-210-250/30-35-40 Dt: 200-237-260/25-35-41	150-160-164/ 110-125-140 (oval to irregular)	35-52-82 (microxeas)	35-53-80 (3-7 actines)	12-14-15 (few)
P. euastrum Banc East Gettysburg, North Atlantic, as *E. stellifer* (*Lévi & Vacelet, 1958*)	95	950/ -	-	Rh: 70/35 Pt:175 Dt:100-160	130/ 100 (oval)	33-40 (microxeas)	25-35 (3-5 actines)	5-14
P. euastrum Canary Islands, North Atlantic (*Cruz, 2002*)	Infralit toral	500-850 (strongyles fusiform)	-	Rh: 220-400 Pt: 120-160 Dt: 80-210	156/ 60 (oval to irregular)	24-40 (microstrongyles)	actines 20-40 long (3-5 actines)	10-16 (microspined)
***P. cavernensis* sp. nov. LIT55, holotype Cova Cala Sa Nau**	3-4	766-1006-1259/ 7-14-22 (N=12)	-	Rh: -/27 Pt: 141/22 Dt: 139/15 (N=1)	74-102-127/ 62-80-96 (discoid to oval, often with thin stumps)	36-45-58/ 2-3-3 (abundant)	32-44-56 (2-5 actines)	8-10-13
***P. cavernensis* sp. nov. LIT45, paratype Cova Cala Sa Nau**	3-4	426-627-853/ 5-8-12 (N=19)	Rh: 426-548/13-18 (N=3) Cl: 155-233-291/7-13-17 (N=5)	Rh:441/20 Pt: 183/15 Dt: 77/10 (N=1)	84-113-135/ 66-84-98 (discoid to oval, often with thin stumps)	35-43-55/ 1-2-3 (abundant)	34-48-68 (2-5 actines)	7-11-14
***P. cavernensis* sp. nov. LIT65, paratype Cova Cala Sa Nau**	6	524-839-1033/ 6-10-15 (N=16)	Rh: 289 (N=1)/9-13 (N=2) Cl: 109-242/8-9 (N=2)	Rh: 407-515(N=3)/7-13-16 (N=4) Pt: 86-134-213/9-12-14 (N=4) Dt:49-66-74/7-10-12 (N=4)	67-97-128/ 54-77-94 (discoid to oval, rarely with thin stumps)	28-36-56/ 1-2-2 (abundant)	32-50-68 (2-4 actines)	6-9-14
P. aspidodiscus holotype, Monaco (*Topsent, 1928*)	123	usually with blunt ends	yes	yes (often Pt>Dt)	130/ 110 (discoid, often with thin stumps)	35-60 (microxeas)	10-55 (3-5 actines)	<16

2167

Spicules

Dichotriaenes (Fig. 4.3.24B), scarce, whose cladome has longer protoclads than deuteroclads. Rhabdome: 344-387/19-36, protoclad: 148-206/20-45, deuteroclad: 46-220/11-36 µm. In the observation of several *P. euastrum* specimens we have observed modified dichotriaenes with one, two and three (orthotriaenes) of its clads non-bifurcated. Also, we observed one rhabdome modified to a rounded end (Fig. 4.3.24B).

Oxeas, with variable morphology; some are straight while others are bend or abruptly curved. Tips may be pointed, stepped or rounded, resembling strongyles, measuring 465-1390/4-38 µm.

Aspidasters (Fig. 4.3.24C-E), shape variable between individuals, some showing a predominance of discoid to oval (POR932_1) or only oval (i529, i530, POR469, POR1253), sometimes irregular (Fig. 4.3.24E). Stumps in the hilum area found only in POR932_1, having several stumps per aspidaster and showing a bulbous shape, type 3 rosettes *sensu* Cárdenas (2020), measuring 97-182/74-142 µm (maximum diameter/min diameter).

Oxyasters I (Fig. 4.3.24F), with 2-10 actines, smooth or with few spines, barely visible with an optical microscope (Fig. 4.3.24G). There is a relationship between size and number of actines, being in general larger those with less actines. Measuring 25-74 µm in diameter.

Oxyasters II (Fig. 4.3.24H-I), with >10 actines, smooth or with few spines, not visible to the optical microscope, measuring 8-28 µm in diameter.

Microrhabds (Fig. 4.3.24J), smooth, centrotylote, with blunt ends 27-74/2-6 µm.

Ecology and distribution

Common species usually found at mesophotic depths: on fishing grounds of the platform, on *Peyssonnelia* and rhodolith bottoms and at the summit of the AM and the EB seamounts. May have several sponge epibiont species like *Timea* sp. and some poecilosclerids.

Genetics

The Folmer short miniCOI was obtained from i530 and POR932_1 (SBP#2683 and SPB#2684), while 28S (C1-C2) (ON133852) was obtained from i530.

Taxonomic remarks. See remarks below for *Penares cavernensis* **sp. nov.**

***Penares cavernensis* sp. nov. Díaz & Cárdenas**

(Figs. 4.3.19 and 4.3.25; Table 4.3.10)

Etymology

Penares cavernensis, from the Latin *cavernae* (cave), referring to the habitat where the species was discovered.

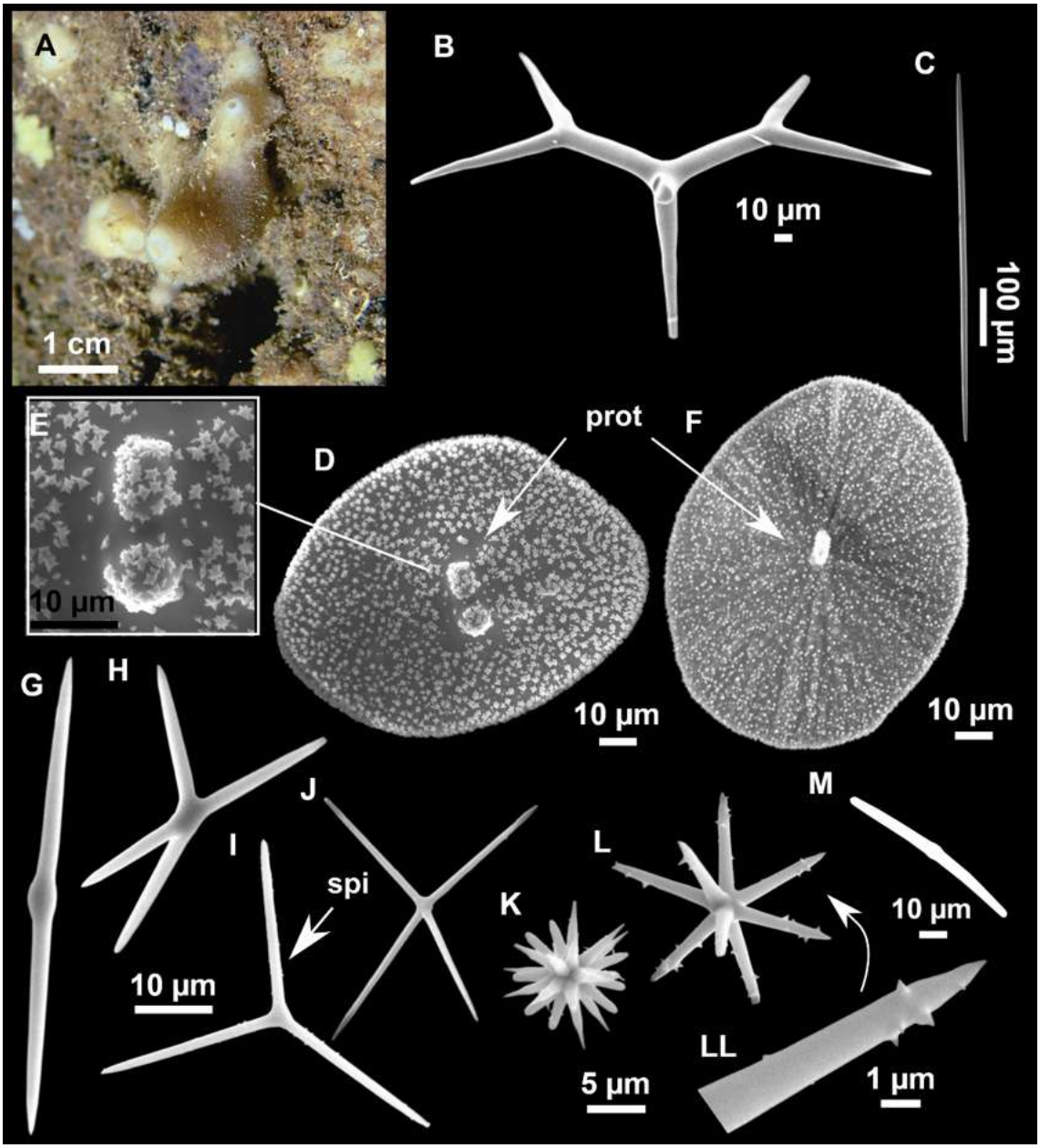

Figure 4.3.25. Holotype of *Penares cavernensis* **sp. nov.**, UPSZTY 190918 (LIT55). (A) Habitus *in situ*, at 3– 4 m depth, Cova Cala Sa Nau. (B–M) SEM images of the spicules. (B) Dichotriaene. (C) Oxea. (D–F) Asp-idaster with (E) detail of the rosettes and the central protuberances. (G–J) Oxyasters I. (K–LL) Oxyasters II with (LL) detail of the spines. (M) Microrhabd. prot, protuberance; spi, spines.

Material examined

Holotype: UPSZTY 190918, field#LIT55, Cova Cala Sa Nau, east of Mallorca, 3-4 m, scuba diving, coll. J. A. Díaz & J. Cabot.

Paratypes: UPSZTY 190917, field#LIT45, Cova Cala Sa Nau, east of Mallorca, 3-4 m, scuba diving, coll. J. A. Díaz; UPSZTY 190919, field#LIT65, Caló des Monjo, west of Mallorca, 6 m, scuba diving, coll. J. A. Díaz & A. Frank.

Outer morphology

Massive-encrusting, lobated sponges (Fig. 4.3.3F, Fig. 4.3.25A), about 2-5 cm in maximum diameter, and 1-3 cm in height. Surface color can be dark brown to beige, whitish rim around the oscula. Choanosome whitish. Same coloration in life and after fixation in ethanol. Several circular oscula located apically, 1-3 mm in diameter, smaller whitish pores are visible with the naked eye. No hispidation present, surface smooth to the touch. Very thin cortex present, about 0.4 mm. Hard but slightly compressible consistency. The skin wrinkles after EtOH preservation. In the holotype, a large cloaca can be observed below the main apical oscula.

Spicules

Dichotriaenes (Fig. 4.3.25B), scarce, morphology and abundance varies with the individuals. They are very scarce in specimens found in Cala sa Nau (LIT45 and LIT55), with robust rhabdome and cladome. In the specimen from Caló des Monjo (LIT65), dichotriaenes are more abundant but with thinner rhabdome and cladome, also showing teratogenic modifications and aborted actines. Overall measuring: rhabdome 407-515/7-27 µm, protoclad: 86-213/9-22 µm, deuteroclad: 49-139/7-15 µm.

Orthotriaenes (not shown), scarce and mostly broken, with long clads slightly curved inwards, rhabdome: 289-548/9-18 µm, cladi: 109-291/7-17 µm.

Oxeas (Fig. 4.3.25C), straight or curved, with slightly stepped tips, 426-1259/5-22 µm.

Aspidasters (Fig. 4.3.25D-F), discoid to oval (the majority are oval), very thin, several having one or more characteristic stump(s) in the hilum area (Fig. 4.3.25E), which are isolated actines; type 3 rosettes *sensu Cárdenas (2020)*, measuring 67-135/54-98 µm (maximum diameter/min diameter). Translucent appearance with an optical microscope due to their extreme thinness.

Oxyasters I (Fig. 4.3.25G-J), with very thin actines, smooth or minutely spined, 2-5 actines, 32-68 µm.

Oxyasters II (Fig. 4.3.25K-LL), many spined actines, (Fig. 4.3.25LL), 6-14 µm.

Microrhabds (Fig. 4.3.25M), smooth, curved and centrotylote, with blunt ends, 28-58/1-3 µm.

Ecology and distribution

Found on vertical walls of shallow caves, Mallorca Island, at 3-4 m depth.

Genetics

The Folmer miniCOI has been obtained from the holotype (SPB#2685).

Taxonomic remarks on *Penares euastrum* and *Penares cavernensis* sp. nov.

Penares euastrum is a former *Erylus* species (i.e. Geodiidae with aspidasters) that was moved to the genus *Penares* by *Cárdenas et al. (2010)* based on its close phylogenetic position with *P. helleri*, the type species of the genus *Penares.* The Schmidt holotype of *P. euastrum* from Algeria was here examined, and all the spicules remeasured for the first time (Fig. 4.3.26A-I, Table 4.3.10). SEM pictures notably showed that the oxyasters I and II can be spiny to slightly spiny (Fig. 4.3.26D-H) and not always smooth as most of the

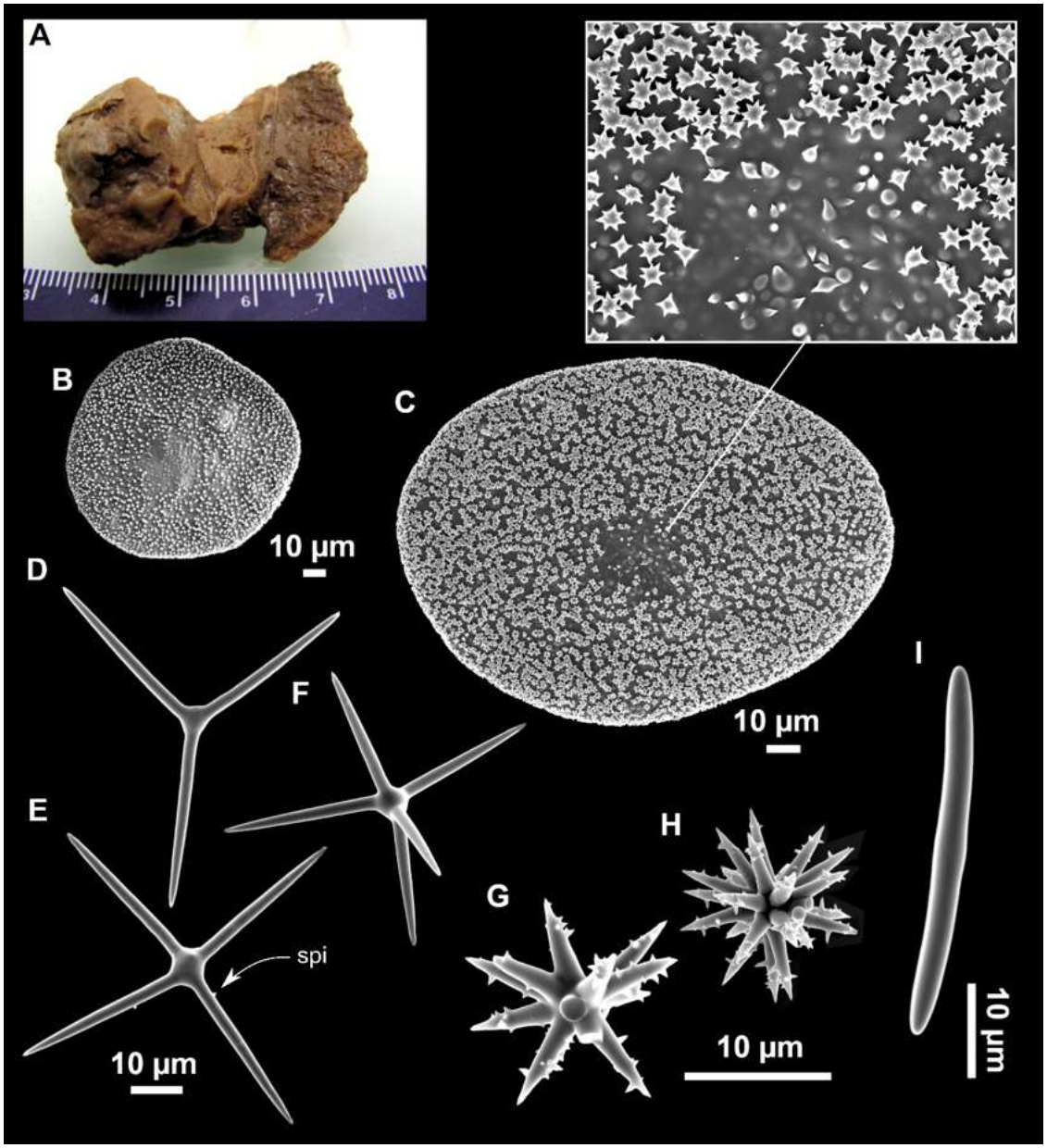

Figure 4.3.26. Holotype of *Penares euastrum*, MNHN Schmidt collection#76, La Calle, Algeria. (A) Habi-tus. (B) Optical microscope image of a thick transversal section. (C) Aspidasters with detail of the rosettes and hilum. (D–F) Oxyasters I with arrow (spi) indicating the spines. (G–H) Oxyasters II. (I) Microrhabd.

previous descriptions suggested. Oxyasters of our *P. euastrum* material (Fig. 4.3.24F-I) were similar, smooth to spiny. *P. euastrum* is a common Mediterranean species, regularly reported from caves to mesophotic depths. We had originally identified our cave specimens from Mallorca as *P. euastrum*, however, while the two miniCOI from our mesophotic specimens (i530 and POR932_1) were a perfect match to the COI of a mesophotic *P. euastrum* from Italy (MT815827), the miniCOI sequence from our cave specimen LIT55 showed a 2 bp difference with the Italian and the Balearic islands mesophotic specimens. This is a significant difference considering how conserved COI is in demosponges (*Schuster et al., 2017*), the geographical closeness of the two habitats and the short size (130 bp) of the miniCOI. In fact, having 2 or more bp differences in a

full (about 640 bp) COI sequence is generally considered indicative of different species. External morphology differences are few and subtle but consistent: mesophotic specimens are larger and with a darker coloration while cave specimens are encrusting to massive-encrusting and of a paler color. Although spicules are very similar with overlapping size ranges (Table 4.3.10), overall cave specimen spicules are thinner and smaller**.** Aspidasters of *P. euastrum* are slightly larger and wider (97-182/74-142 µm vs 67-135/54-96) with rosettes more densely disposed (Figs. 4.3.24D, 4.3.25E and 4.3.26C). Besides, aspidasters of *P. cavernensis* **sp. nov.** are more translucid under the light microscopy than those of *P. euastrum*, probably because of having less densely arranged rosettes and being thinner (although we did not manage to get thickness measurements of the aspidasters). Moreover, aspidasters from cave specimens are occasionally discoid (much rarer in mesophotic specimens) and commonly have ectopic actines in the hilum area, which is quite distinct (Fig. 4.3.25D-F). Ectopic actines have been found in all three specimens of *P. cavernensis* **sp. nov.** examined but only in one of the nine Balearic Islands *P. euastrum* studied (specimen POR932_1), and are absent in the holotype (see Table 4.3.10, Figs. 4.3.24 and 4.3.26). The holotype of *P. euastrum* from Algeria is a large mesophotic specimen (3.5 x 3 cm) (Fig. 4.3.26); its spicule measurements are closer to our mesophotic specimens, which are therefore formally identified as *P. euastrum*. *Topsent (1928)* had also distinguished a variety of *P. euastrum* called *Erylus aspidodiscus,* which, based on its morphological similarity with *P. euastrum* should actually be moved to the genus *Penares* as well, as *Penares aspidodiscus* comb. nov. This species was unfortunately based on a single specimen, from mesophotic depths close to Monaco (123 m) with spicule sizes closer to those of the holotype of *P. euastrum.* It was characterized by having only discoid aspidasters, commonly with ectopic actines, just like in *P. cavernensis* **sp. nov.** Since one of our *P. euastrum* also showed ectopic actins (POR932_1), it seems that this character may be shared by *P. euastrum* and *P. cavernensis* **sp. nov.**, although being much more common in the second. Also, *P. cavernensis* **sp. nov.** does not have exclusively discoidal aspidasters like in *P. aspidodiscus,* in fact the majority of the aspidasters are oval in *P. cavernensis* **sp. nov**. *P. aspidodiscus* thus shares some characters from *P. euastrum* and some from *P. cavernensis* **sp. nov**. and is of uncertain taxonomic status at this point.

Regarding 28S, we only manage to get a C1-C2 fragment of mesophotic *P. euastrum* (i530). Interestingly, it showed 3 bp difference with another mesophotic *P. euastrum* from the 'Banc de l'Esquine' (off La Ciotat, France, AF062600), which may indicate that there is even more diversity than suspected in the *P. euastrum* complex.

Penares candidatus **(Schmidt, 1868)**

(Figs. 4.3.19 and 4.3.27; Table 4.3.11)

Material examined

UPSZMC 190913, field#i143_G, St. 51, INTEMARES0718, MaC (EB), 128 m, beam trawl, coll. F. Ordines; UPSZMC 190914-15, field#i315_A-315_B, St. 124, (INTEMARES1019), MaC (EB), 152 m, beam trawl, coll. J. A. Díaz.

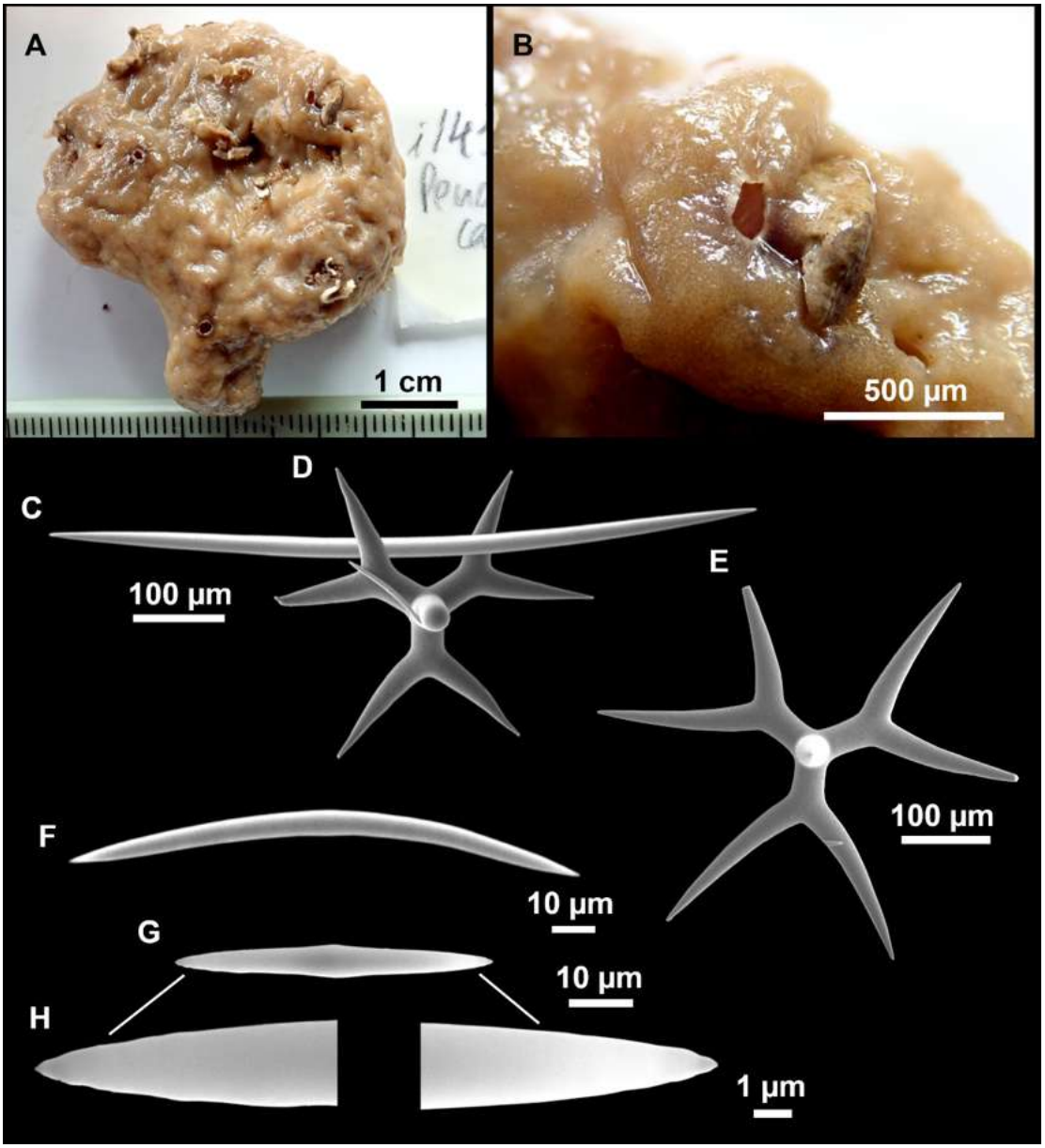

Figure 4.3.27. *Penares candidatus* (*Schmidt, 1868*), specimen i143_G. (A) Habitus after EtOH fixation. (B) Detail of the oscula of i143_G. (C) Oxea. (D–E) Dichotriaene. (F) Large microxea. (G) Small microxea with (H) detail of the tips.

Comparative material

Penares candidatus, holotype, MNHN Schmidt collection#80, wet specimen, Algeria, 'Exploration Scientifique de l'Algérie', 1842.

Outer morphology

Massive, lobated sponges (Fig. 4.3.27A), up to 5 cm in maximal diameter. Greenish to dirty gold in life, light to dark brown with a faint yellowish tinge after preservation in ethanol. Choanosome beige after ethanol, cavernous. Cortex about 0.2 mm thick. Hard consistency, only slightly compressible. No hispidation, smooth surface and heavily wrinkled. Several circular oscula, 2-3 mm in diameter, located at the apex of the lobules

Table 4.3.11. Spicule measurements of *Penares candidatus*, given as minimum-mean-maximum for total length/minimum-mean-maximum for total width; all measurements are expressed in µm. Specimen codes are the field#. Rh: rhabdome; Cl: clad; pc: protoclad; dc: deuteroclad; -:not found/not reported; EB: Emile Baudot.

Material	**Depth** (m)	**Oxeas** (length/width)	**Dichotriaenes** Rhabdome (length/width) Clad (length/width) Protoclade (length/width) Deuteroclade (length/width)	**Microrhabds** (length/width)
i143_G EB	128	402-668-974/ 7-14-25	Rh: 197-229-274/24-31-38 (N=3) Pt: 52-68-97/9-27-39 (N=12) Dt: 37-163-255/6-24-38 (N=12)	35-109-207/3-7-12 (centrotylote or not)
i315_A EB	152	464-774-1156/ 5-16-26	Rh: 225-310/30-34-39 (N=2) Pt: 59-72-87/17-35-49 (N=20) Dt: 66-191-258/15-29-40 (N=20)	35-99-216/2-5-9 (centrotylote or not)
holotype MNHN#86 Algeria (*Sollas, 1888*)	-	816/ -	Rh: short Pt: 71 Dt: 177	50-250 (centrotylote or not)
Cap de Creus & Banyuls Western Mediterranean (*Topsent, 1894*)	30-40 (Banyuls) 90-100 (Cap de Creus)	825-1200/ 23-25	Rh: 265/30 Pt: 76 Dt: 165	30-250 (centrotylote or not)
Blanes Western Mediterranean (*Bibiloni, 1981*)	6 (facies of *Peyssonnelia rubra*)	450-500/ 10	Rh: short Pt: 60 Dt: 100	50-100/4-5 (not centrotylote)
Canary Islands (*Cruz, 2002*)	-	320-700/ -	Rh: 92-160 Pt: 48-92 Dt: 12-96	40-60 (not centrotylote)

and spread over the body. A characteristic dark rim surrounds the oscula (Fig. 4.3.27B). Pores inconspicuous.

Spicules

Dichotriaenes (Fig. 4.3.27D-E), with a short, straight, and sharp rhabdome, measuring 197-310/24-39 µm (N=5). Cladome with cladus of approximately the same length as rhabdome. Protoclads measuring 52-97/9-49 µm, deuteroclads measuring 37-258/6-40 µm.

Oxeas (Fig. 4.3.27C), robust, fusiform, slightly bent, with sharp tips, 402-1156/5-26 µm.

Microrhabds (Fig. 4.3.27F-H), smooth, curved and with sharp ends (Fig. 4.3.27H), measuring 35-216/2-12 µm. Some are very slightly centrotylote, more clear in small spicules.

Ecology notes

Species found at two stations, both at the EB summit: one at 132 m and the other one at 152 m. Both stations corresponded to sponge grounds, with a great sponge diversity and abundance, including large tetractinellids like *Discodermia polymorpha* Pisera & Vacelet, 2011 or *Erylus* spp,, small axinellids and haplosclerids like *Petrosia (Petrosia) ficiformis* (Poiret, 1789) and *Petrosia (Strongylophora) vansoesti* (Boury-Esnault, Pansini & Uriz, 1994).

Genetics

COI (ON130543) and 28S (C1-C2) (ON133857) sequences of specimen i315_B were obtained. The 28S sequence represents the first published sequence of this marker for the species.

Taxonomic remarks

This is the first report of *P. candidatus* in the Balearic Islands, and the deepest for the species, extending its bathymetric range down to 152 m. The species is also reported for the first time on a seamount. *P. candidatus* is easily recognizable by its external appearance and the absence of oxyasters, a unique feature amongst North Atlantic/Mediterranean *Penares* species. However, there is some heterogeneity in the literature regarding spicule sizes (Table 4.3.11). Microrhabds have smaller size ranges in *Bibiloni (1981)* (50-100/4-5 µm), and *Cruz (2002)* (40-60 µm) and are never centrotylote in contrast to the holotype (50-250 µm), specimens from Banyuls, France (30-250 µm) (*Topsent, 1894*) and our material (35-216/2-12 µm). A similar tendency is observed with the oxeas, which are smaller in Bibiloni and Cruz (450-500/10 µm and 320-700 µm, respectively) than in our specimens (825-1200/23-25 µm and 402-1156/5-26 µm, respectively) and the rest of the literature (Table 4.3.11). These discrepancies may be explained by the depth, and thus silica availability, where individuals were collected, as Bibiloni specimens came from shallower waters (Blanes, 6 m), while possibly the holotype and our specimens were collected at greater depths (>30 m, and up to 152 m). Another explanation is that *P. candidatus* represents a species complex between some shallow and deeper populations, as for *Penares helleri* and *Penares euastrum* (see discussion above and below), but this is currently not supported by COI

sequences, which are 100% identical for specimens from 5 m (Berlengas Islands, Portugal, HM592719) and our mesophotic specimens.

Penares helleri (Schmidt, 1864)

(Figs. 4.3.19 and 4.3.28; Table 4.3.12)

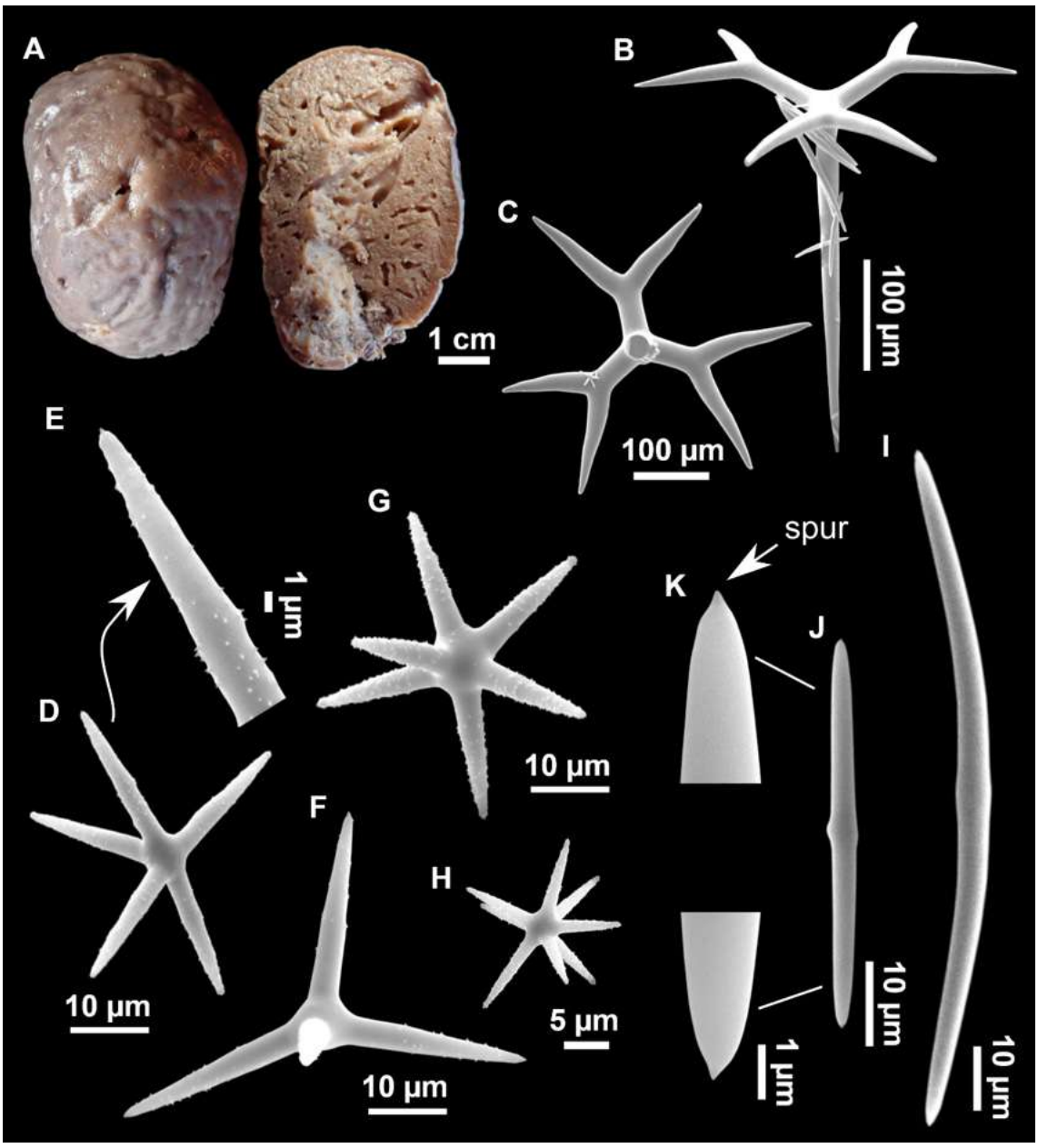

Figure 4.3.28. *Penares helleri* (*Schmidt, 1868*), specimen POR946. (A) Habitus after preservation. (B–C) Dichotriaenes. (D–H) Oxyasters with (E) detail of the spines. (I–K) Microrhabds with (K) detail of the spurs at the tips.

Material examined

UPSZMC 190933, field#i142_D, St. 51 (INTEMARES0718), MaC (EB), 128 m, beam trawl, coll. F. Ordines; UPSZMC 190934, field#i152, St. 52 (INTEMARES0718), MaC (EB), 107-110 m, rock dredge, coll. F. Ordines; UPSZMC 190935, field#i233, St. 48 (INTEMARES1019), MaC (AM), 123 m, beam trawl, coll. J. A. Díaz; UPSZMC

190936, field#i739, St. 52 (INTEMARES0720), MaC (EB), 300-330 m, beam trawl, coll. J. A. Díaz; UPSZMC 190937, field#POR946, St. 76 (MEDITS2020), s'Algar (east of Menorca), 131 m, GOC-73, coll. J. A. Díaz.

Comparative material

Penares sp.1, PC325, 3PP cave, La Ciotat, France, scuba-diving, 28S: AF062598, originally identified as *P. helleri* in Chombard et al. (1998).

Penares sp.2, ZMAPOR 21658, field#FLW.06.48, Gruta Enchareus (cave), Flores, Azores, 12 m, scuba-diving, 11 July 2006, coll: J. R. Xavier, 28S: HM592828, originally identified as *P. helleri* in Cárdenas et al. (2011).

Outer morphology

Massive ovoid and lobated sponges (Fig. 4.3.28A), colors alive are dark brown on its upper side, progressively fading to light brown or whitish in its basal area. Some specimens are entirely whittish (e.g. i739). Colors after ethanol fixation are brown (basal area) to dark brown (apical area). Surface visually smooth but rough to the touch, slightly compressible. Cortex 0.5-0.7 mm thick clearly distinguishable. Choanosome fleshy, light brown after ethanol and showing a well developed aquiferous system. 1-3 small oscules (mm size) irregularly distributed, uniporal pores, much smaller (<1 mm) grouped in some areas. In some specimens the ethanol acquires a dirty gold coloration during the fixation.

Spicules

Dichotriaenes (Fig. 4.3.28B-C), abundant, rhabdome: 236-293/24-62 μm, longer deuteroclad than protoclad: protoclad 51-103/18-59 μm, deuteroclad 99-265/17-50 μm.

Oxeas, robust, fusiform and slightly bent, 684-1641/10-42 μm.

Oxyasters (Fig. 4.3.28D-H), microspined (Fig. 4.3.28E), with 4-10 actines, 11-56 μm.

Microrhabds (Fig. 4.3.28I-K), on a wide but continuous size range, smooth, can have mucronated ends, which are only visible under SEM microscope (Fig. 4.3.28K), centrotylote, measuring 19-171/2-8 μm.

Ecology and distribution

Species found in sedimentary bottoms from mesophotic to upper bathyal depths (100-300 m). It is common at the fishing grounds of the upper slope of the Mallorca and Menorca shelf and at the summit and slopes of the AM and the EB.

Genetics

The COI (ON130538, ON130539) and 28S (C1-C2) fragments (ON133859, ON133858) have been obtained from specimens i739 (EB) and POR946 (s'Agar). These are the first sequences from mesophotic *P. helleri*.

Taxonomic remarks. See below taxonomic remarks for *Penares isabellae* **sp. nov.**

***Penares isabellae* sp. nov. Díaz & Cárdenas**

(Figs. 4.3.19 and 4.3.29; Table 4.3.12)

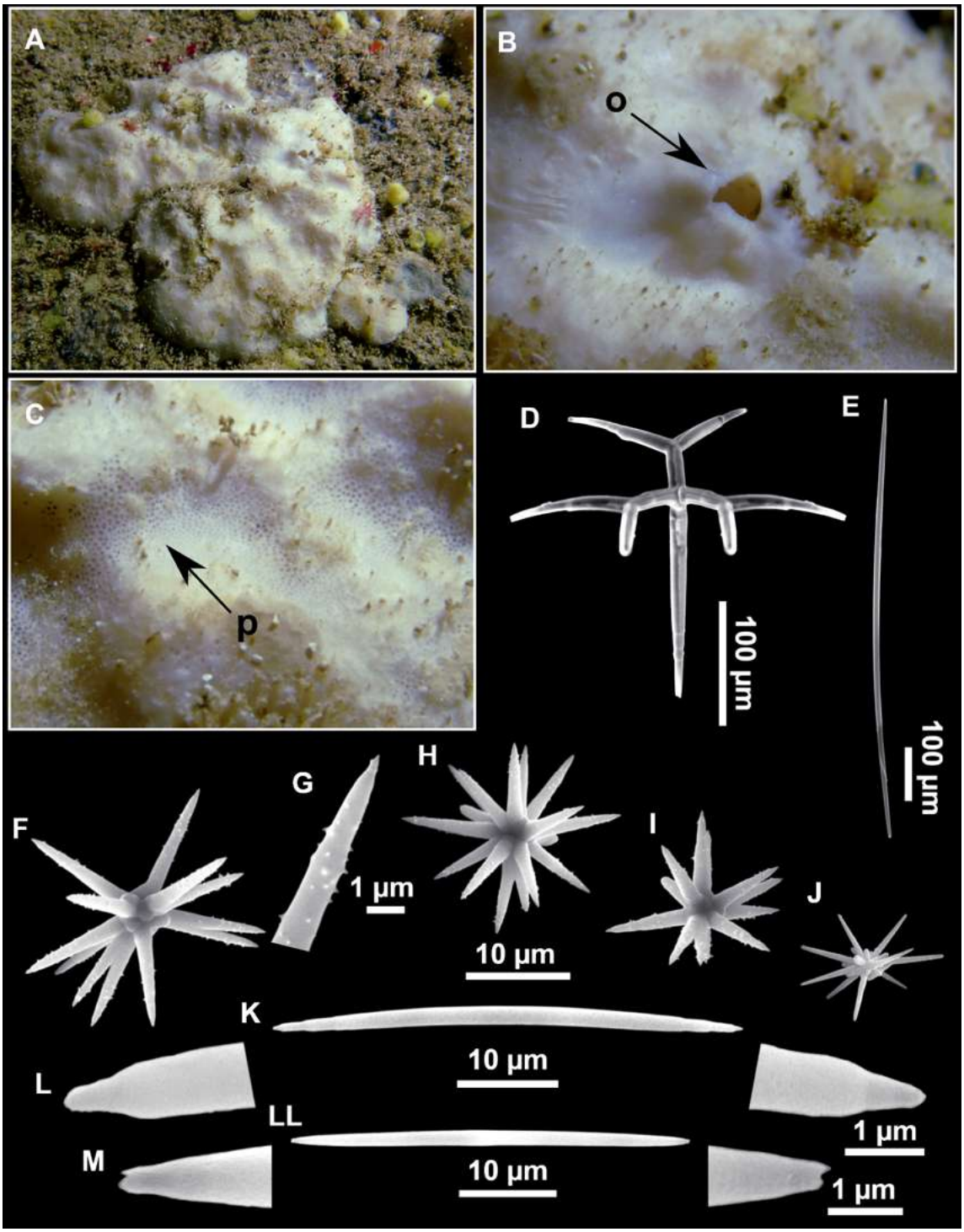

Figure 4.3.29. Holotype of *Penares isabellae* **sp. nov.**, UPSZTY 190938 (LIT48). (A) Habitus *in situ* at 3–5 m depth, Cala sa Nau. (B) Detail of the oscula. (C) Detail of the pores. (D–M) SEM images of the spicules. (D) Dichotriaene. (E) Oxea. (F–J) Oxyasters. (K–LL) Microrhabds with (L–M) detail of the microrhabd tips. o, oscula; p, pores.

Etymology

Named after Isabel Fullana Riera (a.k.a. Bel Fullana), a Mallorcan painter.

Material examined

Holotype: UPSZTY 190938, field#LIT48, Cova Cala Sa Nau, east of Mallorca, 3-4 m, scuba diving, coll. J. A. Díaz.

Paratypes: UPSZTY 190939, field#LIT40_1, Cova Cala Sa Nau, east of Mallorca, 3-4 m, scuba diving, coll. J. A. Díaz; UPSZTY 190940, field#LIT66, Caló des Monjo, west of Mallorca, 6 m, scuba diving, coll. J. A. Díaz and A. Frank.

Outer morphology

Massive-encrusting sponges (Figs. 4.3.4E and 4.3.29A), 8-9 cm in length (sometimes more), 0.5 cm in height. Whitish gray in life and after preservation in ethanol. Surface smooth, slightly rough to the touch. Flexible and compressible. Cortex less than 0.5 mm, clearly distinguishable. Choanosome whitish. Circular oscula 3-5 mm in diameter (Fig. 4.3.29B). Minute pores distinguishable with the naked eye when alive, located on depressed areas present all over the surface (Fig. 4.3.29C), due to body contraction after fixation, these areas are more difficult to see.

Spicules

Dichotriaenes (Fig. 4.3.29D), very scarce (only found in the holotype), with short rhabdome, cladome may show aberrant cladi. Rhabdome: 169 (N=1)/15-22 (N=2) µm, protoclad 38-59/16-19 (N=2) µm, deuteroclad 105-114/12-17 (N=2) µm.

Oxeas (Fig. 4.3.29E), slightly bent, tips may be pointed or blunt (i.e. modifications to style and strongyle), 353-913/6-17 µm.

Oxyasters (Fig. 4.3.29F-J), with up to 17-18 microspined actines (Fig. 4.3.29FG). Overall measuring 9-30 µm.

Microrhabds (Fig. 4.3.29K-M), very abundant, on a wide but continuous size range, measuring 31-168/2-6 µm, smooth, slightly bent (rarely abruptly bent), with stepped tips (Fig. 4.3.29L) that may be mucronated (Fig. 4.3.29M).

Ecology and distribution

This species was discovered in shallow caves, the two exact same localities/habitat as *P. cavernensis* **sp. nov.** (Fig. 4.3.3I) (see above).

Genetics

The Folmer COI (ON130540, ON130541, ON130542) were obtained from holotype LIT48 and paratypes LIT40_1 and LIT66, while a 28S (C1-C2) fragment was obtained from the paratype LIT40_1 (ON133860).

Taxonomic remarks on *Penares helleri* and *Penares isabellae* sp. nov.

Penares helleri is a common Mediterranean species found at both infralittoral caves and the mesophotic zone with one report from the Atlantic side, but close to Gibraltar at 521 m depth, its current deepest record (*Boury-Esnault et al., 1994*). Cave specimens are reported to be massive or encrusting while mesophotic ones tend to be reported as

2470 **Table 4.3.12.** Spicule measurements of *Penares isabellae* **sp. nov.** and *Penares helleri*, given as minimum-mean-maximum for total
2471 length/minimum-mean-maximum for total width; all measurements are expressed in µm. Specimen codes are field#. Rh: rhabdome; Cl:
2472 clad; pc: protoclad; dc: deuteroclad; -=not found/not reported; n.m.= not measured; EB: Emile Baudot, AM: Ausias March.

Material	**Depth** (m)	**Oxeas** (length/width)	**Dichotriaenes** Rhabdome (length/width) Protoclade (length/width) Deuteroclade (length/width)	**Microrhabds** (length/width)	**Oxyasters** (length)
P. helleri **POR946** **Menorca**	131	684-1099-1337/10-22-30	Rh: -/24-44-59 (N=12) Pt: 54-74-86/23-41-59 (N=12) Dt: 99-170-222/17-35-50 (N=12)	31-82-146/2-4-7 (centrotylote)	13-28-45
P. helleri **i739** **EB**	300-330	755-1243-1641/10-26-42	Rh: 236-293 (N=3)/25-36-62 Pt: 51-68-103/18-33-52 (N=17) Dt: 112-179-265/17-28-49 (N=17)	29-94-150/3-5-8 (centrotylote)	12-33-56
P. helleri **i152** **EB**	107-110	n.m.	n.m.	36-72-121/2-3-6 (N=14) (centrotylote)	15-30-53
P. helleri **i233** **AM**	123	n.m.	n.m.	19-98-171/2-4-8 (centrotylote)	11-27-48
P. helleri holotype, Vis (=Lissa), Croatia (*Sollas, 1888*)	64.7	1430/39	Rh: 400/35 Pt: 60-90 Dt: 190-240	32-150/6 (centrotylote)	actin of 20
P. helleri Gibraltar, Atlantic side (*Boury-Esnault et al., 1994*)	521	710-1050-1550/18-28-40	Rh: 345-377-410/28-31-35 Pt: 65-79-90/40-47-55 Dt: 175-222-260/40-45-50	20-105-150/4-8-10 (centrotylote)	30-41-50
P. helleri Gulf of Naples (*Pulitzer-Finali, 1972*)	1-10 m	1100/25 or 600-750/- (slightly centrotylote in shallow specimen)	Rh: short Pt: 86-135/ Dt: 54-145/	30-190/10, reaching 230 in shallow specimen (rarely centrotylote)	13-40
P. helleri Ionian Sea (Porto tricase)*	15 and 30* 15**	1000-1500/15-35	Rh: 200-400/25-40 Cladome: 150-330	30-240	13-50

Ligurian Sea (Bogliasco)** (*Pulitzer-Finali, 1983*)				(moderately centrotylote)	
P. helleri var. *subtilis* Gulf of Naples, rocky bottom (#775:2, #783:2) (*Sarà & Siribelli, 1960*)	20-25	374-510/6-7	only one found	52-80/1-1.7 (#783:2)	-
***P. isabellae* sp. nov. holotype, LIT48 Cala sa Nau**	3-5	661-802-913/7-13-17	Rh: 169 (N=1)/15-22 (N=2) Pt: 38-59/16-19 (N=2) Dt: 105-114/12-17 (N=2)	40-74-145/2-3-5	13-21-30 (11-18 actines)
***P. isabellae* sp. nov. paratype, LIT40_1 Cala sa Nau**	3-5	436-638-821/6-8-14	-	35-84-168/2-3-6	10-17-28 (10-17 actines)
***P. isabellae* sp. nov. paratype, LIT66 Caló des Monjo**	3-5	353-640-854/6-10-14	-	31-98-165/2-3-4	9-17-29 (8-17 actines)

2473

massive. Otherwise cave and open-sea specimens share the same spicular set; smooth microrhabds, oxyasters, oxeas and dichotriaenes. However, reported spicular sizes are very heterogeneous (Table 4.3.12), with some specimens having longer and/or thicker microrhabds/oxeas. Also, dichotriaenes seems to be very common in some specimens, but very scarce in others. The mentioned differences are usually explained in the literature (*Sarà, 1961*) by differences in habitat conditions, for example, currents may affect the growing morphology, leading to encrusting versus massive specimens and depth may influence nutrient availability, affecting the silica content and thus spicule development. Our results reveal that *P. helleri* is a species complex with at least four cryptic but genetically different species, a fact that challenges the use of ecophysiological traits to explain morphological differences.

A first species (POR946, i739, i152 and i233) corresponds to the true *P. helleri,* as macroscopic morphology (massive), spicules (robust and abundant dichotriaenes, thick microxeas and large oxyasters with 4-10 actines) and habitat (mesophotic to upper bathyal) matches the holotype.

A second species was revealed by our molecular markers. The full Folmer COI clearly suggested that our cave specimens (LIT40_1, LIT48 and LIT66) was a different species with a significant 7 bp. difference with the mesophotic *P. helleri*; 28S (C1-C2) shows a 1 bp. difference, knowing that the C1-D1-C2 fragment is quite conserved (we are missing the much more variable D2 part, which is ideal to discriminate species). This whitish encrusting species had thinner microxeas, smaller oxyasters with >10 actines and very scarce dichotriaenes. This species actually resembles *P. helleri* forma *subtilis* Sarà & Sribelli, 1960 found on rocky bottoms in the Gulf of Naples (20-25 m) and in caves. *P. subtilis* is described as whitish encrusting, small, with weak microxeas and with very scarce dichotriaenes, just as in our cave specimens. In fact, in her thesis *Bibiloni (1990)* assigned cave *P. helleri* from Mallorca to the *subtilis* variety. However, the description of *P. subtilis* is incomplete (the size of oxyasters is notably missing) and it suggests there are two distinct sizes of microrhabds (32-80 µm and 103-213 µm) vs. only one in our material (31-165 µm). Furthermore, the type material of *P. helleri* var. *subtilis* (specimens #773:2 and #783:2) could not be revised here, it is unfortunately missing and presumably lost (pers. comm., 'Stazione Zoologica Anton Dohrn', Naples, curator Dr. Andrea Travaglini; 'Museo Civico di Storia Naturale "G. Doria"', Genoa, curator Dr. Maria Tavano; 'Museo zoologico, Naples University', curator Dr. Roberta Improta; 'Museo di zoologia', Bari, Dr. Giovanni Scillitani). Instead of risking to mis-identify this common Mallorcan species, we decided to create *P. isabellae* **sp. nov.**, before someone can sequence several *P. helleri* from the Gaiola area in the Gulf of Naples for comparison.

The fourth species in this complex was originally identified as *P. helleri* in *Chombard et al. (1998)* but is here again revealed different thanks to 28S. The full 28S (C1-D2) fragment of a specimen from the 3PP cave (La Ciotat, France, AF062598) has surprising 12 bp. and 13 bp differences with respectively our mesophotic *P. helleri* and *P. isabellae* **sp. nov.** This specimen (PC325) was re-examined here, it is a cave specimen with many dichotriaenes, large oxyasters (13-47 µm) as in *P. helleri* and non-centrotylote shorter microxeas (25-105/2-4 µm), as in *P. isabellae* **sp. nov**. Interestingly, it has common double-bent microxeas, which were never observed in our

Balearic specimens. More "*P. helleri*" from the 3PP cave need to be sequenced in order to confirm and understand this potential new species. Meanwhile, this brings additional data to possible cryptic cave faunas. Marine caves are often considered isolated habitats, with cave fauna being poorly connected and having low gene flow, a fact that promotes speciation and high levels of endemism (*Juan et al., 2010*). Patterns of genetic connectivity between cave sponges are understudied, but some works pointed to a high isolation pattern (*Muricy et al., 1996*).

Finally, a fifth species is represented by the specimen ZMAPOR 21658 from another shallow cave, this time on Flores Island, in the Azores. This Flores *P. helleri* is genetically much closer to the 3PP cave specimen than to the Balearic specimens. Indeed, This Flores specimen and the 3PP cave specimen group in a well supported clade, along with a sequence of *Penares sclerobesa* Topsent, 1904 , while the Balearic specimen seem to group closer to the *Erylus mamillaris/discophorus/deficiens* complex (Fig. 4.3.19). The Flores specimen also has double-bent microrhabds, like those observed in the 3PP cave specimen, which thus may be a good character for future discrimination.

To conclude, the discovery of a polyphyletic *P. helleri* brings new taxonomic issues because if indeed the type of *P. helleri* from the Adriatic Sea is conspecific with our mesophotic specimens, then the phylogenetic relationship *P. helleri/P. euastrum* (based on the position of the 3PP "*P. helleri"* sequence) is no more. This means that the reallocation of *P. euastrum* (and *P. cavernensis* **sp. nov.**) to the genus *Penares* would not be justified. Our current phylogenetic COI and 28S trees now reveal a complex mix of *Erylus* and *Penares* species, with mostly poorly-supported nodes, thus begging for better and additional markers.

Subfamily Geodiinae Gray, 1867

Genus *Geodia* Lamarck, 1815

Geodia matrix sp. nov. Díaz & Cárdenas

(Figs. 4.3.10 and 4.3.30; Table 4.3.13)

Etymology

Named *matrix* in analogy with something that harbors other elements, because the species always incorporates all kinds of substrata on its body, and also is a substrate to many other sponge epibionts; also after the 1999 film by the Wachowski sisters (https://en.wikipedia.org/wiki/The_Matrix).

Material examined

Holotype: UPSZTY 190881, field#i577_1, St. 21 (INTEMARES0720), MaC (AM), 109 m, beam trawl, coll. J. A. Díaz.

Paratypes: UPSZTY 190876, field#i146_1A, St. 51 (INTEMARES0718), MaC (EB), 128 m beam trawl, coll. F. Ordines; UPSZTY 190879, field#i244_B1, St. 50 (INTEMARES1019), MaC (AM), 102 m, beam trawl, coll. J. A. Díaz; UPSZTY 190880, field#i545, St. 19 (INTEMARES0720), MaC (AM), 111-94 m, rock dredge,

coll. J. A. Díaz; UPSZTY 190882, field#i577_2, St. 21 (INTEMARES0720), MaC (AM), 109 m, beam trawl, coll. J. A. Díaz.

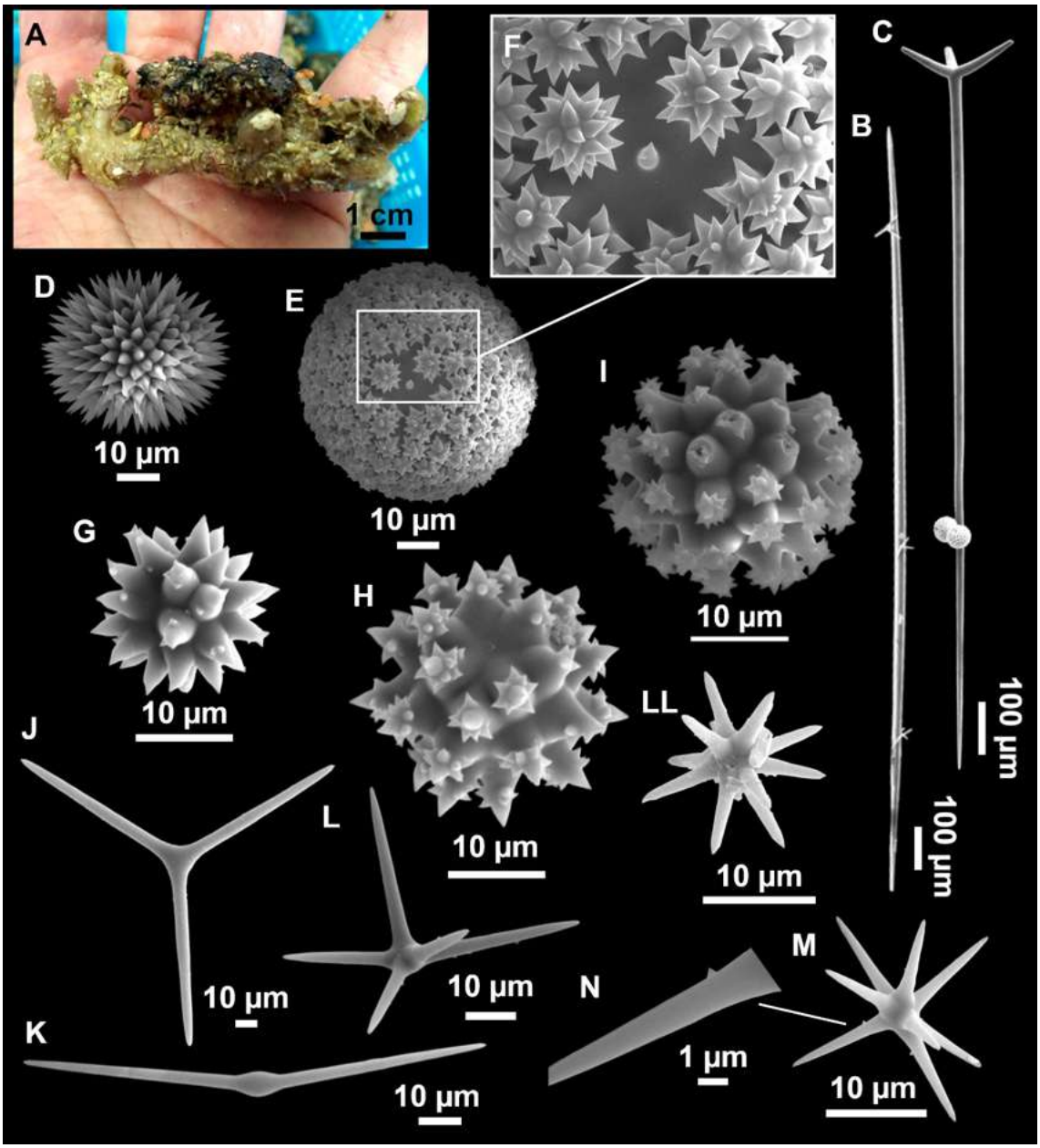

Figure 4.3.30. Holotype of *Geodia matrix* **sp. nov.**, UPSZTY 190881 (i577_1). (A) Habitus on deck with a *Hexadella* sp. epibiont (dark lilac). (B-N) SEM images of the spicules. (B) Oxea. (C) Plagiotriaene. (D) Im-mature sterraster. (E) Sterraster with (F) detail of the rosettes. (G–I) Spherasters. (J–L) Oxyasters I. (LL– N) Oxyasters II with (N) detail of the spines.

Comparative material

Geodia canaliculata Schmidt, 1868, holotype, MNHN-DT750, MNHN Schmidt collection#61, wet specimen and slide, Algeria, 'Exploration Scientifique de l'Algérie', 1842.

Outer morphology

Ramose sponge, growing repent and incorporating all kinds of gravels from the substrate. In life, light brown (Fig. 4.3.30A), dark brown after ethanol fixation. Choanosome dirty beige after ethanol fixation. The holotype is 7x2.5x.5 cm. Surface smooth to hispid. Hard but breakable consistency. Small uniporal openings barely visible, often at the tips of the lobes, probably oscules, but maybe also pores. Cortex 0.3-0.5 µm mm thick. The species is usually covered with other sponges, like *Hexadella* sp. (Fig. 4.3.30A), haplosclerids, poecilosclerids and an orange encrusting *Timea* sp.

Spicules

Oxeas (Fig. 4.3.30B), slightly curved and fusiform, 566-1949/7-28 µm.

Plagiotriaenes (Fig. 4.3.30C), rhabdome stout and long, straight to slightly bent, with a sharp end. Smaller ones with a marked swelling below the cladome. Clads are usually disposed in a 60-70° angle with the rabdome, they are short and triangular, straight or slightly curved upwards, some aberrant or underdeveloped. Rhabdome: 728-1623/9-36 µm, cladi: 29-179/7-29 µm.

Sterrasters (Fig. 4.3.30D-F), spherical, smooth rosettes (Fig. 4.3.30F), measuring 26-71 µm.

Spheroxyasters (Fig. 4.3.30G-I), smooth, with triangular actines. Young spherasters have few spines (Fig. 4.3.30G) while fully developed spheroxyasters have many spines concentrated at the tips of the actines (Fig. 4.3.30H-I), resembling the rosettes of the sterrasters. Measuring 11-33 µm in diameter.

Oxyasters I (Fig. 4.3.30J-L), 2-7 actines. The less actines they have, the larger they are. Actines are essentially smooth with a few occasional small spines. Measuring 36-92 µm in diameter.

Oxyasters II (Fig. 4.3.30LL-N), uncommon, with 4-11 slightly microspined actines (Fig. 4.3.30N), 16-37 µm in diameter.

Ecology and distribution

Always found associated with rhodolith beds at the summit of the AM and the EB seamounts, where it can be very abundant and significantly contribute to the overall biomass in hundreds of kg per m2 (check). Due to its relatively large size and high abundance, the species may play a role as habitat builder, providing shelter to smaller associated fauna. It is always overgrown by other sponges, mostly *Hexadella* sp., *Timea* sp. and several haplosclerids.

Genetics

COI (ON130523, ON130524, ON130525) and 28S (C1-C2) (ON133885, ON133886, ON133887) were obtained from i146_1A, i244_B1, i577_1 (holotype) and i577_2.

Taxonomic remarks

Geodia matrix **sp. nov.** appears to have uniporal oscules/pores, which is only found in a few temperate Atlanto-Mediterranean species, previously grouped in the genus *Isops*: *Geodia geodina* (Schmidt, 1868), *G. canaliculata*, *Geodia globus* Schmidt, 1870 and *Geodia pachydermata* Sollas, 1886. Two more species should be considered for

Table 4.3.13. Spicule measurements of *Geodia matrix* **sp. nov.** and *Geodia canaliculata*, given as minimum-mean-maximum for total length/minimum-mean-maximum for total width; all measurements are expressed in µm. Balearic specimen codes are the field#. Rh: rhabdome; Cl: clad; -=not found/not reported; n.m.= not measured; EB: Emile Baudot; AM: Ausias March.

Material	**Depth** (m)	**Oxeas** (length/width)	**Anatriaenes** Rhabdome (length/width) Clad (length/width)	**Plagiotriaenes** Rhabdome (length/width) Clad (length/width)	**Sterrasters** (diameter)	**Oxyasters I** (length)	**Oxyaster II** (length)	**Spherasters** (length)
***G. matrix* sp. nov. i244_B1 EB**	102	910-1377-1785/ 9-16-24	-	Rh: 748-1113-1615/11-22-32 (N=14) Cl: 41-133-179/8-18-24 (N=17)	40-49-57	36-58-92 2-7 actines	18-26-32 6-11 actines (N=18)	12-23-33
***G. matrix* sp. nov. i146_1A AM**	128	817-1317-1705/ 6-15-23	-	Rh: 728-1038-1415/9-22-36 Cl: 29-93-146/7-17-29	26-49-63	38-55-79 2-6 actines	14-24-28 6-11 actines (N=7)	12-18-22
***G. matrix* sp. nov. Holotype i577_1 AM**	109	867-1454-1879/ 12-21-28 (N=17)	-	Rh: 769-1259-1606/14-23-30 Cl: 78-121-168/15-21-28 (N=17)	44-52-60	43-65-89 2-6 actines	17-22-32 6-9 actines (N=19)	16-20-31
***G. matrix* sp. nov. i577_2 AM**	109	566-1405-1949/ 7-18-28	-	Rh: 786-1193-1623/13-22-31 Cl: 73-97-140/11-18-27 (N=10)	43-55-71	42-64-81 2-7 actines	17-25-37 7-11 actines (N=14)	11-20-31
***G. matrix* sp. nov. i545 EB**	94-111	1016-1477-1713/12-19-23 (N=14)	Rh: 1350/6 Cl: 15/7 (N=1)	Rh: 761-1050-1311/13-18-30 Cl: 71-117-165/11-16-27 (N=9)	41-53-63	50-62-81 2-5 actines (N=18)	16-23-31 4-9 actines (N=17)	17-21-26 (N=13)
***G. canaliculata* holotype, Algeria MNHN DT750**	-	n.m.	n.m.	n.m. (malformed cladomes with large axial canals)	44-50-62	-	12-21-30 (N=20) (few)	20-22-25 (N=5) (very few)
G. canaliculata La Calle, Algeria (*Topsent, 1901*)	*"Corallig en banks"*	1900/ 33	-	Aberrant cladomes Rhabdome robust, >1000/ 30	45-60	-	-	20-25

comparison, since their opening morphologies are unknown: *Geodia echinastrella* Topsent, 1904 and *Geodia spherastrella* Topsent, 1904.

Geodia geodina has smaller spheroxyasters (10-18 µm), which do not develop spines at their tips (cf. below). *G. globus*, is a poorly described species only reported once from Portugal but a re-description of the type suggests it has strongylasters (9 µm), and no spherasters (*Burton, 1946*). *G. pachydermata* has a very typical external warty appearance, and much larger sterrasters (>200 µm). *G. echinastrella* from the Azores, resembles *G. matrix* **sp. nov.** in having similar size spherical sterrasters (47-50 µm) and similar sized smooth oxyasters (22-26 µm), however, it has smaller spherasters (15-18 µm) and is lacking the large oxyaster category. *G. spherastrella* also from the Azores has larger and ellipsoidal sterrasters (90-110 µm), smaller spherasters (14-16 µm) and only one size of spiny oxyasters (25 µm).

Of all known Atlanto-Mediterranean species, *G. matrix* **sp. nov.** is closest to *G. canaliculata,* a poorly-known species reported twice from the coast of Algeria more than 100 years ago (*Schmidt, 1868; Topsent, 1901*). The holotype (Fig. 4.3.31) was revised by *Topsent (1938)* but re-examined here and thick sections were made (Fig. 4.3.31D-G): it is a massive sponge with uniporal openings (Topsent also could not distinguish oscules from pores), which explains its placement in the former genus *Isops* by *Topsent (1901)*. It can be added to the detailed description given by *Topsent (1938)* that the holotype is overgrown by an encrusting poecilosclerid with hymedesmoid skeleton (reddish color, Fig. 4.3.31D-E) and the cortex is 0.25-0.3 mm thick (measured on thick sections). On our sections, oxyasters are essentially found just below the cortex (moderate abundance) while spheroxyasters (at different stages of development) are found throughout the choanosome (low abundance, Fig. 4.3.31F), with rare presence in the cortex. More surprisingly, slightly flexuous microtoxas were found, often slightly centotylote (160-220 µm long; Fig. 4.3.31G); they look like flattened flexuous microtoxas such as the ones from the encrusting sponge *D. annexa,* a common epibiont in the Atlanto-Mediterranean Sea region. They clearly appeared on the thick sections we made, fairly abundant throughout the choanosome, and with no particular orientation. Such spicules have never been observed before in *Geodia* species so we consider them to be probably foreign, but we also note that there are no other spicule contamination in the choanosome than these flexuous microtoxas (i.e. no other typical *D. annexa* spicules). As a result, despite some shared characters with *G. canaliculata* (irregular lobose/ramose shape with numerous foreign bodies and epibionts, uniporal oscules/pores, sterraster size, characteristic spherasters)*, G. matrix* **sp. nov.** has two significant differences: i) well-developed regular plagiotriaenes (vs. aborted cladomes), and ii) large and small oxyasters (vs. only small oxyasters).

Attention should be paid to the fact that *G. matrix* **sp. nov.** tends to be overgrown by *Timea* sp. This species has spheroxyasters of a similar shape and size (6-19-30) as those of *G. matrix* **sp. nov.** and so they mixed in our first spicule preparations. The subtle difference is that spheroxyasters of *G. matrix* **sp. nov.** have a larger centrum and heavily spined actines, especially at their tips. *Timea* sp. has a characteristic orange color in life but it turns brownish after ethanol fixation, so its presence is hard to notice once specimens are fixed. After carefully digesting separately clean cortex and choanosome, we observed that *Geodia* spheroxyasters are much more abundant in the cortex,

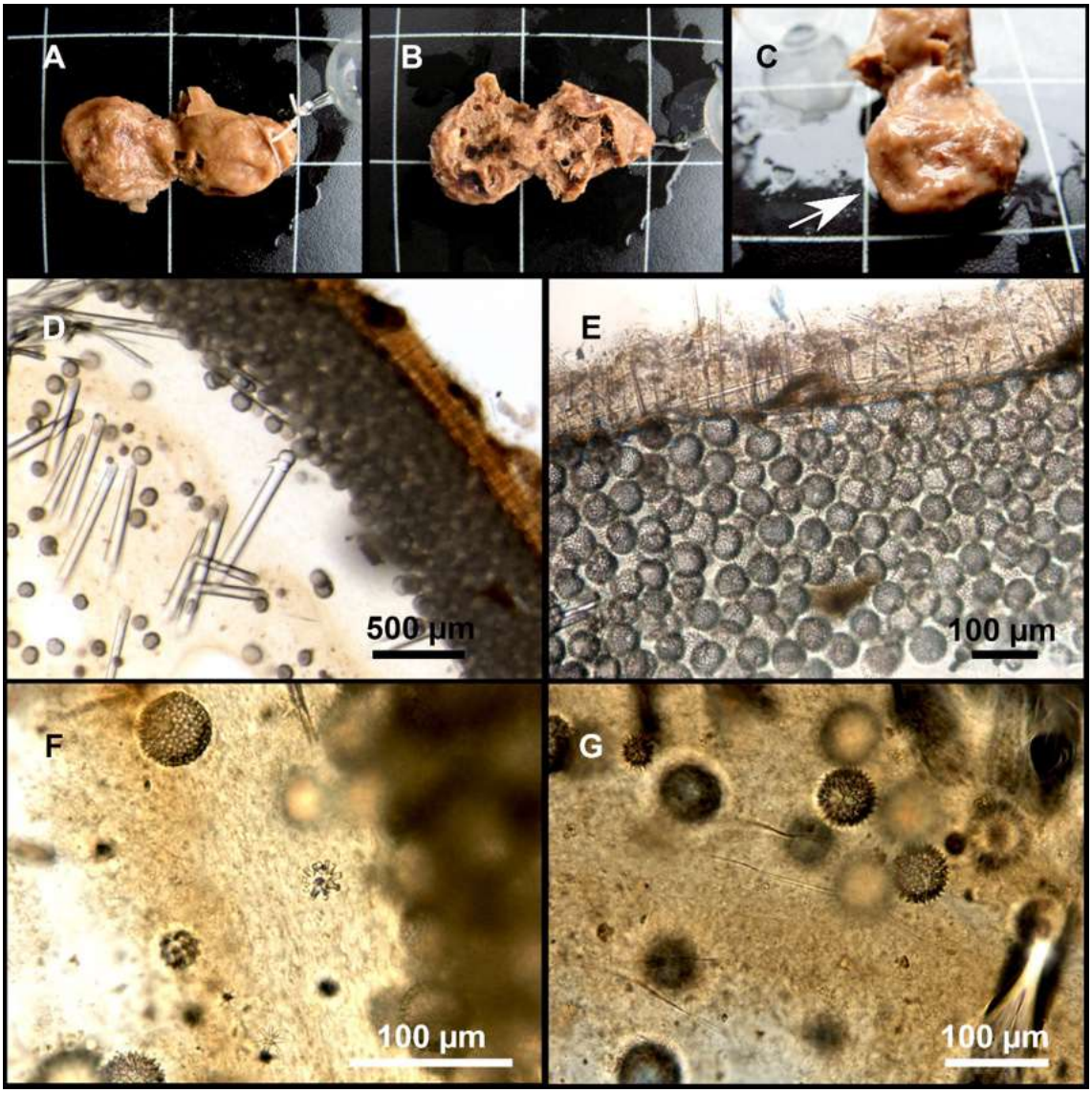

Figure 4.3.31. Holotype of *Geodia canaliculata Schmidt, 1862*, MNHN DT750, Algeria. (A–C) Habitus, notably showing the uniporal openings in C (arrow). (D–G) Optical microscope images of thick sections. (D) Transversal section of the cortex with an underdeveloped triaene. (E) Detail of the cortex and the poe-cilosclerid epibiont. (F) Detail of the choanosome with spheroxyasters. (G) Detail of the choanosome with foreign toxas. Scale rid of A–C: one cm.

suggesting that spheroxyasters could be ectocortical or located just below the cortex. However, we could not confirm this as in the thick sections the cortex was always covered by the *Timea* sp. We further note that spheroxyasters are overall much more abundant in *G. matrix* **sp. nov.** than in the holotype of *G. canaliculata*; this characteristic should be confirmed with new specimens of *G. canaliculata*. According to their similar spicules, *G. canaliculata* and *G. matrix* **sp. nov.** are undoubtedly phylogenetically close species. It is also clear that the typical spheroxyasters in both species are homologous. There has been some confusion regarding these spheroxyasters in *G. canaliculata* (*Topsent, 1901, 1938*), which SEM observations of *G. matrix* **sp. nov.** have helped us to understand. *Schmidt (1868)* and *Topsent (1901)* mention the presence of smaller sterrasters, with less actines than the regular ones, later thought to

be a different category of spicule (*Topsent, 1938*). These are actually fully-developed spheroxyasters with spiny tips, as observed in *G. matrix* **sp. nov.** (Fig. 4.3.30I) or in other species but with a smaller size (*G. pachydermata*, *G. spherastrella*). The confusion arises because these spheroxyasters are almost as large as the sterrasters and sometimes mixed with them in the cortex.

COI and 28S tree suggest that *G. matrix* **sp. nov.** is related to species *Geodia parva* Hansen, 1885, *Geodia phlegraei* (Sollas, 1880)*, G. geodina*, *Rhabdastrella intermedia* Wiedenmayer, 1989 and *Rhabdastrella* sp.1 South Africa. (Fig. 4.3.10). Those species do not belong to the three main *Geodia* clades (*Cydonium*^{P}, *Depressiogeodia*^{P} and *Geodia*^{P}) (*Cárdenas et al., 2011*), and may represent a fourth group in *Geodia* based on shared smooth oxyasters and presence of spheroxyasters, despite no bootstrap support for the clade at the moment.

Geodia geodina (Schmidt, 1868)

(Figs. 4.3.10 and 4.3.32-4.3.34; Table 4.3.14)

Synonym

Stelletta geodina Schmidt, 1868

Cydonium geodina (Schmidt, 1868)

Sidonops geodina (Schmidt, 1868)

Synops anceps Vosmaer, 1894 (new synonym)

Isops anceps (Vosmaer, 1894) (new synonym)

Geodia anceps (Vosmaer, 1894) (new synonym)

Not *Geodia anceps* in *Sitjà et al. (2019)* from the Gulf of Cadiz: renamed in the present paper as *Geodia phlegraeioides* **sp. nov.**

Material examined

UPSZMC 190862-190863, field#i140_A and field#i140_B, St. 51 (INTEMARES0718), MaC (EB), 135 m, beam trawl, coll. F. Ordines; UPSZMC 190868, field#i391_3, St. 158 (INTEMARES1019), MaC (EB), 146 m, beam trawl, coll. J. A. Díaz; UPSZMC 190870-190871, field#i575 and field#i576, St. 21 (INTEMARES0720), MaC (AM), 109 m, beam trawl, coll. J. A. Díaz; UPSZMC 190872, field#i708, St. 45 (INTEMARES0720), MaC (EB), 150 m, beam trawl, coll. J. A. Díaz.

Comparative material

Geodia geodina, lectotype (designated here), MNHN Schmidt collection#91 (large specimen), paralectotype (designated here), MNHN Schmidt collection#93 (small specimen), both specimens in the same jar registered under MNHN DT752, wet specimens, Algeria, 'Exploration Scientifique de l'Algérie', 1842; MNHN DCL728, spicule slide, East Gettysburg, Gorringe Bank, St. 149, trawl, 95 m *(Lévi & Vacelet, 1958)*; MNHN (unregistered), field#JC46, Jean Charcot Madeira 1966, SW of Deserta Islands, 32º21'30''N, 16º30'18''W, 100-130 m, wet specimen, 18 July 1966, id: P. Cárdenas.

Geodia anceps, syntype, NHM 1955.3.24.1 (= RMNH POR0655), wet specimen, label from the 'Rijksmuseum-Leiden' saying 'coll. no. 655, fragment of type sp.', Vosmaer personal number N557, between Capri and Naples, 150-200 m, 12 Feb. 1891.

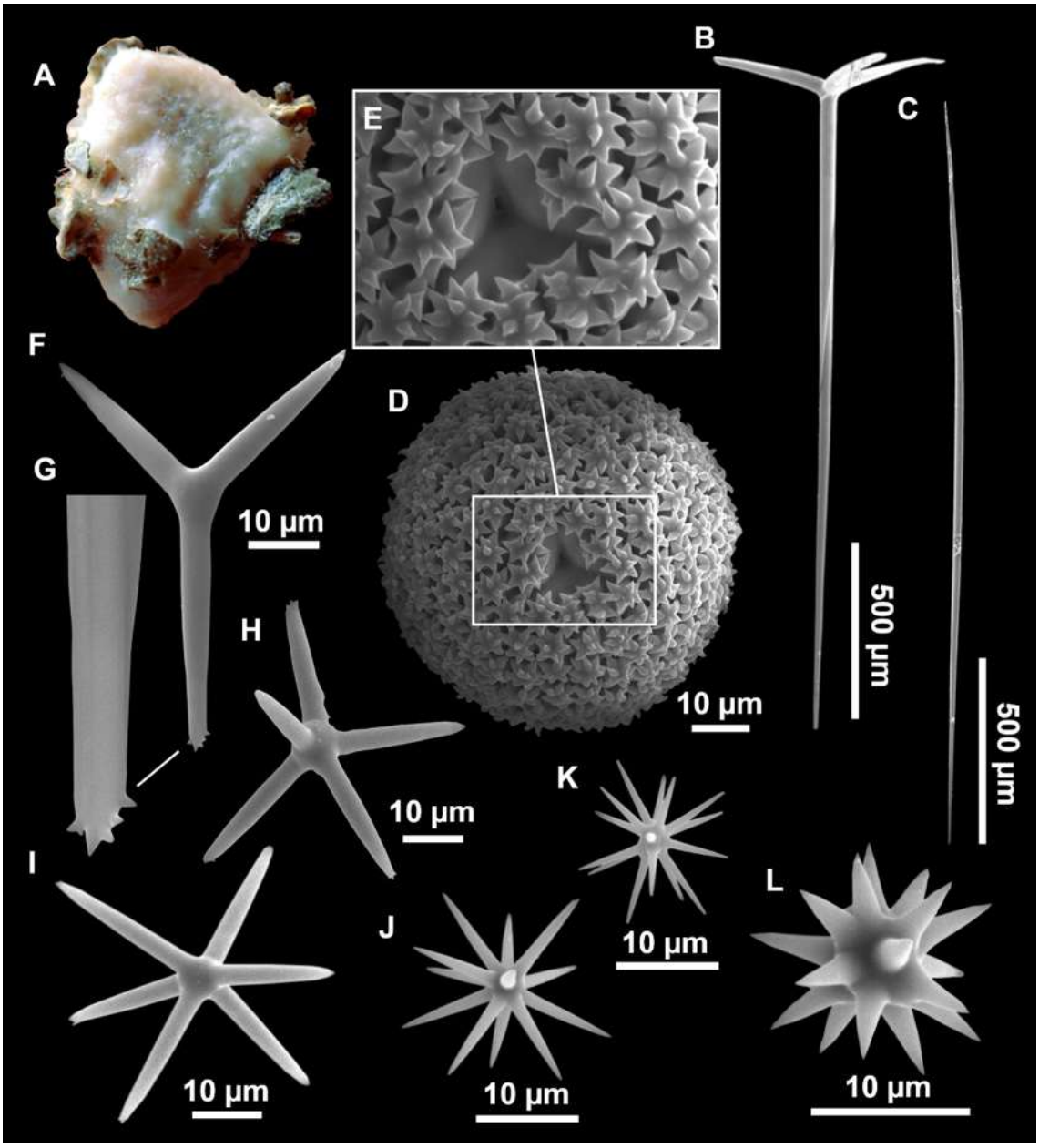

Figure 4.3.32. *Geodia geodina* (*Schmidt, 1868*), specimen i708. (A) Habitus after EtOH. (B) Orthotriaene. (C) Oxea. (D) Sterraster with (E) detail of the rosettes. (F–I) Oxyasters I with (G) detail of the spines. (J– K) oxyasters II. (L) Spheraster.

Outer morphology

Massive, globular (Fig. 4.3.32A), to ramose or lobated. Larger specimens up to 12 cm in maximum diameter. Grayish ocher in life, dark brown after ethanol fixation. Always paler on the lower side of the body (protected from the light). Surface smooth to hispid, smooth to the touch. Hard, only slightly compressible consistency. Cortex less than 0.5 mm thick, clearly distinguishable. Choanosome fleshy, whittish. Uniporal oscules are grouped on the top surface of specimens or at the top of lobes, always contracted on

deck and after ethanol fixation. Uniporal pores gathered in depressed areas, visible to the naked eye in some specimens.

Spicules

Orthotriaenes (Fig. 4.3.32B), rhabdome straight and fusiform; the smaller ones have a triangular swelling at the joint with the cladome. Clads are disposed in a 100° angle with the rhabdome, some being slightly tortuous or having its tips curved inwards. A single cladome modification in the form of dichotriaene was observed. Rhabdome measuring 419-1947/11-54 µm, cladi measuring 71-470/11-50 µm.

Oxeas (Fig. 4.3.32C), slightly curved and fusiform, measuring 748-2614/6-38 µm.

Anatriaenes, uncommon, with straight, fusiform rhabdome, 1180-2687/5-19 µm. Clads with short cladi, evenly curved, measuring 3-97/5-16 µm.

Sterrasters (Fig. 4.3.32D), spherical, with smooth rosettes having 4-12 conical rays (Fig. 4.3.32E) , measuring 41-68 µm.

Oxyasters I (Fig. 4.3.32F-I), large, smooth actines, usually with a few spines at its tips (Fig. 4.3.32G), 36-88 µm (2-10 actines).

Oxyasters II (Fig. 4.3.32J-K), smaller than oxyasters I, smooth actines. Measuring 14-38 µm (~6-19 actines).

Spherasters (Fig. 4.3.32L), with triangular actines that can be smooth or microspined at its tips, measuring 8-22 µm.

Ecology and distribution

Circalittoral species found at the summit of the AM and the EB, although reaching greater depths at the EB. It can be very abundant in some stations, suggesting that it is a habitat-forming species due to its large size and sometimes intricate body shape. It is used as a substrate by epibionts, especially other sponges, like *Hexadella* sp., *Timea* sp., as well as several haplosclerids like *Haliclona poecillastroides* (Vacelet, 1969).

Genetics

COI (ON130519, ON130520, ON130521, ON130522) has been obtained for i575, i708, i576 and i140_A, while 28S (C1-C2) (ON133879, ON133880) were obtained from i575 and i708.

Taxonomic remarks. See taxonomic remarks on *G. geodina* and *G. phlegraeioides* **sp. nov.** below.

Geodia phlegraeioides sp. nov. Díaz & Cárdenas

(Table 4.3.14)

Etymology

Named '*phlegraeioides*' to highlight its phylogenetic and morphological closeness with *Geodia phlegraei* (Sollas, 1880) from boreal waters.

Type material

Holotype, MNCN/1.01/1026 (wet specimen), UPSZTY 190886 (thick sections and spicule slide), Almazán mud volcano, Gulf of Cadiz, 36°3’17.39’’N, 7°19’43.20’’W-36°3’36.6’’N, 7°19’13.2’’W (INDEMARES-CHICA), beam trawl, 894-896 m, 4 March 2011, coll: C. Farias, originally identified as *G. anceps* in *Sitjà et al. (2019)*.

Paratype, UPSZTY 190887, field#DR15-972, Le Danois Bank, Cantabrian Sea, station DR-15, 650 m, 44º6’20.64’’N, 5º9’16.2’’W (SponGES0617), rock dredge, 23 June 2017, coll: P. Rios.

Other non-type material examined

Geodia phlegraeioides **sp. nov.,** CPORCANT, DR10-490 and -500, Le Danois Bank, Cantabrian Sea, station DR-10, 44º6’4.8’’N, 4º38’18’’W, 541 m, 17 June 2017, rock dredge, Expedition SponGES0617, coll: P. Rios; CPORCANT DR15-869c, -862c, -882, same station as paratype; COLETA#5803 (=PC566, spicule slide), Banc Princesse Alice, Azores, 37°49’19.2’’N, 20°27’43.2’’W, 432 m, 28 Feb. 2011, subglobular specimen, bycatch from long line demersal fishery TB/137/MBO/2011; COLETA#6243 (=PC567, spicule slide), Banco Voador, Azores, 37°28’58.8’’N, 30°50’34.8’’W, 418 m, 24 June 2010, fragment of a specimen, Coral Fish D33-V10, Palangre de fundo.

Comparative material

Geodia phlegraei, holotype, NHM 1910.1.1.840, Korsfjord, SW Bergen, Norway, 1878, 60°9′60’’N, 5°10’0’’E, 330 m, coll: Rev. A. M. Norman.

Geodia parva, holotype, ZMBN 100, spicule slide, unknown station, Norwegian North Sea Exp. 1876–78.

Outer morphology and skeleton

Massive, subspherical. External color whitish to light brown, alive and in ethanol; choanosome slightly more tanned. Surface is smooth to hispid. Uniporal oscules (up to ~1 mm in diameter) and minute uniporal pores (~0.2 mm in diameter). Cortex is ~0.5 mm thick. Typical geodiid skeleton with ectocortical spheroxyasters and choanosomal oxyasters. The holotype is the largest specimen we have seen so far, 6.5x5x2.5 cm; for a detailed description of the holotype including its spicules, see *Sitjà et al. (2019)*.

Spicules (Table 4.3.14)

Ortho- and dichotriaenes, robust, straight rhabdome 375-2770/11-70 µm, cladi slightly forward oriented, clads of orthotriaenes: 90-580 µm, protoclads: 28-378, deuteroclads: 53–580 µm.

Oxeas, curved and fusiform, 136-3406/16-45 µm.

Sterrasters, spherical, with smooth rosettes, 41-99µm.

Oxyasters, smooth, 11-93 µm.

Spheroxyasters, smooth with a few microspines at tips essentially, 9-32 µm. Specimens from the Azores tend to have a larger centrum.

Ecological notes

Some specimens were found growing on other sponges: DR15-869c was found on *C. (C.) geodioides*, the holotype was growing on a *Pachastrella* sp. The holotype was budding (*Sitjà et al., 2019*).

Genetics

COI were obtained from the holotype (OR045844), COLETA#5803 (OR045842), COLETA#6243 (OR045843) and DR15-869c (OR045845).

Taxonomic remarks on *G. geodina* and *G. phlegraeioides* sp. nov.

Our material from the EB and AM seamounts matches with *G. geodina*, a species described from Algeria (*Schmidt, 1868*) and subsequently reported in the Gulf of Naples (*Pulitzer-Finali, 1972*) and the Gorringe Bank (*Lévi & Vacelet, 1958*). We have compared our material with the type material from Schmidt (lectotype (#91) and paralectotype (#93), here designated), for which new thick sections and SEM was done (Fig. 4.3.33), and the spicules re-measured (Table 4.3.14). The only differences were in the smaller sizes of sterrasters (35-45 µm vs 41-68 µm) and of the orthotriaenes in the type material (Table 4.3.14). In this process, a close morphological similarity with *G. anceps,* a better-known Mediterranean *Geodia,* was also noticed. A syntype of *G. anceps* (NHM 1955.3.24.1) was examined, with new spicule and SEM preparations (Fig. 4.3.34). The type materials of *G. geodina* and *G. anceps* shared the same external morphology, spicule set and morphologies, with similar size ranges (Table 4.3.14). Again, the only noticeable difference was the smaller size of the sterrasters (35-45 µm vs. 50-70 µm) and of the orthotriaenes in the types of *G. geodina*, which may be a result of different depths or habitats, as it is known that sterraster and triaene size can be influenced by these parameters (*Cárdenas & Rapp, 2013*). All previous records of *G. anceps,* from the Gulf of Naples (*Vosmaer, 1894; Pulitzer-Finali, 1972*) or the Alboran Sea (*Maldonado, 1992*), as well as our material, come from mesophotic depths (70-200 m). Unfortunately, we have no locality/depth data for the types of *G. geodina* so it is impossible to test this hypothesis at the moment. Also, anatriaenes with small cladomes were occasionally found in the syntype of *G. anceps* (this study), in previous reports (*Vosmaer, 1894; Pulitzer-Finali, 1972; Maldonado, 1992*), in a NHM Schmidt type slide of *G. geodina* (*Burton, 1946*) as well as in our material from the Balearic Islands; however, no anatriaenes were found in our preparations of the *G. geodina* types. Not finding anatriaenes is not surprising since they can be rare and are often localized to certain parts of the sponge in some *Geodia,* so they can be easily overlooked. To conclude, we propose that *G. anceps* becomes a junior synonym of *G. geodina.*

One single *G. anceps* report is from the Atlantic: from the Gulf of Cadiz, 895 m depth (*Sitjà et al., 2019*). It was stated at the time that sterrasters were larger than in Mediterranean specimens (*Sitjà et al., 2019*). Besides that, we also noted other unusual features in this specimen, such as a mix of orthotriaenes and dichotriaenes, and very rare oxyasters I. Examination of additional Northeast Atlantic specimens originally identified as *G. anceps* from Le Danois Bank (Cantabrian Sea) at 650 m and two

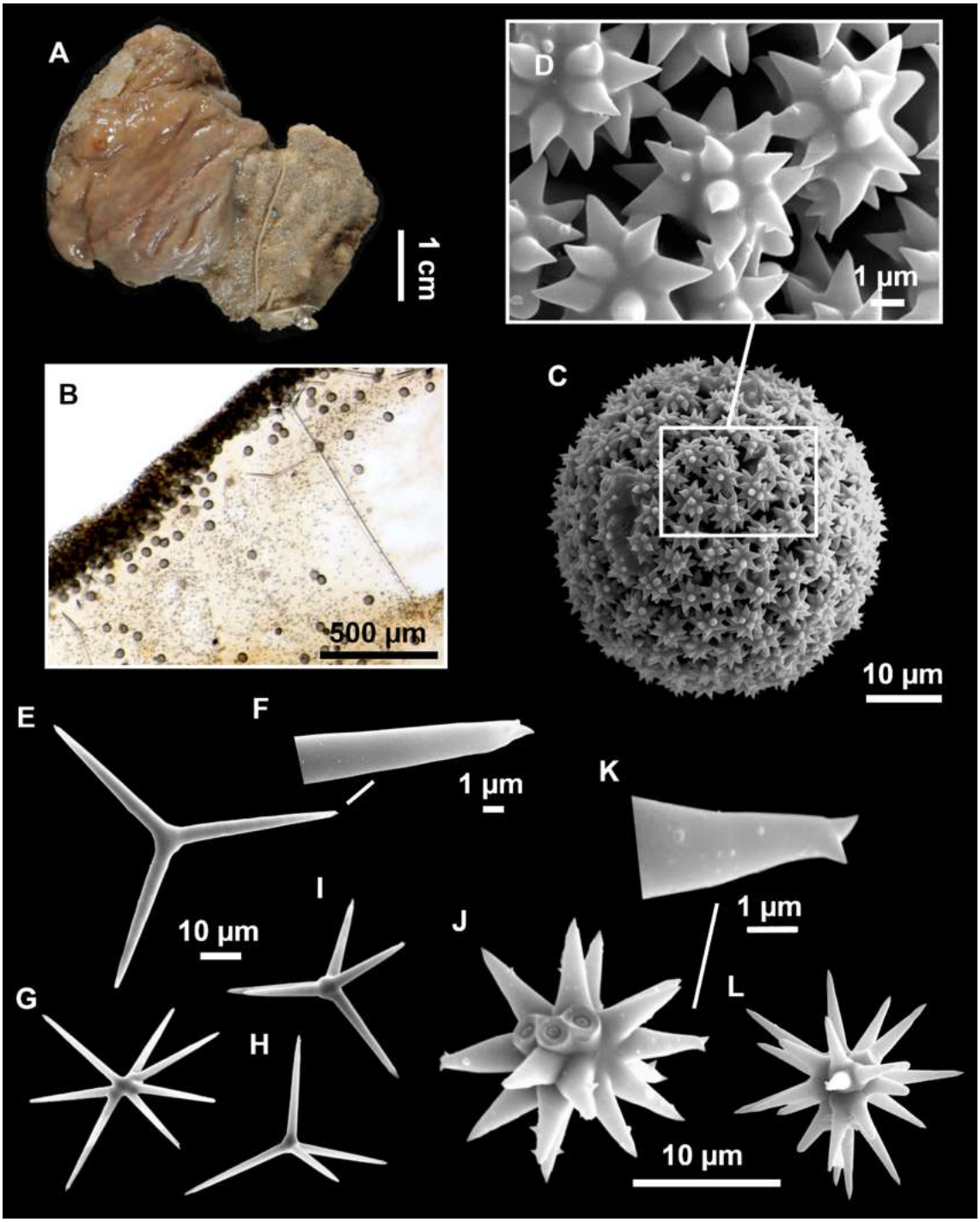

Figure 4.3.33. Lectotype of *Geodia geodina* (*Schmidt, 1868*), MNHN Schmidt collection#91 Algeria. (A) Habitus. (B) Optical microscope image of a thick transversal section. (C) Sterraster with (D) detail of the smooth rosettes. (E–I) Oxyasters I with (F) detail of the spines. (J) Spheraster with (K) detail of the spines. (L) Oxyaster II.

specimens collected South of the Azores (418-432 m) revealed these exact same characters: i) larger sterrasters with an average size of 68-94 µm (vs. 40-61 µm in *G. geodina*), ii) common dichotriaenes mixed with orthotriaenes, iii) usually only one category of oxyasters with a continuum of sizes from 11 to 93 (vs. two separate sizes in *G. geodina*) and iv) slightly larger spheroxyasters with an average size of 14-21 µm (vs. 13-15 µm in *G. geodina*). Although *Sitjà et al. (2019)* report two oxyaster categories,

Table 4.3.14. Spicule measurements of *Geodia geodina, Geodia phlegraeioides* **sp. nov.** and related species *Geodia phlegraei* and *Geodia parva*, given as minimum-mean-maximum for total length/minimum-mean-maximum for total width; all measurements are expressed in µm. Balearic specimen codes are the field#. Rh: rhabdome; OPD: ortho/proto/deuteroclads; -=not found/not reported; n.m.= not measured; EB: Emile Baudot, AM: Ausias March.

Material	**Depth** (m)	**Cortex thickness** (mm)	**Oxeas** (lenght/width)	**Anatriaenes** Rhabdome (length/width) Clad (length/width)	**Orthotriaenes** Rhabdome (length/width) OPD ortho/proto/deuteroclads Clad (length/width)	**Sterrasters** (diameter)	**Oxyasters I** (diameter)	**Oxyasters II** (diameter)	**Spherasters** (diameter)
G. parva holotype ZMBN 100 (*Cárdenas et al., 2013*)	-	-	773-1194-1625/ 14-21-34 (N=6)	-	Rh: 360-697-1000/ 20-26-33 (N=8) OPD: 102-161-232 (N=7)/ 56/44	75-85-93	19-42-64		13-16-21
G. phlegraei holotype NHM 1910.1.1.840 (*Cárdenas et al., 2013*)	330	0.64	1825-3293-448/ 20-41-60	Rh: >3760/ 8-19-25 (N=6) Cl: 48-72-130 (N=6)	Rh: 586-2129-3640(N=10)/ 12-50-72 OPD: 80-416-660/ 220-250(N=2)/ 100-250 (N=2)	82-93-102/76-86-95	17-24-40.8		12-17-24
G. anceps **syntype NHM 1955.3.24.1 Capri-Naples**	150-200	-	900-1907-2580/ 8-28-42	Rh: 1689 (N=1)/ 7-8-9 (N=3) Cl: 20-30-37	Rh: 830-1426-1920/18-39-62 OPD: 130-262-390 160 (N=1)/130 (N=1)	50-61-70	30-51-75 (3-8 actines)	12-17-25 (>8 actines)	10-13-15 (N=10) (sometime spiny at tips)
G. geodina **lectotype MNHN DT752 Algeria**	-	0.15-0.2	1536/20 (N=1)	-	Rh: >1050/8-17-25 (N=12) OPD: 88-199-320/-/-	38-42-45	35-53-65 (3-8 actines) (very abundant)	10-17-27	10-15-18
G. geodina **paralectotype MNHN DT752 Algeria**	-	0.15-0.2	broken	-	Rh: broken/10-17-25 OPD: 100-197-326/-/-	35-40-45	20-40-62 (>3 actines) (very abundant)	8-14-18	8-14-20
G. geodina MNHN syntypes (*Topsent, 1938*)	-	0.5	2200-2400/ 20-25	-	Rh: 1250/ 16-18 OPD: 200-300/-/-	40-45	30 (actine) (4-8 actines)	15-17	-
G. geodina **i140_b EB**	128	-	1494-1856–2534/6-19-31 (N=12)	Rh: 1421-1845-2020/10-14-17 (N=10) Cl: 21-28-37/8-10-13 (N=10)	Rh: 1316/ 27 (n=1) Cl: 206-294-343/ 20-27-33 (n=12)	41-51-59	38-61-86 (2-8 actines)	11-21-27 (8-12 actines)	10-14-18
G. geodina **i708**	130	-	748-1918-2614/8-25-36	Rh: 2006-2687 (N=2)/9-10 (N=3)	Rh: 797-1650-1947/ 16-39-54 (N=11)	46-54-64	41-53-77 (3-8 actines)	14-25-38 (6-15 actines,	11-14-18 (uncommon)

AM				Cl: 3-37/8-10 (N=3)	Cl: 112-279-372/ 13-35-50 (N=10)			largest one has 6 actines)	
G. geodina **i575 AM**	110	-	1208-1668-2176/14-24-35	Rh: 1180 (N=1)/5-17 (N=2) Cl: 22-97/5-16 (N=2)	Rh: 419-1085-1395/ 11-24-32 (n=9) Cl: 71-284-470/ 11-26-36 (n=31)	46-57-66	40-54-74 (3-6 actines)	14-23-30 (8-19 actines)	12-14-15 (uncommon, N=11)
G. geodina **i576 AM**	110	-	1357-1742-2145/11-23-36 (n=20)	Rh: 1597 (n=1)/ 8-14 (n=10) Cl: 20-36/9-14 (n=10)	Rh: 523-1092/ 13-22 (n=2) Cl: 99-246-340/ 10-23-30 (n=17)	47-52-64	38-51-61 (4-9 actines, never 2)	15-25-36 (~7-14 actines)	13-14-17 (n=11)
G. geodina **i140_a EB**	128	-	1185-1740–2500/16-24-38	Rh: 1428/19 (n=1) Cl: 39/16 (n=1)	Rh: all broken Cl: 175-270-330/ 20-28-32 (n=10)	44-56-68	36-61-88 (6-10 actines)	16-22-35 (N=19) (6-13 actines)	8-14-22
G. anceps Alboran Sea (*Maldonado, 1992*)	70-120	0.5-0.7	1085-3000/15-30 600-1812/ 2-4 (flexuous; in 1 specimen)	Rh: 200-961/ 4-10 Cl: 15-25	Rh: 433-1700/ 15-26 OPD: 80-273/ 140-160/113-170	44-68	30-46 (actine length) (2-5 actines)	17-27 (>6 actines)	12-25
G. geodina **MNHN DCL728 Gorringe Bank, (*Lévi & Vacelet, 1958*)**	95	0.5	640-1468-2150/10-18-25	Rh: 1254-1636-1971 (N=5)/4-7-12 Cl: 13-29-50	Rh: 1020-1561 (N=2)/ 13-18-22 (N=10) OPD: 133-258-367	42-48-50	43-54-67 (3-5 actines) (very abundant)	12-20-37	10-13-16
G. phlegraeioides holotype, MNCN-P224-11 Gulf of Cadiz (*Sitja et al., 2019*) **(this study)***	895	0.5	2122-3406/ 16-42	Rh: Up to 1500/ 6-8 Cl: -	Rh: 375-2770/ 14-70 OPD: 97-580/ 122-378/ 121-338	77-91 **75-81-87***	31-50 (2-5 actines) (rare) **-***	18-30 (6-8 actines) **12-19-30***	13-29 (sometime spiny)
G. phlegraeioides **paratype, UPSZTY 190887 (DR15-972) Le Danois Bank**	650	0.5	broken	-	Rh: broken/ 28-61 (N=2) OPD: 93-255-459 (N=5)/ 86-180-247 (N=11)/ 194-269-351 (N=10)	87-94-99	19-36-57		14-21-32
G. phlegraeioides **DR15-869c Le Danois Bank**	650	-	broken	-	Rh: - OPD: 281/ 140/249-254	41-78-92	12-24-61		9-14-17
G. phlegraeioides **DR15-862c Le Danois Bank**	650	-	145-975-2995 (N=12)/ 15-20 (N=2)	-	Rh: 1012-1134 (N=2)/ 37-45 (N=2) OPD: 131-273-508 (N=4)/	76-83-91	42 (N=1)	16-19-25 (N=20)	10-16-20

					28-131-307 (N=5)/ 53-217-580 (N=5)				
G. phlegraeioides **DR15-882 Le Danois Bank**	650	-	136-1161-2892 (N=22)/-	-	Rh: 955-1130-1324 (N=3)/ 37 (N=1) OPD: 90-307-575 (N=9)/ 92-172-220 (N=15)/ 93-201-315 (N=15)	58-83-96	14-36-94		12-18-25
G. phlegraeioides **COLETA#5803 Banc Princesse Alice, Azores**	432	-	>3328/ up to 45	Rh: >3840/ 10-19-25 (N=7) one ana(meso)triaene Cl: 35-58-87 (N=7)	Rh: 1740-2333-2670 (N=16)/ 35-42-50 OPD: 327-336-449/-/-	60-69-87	10-15-25		8-16-25 (large centrum)
G. phlegraeioides **COLETA#6243 Banco Voador, Azores**	418	0.5-0.6	broken	-	Rh: broken/ 20-46-50 (N=11) OPD: 225 (N=1)/ 184-249-357 (N=12)/ 153-252-357 (N=15)	67-78-85	13-22-40		12-15-18 (large centrum)
G. phlegraeioides Italy (*Longo et al., 2005*)	738-809	0.65	1200-1592-2000/20-26-40	Rh: 1100-1900-2500/ 4-8-10 Cl: -/45-70	Rh: 540-1120/- Cl: 90-174-260/- n.m./n.m.	88-99-106	40-56-68 (4-6 actins)	34-48-66 (many actines)	10-14-16
G. echinastrella holotype, Azores (*Topsent, 1904*)	318	"thick"	n.m.	-	orthotriaenes	47-50	22-26		15-18

only one category was found during our re-examination of the specimen. Likewise, only one large oxyaster was found in specimen DR15-862c from Le Danois Bank, suggesting that a second larger category of oxyasters may occasionally be produced in *Geodia phlegraeioides* **sp. nov.** but they are very rare or integrated in a continuum with the first category. On the other hand, large oxyasters are always very common in *G. geodina,* and in a clear separate category. These morphological differences were supported genetically: COI Folmer sequences of these Atlantic specimens had a highly significant 18 bp difference with *G. anceps.* We propose the name *Geodia phlegraeioides* **sp. nov.** for this North Atlantic species resembling *G. anceps* and found deeper, down to the upper bathyal zone (418-895 m). The specimen described by *Sitjà et al. (2019)* is designated as the holotype, while one specimen from Le Danois Bank is designated as a paratype.

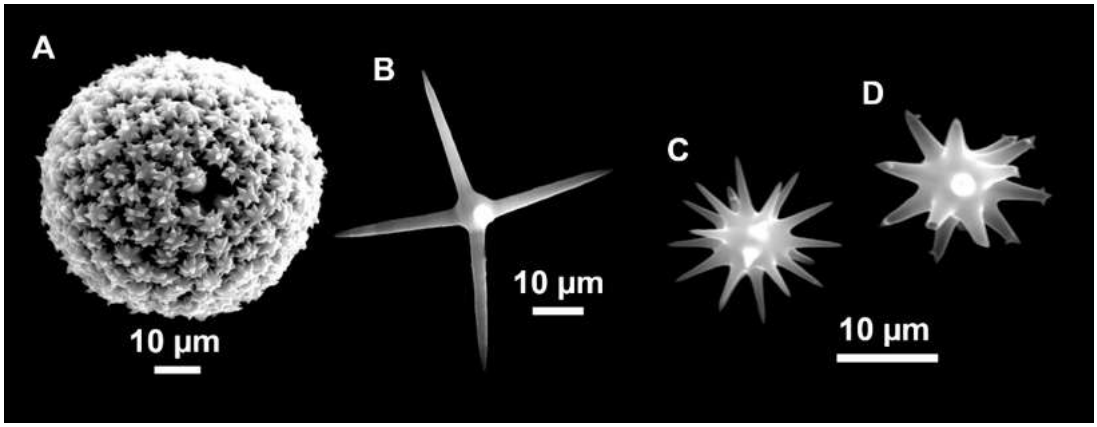

Figure 4.3.34. Syntype of *Geodia anceps* (*Vosmaer, 1894*), NHM 1955.3.24.1, between Capri and Naples, Italy. (A) Sterraster. (B) Oxyaster I. (C) Oxyaster II. (D) Spherasters.

One deep report of *G. anceps* at 738-809 m, from the deep-sea coral reef off Cape Santa Maria di Leuca, Italy (*Longo et al., 2005*) is possibly *G. phlegraeioides* **sp. nov.**: it has larger sterrasters (88-106 µm) and the common dichotriaenes. However, two categories of oxyasters are reported with similar size ranges, which is atypical and needs to be revised. If this was indeed *G. phlegraeioides* **sp. nov.**, it would suggest that this North Atlantic species can also be found in the upper bathyal Mediterranean Sea, below the *G. geodina* zone in the mesophotic area. Likewise, *G. geodina* would also be found in the mesophotic zone in the Atlantic, above the deeper *G. phlegraeioides* **sp. nov.** In fact, a *G. geodina* spicule slide (MNHN-DCL 728) from the Gorringe Bank in the Northeast Atlantic, 95 m depth (*Lévi and Vacelet, 1958*) was re-measured and it fits clearly better the description of *G. geodina* than that of *G. phlegraeioides* **sp. nov.** (Table 4.3.14). This was independently confirmed by the examination of a MNHN large *Geodia* specimen (~12 cm long) from Deserta Islands (close to Madeira) from 100-130 m, that we also identified as *G. geodina*.

With respect to our phylogenetic trees (Fig. 4.3.10), both *G. geodina* and *G. phlegraeioides* **sp. nov.** group with *G. matrix* **sp. nov.**, former species of *Isops (G. phlegraei, G. parva*), which all share as previously said smooth oxyasters, spheroxyasters, and external morphology. In the COI tree, *G. phlegraeioides* **sp. nov.** was the sister species to the clade *G. phlegraei*+*G. parva*; there were respectively 5 and 6 bp differences between them. *G. phlegraei* is a boreal species found from 40 to 3000

m depth, while *G. parva* is its arctic counterpart (*Cárdenas et al., 2013*), so *G. phlegraeioides* **sp. nov.** is the temperate version of *G. phlegraei,* thus explaining our choice for the species name. *G. phlegraeioides* **sp. nov.** seems to have a more irregular shape than *G. phlegraei* (which is subglobular when young and then bowl shaped when larger), with fewer oscules, less visible pores, it can have lots of dichotriaenes (*G. phlegraei* only has orthotriaenes), its sterrasters are round (vs. usually oval in *G. phlegraei*). *G. geodina* is also quite close to *G. phlegraei* but again, the shape is more irregular with smaller, less abundant oscules and invisible pores. *G. geodina* has smaller spherical sterrasters (vs. oval in *G. phlegraei*) with two sizes of oxyasters (vs. one size in *G. phlegraei*), and the large ones have fewer actines than in *G. phlegraei*.

Geodia bibilonae sp. nov. Díaz & Cárdenas

(Figs. 4.3.10 and 4.3.35; Table 4.3.15)

Etymology

Named after Dr. Maria Antònia Bibiloni, who initiated the studies of sponges from the Balearic Islands, from 1982 to 1993.

Material examined

Holotype: UPSZTY 190857, field#i715_1, St. 45 (INTEMARES0720), MaC (EB), beam trawl, 150 m.

Paratypes: UPSZTY 190860-190861, field#i674-field#i675, St. 42 (INTEMARES0720), MaC (EB), 143-139 m, beam trawl, coll. J. A. Díaz; UPSZTY 190858-190859, field#i780-field#i781, St. 54 (INTEMARES0720), MaC (EB), 124-210 m, rock dredge, coll. J. A. Díaz.

Outer morphology

Found in two different morphologies: globose when living in sedimentary bottoms, with a lot of gravel incorporated on its body (i715_1; Fig. 4.3.35A), encrusting, slightly hemispherical, and free of foreign materia when growing on rocks (i674, i675, i780, i781; Fig. 4.3.35B). Relatively small, ~2 cm in diameter. Whitish beige on deck and after ethanol fixation. Choanosome fleshy, pale beige after ethanol fixation. Surface hispid. Hard consistency, incompressible. Small cribriporal openings (about 0.2 mm) present all over the body, visible to the naked eye on deck. After preservation, they are also visible but not so patent. Cortex more than 0.5 mm thick. Typical geodiid skeleton with ectocortical spherasters, endocortical sterrasters and choanosomal oxyasters.

Spicules

Oxeas (Fig. 4.3.35C), thin and long, slightly curved, 1058-2765/12-32 µm. A second category of smaller oxeas were found in small numbers (N=5) and only in i675 (Table 4.3.15). Those spicules are probably contamination, as its shape was similar to the isoactinal oxeas (oxeas II) of *Craniella* cf. *cranium*.

Orthotriaenes (Fig. 4.3.35D), with long, fusiform rhabd and slightly curved clads. The clads may end tipping downward. Sometimes a clad may be bifurcated. Juvenile stages show

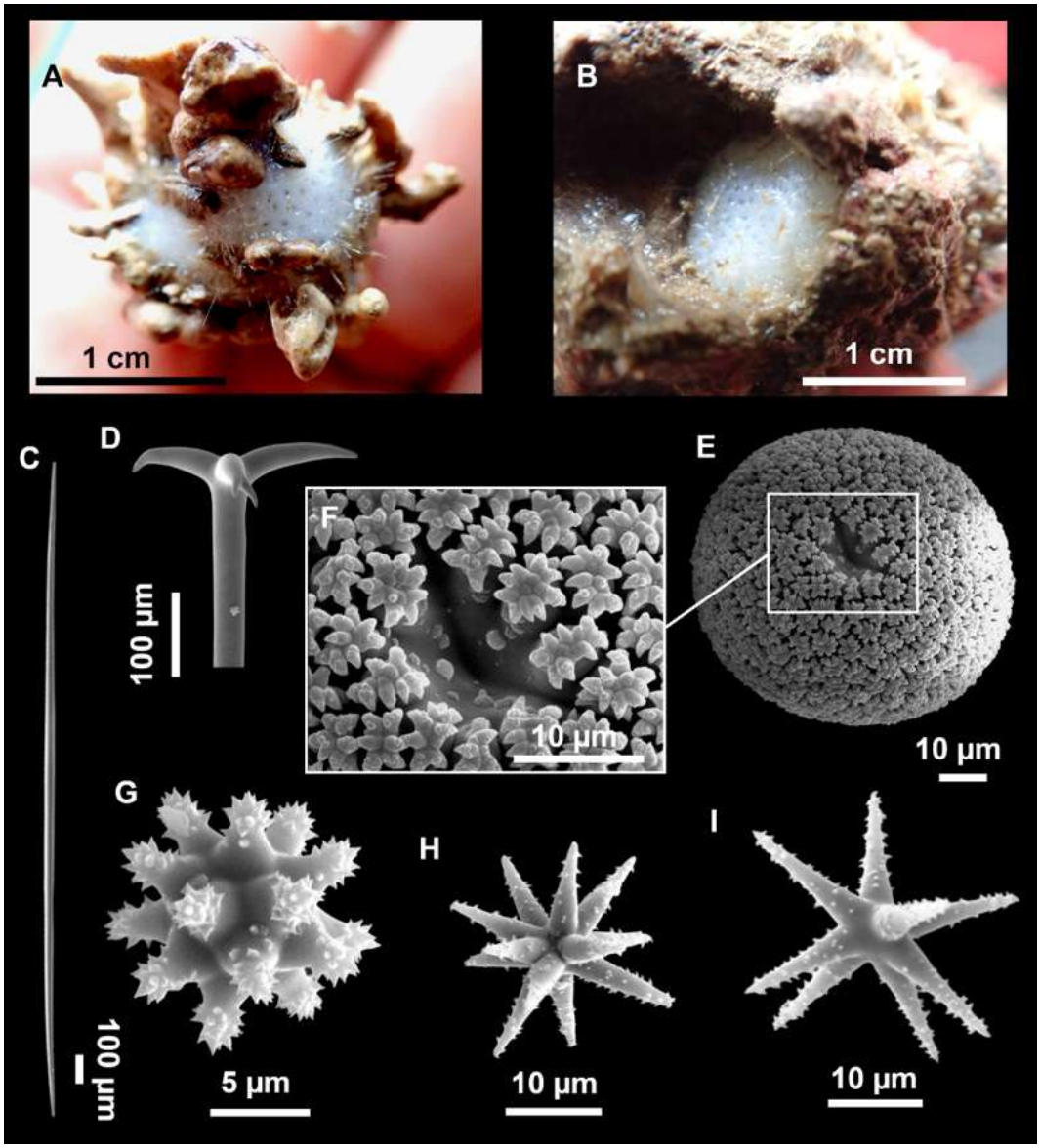

Figure 4.3.35. *Geodia bibilonae* **sp. nov.** (A) Habitus of the holotype UPSZTY 190857 (i715_1) on deck. (B) Habitus of the paratype i780 on deck. (C–H) SEM images of the holotype spicules. (C) Oxea. (D) Ortho-triaene. (E) Sterraster with (E1) detail of the warty rosettes and hilum. (F) Spheraster. (G–H) Oxyasters.

a bulbous swelling at the uppermost part of the rhabd. Rhabdome length: 594-2224/14-59 µm, cladi 78-306/12-49 µm.

Protriaenes (not shown), only found in specimen i675. With long, straight or slightly curved rhabdome and pointed clads. Rhabdome: 1472-2389-3446/9-11-14 µm (N=10), cladome: 69-102-157/8-11-13 µm (N=16).

Anatriaenes (not shown), scarce, rhabdome: 2567 (N=1)/2-10 µm, cladome: 16-86/2-14 µm.

Sterrasters (Fig. 4.3.35E), rounded, with warty rosettes (Fig. 4.3.35F), 39-69 µm in diameter.

Strongylasters-spherasters (Fig. 4.3.35G), with spines on the tips of the actines, 9-18 µm.

Oxyasters (Fig. 4.3.35H-I), normally with 6-12 (sometimes up to 16), spined actines, 21-48 µm.

Ecological notes

Species found in the mesophotic to aphotic zone, in both sedimentary and rocky bottoms. In the sedimentary bottoms the species is collected as a rounded mass with many agglutinated sediments while when found on hard substrata it is encrusting, hidden in crevices of rocks. With that in mind, the spherical morphology is likely an artifact, as a consequence of the body contraction when collected, given that the small sediments that act as substrate in these bottoms are not heavy enough to avoid the body contraction. This, however, must be corroborated through direct observation of living specimens.

Genetics

Folmer COI (ON130526, ON130527 and ON130528) and 28S (C1-C2) (ON133882, ON133883, ON133881) sequences were obtained from i780, i674 and i715_1 (holotype). Two haplotypes were found for COI and 28S, which differed in 1 bp for both markers.

Taxonomic remarks. See taxonomic remarks on *G. bibilonae* **sp. nov.** and *G. microsphaera* **sp. nov.** below.

***Geodia microsphaera* sp. nov. Díaz & Cárdenas**

(Figs. 4.3.10 and 4.3.36; Table 4.3.15)

Etymology

The name '*microsphaera*' refers to the small size of its sterrasters.

Material examined

Holotype: UPSZTY 190883, field#i589_2, St. 21 (INTEMARES0720), MaC (AM), 109 m, beam trawl, coll. J. A. Díaz.

Paratypes: UPSZTY 190884-190885, field#i589_3-i589_8, same station and collector as the holotype.

Comparative material

Geodia cydonium, ZMBN 85220, field#HC1, Hidden Cleft Cave, Brixham, Devon, England, collected above water at low tide, 1 Sept. 2008, colls. F. Crouch and C. Proctor, id: P. Cárdenas, COI: HM592715, 28S: HM592814.

Outer morphology

Small (0.8 cm in diameter), globose sponge almost entirely covered with gravels (Fig. 4.3.34A-B). Color on deck not recorded, of whitish surface and choanosome after fixation in ethanol. Surface fairly hispid, hard consistency. Cortex patent, 0.5 cm thick.

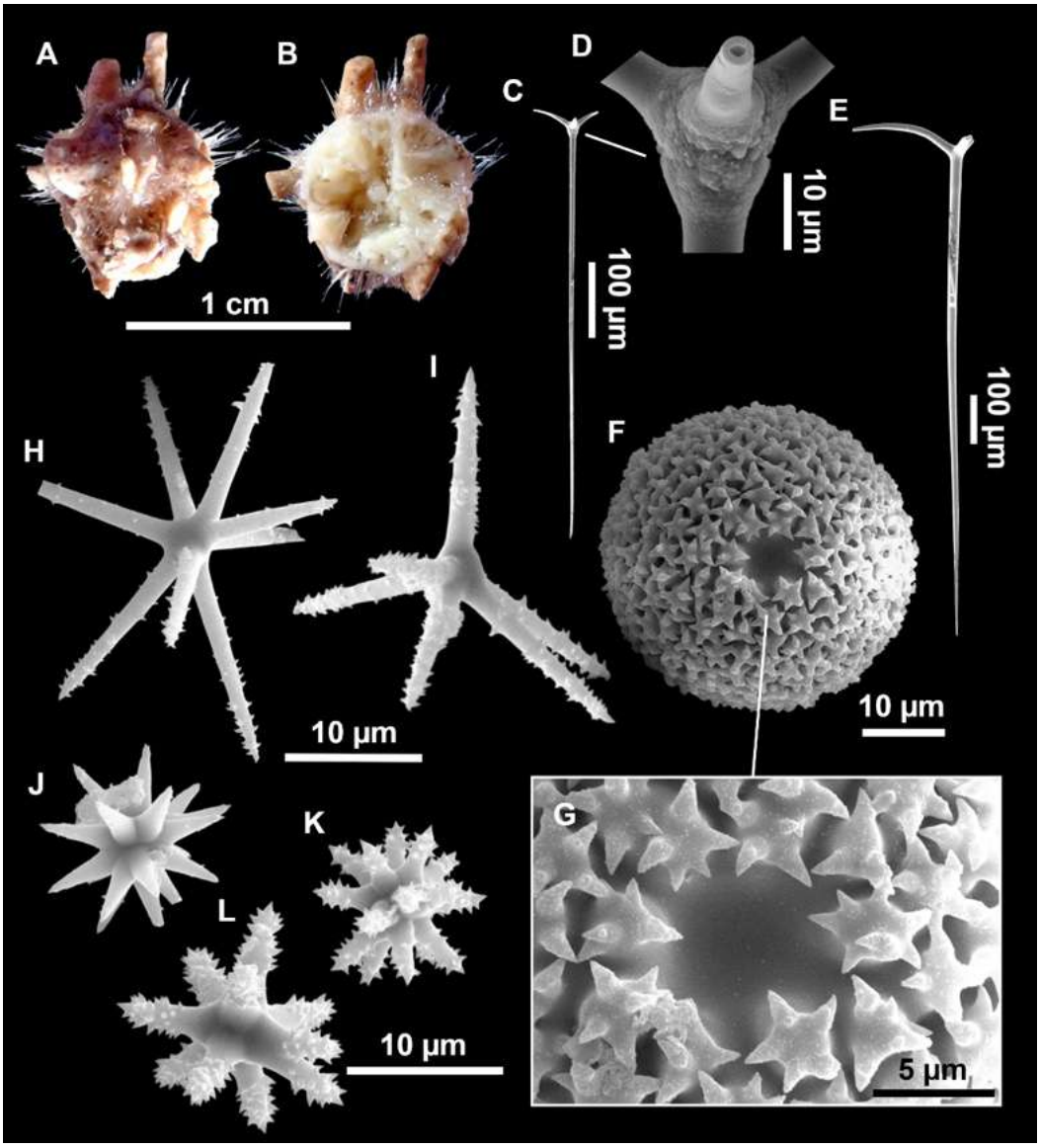

Figure 4.3.36. Holotype of *Geodia microsphaera* **sp. nov.**, UPSZTY 190883 (i589_2). (A–B) Habitus af-ter ethanol fixation. (C–L) SEM images of the spicules. (C) Juvenile orthotriaene with (D) subterminal swelling. (E) Orthotriaene. (F) Sterraster with (G) detail of the warty rosettes and hilum. (H–I) Oxyasters. (J–L) Spherasters.

Openings not visible. Typical geodiid skeleton with ectocortical oxyspherasters, endocortical sterrasters and choanosomal oxyasters. Choanosome fleshy.

Spicules

Orthotriaenes (Fig. 4.3.36C-E), fusiform rhabd and curved cladi. In juvenile forms, swellings present at the uppermost part of the rhabd (Fig. 4.3.34D). Rhabdome length: 311-1558/5-29 µm, cladi: 34-332/4-27 µm.

Protriaenes (not shown), rare in i589_2 and i589_3 but common in i589_8. Long and thin, rhabdome straight, slightly curved or bent, cladome straight. Rhabdome: 1394-3504/7-13 µm, cladi: 44-118/5-13 µm.

Oxeas (not shown), fusiform, usually straight, some slightly bent or curved, 827-1696/9-23 µm.

Sterrasters (Fig. 4.3.36F), small and spherical, with warty rosettes (Fig. 4.3.36G), 31-51 µm.

Oxyasters (Fig. 4.3.36H-I), with 4-10 long and spined actines, overall measuring 16-49 µm

Strongylasters (Fig. 4.3.36J-L), with the spines concentrated at its tips, overall measuring 5-23 µm.

Ecological notes

All specimens were found at a single station: the summit of the AM, in the mesophotic zone, composed of detrital bottoms with gross sand and gravels. Due to its small size and the amount of sediment that it agglutinates, the species may have been neglected from many other stations with similar features. In the field, it was almost indistinguishable from *G. bibilonae* **sp. nov.** and *S. dichoclada.*

Genetics

COI (ON130529) and 28S (C1-C2) (ON133884) sequences were obtained from the holotype (i589_2).

Taxonomic remarks on *Geodia bibilonae* sp. nov. and *Geodia microsphaera* sp. nov.

Both new species have very similar external morphology, spicule sets and yet clearly different COI/28S sequences; they were also found on different seamounts. *Geodia bibilonae* **sp. nov.** probably has cribriporal oscules and pores since only cribriporal openings could be found and we then assumed that some of those were inhalant and others exhalant. It can be therefore compared with North Atlantic/Mediterranean species with indistinctive cribriporal oscules/pores, some of which were formerly grouped in the genus *Cydonium* Fleming, 1828, now a synonym of *Geodia*. These species are the shallow/mesophotic species *Geodia cydonium*, *Geodia conchilega* Schmidt, 1862, *Geodia tuberosa* Schmidt, 1862 and the deep-sea North Atlantic *Geodia macandrewii* and *Geodia nodastrella* Carter, 1876. To this we need to add the poorly described species *Geodia pergamentacea* Schmidt, 1870 from Portugal. We can easily discard *G. macandrewii* and *G. nodastrella*, which are massive sponges found in the North Atlantic at deeper depths (*Cárdenas et al.., 2013; Cárdenas & Rapp, 2015*) and have for the former much larger sterrasters and for the later very characteristic ectocortical spheraster; both have also been sequenced and have different COI and 28S (Fig. 4.3.10). The shallow *G. conchilega* has a characteristic thick cortex and fairly large oval sterrasters, quite different from those in our new species; its COI/28S sequences are also different from those of our new species. As for the two poorly known Schmidt species, *G. pergamentacea* and *G. tuberosa*, for which no illustrations are published, we can rely on redescriptions (*Sollas, 1888; Burton, 1946*) from fragments and/or slides of type material. Although their succinct and incomplete descriptions make it challenging to identify these species, they are clearly different from our new species with much larger sterrasters (spherical 90 µm for *G. tuberosa* and oval 60-80 µm for *G. pergamentacea*). *Burton (1946)* further suggests that *G. pergamentacea* is a synonym of *G. conchilega* but this remains to be confirmed.

Table 4.3.15. Spicule measurements of *Geodia bibilonae* **sp. nov**, *G. microsphaera* **sp. nov.** group and the related species *G. cydonium* (Linnaeus, 1767), given as minimum-mean-maximum for total length/minimum-mean-maximum for total width; all measurements are expressed in µm. Balearic specimen codes are the field#. Rh: rhabdome; Cl: clad; -:not found/not reported; EB: Emile Baudot; AM: Ausias March.

Material	**Depth** (m)	**Oxeas** (length/width)	**Anatriaenes** Rhabdome (length/width) Clad (length/width)	**Protriaenes** Rhabdome (length/width) Clad (length/width)	**Orthotriaenes** Rhabdome (length/width) Clad (length/width)	**Sterrasters** (diameter)	**Oxyasters** (diameter)	**spherasters** (diameter)
***G. bibilonae* sp. nov. holotype, i715_1 EB**	150	I. 1058-1968-2765/ 12-22-32	Rh: 2567/ 8 (N=1) Cl: 32-65/ 9-14 (N=3)	-	Rh: 731-1360-2243/ 24-38-59 Cl: 88-169-246/ 14-30-49	39-51-63	21-29-42 (6-16 actines)	9-12-15
***G. bibilonae* sp. nov. paratype, i675 EB**	141	I. 1478-1970-2213/ 14-20-24 (N=18) II. 247-388/ 4-5 (N=5)	Rh: broken Cl: 16-86/ 2-10 (N=5)	Rh: 1472-2389-3446/9-11-14 (N=10) Cl: 69-102-157/8-11-13 (N=16)	Rh: 594-1524-1885/ 14-35-47 Cl: 78-209-306/ 12-31-46 (N=16)	46-60-69	21-37-48	9-13-18
***G. microsphaera* sp. nov. holotype, i589_2 AM**	109	1057-1696/ 10-16 (N=7)	-	Rh: 1682-2451/8-9 Cl: 66-116/8-9 (N=3)	Rh: 557-1121 (N=7)/ 9-20-25 (N=9) Cl: 57-185-254/ 8-16-25 (N=9)	31-38-44	25-33-49 (N=11)	9-13-20
***G. microsphaera* sp. nov. paratype, i589_3 AM**	109	844-1164-1493/ 10-14-16 (N=19)	-	Rh: 2948-3504/10-10 Cl: 72-116/9-10 (N=2)	Rh: 311-1137-1558/ 5-18-27 Cl: 34-193-294/ 4-15-25(N=15)	30-38-44	16-32-41 (N=10, 4-8 actines)	10-15-21 (N=22)
***G. microsphaera* sp. nov. paratype, i589_8 AM**	109	827-1242-1694/ 9-16-23 (N=22)	-	Rh: 1394-3438 (N=9)/ 7-10-13 (N=18) Cl: 44-93-118/5-8-11 (N=17)	Rh: 583-985-1278/ 9-22-29 Cl: 56-179-332/ 7-18-27 (N=22)	38-44-51	26-40 (5-7 actines, N=6)	5-13-23
G. cydonium Cataluna, Spain Specimen 146 (*Uriz, 1981*)	30-35	I. 2000-2500/25 II. 600-700/10-12	Rh: 3000 Cl: 50	Rh: 3000 Cl: 60	Rh: 1200-1300/ 20-25 Cl: 150-200/-	50	15	Chiasters: 15 Spherasters: 18-20

We are left with *G. cydonium*, a species complex (*Cárdenas et al., 2011*). Both *G. bibilonae* **sp. nov.** and *G. microsphaera* **sp. nov.** seem to be close to *G. cydonium* in terms of spicule set (small spherical sterrasters with warty rosettes, spiny oxyasters, spiny spheraster to strongylasters variations) and without molecular markers we would have been tempted to consider them conspecific with *G. cydonium*. However, although COI/28S trees (Fig. 4.3.10) confirmed that our new species belong to the 'Cydonium' clade, they also suggested that they are different from the *G. cydonium* sequenced so far. Our new species group closer to *G. cydonium* (ZMBN 85220) from Devon, England, which has similar spicules with similar sizes (sterraster size 52-60 µm, closer to those of *G. bibilonae*); however, this *G. cydonium* comes from a different habitat, intertidal shallow cave, sometimes emerged at very low tide. *G. microsphaera* **sp. nov.** even shares the exact same 28S (C1-C2) with the English *G. cydonium*, but a different COI with a 6 pb difference; this is not so surprising since the 28S C1-C2 fragment is more conserved, it is missing the more variable D2 fragment. *G. bibilonae* **sp. nov.** COI is even more different with a 17-18 bp difference with the English *G. cydonium.* So, despite similar spicule sets *G. bibilonae* **sp. nov.** and *G. microsphaera* **sp. nov.** are genetically different and live in different habitats. As for the Mediterranean *G. cydonium*, reports all show two sizes of oxeas, vs. only one in our new species. We hypothesize that several cryptic species are hiding under the overused name *G. cydonium*; *G. bibilonae* **sp. nov.** and *G. microsphaera* **sp. nov.** are the first ones to be formally identified, while others await description (P. Cárdenas, unpublished results) along with a necessary revision of *G. cydonium*, a task beyond the scope of this study.

Geodia bibilonae **sp. nov.** and *G. microsphaera* **sp. nov.** differ in that *G. bibilonae* **sp. nov.** has orthotriaenes with longer and thicker rhabdomes (594-2224/14-59 µm versus 311-1558/5-29 µm), thicker cladomes (12-49 µm versus 4-27 µm), longer oxeas (1058-2765 µm versus 827-1696 µm) and larger sterrasters on average (average 51-60 µm versus 38-44 µm). Genetically, *G. bibilonae* **sp. nov.** and *G. microsphaera* **sp. nov.** differ by 13-14 bp for the COI and 3-4 bp for the 28S (C1-C2) fragment. For *G. bibilonae,* two COI haplotypes with a 1 bp difference were detected (i780/i715_1 versus i674), and two 28S haplotypes with a 1 bp difference were detected (this time i780/#i674 versus i715_1). This reminds us what was reported for *Stelletta dichoclada* except that here there is variation within the same seamount and that both markers do not distinguish two clear populations.

Family Pachastrellidae Carter, 1875

Genus *Characella* Sollas, 1886

Characella pachastrelloides (Carter, 1876)

(Figs. 4.3.6 and 4.3.37; Table 4.3.16)

Material examined

UPSZMC 190815, field#i527, St. 18 (INTEMARES0720), MaC (AM), 116 m, Beam trawl, coll. J. A. Díaz.

Comparative material

Spongosorites maximus Uriz, 1983, CEAB.POR.BIO.89, holotype, Fora de les Garotes, off Blanes, Catalan coast, Spain, trawl fishing ground, 150-250 m (Fig. 4.3.37B).

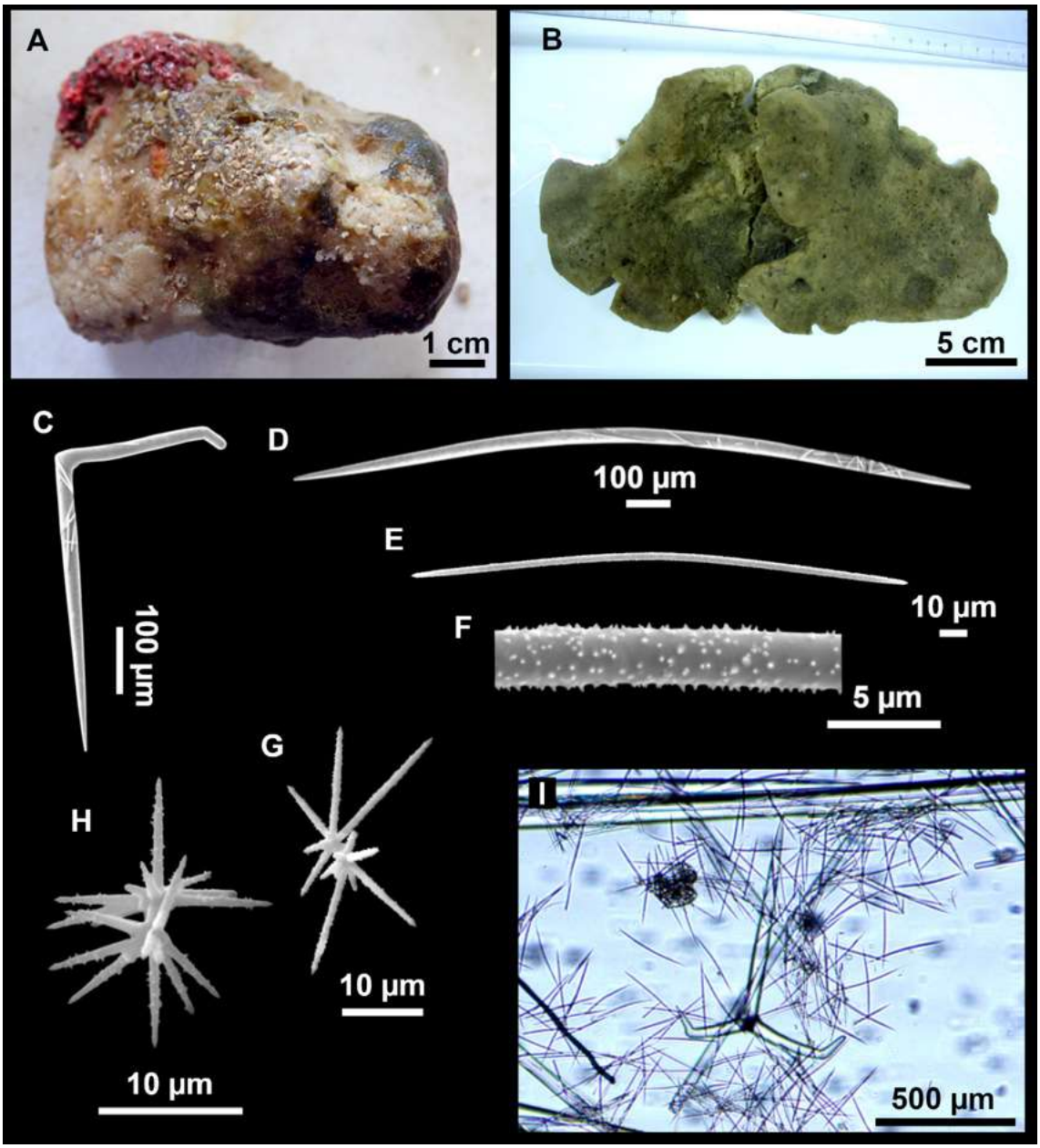

Figure 4.3.37. *Characella pachastrelloides* (*Carter, 1876*). (A) Habitus of specimen i527 on deck. (B) Habi-tus of *Spongosorites maximus Uriz, 1983*, (CEAB.POR.BIO.89) holotype. (C–H) SEM images of spicules from i527 (C) Orthomonoaene. (D) Oxea. (E) Microxea I with (F) detail of the spines. (G–H) Amphi-asters. (I) Optical microscope image of an orthotriaene and microxeas.

Outer morphology

Massive sponge, 9x6x5 cm attached to a rhodolith at its base (Fig. 4.3.37A). Alive, dark olive in the upper area, beige at the base. After ethanol fixation, surface and choanosome pale beige. Surface smooth with only faint hispidation in the groves. Hard but slightly spongy consistency. Diffuse cortex, less than 0.5 mm thick. Choanosome fleshy, not cavernous. Openings not visible.

Table 4.3.16. Spicule measurements of *Characella pachastrelloides* and *Characella tripodaria,* given as minimum-mean-maximum for total length/minimum-mean-maximum for total width; all measurements are expressed in µm. Balearic specimen codes are field#. Rh: rhabdome; Cl: clad; -:not found/not reported; EB: Emile Baudot, AM: Ausias March.

Material	**Depth** (m)	**Oxea** (length/width)	**Anatriaene** Rhabdome (length/width) Clad (length/width)	**Triaene** Rhabdome (length/width) Clad (length/width) Protoclade (length/width) Deuteroclade (length/width)	**Microxea I** (length/width)	**Microxea II** (length/width)	**Amphiaster** (length)
C. pachastrelloides holotype, Portugal (*Sollas, 1888; Maldonado, 1996*)	683	3660-4620/ 84-100	Rh:3660-6640/21 Cl: 100-170/-	Rh: 850/70 Cl: 490/- (orthotriaenes+pseudocalthrops)	245/6	47/9	13
C. pachastrelloides **i527 AM**	116	681-1088-143/8-21-35	-	Rh: 187-320-416/8-16-25 (N=7) Cl: 133-228-334/10-15-21 (N=7) Pr: 116-134/12-14 Dt: 101-110/11-14 (N=2) (orthotriaenes mainly)	93-176-254/ 1-3-4	19-30-44/ 1-2-3	13-26-44 (N=8)
Spongosorites maximus **holotype CEAB.POR.BIO.89 Catalan Coast**	150-250	1004-1696-23/74/10-29-61	-	Rh: 311-495-716/36-56-78 (N=5) Cl: 205-361-555/34-51-78 (N=6) (orthotriaenes)	145-177-225/ 3-4-5	33-48-59/ 2-3-3 (N=19)	11-15-27
C.tripodaria holotype, NHM:68:3:2:36, Algeria (*Maldonado, 1996; Cárdenas & Rapp, 2012*)	-	1000-1600/ 10-40	Rh:-/10 Cl: 25/-	Rh: 180-400/15-22 Cl: 180-400 (plagiotriaene pseudocalthrops)	115-180/ 2-3	35-45/ 2-3	10-18-30 (N=15)
C. tripodaria **i153_1B EB**	107-110	689-1456-2148/ 15-29-49	Rh: 723-1006-1767/7-13-18 Cl: 27-66-108/7-12-18 (N=18)	Rh: 207-298-434/ 16-23-30 (N=17) Cl: 221-315-426/15-22-26 (plagiotriaene pseudocalthrops)	86-126-152/ 2-3-5	25-35-53/ 1-2-4	8-14-27
C. tripodaria **i777 EB**	102-105	697-1369-1909/7-22-41	-	-	86-125-160/ 2-3-4	22-33-40/ 1-2-3 (N=6)	14-17 (N=2)

Spicules

Orthotriaenes (Fig. 4.3.37C, I), most are aberrant, in the form of orthomonoaenes and orthodiaenes, some with aborted cladome, others with ectopic actines on the rhabdome. Rhabdome length: 187-320-416/8-16-25 µm, cladi: 133-228-334/10-15-21 µm (N=7).

Dichotriaenes (not shown), only two found, as modified orthotriaenes. Rhabdome length: 16-332/13-13 µm. Protoclad: 116-134/12-14 µm. Deuteroclad: 101-110/11-14 µm (N=2).

Oxeas (Fig. 4.3.37D), very abundant, centrocurved, 681-1088-1437/8-21-35 µm.

Microxeas I (Fig. 4.3.37E-F), very abundant, thin and centrocurved, microspined (Fig. 4.3.37F), with sharp ends, 93-176-254/1-3-4 µm.

Microxeas II (not shown), rare, spiny, some centrotylote, 19-30-44/1-2-3 µm.

Amphiasters (Fig. 4.3.37G-H), rare, with long spined actines, aborted actines are common, shafts are clear or with aborted actines, length: 13-26-44 µm (N=8).

Ecology and distribution

Species only found once at the top of the AM, on a rhodolith bed.

Genetics

COI (ON130551) and 28S C1-C2 (ON133873) sequenced.

Taxonomic remarks. See below discussion of *C. tripodaria*.

Characella tripodaria (Schmidt, 1868)

(Figs. 4.3.6 and 4.3.38; Table 4.3.16)

Material examined

UPSZMC 190816, field#i153_1B, St. 52 (INTEMARES0718), MaC (EB), rock dredge, 110-107 m, coll. F. Ordines; UPSZMC 190818, field#i777, St. 53, MaC (EB), rock dredge, 108-102 m, coll. J. A. Díaz.

Comparative material

Characella tripodaria, MNHN DT756, holotype, Schmidt collection#107, Algeria, 'Exploration Scientifique de l'Algérie', 1842.

Outer morphology

Massive irregular (i153_1B) or massive elongated (i777), up to 4 cm in diameter. In life, pale beige, gray after ethanol fixation, same color on the surface and in the choanosome. Surface mostly hispid with some smooth areas. Hard consistency. Diffuse cortex, less than 0.5 mm thick. Openings not visible.

Spicules

Plagiotriaene pseudocalthrops (Fig. 4.3.38B-D), only found in i153_1B, the three clades often curved making them look like plagiotriaene. Sometimes triactinals, with an

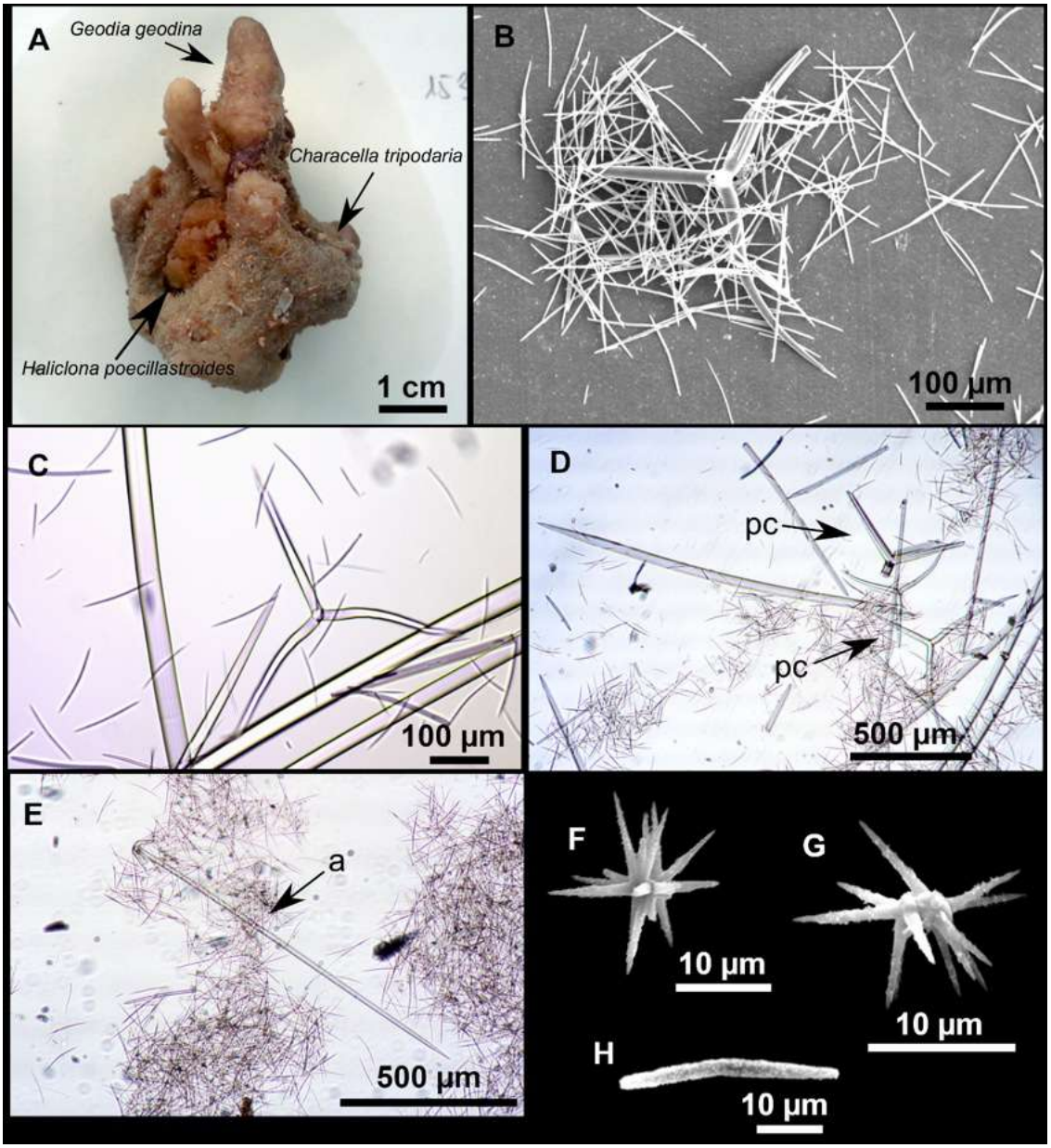

Figure 4.3.38. *Characella tripodaria* (*Schmidt, 1868*). (A) Habitus of i153_1B after ethanol fixation, over-grown with *Geodia geodina* and *Haliclona poecillastroides*. (B–H) Spicule images of i153_1B. (B) SEM im-age showing a plagiotriaene pseudocalthrop and microxeas. (C–D) Several plagiotriaene pseudocalthrops (pc), oxeas and microxeas. (E) Anatriaene (a) and microxeas I. (F–G) Amphiasters. (H) Microxeas II.

aborted actine. Rhabdome length: 207-298-434/16-23-30 µm. Cladi: 221-315-426/15-22-26 µm (N=17).

Anatriaenes (Fig. 4.3.38E), only in i153_1B, scarce, with a fusiform rhabdome, the cladome may have clads projecting straight from the center or drawing a soft curvature. In some cases, there are aborted clads. Rhabdome length: 723-1006-1767/7-13-18 µm, cladome: 27-66-108/7-12-18 µm (N=18).

Oxeas (Fig. 4.3.38D), slightly curved, 689-2148/7-49 µm.

Microxeas I (Figs. 4.3.38B-E), thin and slightly curved in the center, with sharp ends, minutely spined, 86-160/2-5 µm.

Microxeas II (Fig. 4.3.38H), rare (i153_1B) to very rare (i777), thin, some are straight while others are abruptly curved in the center, with some stylote and strongylote modifications, 22-53/1-4 µm.

Amphiasters (Fig. 4.3.38F-G), rare (i153_1B) to very rare (i777), some are normal while others have malformations and aborted actines, 8-27µm.

Ecology and distribution

Both specimens were found at the summit of the EB, together with other massive sponges like *Spongosorites* spp., *Pachastrella monilifera* and several axinellids.

Genetics

COI was obtained from i777 (ON130552) while only the short miniCOI was obtained from i153_1B (SBP#2690). The 28S (C1-C2) fragment was obtained from both i777 and i153_1B (ON133871 and ON133872).

Taxonomic remarks on *C. pachastrelloides* and *C. tripodaria*

There are two *Characella* species documented in the Mediterranean Sea and the nearby North Atlantic, *C. pachastrelloides* and *C. tripodaria,* both sharing an almost identical set of spicules. The taxonomic history, characters and distribution of the two species have previously been discussed (*Maldonado, 1996; Cardenas & Rapp, 2012*). After revision of the holotype of *C. tripodaria*, *Cárdenas & Rapp (2012)* concluded that no clear differences could be made between the two species, even though the amphiasters seemed to have more actines on the shaft in *C. tripodaria*. Our COI and 28S sequences both suggested a partition of i527 versus i153_1B and i777. Specimen i527 from AM Seamount is a perfect COI match with boreal *C. pachastrelloides* (haplotype 1) from Norway (HM592672), Scotland (HM592749) and the Globan Spur (Celtic Sea) (MK085975). The COI of i153_1B and i777 (haplotype 3) has a 2 bp. difference with the boreal sequences and 1 bp. difference with two fairly deep *C. pachastrelloides* from the Gulf of Cadiz (HM592713) and southern Portugal (HM592709) (haplotype 2), both close to the type locality of *C. pachastrelloides*. So we now have three COI haplotypes in this complex. We have looked for morphological differences between i527 versus i153_1B/i777: i527 is large, with a smooth surface while i153_1B/i777 specimens are smaller and very hispid but such shape/surface variations have already been observed by *Topsent (1904)* in the Azores within *C. pachastrelloides,* so they do not seem to be diagnostic. The triaenes however look different: i153_1B has pseudocalthrops often with three curved forward-oriented clades, that we decided to call plagiotriaene pseudocalthrops (Fig. 4.3.38B-D), while i527 has rather irregular orthotriaenes with most of the time straight clades. The taxonomic value of triaene morphological variations in *C. pachastrelloides* has already been raised, but always failed to reveal a phylogenetic pattern (*Topsent, 1904; Maldonado, 1996; Cárdenas & Rapp, 2012*). Looking back on previous descriptions it does seem however that triaenes may reflect different populations or species. We noticed that i) the Norwegian, Scottish and Globan Spur specimens (hap 1, mesophotic to upper bathyal) all had i) short-shafted orthotriaenes (sometimes looking like pseudocalthrops) mixed with dichotriaenes, with

clads usually straight, except when irregular; no anatriaenes found; amphiasters were moderately abundant, usually with a "clean" shaft (i.e. no extra actines there). North Atlantic Iberian specimens (hap 2, upper bathyal), the closest to the type locality of *C. pachastrelloides* in terms of geography and depth, had anatriaenes and the same type of triaenes as hap1 but usually larger/thicker (*Cárdenas & Rapp, 2012*, Table 4.3.2); amphiasters are moderately abundant as well, usually with a "clean" shaft. Finally, our specimens i153_1B/i777 from EB (hap 3, mesophotic zone) have anatriaenes and pseudocalthrops, usually with curved clades, sometimes malformed/aborted, no dichotriaenes; amphiasters are somewhat in lower numbers, with additional actines on the shaft. This description fits the holotype of *C. tripodaria* we examined, and in which we found triaenes with curved clades similar to that drawn by *Schmidt (1868*, pl. III, fig. 10a), no dichotriaenes, and similar amphiasters (*Cárdenas & Rapp, 2012*, Fig. 2J). The triaenes of i527 from AM look more like those in hap1 and hap2, short-shafted orthotriaenes mainly, but they are on average smaller and more irregular than in its North Atlantic counterparts. We concluded that in the Balearic Islands we had *C. pachastrelloides* (i527) and *C. tripodaria* (i153_1B and i777) at the same depth, but so far on different seamounts. Following this, we consider for now hap1 and hap2 (1 bp. difference) to be haplotypes of two distinct populations of *C. pachastrelloides*. Therefore, hap3 with 1-2 bp difference with *C. pachastrelloides* is the first COI sequence of *C. tripodaria*.

Besides, microxea I lengths are identical between *C. tripodaria* specimens (86-152 µm and 86-160 µm, respectively) and much smaller than those of *C. pachastrelloides* (93-254 µm). This pattern in microxea I sizes is consistent with the sizes reported for other *C. pachastrelloides* and *C. tripodaria*: for *C. pachastrelloides*, it matches with the holotype (246 µm) and the Norwegian specimen ZMBN 80248 (80-259 µm; *Cárdenas & Rapp, 2012*). It should be noted that COI and 28S are available for ZMBN 80248, being identical to i527. Conversely, the microxea I sizes for the holotype of *C. tripodaria* are also in the same size range (115-180 µm) than those of the Balearic Islands. Also, as already discussed in the literature, amphiaster morphology seems to be different between *C. pachastrelloides* and *C. tripodaria*. We found that those spicules are rare and may have aborted actines in both species. However, amphiasters of *C. tripodaria* tend to have a more elevated number of actines, which are also shorter, and a shorter shaft, a character already also noted by *Maldonado, (1996)*, and *Cárdenas & Rapp, (2012)*. Notwithstanding the mentioned, amphiaster morphology is, by today, a weak character to discern between *Characella* species, as it is probably influenced by ecophysiological factors and/or intraspecific variability. Further works shall study a larger number of individuals and compare its amphiasters and its genetic sequences to clarify its systematic value.

In the course of another project, the holotype of *Spongosorites maximus* Uriz, 1983 had been examined (Fig. 4.3.37B) with the making of new spicule preparations (Table 4.3.16). Unexpectedly, orthotriaenes and amphiasters were found, which, combined with two sizes of microxeas, suggested that it was in fact a *C. pachastrelloides*. Therefore, *S. maximus* becomes a junior synonym of *C. pachastrelloides*, further confirming the presence of this species in the Mediterranean Sea. This large specimen (25x16 cm) had been collected on the fishing grounds off the Catalan coast (Fora de les Garotes) at mesophotic depths (150-250 m). The third record of a Mediterranean *C.*

pachastrelloides is from south Malta at 607 m depth (*Calcinai et al., 2013*), the description of orthotriaenes, abundant amphiasters with few actines suggest that this is a correct identification. For *C. tripodaria*, it has been previously reported from Algeria and the Alboran Sea (*Maldonado, 1996*) so this is the third report in the Mediterranean Sea. Both species are reported for the first time off Balearic Islands.

Anatriaenes were not found in *C. pachastrelloides* i527 nor *C. tripodaria* i777 but they were relatively common in *C. tripodaria* i153_1B, which further confirms their presence in this species. Since anatriaenes were previously formally reported from *C. pachastrelloides*, including the holotype (*Maldonado, 1996; Cárdenas & Rapp, 2012*), they are not a good character to discern between *C. pachastrelloides* and *C. tripodaria*.

Smooth oxeas II have previously been reported with some doubt in a specimen from Norway (*Cárdenas & Rapp, 2012*). Here, similar smooth smaller oxeas can be found in i153_1B/i777 but the most plausible explanation is that they are contamination by haplosclerid sponges (especially *H. poecillastroides*) overgrowing all the studied specimens. They have the same oxeas, with the same length/width as those found. Similarly, the holotype of *C. tripodaria i*s overgrown by an haplosclerid, and possesses such oxeas (*Topsent, 1938*). The report of oxeas II in *Characella luna* Dias et al., 2019 from Brazil therefore needs to be considered with caution and confirmed.

Genus *Nethea* Sollas, 1888

Nethea amygdaloides (Carter, 1876)

(Figs. 4.3.6 and 4.3.39; Table 4.3.17)

Material examined

UPSZMC 190889, field#POR7(15), St. 181 (MEDITS052016), south west of Cabrera Archipelago, 142 m, GOC-73, coll. P. Ferriol; UPSZMC 190888, field#POR347_b, St. 194 (MEDITS052017), Port d'es Canonge (North of Mallorca), 148 m, GOC-73, coll. J. A. Díaz; UPSZMC 190890, field#i215_b, St. 3 (INTEMARES1019), MaC (SO), 293-255 m, rock dredge, coll. J. A. Díaz.

Comparative material

Nethea amygdaloides, holotype, NHM Norman Coll. slides 1910.1.1.1683-1685, near Cap St. Vincente, Portugal, 534 m, Porcupine Expedition, St. 24, 1870; ZMAPOR 21223, Gulf of Cadiz, 35º18'46.8''N, 6º13'44.4''W, 428 m, 2007, field#CAD07-01, coll: Loïs Maignien, id: P. Cárdenas, 28S: HM592773; MNHN DCL4077, Apulian Platform, off Cape Santa Maria di Leuca, southern Italy, 39º33'54.78''N, 18º26'12.39''E, 562 m, sampling#PBT1(1), ROV dive 327-6, MEDECO leg1 (Ifremer), 17 Oct. 2007, coll: Julie Reveillaud, id: P. Cárdenas, 28S: HM592772; sampling#GBT1-1, Apulian platform, Atlantis mound, off Cape Santa Maria di Leuca, southern Italy, 39º36'43.84''N, 18º30'28.28''E, 648 m, ROV dive 328-7, MEDECO leg1 (Ifremer), 17 Oct. 2007, coll: Julie Reveillaud, id: P. Cárdenas; PC479, SME PL.ACH.P1, Canyon du Planier, off Marseille, France, 43º0'6.08''N, 5º0'12.49''E, 332 m, ROV dive B4-PL-ACH-P01-20091112, 12 Nov. 2009, MedSeaCan campaign, RV *Minibex*, coll: J. Vacelet, id: P. Cárdenas; PC1280, SME TetractCYE8-D2b, Canyon St. Florent, Corsica, 42º45'56.88''N, 9º13'30.72''E, 208 m, 6 Oct. 2018, H-ROV *Ariane*

dive 110-08, Cylice-Eco (CYE) campaign, RV *L'Europe*, coll: P. Chevaldonné, id: P. Cárdenas.

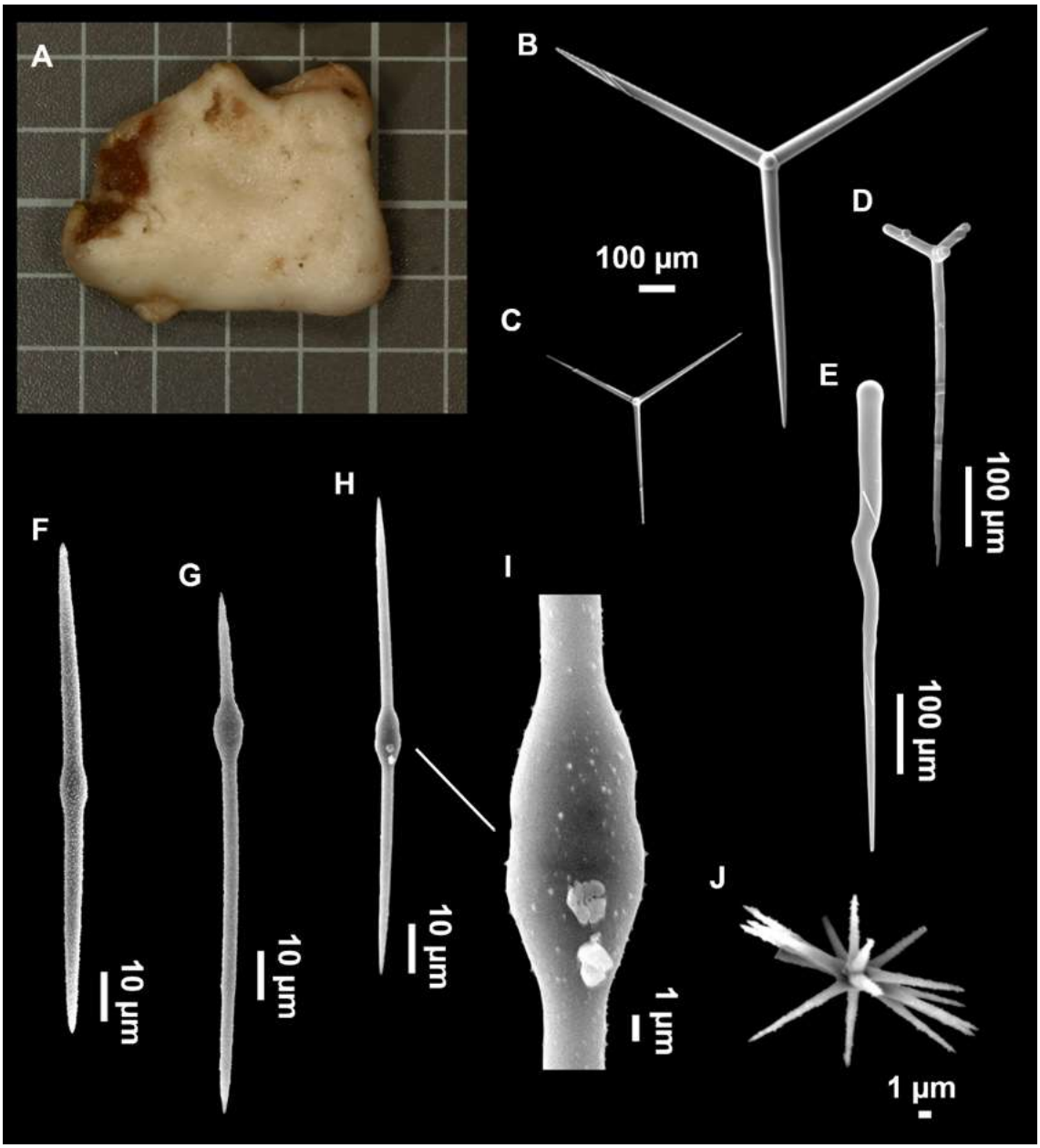

Figure 4.3.39. *Nethea amygdaloides* (*Carter, 1876*). (A) Habitus of specimen POR7(15) on deck. (B–I) SEM images of specimen POR347_B spicules. (B–C) Regular calthrops. (D–E) Underdeveloped calthrops. (F– H) Microxeas with (H1) detail of a central swelling and spines. (I) Amphiaster.

Outer morphology

Massive, or encrusting (i215_b); the largest specimen, POR7(15) (Fig. 4.3.39A) measures 4 cm in diameter and 1 cm in height. The color of POR7(15) was whitish on deck and whitish gray after preservation in alcohol. In Por347_b, the color after preservation is dark gray. The skin of both individuals is slightly rough to the touch with only localized hispidation visible to the naked eye. Consistency stony hard, leaving a mark when pressed. Single oscula observed in both specimens, measuring 2 mm in

POR7(15) and 1 mm in POR347_b. Pores inconspicuous. Specimen POR7(15) had a dark garnet *H. poecillastroides* as epibiont (Fig. 4.3.39A).

Spicules

Cathrops (Fig. 4.3.39B-E). Regular ones are mostly tetractinals (Fig. 4.3.39B-C) with actines disposed in equiangular disposition on a same plane and with one of the actines reduced to a stump, making the spicule look like a triactin. Regular actines are mostly straight, occasionally slightly curved; distinct swellings occasionally occur on the actines in Por7(15); actine ends are progressively sharpened or stepped. In Por347_b and Por7(15), malformed or underdeveloped actines are quite common; as well as reduced triactines to one (Fig. 4.3.39E) or two actines. Actines overall measuring 114-910/5-48 μm.

Oxeas (not shown), long, thin, slightly curved and with sharp tips. Measuring 615-1863/6-24 μm.

Microxeas (Fig. 4.3.39F-I), mostly bent, but some are straight; in i215_b they are quite curvy with sometimes double bends. With a marked (Fig. 4.3.39F) or subtle (Fig. 4.3.39G-H and 39I) microspination. In Por347_b, many microxeas have a distinct swelling in the middle or the upper part; in Por7(15) and i215_b such swellings are very rare. Length: 53-181 μm, width: 2-10 μm.

Amphiasters (Fig. 4.3.39J), moderately abundant, 14-17 actines, both regular and underdeveloped forms are found. Clear shaft, sometimes reduced/absent shaft making some amphiasters look like euasters. Length: 8-31 μm.

Ecology and distribution

Uncommon, found on upper slopes of the Mallorca shelf and SO seamount.

Genetics

The COI of specimens POR347_B, POR7(15) (ON130544 and ON130545), and the miniCOI fragment of i215_b (SBP#2686) have been obtained. The 28S (C1-C2) fragment was obtained from i215_b (ON133878).

Taxonomic remarks

The specimens are assigned to the genus *Nethea* on the basis of the triactinal calthrops with three actines disposed on a single plane and a fourth actine absent or reduced to a stump. When they resurrected *Nethea*, *Cárdenas et al. (2011)* suggested to include all species with triactinal calthrops and amphiasters: *Nethea nana* (Carter, 1880) from the Indian Ocean, *Nethea capitolii* (Mothes et al., 2007) from Brasil and *N. amygdaloides*. The case of *Characella connectens* (Schmidt, 1870) from Florida is unclear since *Maldonado, (2002)* observed in the type material triactinal calthrops but also two sizes of microxeas instead of one, as in *Characella* species: a revision of the type material is necessary.

Table 4.3.17. Spicule measurements of *Nethea amygdaloides,* given as minimum-mean-maximum for total length/minimum-mean-maximum for total width; all measurements are expressed in µm. Balearic specimen codes are the field#. SO: Ses Olives.

Material	Depth (m)	Oxea (length/width)	Calthrops (length/width of actine)	Microxea (length/width)	Amphiaster (length)
holotype NHM 1910.1.1.1683-1685 Cap St. Vincent, Portugal	534	796-1076-1673/ 10-15-20	184-539-755/ 18-47-67	35-94-155/ 2-5-8	17-21-25
Por347_B North of Mallorca	148	682-857-1008/ 9-13-18	250-496-829/ 9-22-34	53-106-178/ 2-4-6	8-15-24
Por7(15) Cabrera archipelago	142	615-1123- 1863/ 6-13-24	114-449-910/ 5-25-48	70-131-181/ 3-6-10	10-16-31
i215_b SO	274	747-1055-1340/ 7-12-17 (N=12)	235-441-670/ 13-28-38	67-123-174/ 2-4-5	13-20-29
MNHN DCL4077 Southern Italy	562	974-1660/ 10-22 (N=5)	181-594-871/ 11-39-59	55-104-169/ 2-3-6	13-25-54
GBT 1(1) Southern Italy	648	1354-2036/ 15-27 (N=6)	256-673-1048/ 12-34-51	80-133-192/ 2-4-6	12-16-27 (N=12)
ZMAPOR 21223 Gulf of Cadiz, Atlantic	428	835-2068/ 12-24 (N=7)	190-734-996/ 10-37-50	63-109-157/ 1-4-6	12-15-19 (N=15)
PC479 Marseille, France	330	914-1770/ 15-28	215-734-1007/ 13-34-47	72-126-171/ 4-5-7	9-18-35
PC1280 Canyon St. Florent Corsica	208	527-1267-1776/ 8-19-29	173-608-871/ 7-25-41	74-133-172/ 2-4-7	9-16-24 (N=14)
NIS.70.1, PF.263 Corsica (*Pullitzer-Finali 1983*)	140 and 200	1200-1600/ 11-14 (rare)	650/37 (some reduced to diactines)	65-140/ 1.5-5.5	Abundant (NIS.70.1), rare (PF.263)

Nethea amygdaloides is occasionally reported from mesophotic to bathyal depths (103-2165 m) of the northeast Atlantic (*Topsent, 1892; 1904; 1928; Sitjà et al., 2019; Ríos et al., 2022*) and shallow to mesophotic depths (25-200 m) of the Western Mediterranean Sea (*Topsent, 1895; Pulitzer-Finali, 1983*). Comparative material from the upper bathyal depths in the Apulian platform (off Cape Santa Maria di Leuca, southern Italy) also shows that this species can be found quite deep also in the Mediterranean. The species was previously reported on a monticule at the southeast of the EB (*Maldonado et al., 2015*; Table 4.3.1) but no description was given. Here, the species is reported for the second time in the Balearic Islands region, and fully described/barcoded. The Folmer primers together do not seem to work for this species (P. Cárdenas, unpublished data) so we tried to sequence COI in two parts (miniCOI + part 2) which worked, thus giving us the first COI sequence for this species. This is an opportunity to test the phylogenetic position of this species which is very uncertain with 28S (C1-D2) (*Cárdenas et al., 2011*; Fig. 4.3.6B). Unfortunately, our COI tree (Fig. 4.3.6A) also gives an uncertain position for *N. amygdaloides,* diverging between the Vulcanellidae and lithistid families, alone on a poorly-supported branch. The two 28S (C1-D2) sequences previously obtained by *Cárdenas et al. (2011)* were quite different: specimen MNHN DCL4077 (HM592772) from Italy and ZMAPOR 21223 (HM592773) from the Gulf of Cadiz had a significant 19 bp difference plus a deletion of 4 bp., a result difficult to explain at the time. Our shorter 28S (C1-C2) fragment (ON133878) is a 100% match to the sequence from Italy confirming this difference. Such a high genetic difference between Northeast Atlantic and Mediterranean specimens suggests two clear different species, and a species complex for *N. amygdaloides*.

In order to explore this hypothesis, we decided to measure spicules from the type, which has never been revised since its original description (*Carter, 1876*). *Maldonado, (2002)* mentions a type slide (NHM 00047; I.1.2) but does not give any measurements or drawings. Here, three slides were examined (NHM 1910.1.1.1683-1685); although not explicitly labeled as type slides, these slides have the label '*Porcupine Exped. Pachastrella amygdaloides Cr*'. Since the holotype is the only specimen collected during the Porcupine Expedition, we can be sure that these spicule slides are from the holotype. These slides also have purple hand-written numbers '43' (1684), '44' (1683) and '45' (1685), which seem older, and may explain why *Maldonado, (2002)* examined a slide with number '47'. On slides 1683 and 1685, the genus has been changed to *Poecillastra* with hand-written ink, maybe after its genus reallocation (Sollas, 1888). In addition to the holotype slides, spicules from other specimens were measured: *N. amygdaloides* off southern Italy (MNHN DCL4077, GBT1(1)), Marseille (PC479), Corsica (PC1280) and the Gulf of Cadiz (ZMAPOR 21223) (Table 4.3.17). The spicule sizes of the three specimens collected from the Balearic Islands match well with those of the holotype (Table 4.3.17): minor differences were found in the size of the calthrops (with thicker actines in the holotype) and the microxeas (slightly shorter in the holotype). Overall, no significant size differences could be identified between the two Northeast Atlantic and the seven Mediterranean specimens. Spicule morphologies were then compared. The triactines can have straight or slightly bent actines: in the holotype the majority of the actines are bent, while actines in Mediterranean species seem to be more straight, but more Atlantic specimen are required to confirm this difference. Besides, the northeast Atlantic specimen ZMAPOR 21223 also had triactines with fairly straight actines, as well as irregular/aborted actines, unlike the holotype. Irregular

triactines were especially common in the most shallow specimens from the Balearic Islands (Por347_B and POR7(15)) where reductions to one-two actines were found, as well as in GBT1(1) from Italy. We also noticed that swellings along the actines were quite common in the Mediterranean specimens (i215b, GBT1(1), PC479, PC1280) albeit not always present (POR347_B, POR7(15)); these were not present on the actines of the northeast Atlantic specimens (type and ZMAPOR 21223). We also compared microxea morphology but no differences could be found: centrotylote microxeas are generally uncommon, but specimen Por347_B had plenty (Fig. 4.3.39F-I), maybe because its microxeas were thinner, which revealed more swellings. Finally, we cannot exclude differences in external morphology between the Atlantic and Mediterranean populations but unfortunately Atlantic specimens are few and either poorly described or only a fragment (e.g. ZMAPOR 21223). To conclude, although 28S suggests *N. amygdaloides* to be a species complex, we refrain from any taxonomical action before more specimens can be revised (e.g. Topsent's numerous specimens from the Azores) and sequenced.

A second size of oxeas, resembling renierid spicules, is quite common in our samples. As for *C. pachastrelloides* and *C. tripodaria* (see above), those spicules are probably foreign, because the species shares habitat with haplosclerids with spicules of a similar size and morphology. In fact, a specimen of *H. poecillastroides* (#CFM-IEOMA-6393) reported by *Díaz et al. (2020)* was collected along with POR347_b, with a similar spicule size. Those spicules were not present in the holotype and in specimens from Corsica (PC1280), Marseille (PC479) and Italy (MNHN DCL4077).

Genus *Pachastrella* Schmidt, 1868

Pachastrella monilifera Schmidt, 1868

(Fig. 4.3.40; Table 4.3.18)

Material examined

UPSZMC 190891-190892, field#i139_A-i139_B, MaC (EB), St. 51 (INTEMARES0718), 128 m, beam trawl; UPSZMC 190893-190894 field#i153_3 and field#i157, MaC (EB), St. 52 (INTEMARES0718), 109 m, rock dredge, coll .F. Ordines; UPSZMC 190897, field#i352_4, MaC (EB), St. 136 (INTEMARES1019), 146 m, beam trawl, coll. J. A. Díaz; UPSZMC 190898, field#i650, MaC (AM), St. 34 (INTEMARES0720), 105-111 m, rock dredge, coll. J. A. Díaz; UPSZMC 190899-190900, field#i687 and field#i688, MaC (EB), St. 43 (INTEMARES0720), 117 m, rock dredge, coll J. A. Díaz; UPSZMC 190901, field#i771, MaC (EB), St. 53 (INTEMARES0720), 104 m, rock dredge, coll J. A. Díaz; UPSZMC 190904, field#i827_2, MaC (EB), St. 25 (INTEMARES0820), 100 m, ROV, coll J. A. Díaz.

Comparative material

Pachastrella monilifera, MNHN-DT-410, holotype, Schmidt collection#65, Algeria, 'Exploration Scientifique de l'Algérie', 1842.

Outer morphology

Massive irregular or cup-shaped, 2-15 cm in diameter. Coralligenous algae (alive and dead), used as substrate and incorporated in the body (Fig. 4.3.40A). Several sponge epibionts, including *H. poecillastroides*, *Jaspis* sp., *P. compressa* and *Craniella* cf. *cranium* (Fig. 4.3.40B-C). No oscula observed. In some specimens, several minute orifices are placed in a central depression (Fig. 4.3.40B). Same color on deck and after ethanol fixation; whitish gray. Stony hard consistency. Surface smooth with localized hispidation areas. Diffuse cortex ca. 500 µm thick.

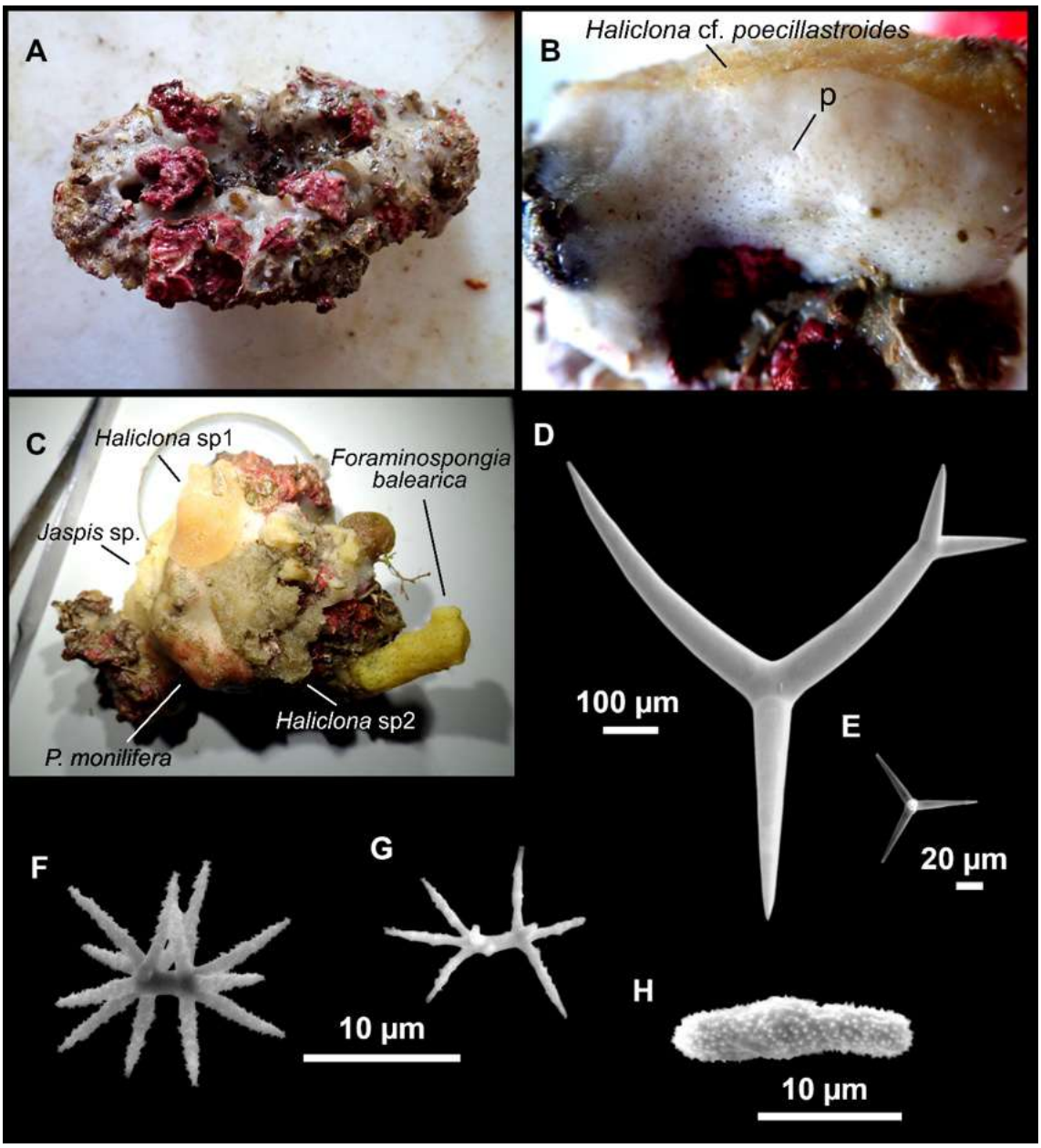

Figure 4.3.40. *Pachastrella monilifera Schmidt, 1868*. (A) Specimen i688 on deck. (B) Specimen i687 on deck, showing the pores (p) and overgrowth by *Haliclona* cf. *poecillastroides*. (C) Specimen i824_1 on deck overgrown by several demosponges. (D–H) SEM images of spicules from i139_A. (D–E) Calthrops. (F–G) Amphiasters. (G) Microrhabd I.

Spicules

Calthrops, large size range (Fig. 4.3.40D-E). Three of its actines are curved, corresponding to the cladome, and a fourth one straight, slightly longer, which is the rhabdome. Differentiation between cladome and rhabdome is obvious in larger spicules, but unclear in medium/small ones. For this reason clads and rhabdome measurements were merged. On the largest calthrops, actines may be rarely dichotomous or aberrant (Fig. 4.3.40D). Actine length: 23-779/4-112 μm.

Oxeas, long and thin, found mostly broken. However, in specimen i153_3A several unbroken ones were measured, length: 972-2326-3907/10-17-24 μm (N=11). It cannot be excluded that longer oxeas may be present.

Amphiasters (Fig. 4.3.40F-G), scarce, microspined rays radiating from two distal axes, sometimes from the shaft, 7-19 μm.

Microstrongyles I (= microrhabds, Fig. 4.3.40H), spiny, sometimes centrotylote, elongated to spherical, 8-21/2-6 μm.

Microstrongyles II (= microrhabdose streptasters), very scarce, spiny, thin, elongated and curved, rarely centrotylote, 17-56/1-2 μm.

Ecology and distribution

Found at the summit of the EB and the AM, on coralligenous algae bottoms (100-146 m) that serve as substrate for growth. It was also found growing on *S. mucronatus* (i827_1). This species is often overgrown with sponge epibionts such as *Jaspis* sp., *H. peocillastroides*, *Vulcanella aberrans* (Maldonado & Uriz, 1996) or *C.* cf. *cranium.*

Genetics

Folmer COI was sequenced from i688 ((ON130559) but only the second part of COI was sequenced for i771 (ON130560); 28S (C1-C2) was obtained only from i688 (ON133874).

Taxonomic remarks. See below discussion of *P. ovisternata*.

Pachastrella ovisternata Lendenfeld, 1894

(Figs. 4.3.2B and 4.3.41, Table 4.3.18)

Material examined

UPSZMC 190905, field#i219_A, MaC (SO), St. 8 (INTEMARES1019), 240 m, rock dredge, coll. J. A. Díaz; UPSZMC 190906-190907, field#i278_B-i278_D, MaC (AM), St. 58 (INTEMARES1019), 139 m, beam trawl, coll. J. A. Díaz; UPSZMC 190908, field#i394_1, MaC (EB), St. 165 (INTEMARES1019), rock dredge, 312 m, coll. J. A. Díaz; UPSZMC 190909, field#i628, MaC (AM), St. 30 (INTEMARES0720), 204 m, rock dredge, coll. J. A. Díaz; UPSZMC 190902, field#i808, small mount west AM, St. 11 (INTEMARES0820), 263 m, ROV, coll. J. A. Díaz; UPSZMC 190911, field#i818_1, small mount east off EB, St. 20 (INTEMARES0820), ROV, 725 m, coll. J. A. Díaz; UPSZMC 190912, field#i820_1, MaC (EB), St. 21 (INTEMARES0820), 425-733 m, ROV, coll. J. A. Díaz

Outer morphology

Massive, irregular, up to 40 cm in diameter (i808, Fig. 4.3.41A), often with several pockets which may develop in deep cavities, these pockets and cavities are covered with minute openings (Figs. 4.3.2B and 4.3.41B); the nature of these openings in the cavities is uncertain. Surface and choanosome whitish in life and after ethanol fixation; strongly hispid surface; hard consistency; diffuse cortex ca. 0.5 cm thick.

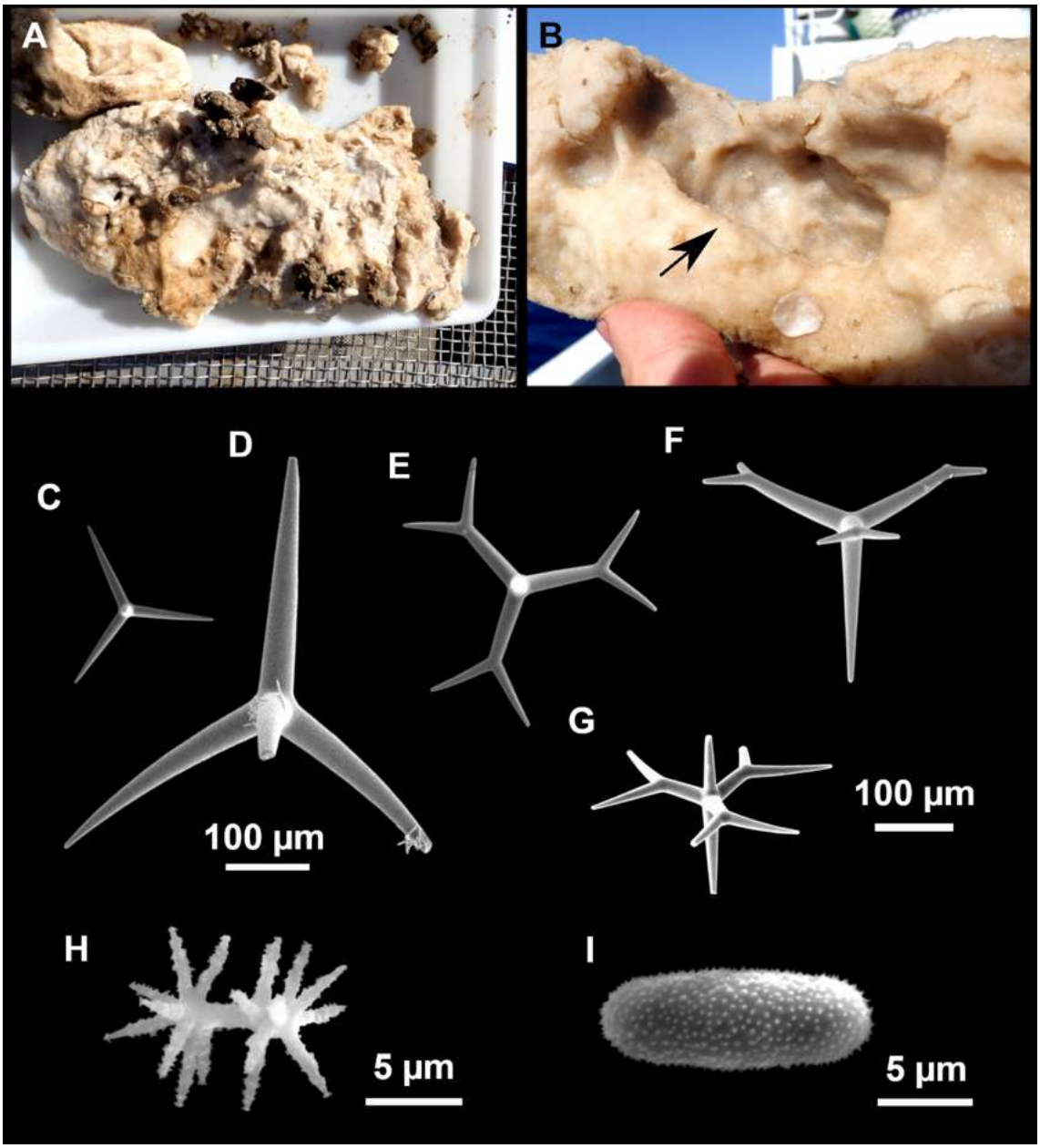

Figure 4.3.41. *Pachastrella ovisternata* Lendenfeld, 1984. (A) Habitus of i808 on deck. (B) Habitus of i628 on deck, showing the minute openings placed in large depressions (arrow). (C–I) SEM images of spicules from i808. (C–D) Calthrops. (E–F) Dichotriaenes. (G) Mesodichotriaene. (H) Amphiaster. (I) Microstrongyle I.

Spicules

Calthrops (Fig. 4.3.41C-D) in a wide size range, with the rhabdome slightly longer and straighter than the clads. In the larger ones, curvature of the clads is more pronounced;

rarely, having only three actines, showing teratogenic modifications or having their actines bifurcated. Actine measurements: 44-1102/7-142 µm.

Meso/dichotriaenes (Fig. 4.3.41E-G), common, rhabdome and epirhabdome are straight and fusiform, the former slightly longer than the latter. Epirhabdome may be absent or poorly developed. Measuring: rhabdome 47-129/5-16 µm, epirhabdome 27-108/4-15 µm. Protoclads are disposed in a 120° angle with the rhabdome, while deuteroclads are in a 90° angle with the rhabdome. Teratogenic modifications are frequent. Protoclads measuring 13-66/3-17 µm, deuteroclads 4-140/4-14 µm.

Oxeas (not shown), long and fusiform, slightly curved, mostly broken, measuring 980-5931/7-50 (N=15) µm.

Amphiasters (Fig. 4.3.41H), abundant, with well developed microspined actines, measuring 7-22 µm.

Microstrongyles I (= microrhabds) (Fig. 4.3.41I), spiny, very abundant, centrotylote or not, elongated straight or slightly curved to spherical, measuring 8-21/1-7 µm.

Microstrongyles II (= microrhabdose streptasters), very scarce, spiny, thin, elongated and curved, 20-47/1-2 µm.

Ecology and distribution

Essentially found in the MaC, below the photic zone (139-733 m). Due to its large size, the species provides habitat to many other invertebrates: sea urchins, brittle stars, shrimps and other small crustaceans, sponges: an unidentified Calcarea, *Haliclona* spp., *Jaspis* sp., *C.* cf. *cranium*, *P. compressa* or *Vulcanella gracilis* (see below).

Genetics

COI from i808 (ON130558) was obtained, while 28S (C1-C2) was obtained for i808 and i820_1 (ON133876 and ON133875).

Taxonomic remarks on *Pachastrella monilifera* and *Pachastrella ovisternata*

To discriminate both species, three spicule characters were particularly used: *P. ovisternata* has i) large calthrops with straight actines with irregular endings (vs. curved regular actines in *P. monilifera*), ii) meso/dichotriaenes (absent in *P. monilifera*) and iii) streptasters as a mix of amphiasters (the majority) along with metasters with less actines (absent in *P. monilifera*). Our specimens of *P. monilifera* also had less abundant amphiasters as well as slightly thinner microstrongyles I (Table 4.3.18). Macroscopically, *P. monilifera* tended to be smaller and much less hispid than *P. ovisternata*. In the MaC both species seems to have overlapping by different bathymetric distributions: *P. monilifera* was always collected in the photic zone, associated to coralligenous algae bottoms while *P. ovisternata* appears below the photic zone and reaches bathyal depths, down to 725 m. This is only the second record of *P. ovisternata* in the Mediterranean Sea after its finding off Malta (*Sitjà, 2020*) at 239 m and 752 m. The mesophotic distribution of *P. monilifera* agrees with most of the previous Mediterranean records (*Topsent, 1934; Pulitzer-Finally, 1972*) while it also has been commonly reported from upper bathyal depths in the North Atlantic (*Cárdenas & Rapp, 2012*), down to 2165 m off Essaouira (=Mogador), Morocco (*Topsent, 1928*).

Table 4.3.18. Spicule measurements of *Pachastrella monilifera* and *Pachastrella ovisternata,* given as minimum-mean-maximum for total length/minimum-mean-maximum for total width; all measurements are expressed in µm. Balearic specimen codes are the field#. Rh: rhabdome; Cl: clad; -:not found/not reported; EB: Emile Baudot; AM: Ausias March; SO: Ses Olives.

Material	**Depth** (m)	**Oxeas** (length/width)	**Calthrops** (length/width of actine)	**Mesodichotriaenes** Rhabdome (length/width) Epirhabdome (length/width) Protoclade (length/width) Deuteroclade (length/width)	**Microrhabds** (length/width)	**Amphiasters** (length)
P. monilifera **i139_A EB**	128	broken	43-183-522/ 7-26-77	-	I. 12-16-18/3-4-6 II. 23-33-56/1-1-2	9-13-19
P. monilifera **i153_3A EB**	109	972-2326-3907/ 10-17-24 (N=11)	23-168-779/ 4-25-106	-	I. 12-17-21/2-4-6 II. 17-27-32/1-1-2 (N=5)	8-11-16
P. monilifera **i688 EB**	117	3129/24 (N=1)	107-300-724/ 8-37-112	-	I. 8-13-18/2-3-5 II. -	7-9-12 (N=9)
P. ovisternata **i219_A SO**	240	n.m.	44-242-1036/ 7-34-142	Rh: 52-67/6-8 (N=3) EpiR: 40-55/7-9 (N=3) Pr: 18-32-44/4-8-12 (N=14) Dt: 25-51-82/4-7-10 (N=14)	I. 9-14-17/4-5-7 II. 23-29-35/1-2-2 (N=5)	8-12-22
P. ovisternata **278_B AM**	139	2691/ 22 (N=1)	59-301-1102/ 8-38-140	Rh: 49-82-129/5-9-16 (N=7) EpiR: 27-59-108/4-8-15 (N=7) Pr: 16-24-30/4-9-17 (N=13) Dt: 4-62-99/4-8-15 (N=13)	I. 9-15-21/1-3-4 II. 29-42/1-2 (N=2)	7-12-16
P. ovisternata **i278_D AM**	139	980-2244-5931/ 7-18-35 (N=10)	49-292-726/ 7-36-99	Rh: 50-65-79/5-7-10 (N=7) EpiR: 31-46-60/4-6-8 (N=6) Pr: 13-28-48/3-8-15 (N= 11) Dt: 26-51-140/4-7-14 (N=11)	I. 10-15-21/2-3-4 II. 20-29-41/1-1-2 (N=11)	8-14-19
P. ovisternata **i628 AM**	240	3222/ 29 (N=1)	62-340-860/ 7-49-140	Rh: 79 (N=1)/8-9-12 (N=5) EpiR: broken Pr: 26-32-43/5-7-9 (N=5) Dt: 23-39-59/5-6-7 (N=5)	I. 11-16-18/3-5-6 II. 36-47/1-2 (N=2)	8-14-19 (N=20)
P. ovisternata **i808 AM**	263	3345-3587/ 31-50 (N=3)	87-294-793/ 11-39-115	Rh: 47-58-68 (N=8)/8-12-15 (N=12) EpiR: 39-56-76/8-11-13 (N=6) Pr: 25-39-66/8-11-15 (N=12) Dt: 28-49-73/5-9-12 (N=5)	I. 8-13-18/3-5-6 II. -	10-13-20 (N=20)

However, we have failed to separate both species genetically: COI and short fragments of 28S (C1-C2) were identical for our specimens of *P. monilifera* and *P. ovisternata*. It is known that in some groups COI shows no variation between sister species, even when apparently strong morphological synapomorphies are present; see the case of *Heteroxya corticata/H. beauforti* (*Morrow et al., 2019*) or *Thenea muricata/T. valdiviae* (*Cárdenas & Rapp, 2012*). Also, we are missing the 28S D2 fragment, which is the most variable. Our COI tree (SuppFig. 2) also suggests that *P. ovisternata* is polyphyletic. A revision of the type material is necessary now to decide which *P. ovisternata* is the right one. In any case, this suggests that there is probably another undescribed *Pachastrella* in the Atlanto-Mediterranean region, and that more specimens need to be sequenced to untangle the matter. However, there may be a second explanation: the discrepancy in spicular set, spicule sizes and abundances may just be a depth-related artifact caused by differences in nutrient content or nutrient availability. Silica concentration is known to directly affect the spiculogenesis in demosponges, and proved to be the cause of the presence/absence of isochelae and desmas in *Crambe crambe* (*Maldonado et al., 1999*). Depth directly affects the silica concentration of the water mass through several processes, but mostly because at the photic zone it is disputed by diatoms. This could explain why the deep species *P. ovisternata* develops mesodichotriaenes and more amphiasters and why "*P. ovisternata"* morphotype only appears below the photic zone while "*P. monilifera" morphotype* is always shallower. Future studies should address this question using molecular markers with greater resolution, like microsatellites or SNPs.

Hastate oxeas are sometimes reported in *Pachastrella* (*Maldonado, 2002; Cárdenas & Rapp, 2012*). While some authors question their origin and point them as foreign, others consider them as proper (*Maldonado, 2002*). We have found both hastate and regular oxeas in most of *Pachastrella* spp. specimens. However, usually those specimens also harbor several haliclonid as epibionts which could act as the source of the oxeas. In order to discern whether they are proper or exogenous, we measured the oxeas found in *Pachastrella* spp. choanosomes and compared them to those of *Haliclona* spp. growing on the same individuals. Hastate oxeas measured 100-195-310/3-6-12 (n=19) μm in the choanosome of i687 (*P. monilifera*) and 114-236-314/3-8-14 μm in i687_1 (*Haliclona* cf. *poecillastroides* epibiont); 199-316/8-13 μm (n=2) in the choanosome of i628 (*P. ovisternata*) and 281-312-349/7-13-18 μm in i628_1 (*H. poecillastroides* epibiont); 263-279-294/7-11-15 μm (n=4) in i808 and 202-281-334/11-13-16 μm in i808_1 (*H. poecillastroides* epibiont). Besides, in the choanosome of *P. monilifera* specimen i824_1 smaller haliclonid spicules were found, 148-158-172/4-6-8 μm (n=4), versus 127-157-181/2-5-7 μm for the oxeas from i824_2, a whitish *Haliclona* sp. epibiont found on that same specimen. The coincidence in sizes and the prevalence of the association between *Pachastrella* and *Haliclona* spp. (mostly *H. poecillastroides*) seems to indicate that both regular and hastate oxeas are foreign, in opposite view to *Maldonado (2002)*. Having those spicules in the choanosome does not mean that they are proper of *Pachastrella*, yet other clearly non-pachastrellid spicules (like sterrasters, clionid microscleres, bubarid vermicular oxeas and *Jaspis* oxyasters and microxeas) have been found in the choanosome of our *Pachastrella* spp. These species act as substrate for many sponges, such as *H. poecillastroides*, *Jaspis* sp., *Craniella* cf. *cranium*, etc. Foreign spicules which end up in the choanosome are perhaps filtered by the aquiferous system of the host and then incorporated in its own body, or possibly

actively stolen from epibionts. It could also be the case that *Pachastrella* kills the epibionts by overgrowing them and then uses its skeleton as a substrate. Epibiont interactions are widespread in deep-sea sponge communities, and may occur in other massive demosponges, a fact that could explain the presence of hastate oxeas in species like *N. amygdaloides* or *C. tripodaria* as well, and their recurrence in the tetractinellid literature.

Genus Discodermia du Bocage 1869

Discodermia polymorpha Pisera & Vacelet, 2011

(Fig. 4.3.42, Table 4.3.19)

Material examined

UPSZMC 190824-190825, field#i141_1-i141_2, MaC (EB), St. 51 (2018), 128 m, beam trawl, coll. F. Ordines; UPSZMC 190829, field#i277_1, MaC (AM), St. 58 (INTEMARES1019), 139 m, beam trawl, coll. J. A. Díaz; UPSZMC 190833-190834, field#i320 and field#i321, MaC (EB), St. 124 (INTEMARES1019), 152 m, beam trawl, coll. J. A. Díaz; UPSZMC 190837, field#i606, MaC (AM), St. 26 (INTEMARES0720), 130 m, beam trawl, coll. J. A. Díaz.

Outer morphology

Extremely variable in shape, some have a slightly ramose tendency, some show bulbous processes and protuberances (Fig. 4.3.42A), others are spherical or cup-shaped (Fig. 4.3.42B). Sizes about 4-9 cm in diameter. Consistency hard and crumbly; surface smooth. Subdermal canals commonly visible by transparency on the surface (Fig. 4.3.42A). Beige with brownish shades on deck (Fig. 4.3.42A-B), whitish after ethanol fixation. Uniporal to cribiporal oscules grouped on the top surface (Fig. 4.3.42A-B), about 1-4 mm in diameter, with a patent thin membrane.

Skeleton

Cortex formed by a layer of discotriaenes, with their rhabdomes pointed inwards and the discs disposed tightly packed. The discs lay on a layer composed by a dense aggregation of microrhabds on a collagenous membrane. Choanosome cavernous, fleshy, with tight fascicles of diactines disposed perpendicular to the cortex and a network of desmas. Many incorporated exogenous particles. Microxeas embedded in the walls of the choanosomal chambers.

Spicules

Tetraclone desmas (Fig. 4.3.42C-D), with smooth clones, zygomes tuberculated, 235-651/13-55 μm.

Discotriaenes (Fig. 4.3.42E), concave disc, highly polymorphic: from circular to elliptical, with regular or irregular margins or with several lobules, diameter of 151-358 μm. Rhabdome is short, triangular, sometimes with a swelling below the disc and with a slightly blunt tip, measuring 63-150/8-48 μm.

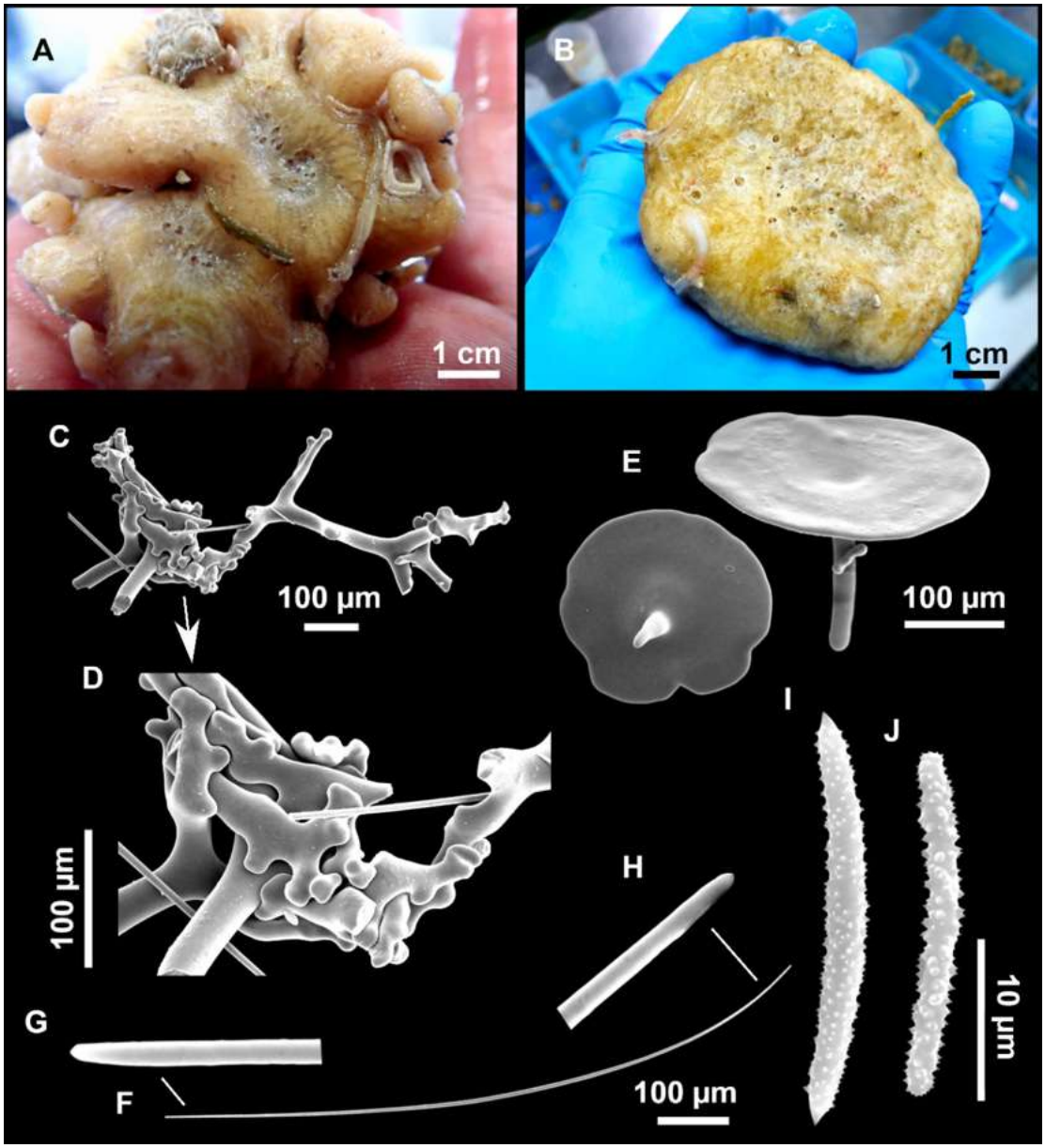

Figure 4.3.42. *Discodermia polymorpha Pisera & Vacelet, 2011*. (A) Habitus of i606 on deck. (B) Habitus of i320 on deck. (C) Tetraclone desmas with (D) detail of the zygosis. (E) Discotriaenes. (F) Diactine with detail of the tips (G–H). (I) Acanthomicroxea. (J) Acanthomicrorhabd.

Diactines (Fig. 4.3.42F), thin, widely curved, with variable tips (rounded, tylote, subtylote or blunt, Fig. 4.3.42G-H), measuring 508-1446/3-10 µm.

Acanthomicroxeas (Fig. 4.3.42I), straight to slightly curved, triangular, with sharp tips, 20-65/1-4 µm.

Acanthomicrorhabds (Fig. 4.3.42J), curved, with round ends, entirely covered with microspines, measuring 13-48/1-3 µm.

Genetics

COI obtained for i606 and i321 (ON130549 and ON130550); 28S (C1-C2) obtained for i606, i321 and i320 (ON133891, ON133890 and ON133889).

Ecology and distribution

Mesophotic species, always collected on the upper slopes of the AM and the EB, just below the photic zone, between 128-152 m depth. Occasional sponge epibionts are a red *Timea* sp., *Hexadella* sp. and *Jaspis* sp. In addition, agglomerations of diatoms attached to the discotriaenes were common, and are probably giving the characteristic brownish shades to their skin.

Taxonomic remarks

Discodermia polydiscus (Bowerbank, 1869), the type species of *Discodermia,* was described from Saint Vincent, in the Caribbean, as "*small, unequally developed, cup-shaped sponge"* with tetraclone desmas, discotriaenes, microrhabds and microxeas. Diactinal spicules were not originally described but found later when revising the holotype (*Pisera & Lévi, 2002*). After its description, the species was reported in Portugal (du Bocage, 1870), Canary Islands (*Cruz, 2002*) and the Mediterranean Sea (*Vacelet, 1969; Pouliquen, 1969, 1972; Voultsiadou, 2005*, Table 4.3.19). The assignment of the northeast Atlantic and Mediterranean specimens to *D. polydiscus* was never satisfactorily argued, especially considering the distance between the type locality (Caribbean) and the Mediterranean Sea. Finally, *Pisera & Vacelet (2011)* described a new species, *D. polymorpha,* to include all the previous *D. polydiscus* Mediterranean records, from shallow caves to mesophotic depths in the Aegean Sea (210-360 m). The identity of the remaining northeast Atlantic records of *D. polydiscus* (*du Bocage, 1969; Cruz, 2002*) are probably inaccurate but require proper revision of this material. Because *D. polymorpha* had extremely variable macroscopic and spicular characters, *Pisera & Vacelet (2011)* cannot exclude that it could represent a species complex. Our sequences match previous *D. polymorpha* sequences from its type locality, the 3PP cave, in La Ciotat, France (*Chombard et al., 1998; Cárdenas et al., 2011*). Our 28S (C1-C2) is 100% identical, while our COI has a 1 bp difference with cave specimens from the type locality. Interestingly, all cave specimens sequenced so far from Medes Islands (Spain), around Marseille (France) and Dugi Otok (Croatia) share the holotype COI (*Pisera & Vacelet, 2011*) which would suggest that western Mediterranean cave populations are somewhat genetically separated from the Balearic mesophotic populations. Several morphological traits observed in our material may support this possibility. *D. polymorpha* from caves were described as small, 1-2 cm in diameter while our specimens are much larger, reaching 8 cm in diameter (i320). Also, *D. polymorpha* overall shape was described as "*nearly spherical to irregular masses with protuberances"* (*Pisera & Vacelet, 2011*). This character was actually used to differentiate *D. polymorpha* from the North Atlantic *Discodermia ramifera* Topsent, 1892 and *D. polydiscus* which are ramose and cup-shaped to irregular, respectively. However, the morphologies of our mesophotic specimens cover all these shapes: spherical or subspherical (i141_1, i141_3), ramose (i277, i321), and cup-shaped (i320, Fig. 4.3.42B). Also, *D. ramifera* and *D. polydiscus* have simple oscules (i.e. uniporal) on elevations, very much like in specimens of *D. polymorpha* from caves that we observed on underwater pictures (courtesy of P. Chevaldonné), looking like white warts. The

Table 4.3.19. Spicule measurements of *Discodermia polymorpha* and related species, given as minimum-mean-maximum for total length/minimum-mean-maximum for total width; all measurements are expressed in µm. Balearic specimen codes are the field#. -=not found/not reported. EB: Emile Baudot; AM: Ausias March.

Species	**Depth** (m)	**Diactines** (length/width)	**Discotriaenas** Rhabdome (length/width) Cladome (diameter)	**Desmas** (length/width)	**Acanthomicrorhabds** (length/width)	**Acanthomicroxeas** (length/width)
D. polymorpha **i141_1** **EB**	128	724-929-1152/ 3-5-8	Rh: 63-93-125/18-22-28 Cl: 151-261-319	264-422-651/ 28-35-46	13-21-31/1-2-3	20-40-51/2-2-3
D. polymorpha **i141_2** **EB**	128	673-905-1126/ 3-5-8	Rh: 71-96-110/16-25-48 Cl: 207-247-295	255-393-582/ 38-42-54	15-22-27/2-2-3	23-38-48/2-2- 4
D. polymorpha **i321** **EB**	152	683-1023-1367/ 3-6-8	Rh: 85-97-105/8-14-20 Cl: 155-262-347	235-377-520/ 13-29-55	13-20-28/2-2-3	43-51-65/2-2-3
D. polymorpha **i606** **AM**	130	508-945-1446/ 5-7-10	Rh: 63-115-150(N=5)/ 11-19-26 Cl: 157-267-358	295-405-508/ 34-40-46 (N=9)	16-25-48/1-2-3	48-54-61/1-3-4
D. polymorpha Marseille (caves) (*Pouliquen, 1972*)	4-25	-/5-8	Rh: 30-50/ - Cl: 200-300	-/40	10-25 /2	40-60/3
D. polymorpha Western Mediterranean and Aegan Sea (*Pisera & Vacelet, 2011*)	littoral caves and deep sea (360 m)	-	Rh: 60-65/- Cl: 174-366/-	370-718 µm in diameter	13-44-37/2-5-4	25-68/2-4
D. polydiscus Canary Islands (caves) (*Cruz, 2002*)	-	1200-1500/-	Rh: - Cl: 160-440	-/30-60	12-20	36-60
*D. polydiscus (*holotype) Saint Vincent, Caribbean (*Bowerbank, 1869*)	-	present	-	-	-	-
D. ramifera holotype, Azores (*Topsent, 1892*)	318	present	Cl: 300 Cl: -	Desmas rays full of tubercles in the extremities	20-25	40-45

oscula morphology of our specimens is more diverse and complex than this, with uniporal to cribriporal oscules, usually placed on depressed or flat areas located apically (Fig. 4.3.42A). One reason for that may be that we examined live specimens; once fixed in ethanol, many of these oscule groups contract and become less visible to invisible. However, the clear difference between the warty uniporal oscules in live cave specimens versus our oscule complexes remains and may be due to difference in depth, habitat differences such as water flow/currents. Similar oscule differences were also observed between cave *Caminella* and mesophotic ones, where oscule walls disappeared in deeper specimens (*Cárdenas et al., 2018*): reduced water flow in caves may stimulate the formation of raised oscules.

Another significant difference of our specimens is the presence of diactines in relatively high abundance, packed together on choanosomal tracks, a spicule only previously reported by *Pouliquen (1972)* but not mentioned by *Pisera & Vacelet (2011)*. Again, the abundance of this spicule may be linked to the mesophotic depths of our specimens. Interestingly, according to *Carvalho et al. (2020)*, diactines are always present in the Northeast Atlantic *D. ramifera,* found at 98-673 m in the Azores (*Topsent, 1892*) the Gulf of Cadiz (*Sitjà & Maldonado, 2019*) and the Great Meteor Seamount (*Carvalho et al., 2020*). The similarity of spicular set, spicule morphometrics, macroscopic shape and deep-sea habitat of *D. ramifera* and *D. polymorpha* indicate that both are phylogenetically closely related. Indeed, specimens of *D. ramifera* from the Azores (COI: MW000696; 28S: MW006540-6541) are clearly different genetically but sister to *D. polymorpha* (COI: 4-5 bp. difference; 28S (C1-D2): 13-14 bp difference), and are actually 1 bp. closer (with COI) to our mesophotic specimens than to the cave ones, which suggests that the shallow cave populations appeared after the deep ones.

Family Theneidae Gray, 1872

Genus *Thenea* Gray, 1867

Thenea muricata (Bowerbank, 1858)

Material examined

UPSZMC 190967, field#i232_1, St. 36 (INTEMARES1019), MaC (SO), beam trawl, 619 m.

Outer morphology

Spherical to hemispherical sponges with basal root-like projections. Sizes are variable between areas: 0.3-1.5 cm in maximum diameter at the seamounts off MaC and 2-5 cm in maximum diameter in some fishing grounds, especially in some stations found north off MeC. Hispid surface, slightly compressible. Colour whitish on deck and after preservation. Apical, circular oscula, from <0.1 mm to about 0.4 cm in the larger ones. Equatorial sieved poral area, barely distinguishable in smaller specimens. The ectosome is visible to the naked eye, measuring about 0.1 mm in thickness.

Genetics

COI and 28S (C1-C2) were obtained from i232_1 (ON130569 and ON133888).

Ecology

The species is widely present in the detrital mud stations of both the MaC and the fishing grounds of the Mallorca and Menorca shelf. Large aggregations of the species are annually found in a fishing ground North of Mallorca (MeC), constituted by individuals that reach 5 cm in diameter. However, most of the specimens collected in the MaC seamounts and the adjacent bottoms were much smaller, barely reaching 1 cm in diameter. This may be caused by nutrient differences between both areas, and be related to the fact that the MeC is narrower and shallower and more influenced by the strong storms from the north. The species is usually epyphyted by *Epizoanthus* sp., a relationship more common in larger specimens.

Taxonomic remarks

The species is well known and documented in the literature. The spicular complement agrees with those provided previously (*Cárdenas & Rapp, 2012*). COI and 28S (C1-C2) are a 100% match with already-existing sequences for this species.

Family Vulcanellidae Cárdenas, Xavier, Reveillaud, Schander & Rapp, 2011

Genus *Poecillastra* Sollas, 1888

***Poecillastra compressa* (Bowerbank, 1866)**

(Fig. 4.3.43)

Material examined

UPSZMC 190941-190942, field#i808_9-#i809, small mount west of AM (MaC), St. 11 (INTEMARES0820), 263 m, ROV, coll. J. A. Díaz.

Ecology and distribution

Very abundant species, at seamounts it was found associated with rhodolith beds at the EB and AM summits (98-150 m), and in greater depths living on hard and gravel bottoms (down to 511 m). On trawl fishing grounds, it was found on the shelf break and upper slopes, on a more restricted depth range (104-257 m).

Genetics

COI was obtained from i808_9 and i809 (ON130553 and ON130554), as well as 28S (C1-C2) for i809 (ON133870).

Taxonomic remarks

Spicule size/morphology perfectly agree with previous descriptions (*Cárdenas & Rapp, 2012*). COI and 28S (C1-C2) are 100% match with already-existing sequences for this species. This deep-sea species is common throughout the Eastern Atlantic and Mediterranean Sea (*Cárdenas & Rapp, 2012; Cárdenas & Rapp, 2015*). It can present different external colors, from white, grayish, yellow to orange (*Cárdenas & Rapp, 2012*). Samples UPSZMC 190941-190942 were of the white morphotype but other examined specimens were also orange, yellowish or grayish. *Cárdenas & Rapp (2012)* suggested that color was a morphological variety not related to light irradiance because

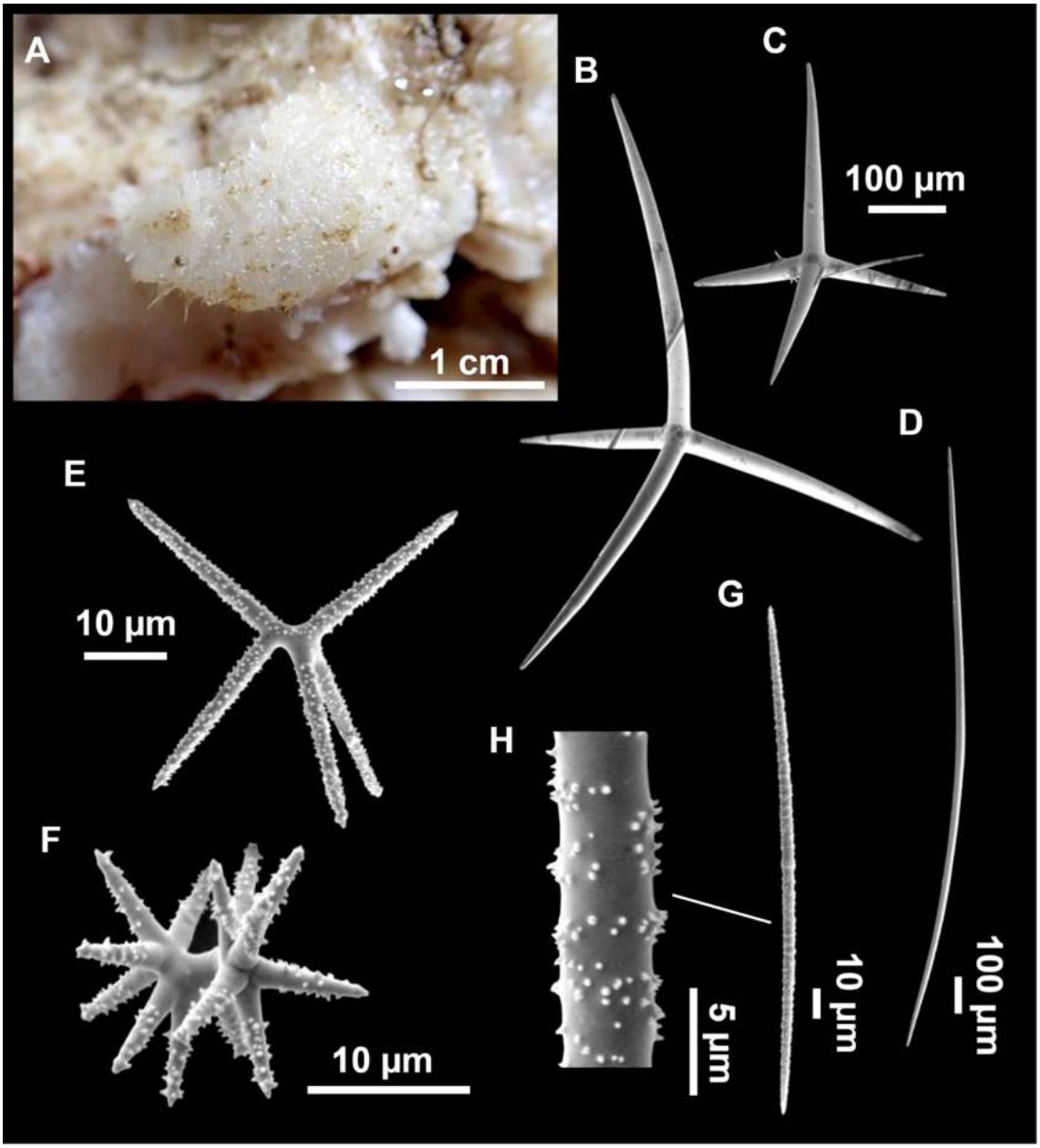

Figure 4.3.43. *Poecillastra compressa* (*Bowerbank, 1866*), specimen i808_9. (A) Habitus on deck. (B–C) Pseudocalthrops. (D) Oxea. (E) Plesiaster. (F) Metaster. (G) Microxea with (H) details of the spines.

of bicolor specimens and colored specimens at depths deeper than 100 m. However, in the Balearic islands, orange to yellowish specimens are always found at mesophotic depths, 100-150 m, while non-colored specimens (white and grayish), are present in both mesophotic and aphotic zones. This seems to indicate that colored specimens are conditioned by light irradiance at the bottom while non-colored specimens are more widespread. In other sponge species like *Suberites domuncula* (Olivi, 1792), blue, orange and yellowish colorations are given by carotenoids acquired from bacteria and microalgae (*Cariello & Zanetti, 1981; Maia et al., 2021*), which may be lost or not produced when inhabiting deeper waters (deeper *S. domuncula* specimens are grayish, personal observation). In fact, in marine invertebrates, orange and yellow colors that cannot be produced intrinsically are usually linked to carotenoids accumulated in the

body and acquired from the medium through feeding on photosynthetic microorganisms. In some cases, colors are lost when inhabiting shaded or cryptic spaces or deeper waters (*Bandaranayake, 2006*). In the case of *P. compressa*, the loss of coloration when the sponge lives in aphotic habitats may be caused by the lack of light or photosynthetic microorganisms in the surrounding waters. However, this does not explain why there are white and bicoloured individuals in the mesophotic zone. Perhaps, those specimens are placed in cryptic areas, hidden from the sunlight, or perhaps they do not have the time to acquire the pigments. In any case, those questions should be addressed in future works exploring the pigment contents of *P. compressa*.

Genus *Vulcanella* Sollas, 1886

Vulcanella aberrans (Maldonado & Uriz, 1996)

(Fig. 4.3.44, Table 4.3.20)

Material examined

UPSZMC 190971, field#i139_B1, MaC (EB), St. 51 (INTEMARES0718), 128 m, beam trawl, coll. F. Ordines.

Comparative material

Vulcanella aberrans, paratype, CEAB.BIO.POR.021B, slope of Alboran Island, 70-120 m.

Outer morphology

Small massive encrusting specimen, subdiscoid (~4 cm in diameter), with a few foreign pebbles, growing on *P. monilifera* (i139_B). External color is light brown in ethanol, same color as *P. monilifera*; internal color is the same. Surface is slightly hispid. Compressible. No oscula or pores observed.

Spicules

Plagiotriaenes (Fig. 4.3.44B-D), scarce, with malformations such as aborted, missing clads and stumps, affecting both cladome and the rhabdome. Rhabdome measures 478-549-591/21-22-23 µm (N=3), cladi measures 85-191-275/20-24-28 µm (N=4).

Oxeas I (Fig. 4.3.44E), abundant, robust and fusiform, slightly or markedly curved, occasionally double bent. Some modified to styles, 1115-1580-2185/11-21-34 µm.

Oxeas II, rare, thin and slender, sometimes centrotylote, smooth, 950-1269-1537/6-8-10 (N=4) µm.

Metasters to plesiasters (Fig. 4.3.44F-H), abundant, microspined, short axis and long, robust actines, some of which may be aborted, 13-27-43 µm.

Spirasters, uncommon, may be immature stages of metasters 14-18-20 µm (N=5).

Microxeas (Fig. 4.3.44I), thin, slightly curved, some centrotylote, finely microspined (Fig. 4.3.41J), sometimes in larger ones a subtle ring-pattern of spines can be seen at the central part. On a wide but continuous size range, 83-196-371/1-3-5 µm.

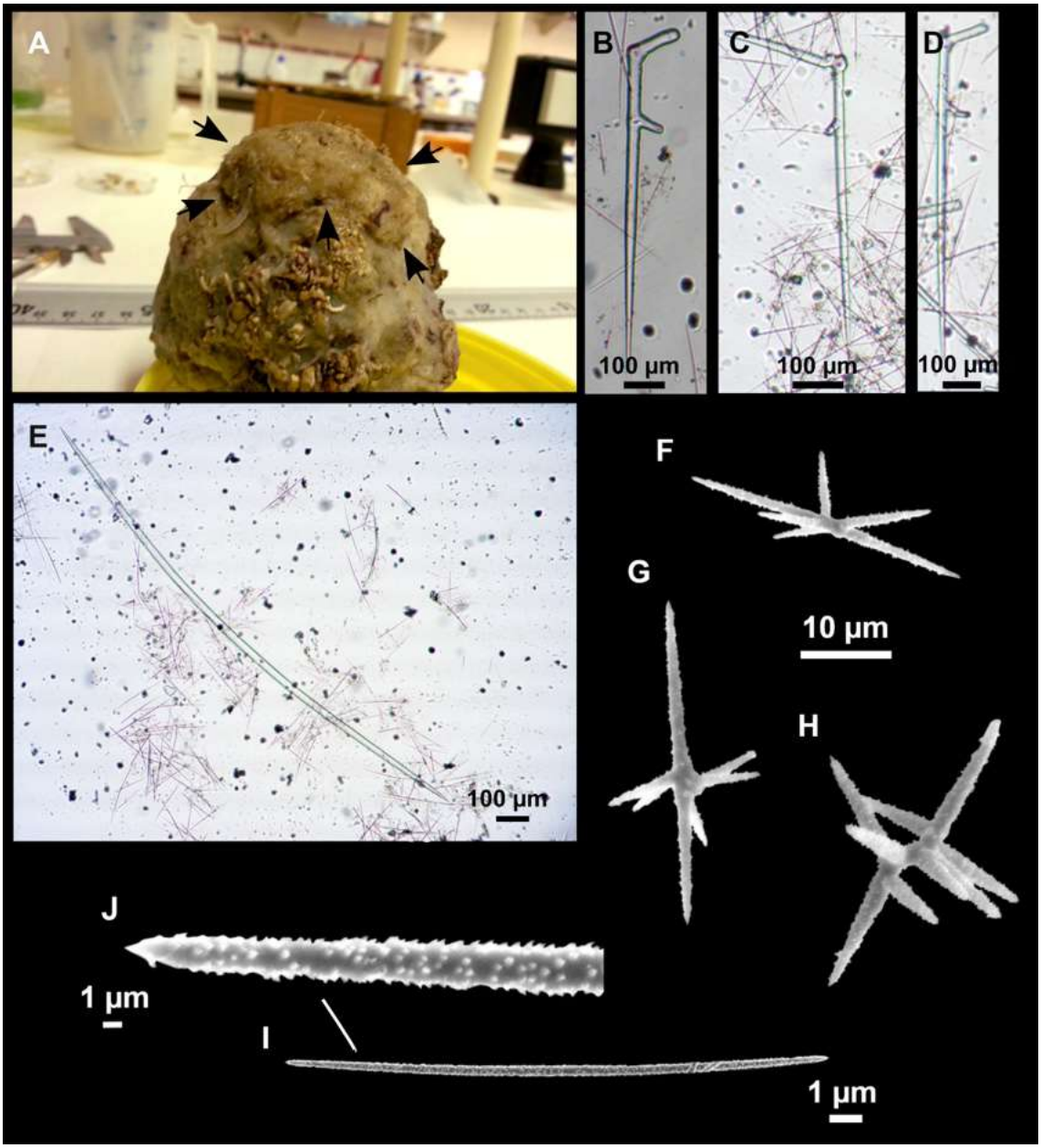

Figure 4.3.44. *Vulcanella aberrans* (*Maldonado & Uriz, 1996*). (A) Habitus of i139_B1 after ethanol (ar-rows) growing on a *P. monilifera* specimen (i139_B). (B–D) Irregular plagiotriaenes. (E) Oxeas I and mi-croxeas. (F–H) Metasters to plesiasters. (I) Microxea with (J) detail of the spines.

Ecology and distribution

Only a single specimen was collected, growing in epibiosis on a large *P. monilifera* specimen, at the mesophotic zone off EB.

Genetics

No sequences were obtained.

Taxonomic remarks

The material is assigned to *V. aberrans* essentially on the basis of the presence of malformed plagiotriaenes, of the same size and morphology as those described in the original description, and also similar to those found in the paratype CEAB-BIO POR021, from the closeby Alboran Sea. *Maldonado & Uriz (1996)* describe two categories of microxeas with very close sizes (150-315/3-7 and 65-140/2-2.5) with the largest size being sometimes centrotylote and with spines distributed in a ringed pattern. After measuring a large number of microxeas in our specimen, we concluded that they belonged to one category: size was continuous, with similar morphology, except for larger ones where a weak spiny ringed pattern was sometimes observed. However, this was not always the case, and some large microxeas were identical to small ones. Considering that, the sizes of the microxeas from the paratype and specimen i139_B1 are very similar (53-165-361/1-3-8 µm versus 83-196-371/1-3-5 µm). This is the first report of the species in the Balearic Islands after its description in the Alboran sea, slightly extending its distribution in the Western Mediterranean. A potential different population whose status remains to assess, occurs in Norway (*Cárdenas & Rapp, 2012*).

Vulcanella gracilis (Sollas, 1888)

(Fig. 4.3.45, Table 4.3.20)

Material examined

UPSZMC 190974, field#i303_B, MaC (AM), St. 103 (INTEMARES1019), 231-302 m, rock dredge, coll. J. A. Díaz; UPSZMC 190977, field#i818_2, small mount east of EB, St. 20 (INTEMARES0820), 725 m, ROV, coll. J. A. Díaz.

Comparative material

Vulcanella gracilis, MNHN DCL4082, Apulian Platform, off Cape Santa Maria di Leuca, southern Italy, 39º33’36’’N, 18º25’48’’E, 560-580 m, ROV dive 327-6, field#ASC-9/327-6, MEDECO leg1 (Ifremer), 17 Oct. 2007, coll: J. Reveillaud, id: P. Cárdenas, COI: HM592704, 28S: HM592760.

Outer morphology

Ovoid, massive or encrusting sponges (Fig. 4.3.45A), slightly compressible, hispid, up to 2 cm in diameter. Pale gray in life and after ethanol fixation. Small specimens have a single oscular basket while larger ones can have several (Fig. 4.3.45A). Oscular baskets are composed of an atrial sieve with a characteristic smooth thin membrane with openings 0.5-1 mm wide, surrounded by long thin oxeas. i818_2 (Fig. 4.3.45A) represents multiple small *V. gracilis* growing on a *P. ovisternata* (i818_1).

Spicules

Plagiotriaene pseudocalthrops (Fig. 4.3.45B-C) with a very short rhabdome. Some malformations (additional/aborted actines and stylote terminations) may be present. The rhabd measures 254-1111/36-77 µm (N=9) while clads measure 181-655/24-85 µm (N=20).

Oxeas I, around the atrial sieve, very long and thin, smooth, most broken when digested, measuring 4550-7406/9-21 µm (N=3).

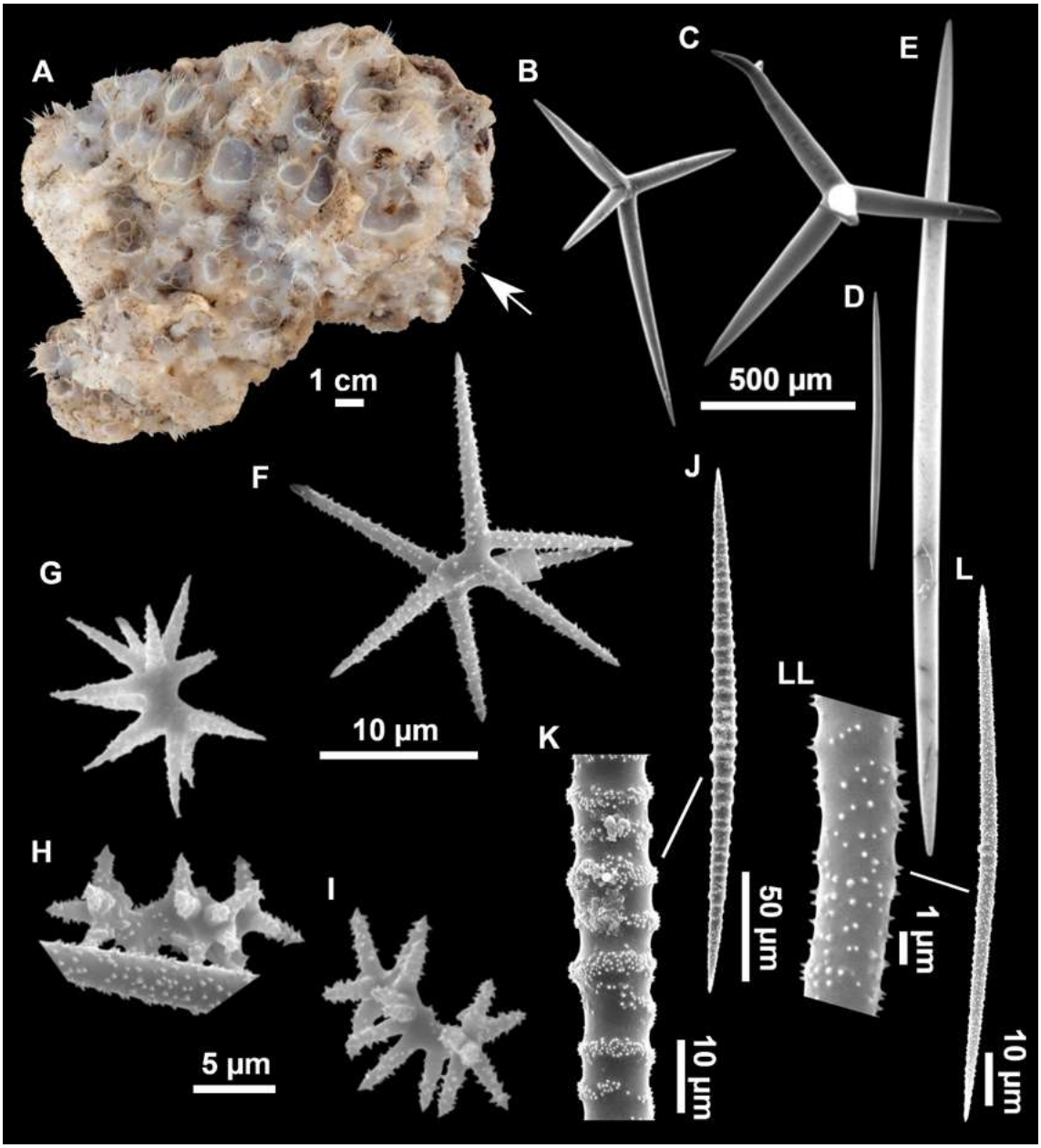

Figure 4.3.45. *Vulcanella gracilis* (*Sollas, 1888*). (A) Habitus of the association between a large *P. ovister-nata* specimen (i818_1) acting as substrate for several *V. gracilis* epibionts (arrow), including the specimen i818_2. (B–C) Pseudocalthrops. (D–E) Oxeas. (F) Metaster. (G–I) Metasters to spirasters. (J) Microxea I with (K) detail of the ringed microspination. (L) Microxea II with (LL) detail of the microspination.

Oxeas II (Fig. 4.3.45D-E), fusiform, smooth, thick, measuring 911-1795/29-107 (N=8).

Metasters (Fig. 4.3.45F), spiny, with a short, thin axis and long actines, measuring 12-25 µm.

Spirasters (Fig. 4.3.45G-I), uncommon, with short spined actines and an axis that can be thick or thin, 10-18 µm.

Microxeas I (Fig. 4.3.45J), with a very patent and regular spiny annulation clearly visible with the optical microscope (Fig. 4.3.45K), straight to gently curved. Overall measuring 155-341/6-19 µm.

Microxeas II (Fig. 4.3.45L), microspined but not annulated, (Fig. 4.3.45LL) gently curved, 77-171/2-8 µm.

Ecology and distribution

Very abundant species in the summits of the AM and the EB Seamounts, where it grows on epibiosis with *Hexadella* sp. individuals. It has also been collected growing on rocks on the slopes of the seamounts EB and AM.

Genetics

Folmer COI and the 28S (C1-C2) fragment were obtained from i818_2 (ON130555 and ON133869).

Taxonomic remarks

Vulcanella gracilis is easily recognizable due to the possession of characteristic strongly tuberculated microxeas, together with a second smaller category of spiny, non annulated, microxeas. Spicule size/morphology (Table 4.3.20) agree with previous descriptions from the Mediterranean Sea and measurements from comparative material from Italy (MNHN DCL4082). This is the first record of the species at the Balearic Islands. COI and 28S (C1-C2) are 100% match with already-existing sequences for this species off Cape St. Maria di Leuca, Italy (560-580 m) and off Tangers, Morocco (529 m). However, sequences from the somewhat remote type locality (Cape Verde Islands) and a careful comparison with the type is warranted in the future. Indeed, the type material (*Sollas, 1888*) did not seem to have rare spirasters as in our specimens (and comparative material), and the microxeas II were smooth and suddenly bent vs. spiny and gently bent in our material (and comparative material). Previous sequencing of Cape Verde *(Cárdenas et al., 2018)* or Canary Island specimens (*Caminus xavierae* **sp. nov.**, this study) have shown that the sponge faunas there may be different.

Vulcanella cf. *gracilis* (Sollas, 1888)

(Fig. 4.3.46, Table 4.3.20)

Material examined

UPSZMC 190972-190973, field#i279_A-i279_B, MaC (AM), St. 58 (INTEMARES1019), 139 m, beam trawl, coll. J. A. Díaz.

Outer morphology

Small hispid basket-like sponges, 0.5-0.7 cm long. Whitish alive and in ethanol discolored to deep purple by neighboring *Hexadella* sp.

Spicules

Plagiotriaene pseudocalthrops (Fig. 4.3.46), abundant, small (Fig. 4.3.46B), straight to slightly distorted, many dichotomized and/or with some degree of malformation, 114-369-523/13-32-45 µm.

Oxeas I, atrial oxeas, long and thin, all broken.

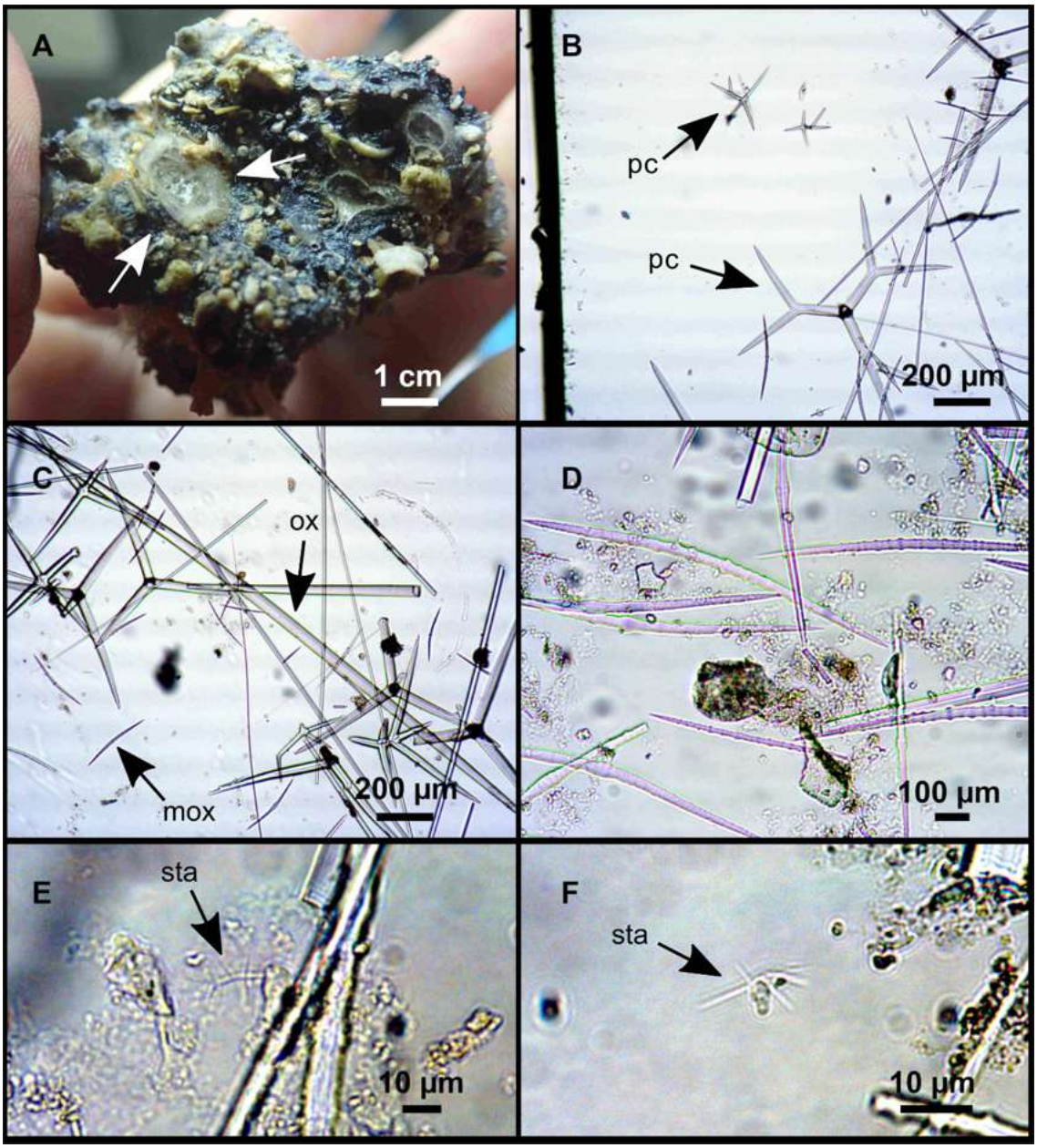

Figure 4.3.46. *Vulcanella* cf. *gracilis* (*Sollas, 1888*). (A) Habitus of i279_A on deck (arrows) growing on *Hexadella* sp. (B–F) Optical microscope images of i279_A (B–D) and i279_B (E–F). (B) Pseudocalthrops (pc). (C) Microxeas I (mox), oxeas (ox), and pseudocalthrops. (D) Microxeas I. (E–F) Streptasters (sta).

Oxeas II (Fig. 4.3.46C), fusiform, thick, slightly curved, measuring 1149-1712-2565/12-25-53 µm (N=16);two oxeas thin and centrotylote, may represent immature stages of Oxea I, 670-1300/7-8 µm (N=2).

Table 4.3.20. Spicule measurements of *Vulcanella aberrans, Vulcanella gracilis* and *Vulcanella* cf. *gracilis* given as minimum-mean-maximum in µm. Balearic specimen codes are the field#. -:not found/not reported; n.m.: not measured; EB: Emile Baudot; AM: Ausias March.

Material	**Depth** (m)	**Oxeas** (length/width)	**Pseudo-calthrops/calthrops** Rhabdome (length/width) Clad (length/width)	**Microxeas I** (length/width)	**Microxeas II** (length/width)	**Metaster/ plesiasters** (length)	**Spirasters** (length)
Vulcanella aberrans **paratype CEAB-BIO POR021B Alboran Island**	70-120	602-2059-2553/13-33-47 Styles: 674-1409-1892/19-28-38 (N=4)	Rh: 596-798/14-24 (N=4) Cl: 110-390/15-25 (N=4) (rare)	53-165-361/ 1-3-8	-	8-17-28	10-15-23
Vulcanella aberrans **i139_B1 EB**	128	I. 1115-1580-2185/11-21-34 (styles, same size) II. 951-1537/6-10 (N=4)	Rh: 478-591/21-23 (N=3) Cl: 85-275/20-28 (N=4) (rare)	83-196-371/ 1-3-5	-	13-27-43	14-18-20 (N=4) scarce
Vulcanella gracilis **MNHN DCL4082 Southern Italy**	560-580	between 1500 and > 2000/16-39-64	Rh: 481-589-767/38-52-62 (N=11) Cl: 229-336-410/36-51-64 (N=11)	112-209-326/ 6-9-13	80-120-169/ 2-3-6	28 (N=1)	11-19-26
Vulcanella gracilis **i303_B AM**	231-303	I. 4550-7406/9-21 (N=3) II. 1736-2663/32-76 (N=3)	Rh: 563-798-1111/60-70-77 (N=5) Cl: 354-551-661/50-66-72 (N=5)	155-254-324/ 6-10-12 (N=11)	94-116-151/ 2-2-3 (N=11)	12-18-24 (N=18)	14-16-18 (N=4)
Vulcanella gracilis **i818_2 EB**	725	I. long and thin, broken II. 911-1884-2795/29-60-107 (N=5)	Rh: 254-507-717/36-54-70 (N=4) Cl: 181-454-655/24-54-85 (N=15)	194-262-341/ 9-14-19	77-109-171/ 2-4-8 (N=20)	13-19-25 (N=10)	10-13-16 (N=3)
Vulcanella* cf. *gracilis **i279_A AM**	139	I. long and thin, broken II. 1149-1712-2565/12-25-53 (N=16)	114-369-523/13-32-45	105-222-351/ 3-6-11	-	-	-
Vulcanella* cf. *gracilis **i279_B AM**	139	n.m.	n.m.	n.m.	-	13-20-29 (N=8)	-

Microxeas I (Fig. 4.3.46D), slightly curved, centrotylote, with an irregular annulation more patent at the central part of the spicule, measuring 105-222-351/3-6-11 µm.

Streptasters (Fig. 4.3.46E-F), only found in 279_B, rare, spiraster to metaster morphology, 13-20-29 µm (N=8).

Ecology and distribution

Found as epibiont of *Hexadella* sp., at the upper slope of the AM.

Genetics

No sequences obtained.

Taxonomic remarks

The material is assigned to *Vulcanella* cf. *gracilis* because it has similarities but also several spicule differences with *V. gracilis.* The macroscopic morphology is identical, having a clear fenestration surrounded by a ridge of long oxeas. Like *V. gracilis,* it has pseudocalthrop plagiotriaenes, however, i) they are more abundant, ii) their rhabdome is proportionally shorter, compared to the cladi, than in *V. gracilis*, and iii) clads are shorter and thinner, and iv) commonly bifurcated, a modification also observed in *V. gracilis,* but less common (*Uriz, 1981; Pulitzer-Finali, 1983; Boury-Esnault, Pansini & Uriz, 1994*). On the other hand, oxeas are shorter and thinner than in *V. gracilis*. Regarding microscleres, *V.* cf. *gracilis* is missing the microxeas II found in *V. gracilis*. Also, the microxeas sometimes show an irregular annulation pattern, which contrasts with the regular tuberculated annulation of *V. gracilis*. Finally, streptasters are very scarce, only found in i279_B but not in i279_A, while these are relatively common in *V. gracilis*. To conclude, these two samples from the same station might represent a new species or atypical shallower specimens of *V. gracilis*. Genetic markers and additional specimens are necessary to test our hypotheses.

Family Thrombidae Sollas, 1888

Genus *Thrombus* Sollas, 1886

***Thrombus abyssi* (Carter, 1873)**

(Fig. 4.3.47)

Material examined

UPSZMC 190968-190969, field#i391_5_1 and field#i391_6, MaC (EB), St. 158 (INTEMARES1019), 146 m, beam trawl, coll. J. A. Díaz; UPSZMC 190970, field#i470, MaC (SO), St. 8 (INTEMARES0720), 244-251 m, rock dredge, coll. J. A. Díaz.

Outer morphology

Small encrusting sponges, spreading 1-3 cm on rocks and other sponges. Beige in life (Fig. 4.3.47A), and beige to grayish beige (Fig. 4.3.47B) after ethanol fixation. Smooth surface, hard but slightly compressible. Cortex not visible to the naked eye. Pores and oscules inconspicuous.

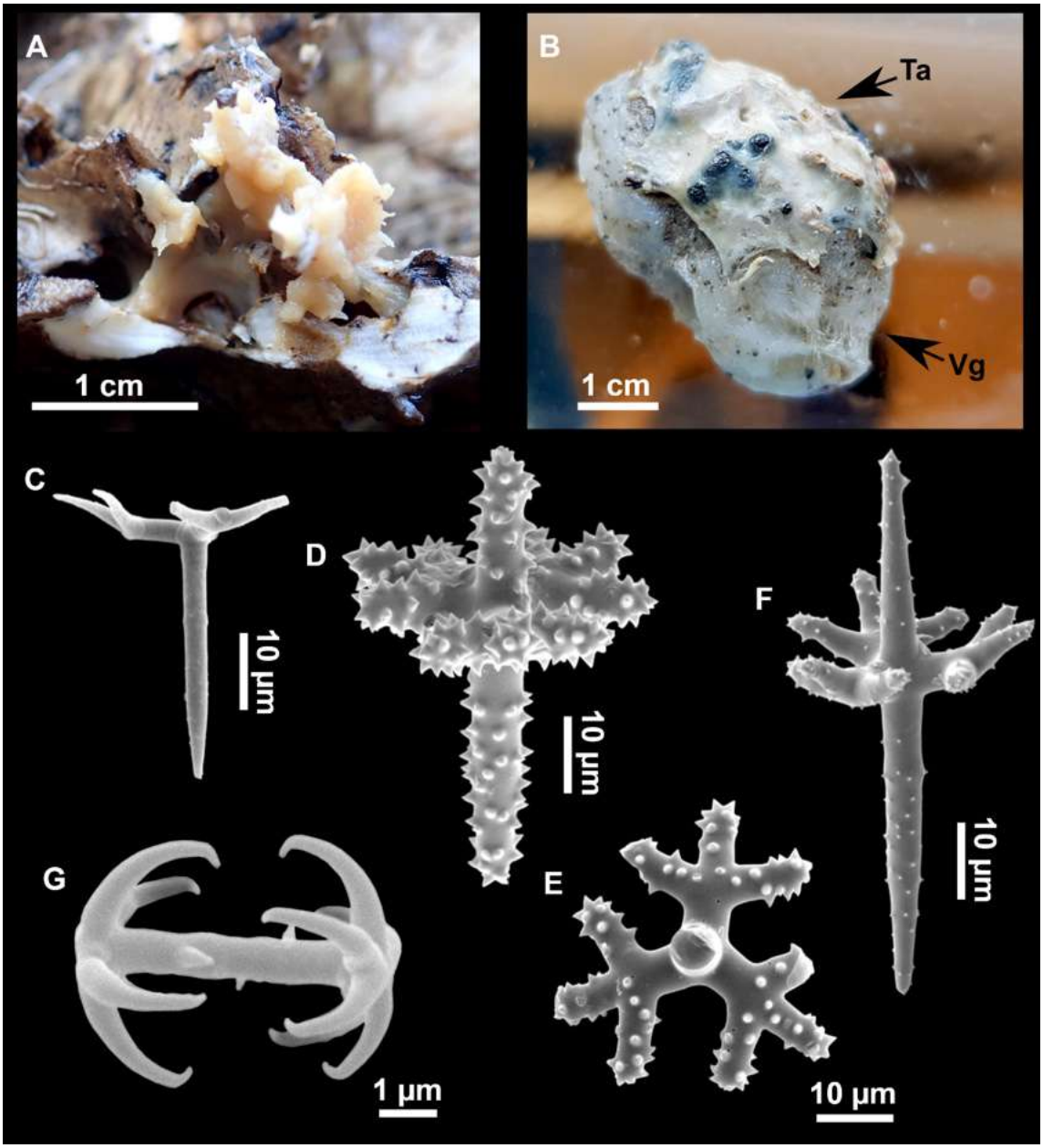

Figure 4.3.47. *Thrombus abyssi* Carter, 1873. (A) Habitus of i470 on deck. (B) Habitus of i391_5_1 (Ta) af-ter ethanol fixation, growing on a *Vulcanella gracilis* (Vc) specimen i391_5. (C–G) SEM images of i470. (C) Juvenile acanthotrichotriaene. (D–F) Acanthotrichotriaenes. (G) Amphiaster.

Spicules

Acanthotrichotriaenes (Fig. 4.3.47C-F), several morphologies probably representing different developmental stages. Small ones (Fig. 4.3.47C), microspined, with a smooth appearance under the light microscope; clads sometimes not bifurcated, and sometimes without an epirhabdome. Large ones appear in two morphologies, with overlapping sizes, mostly trichotomous but also dichotomous or unbifurcated. Often, one morphology (Fig. 4.3.47D-E) is robust with strong and large spines and short epirhabdome, while a second morphology (Fig. 4.3.47F), is more slender, has less and smaller spines and a longer epirhabdome. Overall measuring: rhabdome 25-45/2-9 µm, epirhabdome 8-34/4-9 µm, protocladi 2-9/2-8 µm, deuterocladi 5-15/2-7 µm.

Amphiasters (Fig. 4.3.47G), common, rays curved and directed inwards, at the end of both axes. Axis is straight and may have some isolated spines. Overall measuring 4-6 μm.

Ecology and distribution

The species has been found as epibiont of tetractinellid sponges *G. geodina* (i391_6_1) and *V. gracilis* (i391_5_1), and also growing on a dead oyster *Neopycnodonte* sp. shell (i470).

Genetics

Folmer COI and 28S C1-D2 fragments were obtained from i470 (ON130561 and ON133868).

Taxonomic remarks

Easily recognizable species due to the presence of trichotriaenes with both rhabdome and epirhabdome together with characteristic "amphiasters". Its sister species *Thrombus niger* Topsent, 1904 differs with *T. abyssi* by its black color and the absence of epirhabdome in its trichotriaenes. We have however found trichotriaenes with and without epirhabdome in *T. abyssi* but the former are more abundant. Interestingly, all trichotriaenes observed under SEM had epirhabdomes, but in many cases it was broken, which may suggest an artifact when these spicules are observed under light microscope. The small size of the spicules and the epirhabdome itself could make it difficult to distinguish this break, and thus the observer may assume that the epirhabdome is not present. The unique morphology of the "amphiasters" indicates that they are not homologous to the amphiasters found in the Astrophorina (e.g. Pachastrellidae, Vulcanellidae, Theneidae). This is the first time COI is sequenced for this species. As for 28S, two haplotypes were previously sequenced from Rockall Bank, 751-784 m (HM592755) and Mingulay Reef in Scotland, 151-159 m (HM592756), with a 1 bp difference; our 28S sequence is the same haplotype as that of the specimen from Rockall Bank.

Suborder Spirophorina Bergquist & Hogg, 1969

Family Tetillidae Sollas, 1886

Genus *Craniella* Schmidt, 1870

***Craniella* cf. *cranium* (Müller, 1776)**

(Fig. 4.3.48)

Material examined

UPSZMC 190910 (spicule preparation), field#i151_1B and UPSZMC 190873 (spicule preparation), field#i153_4_1, MaC (EB), St. 52 (INTEMARES0718), 109 m, rock dredge, coll. F. Ordines; UPSZMC 190819, field#i172_1A, MaC (EB), St. 60 (INTEMARES0718), 138 m, beam trawl, coll. F. Ordines; UPSZMC 190820, field#i339_5, St. 124 (INTEMARES1019), MaC (EB), 152 m, beam trawl; UPSZMC 190821, field#i409_1_1, MaC (EB), St. 167 (INTEMARES1019), 151 m, beam trawl, coll. J. A. Díaz; UPSZMC 190822, field#i416_D, EB, St. 177 (INTEMARES1019), 155

m, beam trawl, coll. J. A. Díaz; UPSZMC 190823, field#i826_7_1(G), MaC (EB), St. 24 (INTEMARES0820), 150-134 m, ROV, coll. J. A. Díaz.

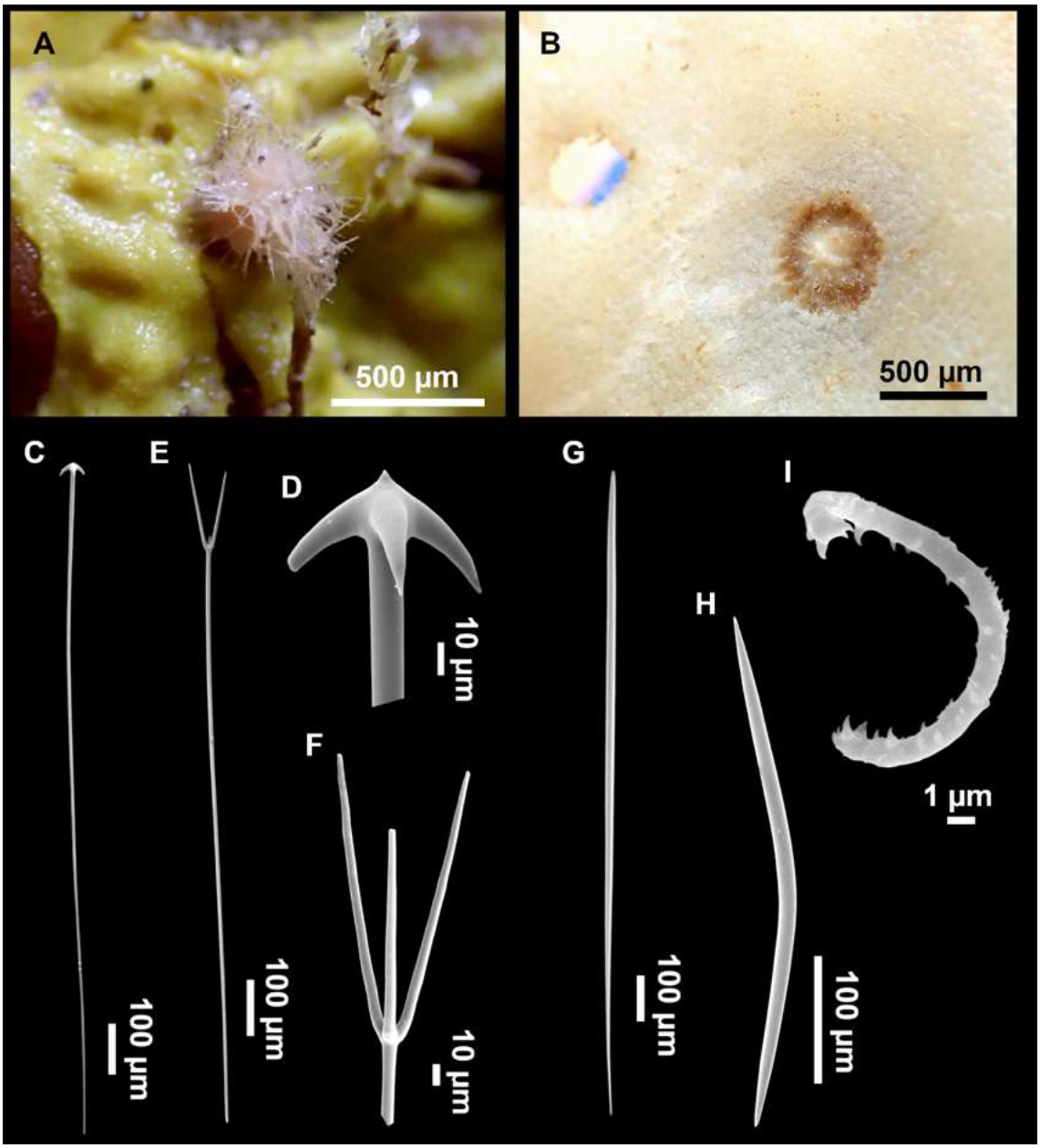

Figure 4.3.48. *Craniella* cf. *cranium* (Müller, 1776). (A) Habitus of i826_7_1(G) growing on *Spongosorites* sp., picture taken on deck. (B) Habitus of i409_1_1 after ethanol fixation, growing on/in *Phakellia robusta* and causing necrosis to the host. The hole on the left may be the remain of another of these interactions. (C–I) SEM images of i827_7_1(G). (C) Anatriaene with (D) detail of the cladome. (E) Protriaene with (F) detail of the cladome. (G) Oxea I (anisoxea). (H) Oxea II. (I) Sigmaspire.

Outer morphology

Small, 0.3-1 cm in diameter (Fig. 4.3.48A), circular to hemispherical, encrusting or slightly insinuating sponges (Fig. 4.3.48B). Pale beige in life and after ethanol fixation. Very hispid, hard and compressible consistency. Choanosome flexy, thin cortex, less than 0.1 mm width. Pores and oscules inconspicuous.

Spicules

Anatriaenes (Fig. 4.3.48C), with long, thin and flexuous rhabdomes, measuring 744-1364-2436/4-7-15 µm (N=14). Cladomes with short pointy clads, usually with a small spine at its top. (Fig. 4.3.48D), 13-21-51/5-8-15 µm.

Protriaenes (Fig. 4.3.48E), abundant, with long rhabdome, straight at most of its length but ending in a flexuous tip, measuring 777-900-1045/6-6-7 µm. Cladome with 2-3 clads, often of an unequal length, straight or slightly curved inwards at the tips (Fig. 4.3.48F), 25-63-135/4-6-10 µm.

Oxea I (Fig. 4.3.48G), anisoactinal (anisoxeas), straight and fusiform, 427-821-1307/5-11-27 µm.

Oxea II, isoactinal, fusiform, slightly curved, 177-281-470/5-10-23 µm.

Microxea (Fig. 4.3.48H), curved, measuring 80-173-243/1-5-5 µm (N=18)

Sigmaspires (Fig. 4.3.48I), very abundant, spiny, most C-shaped but also S-shaped, fairly small and measuring 7-8-10 µm in chord.

Ecology and distribution

Found at the summit and upper slope of the EB, on gravel bottoms. The sponge has been found growing on other sponges like *Spongosorites* sp. (i826_7_1) (Fig. 4.3.48A), *Phakellia robusta* Bowerbank, 1866 (i409_1_1) (Fig. 4.3.48B), *Foraminospongia balearica* Díaz, Ramírez-Amaro & Ordines, 2021 (i172-1A), *P. monilifera* (i151_1B and i153_4_1) or directly on the substrate (i339_5). Interestingly, when growing on *P. robusta* it erodes its tissue, which at the end is cut off, leaving a characteristic hole (Fig. 4.3.48B). In ROV records of the MaC seamounts, perforated *P. robusta* specimens are commonly seen. It is unknown if this process is a defense mechanism of the host (potentially mediated through secondary metabolites) or an indirect effect of the epibiosis (like tissue decay due to pore obstruction).

Genetics

The COI Folmer-Erpenbeck fragments were obtained for i172-1A and i416_D (OR045914 and OR045913), as well as the 28S (C1-C2) fragments of the same specimens (ON133849 and ON133850).

Taxonomic remarks

A comprehensive revision of *Craniella cranium* is greatly needed, it has been widely reported from the Mediterranean (e.g. *Vacelet, 1969, Pulitzer-Finali, 1983*), including the MeC (*Santín et al., 2018*). It is also recorded from the eastern, central and western Atlantic, including both north and south America coasts, and on a broad range of depths and habitats (caves, mesophotic zone, deep sea; see WPD for an overview). Most of the records have not been accompanied by proper descriptions and/or type redescriptions, nor sequencing. Here, we prefer to identify our material *Craniella* cf. *cranium*, until a future revision of the species is done.

Discussion

Hidden diversity in mesophotic west Mediterranean waters

The Mediterranean Sea is considered one of the best known marine areas of the world (*Coll et al., 2010*). Regarding sponges, this study challenges this assumption. In a small area such as the Balearic Islands, we are reporting the discovery of six new tetractinellid species: *Stelletta mortarium* **sp. nov.**, *Penares cavernensis* **sp. nov.**, *Penares isabellae* **sp. nov.**, *Geodia bibilonae* **sp. nov.**, *Geodia microsphaera* **sp. nov.** and *Geodia matrix* **sp. nov.**. Also, *Stelletta dichoclada* and *Erylus corsicus* are reported here for the second time since their description 40 years ago. *Pachastrella ovisternata, Vulcanella aberrans* and *Characella pachastrelloides* are reported only for the second time in the Mediterranean. Others are reported for the first time in the Balearic Islands region: *C. pachastrelloides, C. tripodaria, Stelletta mediterranea*, *Caminus vulcani, Caminella intuta, G. geodina*, *Erylus* cf. *deficiens*, *Erylus mamillaris*, *Discodermia polymorpha, Thrombus abyssi* and *Vulcanella gracilis*. With this work the number of Mediterranean tetractinellid species is raised from 83 to 89, while in the Balearic Islands, their number more than doubles, from 16 to 39, thus becoming one of the regions with the highest tetractinellid diversity of the Mediterranean (*de Voogd et al., 2024*). The only species that we have not found but that are reported in the Balearic Islands are *Dercitus (Stoeba) plicatus* (Schmidt, 1868) and *Geodia cydonium*, both reported by Bibiloni (1990) and the lithistids *Neophrissospongia nolitangere* and *Leiodermatium pfeifferae* reported from the MaC and MeC, respectively (*Santin et al., 2018; Maldonado et al., 2015*). *Dercitus (S.) plicatus* is an encrusting to excavating sponge, maybe missed due to its cryptic habit. Regarding *G. cydonium,* it is interesting that *Bibiloni (1990)* mentioned the presence of two types of morphologies, one large/massive and one small/encrusting. We suspect that small encrusting individuals belong in fact to *G. bibilonae* **sp. nov.**, but we did not have access to this material for comparison.

Interestingly, in the MaC Seamounts we have found 29 of the 34 species here reported, a number that contrasts with the seven species previously found in the MeC (*Santín et al., 2018*). This may be explained by the higher habitat heterogeneity of the MaC seamounts, but also could be an artifact caused by differences in sampling methodologies, use of molecular markers, lack of specialists and sampling intensity.

Also, *Uriz (1981)* reported 10 species of tetractinellids in the northeastern Iberian Peninsula, three of which (*Stelletta dorsigera*, *Stelletta grubii* and *Stelletta hispida*) were not reported in the Balearic Islands. The shallower distribution of these species may explain why these were not found in the present study. The high oligotrophy of the Balearic Islands may also be a contributing factor. Indeed, nutrient scarcity can have a negative effect on eutrophic species by limiting its physiological demands. Also, oligotrophy causes water transparency which in turn promotes a shift in the taxonomic composition of the benthos, promoting the development of photosynthetic algae and seagrass communities that compete with filter-feeders. In fact, shallow bottoms of the Balearic Islands are dominated by vast meadows of *Posidonia oceanica* (L.) Delille, 1813 and also brown and green algae like *Cystoseira* spp., *Halimeda* or *Caulerpa*, among others. At mesophotic depths, red algae are dominant from 30-40 m to 130-140 m. However, the deepest red algae may not be as efficient in competing for space as the

heterotrophic or mixotrophic organisms. The low nutrient content and the intense competition for space in shallow Balearic Islands waters may explain why most of the tetractinellids have been found associated with deep red algae beds, and why some shallow water species are not found.

Sitjà & Maldonado (2014) listed 26 tetractinellid species in the Alboran Island and surrounding abyssal plains. The upper shelf of the Alboran Island is a Specially Protected Areas of Mediterranean Importance (SPAMI), extensively studied and considered one of the richest spots of the Alboran Sea (*Rueda et al., 2021*), with a surface area comparable to the MaC seamounts. The fact that we found three more tetractinellid species than in the emblematic area of the Alboran Island is a strong argument towards the inclusion of these seamounts in the Natura 2000 framework.

Some of the new species described here are large and massive (*G. matrix* **sp. nov.** and *S. mortarium* **sp. nov.**), and have large population biomasses, which could signify potential sponge ground habitats in these areas (Díaz et al., unpublished data). Those species, together with other large tetractinellids reported (*P. monilifera, P. ovisternata, C. (C.) pathologica, S. fortis* and *S. mucronatus*) are habitat builders that provide three dimensional structure, shelter, and settlement substrate for other organisms like small crustaceans, ophiuroidea, worms and other sponges. Recently, *Díaz, Ramírez-Amaro & Ordines (2021)* described the agelasid genus *Foraminospongia Díaz, Ramirez & Ordines, 2021* at the MaC Seamounts. Its type species, *Foraminospongia balearica Díaz, Ramírez-Amaro & Ordines, 2021*, shares habitat with *G. matrix* **sp. nov.**, *G. geodina* and *S. mortarium* **sp. nov.**, and like those it is an abundant, large and characteristic habitat builder. The fact that those large key species have only been recently described indicates that more large species may be waiting to be discovered. This highlights how poorly explored Mediterranean deep-sea habitats are, especially seamounts, and the importance of future seamount research and conservation.

Sampling was done on a broad bathymetric scale (0-725 m) and heterogeneous habitats: from littoral caves, to different sedimentary bottoms (with mud, gravels, soft and coralline red algae), located at trawling grounds and seamounts, and also on the rocky slopes and summits of the seamounts SO, AM and EB. Of the 34 species recorded here, only five were not recorded from the seamounts (*C. intuta, P. isabellae* **sp. nov.**, *P. cavernensis* **sp. nov**., *E.* cf. *deficiens* and *E. discophorus*), which shows the importance of the MaC seamounts in terms of species richness. On the contrary, on the trawl fishing grounds off Mallorca, Menorca and Ibiza-Formentera, only six species were found (*Poecillastra compressa*, *Nethea amygdaloides*, *P. euastrum*, *P. helleri*, *S. mucronatus, Thenea muricata*), all of them also present in the MaC seamounts. MaC has been proposed to be part of the Natura 2000 network due to its highly rich ecosystems and presence of vulnerable marine habitats (*Ordines et al., 2019c; Díaz et al., 2021; Massuti et al., 2022*). The present study strengthens this proposal.

Species complexes revealed by molecular markers

The combined use of morphology and molecular markers has allowed us to detect several species complexes: *Geodia bibilonae* **sp. nov.** and its sister species *Geodia microsphaera* **sp. nov.**, both related to the Northeast Atlantic *G. cydonium*. Their almost identical macroscopic morphology, added to their small sizes and similar spicular set

(only distinguishable by differences in spicule size and morphology) makes their distinction and determination by means of morphology alone challenging. Another species complex concerns the species *G. geodina* (previously called *G. anceps* for most records), that we now split in two species: *Geodia phlegraeioides* **sp. nov.** in the upper bathyal Atlantic (phylogenetically closer to *G. phlegraei/parva*) and *G. geodina* in the mesophotic Mediterranean and the mesophotic North Atlantic. This was discovered thanks to the barcoding and careful spicule comparison of several specimens of Mediterranean and Atlantic representatives. Likewise with the species *C. vulcani* and *Caminus xavierii* **sp. nov.**, the first being now restricted to the Mediterranean and the second to the Canary Islands for the moment. Those cases are direct evidence of how the Atlanto-Mediterranean barriers, as well as water masses, have strongly affected sponge speciation. Two major genetic barriers are present between the north Atlantic and the Western Mediterranean: the Strait of Gibraltar, which separates the North Atlantic from the sea of Alboran, and the Almeria Oran front, that separates Alboran from the western Mediterranean. These barriers are known to affect a vast number of marine organisms, including sponges (*Patarnello et al., 2007; Riesgo et al., 2019*). Besides, a minor genetic barrier is also known at the Ibiza Channel, between the island off Ibiza and Valencia (*García-Merchán et al., 2012*). In light of that, many sponge species previously thought to have an Atlanto-Mediterranean distribution may in fact represent species complexes, with separate North Atlantic and Mediterranean representatives. The case of *G. geodina* also illustrates that mesophotic Mediterranean species can be found in the Atlantic at similar depths, highlighting the importance of water masses as barriers, already suggested for deep-sea sponge distribution (*Roberts et al., 2021; Steffen et al., 2022*).

Shallow-water caves connections with the deep sea

It is usually assumed that the shallow-water cave fauna is tightly connected to the deep-sea fauna, with some species common to both habitats: the fish *Conger conger* (Linnaeus, 1758), the hexactinellid sponge *Oopsacas minuta* Topsent, 1927 and the carnivorous sponge *Lycopodina hypogea* (Vacelet & Boury-Esnault, 1996*) (Bakran-Petricioli et al., 2007*) are only a few examples. This happens in ecosystems that may be separated by hundreds of km, and is explained by the similarities between both habitats: lack of light (and thus lack of photosynthetic communities), scarcity of nutrients and low hydrodynamic energy (*Vacelet et al., 1994*). However, our results nuance this assumption: we have shown that several species that were previously thought to inhabit both shallow water caves and deep sea habitats can sometimes have diverged enough to reach species status. This is the case of sister species *P. helleri* (deep sea) / *P. isabellae* **sp. nov.** (caves), and *P. euastrum* (deep sea) / *P. cavernensis* **sp. nov** (caves), both traditionally considered a single species. Also, the COI sequence of deep sea *D. polymorpha* showed 1 bp. difference with cave specimens off Marseille, a genetic differentiation not sufficient alone to justify describing a new species but that suggest some kind of population differentiation.

Sponges are main contributions to the overall diversity and biomass elements in both deep sea and cave habitats (*Gerovasileiou & Voultsiadou, 2012; Maldonado et al., 2017*). Mesophotic and cave species may be more susceptible to undergo speciation driven by oceanographic barriers, because of the added effects of habitat discontinuities

(habitat patchiness or limited ecological threshold). Different speciation scenarios may have taken place: ancient species with broad bathymetric distribution inhabiting both deep sea and littoral caves, becoming isolated and later differentiated in two different species. Also, throughout new environment colonization (deep-sea species colonizing caves, as suggested in the case of *D. polymorpha*, or vice versa) and posterior reproductive isolation. In some cases the dispersal potential may have been high enough to maintain the gene flow between both ecosystems, in which case a single species remained. This may be the case of the mentioned *D. polymorpha*, but also of *Erylus discophoru*s. For the latter, we have found 0-2 bp differences between specimen POR785, found on a fishing ground, and Mallorca shallow water cave specimens LIT71, LIT72 and LIT74. Further works with higher resolution markers are necessary to clarify these questions. Cave and deep-sea sponges would probably represent a good model to study speciation in low-dispersal invertebrates.

Finally, it important to highlight the importance of using molecular markers when studying species inhabiting this kind of ecosystems, especially if they are found in both shallow caves and deeper waters. In those cases, molecular markers represent an independent dataset to test the relevance of possible morphological discrepancies, which may be related to environmental parameters, such as different silica concentration, and/or genetics. In the course of this study, we have always found larger spicules on deeper waters, in both cases: when a single species inhabits caves and the deep-sea (like *D. polymorpha* or *E. discophorus*), and in cases when there are two sister species, one from the deep-sea and one inhabiting the caves (like *P. helleri/ P. isabellae* **sp. nov** or *P. euastrum/ P. cavernensis* **sp. nov.**). Translocation experiments or laboratory experiments under different silica concentrations could eventually show if these size characters are fixed in the genetics of the species/populations or simply part of their spicule plasticity range.

4.4. First record of the recently described *Axinella venusta* Idan, Shefer, Feldstein & Ilan, 2021 (Demospongiae: Axinellidae) in the western Mediterranean

Julio A. Díaz[1, 2], Francesc Ordines[1] & Enric Massutí[1]

[1]Centre Oceanogràfic de les Balears (COB-IEO), CSIC, Moll de Ponent s/n, 07015 Palma (Illes Balears), SPAIN.

[2] Laboratori de Genètica, Biology Department, University of the Balearic Islands, Carretera de Valldemossa km 7.5, 07122 Palma (Spain).

Abstract

The sponge *Axinella venusta* Idan, Shefer, Feldstein & Ilan, 2021, recently described from the mesophotic zone off the coast of Israel (Levantine Sea), is recorded for second time from the western Mediterranean. Two specimens of *A. venusta* were collected at the summit of the Emile Baudot seamount, at the Mallorca channel (Balearic Islands). The specimens are described and the COI and 28S C1-C1 fragments sequenced. This record underlines the importance of seamounts as ecosystems of special interest for biodiversity research.

Introduction

In recent times, the study of Mediterranean mesophotic habitats has allowed the discovery of rich and poorly-known benthic communities. The lack of data is more accused in deep-sea ecosystems like seamounts (e.g. *Massuti et al., 2022*), whose exploration presents logistic difficulties. At seamounts, benthic communities are favored by particular oceanographic features, like the presence of hard bottoms and enhanced currents, particularly near the summits and prominent features, which increase the availability of food to suspension feeders (*Watling and Auster, 2017*). In these habitats, corals and sponges often present high densities (e.g. *Ramiro-Sánchez et al., 2019*). Besides, low anthropogenic impacts led many of those communities barely pristine. In the case of sponges, the recent increase and interest of seamounts studies has led to the discovery of many new species and new biogeographic reports (*Idan et al., 2021; Diaz et al., 2021*).

The Balearic Promontory is an area of high biodiversity of sponges (*Bibiloni, 1990; Guzzetti et al., 2019; Díaz et al., 2020, 2021*). The Emile Baudot, Ausias March and Ses Olives seamounts are located at the Mallorca Channel, between the islands of Mallorca and Eivissa-Formentera. Recently, within the framework of LIFE IP INTEMARES project, several oceanographic research surveys have been conducted to improve the scientific knowledge of these seamounts for their further inclusion, as Site of Community Importance (SCI), within the Natura 2000 framework (*Massutí et al., 2022*). The first results have reported the presence of uncommon and new invertebrate species (*Ordines et al., 2019c; Díaz et al., 2021*). These surveys were particularly rewarding in the case of sponges, showing high biodiversity and abundance, especially at the shallow summits of Emile Baudot and Ausias March, where sponge gardens develop mostly associated with rhodoliths beds and rocky outcrops (*Massutí et al., 2022*).

The species *Axinella venusta* Idan, Shefer, Feldstein & Ilan, 2021 has been recently described at 97 m depth off Levantine Sea, in the eastern Mediterranean (Fig. 4.4.1A). The aim of this work is to report the presence of this species in the western Mediterranean and to provide a morphological description complemented by molecular barcoding.

Material and Methods

Two specimens of *Axinella venusta* were found and in two stations between 99 and 118 m depth, located at rocky bottoms of the summit of the Emile Baudot seamount (Fig. 4.4.1A, B), using a rock dredge during the INTEMARES_A22B_0720 survey carried out in July 2020.The two specimens were preserved in absolute ethanol (EtOH) for further morphological and molecular analysis at the laboratory. They are deposited in the zoological collection at the Museum of Evolution, Uppsala University (Uppsala, Sweden), under the reference UPSZMC 190204-190205. A fragment of each specimen has been kept at the Oceanographic center of the Balearic Islands (COB) collection under the codes i695 and i760.

To obtain dissociated spicules preparations, a fragment of tissue was digested with bleach and the remaining spicules were cleaned with pure water first, and then with EtOH at 50% and 96%. Spicules were observed and measured with an optical

microscope Nikon S-ke. For each sample, 25 spicules per spicule category were counted. The terminology applied for the morphological description of the spicules *follows Boury-Esnault & Rützler (1997)*.

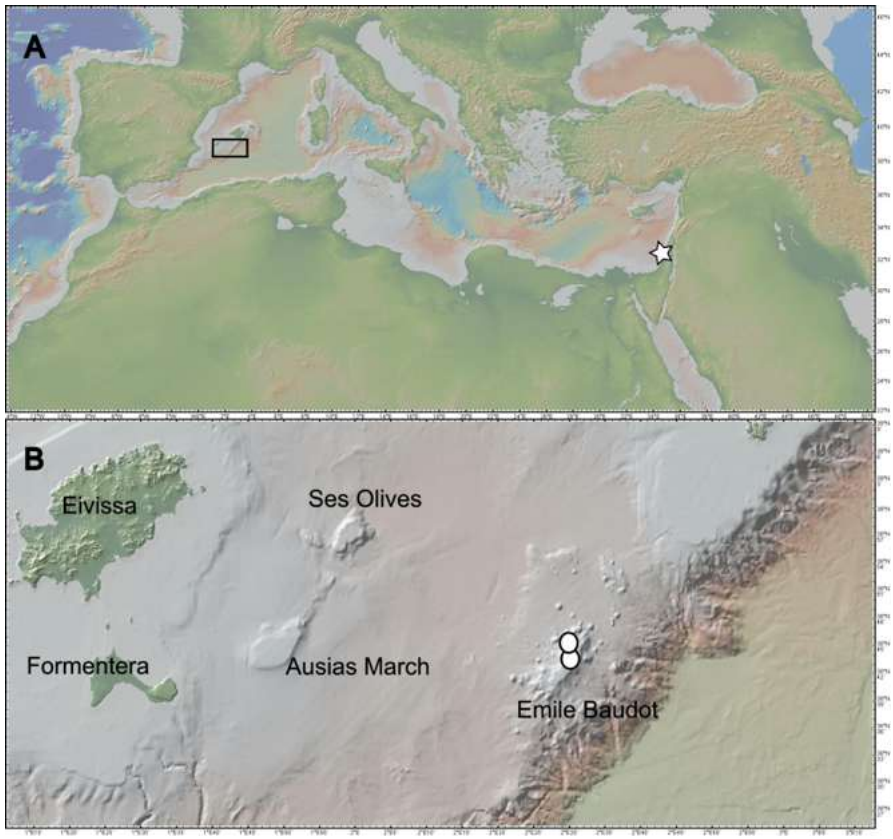

Figure 4.4.1. A: Map of the Mediterranean Sea, showing the type locality of *Axinella venusta* Idan, Shefer, Feldstein & Ilan, 2021 at the Levantine Sea (marked as star) and the area of the present record (marked as rectangle). B: Detail of the Mallorca Channel (Balearic Islands, western Mediterranean), with Ses Olives, Ausias March and Emile Baudot seamounts, showing the two stations where specimens of *A. venusta* were collected.

DNA was extracted from a piece of choanosomal tissue (~2 cm^3) using the DNeasy Blood and Tissue Extraction kit (QIAGEN). Polymerase chain reaction (PCR) was used to amplify the the first 130 bp of the Folmer marker, (minibarcode, Cárdenas & Moore, 2019) and the C1-C2 (~369 bp) fragment of the nuclear rDNA 28S gene. COI minibarcode and 28S C1-C1 were amplified with the primers LCO/Tetractminibarcode and C1'/Ep3, respectively. PCR was performed in 50 µl volume reaction (34.4 µl ddH20, 5 µl Mangobuffer, 2 µl DNTPs, 3.5 $MgCl_2$, 1 µl of each primer, 1 µl BSA, 0.1 µl TAQ and 2 µl DNA). PCR thermal profile used for amplification was [94°C / 5 min; 37 cycles (94°C / 15 s, 46°C / 15 s, 72°C / 15 s); 72°C / 7 min]. PCR products were

visualized with 1% agarose gel and purified using the QIAquickR PCR Purification Kit (QIAGEN) and sequenced at Macrogen Inc. (South Korea). Sequences were imported and edited with BioEdit 7.0.5.2. (*Hall, 1999*). The 28S sequence was deposited in Genbank (http://www.ncbi.nlm.nih.gov/genbank/) with the accession number PP377811.1, while the minibarcode was deposited on the Sponge Barcoding Project (https://www.spongebarcoding.org) with the accession number SBD#2884.

Results and discussion

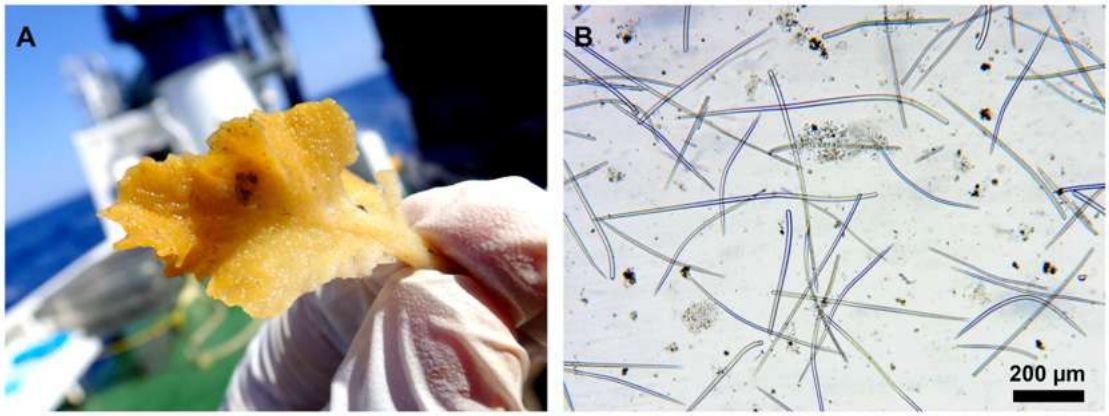

Figure 4.4.2. *Axinella venusta* Idan, Shefer, Feldstein & Ilan, 2021. A: Photograph of the fresh specimen i760 before preservation; B: Optical microscope image of the spicules of specimen i695.

The two specimens of *Axinella venusta* were associated to rhodoliths and coralligenous outcrops. External morphology matches the type material: erect, foliaceous sponge, 4-6 cm in height and 2-3 cm in width, having 3-4 foliaceous processes fused to the main body; bright orange-yellow in color; microhispid to the naked eye (Fig. 4.4.2A). Spicules are contoured oxeas (Fig. 4.4.2B), with stepped tips measuring 303-412-504/5-9-13 µm (minimum-mean-maximum length and width, respectively) in i695 and 261-420-528/6-9-12 µm in i760, and styles probably divided in two overlapping categories, small and thick and long and thin, overall measuring 240-480-1244/5-11-16 µm in i695 and 220-460-830/7-10-15 µm in i760. We could only get the minibarcode and the C1-C2 fragment of the 28S from specimen i695. The minibarcode shows no differences with the holotype and paratypes of *A. venusta* while 28S differed in 1 bp with the holotype, a minor difference that could underlie a population differentiation.

The type locality of *A. venusta* is a sandstone ridge at the Levantine Sea, where the species is very abundant and always associated to rocky substrates. However, at the seamounts of the Mallorca Channel the species seems to be rather scarce, being only found twice at the summit of the Emile Baudot. This may be explained by the differences in the water conditions, since the coast of Israel has higher temperature and salinity levels than the Balearic Islands (*Lavigne et al., 2015*). However, differences in *A. venusta* abundances can also be attributed to sampling bias. In fact, the species grows on rocky bottoms, a habitat not intensively sampled at the seamounts of the Mallorca Channel, in comparison with sedimentary bottoms (*Massutí et al., 2022*).

The lack of reports of the species in areas located between the type locality and the present report, in the most eastern and western part of the Mediterranean, respectively, may be explained by the low number of studies on benthic biota in mesophotic ecosystems of this sea. The present report remarks the important role of seamounts for biodiversity in the Mediterranean and highlights the need to keep exploring those habitats.

4.5. First documented report and barcoding of the sponge *Placospongia decorticans* (Hanitsch, 1895) in the North-Western Mediterranean

J. A. Díaz

Abstract

The demosponge Placospongia decorticans (Hanitsch, 1895) *is documented for first time in the North-Western Mediterranean. Patches of* P. decorticans *have been observed in marine caves in the island of Mallorca (Balearic Islands, Spain) and in the Gulf of Lion (La Ciotat and Marseille, France). The morphology of those specimens is studied in basis of micro and macroscopical characters using Scanning Electron Microscopy (SEM). In addition, the standard barcoding fragment (Cytochrome Oxidase subunit I) and the C1-C2 fragment of the nuclear 28S gen are provided. The results are compared with previous reports of the species in the Mediterranean and the North-Atlantic Ocean, whose characters are here summarized.*

Keywords DNA Barcoding, Porifera, Marine Diversity, Sea Caves

Introduction

The genus *Placospongia* Gray, 1867 (Family Placospongiidae), comprises 13 species of marine sponges distributed in tropical and temperate latitudes, found from the intertidal area to 80-90 m. Growth form varies from encrusting to branching and color from orange to reddish brown or tan. The genus is well characterized by the possession of a characteristic dermal crust of selenasters, forming polygonal and contractile plates separated by grooves. The choanosomal structure is composed by radial tracks of tylostiles emerging from a basal crust or a central axis (branching specimens) and supporting the plates. Other spicules that may be present are spherasters, amphiasters/streptasters, spirasters and microrhabds (*Hooper & Van Soest, 2002; Becking, 2013*).

In the North-west Atlantic and the Mediterranean Sea, all the records of the genus *Placospongia* belong to *Placospongia decorticans* (*Hanitsch, 1895*), a shallow water species commonly found at the intertidal zone (Table 4.5.1). The species was originally described off Portugal (Sines) and reported off the Canary Islands (Spain) and the West coast of Africa (Senegal), Cape Verde (*Van Soest, 1993*), the Tyrrhenian, the Adriatic, the Ionian, the Aegean and the Levantine Seas (Fig. 4.5.1).

The island of Mallorca (Balearic Islands, Spain) represents a poorly explored yet highly interesting spot for the sponge fauna (*Bibiloni & Gili, 1982; Bibiloni et al, 1989, 1998; Bibiloni, 1990, 1993; Santin et al., 2018; Díaz et al., 2020, 2021*). Here, marine caves of karstic nature are very abundant (*Ginés et al., 2013*). The caves are known to be a hotspot of sponge diversity, since sponges are good competitors in lack of light (*Gerovasileiou & Voultsiadou, 2012*). However, the sponge fauna from the caves of the Balearic Islands remains poorly known, and only a few works have focused on it

(*Bibiloni & Gili, 1982; Bibiloni et al., 1989; Vacelet & Uriz, 1991*). On the other side, marine caves of the Provence region have been widely studied and are known for their rich sponge repertoire (*Grenier et al, 2018*).

The aim of the present work is to document, for first time, the species in the North-Western Mediterranean and to provide a complete morphological description complemented by molecular barcoding of the Cytochrome oxygenase I (*COI*) and the subunits C1-C2 of the 28S. The morphological differences found between the north-western Mediterranean specimens and the published descriptions are also discussed.

Material and Methods

Sampling

Patches of *Placospongia decorticans* were found at several marine littoral caves off Balearic Islands (Spain) and the Provence region (France) (Table 4.5.1; Fig. 4.5.1)

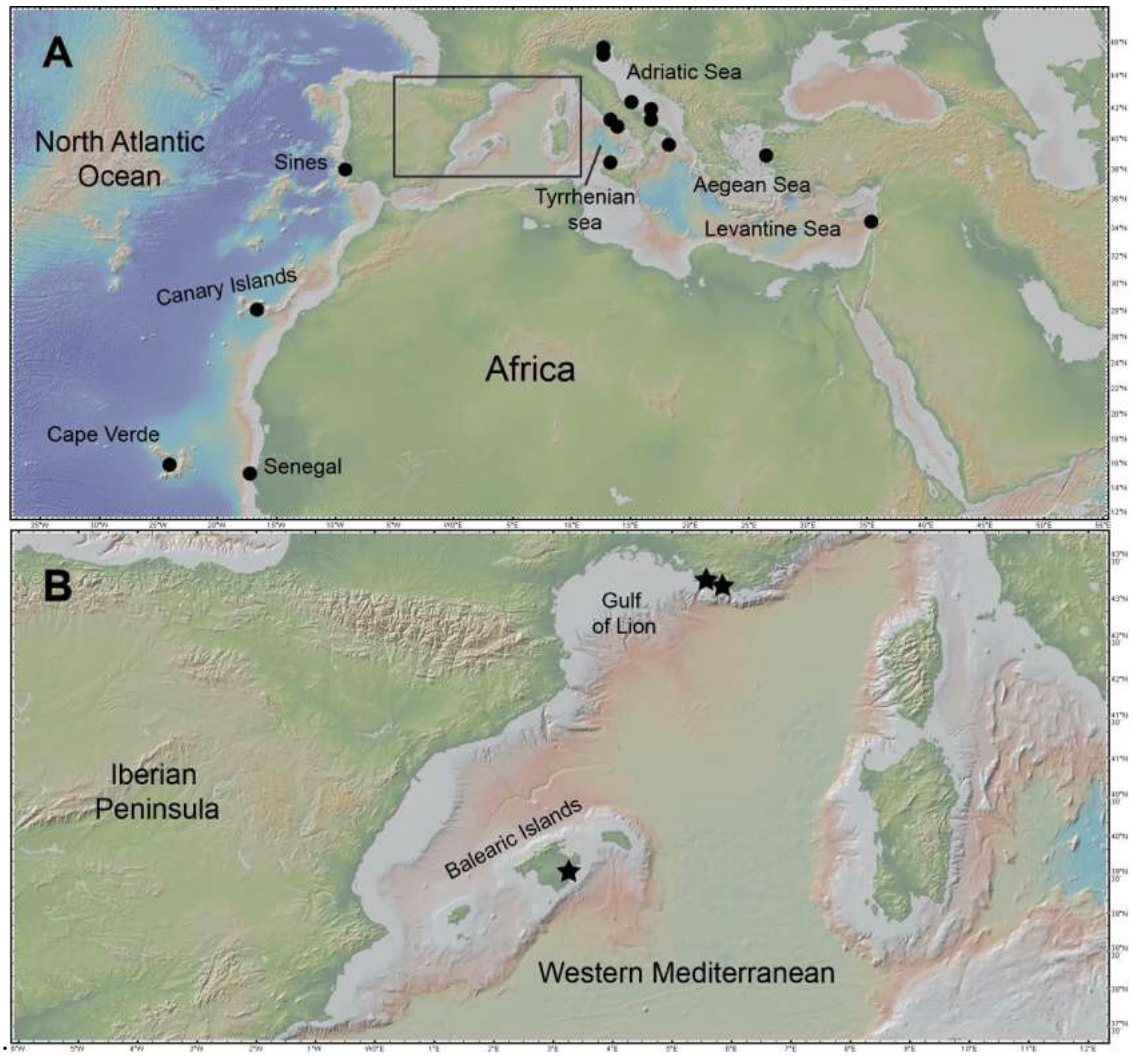

Fig. 4.5.1 (A) Map of the northwestern Atlantic Ocean showing previous reports of *Placospongia decorticans* (Hanitsch, 1895). (B) present reports of *P. decorticans* in the North-Western Mediterranean. Maps made with GeoMapApp v.3.6.15 (http://www.geomapapp.org).

For each location, a small fragment was collected by free apnea or scuba diving and stored in EtOH 96% or formaldehyde for posterior taxonomic and molecular analysis. *In situ* photographs were taken with an Olympus TG5 digital camera.

Morphological analysis

Phenotypic characters like morphology, color and texture were annotated prior to the sample conservation. To obtain dissociated spicules preparations and histological sections, all procedures were made by following standard methods (*Hooper, 2003*).

Spicules were observed with a Nikon S-Ke optical microscope and photographed with a CMOS digital camera. For each sample, 30 spicules per spicule class or category were counted. Thick sections of both tangential-surface and transversal-surface sections were made with a scalpel and, when necessary, dehydrated with alcohol and cleared with xylene. Cleared sections were re-hydrated with water, included in mounting media and observed with the microscope or a Leica M165C stereomicroscope. Aliquots of suspended spicules were transferred onto aluminum foil, air dried, sputter coated with gold and observed under a HITACHI S-3400N scanning electron microscope (SEM).

The terminology applied for the morphological description follows *Boury-Esnault & Rützler (1997)* and the systematics follow those of the World Porifera Database (de Voogd *et al.*, 2024).

Sponge specimens were deposited in the zoological collection at the Museum of Evolution, Uppsala University (Uppsala, Sweden) with UPSZMC#. The numbers of the author collection are referred as LIT#.

Results

Systematics

Class DEMOSPONGIAE *Sollas, 1885*

Subclass HETEROSCLEROMORPHA *Cárdenas, Perez and Boury-Esnault, 2012*

Order Clionaida *Morrow & Cárdenas, 2015*

Family Placospongiidae *Gray, 1867*

Genus *Placospongia Gray 1867*

***Placospongia decorticans* (*Hanitsch, 1895*)**

Material examined

Gulf of Lion (Western Mediterranean): Triperie Cave, (between Marseille and Cassis). One specimen. 43°12’ 12’’ N, 5° 27’ 04’’ E. Depth unknown. Collected June 9,1983. Collector: Jean-Georges Harmelin; Fauconiére cave (La Ciotat). Two specimens. 43° 09’ 18’’ N, 5°40’ 58’’ E. Depth 8 m. Collected June 3, 2009. Collector Jean Vacelet.

Balearic Islands (Mallorca): LIT09/UPSZMC190206 small cave, “Caló de’n Rafelino”. 39° 33’ 33’’ N, 3° 22’ 01’ E. Depth 0-0.2 m. Collected May 23, 2020. Collector J.A.

Díaz; LIT67/UPSZMC190207 “des Pilar” cave. 39° 29’ 26’’ N, 3° 17’ 50’’ E. Depth 0-0.2 m. Collected June 26, 2021. Collector J.A. Díaz; LIT70/UPSZMC190208 “Sa Merdera” cave. 39° 35’ 40’’ N, 3° 20’ 08’’ E. Depth 0-0.5 m. Collected July 17, 2021. Collector J.A. Díaz.

Macroscopic description (Fig. 4.5.2)

Encrusting patches, up to 0.5 mm in width and extending horizontally in an irregular way (Fig. 4.5.2, A-D). In life pale orange ectosome and bright orange choanosome.

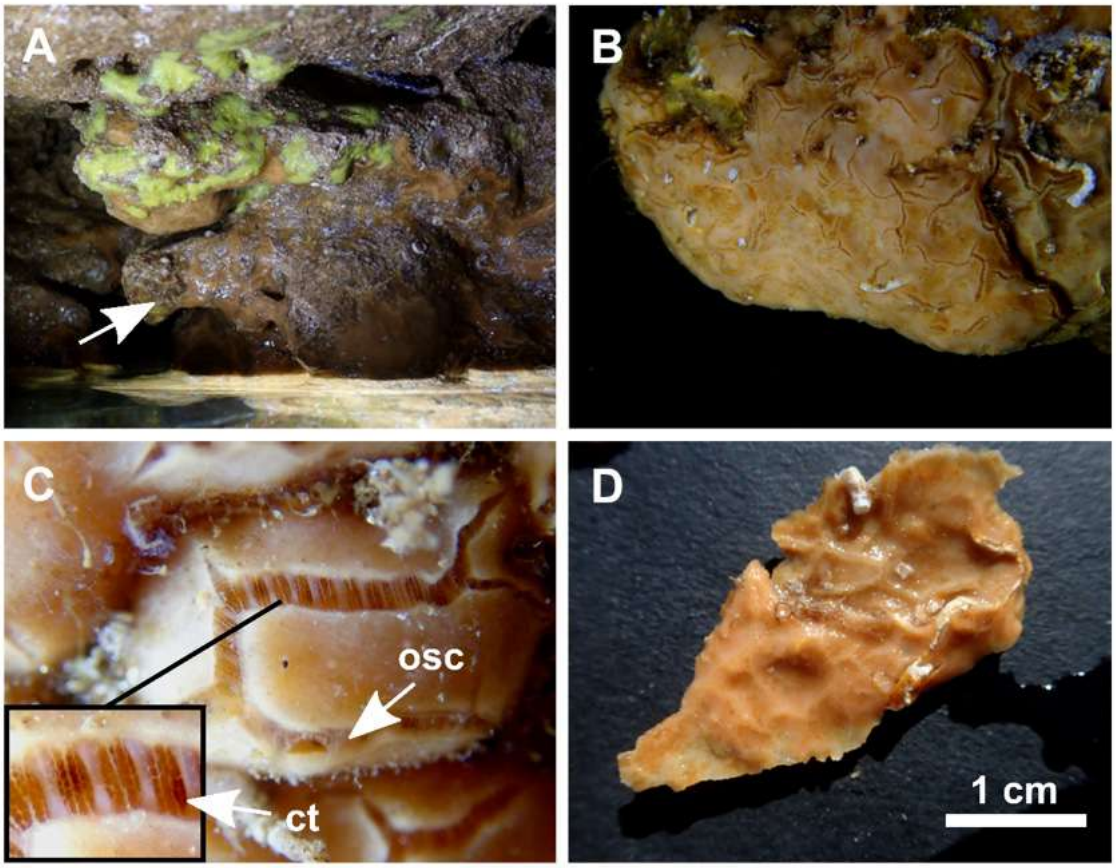

Fig. 4.5.2 (A) Portion of Lit09/UPSZMC190206 in the intertidal zone, exposed part. (B) Portion of Lit09/ UPSZMC190206 inside the water, submerged part. (C) Detail of the groove and plates of A (arrow). (D) Lit09/ UPSZMC190206 just after collection, with contracted plates. (P) *Placospongia decorticans*; osc, oscula; ct, connective tissue.

Both ectosome and choanosome turn beige after spirit. Smooth surface of a coriaceous consistency, divided into polygonal plates of a variable size, separated by grooves 2-3 mm width. Oscula (Fig. 4.5.2, C), circular, placed in the grooves and delimited by a translucid membrane. A system of organic filaments joins the plates, structured in two layers; an inner layer composed of wide filaments disposed regularly and perpendicular to the plates, and a second layer of thinner filaments drawing a circular mesh and placed upon the first (Fig. 4.5.2, C, detail). The patches were growing at the intertidal zone, with a large portion of its body outside the water (Fig. 4.5.2, A). The portion of the patch placed outside the water presents its patches contracted, while submerged parts are fully opened (Fig. 4.5.2C).

Spicules (Fig. 4.5.3)

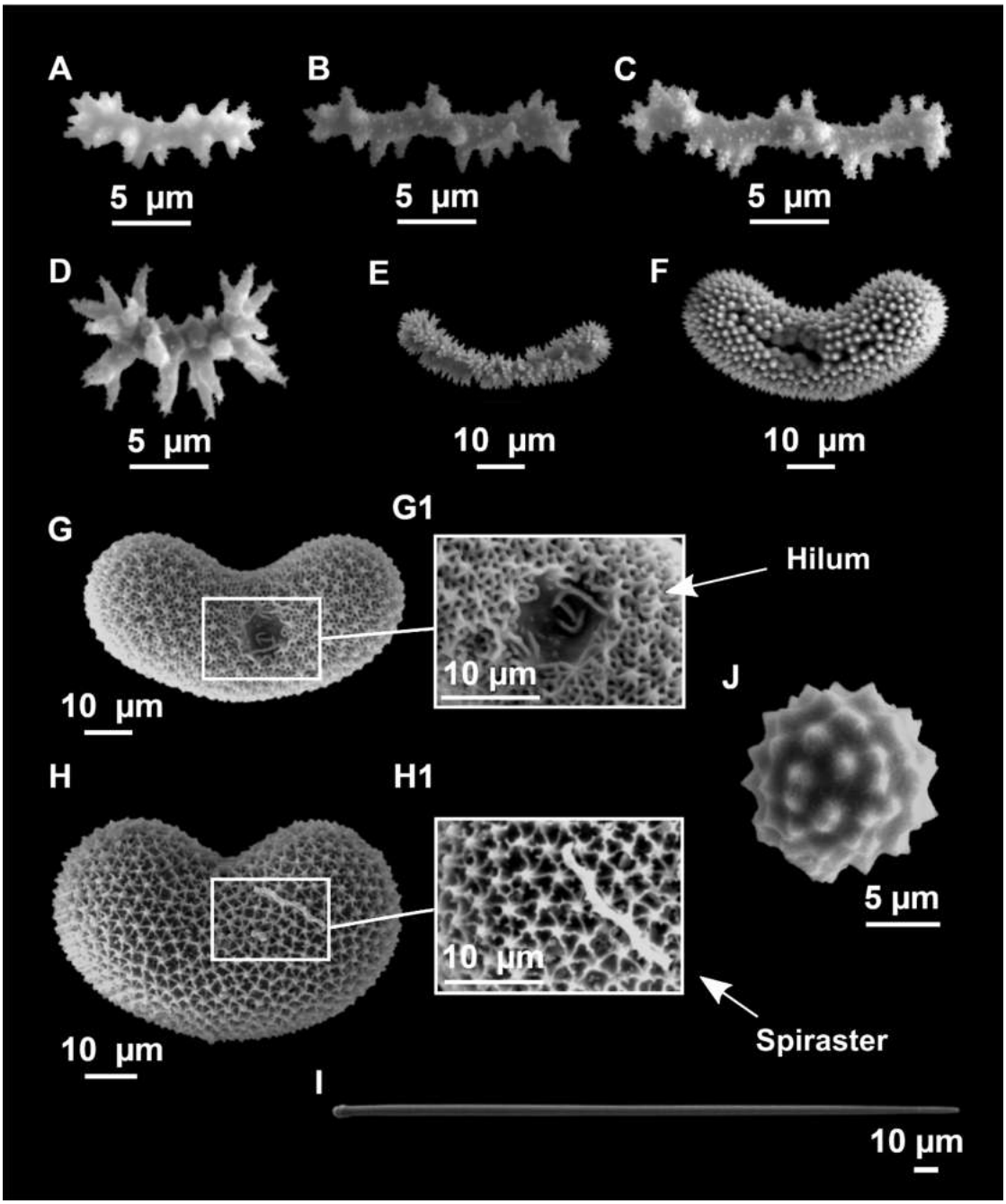

Fig. 4.5.3. SEM images of Placospongia decorticans (Hanitsch, 1895), specimen Lit09/UPSZMC190206. (A-C) Spirasters I. (D) Streptasters. (E-H) Different maturation stages of selenasters. (G1) detail of hilum of G. (H1) Detail of spines of mature selenasters. (J) spheraster. (I) tylostyle.

Spirasters, (Fig. 4.5.3A-C), with straight shafts, twisted twice in small and three times in longer forms. Thick rays, conical and disposed following the twist. Small spines distributed on shaft and rays. Measuring 10-20/1-4 µm.

Streptasters (Fig. 4.5.3D), uncommon. Twist starts independently from both ends, generating a symmetric, specular morphology. Rays disposed in the twist or aborted. Spines located on both rays and shaft. Measuring 8-22/2-6 µm.

Spherasters (Fig. 4.5.3J), with large centers and conical actines, measuring 6-20 µm.

Styles, tylostyles and subtylostyles (Fig. 4.5.3, I), not clearly divisible in categories, straight to slightly bent, with ovoid tips, measuring 184-537/4-16 µm.

Selenasters, beam shaped. Immature ones with underdeveloped spines free and sharp, (Fig. 4.5.3E) while conical in intermedium stages (Fig. 4.5.3F). In mature forms spines are joined with a septa, which generates a triangular pattern (Fig. 4.5.3G-G1, H-H1). Prominent hilum, circular in well-developed stages, twisted and elongated in immature ones. Mature selenasters measure 52-86/20-41 µm (chord/width).

Skeletal arrangement (Fig. 4.5.4)

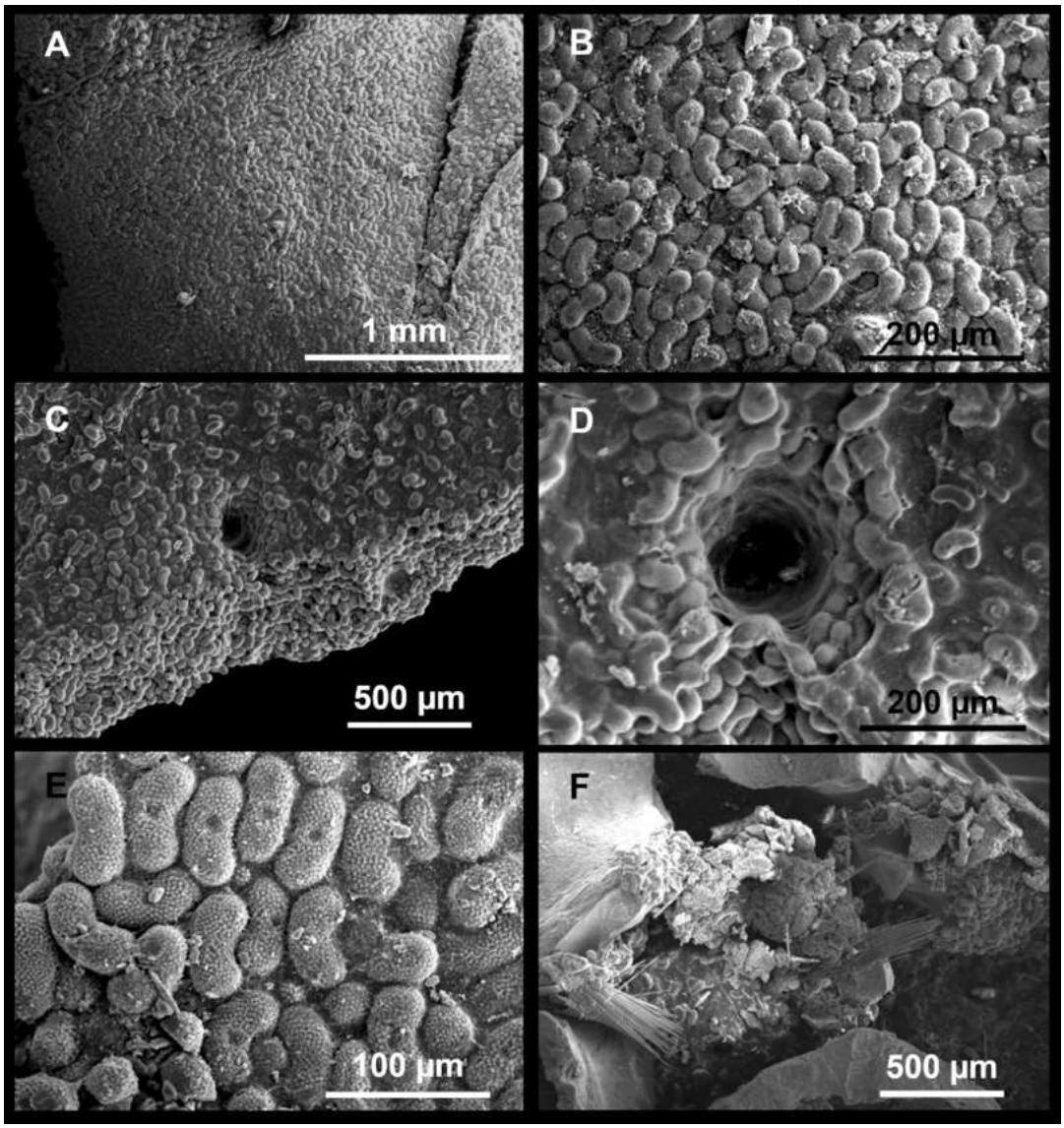

Fig. 4.5.4. Skeletal arrangement of *Placospongia decorticans* (Hanitsch, 1895) specimen Lit09/UPSZMC190206. (A-B) View of the ectosomal plates. (C-D) Ectosomal pore located in a plate. (E) Inner view of an ectosomal plate. (F) Choanosomal tracks of tylostyles emerging from the substrate.

Ectosomal plates composed by selenasters and spherasters tightly packed and cemented with a layer of connective tissue (Fig. 4.5.4A-E), the latter being much less abundant. Upon the plates there are the spirasters and streptasters, scattered here and there but without forming a distinguishable layer. Some circular pores are visible in the plates,

100 µm in diameter (Fig. 4.5.4C-D). Choanosome cavernous, with tracks of tylostyles running from the substrate towards the ectosomal plates (Fig. 4.5.4F). The tracks protrude the ectosome and are visible here and there under a tangential view. No microscleres were observed in the choanosome.

Genetics

Folmer COI (709 bp; OQ214203) and 28S (C1-C2) (382 bp; OQ211106) were obtained from specimen Lit09. The COI sequence shows 7-15 bp differences with the other *Placospongia* spp. sequences found at the Genbank while the short 28S fragment shows 1-2 bp differences with other published sequences.

Current Distribution and Ecology

This report extends the geographic location of the species, previously only known from the North Atlantic, the Tyrrhenian and the Eastern Mediterranean (Fig. 4.5.1, Table 4.5.1 and *Saritas, 1972*, *Corriero et al., 1997, 2000, Sarà, 1958b, 1961*). It has always been found in shallow water caves, reaching the intertidal zone. This may indicate a dependence of the species to freshwater inputs, which are known to be rich in silica, in a similar way that is observed by other sponge species (*Pisera & Gerovasileiou, 2021*).

Remarks

The characters of the specimens here reported match those from the literature with some exception (Table 4.5.1). *Lévi (1956)* reported much longer selenasters (300-360 µm), but this seems to be a mistake since the size range that he provides for the selenasters is the same as the styles (300-360 µm), which suggests a mistranscription of both spicules, moreover when considering that selenasters size is very conserved, falling in a much smaller range (≈50-83/20-41 µm). In the original description of the holotype (*Hanitsch, 1895*) and in Canary Island specimens (*Cruz, 2002*) a second category of spherasters is reported (spheraster II), a spicule that has no longer been found in any other specimen (Table 4.5.1). This could mean that those spicules are not always present in the species. Another explanation is that *Hanitsch (1985)* and *Cruz (2002)* confused the spherasters II with a sagittal view of the streptasters, which is plausible since the reported sizes of the spherasters II (16 µm and 10-12 µm) are in the size range of the streptasters (8-22 µm). A re-examination of the holotype (Hanitsch, 1895) and *Cruz (2002)* specimens should be necessary to clarify this point.

The streptasters found in the specimens here studied have never been reported in the past. Again, this may indicate that these spicules are not always present in the species or that its presence has been disregarded or confused with the spirasters. Streptasters are very uncommon and under optical microscope they look very similar to the spirasters. *Lendenfeld (1898)* pointed to differences in the spine number and length of the spirasters, similar to the differences in the spines between the spirasters and streptasters, a fact that suggest that streptasters were present on its specimen but confused with spirasters.

Table 4.5.1. Summary of the characters, depth, and location of the documented reports of *Placospongia decorticans* (Hanitsch, 1895) in the literature. Spicule measures are given as minimum-mean-maximum for total length/minimum-mean-maximum for total width. All measurements are expressed in µm. Specimens here measured are in bold. Specimen codes are the field codes of the author collection (Lit#) and UPSZMC# for the Uppsala University Museum of Evolution. n.r.: not reported; n.f.: not found.

Specimen	Tylostyle/ Subtylostyle/ Style	Selenasters	Spherasters I (large centre small rays)	Spherasters II (small centre long rays)	Spirasters	Streptasters	Cortex arrangement	Colour	Depth
Triperie cave, Gulf of Lion (Western Mediterranean)	318-375-427/6-9-11 (N=8)	52-65-74/20-26-32	9-12-15 (N=7)	n.f.	11-15-18/2-3-3	10-14/3-4 (N=2)	Not studied	Orange in life, pale beige in spirit	Shallow
Fauconière cave, Gulf of Lion (Western Mediterranean)	234-388-434/4-8-11 (N=10)	58-66-75/20-27-34	6-12-18	n.f.	10-13-17/2-2-3 (N=8)	10/4 (N=1)	Not studied	Orange in life, pale beige in spirit	8
Fauconière cave (Western Mediterranean) (labelled #1525)	268-365-417/6-8-11 (N=12)	58-66-78/16-23-29	8-12-15 (N=15)	n.f.	10-14-17/2-2-3 (N=7)	10/3 (N=1)	Not studied	Orange in life, pale beige in spirit	8
Lit09/UPSZMC190206 Balearic Islands (Western Mediterranean)	184-395-537/4-7-9	52-66-77/20-27-38	8-12-14	n.f.	11-15-19/1-2-2	8-13-22/2-3-3	Ectosomal plates of selenasters and spherasters I, with disperse spirasters laying upon it.	Orange in life, pale beige in spirit	0-0.2
Lit67/UPSZMC190207 Balearic Islands (Western Mediterranean)	283-363-494/6-10-13	64-75-86/28-36-41	12-15-20	n.f.	13-16-19/1-3-4	14/5 (N=1)	Not studied	Orange in life, yellowish white in spirit	0-0.2
Lit70/UPSZMC190208 Balearic Islands (Western Mediterranean)	252-383-449/7-11-16	65-77-83/28-33-39	7-14-18 (N=12)	n.f.	12-15-20/2-3-4	14-17-20/4-5-6 (N=7)	Not studied	Orange in life, yellowish white in spirit	0-0.5
Hanitsch, 1895 (holotype) Sines (North-East Atlantic)	510/8	80/28	12	16 (resembling streptasters)	14	No	Outermost part with spherasters I followed by a layer of spirasters and then selenasters.	Orange in life, pale beige in spirit	n.r.
Lendenfeld, 1898 Adriatic	400-540/4	67/30	Interpreted as young stages of selenasters. Size n.r.	n.r.	6-13/1	n.r.	Outermost part with spirasters followed by a layer of selenasters.	Brownish yellow	n.r.
Lévi 1956 Dakar (North-East Atlantic)	300-360/7	300-360/22-25	13-18	n.r.	15-25	n.r.	Outermost part with spirasters I and spherasters I followed by a layer of selenasters.	Ochre	n.r.
Pulitzer-Finali, 1983 Bari, Santa Maria di Leuca (Adriatic). Naples (Tyrrhenian)	160-540/5-8	55-75	10-14	n.r.	7-15	n.r.	n.r.	Brownish yellow	0.3-15
Labate 1964 Adriatic	550/10	55/20	size n.r.	n.r.	Size n.r.	n.r.	n.r.	Roseate	Intertidal zone
Rützler 1965 Adriatic	240-550/5-10	55-70	10-13	n.r.	10-15	n.r.	Outermost part with spirasters I and spherasters I followed by a layer of selenasters.	Dark Brown	Intertidal zone
Carteron (2002) Lebanon (Levantine Sea)	150-430/3-13	60-80	10-20	n.r.	8-27	No		Beige after alcohol	5
Cruz, 2002 Canary Islands (North-east Atlantic)	200-440	56-62/16-20	12-14	10-12	12-20	No	n.r.	Orange in life	Intertidal zone

Regarding the skeletal arrangement, the presence of a three-layered cortex described in the holotype hasn't been found here. Instead, spirasters and streptasters are very scarce, not conforming a distinguishable layer but being scattered upon the selenasters.

The morphological differences observed between the present specimens and those from the literature could reflect the presence of a species complex. Genetic connectivity in animals inhabiting marine caves tends to be limited, many having a strong genetic structure (*Padua et al., 2018*) and a tendency to endemism (*Culver & Pipan, 2009*). This could be more accentuated in sponges, yet the group is known for having low dispersal capabilities and strongly structured populations (*Shaffer et al., 2020*). In fact, *Nichols & Barnes, (2005)* explored the genetic structure of *Placospongia* sp. from Central America, Southeastern Asia, Australia and the Seychelles and concluded that morphology was not always correlated with the genetic diversity, and that cryptic lineages seems to occur in distant locations.

However, the observed differences could also be caused by ecological variations of the environment (e. g., nutrient availability, temperature, seasonality), facts that are known to determine the presence/absence of a given spicule or its size range (*Uriz et al., 2003a-b*). We have sequenced for the first time the COI and the C1-C2 28S fragment of one specimen, expecting that it would help further studies to clarify the correct relationship in *P. decorticans* populations.

Conclusion

The sponge *P. decorticans* is reported for the first time in the North-western Mediterranean. A detailed description of its skeletal elements revealed the presence of streptasters, a spicule never reported in the species and that may suggest the presence of a species complex. A specimen from the Balearic Islands has also been barcoded (COI and 28S). Future work should collect and sequence new material from the type locality and compare it with the Mediterranean to confirm or deny its conspecificity.

29

4.6. Sponge assemblages in fishing grounds and seamounts of the Balearic Islands (Western Mediterranean)

*Julio A. Díaz[1], Francesc Ordinas[1], M. Teresa Farriols[1], Camilo Melo-Aguilar[2] and Enric Massutí[1]
[1]Centre Oceanogràfic de les Balears (COB-IEO), CSIC, Moll de Ponent s/n, 07015 Palma, SPAIN.
[2]Universidad Complutense de Madrid, Dpto. de Física de la Tierra y Astrofísica, Pl. de las Ciencias, 1, 28040 Madrid

Abstract

The Balearic Archipelago (western Mediterranean) is an area of great ecological interest due to the combination of complex geomorphology, highly oligotrophic waters and low fishing pressure. Sponges play a key role in benthic habitats, providing structural complexity and significantly contributing to their diversity and biomass. Here, we present an insight into the sponge communities of this archipelago from the analysis of samples collected during several scientific research surveys carried out on bottom trawl fishing grounds around the Balearic Islands and on sedimentary and rocky bottoms of the Mallorca Channel seamounts. Sampling was carried out with experimental bottom trawl, beam trawl, rock dredge and remotely operated vehicle (ROV). We analyzed species presence/absence data using multivariate methods in order to identify assemblages. Once identified, we characterized their biodiversity, biomass and taxonomic composition. A dbRDA analysis was conducted to test the influence of environmental variables and fishing pressure on the sponge communities. Up to 350 species are reported: 220 at bottom trawl fishing grounds and 189 at seamounts. Communities were structured by depth, temperature, currents, substrate and fishing pressure with sponge presence/absense, biomass and diversity also linked to the presence of deep algae beds. Taxonomic composition differed between bottom trawl fishing grounds and the seamounts, where this fishing activity is almost negligible, pointing to different sensitivity to this fishing impact among the different orders, particularly for Tetractinellida, which was much more diverse and abundant at seamounts.

Keywords: Biodiversity, Sponge grounds, Porifera, Fishing pressure, Sponge communities

Introduction

Sponges are key components of worldwide benthic biocenosis, usually being main contributors to biomass and biodiversity (*Bell, 2008*; and references therein). They also provide several important ecosystem services like the enhancement of bottom structural complexity, providing shelter and nursery areas to crustaceans, mollusks and fish, and contributing to nutrient recycling (*Van Soest et al., 2012; Maldonado et al., 2017*). The role of sponges in maintaining some ecosystems has proved to be important at oligotrophic areas, like tropical reefs and the deep sea, and it is probably critical in some areas of the Mediterranean (*Maldonado et al., 2012; Rix et al., 2018; Bart et al., 2021*). At those ecosystems, sponges optimize the nutrient fluxes by feeding on dissolved organic matter, which is recycled for the food web in a process involving particulate organic matter release in form of fecal pellets, which are subsequently consumed by detritivores (*de Goeij et al., 2013*).

The Mediterranean is a highly studied area regarding sponge taxonomy (e.g. *Topsent, 1928; Vacelet., 1969; Pulitzer-Finali, 1983; Boury-Esnault, Pansini & Uriz., 1994*). It is considered a hotspot of diversity for this group (e.g. *Xavier & van Soest, 2012*; *van Soest et al. 2012*), with more than 700 reported species (*de Voogd et al., 2024*), a number that grows periodically with descriptions of new species and addition of new records (e.g. *Sitjà & Maldonado, 2014; Díaz et al., 2021*). However, studies focusing on the factors shaping sponge distribution and their communities are scarce. *Sarà (1962)* and *Boury-Esnault (1971)* emphasized the importance of depth and substrate orientation on the distribution of infralittoral sponges. *Uriz et al. (1992)* pointed out the importance of light irradiation in structuring infralittoral sponge communities in the oligotrophic waters of Cabrera, in the Balearic Islands. According to these authors, because light had a direct effect on algae growth, competition for the substrate between algae and sponges was higher in oligotrophic areas with clear waters. A similar conclusion was reached by *Kefalas (2003)*, who studied the circalittoral sponge communities of the Aegean Sea, finding light irradiation as the factor causing a markedly different distribution than in other areas with less transparent waters. Due to sampling limitations, less and more fragmentary information is available for deeper strata. Some of the available studies highlight substrate, sedimentation rate and currents as main factors in absence of photosynthesis, also pointing out the similarity of some deep sea communities with those of dark caves (*Vacelet, 1969, Vacelet et al., 1994*). *Pansini & Musso (1991)* conducted a large study on bottom trawl fishing grounds of the Ligurian Sea, down to a depth of 700 m, identifying 66 species, not finding any significant environmental factor determining sponge assemblages, but indicating that trawling could have a major impact in structuring soft bottom communities. Other studies highlighted the differentiation between sponge communities associated with deep-sea coral banks and soft bottom communities (*Longo et al., 2005; Calcinai et al., 2013*).

More recently, the improvement of sampling technologies and knowledge of seafloor topography fostered a growing interest in studying less accessible deep-sea habitats, like seamounts or canyons (*Morato et al., 2013; De la Torriente et al., 2018; Grinyo et al., 2018; Corbera et al., 2019; Bo et al., 2021; Massutí et al., 2022*), leading to the discovery of singular sponge communities, like keratose-dominated grounds in the Ligurian Sea (*Enrichetti et al., 2019*), diverse mesophotic grounds in the Levantine Sea (*Idan et al., 2018, 2021*) and a deep-sea lithistid reef in the Balearic Sea (*Maldonado et al., 2015*).

The aim of this work is to characterize the sponge communities of the Balearic Islands, including sedimentary and rocky bottoms of the circalittoral and bathyal domains in bottom trawl fishing grounds and seamounts. To do that, we have analyzed data and samples obtained with different sampling methods during several scientific research surveys.

Material and Methods

Study area

The Balearic Promontory (western Mediterranean) is composed of four main islands and several islets, channels and seamounts (*Acosta, 2003;* Fig. 4.6.1). It is characterized by clear waters, as a consequence of lack of river runoff, the scarcity of rain and the high distance from the Iberian Peninsula, where terrigenous-muddy sediments from river discharges are widely distributed. By contrast, the sand and gravel calcareous biogenic sediments predominate in the Balearic Islands (*Alonso et al., 1988*). These oceanographic characteristics allow light intensity to reach 0.05% of surface values as deep as 110 m, enabling the growth of seaweeds in most of the continental shelf of the Archipelago (*Canals and Ballesteros 1997*). As a consequence, benthic communities distribution and composition varies from that of the adjacent Iberian Peninsula and other Mediterranean areas (*Pérès and Picard, 1964, Ballesteros, 1994*).

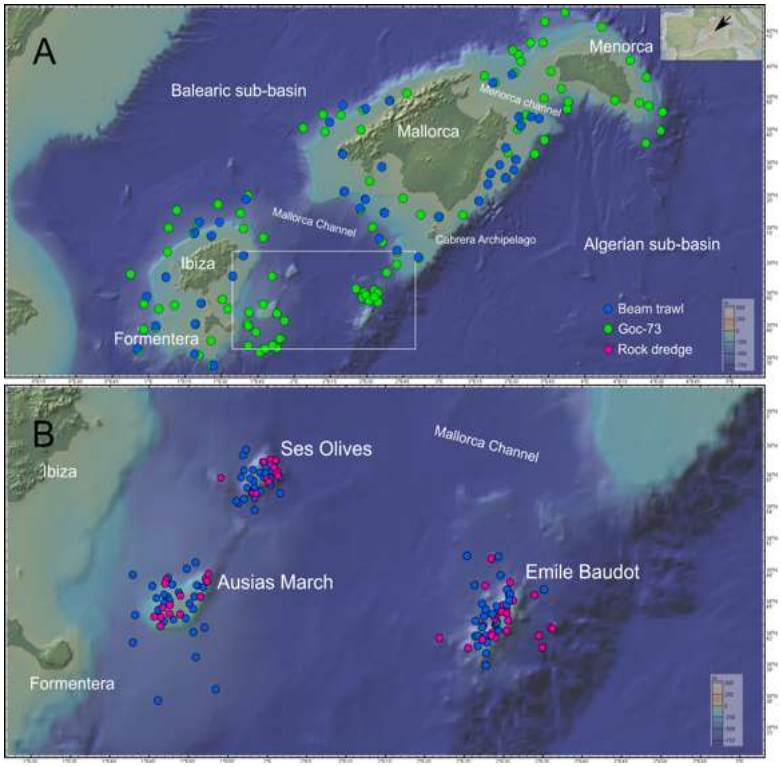

Figure 4.6.1. Maps of the studied area showing the location of the sampling stations. A: Trawl fishing grounds at sedimentary bottoms on the continental shelf and slope around the Balearic Islands; B: Mallorca Channel with the seamounts Ses Olives, Ausias March and Emile Baudot.

According to *Ordines and Massutí (2009)*, seaweed communities including maërl, *Peysonellia* spp., *Osmundaria vulubilis* and *Laminaria rodriguezii* beds predominate in the coastal shelf of the Balearic Islands, while sedimentary bottoms of the deep shelf and upper slope show some other habitats of interest, like crinoids beds. Despite the pronounced oligotrophy of this Archipelago, the red algae beds show high diversity and benthic productivity (*Ordines and Massutí, 2009*), being the sponges one of the main benthic groups associated to these algal communities (*Ordines et al., 2017*).
Two main channels are present in the Balearic Archipelago: the Menorca Channel, between the islands of Mallorca and Menorca, and the Mallorca Channel, between the Pitiusas Islands (Ibiza and Formentera) and Mallorca. These channels are situated

northern and southern of the Archipelago, being influenced by the oceanographic conditions of the Balearic and the Algerian sub-basins, respectively and playing an important role in the regional circulation, as passages for the exchange of water masses between them (*Massutí et al., 2014*; and references cited therein).

The Menorca Channel is characterized by having relatively shallow waters, a consequence of the continuity of the continental shelf between Mallorca and Menorca. It is influenced by atmospheric forcing (Monserrat et al., 2008; López-Jurado et al., 2008) and by the Balearic Current, which flows along the northern shelf margin and upper slope of the Balearic Promontory. This current, jointly with frontal meso-scale events between Mediterranean and Atlantic waters and input of old northern water into the channels, can acts as external fertilization mechanism that enhance productivity off the Balearic Islands (Pinot et al., 1995; Fernández de Puelles et al., 2004). This channel harbors rich and diverse benthic habitats (Grinyó et al., 2018) and hence in 2014 it was declared a Site of Community Importance (SCI), under the Natura 2000 framework.

The Mallorca Channel is a seaway composed of diverse geomorphological features, with an bathyal plain descending to 1050 m depth that separate the continental shelves of Mallorca-Menorca and Ibiza-Formentera. It is mainly affected by density gradients and the warmer and less saline Atlantic waters (Monserrat et al., 2008; López-Jurado et al., 2008) and the trophic webs of the deep-water ecosystems are supported more by plankton biomass than by benthic productivity (Maynou and Cartes, 2000; Cartes et al., 2001). At the southern part of the Mallorca Channel there are three seamounts: Ses Olives and Ausias March of orogenic origin, and the Emile Baudot of volcanic origin. These seamounts have been recently studied, within the LIFE IP INTEMARES project (https://intemares.es/en) and the first results have mapped their geomorphological features showing a high diversity of species, especially benthic filter feeders like sponges, and habitats of special interest for conservation, including coralligenous outcrops and maërl beds at summits, deep-sea coral reefs at rocky escarpments and *Isidella elongata* and pockmarks fields on sedimentary bathyal bottoms (*Massutí et al., 2022*).

Historically, the number of trawl fishing boats has remained very low in the Balearic Islands, compared to other areas of the Mediterranean coast of the Iberian Peninsula (*Quetglas et al., 2012*). According to these authors, the number of vessels per potential fishing ground surface, as a simple indicator of the fishing effort exerted, is one order of magnitude lower in the Balearic Islands than in the adjacent Peninsula coast. In the Archipelago bottom trawling is conducted on the shelf and slope (from 50 to about 750 m depth), with the upper bathymetric limit delimited by the end of *Posidonia oceanica* meadows. However, fishing grounds between 50 and 100 m depth can overlap with red algae beds, which explains the high quantity of algae and benthic invertebrates in the discards of this fleet (*Ordines et al., 2006*). Some demersal fisheries are developed in the Mallorca Channel, mainly focused on the deep water decapod crustaceans shrimp (*Ariesteus antennaus*) and the pandalid shrimp *Plesionika edwardsi* using bottom trawl in the adjacent bottoms of SO and AM and traps at the flanks and summits of the three seamounts, respectively (*Massutí et al., 2022*).

Sampling

Samples were collected during 12 oceanographic research surveys carried out from 2016 to 2021 in two main areas of the Balearic Islands: trawl fishing grounds on sedimentary bottoms of the continental shelf and upper and middle slope around the Balearic Islands, and the seamounts Emile Baudot (EB), Ausias March (AM) and Ses Olives (SO) at the Mallorca Channel (Fig. 4.6.1). These surveys were developed within the MEDITS (6 annual surveys from 2016 to 2021) and the Marine Strategy Framework (MSF; one survey in 2021) programs and the LIFE IP INTEMARES project (4 surveys in seamounts from 2018 to 2020 and one survey in Menorca Channel in 2019). The bathymetric ranges were 50-758 m depth at trawl fishing grounds and 89-1169 m depth at seamounts and surrounding areas.

Trawl fishing grounds were sampled by a Jennings type beam trawl (BT), designed to collect epi-benthos (*Jennings et al., 1999*) whose efficiency has been estimated by *Reiss et al. (2006)*, and the experimental bottom trawl GOC-73 (GOC), a sampling device widely used in MEDITS surveys along the northern Mediterranean, to estimate the abundance and distribution of demersal resources and the impact of the fishing activity on benthic ecosystems (*Spedicato et al., 2019*). Sampling at the seamounts used the same BT for sedimentary bottoms and a rock dredge (RD) for rocky bottoms. The Remotely Operated Vehicle (ROV) *Liropus* 2000 was also used to collect samples and images at the seamounts. More details of these surveys and sampling stations can be found in Table 4.6.1.

The BT has horizontal and vertical openings of 2 and 0.5 m, respectively, and a cod-end mesh size of 5 mm. Sampling was conducted at 2 knots, with an effective sampling duration between 5 and 15 minutes depending on depth. The GOC has horizontal and vertical net openings ranging 18–22 and 2.5-3 m, respectively, and a cod-end mesh size of 10 mm. Sampling was conducted at 2.8-3.0 knots, with an effective sampling duration between 20 and 60 minutes depending on depth. The RD is composed of a rectangular metallic frame with beveled edges, equipped with a 10 mm mesh cod-end, protected by another net of 20 mm meshes and leather covers on bottom and top sides. It was trawled in an upward direction over the seafloor at 0.5-1 knots, during 5 to 10 minutes.

There are significant differences in the catch efficiency and sampled surface between GOC, RD and BT devices. The BT is the most efficient one regarding benthic species, resulting in higher biomasses, while GOC is less efficient but sweeps much larger areas than the BT: 40000-120000 *vs* 370-1900 m^2, respectively depending on depth. The surface sampled using the RD is difficult to estimate and it is specially misleading at rocky slopes, with high inclination such as those of the seamounts, whereas its efficiency largely depends on the nature of the rocky bottom and the capability of the dredge to pull off it.

Once samples were on deck, all the specimens were identified to the lowest taxonomic level by examining macroscopical and microscopical characters. Specimens that could not be identified on board were stored for further analyses in the laboratory, including the use of molecular markers (COI and 28S). Part of the taxonomic work has already been published (*Díaz et al., 2020, 2021*). After identification, wet biomass was weighted, and the number of individuals and/or fragments (for non-encrusting species) annotated.

Table 4.6.1. Summary of the sampling used in the present study, indicating the research survey, the sampling area (trawl fishing grounds) and sampling device (RD: rock dredge; BT: beam trawl; GOC: the experimental bottom trawl GOC), as well as the stations analyzed in each survey and the number and percentages of samples with and without sponges by bathymetric range (50-90, 91-200 and 201-1000 m), corresponding to euphotic, mesophotic and aphotic Zones, respectively. During the INTEMARESA22B0720 survey, 37 stations with ROV were also developed along the whole bathymetric range. n.s.: bathymetric range not sampled.

Survey	Area	Device	Stations with sponges				Stations without sponges				TOTAL
			50-90	91-200	201-1000	Total	50-90	91-200	201-1000	Total	
trawl fishing grounds											
MEDITS 2016	Mallorca-Menorca	GOC	16	10	4	30	0	7	14	21	51
MEDITS 2017	Mallorca-Menorca	GOC	18	11	2	31	0	5	15	20	51
MEDITS 2018	Mallorca-Menorca	GOC	17	7	3	27	0	10	14	24	51
MEDITS 2019	Mallorca-Menorca	GOC	17	8	5	30	0	8	12	20	50
MEDITS 2020	Mallorca-Menorca	GOC	18	10	7	35	0	6	14	20	55
MEDITS 2021	Mallorca-Menorca	GOC	22	6	6	34	0	9	18	27	61
MEDITS 2021	Ibiza-Formentera	GOC	7	6	5	18	0	1	16	17	35
CIRCALEBA1121	Balearic Islands	BT	21	5	7	33	0	4	5	9	42
INTEMARES-A4	Menorca Channel	BT	43	n.s.	n.s.	43	0	n.s.	n.s.	n.s.	43
	Sub-Total	**Sum**	179	63	39	281	0	50	108	158	439
		%	100	56	27	64	0	44	73	36	
Seamounts											
INTEMARES-A22B0718	Mallorca Channel	BT	n.s.	7	4	11	n.s.	0	6	6	17
		RD	n.s.	6	3	9	n.s.	0	0	0	9
INTEMARES-A22B1019	Mallorca Channel	BT	n.s.	13	29	42	n.s.	0	3	3	45
		RD	n.s.	5	9	14	n.s.	0	1	1	15
		GOC	n.s.	n.s.	10	10	n.s.	0	8	8	18
INTEMARES-A22B0720	Mallorca Channel	BT	n.s.	6	16	22	n.s.	0	1	1	23
		RD	n.s.	9	12	21	n.s.	0	3	3	24
	Sub-Total	**Sum**	0	46	83	130	0	0	22	22	151
		%	n.s.	100	79	86	n.s.	0	21	15	
Total			179	109	122	410	0	50	130	180	590

Data analysis

The first three MEDITS surveys (2016-2018) and the first INTEMARES (2018) survey were used only for taxonomic purposes, while biomass and abundances were also annotated for the rest of surveys: MEDITS from 2019 to 2021, CIRCA-LEBA-1121 (MSF) and INTEMARES from 2019 to 2020 (Table 4.6.1).

In the case of GOC, biomass data was standardized to surface using the SCANMAR or MARPORT systems to determine the arrival and departure of the net to the bottom and its horizontal opening, and the distance covered in each haul. This method was also applied to standardize BT data, but using the width of the beam as horizontal opening. The data was then transformed to presence/absence for multivariate analyses purposes. RD data was also transformed to presence absence to be used in the multivariate analyses, but could not be standardized due to the difficulties to estimate the effective sampled surface. No ROV data was used in multivariate analyses. Faunistic lists were elaborated using the data collected from all surveys since 2016 and using all gears and ROV.

With the Primer 6 software (Primer, Plymouth, UK) we carried out independent multivariate analyses for GOC and BT samples collected from trawl fishing grounds, and BT and RD collected from seamounts. These analyses included a Cluster Analysis to detect assemblages and a Similarity Percentage Analysis (SIMPER; Clarke and Warwick, 1994), as well as number of species and biomass to describe them. To do so, the Sørensen-Dice coefficient was used to calculate a between-sample similarity matrix from biomass data previously transformed into presence/absence. Then samples were linked into clusters using the Unweighted Pair-Group Method with Arithmetic Mean. The resulting dendrogram was analyzed to detect significantly different groups using the Similarity Profile Routine test (SIMPROF; *Clarke et al., 2008*). These groups detected were considered assemblages. Then, SIMPER analysis was used to identify the most important species contributing to within group similarity. The total and mean species richness (S) and the mean standardized biomass of both sponges and algae (in terms of grams per 100 m^2) were also estimated by each assemblage, except for those exclusively composed of samples from RD, in which it was not possible to estimate the standardized biomass, due to the low efficiency of this gear and the impossibility to calculate the surface effectively sampled. The S was estimated for each seamount separately, as well as for all seamounts together and the trawl fishing grounds. Rarefaction species curves were calculated for seamounts and trawl fishing grounds, and in trawl fishing grounds also for each sampling method (GOC and BT).

We also investigated the taxonomic composition of the assemblages. To do that, we have calculated the number of orders and the number of species per order in seamounts and trawl fishing grounds, and for each of the assemblages detected.

Environmental and fishing conditions

To characterize oceanographic variables, the outputs of the WMOP (Western Mediterranean Operational forecasting system) model, available in the Balearic Islands Coastal Observing and Forecasting System (SOCIB from its acronym in Spanish) have been considered (*Tintoré et al., 2013*): https://www.socib.es/?seccion=modelling&facility=forecast_system_description.

WMOP is a high-resolution (2.6 km) 3D ROMS (Regional Ocean Modeling System) model, implemented in the western Mediterranean with a daily temporal resolution (Juza et al., 2016, Mourre et al., 2018). Values of water temperature and irradiance above the bottom, speed and direction of bottom currents and chlorophyll a concentration at the surface, as a proxy of primary production, were obtained by each of the sampling station during the period 2016-2021.

The EMODNET (European Marine Observation and Data Network) broad-scale seabed habitat map for Europe (EUSEaMap) has been used for benthic habitat characterization: https://emodnet.ec.europa.eu/en/seabed-habitats. The EUSeaMap includes several seafloor habitat classifications (Vasquez et al., 2021). For the present study, the kind of substrate included in this database has been used. In the Mallorca Channel seamounts, the habitat type of some sampling stations was checked according to the more accurate mapping of the seafloor recently obtained by the INTEMARES project (Massutí et al., 2022). Finally, due to the low concordance between the observations from scientific surveys and EMODNET data, samples from Mallorca Channel were also assigned to a nominal explanatory variable, but with only two categories: Rocky vs. Sedimentary bottoms.

In addition to the seafloor type, it has also been taken into account as an environmental variable, the density of rhodoliths-forming species and total algae, estimated during the same surveys as the sponge assemblages studied. The rhodoliths-forming species are considered as bioengineers (*Foster, 2001; Nelson, 2009; Teichert, 2014*). For each BT and GOC stations, the standardized rhodoliths and total algae biomass (g/100 m2) was estimated. For the seamounts this variable was not included in the analysis because at seamounts we included stations sampled with RD, a sampling device not apropiate for biomasse estimations.

The fishing effort of the bottom trawl fleet was estimated from information collected by the Vessel Monitoring System (VMS). These data are available since 2006 and consist of position and instantaneous velocity that each fishing vessel sends automatically via satellite communications every two hours. VMS signals generated during navigation were excluded from the analyses, by considering only those signals with instantaneous velocities ranging from 2 to 3.6 knots, which is the towing speed used by trawlers in the area. This information has been used to model the geographic distribution of bottom trawl fishing effort in the area and to estimate the fishing effort by fishing ground (*Farriols et al., 2017; Guijarro et al., 2020*). Each sampling station on the continental shelf and slope around the Balearic Islands was associated to a bottom trawl fishing ground and consequently to its fishing effort. The fishing effort represents the annual number of fishing trips that the fleet works in each fishing ground in the year in which each sampling station was surveyed.

There is no bottom trawling on the summits, flanks and nearby bottoms around the Mallorca Channel seamounts (*Massutí et al., 2022*), where the sampling effort was concentrated. In this area, bottom trawling is only carried out at three fishing grounds on adjacent sedimentary bottoms located at a certain distance from the seamounts, which show a similar fishing effort (Massutí et al., 2022). Therefore, in this area fishing effort

has been considered as a quantitative explanatory variable, assigning sampling stations to two categories: Not Trawling vs. Trawling.

Relationships with environmental parameters

A distance-based-Redundancy Analysis(dbRDA), available in the CANOCO 5.1 package (*ter Braak and Smilauer, 2018*), was used to model the effect of environmental and fishing variables on the distribution of sponge species. Unlike multivariate indirect gradient analyses, canonical analyses such as RDA provide the means for conducting direct explanatory analyses in which the association among species can be studied with respect to their common and unique relationships with environmental variables *(Peres-Neto et al., 2006*). In dbRDA, case scores, obtained by a principal coordinate analysis (PCO) of a distance matrix, are further constrained by explanatory variables using RDA (*Legendre and Anderson, 1999*). Dependent variables were presence/absence of sponge species, while depth (m) and the environmental and fishing variables explained above (see Section Environmental and fishing conditions) were included in the RDA as continuous (temperature, irradiance, speed and direction of currents, chlorophyll a concentration, rhodoliths and total algae biomass and fishing effort on the Balearic Islands bottom fishing grounds) or nominal/categorical (seafloor type on the Balearic Islands bottom trawl fishing grounds, and rocky vs. sedimentary and trawling or not trawling in the Mallorca channel seamounts) explanatory variables. The distance matrix was conducted using the Bray-Curtis distance for presence/absence data.

The explanatory variables included in the db-RDA were selected by means of a protected forward selection (*Blanchet et al. 2008; ter Braak and Smilauer, 2018*) and the correlation between them was checked with the inflation factor, the Variance Inflation Factor of a variable in a multiple regression equation (*Montgomery and Peck 1982*). The effect of each variable was tested using partial dbRDA models, which allow the effect of a particular explanatory variable to be analyzed after the rest of the variables have been set as covariables (variables that are fitted to the species data before the ordination, which is carried out afterwards using only the residual variation). The significance of the models was assessed using the Monte Carlo permutation-based test (*Manly, 1991*).

Results

Sponges were found in 69% of the 590 stations sampled with GOC, BT and RD, in 85% of the 151 stations sampled in seamounts and in 64% of the 439 stations sampled in trawl fishing grounds (Table 4.6.1). Sponges appeared in all the 37 ROV transects carried out in seamounts. Species accumulation curves from both seamounts and trawl fishing ground showed similar tendencies, being close to plateau, which indicates that a large fraction of the sponge diversity has been sampled and documented (Fig. 4.6.2).

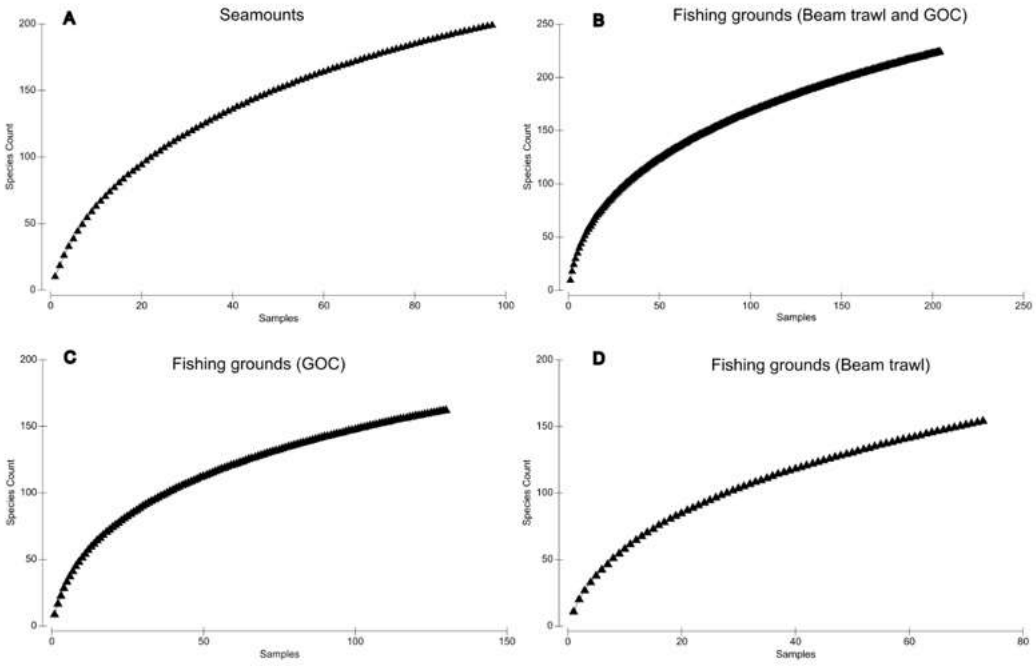

Figure 4.6.2. Species accumulation curves for the Seamounts (A) and fishing grounds (B-D). Graphs B-C shows the accumulation curves obtained with the different sampling methods on the fishing grounds (beam trawl and GOC), while graph D shows the accumulation curve for the total of species of the fishing grounds, including both sampling methods.

Sponge diversity

A total of 2800 samples were collected and kept in the authors collection in the Centre Oceanogràfic de les Balears, while some specimens have been deposited in the Marine Fauna Collectionbased at the Centro Oceanográfico de Málaga (Instituto Español de Oceanografía) and at the Museum of Evolution, Uppsala University (Uppsala, Sweden). So far, 350 species or taxa were identified: 189 at seamounts and 220 at trawl fishing grounds (Annex Table S4.6.1). Of those, only 61 were shared between both areas. The most diverse seamount was EB (S= 140 species or taxa), followed by AM (S= 111) and SO (S= 36) seamounts.

The species *Timea chondrilloides, Forcepia (Leptolabis) luciensis* and *Callyspongia septimaniensis* are new records for the Balearic Islands, although *C. septimaniensis* may have been reported by Bibiloni (1990) under the name of *Adocia simulans* (Johnston, 1842). Taxa not identified to the species level will be described on taxonomic articles elsewhere (Diaz et al., in prep.). At trawl fishing grounds, *Haliclona* sp3, *Suberites domuncula, Haliclona (Reniera) mediterranea* and *Lissodendoryx (Lissodendoryx) cavernosa* were the most frequent species, collected in 95 (33%), 88 (31%), 72 (25%) and 63 (22%) stations, respectively, while *Phorbas tenacior, Myxilla (Myxylla) iotrochotina*, *Haliclona (Reniera) mediterranea* and *Haliclona* sp3 were the species with more biomass. At seamounts, *Thenea muricata, Poecillastra compressa, Desmacella inornata* and *Foraminospongia balearica* were the most frequent species, being present in 41 (33%), 40 (32%), 36 (29%) and 28 (22%) stations, respectively, while *Hexadella* sp1, *Haliclona (Halichoclona)* sp. and *Geodia sp1* were the species with more biomass.

Sponge assemblages

We obtained three different dendrograms: one for the seamounts, resulting from the analyses of BT and RD samples (Fig. 4.6.3 and Table 4.6.2) and two for the trawl fishing grounds, one resulting from the analyses of GOC samples (Fig. 4.6.4 and Table 4.6.3) and other resulting from the analysis of BT samples (Fig. 4.6.5 and Table 4.6.4). The maps showing the distribution of assemblages in each dendogram are shown in Figure 4.6.6.

Seamounts

Dendrogram showed 6 different clusters (Fig. 4.6.3). Shallow summits of the AM and the EB seamounts (94-193 m) formed a main group that was subdivided in two groups corresponding to sedimentary assemblages (sB and sC), which clustered together, and a rocky group (sD). The other three groups were deeper (151 -740 m), found in SO, AM and EB seamounts (assemblages sA, sE and sF).

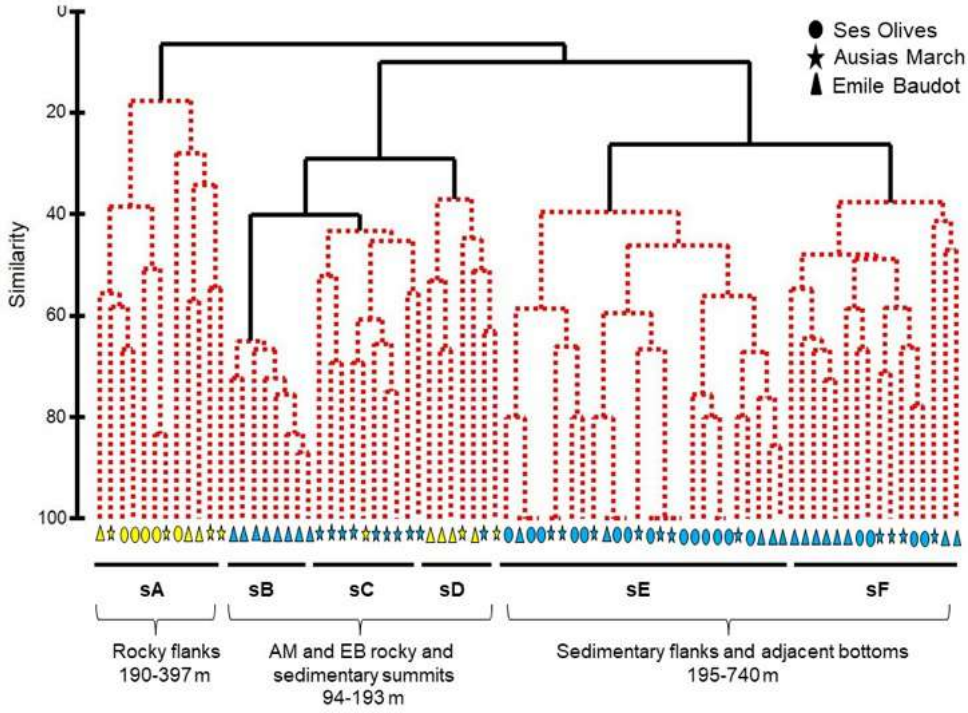

Figure 4.6.3. Dendrogram of seamounts assemblages identified from cluster analysis. Statistically significant groups are defined by the SIMPROF test and illustrated by discontinuous red lines. Samples are represented in circles (Ses Olives), triangles (Emile Baudot) and stars (Ausias March). Color represents the sampling device used in each station, with yellow indicating rock dredge and blue indicating beam trawl. Depth range, zone and bottom type are indicated by each cluster.

Within the shallower assemblages, sC (97-135 m depth) was composed of samples from sedimentary bottoms (with the exception of one rocky station) at AM seamount. It showed high values of total and mean S (70 and 16.9±1.9 species, respectively) and the highest mean sponge and algae biomass (1342±840 g/100m^2 and 4042±8178 g/100m^2, respectively) of the seamounts (Table 4.6.2), with the second highest sponge biomass value on a single station of all the study (7685 g/100m^2). This group was characterized by *P. compressa*, *F. balearica*, *Calcarea* sp6 and *Hexadella* sp1 (Table 4.6.5; Fig. 4.6.7A and 7B). The group sB (141-154 m depth) was composed exclusively of sedimentary

bottoms at EB seamount. This was the most diverse group of the seamounts, with total and mean *S* values of 71 and 30.6±2.7 species, respectively, and it also showed high sponge biomass, with a mean value of 771±189.8 g/100m^2, but low algae biomass (Table 4.6.2). This group contained the station with more species of all the study, with up to 42 species and a biomass of 1843 g/100m^2. It was characterized by *P. compressa*, *Hemiasterella elongata*, *Penares helleri* and *Chelonaplysilla* sp. (Table 4.6.5; Fig. 4.6.7C-7E). The group sD (94-193 m depth) was composed of stations located in rocky bottoms (except one which was sedimentary) from AM and EB seamounts. Their total and mean S values were also high, up to 69 and 18.4±2.7 species, respectively (Table 4.6.2), but biomass could not be estimated because all samples were collected using RD, except one using BT with 19.8 g/100m^2 of sponge biomass. This group was characterized by *Spongosorites* sp1, *Haliclona poecillastroides*, *F. balearica* and *Polymastia* sp3 (Table 4.6.5; Fig. 4.6.7F and 7G).

Within the deeper assemblages, sA (151-458 m depth) was composed by stations in rocky bottoms, showing total and mean S values of 31 and 5.4±0.5 species, respectively. No biomass values were estimated for this group as it only contains samples collected with RD (Table 4.6.2). This group was characterized by *Jaspis* sp2, *Heteroxya* cf. *beauforti*, *Hamacantha* (*Hamacantha*) sp2 and *P. compressa* (Table 4.6.5; Fig. 4.6.7H and 7I). The group sF (195-511 m depth) was composed of samples collected at the SO summit and sedimentary bottoms of the flanks of the three seamounts. It showed low total and mean S values (55 and 12.3±(1.3) species, respectively) and relatively low mean biomass (25.9±7.7 g/100m^2; Table 4.6.2). It was characterized by *P. compressa*, *D. inornata*, *T. muricata*, *Hamacantha* (*Hamacantha*) sp1, *Dragmatella aberrans* and *Desmacella annexa* (Table 4.6.5). The group sE (278-740 m depth) was composed of samples collected at sedimentary bottoms of all seamounts. It showed low total and mean S values (20 and 3.4±(0.4) species, respectively) and a mean biomass of 8.26±6.5 g/100m^2 (Table 4.6.2). It was characterized by *T. muricata*, *D. innornata* and *D. annexa* (Table 4.6.5).

Trawl Fishing grounds

Both GOC (Fig. 4.6.4) and BT (Fig. 4.6.5) based dendrograms showed two main groups, one with coastal shelf groups (45-93 m) and the other with deep shelf to middle slope groups

Table 4.6.2. Summary of results by each sponge assemblage detected at seamounts. Depth, mean and total species richness (Smean and Stotal), sponge biomass (Bmean) and algae biomass (Bamean) are expressed in terms of mean value (±standard error) and range values (minimum-maximum). Biomass values are only given for stations sampled with beam trawl and expressed in g/100 m2. The total values of S, as well as the sampling devices (BT: beam trawl; RD: rock dredge) are also shown.

Assemblage	N	Substrate	Device	Depth (m)	S_{mean}	S_{total}	B_{mean}	Ba_{mean}
sB	8	Sedimentary	BT	148±1.2 (141-154)	30.6±2.7 (20-42)	71	771.7±189.8 (94-1843)	26±43 (0-130)
sC	9	Mostly Sedimentary	BT/RD	115±3.9 (97-135)	16.9±1.9 (9-30)	70	1342.3±839.8 (17-7684)	4042±8178 (0-24151)
sD	7	Mostly rocky	BT/RD	117±8.1 (94-193)	18.4±2.7 (10-26)	69	19.77*	2756*
sE	26	Sedimentary	BT	513±31.0 (278-740)	3.4±0.4 (1-8)	20	8.3±6.5 (0.01-169)	--
sF	16	Sedimentary	BT	338±24.0 (195-511)	12.3±1.3 (4-22)	55	25.9±7.7 (1.8-90)	--
sA	12	Rocky	RD	277±15.6 (191-397)	5.4±0.5 (3-9)	31	--	--
Total	78	--	BT/RD	--	14.5±1.1 (1-42)	185	433.6±78.0 (0.01-7684)	2275±483.3 (0-24151)

*The value corresponds to the only station sampled with beam trawl at that assemblage.

(106-750 m). Coastal shelf stations showed diverse types of algae assemblages, being dominated by red algae beds.

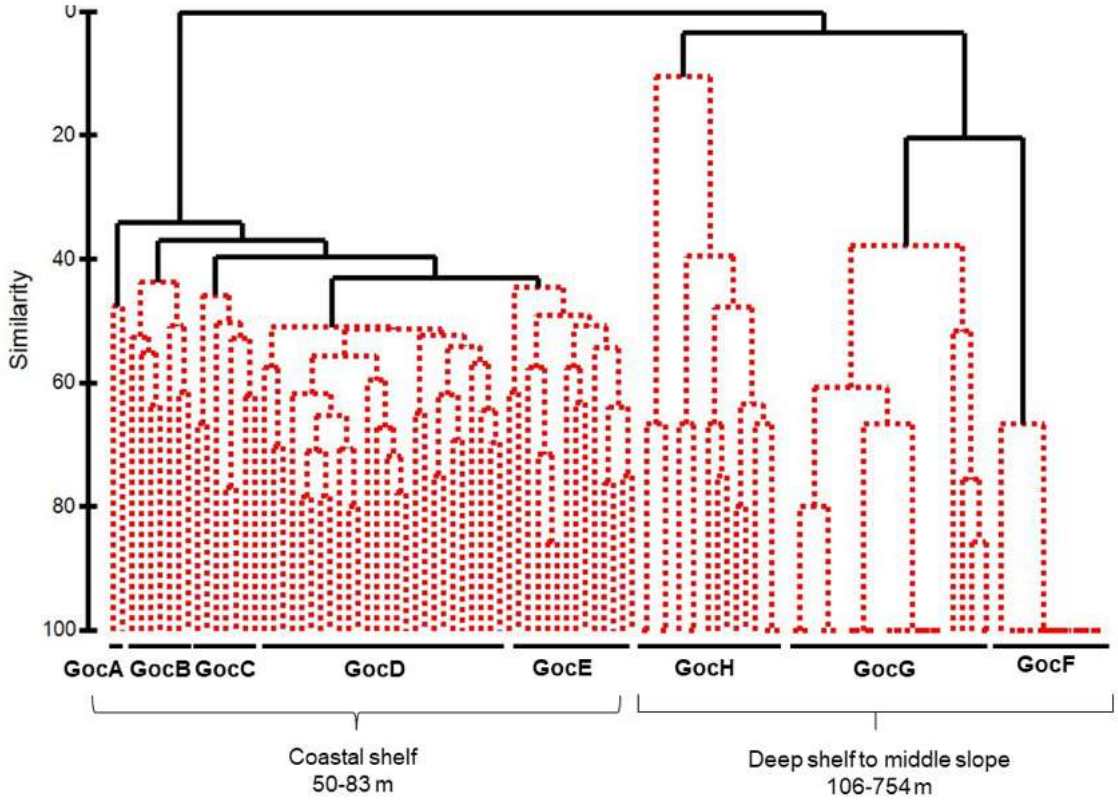

Figure 4.6.4. Dendrogram of trawl fishing grounds assemblages identified from cluster analysis of the GOC samples. Statistically significant groups are defined by the SIMPROF test, and illustrated by discontinuous red lines. Depth range and zone are indicated by each cluster.

Regarding GOC dendrogram, coastal shelf group GocA was composed only of two samples at 61 and 70 m depth, with a total and mean *S* values of 21 and 13.5±2.5 species, respectively and mean sponge and algae biomass of 8.7±3.7 g/100m^2 and 527±37 g/100m^2 (Table 4.6.3). It was characterized by *S. domuncula*, *Haliclona* sp3, *C. septimaniensis*, *Baztella inops* and Calcarea sp4 (Table 4.6.6). GocB (54-83 m depth) showed a value of total *S* (n=38 species) higher than the previous group, but it had similar values of mean *S* (11±0.8 species) and sponge and algae biomasses (8±4.7 g/100m^2 and 658±275 g/100m^2) (Table 4.6.3). It was characterized by *S. domuncula*, *Axinella damicornis*, *Axinella verrucosa* and *Siphonochalina* sp. (Table 4.6.6). The group GocC (55-78 m depth), had a total S of 36 species and a mean *S* similar to previous groups (13.1±1.2 species) and mean sponge and algae biomasses of 17.6±12.3 g/100m^2 and 407±162 g/100m^2 (Table 4.6.3). It was characterized by *S. domuncula*, *H. (R.) mediterranea*, *Siphonochalina balearica* and *Haliclona* sp3 (Table 4.6.6). The other two clusters of the coastal shelf grouped most of the samples, and showed higher *S* and biomasses values. The group GocD (54-79 m depth) had a total and mean *S* values of 95 and 20.8±1.3 species, respectively and a mean sponge and algae biomasses of 33.3±11.3 g/100m^2 and 788±214 g/100m^2 (Table 4.6.3). It was characterized by *Mycale* (*Aegogropila*) *syrinx*, *Haliclona* sp3 and *S. domuncula* (Table

Table 4.6.3. Summary of results by each sponge assemblage detected at trawl fishing grounds with GOC. Depth, mean and total species richness (Smean and Stotal), sponge biomass (Bmean) and algae biomass (Bamean) are expressed in terms of mean value (±standard error) and range values (minimum-maximum). Biomass values are expressed in g/100 m2. The total values of S are also shown.

Assemblage	N	Substrate	Depth (m)	S_{mean}	S_{total}	B_{mean}	Ba_{mean}
GocE	14	Sedimentary	57±1.1 (50-63)	13.1±0.8 (8-19)	55	28.5±8.0 (2.5-110.0)	572±117 (157-1558)
GocB	7	Sedimentary	73±4.1 (54-83)	11±0.8 (7-13)	38	8±4.7 (0.5-33.2)	658±275 (19-1921)
GocD	26	Sedimentary	68±1.5 (54-79)	20.8±1.3 (12-36)	95	33.3±11.3 (0.6-252.2)	788±214 (45-4426)
GocC	7	Sedimentary	67±3.4 (55-78)	13.1±1.2 (7-16)	36	17.6±12.3 (1.6-91.5)	407±162 (111-1103)
GocA	2	Sedimentary	65±3.5 (61-68)	13.5±2.5 (11-16)	21	8.7±3.7 (5.0-12.4)	527±37 (490-564)
GocH	16	Sedimentary	195±36.6 (106-625)	3.6±0.8 (1-13)	27	0.6±0.25 ($2.7*10^{-3}$-3.9)	--
GocG	22	Sedimentary	356±46.1 (112-738)	2.6±0.4 (1-8)	16	0.6±0.4 ($4.6*10^{-4}$-8.2)	--
GocF	12	Sedimentary	459±69 (111-754)	1.1±0.1 (1-2)	2	0.02±0.02 ($8.4*10^{-4}$-0.2)	--
Total	106	--	--	9.9±0.7 (1-36)	158	12.2±1.3 ($8.4*10^{-4}$-252.2)	590±19.11 (19-4426)

6). GocE (50-63 m depth) had total and mean *S* values of 55 and 13.1±0.8, respectively and a mean sponge and algae biomasses of 28.5±8.0 g/100m^2 and 572±117 g/100m^2 (Table 4.6.3). It was characterized by *S. domuncula*, *Haliclona* sp3, *Dysidea* sp1, *M.* (*A.*) *syrinx* and *P. tenacior* (Table 4.6.6).

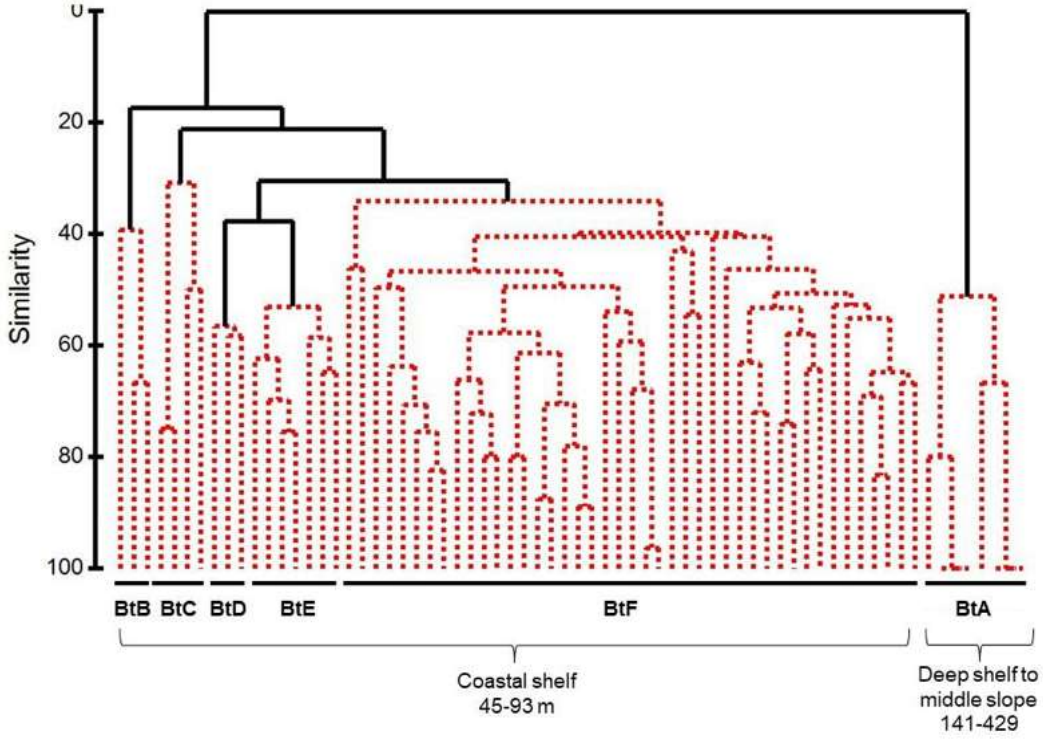

Figure 4.6.5. Dendrogram of trawl fishing ground assemblages identified from cluster analysis of the beam trawl samples. Statistically significant groups are defined by the SIMPROF test, and illustrated by discontinuous red lines. Depth range and zone are indicated by each cluster.

The clusters from the deep shelf to the middle slope showed very low values of *S* and biomass. The group GocF (111-754 m depth) had total and mean *S* values of 2 and 1.1±0.1 species, respectively and a mean biomass of 0.024±0.02 g/100m^2 (Table 4.6.3). It was composed exclusively by *D. annexa*, except for a single specimen of *Petrosia (Petrosia) raphida*. The group GocG (112-738 m depth) had a total and mean *S* of 16 and 2.6±0.4 species, respectively and a mean biomass of 0.6±0.4 g/100m^2 (Table 4.6.3). It was characterized by *T. muricata*, with a much lower contribution of *D. annexa* (Table 4.6.6). The group GocH (106-625 m depth) had total and mean *S* values of 27 and 3.6±0.8 species, respectively and a mean biomass of 0.6±0.25 g/100m^2 (Table 4.6.3). It was characterized by *P. compressa*, *H. poecillastroides*, *P. helleri* and *P. (P.) raphida* (Table 4.6.6).

Regarding BT dendrogram, coastal shelf BtB (50-72 m depth) was the group with the

Table 4.6.4. Summary of results by each sponge assemblage detected at trawl fishing grounds with beam trawl. Depth, mean and total species richness (Smean and Stotal), sponge biomass (Bmean) and algae biomass (Bamean) are expressed in terms of mean value (±standard error) and range values (minimum-maximum). Biomass values are expressed in g/100 m2. The total values of S are also shown.

Assemblage	$N_{stations}$	Substrate	Depth (m)	S_{mean}	S_{total}	B_{mean}	Ba_{mean}
BtF	43	Sedimentary	64±1.3 (45-93)	10.8±0.7 (5-21)	83	364,2±27.1 (2.0-7720.3)	23981±3441 (990-92493)
BtB	3	Sedimentary	59±6.8 (50-72)	3.7±1.7 (2-7)	8	18,1±17.2 (0.6-52.5)	9326±7946 (445-25179)
BtC	4	Sedimentary	71±3.4 (67-71)	6.3±1.1 (4-8)	16	16,8±4 (6.1-24.2)	2056±993 (9-3996)
BtD	3	Sedimentary	76±4.3 (69-84)	18.3±1.3 (17-21)	35	1478,6±917.6 (121.6-3227.1)	36773±17305 (4532-63791)
BtE	7	Sedimentary	73±2.7 (62-81)	26.3±1.9 (22-36)	68	553,8±125.8 (134.9-1136.4)	30504±12991 (3513-85607)
BtA	8	Sedimentary	248±35.5 (141-429)	5.9±2.2 (2-20)	26	15±12.4 (0.05-101.3)	--
Total	68	--	--	11.9±1.1 (2-36)	149	407.8±69.2 (0.05-7720.3)	20528±1873 (445-92493)

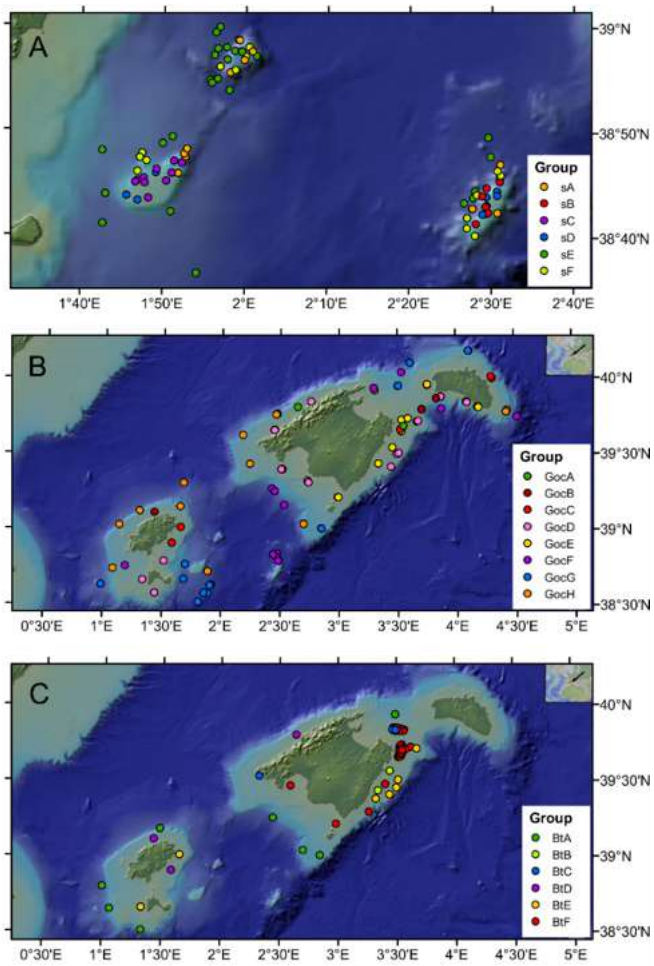

Figure 4.6.6. Maps showing the location of the sampling stations corresponding to each sponge assemblage obtained. A: Seamount groups. B-C: Fishing grounds groups obtained with GOC (B) and beam trawl (C).

lowest value of total *S* (8 species) and also had low values of mean *S* (3.7±1.7 species) and sponge and algae biomasses with 18±17.2 g/100 m^2 and 9326±7946 g/100 m^2 (Table 4.6.4). It was characterized by *S. domuncula* and *C. septimaniensis* (Fig. 4.6.8A-B, Table 4.6.7). The group BtC (67-71 m depth) had a total and mean *S* of 16 and 6.3±1.1 species, respectively and low mean sponge and algae biomasses, with 17±4 g/100 m^2 and 2056±993 g/100 m^2 (Table 4.6.4). It was characterized by *C. septimaniensis*, *Calcarea* sp1*, L.* (*L.*) *cavernosa, M.* (*A.*) *syrinx* and *Haliclona* sp4 (Table 4.6.7). The group BtD (69-84 m depth) had a total and mean *S* of 35 and 18±1.3 species, respectively and showed the highest mean biomasses values for both sponges and algae with 1479±917.6 g/100m^2 and 36773±17305 g/100m^2 (Table 4.6.4). It was characterized by *Raspaciona aculeata, A. damicornis, Tethya* sp2*, Phorbas* sp3 and *Paratimea* sp. (Fig. 4.6.8C, Table 4.6.7). The group BtE (62-81 m depth) had a total and mean *S* of 68 and 26.3±1.9 species, respectively and a mean sponge and algae biomasses of 554±125.8 g/100m^2 and 30504±12991 g/100m^2 (Table 4.6.4). It was characterized by *Haliclona* sp3, *H. mediterranea*, *A. damicornis*, *P. tenacior*, *Chelonaplysilla* sp. and *B. inops* (Fig. 4.6.8D-8F; Table 4.6.7). BtF group (45-93 m depth) showed the highest total *S*,

Table 4.6.5. SIMPER results for the seamounts assemblages identified from cluster analysis and SIMPROF test. S_i: average similarity; % $S\hat{}_i$, percentage contribution to similarity.

Assemblages	Species	S_i	%$S\hat{}_i$	Assemblages	Species	S_i	%$S\hat{}_i$
	Jaspis sp2	44.99	44.99		*Jaspis* sp1	5.62	74.1
	Heteroxya cf. *beauforti*	13.94	58.93		*Haliclona poecillastroides*	5.4	79.5
sA	*Hamacantha (Hamacantha)* sp2	13.27	72.2	**sC**	*Discodermia* sp.	4.36	83.86
S_i: 29.92	*Poecillastra compressa*	8.98	81.18	S_i: 49.58	*Chelonaplysilla* sp.	3.84	87.7
	Tretodictyum reiswigi	7.15	88.33		*Penares helleri*	2.2	89.9
	Phakellia robusta	6.9	95.23		*Axinella* sp2	2.2	92.1
	Poecillastra compressa	6.61	6.61		*Spongosorites* sp1	21.51	21.51
	Hemiasterella elongata	6.61	13.23		*Haliclona poecillastroides*	16.09	37.6
	Penares helleri	6.61	19.84		*Foraminospongia balearica*	9.94	47.54
	Chelonaplysilla sp.	6.61	26.45		*Polymastia* sp3	9.08	56.62
	Haliclona (Halichoclona) sp.	6.61	33.07		*Hamacantha (Vomerula) falcula*	6.11	62.73
	Phakellia robusta	5	38.07	**sD**	*Pachastrella monilifera*	5.8	68.53
	Foraminospongia balearica	5	43.07	S_i: 43.69	*Jaspis* sp1	5.17	73.7
	Jaspis sp1	4.9	47.97		*Hexadella* sp1	5.17	78.87
	Hexadella sp1	4.83	52.8		*Axinella* sp7	3	81.87
sB	*Discodermia* sp.	4.83	57.63		*Hymedesmia (Hymedesmia)* sp2	3	84.87
S_i: 69.82	*Dragmatella aberrans*	4.71	62.34		*Scopalinidae* sp1	3	87.88
	Haliclona sp13	4.71	67.06		*Timea* sp1	2.65	90.53
	Vulcanella sp.	3.61	70.67		*Thenea muricata*	71.77	71.77
	Desmacella inornata	3.61	74.27	**sE**	*Desmacella inornata*	9.8	81.57
	Halichondriidae sp2	3.32	77.59	S_i: 50.10	*Desmacella annexa*	8.47	90.04
	Tretodictyum reiswigi	3.24	80.83		*Poecillastra compressa*	20.09	20.09
	Dendroceratida sp3	2.37	83.21		*Desmacella inornata*	19.7	39.79
	Petrosia raphida	2.37	85.58		*Thenea muricata*	12.58	52.37
	Petrosia (Strongylophora) vansoesti	2.25	87.83		*Hamacantha (Hamacantha)* sp1	7.7	60.07
	Haliclona poecillastroides	2.19	90.02		*Dragmatella aberrans*	7.67	67.74
	Poecillastra compressa	18.18	18.18	**sF**	*Desmacella annexa*	7.39	75.13
	Foraminospongia balearica	14.52	32.7	S_i: 47.37	*Hamacantha (Vomerula)* sp5	5.11	80.24
sC	*Calcarea* sp6	10.96	43.66		*Tretodictyum reiswigi*	3.85	84.09
S_i: 49.58	*Hexadella* sp1	10.84	54.51		*Haliclona (Rhizoniera) rhizophora*	3.34	87.42
	Petrosia raphida	8.22	62.72		*Hemiasterella elongata*	2	89.42
	Pennares euastrum	5.75	68.47		*Jaspis* sp2	1.94	91.36

Table 4.6.6. SIMPER results for the trawl fishing grounds (GOC) assemblages identified from cluster analysis and SIMPROF test. S_i: average similarity; % $S\hat{}_i$, percentage contribution to similarity.

Assemblages	Species	S_i	%$S\hat{}_i$	Assemblages	Species	S_i	%$S\hat{}_i$
GocB S_i: 48.53	*Suberites domuncula*	25.09	25.09		*Axinella damicornis*	7.08	69.88
	Axinella damicornis	25.09	50.18		*Callyspongia septimaniensis*	6.76	76.63
	Axinella verrucosa	18.52	68.7		*Hymedesmia (Stylopus)* sp1	3.99	80.63
	Siphonochalina sp.	10.81	79.51		*Lissodendoryx (Lissodendoryx) cavernosa*	2.74	83.37
	Raspaciona aculeata	6.46	85.97		*Siphonochalina* sp.	2.74	86.1
	Callyspongia septimaniensis	2.96	88.93		*Phorbas tenacior*	2.26	88.37
	Antho (Antho) oxeifera	2.96	91.89		*Axinella verrucosa*	2.15	90.51
GocD S_i: 54.35	*Mycale (Aegogropila) syrinx*	10.14	10.14	**GocA** S_i: 47.62	*Suberites domuncula*	20	20
	Haliclona sp3	9.27	19.41		*Haliclona* sp3	20	40
	Suberites domuncula	8.4	27.8		*Callyspongia septimaniensis*	20	60
	Axinella damicornis	6.88	34.68		*Baztella inops*	20	80
	Haliclona mediterranea	6.86	41.54		*Calcarea* sp4	20	100
	Dictyonella incisa	6.69	48.23	**GocE** S_i: 51.26	*Suberites domuncula*	15.45	15.45
	Antho (Antho) oxeifera	4.76	52.99		*Haliclona* sp3	12.87	28.33
	Tethya sp1	4.02	57		*Dysidea* sp1	10.31	38.64
	Dictyonella sp2	3.89	60.9		*Mycale (Aegogropila) syrinx*	10.08	48.72
	Dysidea sp1	3.85	64.75		*Phorbas tenacior*	8.62	57.34
	Phorbas tenacior	3.75	68.5		*Lissodendoryx (Lissodendoryx) cavernosa*	7.52	64.85
	Aaptos sp1	3.71	72.21		*Acarnus levii*	7.14	72
	Axinella verrucosa	3.51	75.71		*Siphonochalina* sp.	5.55	77.54
	Callyspongia septimaniensis	3.07	78.78		*Mycale (Aegogropila) contarenii*	4.64	82.18
	Acarnus levii	3.03	81.81		*Myxilla (Myxilla) iotrochotina*	2.77	84.96
	Raspaciona aculeata	2.32	84.13		*Haliclona mediterranea*	2.75	87.71
	Siphonochalina sp.	2.28	86.41		*Raspaciona aculeata*	2.57	90.28
	Chelonaplysilla sp.	1.91	88.32	**GocH** S_i: 36.89	*Poecillastra compressa*	42.43	42.43
	Phorbas sp3	1.84	90.16		*Haliclona poecillastroides*	30.7	73.13
GocC S_i: 51.22	*Suberites domuncula*	16.03	16.03		*Penares helleri*	15.01	88.14
	Haliclona mediterranea	16.03	32.06		*Petrosia (Petrosia) raphida*	10.58	98.72
	Siphonochalina balearica	11.56	43.62	**GocG** S_i: 59.81	*Thenea muricata*	84	84
	Haliclona sp3	11.24	54.86		*Desmacella annexa*	7.95	91.96
	Tethya sp1	7.94	62.8	**GocF** S_i: 94.44	*Desmacella annexa*	100	100

Table 4.6.7. SIMPER results for the assemblages identified from cluster analysis and SIMPROF test. S_i: average similarity; % $S\hat{}_i$, percentage contribution to similarity.

Assemblages	Species	S_i	%$S\hat{}_i$	Assemblages	Species	S_i	%$S\hat{}_i$
BtF S_i: 44.36	*Haliclona* sp3	20.9	20.9		*Dysidea* sp1	2.66	76.66
	Lissodendoryx (Lissodendoryx) cavernosa	16.47	37.37		*Suberites domuncula*	2.42	79.08
	Bubaris vermiculata	10.39	47.76		*Siphonochalina* sp.	2.42	81.49
	Suberites domuncula	8.21	55.97		*Dictyonella* sp2	2.42	83.91
	Calcarea sp1	8.17	64.15		*Haliclona* sp9	2.42	86.33
	Haliclona mediterranea	6.65	70.8		*Callyspongia septimaniensis*	2.38	88.71
	Baztella inops	5.89	76.69		*Phorbas* sp3	2.38	91.09
	Myxilla (Myxilla) iotrochotina	3.47	80.15	**BtB** S_i: 48.41	*Suberites domuncula*	82.79	82.79
	Dysidea sp1	3.24	83.39		*Callyspongia septimaniensis*	17.21	100
	Mycale (Aegogropila) contarenii	3.24	86.63	**BtA** S_i: 66.43	*Thenea muricata*	77.42	77.42
	Callyspongia septimaniensis	3.14	89.77		*Desmacella inornata*	14.52	91.94
	Siphonochalina sp.	2.62	92.39	**BtD** S_i: 57.16	*Raspaciona aculeata*	15.08	15.08
BtE S_i: 58.16	*Haliclona* sp3	8.78	8.78		*Axinella damicornis*	15.08	30.16
	Haliclona mediterranea	8.78	17.56		*Tethya* sp2	15.08	45.24
	Axinella damicornis	8.78	26.34		*Phorbas* sp3	15.08	60.32
	Phorbas tenacior	6.24	32.58		*Paratimea sp.*	15.08	75.4
	Chelonaplysilla sp.	6.24	38.82		*Raspailia viminalis*	5.55	80.95
	Baztella inops	6.18	45.01		*Diplastrella bistellata*	4.86	85.81
	Microcionidae sp1	4.36	49.36		Dictyoceratida sp3	4.86	90.67
	Antho (Antho) oxeifera	4.13	53.49	**BtC** S_i: 41.47	*Callyspongia septimaniensis*	33.01	33.01
	Dictyonella incisa	4.13	57.62		*Calcarea* sp1	27.91	60.93
	Haliclona sp10	4.13	61.75		*Lissodendoryx (Lissodendoryx) cavernosa*	10.05	70.97
	Calcarea sp1	4.08	65.83		*Mycale (Aegogropila) syrinx*	10.05	81.02
	Raspaciona aculeata	4.08	69.92		*Haliclona* sp4	10.05	91.07
	Halichondria (Halichondria) sp1	4.08	74				

with 83 species, and a mean S value of 10.8±0.7 species, with a mean sponge and algae biomasses of 364±27.1 g/100m^2 and 23981±3441g/100m^2, respectively (Table 4.6.4). This group included the sample with the highest sponge and algae biomasses of all the study (7720 g/100m^2 and 92493 g/100m^2). It was characterized by *Haliclona* sp3, *L. (L.) cavernosa*, *B. vermiculata*, *S. domuncula* and Calcarea sp1 (Fig. 4.6.8G-8H, Table 4.6.7). The cluster BtA (141-429 m depth), similarly to the deep samples obtained with GOC, showed low values of *S* and biomass. It had a total and mean S of 26 and 5.9±2.2 species, respectively and a mean sponge biomass of 15±12.4 g/100m^2 (Table 4.6.4). It was characterized by *T. muricata* and *D. innornata* (Fig. 4.6.8I, Table 4.6.7).

Taxonomic composition

A total of 22 orders have been documented (Fig. 4.6.10), of which 19 belonging to the class Demospongiae. Of the total Demosponge orders, only Trachycladida and Sphaerocladina were not found at the present study. Twenty orders were found at seamounts, 21 at trawl fishing grounds and 18 were shared by both areas. Biemnida was exclusively found at seamounts and Chondrillida and Chondrosida were only found at trawl fishing grounds.

At seamounts, AM seamount had the highest number of orders (n= 20), followed by EB (n= 19) and SO (n= 12) seamounts. Clionaida was only found at AM seamount, while no orders were exclusive from neither the EB nor SO seamounts. In seamounts, the most diverse order was Tetractinellida with 28 species (Fig. 4.6.10A), followed by Haplosclerida, Axinellida, Suberitida, Poecilosclerida and Bubarida with 26, 21, 19, 18 and 15 species, respectively. Besides, Tetractinellida was the most diverse order in both EB, as in AM and SO seamounts, with 25, 19 and 7 species, respectively.

By assemblages, in groups sB, sC and sD, at the shallow summits of AM and EB seamounts, Tetractinellida was also the most diverse order, with 17, 16 and 11 species, respectively. Axinellida was the second most diverse order in sD (12 species), while Haplosclerida was the second most diverse order in sB and sC (15 and 12 species, respectively). In the group sA, at rocky bottoms, Tetractinellida (7 species) and Axinellida (5 species) were the most diverse orders. At sedimentary bottoms, the group sE had Desmacellida as the most diverse order (4 species), followed by Bubarida, Merliida and Polymastida, each one with 3 species, while at group sF, Bubarida was the most diverse group (8 species), followed by Axinellida, Suberitida and Polymastida, with 7 species each one. Only one species of Tetractinellida in group sE and 6 in group sF were found.

At trawl fishing grounds (Fig. 4.6.10B), and considering both BT and GOC samples, the most diverse order was Poecilosclerida (47 species), followed by Axinellida, Haplosclerida, Dictyoceratida, Bubarida and Suberitida with 32, 27, 21, 19 and 16 species, respectively. Only Sceptrulophora was exclusively found in GOC samples, while Lyssacinosida and Scopalinida were only found in BT samples. Contrarily to the seamounts, at trawl fishing

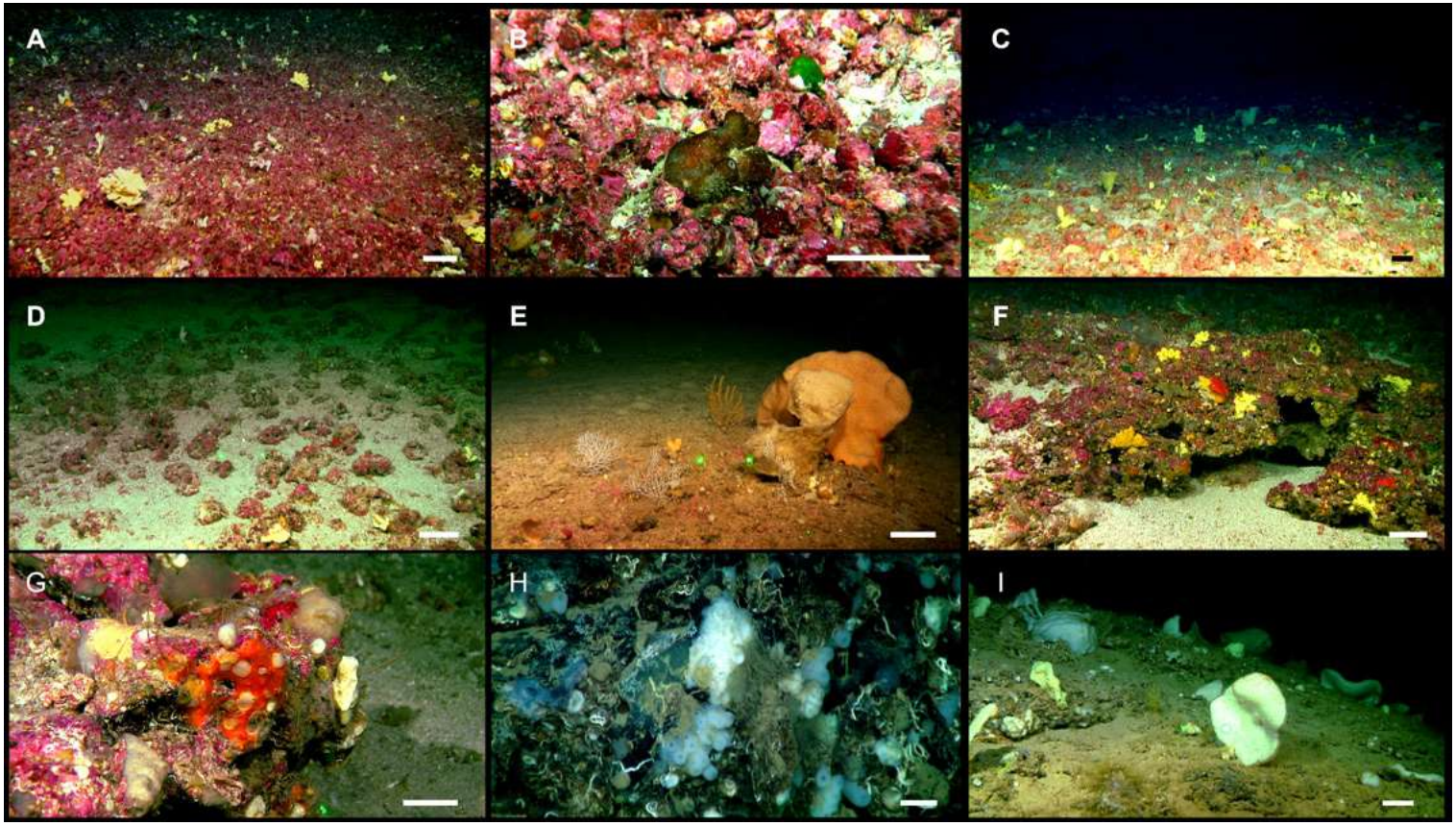

Figure 4.6.7. ROV images of sponge communities identified in the seamounts of the Mallorca Channel (Balearic Islands, western Mediterranean). A: sponge gardens associated with rhodolith beds with high coverage in the AM seamount at 91 m depth; B: detail of a *Penares euastrum* individual at the AM seamount rhodolith beds, at 90 m depth; C-D: sponge gardens associated with rhodolith beds with middle coverage in the EB seamount at 132 m and 141 m depth; E: sponge garden at the deepest part of the mesophotic zone in the EB seamount at 149 m depth; F: sponges at rocky outcrops in the AM at 100 m depth; G: sponges at rocky outcrops in the EB seamount at 146 m depth; H-I: sponge gardens of the aphotic rocky bottoms in the EB (H) and the AM (I) seamounts at 326 m and 354 m depth, respectively. Scale bar 15 cm (A, C-F, I), 5 cm (B, G-H).

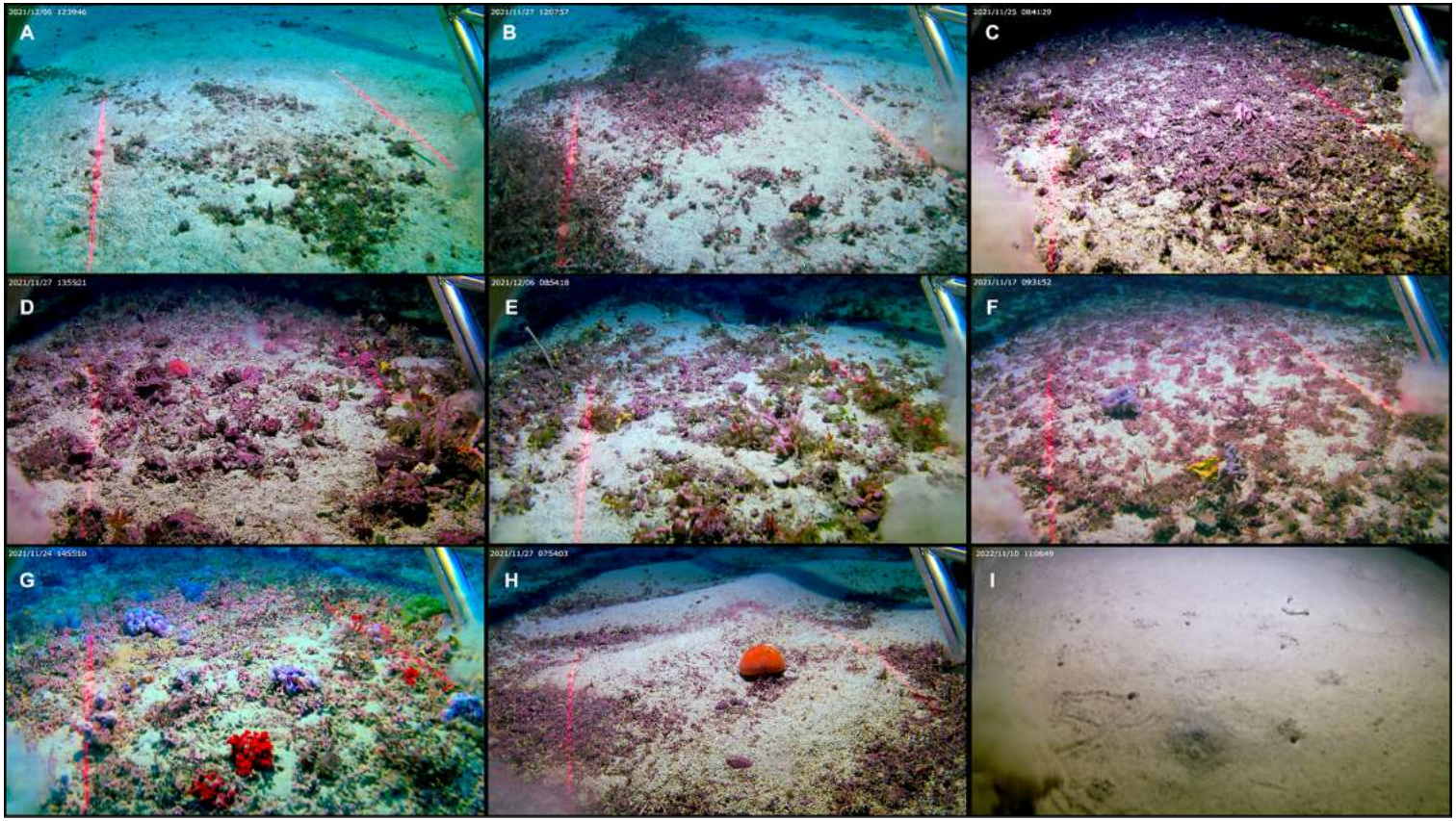

Figure 4.6.8. Sponge communities identified in the Balearic Islands trawl fishing grounds. A-H: typical sponge assemblage from the euphotic zone associated with red algae beds. A-B: stations corresponding to the BtB assemblage, located at the east of Mallorca at 53 m (A) and 51 m (B), with low algae coverage. C: station corresponding to the BtD assemblage, located at north of Mallorca (73 m), with high algae cover and high sponge biomass. D-F: stations corresponding to the BtE assemblage, located at the east of Mallorca (D-E, 78 and 77 m, respectively) and west of Formentera (F, 69 m). G-H: station corresponding to the BtF assemblage, located west of Mallorca (G, 49 m), and east of Mallorca (H, 59 m) with high algae cover and high sponge biomass. I: station corresponding to the BtA assemblage, located east of Formentera, at 377 m. Distance between lasers: 75 cm. Images acquired through the HORUS photogrammetric sled.

grounds we found 21 Dictyoceratida species (against 5) and only 7 Tetractinellida (against 28).

Regarding GOC assemblages at trawl fishing grounds, coastal shelf groups (GocA-GocE) showed a similar composition, with Poecilosclerida, Haplosclerida, Axinellida and Dictyoceratida as the most diverse orders. At deep shelf and upper to middle slope, group GocF was exclusively composed of Desmacellida and Haplosclerida, while in groups GocG and GocH, Suberitida was the most diverse order with 4 species. In the group GocG, it was followed by Desmacellida and Axinellida with 3 and 2 species, respectively, while in group GocH the second most diverse orders were Axinellida and Haplosclerida, with 4 species each one.

For BT assemblages at trawl fishing grounds, coastal shelf groups (BtB-BtF) also showed a similar order composition, with Poecilosclerida as the most common and diverse order, followed by Haplosclerida and Axinellida. In group BtA, Bubarida, Desmacellida, Polymastida and Tetractinellida were the most diverse orders, each one with three species.

Relationship with environmental variables

We constructedducted three dbRDA models: one for seamounts (Fig. 4.6.9A), one for trawl fishing grounds using GOC data (Fig. 4.6.9B), and anotherthe last one for trawl fishing grounds using BT data (Fig. 4.6.9C). The Seamount model explained the 36.8% of the sponge presence/absence variance while at fishing grounds, the BT model and the GOC model explained the 298.7% and the 33% of its variance, respectively. The significant variables of the seamount model were depth (variance explained: 7.25%; p-value=0.001), substrate type (variance explained: 11.41%; p-value=0.001), mean annual temperature at the bottom (variance explained: 10.71%; p-value=0.001) and trawling activity (variance explained: 3.24%; p-value=0.005). At trawl fishing grounds, the significant variables of the GOC model were depth (variance explained: 3.43%; p-value=0.002), annual mean temperature (variance explained: 13.37%; p-value=0.001) , fishing effort (variance explained: 0.94%; p-value=0.009) and maxim flow velocity (variance explained: 3.6%; p-value=0.001) while the significant variables for the BT model were depth (variance explained: 5.11%; p-value=0.001), total algae biomass (variance explained: 4.1%; p-value=0.002), mean annual temperature (variance explained: 5.74%; p-value=0.001) and maxim flow velocity (variance explained: 3.76%; p-value=0.007).

At seamounts, most of the species were correlated with depth and mean temperature (Fig. 4.6.9A). Large mesophotic species like *H. poecillastroides*, *P. compressa*, *F. balearica*, *Hexadella* sp1 and *Spongosorites* sp1 were inversely related with depth and positively related with temperature. Those species characterize the assemblages sB, sC and sD, located at the shallow summits of the AM and the EB seamounts. Species more closely correlated to the substrate type were *D. innornata, D. annexa, C. abyssicola, T. muricata, Hamacantha (H)* sp1, *Hamacantha (Vomerula)* sp5, and *Monocrepidium* sp2 for sedimentary bottoms (found in assemblages sE and sF) and *Jaspis* sp2, *Hamacantha (H)* sp2, and *Heteroxya* cf. *beauforti* for rocky bottoms (assemblage sA). Fishing was only present on deep sedimentary bottoms where showed some negative correlation on small sedimentary species like *Hamacantha (H)* sp1, *Hamacantha (Vomerula)* sp5, *Monocrepidium* sp2 and *Bubaris* sp5.

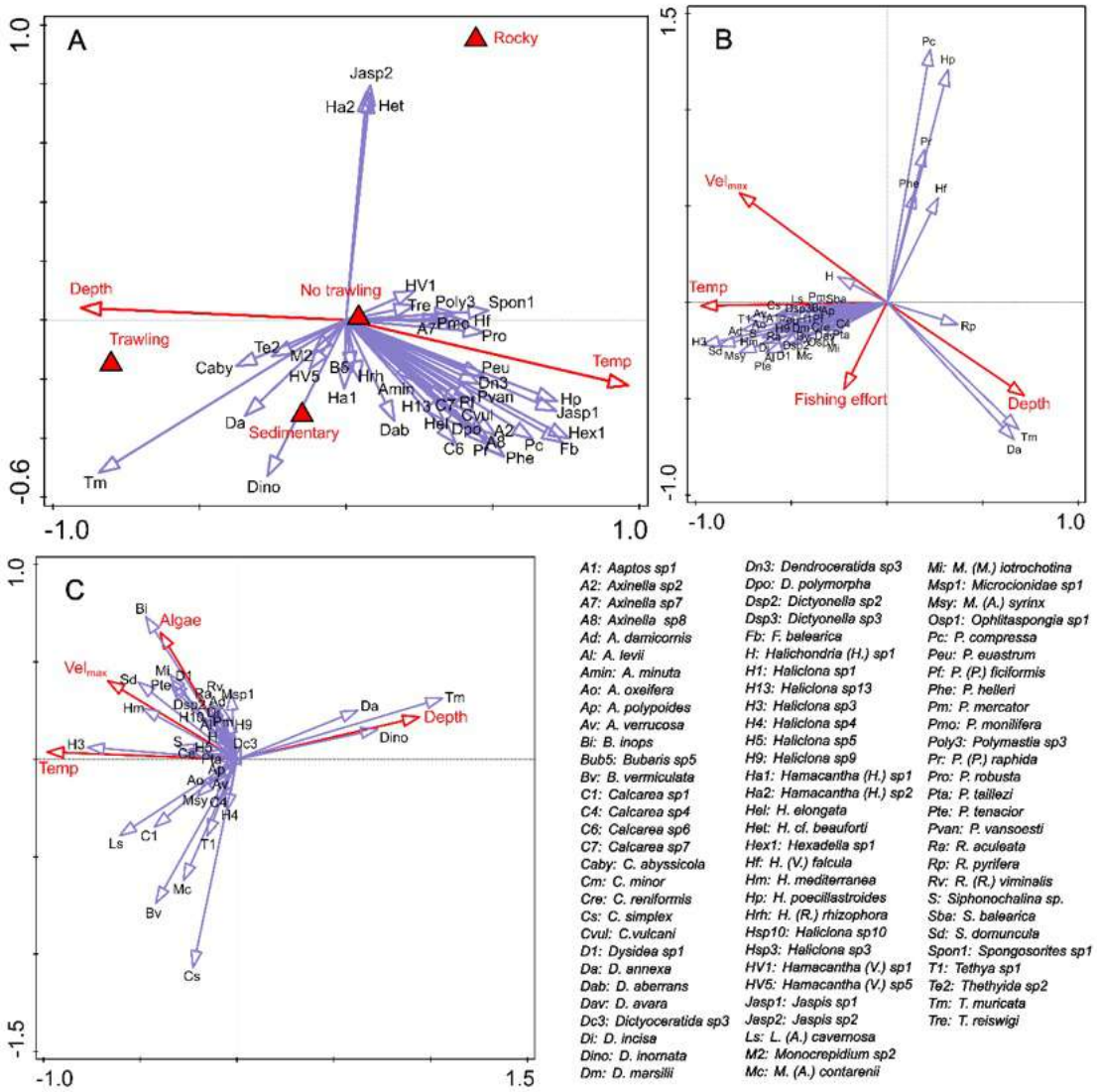

Figure 4.6.9. Biplot for the dbRDA models with the species abbreviation correspondences. A: Seamounts data (beam trawl and rock dredge data); B: trawl fishing grounds (GOC data); C: trawl fishing grounds (beam tralw data).

The GOC model showed a strong correlation between sponge presence/absence with depth and mean annual temperature (Fig. 4.6.9B). Depth was positively related to the deep sea species *T. muricata* and *D. annexa* and *R. pyrifera* (found in assemblages GocF and GocG) and negatively related to coastal shelf species like *P. tenacior, L (L) simplex, Haliclona* sp3 or *S. domuncula* (found in assemblages GocA-GocE). Also, *T. muricata, D. annexa* and *R. pyrifera* were negatively related to maxim flow velocity. Temperature showed a similar but inverse pattern with the same species. Fishing effort was negatively related to the presence of the large species *P. helleri, P. raphida, P. compressa, H. poecillastroides* and *H. (V.) falcula* (assemblage GocH).

As the previous models, the BT model showed a strong correlation with depth and mean annual temperature (Fig. 4.6.9A). Like in the previous GOC model, depth was positively related with *T. muricata* and *D. annexa*, but also with *D. innornata* (corresponding to BtA). Those species were negatively correlated with mean annual temperature, which was positively correlated with the presence of *Haliclona* sp3. Several species like the

encrusting *B. innops* or the massive encrusting *M. (M.) iotrochotina* and *P. tenacior* showed a positive correlation with the total benthic algae biomass. Inversely, species like *C. simplex, M. (A.) contarenii, B. vermiculata* or *Tethya* sp1 showed a negative correlation with total benthic algae biomass. Finally, species like *S. domuncula* and *H. mediterranea* were highly correlated to maxim flow velocity and, to a lesser extent, to total benthic algae biomass.

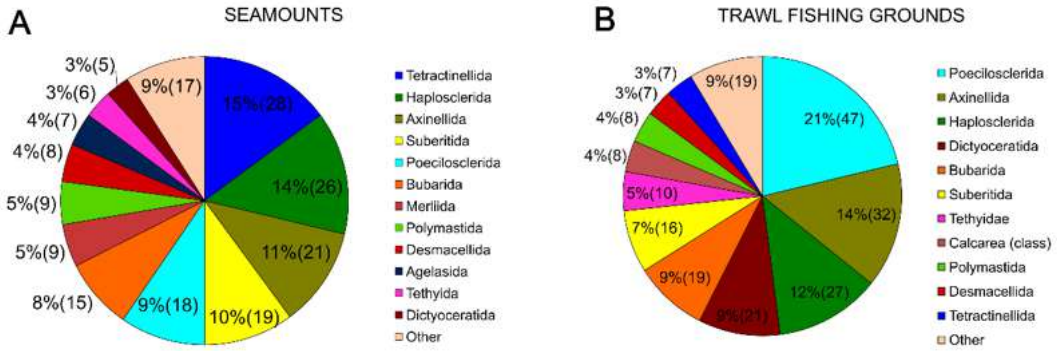

Figure 4.6.10. Percentage of number of taxa in each order, in relation to the total species richness in seamounts and trawl fishing grounds samples. The number of species is also shown between brackets.

Discussion

Sponge diversity

Our results, with 350 species, is one of the larger inventories of sponges published in the Mediterranean. Previous works reported 114 species from the Gulf of Lions, the Ligurian Sea and some areas of the Aegean Sea, between 90 and 765 m depth (*Vacelet, 1969*), 197 species from the Adriatic, Tyrrhenian, Ionian and Aegean seas between 0 and 700 m depth (*Pulitzer-Finali, 1983*), 173 species from the Balearic Islands (*Bibiloni, 1990*) and 96 species from a large region including the Gulf of Cadiz, the Strait of Gibraltar and the Alboran Sea, between 115 and 2110 m depth (*Boury-Esnault, Pansini & Uriz, 1994*).
Among the detected species, *Prosuberites longispinus*, *Bubaris vermiculata*, *Desmacella annexa*, *Mycale (Aegogropila) rotalis, Timea chondrilloides, Forcepia (Leptolabis) luciensis, Spinularia sarsii, Polymastia tissieri* and *Callyspongia septimaniensis* represent new records for the Balearic Islands, although *C. septimaniensis* may have been reported by *Bibiloni (1990)* under the name of *Adocia simulans* (Johnston, 1842). Taxa not identified to the species level will be published on taxonomic articles elsewhere.
The high sponge diversity reported in the present study can be explained by several factors. First, the higher intensity of sampling (590 stations, on which sponges were present in 439), than in the mentioned previous works: 53, 64 and 122 sampling stations in *Vacelet (1969)*, *Pulitzer-Finalli (1983)* and *Boury-Esnault, Pansini & Uriz (1994)*, respectively. This high number of sampling stations could allow us to find rare species or species that appear sporadically. For example, *Axinella vellerea, Lanuginella pupa, Melonanchora emphysema* and *Stryphnus ponderosus* were recorded only once. Second, the combination of sampling methodologies (BT, RD, GOC and ROV) allowed sampling of different habitats (in rocky and sedimentary bottoms, including different levels of

fishing pressure, from trawl fishing grounds to the bottoms not exploited by bottom trawling in the flanks and summits of the seamounts).

The oceanographic characteristics of the Balearic Iºslands must also play a role in the observed sponge diversity values. In fact, large faunistic lists were also documented in previous works performed in this area, even with fewer stations. *Bibiloni (1990)* reported 173 species from 83 sampling stations in caves and trawl fishing grounds between 0 and 200 m depth, *Uriz et al. (1992)* reported 98 species in only 13 sampling stations from 0 to 55 m depth at the Cabrera National Park southern Mallorca and, more recently, *Santin et al. (2018)* reported 109 species in the Menorca Channel between 50 and 350 m depth. Waters around the Balearic Archipelago are much more oligotrophic than those of the adjacent Iberian Peninsula. The transparency of the waters could allow certain sponges to keep their photosynthetic symbionts deeper than in other areas, providing photosynthetic products, which can be a potential advantage on mesophotic depths (*Keesing et al., 2012*) and within an oligotrophic environment as the Mediterranean. For instance, we found some *Petrosia (P.) ficiformis* individuals with red cyanobacterial pigmentation down to 135-140 m depth, at the summit of EB seamount (Annex Table S4.6.1).

The water transparency also allows algae to develop much deeper than in other areas. Total algae biomass was positively related to the presence of a majority of species on the BT dbRDA (Fig. 4.6.9C). Several types of red algae communities can be found down to 90 m depth at trawl fishing grounds, including soft (*Peysonnellia* spp., *Osmundaria volubilis*, *Phyllophora crispa* and *Halopteris filicina*) and calcareous (rhodoliths) species (Joher et al., 2012, 2015), while rhodoliths beds have been found down to 140 m depth in the Mallorca Channel seamounts (*Massutí et al., 2022*). Deep red algae beds can enhance sponge biodiversity and biomass in several ways. Sedimentary bottoms covered by red algae can act as rocky bottoms by providing substrate, a key limiting factor for aquatic sessile invertebrates (*Maldonado et al., 2017*). Although algae and sponges compete for the substrate, algae growing under low irradiances may show lower vitality (*Bahia et al., 2010*) and/or diminished allochemical production (*Amade & Lemee, 1998; Pavia & Toth, 2000; Hellio et al., 2004*) compared to mixotrophic and heterotrophic animals (*Lesser, 2019*) offering a more accessible substrate for sponges or other invertebrates to colonize (*Gherardi, 2004*).

Some authors have also suggested that the structural complexity provided by the red algae create shaded habitats, in which sciaphilous sponge species can develop (*Santin et al., 2018*), although at our study zone we did not find evidence of shading as an important process in the studied red algae beds. Most of the erect and massive sponge species as well as many of the epiphytic encrusting species grow next to the pigmented areas of the algae (Fig. 4.6.11A-E) suggesting a sun-exposed growth.

In addition to structural complexity enhancement, red algae beds release dissolved organic matter (DOM) to the water column in form of exudates that can be consumed by sponges (*de Goeij et al., 2013*), hence boosting their presence and diversity.

Sponge assemblages

Seamounts

The shallow summit sedimentary groups sB and sC were exclusive from the EB and the AM seamounts, respectively. However, differing depths between both groups, with sC being slightly shallower (97-135 m) than sB (141-154 m), indicate that differences found in EB/AM were rather due to depth than to differences in the fauna composition in each seamount. This seems to be corroborated by the fact that the other group of the shallow summit (sD; 94-193 m), included both AM/EB seamounts, having a mixture of characterizing species. Interestingly the shallower sC has higher biomass values, which could be related to the growth of sponges with photosymbionts and by differences in DOM available in the environment released by red algae (*Haas et al., 2010; Mueller et al., 2014; Lesser, 2019*). This points out the importance of light penetration as a determining factor on the temperate mesophotic sponge communities (*Uriz, 1992, Harris, 2022*).

Assemblage sA shows some similarity with the "Hamacantha-Tretodictyum" assemblage described by *Santin et al. (2018)* at similar depths (250-350 m) in the Menorca channel, characterized by *Hamacantha (Vomerula) falcula, T. reiswigi*, *Haliclona mucosa* and *Hexadella* cf. *dedritifera*. However, no *Jaspis* species was reported in that work, and conversely, we recorded *Hamacantha (Hamacantha)* sp2 instead of *Hamacantha (Vomerula) falcula* (Bowerbank, 1874), a thin blue-grayish species very similar in external morphology than the one indicated as *H (v.) falcula* by those authors (see Fig 8 h in *Santin et al., 2018*). In contrast, at Seamounts and trawl fishing grounds we always collected *H. (V) falcula* on sedimentary stations between 102-149 m. Besides, sA was also characterized by *Heteroxya* cf. *beauforti*, *P. compressa* and *P. robusta*. This discrepancy in taxa composition at ecologically similar assemblages of two close areas, suggest that equivalent sponge communities may present significant variations, even when separated by short distances. *T. reiswigi* is an hexactinellid reported in the western Mediterranean, mostly from vertical walls down to 632 m depth (*Boury-Esnault et al., 2017*). At the Cassidaigne canyon, it is known to occur together with other hexactinellids like *Farrea* sp. or *Oopsacas* cf. *minuta*, an association never observed in the present work (*Fabri et al., 2017*).

We detected two assemblages in deep sedimentary stations of the seamounts. The sF included the tetractinellids *P. compressa* and *T. muricata* and a very diverse group of small encrusting and vesicular species like *D. innornata*, *D. aberrans, Hamacantha*

Figure 4.6.11. Several examples of substrate used by sponges in the Balearic Islands trawl fishing grounds (A-G) and Seamounts (H-I). A: *Phorbas tenacior* using *Peyssonnelia* sp as substrate off west Mallorca, at 45 m depth; B: *Myxilla (Myxilla) iotrochotina* using a soft red algae as substrate, at 69 m depth; C: Irciniidae sp3 using soft red algae as substrate, having incorporate most of the algae to its tissue, at 52 m depth; D-E: *Axinella damicornis* and *Raspailia (Raspailia) viminalis* using a rhodolith as substrate at 68 m and 72 m, respectively; F: *Penares helleri* using a dead rhodolith discarded by the trawling fleet as substrate, at 108 m depth; G: *Geodia sp1* using biogenic debris as substrate, with *Hexadella* sp. and other sponges growing in ephybiosis, at 108m depth off AM seamount; H: encrusting sponges and small Axinellids growing on a partially dead rhodolith found at 102-138 m depth, off EB. I: Sample showing small encrusting species common at sF assemblage, using small organogenic sediments as substrate, at 320 m, off EB.

(Hamacantha) sp1, *Hamacantha (Vomerula)* sp5*,* small encrusting species of the genus *Bubaris* and *Eurypon*, and small species of the genus *Axinella* and *Polymastia*, among others. These are minute species grown on organogenic sediments like small pieces of shells, sea urchin spines and gravels (Fig. 4.6.11I and personal observation), which gave these groups a high diversity. This assemblage shows some similarity to those described at 639-1130 m by *Longo et al (2005)* (Cape St. Maria di Leuca, southern Italy), associated to a deep-sea coral bank. Assemblage sE is similar to sF, but it shows much lower diversity and biomass values, probably because there were less organogenic sediments and higher proportion of muds of the area (*Massuti et al., 2022*). Besides, trawling occurs in a few stations of Se corresponding to the lower parts of the seamounts and the adjacent areas, a fact that could also explain the lower biodiversity in that assemblage, and the presence of resilient species like *T. muricata* and *D. annexa*, typically found at trawl fishing grounds (*Pansini & Musso, 1991*) (Table S4.6.1).

Trawl fishing grounds

At trawl fishing grounds coastal shelf sponge assemblages were always associated with red algae beds, used by many sponges as substrate (Fig. 4.6.11A-10E), a correlation also reflected in the BT dbRDA model (Fig. 4.6.9C). Algae colonization by sponges seems to have a phylogenetic component, as according to our observations, boxwork to pralines rhodolith species like *Spongites fruticulosus* seems to be more easily colonized than ramose species like *Lithothamnion corallioides* or *Phymatolithon calcareum*, perhaps because of its rugosity and/or deterrent metabolite production. Besides, massive rhodoliths create small crevices with no living algae that may induce sponge adherence, while ramose rhodoliths have smooth surfaces and are less cavernous (*Basso, 1998*). This pattern was also observed in a shallow rhodolith bed off the Pacific coast of Mexico (average depth of 3.5 m), *Ávila et al. (2013)* also reported a positive correlation between sponge abundance and diversity with rhodolith beds, finding highest levels of sponge diversity and abundance in areas dominated by spherical forms. On the other hand, soft algae like *Peysonnellia* spp. or *Osmundaria volubilis* seem to limit the growth of erect or arborescent sponges, maybe because they offer a less stable substrate than rhodoliths.
Assemblages BtB-BtC and GocA-GocB, with low diversity and sponge biomass values, were located at sandbanks with low algae biomass. Again, the correspondence with low sponge biomass and diversity and low algae is in consonance with the results by *Ávila et al. (2013)* off the Pacific coast of Mexico and highlighting the importance of algae for the development of sponge communities.
A striking difference between assemblages collected with BT and GOC was the dominance of *S. domuncula* for many GOC samples. It is the species that most contributes to similarity in all but one (GocD) coastal shelf assemblages, while its importance in BT assemblages is much lower. This may indicate a sparse distribution area yet GOC has a much higher effective sampling area than BT. *S. domuncula* is very abundant at trawl fishing grounds and probably resilient to trawling (*Ordines et al., 2017*). It quickly contracts when landed on board fishing vessels, a fact that may avoid air cavitation into the aquiferous system (*Hamer et al., 2007*). Contraction may also increase its density and

favor the quick sinking after discard, and hence the survival to capture of this species, which could be related to its high abundances at trawl fishing grounds. This may also be the case of other massive free-living species like *Dictyonella incisa*, which is also very abundant in certain areas of the coastal shelf.

Below 90 m depth irradiance diminishes, red algae beds disappear and diversity and biomass of sponges drastically plummets. Some of the most abundant species in the deeper water assemblages were *T. muricata* and *D. annexa*. The first species has special root-like adaptations to anchor the substrate, a strategy that is also followed by other less common species like *R. pyrifera*, which also have distinct floor attaching modifications. Those species are also negatively correlated to maxim flow velocity, a fact that points its preference for areas with low hydrodynamic conditions, which generally have muddy bottoms and increased sedimentation rates (*Rosenberg, 1995*) (Fig. 4.6.9B-C). Some large massive species found at these assemblages (like *Penares helleri*), were mostly growing on dead coralligenous red algae, probably released by trawl fishing fleet from shallower hauls (Fig. 4.6.11F), indicating that substrate is an important factor in absence of photosynthesis. Besides, another issue is that species inhabiting this group must face its aquiferous system obstruction by sedimentation. Mud resuspension can be caused by currents or by trawling (*Arjona-Camas et al., 2022*) and is potentially harmful for sponges. It is known that certain species develop strategies to face sedimentation, like mucus production to avoid pore obstruction (*McGrath et al., 2017, Kornder et al., 2022*). This may be the case of *D. annexa*, which expels mucus on deck and is very abundant in the deep shelf and shelf break, and can be found in great biomasses in several stations north off the Menorca channel (personal observation).

Seamounts vs *Trawl Fishing Grounds*

A striking difference between seamounts and trawl fishing grounds is the low number of shared species between the two areas (S= 61, 17% of the total here reported). Part of this is explained by bathymetric differences (the shallowest station at trawl fishing grounds was at 45 m while the shallowest station at seamounts was at 93 m), meaning that at trawl fishing grounds there are shallow water communities not expected to be present at seamounts. However, the difference is also patent at deeper, overlapping bathymetric ranges (below 90-100 m), where only 28 species are shared. Interestingly, those 28 species represent 61% of the total (S=46) number of species at that depth range on the trawl fishing grounds, but only 15% at seamounts (of a total S of 190, or 135 if we stick to sedimentary bottoms). This indicates that at trawl fishing grounds the sponge diversity is concentrated on the coastal shelf and it suffers a dramatic decrease below, by contrast to seamounts, which are very diverse at deep waters. As shown in the dbRDA GOC model (Fig. 4.6.9B), fishing pressure seem to affect more intensively lower mesophotic species, like *P. compressa, H. poecillastroides, P. (P.) raphida H. (V.) falcula* and *P. helleri*. In this regard, sponge assemblages found at the lower mesophotic AM and the EB seamounts summits probably represent ancestral, undisturbed stages of the same communities.

In both trawl fishing grounds and seamounts, depth was the main factor determining sponge assemblages, separating shallow and deep groups. As discussed before, separation between shallow and deep assemblages was probably caused by the levels of light irradiance at the bottom, yet the boundaries determined by SIMPER tests match well with the disappearance of red algae beds. However, those limits differ between the two areas, being found at 90-100 m depth at trawl fishing grounds and at ~135-140 m depth at seamounts. This large difference can be explained by several factors, like the higher water transparency at the seamounts (*Massutí et al., 2022*) and by the effect of bottom trawling, which may create nepheloid layers that reduce the light penetrance at trawl fishing grounds (restricting the red algae beds development below 90-100 m) (*Minnery, 1990*).
This difference in light penetration and fishing pressure may explain why some shallow species that are very common at coastal shelf trawl fishing grounds are found on greater depths at the seamount summits. Some examples are: *A. vaceleti* (84 *vs.* 116m, respectively), *A. verrucosa* (83 *vs.* 127m), *A. polypoides* (80 *vs.* 99 m), *P. (P.) ficiformis* (81 *vs.* 151m), *Pennares euastrum* (79 *vs.* 127m), *B. vermiculata* (93 *vs.* 98m) and *D. incisa* (82 *vs.* 98m). Besides, the shallower presence of *T. muricata* (112 *vs.* 122 m) and *R. pyrifera* (110 *vs.* 225 m), at trawl fishing grounds may be related to an increased presence of fine sediments and mud in the seafloor near the islands, in comparison with the prevalence of coarser sediments in the seamount summits (*Massuti et al., 2022*).
Taxonomic composition also changes between both areas, at least for some groups like Tetractinellida or Dictyoceratida. In part, these differences can be attributed to bathymetric differences, especially in orders typical of shallow waters, like Dictyoceratida, more represented in trawl fishing grounds than in Seamounts (21 *vs* 5 spp, respectively). These sponges have no spicules, a fact that has been interpreted as a consequence of evolutionary adaptation to shallow habitats with high temperature and low silica concentrations (*Alvarez et al., 2017*).
More surprising is the different number of Tetractinellida between trawl fishing grounds and Seamounts (28 *vs.* 7 species, respectively). This could indicate a special sensitivity of Tetractinellids to bottom trawling, as has been suggested by *Colaço et al. (2022)* in grounds of *Geodia* species in the Barents Sea. In fact, we didn't observe mucus production in any of the tetractinellids collected. This is a typical physiological response associated with mechanical damage, air exposure or high sedimentation rates, which is widespread in trawl fishing grounds species like *L. (L.) cavernosa, M. (M.) iotrochotina, H. mediterranea, Haliclona* sp3*, H. poecillastroides, D. annexa* and *Ophlitaspongia* sp. Besides, low growing rates can also make the group more susceptible to anthropogenic impacts. Recently, *Morganti et al., (2022)* estimated the age and annual growth of several specimens of *Geodia parva* and *Geodia hentscheli*, two species constituting a dense sponge ground at Langseth Ridge (Central Arctic Ocean), to be hundreds of years (with a community average age of 300 years) and having growths of 0.55 mm/year. At trawl fishing grounds we have observed many species having soft algae embedded in its tissue, which suggest a fast growth (Fig. 4.6.11B-C). It is plausible that trawling selected the fast growing and more resilient sponges to the detriment of slow growing (and probably long lived) species or groups of sponges. In fact, two *Geodia* species (*Geodia* sp1 and *Geodia* sp3) as well as other tetractinellids like *Pachastrella monilifera* are very common at the

summits of AM and EB seamounts (Fig. 4.6.11G), but absent at trawl fishing grounds. Those large species are habitat builders that probably contribute to the overall maintenance of the ecosystem.

The present work confirms the Balearic Islands as an area of great diversity of sponges within the Mediterranean, which can be explained by its particular oceanographic features. This is notable at the trawl fishing grounds of the coastal continental shelf around the Archipelago and at the shallow summits of the Mallorca Channel seamounts AM and EB. The development of deep red algae beds seems to be one of the main reasons, because they offer a suitable habitat, substrate and potential source of food in the form of DOM. The distribution of deep algae beds determines the sponge communities in both trawl fishing grounds and seamounts. Below the limit of presence of those beds, sponges are conditioned by substrate type and probably by the effects of bottom trawling. Further works must include those areas that have been neglected in this work: the rocky bottoms of the continental shelf and slope. Its study will also show if the differences that we detect between the seamounts and the trawl fishing grounds are caused by fishing impacts or can be explained by the different nature of trawl fishing grounds and the Mallorca channel seamounts. Overall, our results highlight the importance and complexity of the relationship with red algae for the sponge communities of the Balearic Islands and points those ecosystems as sponge biodiversity reservoirs.

Acknowledgements

This research was performed in the scope of the LIFE IP INTEMARES project, coordinated by the Biodiversity Foundation of the Spanish Ministry for the Ecological Transition and the Demographic Challenge. It receives financial support from the European Union's LIFE program (LIFE15 IPE ES012). The MEDITS surveys are co-funded by the European Union through the European Maritime and Fisheries Fund (EMFF), being included in the National Program of collection, management, and use of data in the fisheries sector and support for scientific advice regarding the Common Fisheries Policy (Data Collection Framework). CIRCA-LEBA survey is part of the project 18-ESMARES2-CIRCA, included in the program "Asesoramiento científico-técnico para la protección del medio marino: Evaluación y seguimiento de las Estrategias Marinas, Seguimiento de los espacios marinos protegidos de competencia estatal (2018-2021)", co-funded by Spanish Ministry for the Ecological Transition and the Demographic Challenge. J.A. Díaz was supported by a predoctoral contract, co-funded by the Regional Government of the Balearic Islands and the European Social Fund (FPI/2178/2018). Thanks to Sergi Johrer for their comments regarding red algae and to the crew and scientific members of the MEDITS, INTEMARES and ESTRATEGIAS surveys.

GENERAL DISCUSSION

5. General discussion

This PhD thesis highlights how unknown sponges are, even in apparently well-explored regions such as the western Mediterranean (*Van Soest, 2012*). The scope of this study encompassed sponge communities in a wide bathymetric range (from 0 to 1050 m) and diverse habitats, including littoral caves, coralligenous concretions, red algal beds, sandy and muddy circalittoral and bathyal bottoms and rocky outcrops. Consequently, a diverse sampling methodology was employed, including scuba-diving, dredges, beam trawl, experimental bottom trawl and ROV. In addition to this great diversity of marine environments, the sampled areas also include different degrees of fishing pressure, ranging from traditional bottom trawl fishing grounds of the continental shelf and upper to middle slope, to areas recently protected from this fishery, like the continental shelf of the Menorca Channel, and minimally impacted areas, like the seamounts of the Mallorca Channel.

A collection of over 2800 samples has been created, with 350 taxa documented and inventoried. Among these, 122 were identified at species level, 190 at genus level, 21 at family level, and 17 at order or class level. Overall, this work expands the MITECO Master list of wild species present in Spain (https://www.miteco.gob.es/es/biodiversidad/servicios/banco-datos-naturaleza/informacion-disponible/bdn_listas_patron.html#lista-patron-de-los-habitats-terrestres-presentes-en-espana) by 20 additions: *A. levii*, *A. spatula, A.venusta*, *D. polymorpha*, *E. corsicus*, *E. mamillaris*, *F. balearica*, *F. minuta*, *G. bibilonae*, *G. matrix*, *G. microsphaera*, *H. (Soestella) fimbriata*, *H. cf. beauforti*, *P. massutii*, *P. cavernensis*, *P. deficiens*, *P. isabellae*, *R. implicata*, *S. mortarium*, *T. chondrilloides*. Additionally, the species *S. maximus* and *G. anceps* should be synonimyzed with *C. pachastrelloides* and *G. geodina*, respectively.

Prior to this PhD, *Santin (2022)* listed up to 284 species reported at the Balearic Islands. That number raises to 330 by adding the newly described species and the new reports documented in this PhD. Moreover, up to 228 taxa were not identified to species level and most probably will contribute to enlarge the sponge biodiversity in the Archipelago with new species or records. In fact, despite that an in-depth morphological and/or genetic study has only been performed on 57 (16%) of the total documented taxa, it resulted in the description of 9 new species, one new genus and 38 new records for the Balearic Islands, including 4 records for the Mediterranean. Some of the most speciose groups collected in this thesis, like the Haplosclerids, the Poecilosclerids and the Axinellids, still remain with most of their taxa unidentified, with species-level identification lacking for 32, 41, and 27 species, respectively. The Tetractinellida is the only large order fully reviewed, unrevealing 6 new species and 19 new Balearic records. Considering that there are 27 sponge orders in the Balearic Islands, it is plausible to conclude that a large number of new taxa remains to be found.

Given this context, our estimation suggest that the total number of sponge species from the Balearic Islands could approach 400. This holds particular significance when

juxtaposed with the Mediterranean, renowned as a sponge diversity hotspot (*Van Soest et al. 2012*) (Fig. 5.1). Presently, the Mediterranean boasts approximately 778 species, with 440 reported in the western Mediterranean alone (*de Voogd et al., 2024*). Notably, the Balearic Promontory only represents about 0,5% of the entire Mediterranean area. A review by *Voultsiadou (2009*) indicated that the zones with highest sponge diversity of the Mediterranean were the Tyrrhenian Sea (309 species) followed by the Ligurian Sea (289 species) and the French coast with 255 species (Fig. 5.2). All these areas present lower biodiversity than that reported in this thesis. Furthermore, *Santin (2022)* listed in 363 the total number of sponges reported from the "Catalano-Balearic sea", an area including the Balearic Islands and the Catalan coast.

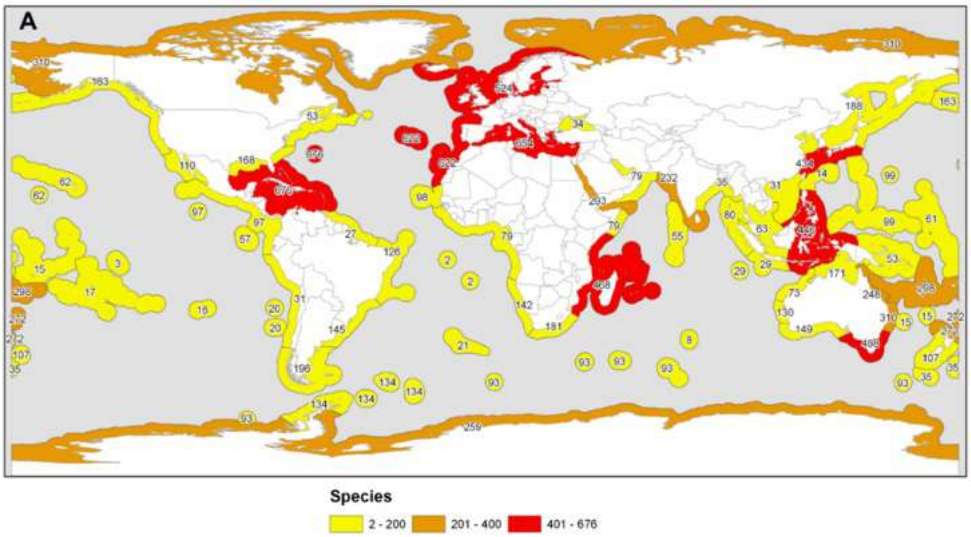

Figure 5.1. Map showing numbers of recent sponge species found in each of 62 Marine Provinces. Source: *Van Soest et al. (2012)*.

As mentioned before, the broad biodiversity here documented can be explained by the intensity of sampling and the heterogeneity of the habitats that were sampled (Chapter 4.5). However, the integrative taxonomy approach applied in this PhD, combining the use of morphology and molecular markers, has also helped in finding cryptic species, which couldn't otherwise be detected using morphological analyses alone. This is the case of *Geodia microsphaera* **sp. nov.** and *Geodia bibilonae* **sp. nov.**, which are almost identical and only distinguished by minor differences in the spicule sizes or *Paratimea massutii*, which is very similar to other *Paratimea* species being only differentiated by minor morphometric characters (Chapters 4.2 and 4.3).

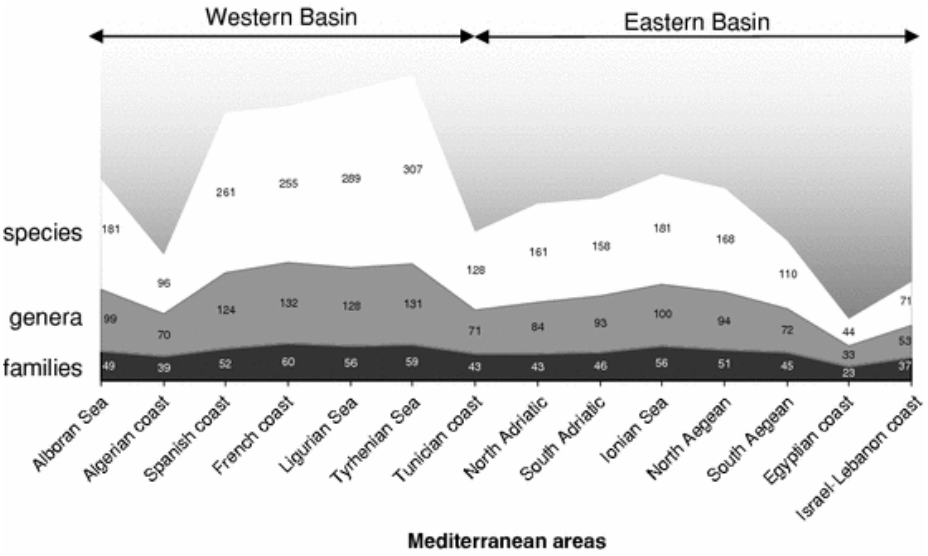

Figure 5.2. Species, genera and families richness of sponges in the Mediterranean areas, presented in a West to East order. Source: *Voultsiadou (2009)*.

Molecular markers are also useful for testing the strength of a certain morphological character such as the presence, absence or abundance of a given spicule or its width and length. Spicule variability depends on ecological factors such as nutrient availability, temperature or depth, and may have a population component, implying that its spatial variability may or may not have a genetic basis. In several cases, this study identified intraspecific variability in spicule morphometrics, suggesting the potential presence of cryptic species. However, we refrained from proposing new species either because there was no genetic information available for comparison or because we failed to get sequences from our specimens. Such is the case for species like *Melonanchora emphysema, Calyx* cf. *tufa* or *Lanuginella pupa*. Conversely, in the case of *Heteroxya* cf. *beauforti*, despite substantial morphological differences between Atlantic and Balearic populations, the lack of variability in COI sequences prevented us from describing a new species (Chapter 4.2).

An additional reason to use genetic markers in sponge taxonomy and phylogeny is avoiding wrong ecological, evolutive and biogeographical interpretations. For instance, *C. vulcanii*, a species previously thought to have an Atlanto-Mediterranean distribution was in fact a species complex, and we erected the species *C. xavierae* **sp. nov.** for the Atlantic reports. A similar case happens with the species *P. helleri* and *P. euastrum*. Those were thought to inhabit both the deep sea and coastal caves. However, when we compare the sequences from cave specimens with those from deep sea specimens, they showed to be different. The lack of this kind of knowledge may lead to wrong interpretation of the Atlanto-Mediterranean faunal affinities, as well as colonization and connectivity patterns (Chapter 4.4.) .

In some groups, molecular markers are also helpful to disentangle problematic phylogenetic relationships. For example, in Chapter 4.1 we show that the genus *Acarnus* is wrongly assigned to Acarnidae, and that it should be placed in Microcionidae. Also,

we show that the genus *Xestospongia* is polyphyletic, with Mediterranean representatives phylogenetically distant from the tropical ones. Besides, the genus *Stelletta* is polyphyletic, as already pointed out in *Cardenas et al. (2011)* and includes species assigned until now to Geodiidae. In this regard, in Chapter 4.3 the newly described species *Stelletta mortarium* **sp. nov.**, belongs to Geodiidae, but not *S. dichoclada* nor *S. mediterranea*, which are true Ancorinids. A future revision of the genus *Stelletta* and *Geodia* is needed to accommodate *Stelletta*-like *Geodia* species.

In Chapter 4.2 we described one of the most abundant species of the mesophotic area (*Foraminospongia balearica*) and its sister, cryptic and smaller species (*F. minuta*). Regarding the first, it is surprising that such a large and easy to spot and identify species,even without studying its spicules, had remained unknown. Individuals of *F. balearica* usually have small crustaceans and other invertebrates hiding inside its tubes or hiding between the crevices of its body, indicating the species is an habitat engineer for other benthic species of the mesophotic zone. Furthermore, the ecological success of this and several other commonly overlooked species prompts inquiries into their physiology, feeding habits, resilience to fishing impacts, reproductive strategies, and toxicity. In order to understanding their role in the ecosystems of the Balearic Islands, these aspects should be addressed in future research.

In Chapter 4.6 sponge communities from the trawl fishing grounds of the continental shelf and from the Mallorca Channel seamounts were identified and characterised. Depth was the main factor determining the sponge communities, together with other factors like temperature, currents, substrate type, fishing effort and algae biomass. Deep mesophotic communities were positively associated with the presence of soft and calcareous red algae deep beds, like *Peyssonellia* spp. or *Osmundaria volubilis* beds and rhodolith or coralligenous outcrops, respectively. Those habitats showed very high levels of sponge diversity and biomass. In the highly oligotrophic waters of the Balearic Islands, red algae can develop until 130-140 m depth. Those algae serve as substrate for many sponge species, allowing the development of hard substrate species in soft bottoms. For this reason, sedimentary areas covered with red algae beds may act like rocky bottoms, a fact that fuels the diversity of sponges and probably other benthic species. Besides, red algae may feed sponges through the release of dissolved organic matter, a question that should be addressed in future works. These red algae beds have already been considered *sensitive habitats* in the case of rodholith beds, and *essential fish habitats* in general, due to their potential role in the sustainability of demersal fishing resources populations (*Ordines et al., 2015*). The fact that algae beds are hotspots of sponge abundance and diversity in the continental shelf of the Balearic Islands, and their potential overlapping in some areas with trawling fishing grounds, provides another reason that justify the necessity for an urgent detailed cartography of benthic habitats and fishing grounds for the whole the Balearic shelf, in order to be able to manage them according to their ecological importance.

By comparing the sponge communities of the Mallorca Channel seamounts with those from the traditional trawling grounds of the continental shelf, we observed significant

differences, with the seamounts exhibithing higher diversity and biomass. This pattern was particularly evident in the lower mesophotic zone (between 90 and 200 m depth approximately). Many species found within this depth range at seamounts, such as *Geodia geodina*, *S. mortarium*, *Pachastrella monilifera* or *Jaspis* sp1, were absent in the trawl fishing grounds. Moreover, species present in both areas, like *Poecillastra compressa*, *Penares helleri*, *Hamacantha (Vomerula) falcula* or *Petrosia (Petrosia) raphida*, were significantly less abundant in the trawl fishing grounds.

Key components of the mesophotic summits of the seamounts, such as *F. balearica* or *Spongosorites* sp1, were rarely collected in the trawl fishing grounds (see Table S4.6.1, Chapter 4.6. In fact, in trawl fishing grounds, species most negatively affected by fishing pressure were typical lower mesophotic species, including the aforementioned *P. compressa*, *P. helleri*, *H. (V.) falcula* or *P. (P.) raphida* (See Fig. 4.3.2A from Chapter 4.3 and Figs 4.6.9A-B and 4.6.11F from chapter 4.6). In contrast, considering the high diversity and abundance of sponges in shallower trawling grounds of the coastal shelf between 45 and 90 m depth approximately), it appears that in these communities, fishing has a comparatively milder effect, at least at the trawling fishing effort level of the Balearic Islands, fairly lower than other adjacent areas of the Iberian Peninsula (*Quetglas et al., 2012*). This seems to indicate that fishing exploitation have significant effects on deep sea sponge communities, particularly at the lower mesophotic zone. It raises questions about the resilience and physiological thresholds of the deep shelf sponge communities, which might be more sensitive to anthropogenic impacts like bottom trawling. Perhaps, deep mesophotic species that thrive in the lowermost photosyntetic irradiance threshold are the first to be affected by the effects of bottom trawling. It is documented that this activity resuspends sediments and creates nepheloid layers near the bottom that might mitigate the light, affecting photosynthetic or mixotrophic communities (*Arjona-Camas et al., 2022*).

We also observed taxonomic composition changes between areas, with tetractinellids dominating in the seamounts but showing low presence in trawled grounds. This group of sponges may have slow growing rates or be more sensitive to the effects of trawling, like physical removal or damage, sediment resuspension or light attenuation. In contrast, in trawl fishing grounds we found dominance of species like *Desmacella annexa* or *Suberites domuncula*. The former produces mucus when disturbed, while the latter is known to perform a very fast body contraction reaction when collected with a trawling net (personal observations). Those responses may be widespread throughout the sponge communities impacted by trawling, allowing a certain degree of survival after they are discarded. Fast growing species with short life spans may also be present in a higher proportion. In the red algae beds, we found many species with soft red algae leaves embedded in his body, which indicates that the sponge has a similar age than the algae. Identifying the biological traits that determine sensitivity to fishing impacts is crucial for developing management plans addressed to sponge communities.

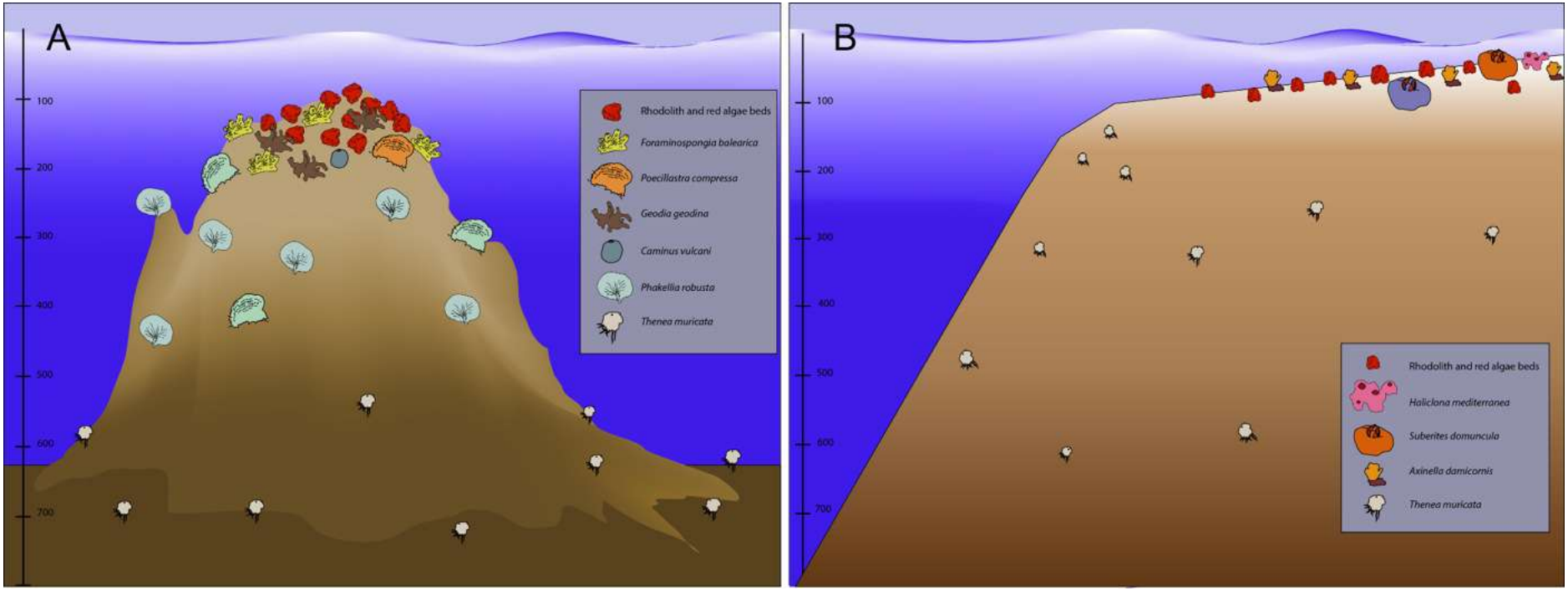

Figure 5.3. Graphical comparisson between the sponge communities of the Ausias March (A) and the trawl fishing grounds (B).

CONCLUSIONS

6. Conclusions

General conclusions

- The Balearic Islands are an area of high sponge diversity and abundance, with an elevated potential for new species discovery. In this PhD, 9 new species and one genus have been described from the Archipelago, along with 38 new geographical records, including 4 new records for the Mediterranean. These results point out that this sea still has a long path to go until the knowledge on sponge communities is complete.

- The combined use of morphological and genetic analyses has allowed the discovery of cryptic species and species complexes, and has helped in understanding the phylogenetic relationship of poorly known groups.

- The elevated diversity and biomass observed in the mesophotic area of the Balearic Islands can be explained by the particularities of the Archipelago, like the heterogeneity of habitats, the elevated oligotrophy and the low trawl fishing pressure. The high water transparency promotes the development of photosynthetic and mixotrophic communities down to 90-100 m on the trawl fishing grounds of the Balearic shelf and to 130-140 m on the seamounts of the Mallorca Channel. The prevalence of coralligenous red algae beds in such depths also provides substrate to the sponges.

Taxonomy

- COI phylogenetics showed that the family Acarniidae is polyphyletic with the genus *Acarnus* belonging to Microcionidae and that the species *Haliclona poecillastroides* is wrongly assigned to the family Chaliniidae.

- The sponge communities of the Mallorca Channel seamounts host many rare or unknown sponge species, including the newly described genus *Foraminospongia*, and the species *Foraminospongia balearica, Foraminospongia minuta* and *Paratimea massutii*.

- *Foraminospongia balearica* is one of the most abundant species of the summits of Emile Baudot and Ausias March seamounts and is also a habitat engineer. The description of such relevant species highlights the importance of deep-sea exploration.

- A thorough study of the order Tetractinellida reveals that this group is one of the most speciose of the Balearic Islands. With the description of six new species and 18 new records from the Archipelago, this order currently accounts for a total of 39 species.

- The use of integrative taxonomy has revealed two patterns of species complexes: 1) species thought to have an Atlantic-Mediterranean distribution have been shown to be two separate species, such as *Caminus vulcanii* and *Caminus xavierae* **sp. nov.**; and 2) species believed to be distributed in caves and deep-sea environments also proved to be different, such as *Penares euastrum* and *P. cavernensis* **sp. nov.**, and *P. helleri* and *P. isabellae* **sp. nov.** This should be considered in future biogeography and connectivity studies, emphasizing the importance of employing an integrative approach.

- Taking into account the relatively low sampling developed in littotal caves, these are promising ecosystems for increasing the sponge biodiversity knowledge of the Balearic Islands, as shown by the description of *Penares cavernensis* **sp. nov.** and *Penares isabellae* **sp. nov.** and by several new records.

Communities

- 6 assemblages were identified at seamounts and 14 assemblages were identified at trawl fishing grounds. At trawl fishing grounds, 8 assemblages were identified from experimental bottom trawl samples, and 6 assemblages were identified from beam trawl samples, suggesting potential overlap. In both seamounts and trawl fishing grounds, depth was the main factor affecting their distribution. Besides, sponge biodiversity and biomass was concentrated in the photic zone and tighly related to the presence of red algae beds. When red algae beds disappear, sponge presence becomes less important. Moreover, substrate type, temperature, current velocity and fishing effort also affect the distribution of sponge communities.

- The limit at which red algae and the associated sponges thrive is different in the trawl fishing grounds than in the untrawled summits and flanks of the Mallorca Channel seamounts, being shallower at trawl fishing grounds (90 *vs.* 130-140 m depth). This suggests that trawling significally impacts deep sea mesophotic communities.

Conclusions Generals

- Les Illes Balears són una zona d'alta diversitat i abundància d'esponges, amb un elevat potencial per al descobriment de noves espècies. En aquesta tesi doctoral, s'han descrit 9 noves espècies i un nou gènere, juntament amb 38 noves cites geogràfiques, incloent 4 noves cites per a la Mediterrània. Aquests resultats indiquen que encara queda molt camí per recórrer fins a completar el coneixement de les comunitats d'esponges a les nostres aigues.

- L'ús combinat d'anàlisis morfològiques i genètiques ha permès descobrir espècies críptiques i complexos d'espècies, i ha ajudat a comprendre les relacions filogenètiques de grups poc coneguts.

- La diversitat i biomassa elevades observades a la zona mesofòtica de les Illes Balears es poden explicar per les particularitats de l'arxipèlag, com ara l'heterogeneïtat dels hàbitats, l'alta oligotròfia i la baixa pressió pesquera. L'alta transparència de l'aigua afavoreix el desenvolupament de comunitats fotosintètiques en un ampli rang batimètric, fins a uns 130-140 m aproximadament, proporcionant substrat a les esponges i afavorint el desenvolupament d'espècies amb fotobionts.

Taxonomia

- La filogenia basada en el COI indica que la família Acarniidae és polifilètica, amb el gènere *Acarnus* pertanyent a la familía Microcionidae, i també que l'espècie *Haliclona poecillastroides* està incorrectament assignada a la amilia Chalinidae.

- Les comunitats d'esponges dels monts submarins del Canal de Mallorca alberguen un gran nombre d'espècies rares o desconegudes, incloent-hi el nou gènere *Foraminospongia* i les noves espècies *F. baleárica* **sp. nov.**, *F. minuta* **sp. nov.** i *Paratimea massutii* **sp. nov.**.

- *Foraminospongia balearica* **sp. nov.** és una de les espècies més abundants als cims dels monts submarins Emile Baudot i Ausias March i també una espècie que crea hàbitats. La descripció d'una espècie tan rellevant com aquesta remarca la importància de l'exploració en aigües profundes.

- Un estudi detallat de l'ordre Tetractinellida ha revelat que aquest grup és un del més diversos de les Illes Balears. Amb la descripció de 6 noves espècies i 18 noves cites per a l'arxipèlag, aquest ordre actualment compta amb un total de 39 espècies. A més, s'han descrit dues noves espècies per a l'oceà Atlàntic Nord.

- L'ús de la taxonomia integrativa ha posat de manifest dos patrons de complexes d'espècies: 1) s'ha demostrat que espècies que es pensava que tenien una distribució atlàntico-mediterrània en realitat son dues espècies separades, com

Caminus vulcanii Caminus xavierae **sp. nov.** i *Geodia geodina*/*Geodia phlegraeioides* **sp. nov.**; i 2) espècies que es pensava que es distribuïen en coves i ambients marins profunds també van demostrar ser diferents, com *Penares euastrum* i *P. cavernensis* **sp. nov.** i *P. helleri* i *P. isabellae* **sp. nov.** Això ha de tenir-se en compte en futurs treballs de biogeografia i connectivitat, destacant la importància de l'ús d'un enfocament integratiu.

- Tenint en compte la baixa intensitat de mostreig realitzat a les coves litorals i els notables resultats obtinguts, aquests ecosistemes són prometedors per augmentar el coneixement de la biodiversitat d'esponges a les Illes Balears, com es mostra amb la descripció de *P. cavernensis* **sp. nov.** i *P. isabellae* **sp. nov.** i diverses noves cites de tetractinèl·lides.

Comunitats

- S'han identificat 6 agrupacions als monts submarins i 14 agrupacions a zones de pesca de ròssec, essent la profunditat el principal factor que afecta la seva distribució. A més, la diversitat i biomassa d'esponges es concentra a la zona fòtica i està relacionada amb la presència de fons d'algues vermelles. Quan aquests desapareixen, la presència d'esponges esdevé menys rellevant. Per altra banda, s'ha vist que el tipus de substrat, la temperatura, la velocitat dels corrents i l'esforç de pesca també afecten la distribució de les comunitats d'esponges de les Illes Balears.

- El límit en què prosperen les algues vermelles i les esponges associades és diferent a les zones de pesca de ròssec que als cims i vessants no explotats de les muntanyes submarines del Canal de Mallorca, sent menys profund a les zones de pesca de ròssec (90 *vs.* 130-140 m). Això suggereix que el ròssec impacta especialment a les comunitats mesofòtiques de fondària.

Conclusiones Generales

- Las Islas Baleares son una zona de alta diversidad y abundancia de esponjas, con un elevado potencial para el descubrimiento de nuevas especies. En esta tesis doctoral, se han descrito 9 especies nuevas y un género nuevo, junto con 38 nuevas citas geográficas, incluyendo 4 nuevas citas para el Mediterráneo. Estos resultados indican que aún queda un largo camino por recorrer hasta completar el conocimiento sobre las comunidades de esponjas en nuestras aguas.

- El uso combinado de análisis morfológicos y genéticos ha permitido descubrir especies crípticas y complejos de especies, y ha contribuido a comprender las relaciones filogenéticas de grupos poco conocidos.

- La diversidad y biomasa elevadas observadas en la zona mesofótica de las Islas Baleares se pueden explicar por las particularidades del archipiélago, como la heterogeneidad de hábitats, la alta oligotrofia y la baja presión pesquera. La alta transparencia del agua favorece el desarrollo de comunidades fotosintéticas en un amplio rango batimétrico, hasta unos 130-140 m aproximadamente, proporcionando sustrato a las esponjas y favoreciendo el desarrollo de especies con fotobiontes.

Taxonomía

- La filogenia basada en el COI indica que la familia Acarniidae es polifilética, con especies del género *Acarnus* que pertenecen a Microcionidae, y también que la especie *Haliclona poecillastroides* está incorrectamente asignada a la familia Chalinidae.

- Las comunidades de esponjas de los montes submarinos del Canal de Mallorca albergan un gran número de especies raras o desconocidas, incluyendo el nuevo género *Foraminospongia* y las nuevas especies *F. balearica* **sp. nov.**, *F. minuta* **sp. nov.** y *Paratimea massutii* **sp. nov.**

- *Foraminospongia balearica* **sp. nov.** es una de las especies más abundantes en las cimas de los montes submarinos Emile Baudot y Ausias March y también es una especie ingeniera de hábitats. La descripción de una especie tan relevante como esta destaca la importancia de la exploración en aguas profundas.

- Un estudio detallado del orden Tetractinellida ha revelado que este grupo es uno de los más diversos de las Islas Baleares. Con la descripción de 6 nuevas especies y 18 nuevos registros para el archipiélago, este orden actualmente cuenta con un total de 39 especies. Además, se han descrito dos nuevas especies para el oceano Àtlantico Norte.

- El uso de la taxonomía integrativa ha puesto de manifiesto dos patrones de complejos de especies: 1) se ha demostrado que especies que se pensaba que

tenían una distribución atlántico-mediterránea resultaron ser diferentes, como *Caminus vulcanii* y *Caminus xavierae* **sp. nov.**, *Geodia geodina* y *Geodia phlegraeioides* **sp. nov.**; y 2) especies que se pensaba que se distribuían en cuevas y ambientes marinos profundos también resultaron ser diferentes, como *Penares euastrum* y *P. cavernensis* **sp. nov.** y *P. helleri* y *P. isabellae* **sp. nov.**. Esto debe tenerse en cuenta en futuros trabajos de biogeografía y conectividad, destacando la importancia de utilizar un enfoque integrativo.

- Teniendo en cuenta la baja intensidad de muestreo realizada en cuevas litorales, estos ecosistemas son prometedores para aumentar el conocimiento de la biodiversidad de esponjas en las Islas Baleares, como se muestra con la descripción de *P. cavernensis* **sp. nov.** y *P. isabellae* **sp. nov.** y diversas nuevas citas de tetractinélidas.

Comunidades

- Se han identificado 6 agrupaciones en montes submarinos y 14 agrupaciones en zonas de pesca de arrastre, siendo la profundidad el principal factor que afecta su distribución. Además, la diversidad y biomasa de esponjas se concentran en la zona fótica y están relacionadas con la presencia de fondos de algas rojas. Cuando estos fondos desaparecen, la presencia de esponjas se vuelve menos relevante. Por otro lado, se ha visto que el tipo de sustrato, la temperatura, la velocidad de las corrientes y el esfuerzo de pesca también afectan la distribución de las esponjas.

- El límite en el que prosperan las algas rojas y las esponjas asociadas es diferente en las zonas de pesca de arrastre que en las cimas y laderas no explotadas de los montes submarinos del Canal de Mallorca, siendo menos profundo en las zonas de pesca de arrastre (90 *vs.* 130-140 m). Esto sugiere que la pesca de arrastre impacta especialmente a las comunidades mesofóticas de aguas profundas.

REFERENCES

7. References

Abdul Wahab MA, Wilson NG, Prada D, Gomez O, and Fromont J. 2020. Molecular and morphological assessment of tropical sponges in the subfamily Phyllospongiinae, with the descriptions of two new species. *Zoological Journal of the Linnean Society.* 1931, 319-335.

Acosta J, Canals M, López-Martınez J, Munoz A, Herranz P, Urgeles R, Palomo C, and Casamor JL. 2002. The Balearic Promontory Geomorphology Western Mediterranean: morphostructure and active processes. *Geomorphology.* 49, 177-204

Acosta J, Ancochea E, Canals M, Huertas MJ, and Uchupi E. 2004. Early Pleistocene volcanism in the Emile Baudot Seamount, (Balearic Promontory, western Mediterranean Sea). *Marine Geology*. 207, 247-257.

Aguilar R, López-Correa M, Calcinai B, Pastor X, de la Torriente A, and García S. 2011. First records of *Asbestopluma hypogea* Vacelet and Boury-Esnault, 1996 (Porifera, Demospongiae Cladorhizidae) on seamounts and in bathyal settings of the Mediterranean Sea. *Zootaxa*. 2925, 33-40.

Aguilar-Camacho JM*,* Carballo JL*,* and Cruz-Barraza JA. 2013. Acarnidae (Porifera: Demospongiae: Poecilosclerida) from the Mexican Pacific Ocean with the description of six new species. *Scientia Marina.* 77, 677-696.

Alonso B. Guillén J, Canals M, Serra-Kiel J, Acosta, J, Herranz P, Sanz-Alonso JL, Calaf A. & Catafau E. 1988. Los sedimentos de la plataforma continental balear. Ávila, E, Riosmena-Rodríguez, R, & Hinojosa-Arango, G. 2013. Sponge–rhodolith interactions in a subtropical estuarine system. *Helgoland Marine Research*, 67, 2, 349-357.

Altschul SF, Gish W, Miller W, Myers EW, and Lipman DJ. 1990. Basic local alignment search tool. *Journal of Molecular Biology*. 215, 403-410.

Alvarez B, Hooper JNA. 2002. Family Axinellidae Carter, 1875. Pp. 724-747. In: Hooper, JNA, and Van Soest RWM. ed. *Systema Porifera. A guide to the classification of sponges*. 1 Kluwer Academic/ Plenum Publishers: New York, Boston, Dordrecht, London, Moscow.

Alvarez B, Frings PJ, Clymans W, Fontorbe G, and Conley DJ. 2017. Assessing the potential of sponges (Porifera) as indicators of ocean dissolved Si concentrations. *Frontiers in Marine Science*. 4, 373.

Amade P, and Lemee R. 1998. Chemical defence of the Mediterranean alga Caulerpa taxifolia: variations in caulerpenyne production. *Aquatic toxicology*. 434, 287-300.

Anon. 2017. MEDITS Handbook Version nº 9, 106 pp.

Arjona-Camas M, Puig P, De Leo FC, Garner G, Paradis S, Durán R, and Palanques A. 2022. Influence of Natural Processes and Bottom Trawling in the Nepheloid Layer Structure Off Vancouver Island British Columbia, Canada, NE Pacific. *Frontiers in Marine Science*. 8, 2111.

Babiç K. 1922. Monactinellida und Tetractinellida des Adriatischen Meeres. Zoologische Jahrbücher. Abteilung für Systematik, Geographie und Biologie der Tiere. 462: 217-302, pls 8-9.

Bahia RG, Abrantes DP, Brasileiro PS, Pereira Filho GH, and Amado Filho GM. 2010. Rhodolith bed structure along a depth gradient on the northern coast of Bahia State, Brazil. *Brazilian journal of oceanography*. 58, 323-337.

Bakran-Petricioli T, Vacelet J, Zibrowius H, Petricioli D, Chevaldonné P, Raa T. 2007. New data on the distribution of the 'deep-sea' sponges *Asbestopluma hypogea* and *Oopsacas minuta* in the Mediterranean Sea. *Marine Ecology*. 28, Suppl. 1, 10-23.

Ballesteros E. 1992. Els fons rocosos profunds amb *Osmundaria volubilis* Linné. R.E. Norris a les Balears. *Bolletí de la Societat d'Història Natural de les Illes Balears.* 35, 33-50.

Ballesteros E. 1994. The Deep-Water Peyssonnelia Beds from the Balearic Islands (Western Mediterranean). *Marine Ecology*. 153-4, 233-253.

Bandaranayake WM. 2006. The nature and role of pigments of marine invertebrates. *Natural Product Reports*. 232, 223-255.

Barberá C, Bordehore C, Borg J.A, Glémarec M, Grall J, Hall-Spencer J.M, de la Huz C, Lanfranco E, Lastra M. and Moore P.G. 2003. Conservation and management of northeast Atlantic and Mediterranean maerl beds. *Aquatic Conservation: Marine and Freshwater Ecosystems*, 13, S65-S76.

Barberá C, Moranta J, Ordines F, Ramón M, De Mesa A, Díaz-Valdés M, Grau AM, and Massutí E. 2012. Biodiversity and habitat mapping of Menorca Channel (western Mediterranean): implications for conservation. *Biodiversity and conservation*. 21, 701-728.

Barcelona SG, De Urbina JMO, De La Serna JM, Alot E, Macías D. 2010. Seabird bycatch in Spanish Mediterranean large pelagic longline fisheries, 2000–2008. *Aquatic Living Resources*, 23, 363-371.

Bart MC, Hudspith M, Rapp HT, Verdonschot PF, and De Goeij JM. 2021. A deep-sea sponge loop? sponges transfer dissolved and particulate organic carbon and nitrogen to associated fauna. *Frontiers in Marine Science*. 8, 604879.

Basso D. 1998. Deep rhodolith distribution in the Pontian Islands, Italy: a model for the paleoecology of a temperate sea. *Palaeogeography, palaeoclimatology, palaeoecology*. 1371-2, 173-187.

Bavestrello G, Bonito M, and Sarà M. 1993. Influence of depth on the size of sponge spicules. *Scientia Marina.* 57, 415-420.

Beazley LI, Kenchington EL, Murillo FJ, and Sacau MDM. 2013. Deep-sea sponge grounds enhance diversity and abundance of epibenthic megafauna in the Northwest Atlantic. *ICES Journal of Marine Science*. 70, 7, 1471-1490.

Becking LE. 2013. Revision of the genus *Placospongia* (Porifera, Demospongiae, Hadromerida, Placospongiidae) in the Indo-West Pacific. *ZooKeys*. 298, 39.

Bell JJ. 2008. The functional roles of marine sponges. *Estuarine, Coastal and Shelf Science.* 79, 341-353.

Bellas J. 2014. The implementation of the Marine Strategy Framework Directive: Short comings and limitations from the Spanish point of view. *Marine Policy*, 50, 10-17.

Bertolino M, Cerrano C, Bavestrello G, Carella M, Pansini M, Calcinai B. 2013. Diversity of Porifera in the Mediterranean coralligenous accretions, with description of a new species. *ZooKeys*. 336, 1-37.

Bertolino M, Bo M, Canese S, Bavestrello G, and Pansini M. 2015. Deep sponge communities of the Gulf of St Eufemia (Calabria, southern Tyrrhenian Sea), with description of two new species. Marine Biological Association of the United Kingdom. *Journal of the Marine Biological Association of the United Kingdom*. 957, 1371.

Bertrand JA, de Sola LG, Papaconstantinou C, Relini G, and Souplet A. 2002. The general specifications of the MEDITS surveys. *Scientia Marina*. 66, 9-17.

Biagi F, Sartor P. Ardizzone G.D, Belcari P, Belluscio A. & Serena F. 2022. Analysis of demersal assemblages off the Tuscany and Latium coasts (north-western Mediterranean). *Scientia Marina*, 66 (Supplement 2): 233-242.

Bibiloni MA. 1981. Estudi faunistic del litoral de Blanes (Girona), II. Sistemàtica d'esponges, *Butlletí de la Institució Catalana d'Història Natural.* 47, 5-59.

Bibiloni MA. 1990. *Fauna de Esponjas de las Islas Baleares. Variación cualitativa y cuantitativa de la población de esponjas en un gradiente batimétrico. Comparación Baleares-Costa Catalana*. PhD Thesis. Universitat de Barcelona, Barcelona, Spain.

Bibiloni MA. 1993. Some new or poorly known sponges of the Balearic Islands (western Mediterranean). *Scientia Marina*. 574, 307-318.

Bibiloni MA, and Gili JM. 1982. Primera aportación al conocimiento de las cuevas submarinas de la isla de Mallorca. *Oecologia aquatica*. 66, 227-234.

Bibiloni MA, Uriz MJ, and Gili JM. 1989. Sponge communities in three submarine caves of the Balearic Islands (Western Mediterranean): adaptations and faunistic composition. *Marine Ecology.* 10, 317-334.

Bibiloni MA, Uriz MJ, and Ros JD. 1998. Faunal affinities of the Sponges (Porifera) of the Balearic Islands with those of other biogeographical areas. *Oecologia aquatica*. 11.

Bidder GP, 1923. The relation of the form of a sponge to its currents. *The Quarterly Journal of Microscopical Science*. 67, 293-323.

Blanchet F.G, Legendre P. & Borcard D. 2008. Forward selection of explanatory variables. *Ecology*, 89, 2623-2632.

Blanquer A, and Uriz MJ. 2008. 'A posteriori' searching for phenotypic characters to describe new cryptic species of sponges revealed by molecular markers (Dictyonellidae: Scopalina). *Invertebrate Systematics*. 22, 5, 489-502.

Bo M, Bertolino M, Borghini M, Castellano M, Harriague AC, Di Camillo CG, Gasparini G, Gasparini C, Paolo M, Povero P, Pusceddu A, Schroeder K, and Bavestrello G. 2011. Characteristics of the mesophotic megabenthic assemblages of the Vercelli seamount North Tyrrhenian Sea. *PLoS One*. 62, e16357.

Bo M, Coppari M, Betti F, Enrichetti F, Bertolino M, Massa F, Bava S, Gay G, Cattaneo-Vietti R, and Bavestrello G. 2020. The high biodiversity and vulnerability of two Mediterranean bathyal seamounts support the need for creating offshore protected areas. *Aquatic Conservation: Marine and Freshwater Ecosystems*. 1-24.

Borja A, Elliott M, Carstensen J, Heiskanen A.-S, van de Bund W. 2010. Marine management - towards an integrated implementation of the European Marine Strategy Framework and the Water Framework Directives. *Marine Pollution Bulletin*, 60, 2175-2186.

Bosc E, Bricaud A, and Antoine D. 2004. Seasonal and interannual variability in algal biomass and primary production in the Mediterranean Sea, as derived from 4 years of SeaWiFS observations. *Global Biogeochemichal Cycles*. 18, GB1005.

Boury-Esnault N. 1971. Spongiaires de la zone rocheuse de Banyuls-sur-Mer. II. Systématique. *Vie et Milieu*. 222, 287-349

Boury-Esnault N. 1971. spongiaires de la zone rocheuse littorale de Banyuls-sur-mer I. Écologie et répartition. *Vie et Milieu*. 159-191.

Boury-Esnault N, and Lopes MT. 1985. Les Démosponges littorales de l'Archipel des Açores. *Annales de l'Institut océanographique*. 612, 149-225.

Boury-Esnault N, and Rützler K. 1997. Thesaurus of sponge morphology. *Smithsonian contributions to zoology.* 596, 1-55.

Boury-Esnault N, Pansini M, and Uriz MJ. 1994. Spongiaires bathyaux de la mer d'Alboran et du golfe ibéro-marocain. *Mémoires du Muséum national d'histoire naturelle.* 1993, 160.

Boury-Esnault N, Vacelet J, Dubois M, Goujard A, Fourt M, Perez T, & Chevaldonne P. 2017. New hexactinellid sponges from deep Mediterranean canyons. *Zootaxa*, 4236, 1, 118-134.

Bowerbank JS. 1866. A Monograph of the British Spongiadae. Volume 2. Ray Society: London: i-xx, 1-388.

Braak CJF. & Smilauer P. 2018. Canoco reference manual and user's guide: software for ordination (version 5.10). *Microcomputer Power* (Ithaca, NY, USA), 536 pp.

Bucchich G. 1886. Alcune spugne dell' Adriatico sconosciute en nuove. *Bollettino della Società Adriatica di Scienze Naturali in Trieste*. 9, 222-225.

Burton M. 1931. The Folden Fiord. Report on the sponges collected by Mr. Soot-Ryven in the Folden Fiord in the year 1923. *Tromsø Museum Skrifter.* 1, 1-8.

Burton M. 1946. Notes on certain species of Geodia described by Oscar Schmidt. *Annals and Magazine of Natural History*, Ser. 11, vol. xiii, 856-860.

Burton M. 1956. The sponges of West Africa. Atlantide Report Scientific Results of the Danish Expedition to the Coasts of Tropical West Africa, 1945-1946, Copenhagen. 4, 111-147.

Calcinai B, Moratti V, Martinelli M, Bavestrello G, and Taviani M. 2013. Uncommon sponges associated with deep coral bank and maerl habitats in the Strait of Sicily (Mediterranean Sea). *Italian Journal of Zoology*. 803, 412-423.

Canals M, and Ballesteros E. 1997. Production of carbonate particles by phytobenthic communities on the Mallorca-Menorca shelf, northwestern Mediterranean Sea. *Deep Sea Research Part II: Topical Studies in Oceanography*. 443-4, 611-629.

Cárdenas P. 2020. Surface microornamentation of demosponge sterraster spicules, phylogenetic and paleontological implications. *Frontiers in Marine Science*. 7, 613610.

Cárdenas P, and Rapp HT. 2012. A review of Norwegian streptaster-bearing Astrophorida (Porifera: Demospongiae: Tetractinellida), new records and a new species. *Zootaxa*. 3253, 1-53.

Cárdenas P, and Rapp HT. 2013. Disrupted spiculogenesis in deep-water Geodiidae (Porifera, Demospongiae) growing in shallow waters. *Invertebrate Biology*. 1323, 173-194.

Cárdenas P, and Rapp HT. 2015. Demosponges from the Northern Mid-Atlantic Ridge shed more light on the diversity and biogeography of North Atlantic deep-sea sponges. *Journal of the Marine Biological Association of the United Kingdom*. 957, 1475-1516.

Cárdenas P, and Moore JA. 2019. First records of Geodia demosponges from the New England seamounts, an opportunity to test the use of DNA mini-barcodes on museum specimens. *Marine Biodiversity*. 491, 163-174.

Cardenas P, Menegola C, Rapp HT, and Díaz MC. 2009. Morphological description and DNA barcodes of shallow-water Tetractinellida (Porifera: Demospongiae) from Bocas del Toro, Panama, with description of a new species. *Zootaxa*. 22761, 1-39.

Cárdenas P, Rapp HT, Schander C, and Tendal OS. 2010. Molecular taxonomy and phylogeny of the Geodiidae (Porifera, Demospongiae, Astrophorida)-combining phylogenetic and Linnaean classification. *Zoologica scripta*. 391, 89-106.

Cárdenas P, Xavier JR, Reveillaud J, Schander C, and Rapp HT. 2011. Molecular phylogeny of the Astrophorida (Porifera, Demospongiae) reveals an unexpected high level of spicule homoplasy. *PLoS One*. 64.

Cárdenas P, Pérez T, and Boury-Esnault N. 2012. Sponge Systematics Facing New Challenges. In: Becerro MA, Uriz MJ, Maldonado M, and Turon X. (eds). *Advances in Sponge Science: Phylogeny, Systematics, Ecology. Advances in Marine Biology.* 61, 79-209.

Cárdenas P, Vacelet J, Chevaldonne P, Pérez T, and Xavier JR. 2018. From marine caves to the deep sea, a new look at Caminella (Demospongiae, Geodiidae) in the Atlanto-Mediterranean region. *Zootaxa*. 44661, 174-196.

Cariello L, and Zanetti L. 1981. A blue carotenoprotein from the marine sponge *Suberites domuncula*: purification and properties. *Marine Biology*. 62, 151-155.

Carter HJ. 1873. On the Hexactinellidae and Lithistidae generally, and particularly on the Aphrocallistidae, Aulodictyon, and Farreae, together with Facts elicited from their Deciduous Structures and Descriptions respectively of Three New Species. *Annals and Magazine of Natural History*. (4) 12, 71, 349-373, 437-472

Carter HJ. 1876. Descriptions and Figures of Deep-Sea Sponges and their Spicules, from the Atlantic Ocean, dredged up on board H.M.S. ‘Porcupine', chiefly in 1869 concluded. *Annals and Magazine of Natural History*. 4. 18105, 226-240; 106, 307-324; 107, 388-410; 108, 458-479.

Carteron S. 2002. Étude taxonomique des Spongiaires du Liban. *Rapport de Maitrise, Centre d'Océanologie de Marseille*. 1-26.

Cartes J. E, Maynou F, Morales-Nin B, Massutí E & Moranta J. 2001. Trophic structure of a bathyal benthopelagic boundary layer community south of the Balearic Islands (southwestern Mediterranean). *Marine Ecology Progress Series*, 215, 23-35.

Cartes JE, Papiol V, & Guijarro B. 2008. The feeding and diet of the deep-sea shrimp Aristeus antennatus off the Balearic Islands (Western Mediterranean): Influence of environmental factors and relationship with the biological cycle. *Progress in Oceanography*, 79, 1, 37-54.

Carvalho FC, Cárdenas P, Ríos P, Cristobo J, Rapp HT, and Xavier JR. 2020. Rock sponges (lithistid Demospongiae) of the Northeast Atlantic seamounts, with description of ten new species. *PeerJ*, 8, e8703.

Carvalho MDS, Lopes DA, Cosme B, and Hajdu E. 2016. Seven new species of sponges (Porifera) from deep-sea coral mounds at Campos Basin SW Atlantic. *Helgoland marine research.* 70, 10.

Castelin M, Lambourdiere J, Boisselier MC, Lozouet P, Couloux A, Cruaud C, and Samadi S. 2010. Hidden diversity and endemism on seamounts: focus on poorly dispersive neogastropods. *Biological Journal of the Linnean Society*. 1002, 420-438.

Cedro VR, Hajdu E, and Correia MD. 2013. Three new intertidal sponges Porifera: Demospongiae from Brazil's fringing urban reefs Maceió, Alagoas, Brazil, and support for Rhabderemia's exclusion from Poecilosclerida. *Journal of Natural History*. 4733-34, 2151-2174.

Chombard C, Boury-Esnault N, and Tillier S. 1998. Reassessment of homology of morphological characters in tetractinellid sponges based on molecular data. *Systematic Biology*. 473, 351-366.

Clark MR, Schlacher TA, Rowden AA, Stocks KI, and Consalvey M. 2012. Science priorities for seamounts: research links to conservation and management. *PloS one*. 71, e29232.

Clarke KR, and Warwick RM. 1994. Similarity-based testing for community pattern: the two-way layout with no replication. *Marine biology*. 118, 167-176.

Clarke KR, Somerfield PJ, and Gorley RN. 2008. Testing of null hypotheses in exploratory community analyses: similarity profiles and biota-environment linkage. *Journal of Experimental Marine Biology and Ecology.* 366, 56-69.

Colaço A, Rapp HT, Campanyà-Llovet N, and Pham CK. 2022. Bottom trawling in sponge grounds of the Barents Sea (Arctic Ocean): A functional diversity approach. *Deep Sea Research Part I: Oceanographic Research Papers*. 183, 103742.

Coll M, Piroddi C, Steenbeek J, Kaschner K, Ben Rais Lasram F, Aguzzi J, Ballesteros E, Bianchi CN, Corbera J, Dailianis T, Danovaro R, Estrada M, Froglia C, Galil BS, Gasol JM, Gertwagen R, Gil J, Guilhaumon F, Kesner-Reyes K, Kitsos MS, Koukouras A, Lampadariou N, Laxamana E, López-Fé de la Cuadra CM, Lotze HK, Martin D, Mouillot D, Oro D, Raicevich S, Rius-Barile J, Saiz-Salinas JI, San Vicente C, Somot S, Templado J, Turon X, Vafidis D, Villanueva R, and Voultsiadou E. 2010. The Biodiversity of the Mediterranean Sea: Estimates, Patterns, and Threats. *PloS one*. 58, e11842.

Corbera G, Iacono CL, Gràcia E, Grinyó J, Pierdomenico M, Huvenne VA, Aguilar R, and Gili JM. 2019. Ecological characterisation of a Mediterranean cold-water coral reef: Cabliers Coral Mound Province (Alboran Sea, western Mediterranean). *Progress in Oceanography*. 175, 245-262.

Corriero G, Scalera-Liaci L, Gristina M, Riggio S, Mercurio M. 1997. Composizione tassonomica e distribuzione della fauna e Poriferi e Briozoi in una grotta semisommersa

della riserva naturale marina "Isola di Ustica". *Biologia Marina Mediterranea*. 4, 1, 34-43.

Corriero G, Scalera-Liaci L, Ruggiero D, Pansini M. 2000. The sponge community of a semi-submerged Mediterranean cave. *Marine Ecology*. 21, 1, 85-96.

Corriero G, Gadaleta F, and Bavestrello G. 2015. A new Mediterranean species of *Tethya* (Porifera: Tethyida: Demospongiae). *Italian Journal of Zoology.* 82, 535-543.

Costa G, Bavestrello G, Micaroni V, Pansini M, Strano F, and Bertolino M. 2019. Sponge community variation along the Apulian coasts Otranto Strait over a pluri-decennial time span. Does water warming drive a sponge diversity increasing in the Mediterranean Sea? *Journal of the Marine Biological Association of the United Kingdom*. 99, 7, 1519-1534.

Costello MJ, Emblow C, and White RJ. 2001. European register of marine species: a check-list of the marine species in Europe and a bibliography of guides to their identification.

Crochelet E, Barrier N, Andrello M, Marsac F, Spadone A, and Lett C. 2020. Connectivity between seamounts and coastal ecosystems in the Southwestern Indian Ocean. *Deep Sea Research Part II: Topical Studies in Oceanography*. 104774.

Cruz T. 2002. *Esponjas marinas de Canarias*. Consejería de Política Territorial y Medio Ambiente del Gobierno de Canarias, S/C Tenerife, 260 pp.

Culver DC, and Pipan T. 2009. Caves, as islands. p. 150-153. In: *Encyclopedia of islands*. Gillespie RG, Clague DA, Eds. University of California Press.

Danovaro R, Corinaldesi C, D'Onghia G, Galil B, Gambi C, Gooday AJ, Lampadariou N, Luna GM, Morigi C, Olu K, Polymenakou P, Ramirez-Llodra E, Sabbatini A, Sardà F, Sibuet M, and Tselepides A. 2010. Deep-sea biodiversity in the Mediterranean Sea: the known, the unknown, and the unknowable. *PloS one.* 5, e11832.

Danovaro R, Fanelli E, Canals M, Ciuffardi T, Fabri MC, Taviani M, Argyrou M, Azurro E, Bianchelli S, Cantafaro A, Carugati L, Corinaldesi C, P De Haan W, Dell'Anno A, Evans J, Foglini F, Galil B, Gianni M, Goren M, Greco S, Grimalt J, Güell-Bujons Q, Jadaud A, Knittweis L, Lopez JL, Sanchez-Vidal A, Schembri PJ, Snelgrove P, Vaz S, Angeletti L, Barsanti M, Borg JA, Bosso M, Brind'Amour A, Castellan G, Conte F, Delbono I, Galgani F, Morgana G, Prato S, Schirone A, and Soldevilla E. 2020. Towards a marine strategy for the deep Mediterranean Sea: Analysis of current ecological status. *Marine Policy*. 112, 103781.

de Forges BR, Koslow JA, and Poore GCB. 2000. Diversity and endemism of the benthic seamount fauna in the southwest Pacific. *Nature*. 4056789, 944-947.

De Goeij JM, Van Oevelen D, Vermeij MJ, Osinga R, Middelburg JJ, De Goeij AF, and Admiraal W. 2013. Surviving in a marine desert: the sponge loop retains resources within coral reefs. *Science*. 3426154, 108-110.

De la Torriente A, Serrano A, Fernández-Salas LM, García M, and Aguilar R. 2018. Identifying epibenthic habitats on the Seco de los Olivos Seamount: Species assemblages and environmental characteristics. *Deep Sea Research Part I: Oceanographic Research Papers*. 135, 9-22.

de Voogd NJ, Alvarez B, Boury-Esnault N, Cárdenas P, Díaz MC, Dohrmann M, Downey R, Goodwin C, Hajdu E, Hooper JNA, Kelly M, Klautau M, Lim SC, Manconi R, Morrow C, Pinheiro U, Pisera AB, Ríos P, Rützler K, Schönberg C, Turner T, Vacelet J, van Soest RWM, Xavier J. 2024. World Porifera Database. Accessed at https://www.marinespecies.org/porifera on 2024-03-20.

de Weerdt WH. 2000. A monograph of the shallow-water Chalinidae (Porifera, Haplosclerida) of the Caribbean. *Beaufortia*. 50, 1-67.

Desqueyroux-Faundez R, and Valentine C. 2002. Family Petrosiidae Van Soest, 1980. In Hooper JNA and van Soest RWM eds, *Systema Porifera: A Guide to the Classification of Sponges*, vol 1. New York, NY: Kluwer Academic/Plenum, pp. 906-917.

Dias A, Santos GG, Pinheiro U. 2019. A new species of *Characella* Sollas, 1886 Tetractinellida, (Demospongiae; Porifera) from deeper waters off the coast of Brazil. *Zootaxa*. 45591, 196-200.

Díaz JA, Movilla-Martín J, Ferriol P. 2019. Individualistic patterns in the budding morphology of the Mediterranean demosponge *Aplysina aerophoba*. *Mediterranean Marine Science*. Vol. 20, no 2, p. 282-286.

Díaz JA, Ramírez-Amaro S, Ordines F, Cárdenas P, Ferriol P, Terrasa B, and Massutí E. 2020. Poorly known sponges in the Mediterranean with the detection of some taxonomic inconsistencies. *Journal of the Marine Biological Association of the United Kingdom*. 1008, 1247-1260.

Díaz JA, Ramírez-Amaro S, Ordines F. 2021. Sponges of Western Mediterranean seamounts: New genera, new species and new records. *PeerJ*. 9, e11879.

Díaz JA, Ordinas F, Farriols MT, Melo-Aguilar C, & Massutí E. 2024. Sponge assemblages in fishing grounds and seamounts of the Balearic Islands (western Mediterranean). *Deep Sea Research Part I: Oceanographic Research Papers*, 203, 104211.

Dinn C. 2020. A new species of *Haliclona (Flagellia)* Van Soest, 2017 (Porifera, Demospongiae, Heteroscleromorpha) from the Gulf of St. Lawrence, Canada. *Zootaxa.* 4778, 391-395.

D'Onghia G, Capezzuto F, Cardone F, Carlucci R, Carluccio A, Chimienti G, Corriero G, Longo C, Maiorano P, Mastrototaro F, Panetta P, Rosso A, Sanfilippo R, Sion L, and Tursi A. 2015. Macro- and megafauna recorded in the submarine Bari Canyon (southern Adriatic, Mediterranean Sea) using different tools. *Mediterranean Marine Science*. 161, 180-196.

Dremière P-Y, Fiorentini L, Cosimi G, Leonori I, Sala A, and Spagnolo A. 1999. Escapement from the main body of the bottom trawl used for the Mediterranean international trawl survey MEDITS. *Aquatic Living Resources.* 12, 207-217.

Duran S, Pascual M, Estoup A, and Turon X. 2004. Strong population structure in the marine sponge *Crambe crambe* (Poecilosclerida) as revealed by microsatellite markers. *Molecular Ecology.* 13, 511-522.

Ekins M, Erpenbeck D, Wörheide G, and Hooper JN. 2016. Staying well connected-Lithistid sponges on seamounts. *Journal of the Marine Biological Association of the United Kingdom*. 2, 437-451.

Enrichetti F, Bavestrello G, Betti F, Coppari M, Toma M, Pronzato R, Canese S, Bertolino M, Costa G, Pansini M, and Bo M. 2020. Keratose-dominated sponge grounds from temperate mesophotic ecosystems (NW Mediterranean Sea). *Marine Ecology*. e12620.

Erpenbeck D, Breeuwer JAJ, Parra-Velandia FJ, and Van Soest RWM. 2006. Speculation with spiculation?—Three independent gene fragments and biochemical characters versus morphology in demosponge higher classification. *Molecular Phylogenetics and Evolution*. 38, 2, 293-305.

Estrada M. 1996. Primary production in the northwestern Mediterranean. *Scientia Marina*. 60, 55-64.

Evans D, Aish A, Boon A, Condé S, Connor D, Gelabert E, Michez N, Parry M, Richard D, Salvati E, and Tunesi L. 2016. Revising the marine section of the EUNIS Habitat classification. *Report of a workshop held at the European Topic Centre on Biological Diversity*. 12-13 May 2016. ETC/BD report to the EEA.

Evcen A, and Çinar ME. 2012. Sponge (Porifera) species from the Mediterranean coast of Turkey (Levantine Sea, eastern Mediterranean), with a checklist of sponges from the coasts of Turkey. *Turkish Journal of Zoology*. 36, 460-464.

Fabri M. C, Bargain A, Pairaud I, Pedel L, & Taupier-Letage I. 2017. Cold-water coral ecosystems in Cassidaigne Canyon: an assessment of their environmental living conditions. Deep Sea Research Part II: Topical Studies in Oceanography, 137, 436-453.

FAO. 2009. Management of Deep-Sea Fisheries in the High Seas. FAO, Rome, Italy .

Farias C, Ordines F, García-Ruiz C, and Fricke R. 2016. *Protogrammus alboranensis* n. sp. (Teleostei: Callionymidae), a new species of dragonet from the Alboran Sea, western Mediterranean Sea. *Scientia Marina.* 80, 51-56.

Farriols MT, Ordines F, Somerfield PJ, Pasqual C, Hidalgo M, Guijarro B, and Massutí E. 2017. Bottom trawl impacts on Mediterranean demersal fish diversity: Not so obvious or are we too late? *Continental Shelf Research*. 137, 84-102.

Fernández de Puelles M. L, Valencia J, Jansá J, & Morillas A. 2004. Hydrographical characteristics and zooplankton distribution in the Mallorca channel (Western Mediterranean): spring 2001. ICES Journal of Marine Science, 61(4), 654-666.

Ferrer Hernández F. 1914. Esponjas del Cantábrico. Parte 2. III. Myxospongida. IV. Tetraxonida. V. Triaxonida. *Trabajos del Museo Nacional de Ciencias Naturales Zoológica*. 17, 1-46.

Ferrer-Hernández F. 1916. Fauna del Mediterráneo Occidental. Esponjas españolas. *Trabajos del Museo Nacional de Ciencias Naturales. Serie Zoológica,* 27, 1-52

Ferrer-Hernández F. 1921. Esponjas recogidas en la campaña preliminar del "Giralda". *Boletín de Pescas*. 6, 161-177.

Ferrer-Hernández F. 1934. Prima campaña biológica a bordo del ~Xauen~ en aguas de Mallorca. *Instituto Español de Oceanografía. Notas y Resúmenes*. Serie II, 80, 1-3.

Fiorentini L, Dremière P.-Y, Leonori I, Sala A. & Palumbo V. 1999. Efficiency of the bottom trawl used for the Mediterranean international trawl survey (MEDITS). *Aquatic Living Resources*, 12, 3, 187-205.

Folmer O, Black M, HoehW, Lutz R, and Vrijenhoek R. 1994. DNA Primers for amplification of mitochondrial cytochrome c oxidase subunit I from diverse metazoan invertebrates. *Molecular Marine Biology and Biotechnology*. 3, 294-299.

Foster M.S. 2001. Rhodoliths: Between rocks and soft places. Journal of Phycology, 37: 659–667.

Fourt M, Goujard A, Pérez T, and Chevaldonné P. 2017. Guide de la faune profonde de la mer Méditerranée. Explorations des roches et des canyons sous-marins des côtes françaises. Patrimoines naturels. *Publications scientifiques du Museum national d'Histoire naturelle Paris.* 75, 1-184.

Fricke R, and Ordines F. 2017a. First record of the reticulated dragonet, *Callionymus reticulatus* Valenciennes, 1837 (Actinopterygii: Callionymiformes: Callionymidae), from the Balearic Islands, western Mediterranean. *Acta Ichthyologica et Piscatoria.* 47, 163-171.

Fricke R and Ordines F. 2017b. First record of the Alboran dragonet, *Protogrammus alboranensis* (Actinopterygii: Callionymiformes: Callionymidae), from the Balearic Islands western Mediterranean. *Acta Ichthyologica et Piscatoria.* 47, 289-295.

Galarza JA, Carreras-Carbonell J, Macpherson E, Pascual M, Roques S, Turner GF, and Rico C. 2009. The influence of oceanographic fronts and early-life-history traits on connectivity among littoral fish species. *Proceedings of the National Academy of Sciences.* 106, 1473-1478.

Galil B, and Zibrowius H. 1998. First benthos samples from Eratosthenes Seamount, eastern Mediterranean. *Senckenbergiana maritima*. 284-6, 111.

Garcia-Ladona E, Castellon A, Font J, and Tintore J. 1996. The Balearic current and volume transports in the Balearic basin. *Oceanologica Acta.* 19, 489-498.

García-Merchán VH, Robainas-Barcia A, Abelló P, Macpherson E, Palero F, García-Rodríguez M, de Sola LG, and Pascual M. 2012. Phylogeographic patterns of decapod crustaceans at the Atlantic-Mediterranean transition. *Molecular Phylogenetics and Evolution*. 622, 664-672.

García-Rodríguez M. & Esteban E. 1999. On the biology and fishery of *Aristeus antennatus* (Risso, 1816), (Decapoda, Dendrobranchiata) in the Ibiza Channel (Balearic Islands, Spain). *Scientia Marina*, 63,1, 27-37.

García-Rodríguez M, Esteban A. & Gil JLP. 2000. Considerations on the biology of *Plesionika edwardsi* (Brandt, 1851) (Decapoda, Caridea, Pandalidae) from experimental trap catches in the Spanish western Mediterranean Sea. *Scientia Marina*, 64: 369-379.

Geller J, Meyer C, Parker M, and Hawk H. 2013. Redesign of PCR primers for mitochondrial cytochrome c oxidase subunit I for marine invertebrates and application in all-taxa biotic surveys. *Molecular ecology resources*. 135, 851-861.

Gerovasileiou V, Voultsiadou E. 2012. Marine caves of the mediterranean sea: a sponge biodiversity reservoir within a biodiversity hotspot. *PLoS ONE*. 7, e39873.

Gherardi DF. 2004. Community structure and carbonate production of a temperate rhodolith bank from Arvoredo Island, southern Brazil. *Brazilian Journal of Oceanography*. 52, 207-224.

Ginés A, Ginés J, and Gràcia F. 2013. Cave development and patterns of caves and cave systems in the eogenetic coastal karst of southern Mallorca (Balearic Islands, Spain). p. 245-260. In: *Coastal Karst Landforms*. Springer, Dordrecht.

Gómez-Ballesteros M, Vazquez JT, Palomino D, Rovere M, Bo M, Alessi J, Fiori C, and Würtz M. 2015. Seamounts and Seamount like Structures of the Western Mediterranean. In: *Atlas of the Mediterranean Seamounts and Seamount-like Structures*. Würtz M, and Rovere M. (eds). IUCN: Gland, Switzerland. Málaga, Spain, 59-109.

Gordoa A, Rouyer T, Ortiz M. 2017. Review and update of the French and Spanish purse seine size at catch for the Mediterranean bluefin tuna fisheries 1970–2010. *ICCAT Collective Volume of Scientific Papers*, 75, 1622-1633.

Gràcia F, Clamor B, and Watkinson P. 1998. La cova d'en Passol i altres cavitats litorals situades entre cala sa Nau i cala Mitjana (Felanitx, Mallorca). *Endins: publicació d'espeleologia*. 5-18.

Gràcia F, Clamor B, Jaume D, Fornós JJ, Uriz MJ, Martín D, Gil J, Gracia P, Febrer M, and Pons GX. 2005. La cova des Coll Felanitx, Mallorca. Espeleogènesi, geomorfologia, hidrologia, sedimentologia, fauna i conservació. *Endins.* 27, 141-186.

Gràcia F, Clamor B, Gamundí P, Cirer A, Fenández JF, Fornós JJ, Ginés A, Ginés J, Uriz MJ, Munar S, Vicens D, Ginard A, Betton N, Vives MA, Jaume D, Mas G, Perelló MA, Cardona F, and Timar-Gabor A. 2014. Es Dolç (Colònia de Sant Jordi, Ses Salines, Mallorca). Cavitat litoral amb influències hipogèniques excavada a les eolianites quaternàries i als materials del Pliocè. *Endins.* 36, 69-96.

Gray JE. 1867. Notes on the Arrangement of Sponges, with the descriptions of some new Genera. *Proceedings of the Zoological Society of London*. 2, 492-558.

Grenier M, Ruiz C, Fourt M, Santonja M, Dubois M, Klautau M, Vacelet J, Boury-Esnault N, and Pérez T. 2018. Sponge inventory of the French Mediterranean waters, with an emphasis on cave-dwelling species. In: Deep Sea and Cave Sponges. Klautau M, Pérez T, Cárdenas P, and de Voogd N. (eds). *Zootaxa*. 4466, 205-228.

Griessinger JM. 1971. Etude des Réniérides de Méditerranée (Démosponges Haplosclérides). *Bulletin du Muséum National d'Histoire Naturelle Zoologie.* 3, 97-182.

Griffiths SM, Butler MJ, Behringer DC, Pérez T, and Preziosi RF. 2021. Oceanographic features and limited dispersal shape the population genetic structure of the vase sponge *Ircinia campana* in the Greater Caribbean. *Heredity*. 126, 63-76.

Grinyó J, Gori A, Greenacre M, Requena S, Canepa A, Iacono CL, Ambroso S, Purroy A, and Gili JM. 2018. Megabenthic assemblages in the continental shelf edge and upper slope of the Menorca Channel, Western Mediterranean Sea. *Progress in Oceanography*. 162, 40-51.

Guardiola M, Frotscher J, and Uriz MJ. 2012. Genetic structure and differentiation at a short-time scale of the introduced calcarean sponge *Paraleucilla magna* to the western Mediterranean. *Hydrobiologia*. 687, 71-84.

Guijarro B, Ordines F, Pasqual C, Valls M, Quetglas A. & Massutí E. 2020. La pesca de ròssec al voltant de l'arxipèlag de Cabrera. In: Grau A.M, Fornós J.J, Mateu G, Oliver P.A. & Terrasa B. 2020. Arxipèlag de Cabrera: Història Natural. *Monografies de la Societat d'Història Natural de les Balears*, 30. pp. 375-391.

Guijarro B, Ordines F, Pasqual C, Valls M, Quetglas A. & Massutí, E. 2020. La pesca de ròssec al voltant de l'arxipèlag de Cabrera. In: Arxipèlag de Cabrera: Història Natural (A.M. Grau, J.J. Fornós, G. Mateu P.A. Oliver and B. Terrasa, Editors). *Monografies de la Societat d'Història Natural de les Balears*, 30, 375-391.

Guzzetti E, Salabery E, Ferriol P, Díaz JA, Tejada S, Faggio C, and Sureda A. 2019. Oxidative stress induction by the invasive sponge *Paraleucilla magna* growing on *Peyssonnelia squamaria* algae. *Marine Environmental Research*. 150, 104763.

Haas AF, Naumann MS, Struck U, Mayr C, el-Zibdah M, and Wild C. 2010. Organic matter release by coral reef associated benthic algae in the Northern Red Sea. *Journal of Experimental Marine Biology and Ecology*. 3891-2, 53-60.

Hajdu E, de Paula TS, Redmond NE, Cosme B, Collins AG, and Lôbo-Hajdu G. 2013. Mycalina: another crack in the Poecilosclerida framework. *Integrative and Comparative Biology.* 53, 462-472.

Hall T. 1999. Bioedit: a user-friendly biological sequence alignment editor and analysis program for Windows 95/98/NT. *Nucleic Acids Symposium Series*. 41, 95-98.

Hamer B, Jaklin A, Pavicic-Hamer D, Brummer F, Muller W. E. G, Zahn R. K, & Batel R. 2007. Contribution to the ecology of the sponge *Suberites domuncula* (Olivi, 1792) (Porifera, Demospongiae, Hadromerida): Sponge contraction. *Fresenius Environmental Bulletin*, 16, 8, 980.

Hanitsch R. 1895. Notes on a collection of sponges from the west coast of Portugal. *Transactions of the Liverpool Biological Society*. 9, 205-219.

Harris B. 2022. *The distribution and feeding ecology of temperate marine sponges through shallow and mesophotic habitats*. Doctoral dissertation, Open Access Te Herenga Waka-Victoria University of Wellington.

Hasegawa M, Kishino H, and Yano T. 1985. Dating of the human-ape splitting by a molecular clock of mitochondrial DNA. *Journal of Molecular Evolution.* 22, 160-174.

Hellio C, Marechal JP, Véron B, Bremer G, Clare AS, and Le Gal Y. 2004. Seasonal Variation of Antifouling Activities of Marine Algae from the Brittany Coast France. *Marine Biotechnology*. 6, 67-82.

Hentschel E. 1929. Die Kiesel- und Hornschwämme des Nördlichen Eismeers. Pp. 857-1042, pls XII-XIV. In: Römer, F, Schaudinn, F, Brauer, A. and Arndt, W. Eds, Fauna Arctica. Eine Zusammenstellung der arktischen Tierformen mit besonderer Berücksichtigung des Spitzbergen-Gebietes auf Grund der Ergebnisse der Deutschen Expedition in das Nördliche Eismeer im Jahre 1898, 5, 4 (G. Fischer, Jena).

Hooper JNA. 2003. Sponguide. Guide to sponge collection and identification. Hooper JNA. Qld. Museum, Australia.

Hooper JNA, and Levi C. 1993. Poecilosclerida (Porifera: Demospongiae) from the New Caledonia Lagoon. *Invertebrate Systematics.* 7, 1221-1302.

Hooper JNA, Van Soest RW. 2002. Systema Porifera. A guide to the classification of sponges. Kluwer Academic/Plenum Publishers, New York.

Idan T, Shefer S, Feldstein T, Yahel R, Huchon D, and Ilan M. 2018. Shedding light on an East-Mediterranean mesophotic sponge ground community and the regional sponge fauna. *Mediterranean Marine Science*. 191, 84-106.

Idan T, Shefer S, Feldstein T, and Ilan M. 2021. New discoveries in Eastern Mediterranean mesophotic sponge grounds: updated checklist and description of three novel sponge species. *Mediterranean Marine Science*. 222, 270-284.

Jennings S, and Kaiser MJ. 1998. The effects of fishing on marine ecosystems. *Advances in marine biology*. 34, 201-352.

Jennings, S, Alvsvåg J, Cotter AJR, Ehrich S, Greenstreet SPR, Jarre-Teichmann A, Mergardt N, Rijnsdorp AD, & Smedstad, O. 1999. Fishing effects in northeast Atlantic shelf seas: patterns in fishing effort, diversity and community structure. III. International trawling effort in the North Sea: an analysis of spatial and temporal trends. *Fisheries Research*, 40, 2, 125-134.

Joher S, Ballesteros E, Cebrian E, Sánchez N & Rodríguez-Prieto C. 2012. Deep-water macroalgal-dominated coastal detritic assemblages on the continental shelf off Mallorca and Menorca (Balearic Islands, Western Mediterranean), *Botanica Marina*, 55, 5, 485-497.

Joher S, Ballesteros E. & Rodríguez-Prieto C. 2015. Contribution to the study of deep coastal detritic bottoms: the algal communities of the continental shelf off the Balearic Islands, Western Mediterranean. *Mediterranean Marine Science*, 163, 573-590.

Juan C, Guzik MT, Jaume D, and Cooper SJ. 2010. Evolution in caves: Darwin's 'wrecks of ancient life' in the molecular era. *Molecular Ecology*. 1918, 3865-3880.

Juza M, Mourre B, Renault L, Gómara S, Sebastián K, Lora S, Beltran JP, Frontera B, Garau B, Troupin C, Torner M, Heslop E, Casas B, Escudier R, Vizoso G. & Tintoré J. 2016. SOCIB operational ocean forecasting system and multi-platform validation in the Western Mediterranean Sea. *Journal of Operational Oceanography*, 9, s155-s166.

Kaandorp JA, and De Kluijver MJ. 1992. Verification of fractal growth models of the sponge *Haliclona oculata* (Porifera) with transplantation experiments. *Marine Biology*. 113, 1, 133-143.

Kallianiotis A, Sophronidis K, Vidoris P. & Tselepides A. 2000. Demersal fish and megafaunal assemblages on the Cretan continental shelf and slope (NE Mediterranean): seasonal variation in species density, biomass and diversity. *Progress in Oceanography*, 46, 429–455.

Katoh K, Misawa K, Kuma K, and Miyata T. 2002. MAFFT: a novel method for rapid multiple sequence alignment based on fast Fourier transform. *Nucleic Acids Research.* 30, 3059-3066.

Keesing JK, Usher KM, and Fromont J. 2012. First record of photosynthetic cyanobacterial symbionts from mesophotic temperate sponges. *Marine and freshwater research*. 635, 403-408.

Kefalas E, Tsirtsis G, & Castritsi-Catharios J. 2003. Distribution and ecology of Demospongiae from the circalittoral of the islands of the Aegean Sea (Eastern Mediterranean). *Hydrobiologia*, 499, 125-134.

Klautau M, Monteiro L, Borojevic R. 2004. First occurrence of the genus *Paraleucilla* (Calcarea, Porifera) in the Atlantic Ocean: *P. magna* sp. nov. *Zootaxa*. 710: 1-8.

Klitgaard AB, and Tendal OS. 2004. Distribution and species composition of mass occurrences of large-sized sponges in the northeast Atlantic. *Progress in oceanography*. 611, 57-98.

Klitgaard AB. 1995. The fauna associated with outer shelf and upper slope sponges (Porifera, Demospongiae) at the Faroe Islands, northeastern Atlantic. *Sarsia*. 801, 1-22.

Kornder NA, Esser Y, Stoupin D, Leys SP, Mueller B, Vermeij MJ, Huisman J, & de Goeij J. M. 2022. Sponges sneeze mucus to shed particulate waste from their seawater inlet pores. *Current Biology*, 32, 17, 3855-3861.

Kovačić M, Ordines F, and Schliewen UK. 2017 A new species of Buenia (Teleostei: Gobiidae) from the western Mediterranean Sea, with the description of this genus. *Zootaxa*. 4250, 447-460.

Kovačić M*,* Ordines F, and Schliewen UK. 2018. A new species of *Buenia* (Perciformes: Gobiidae) from the western Mediterranean slope bottoms, the redescription of *Buenia jeffreysi* and the first Balearic record of *Buenia affinis*. *Zootaxa.* 4392, 267-288.

Kovačić M*,* Ordines F*,* Ramirez-Amaro S, and Schliewen UK. 2019. *Gymnesigobius medits* (Teleostei: Gobiidae), a new gobiid genus and species from the western Mediterranean slope bottoms. *Zootaxa.* 4651, 513-530.

Kumar S, Stecher G, Li M, Knyaz C, and Tamura K. 2018. MEGA X: molecular evolutionary genetics analysis across computing platforms. *Molecular biology and evolution*. 356, 1547.

Labate M. 1964. Poriferi di grotta superficiale del litorale adriatico pugliese. *Annali del Pontificio Istituto Scienze e Letteres*. 14, 319-342.

Lackschewitz P. 1886. Über die Kalkschwämme Menorcas. *Zoologische Jahrbücher.* 1, 297-310.

Lambe LM. 1900. Sponges from the coasts of north-eastern Canada and Greenland. *Transactions of the royal Society of Canada*. 6, 19-49.

Laubenfels MD. 1932. The marine and fresh-water sponges of California. *Proceedings of the United States National Museum*. 81, 1-140.

Lauria V, Garofalo G, Fiorentino F, Massi D, Milisenda G, Piraino S, Russo T, and Gristina M. 2017. Species distribution models of two critically endangered deep-sea octocorals reveal fishing impacts on vulnerable marine ecosystems in central Mediterranean Sea. *Scientific Reports.* 7, 8049.

Lavigne H, D'ortenzio F, Ribera D'Alcalà M, Claustre H, Sauzède R. & Gacic M. 2015. On the vertical distribution of the chlorophyll a concentration in the Mediterranean Sea: a basin-scale and seasonal approach. *Biogeosciences*, 12: 5021-5039.

Lendenfeld RV. 1898. Die Clavulina der Adria. *Nova acta Academiae Caesareae Leopoldino Carolinae germanicae naturaecuriosorum*. Ehrhardt Karras, Halle, 251 pp.

Lesser MP, Slattery M, Laverick JH, Macartney KJ, and Bridge TC. 2019. Global community breaks at 60 m on mesophotic coral reefs. *Global Ecology and Biogeography*. 2810, 1403-1416.

Lévi C. 1956. Spongiaires de la région de Dakar. *Bulletin de l'Institut français d'Afrique noire. A, Sciences naturelles*. 18, 2, 391-405.

Lévi C. 1973. Systématique de la classe des Demospongiaria Démosponges. In: Grassé PP ed. *Traité de Zoologie Spongiaires*. Paris, pp. 577-632.

Lévi C, and Vacelet J. 1958. Éponges récoltées dans l'Atlantique oriental par le 'Président Théodore-Tissier' (1955-1956). Revue des Travaux de l'Institut des Pêches maritimes. 22, 2, 225-246.

Linnaeus C. 1759. Systema naturæ per regna tria naturæ, secundum classes, ordines, genera, species, cum characteribus, differentiis, synonymis, locis. Tomus II. Editio decima, reformata. - pp. [1-4], 825-1384. Holmiæ. (L. Salvii).

Lloret J, Marin A, Marin-Guirao L, Carreno MF (2006) An alternative approach for managing scuba diving in small marine protected areas. *Aquatic Conservation: Marine and Freshwater Ecosystems*. 16, 579-591.

Longo C, Cardone F, Pierri C, Mercurio M, Mucciolo S, Marzano CN, and Corriero G. 2018. Sponges associated with coralligenous formations along the Apulian coasts. *Marine Biodiversity*. 484, 2151-2163.

Longo C, Mastrototaro F, and Corriero G. 2005. Sponge fauna associated with a Mediterranean deep-sea coral bank. *Journal of the Marine Biological Association of the United Kingdom*. 856, 1341-1352.

López-Jurado JL, Marcos M & Monserrat S. 2008. Hydrographic conditions affecting two fishing grounds of Mallorca island (Western Mediterranean): during the IDEA Project (2003–2004. *Journal of Marine Systems*, 71, 3-4, 303-315.

Łukowiak M, Van Soest R, Klautau M, Pérez T, Pisera A, & Tabachnick K. 2022. The terminology of sponge spicules. *Journal of Morphology*. 283, 12, 1517-1545.

Lundbeck W. 1905. Porifera. Part II. Desmacidonidae. The Danish Ingolf-Expedition. 62, 1-219

Lundbeck W. 1909. The Porifera of East Greenland. Meddelelser om Grønland, 29, 423-464.

Maia LF, Gonzaga TA, Campos MT, Lobo-Hajdu G, Edwards HG, and de Oliveira LF. 2021. Coloration patterns of marine sponges assessed by vibrational spectroscopy. *Journal of Raman Spectroscopy*. 5212, 2581-2596.

Maldonado M. 1992. Demosponges of the red coral bottoms from the Alboran Sea. *Journal of Natural History*. 26, 1131-1161.

Maldonado M. 2002. Family Pachastrellidae Carter, 1875. Pp.141-162. In: Hooper, JNA, van Soest RWM. (eds). Systema Porifera. A Guide to the Classification of Sponges (2 volumes). Kluwer Academic/Plenum Publ, New York. 1708+xvliii, ISBN 0-306-47260-0.

Maldonado M. 2006. The ecology of the sponge larva. *Canadian Journal of Zoology*. 842, 175-194.

Maldonado M, Aguilar R, Bannister RJ, Bell JJ, Conway KW, Dayton PK, Díaz C, Gutt J, Kelly M, Kenchington ELR, Leys SP, Pomponi SA, Rapp HT, Rützler K, Tendal OS, Vacelet J, Young CM. 2016. Sponge grounds as key marine habitats: a synthetic review of types, structure, functional roles, and conservation concerns. In: Rossi S. (eds). *Marine animal forests*. Switzerland: Springer International Publishing. p. 1-39.

Maldonado M, and Uriz MJ. 1996. A new species of *Sphinctrella* (Demospongiae: Astrophorida) and remarks on the status of the genus in the Mediterranean. *Bulletin de l'Institut Royal des Sciences Naturelles de Belgique*, 66, 175-184. History. 26, 1131-1161

Maldonado M, and Young CM. 1996. Bathymetric patterns of sponge distribution on the Bahamian slope. *Deep Sea Research Part I: Oceanographic Research Papers*. 436, 897-915.

Maldonado M, Carmona MC, Uriz MJ, and Cruzado A. 1999. Decline in Mesozoic reef-building sponges explained by silicon limitation. *Nature*. 401, 785-788 1999.

Maldonado M, Ribes M, and van Duyl FC. 2012. Nutrient fluxes through sponges: biology, budgets, and ecological implications. *Advances in marine biology*. 62, 113-182.

Maldonado M, Aguilar R, Blanco J, Garcia S, Serrano A, and Punzon A. 2015. Aggregated clumps of lithistid sponges: a singular, reef-like bathyal habitat with relevant paleontological connections. *PLoS One*. 105, e0125378.

Manconi R, Padiglia A, Cubeddu T, and Pronzato R. 2019. Long-term sponge stranding along the shores of Sardinia Island Western Mediterranean Sea. *Marine Ecology*. 406, e12567.

Manly BFJ. 1991. Randomization and Monte Carlo Methods in Biology, Chapman and Hall, London, UK.

Marenzeller E. 1889. Ueber die adriatischen Arten der Schmidt'schen Gattungen Stelletta und Ancorina. *Annalen des K.K. naturhistorischen Hofmuseums*. 4, 7-20, pls II-III.

Marín P, Aguilar R, Garcia S. & Fournier N. 2011. A Complementary Approach for the Mediterranean N2000 in Open and Deep Sea. *OCEANA*, 17 pp.

Martí R, Uriz MJ, Ballesteros E, and Turon X. 2004. Temporal variation of several structure descriptors in animal-dominated benthic communities in two Mediterranean caves. *Journal of the Marine Biological Association of the United Kingdom.* 84, 573-580.

Massutí M. 1959. La pesca de la gamba y de la langosta. Boletín de la Cámara oficial de Comercio, Industria y Navegación de Palma de Mallorca, 625, 185-192.

Massutí M. 1973. Evolución de los esfuerzos y rendimientos de pesca en la región Balear entre los años 1940 y 1970. *Publicaciones Técnicas Dirección General Pesca Marítima*, 10, 37-54.

Massutí E, and Reñones O. 2005. Demersal resource assemblages in the trawl fishing grounds off the Balearic Islands (western Mediterranean). *Scientia Marina*. 691, 167-181.

Massutí E, Olivar MP, Monserrat S, Rueda L & Oliver P. 2014. Towards understanding the influence of environmental conditions on demersal resources and ecosystems in the western Mediterranean: Motivations, aims and methods of the IDEADOS project. *Journal of Marine Systems*, 138, 3-19.

Massutí E, Sánchez-Guillamón O, Farriols MT, Palomino D, Frank A, Bárcenas P, Rincón B, Martínez-Carreño N, Keller S, López-Rodríguez C, Díaz JA, López-González N, Marco-Herrero E, Fernandez-Arcaya U, Valls M, Ramírez-Amaro S, Ferragut F, Joher S, Ordinas F, and Vázquez J-T. 2022. Improving Scientific Knowledge of Mallorca Channel Seamounts (Western Mediterranean) within the Framework of Natura 2000 Network. *Diversity*. 144.

Maynou F & Cartes JE. 2000. Community structure of bathyal decapod crustaceans off south-west Balearic Islands (western Mediterranean): seasonality and regional patterns in zonation. *Journal of the Marine Biological Association of the United Kingdom*, 80, 5, 789-798.

McClain CR, and Hardy SM. 2010. The dynamics of biogeographic ranges in the deep sea. *Proceedings of the Royal Society B: Biological Sciences*. 2771700, 3533-3546.

McDonald JI, Hooper JN and McGuinness KA. 2002. Environmentally influenced variability in the morphology of *Cinachyrella australiensis* (Carter 1886) (Porifera: Spirophorida: Tetillidae). *Marine and Freshwater Research*. 53, 1, 79-84.

McGrath EC, Smith DJ, Jompa J & Bell JJ. 2017. Adaptive mechanisms and physiological effects of suspended and settled sediment on barrel sponges. *Journal of Experimental Marine Biology and Ecology*, 496, 74-83.

Melis P*,* Riesgo A*,* Taboada S, and Manconi R. 2016. Coping with brackishwater: A new species of cave-dwelling *Protosuberites* (Porifera: Demospongiae: Suberitidae) from the Western Mediterranean and a first contribution to the phylogenetic relationships within the genus. *Zootaxa.* 4208, 349-364.

Meylan A. 1988. Spongivory in hawksbill turtles: a diet of glass. *Science*. 239, 4838, 393-395.

Milazzo M, Chemello R, Badalamenti F, Camarda R, and Riggio S. 2002. The impact of human recreational activities in marine protected areas: what lessons should be learnt in the Mediterranean Sea? *PSZNI Marine Ecology*. 23, 280-290.

Miller MA, Pfeiffer W, and Schwartz T. 2010. Creating the CIPRES Science Gateway for inference of large phylogenetic trees. *Proceedings of the Gateway Computing Environments Workshop.* GCE, pp. 1-8.

Minnery GA. 1990. Crustose coralline algae from the Flower Garden Banks, Northwestern Gulf of Mexico; controls on distribution and growth morphology. *Journal of Sedimentary Research*. 606, 992-1007.

Mioso R, Marante FJT, Bezerra RDS, Borges FVP, Santos BV, and Laguna IHBD. 2017. Cytotoxic compounds derived from marine sponges. A review (2010-2012). *Molecules*. 222, 208.

Mokhtar-Jamaï K, Pascual M, Ledoux JB, Coma R, Féral JP, Garrabou J, and Aurelle D. 2011. From global to local genetic structuring in a red gorgonian *Paramuricea clavata*: the interplay between oceanographic conditions and limited larval dispersal. *Molecular Ecology.* 20, 3291-3305.

Monserrat S, López-Jurado JL, and Marcos M. 2008. A mesoscale index to describe the regional circulation around the Balearic Islands. *Journal of Marine Systems*. 713-4, 413-420.

Montgomery DC. & Peck EA. 1982. Introduction to linear regression analysis. Wiley, New York, 504 pp.

Morato T, Kvile KØ, Taranto GH, Tempera F, Narayanaswamy BE, Hebbeln D, Menezes GM, Wienberg C, Santos RS, and Pitcher TJ. 2013. Seamount physiography and biology in the north-east Atlantic and Mediterranean Sea. *Biogeosciences*. 105, 3039.

Morganti TM, Slaby BM, de Kluijver A, Busch K, Hentschel U, Middelburg JJ, Grotheer H, Mollenhauer G, Dannheim J, Rapp HT, Purser A, and Boetius A. 2022. Giant sponge grounds of Central Arctic seamounts are associated with extinct seep life. *Nature Communications.* 13, 638 2022.

Morrow C, Cárdenas P. 2015. Proposal for a revised classification of the Demospongiae (Porifera). *Frontiers in Zoology*. 12: 7.

Morrow C, Cárdenas P, Boury-Esnault N, Picton B, McCormack G, Van Soest R, Collins A, Redmond N, Maggs C, Sigwart J, and Allcock LA. 2019. Integrating morphological and molecular taxonomy with the revised concept of Stelligeridae (Porifera: Demospongiae). *Zoological Journal of the Linnean Society*.

Mothes B, Maldonado M, Eckert R, Lerner C, Campos M, and Carraro JL. 2007. A new species of *Characella* (Demospongiae, Astrophorida, Pachastrellidae) from the south Brazilian continental shelf. In: Custódio MR, Lôbo-Hajdu G, Hajdu E, Muricy G. (eds). 2007. *Porifera Research: Biodiversity, Innovation and Sustainability*. Museu Nacional, Rio de Janeiro, Brazil, 477-482.

Morató M, Quiles-Pons C, Mallol S, Baena I, de la Ballina NR, Díez S, Maresca F, Muñoz A, Real E. & Díaz, D. 2022. Cartografiat i pressió de busseig en l'hàbitat 8330 a les Illes Balears a través de la participació ciutadana. *VIII Jornades de Medi Ambient de les Illes Balears*.

Mourre B, Aguiar E, Juza M, Hernandez-Lasheras J, Reyes E, Heslop E, Escudier R, Cutolo E, Ruiz S, Mason E, Pascual A. & Tintoré, J. 2018. Assessment of high-resolution regional ocean prediction systems using multi-platform observations: illustrations in the Western Mediterranean Sea. In: *New Frontiers in Operational Oceanography* (E. Chassignet, A. Pascual, J. Tintoré and J. Verron, Editors), GODAE Ocean View, pp. 663-694.

Mueller B, Van Der Zande RM, Van Leent PJM, Meesters EH, Vermeij MJ, and Van Duyl FC. 2014. Effect of light availability on dissolved organic carbon release by Caribbean reef algae and corals. *Bulletin of Marine Science*. 903, 875-893.

Muricy G, Solé-Cava AM, Thorpe JP, and Boury-Esnault N. 1996. Genetic evidence for extensive cryptic speciation in the subtidal sponge *Plakina trilopha* (Porifera:

Demospongiae: Homoscleromorpha) from the Western Mediterranean. *Marine Ecology Progress Series*. 138, 181-187.

Nardo GD. 1833. Auszug aus einem neuen System der Spongiarien,wonach bereits die Aufstellung in der Universitäts-Sammlung zu Padua gemacht ist. Pp. 519-523. In: *Isis, oder Encyclopädische Zeitung Coll. (Oken: Jena).*

Nardo GD. 1847. Prospetto della fauna marina volgare del Veneto estuario con cenni sulle principali specie commestibili dell'Adriatico, sulle venete pesche, sulle valli, ecc. Pp. 113-156 1-45 in reprint. In: Venezia e le sue Lagune. Volume Secundo. G. Antonelli: Venezia.

Nelson WA. 2009. Calcified macroalgae: Critical to coastal ecosystems and vulnerable to change. *Marine and Freshwater Research*, 60, 787-801.

Nichols SA, and Barnes PA. 2005. A molecular phylogeny and historical biogeography of the marine sponge genus *Placospongia* (Phylum Porifera) indicate low dispersal capabilities and widespread crypsis. *Journal of Experimental Marine Biology and Ecology*. 323 1, 1-15.

OCEANA 2011. Montañas submarinas de las Islas Baleares: Canal de Mallorca. Propuesta de protección para Ausias March, Emile Baudot y Ses Olives. OCEANA, 64 pp.

OCEANA 2015. Expedition 2014 Balearic Islands: Cabrera National Park and Mallorca Channel Seamounts. *OCEANA*, 21 pp.

Oliver P. 1983. Los recursos pesqueros del Mediterráneo. Primera parte: Mediterráneo Occidental. Studies and Reviews. *General Fisheries Council for the Mediterranean*, 59: 1-141.

Ordines F, and Massutí E. 2009. Relationships between macro-epibenthic communities and fish on the shelf grounds of the western Mediterranean. *Aquatic Conservation: Marine and freshwater ecosystems*. 194, 370-383.

Ordines F, Massutí E, Guijarro B, and Mas R. 2006. Diamond vs. square mesh codend in a multi-species trawl fishery of the western Mediterranean: effects on catch composition, yield, size selectivity and discards. *Aquatic Living Resources*. 194, 329-338.

Ordines F*,* Quetglas A*,* Massutí E, and Moranta J. 2009. Habitat preferences and life history of the red scorpion fish, *Scorpaena notata*, in the Mediterranean. *Estuarine, Coastal and Shelf Science.* 85, 537-546.

Ordines F, Jordà G, Quetglas A, Flexas M, Moranta J, and Massutí E. 2011. Connections between hydrodynamics, benthic landscape and associated fauna in the Balearic Islands, western Mediterranean. *Continental Shelf Research*. 31 17, 1835-1844.

Ordines F, Ramón M, Rivera J, Rodriguez-Prieto C, Farriols MT, Guijarro B, Pascual C, and Massutí E. 2017. Why long term trawled red algae beds off Balearic Islands western Mediterranean. still persist? *Regional Studies in Marine Science.* 15, 39-49.

Ordines F, Fricke R, Williston A, Guijarro B, and Massuti E. 2018. First record of *Microichthys coccoi* (actinopterygii: perciformes: epigonidae) from the Balearic Islands western Mediterranean. *Acta Ichthyologica et Piscatoria.* 48, 19-25.

Ordines F, Ferriol P, Moya F, Farias C, Rueda JL, and Garcia-Ruiz C. 2019a. First record of the sea cucumber *Parastichopus tremulus* (Gunnerus, 1767) (Echinodermata: Holothuroidea: Aspidochirotida) in the Mediterranean Sea (Alboran Sea, western Mediterranean). *Cahiers De Biologie Marine.* 60, 111-115.

Ordines F, Kovačić M, Vivas M, García-Ruiz C, and Guijarro B. 2019b. Westernmost Mediterranean records of three gobiid species (actinopterygii: perciformes: gobiidae). *Acta Ichthyologica et Piscatoria*. 49, 265-272

Ordines F, Ramírez-Amaro S, Fernandez-Arcaya U, Marco-Herrero E, and Massutí E. 2019c. First occurrence of an Ophiohelidae species in the Mediterranean: the high abundances of *Ophiomyces grandis* from the Mallorca Channel seamounts. *Journal of the Marine Biological Association of the United Kingdom*. 998, 1817-1823.

Padial JM, Miralles A, De la Riva, and Vences M. 2010. The integrative future of taxonomy. *Frontiers in Zoology*. 7:16. doi: 10.1186/1742-9994-7-16

Padua A, Cunha HA, and Klautau M. 2018. Gene flow and differentiation in a native calcareous sponge (Porifera) with unknown dispersal phase. *Marine Biodiversity*. 48, 4, 2125-2135.

Palmer M, Quetglas A, Guijarro B, Moranta J, Ordines F. and Massutí E. 2009. Performance of artificial neural networks and discriminant analysis in predicting fishing tactics from multispecific fisheries. *Canadian Journal of Fisheries and Aquatic Sciences*, 66, 2, 224-237.

Palomino D, Vázquez JT, Ercilla G, Alonso B, López-González N, and Díaz-Del-Río V. 2011. Interaction between seabed morphology and water masses around the seamounts on the Motril Marginal Plateau (Alboran Sea,Western Mediterranean). *GeoMarine Letters*. 31, 465-479.

Pansini M. 1984. Notes on some Mediterranean Axinella with description of two new species. *Bollettino dei Musei e degli Istituti Biologici dell'Universitá di Genova*. 50-51, 79-98

Pansini M. 1987. Littoral demosponges from the banks of the Strait of Sicily and the Alboran Sea. In: Vacelet J, Boury-Esnault N. (eds). *Taxonomy of Porifera from the N.E. Atlantic and the Mediterranean Sea*. NATO Advanced Science Institutes Series G, Ecological Sciences Springer, Heidelberg, 13, 149-185.

Pansini M, and Musso B. 1991. Sponges from Trawl-Exploitable Bottoms of Ligurian and Tyrrhenian Seas: Distribution and Ecology. *Marine Ecology*. 124, 317-329.

Pansini M, and Longo C. 2003. A review of the Mediterranean Sea sponge biogeography with, in appendix, a list of the demosponges hitherto recorded from this sea. *Biogeographia-The Journal of Integrative Biogeography.* 24, 57-73

Pansini M, Manconi R, and Pronzato R. 2011. Porifera I. Calcarea, Demospongiae (partim), Hexactinellida, Homoscleromorpha. Fauna d'Italia, Vol. 46. Bologna: Calderini-Il Sole 24 Ore. 554 pp. ISBN: 978-88-506-5395-9

Pardo E, Rubio RA, García S, and Ubero J. 2011. Documentación de arrecifes de corales de agua fría en el Mediterráneo occidental Mar de Alborán. *Chronica naturae*. 1, 20-34.

Pascual M*,* Palero F*,* García-Merchán VH*,* Macpherson E*,* Robainas-Barcia A*,* Mestres F*,* Roda T, and Abelló P. 2016. Temporal and spatial genetic differentiation in the crab *Liocarcinus depurator* across the Atlantic-Mediterranean transition. *Scientific reports.* 6, 29892.

Patarnello T, Volckaert FA, and Castilho R. 2007. Pillars of Hercules: is the Atlantic-Mediterranean transition a phylogeographical break? *Molecular ecology*. 1621, 442.

Pavia H, and Toth GB. 2000. Influence of light and nitrogen on the phlorotannin content of the brown seaweeds *Ascophyllum nodosum* and *Fucus vesiculosus*. *Hydrobiologia*. 4401-3, 299-305.

Pérès JM, and Picard J. 1964. Nouveau manuel de bionomie benthique de la mer Méditerranée. Station Marine d'Endoume.

Peres-Neto PR, Legendre P, Dray S. & Borcard D. 2006. Variation partitioning of species data matrices: estimation and comparison of fractions. *Ecology*, 87, 10, 2614-2625.

Pérez-Portela R*,* Noyer C, and Becerro MA. 2015. Genetic structure and diversity of the endangered bath sponge *Spongia lamella*. *Aquatic Conservation: Marine and Freshwater Ecosystems.* 25, 365-379.

Pham CK, Murillo FJ, Lirette C, Maldonado M, Colaço A, Ottaviani D, and Kenchington E. 2019. Removal of deep-sea sponges by bottom trawling in the Flemish Cap area: conservation, ecology and economic assessment. *Scientific reports*, 9(1), 15843.

Pinot JM, López-Jurado JL, and Riera M. 2002. The CANALES experiment 1996-1998. Interannual, seasonal, and mesoscale variability of the circulation in the Balearic Channels. *Progress in Oceanography*. 553-4, 335-370.

Pinot JM, Tintoré J, & Gomis, D. 1995. Multivariate analysis of the surface circulation in the Balearic Sea. *Progress in Oceanography*, 36, 4, 343-376.

Pisera A, and Vacelet J. 2011. Lithistid sponges from submarine caves in the Mediterranean: taxonomy and affinities. *Scientia Marina*. 751, 17-40.

Pisera A, and Lévi C. 2002. Family Theonellidae Lendenfeld, 1903. In Hooper JNA, and van Soest RWM. (eds). Systema Porifera. A Guide to the classification of Sponges. vol. 1, New York: Kluwer Academic / Plenum Publishers, pp 327-337.6-4444.

Pisera A, and Gerovasileiou V. 2021. Lithistid demosponges of deep-water origin in marine caves of the north-eastern Mediterranean Sea. *Frontiers in Marine Science*. 8, 630900.

Plotkin A, Gerasimova E, and Rapp HT. 2011. Phylogenetic reconstruction of Polymastiidae (Demospongiae: Hadromerida) based on morphology. In: *Ancient Animals, New Challenges,* pp. 21-41. Springer, Dordrecht.

Pöppe J, Sutcliffe P, Hooper JNA, Wörheide G, and Erpenbeck D. 2010. COI barcoding reveals new clades and radiation patterns of Indo-Pacific sponges of the family Irciniidae (Demospongiae: Dictyoceratida). *PLOS ONE*. 5, e9950.

Pouliquen L. 1969. Remarques sur la présence d'éponges de l'étage bathyal dans les grottes sous-marines en Méditerranée. Comptes rendus hebdomadaires des séances de l'Académie des sciences de Paris. 268, 1324-1326.

Pouliquen L. 1972. Les spongiaires des grottes sous-marines de la région de Marseille: écologie et systématique. *Téthys*. 34, 717-758.

Pulitzer-Finali G. 1972 [1970]. Report on a collection of sponges from the Bay of Naples. 1. Sclerospongiae, Lithistida, Tetractinellida, Epipolasida. *Pubblicazioni della Stazione zoologica di Napoli*. 38, 2, 328-354.

Pulitzer-Finali G. 1978. Report on a collection of sponges from the bay of Naples. III Hadromerida, Axinellida, Poecilosclerida, Halichondrida, Haplosclerida. *Bollettino dei Musei e degli Istituti Biologici dell'Universitá di Genova*. 45, 7-89.

Pulitzer-Finali G. 1983. A collection of Mediterranean Demospongiae (Porifera) with, in appendix, a list of the Demospongiae hitherto recorded from the Mediterranean Sea. *Annali del Museo civico di storia naturale Giacomo Doria*. 84, 445-621.

Quetglas A*,* Guijarro B*,* Ordines F, and Massutí E. 2012. Stock boundaries for fisheries assessment and management in the Mediterranean: the Balearic Islands as a case study. *Scientia Marina.* 76, 17-28.

Ramiro-Sánchez B, González-Irusta JM, Henry L-A, Cleland J, Yeo I, Xavier JR, Carreiro-Silva M, Sampaio Í, Spearman J, Victorero L, Messing CG, Kazanidis G, Roberts JM. & Murton B. 2019. Characterization and mapping of a deepsea sponge ground on the Tropic Seamount (Northeast Tropical Atlantic): implications for spatial management in the high seas. *Frontiers in Marine Science*, 6:278.

Redmond NE, Morrow CC, Thacker RW, Diaz MC, Boury-Esnault N, Cárdenas P, Hajdu E, Lobo-Hajdu G, Picton BE, Pomponi SA, and Kayal E. 2013. Phylogeny and systematics of Demospongiae in light of new small-subunit ribosomal DNA (18S) sequences. *Integrative and comparative biology.* 53, 388-415.

Redmond NE, Raleigh J, van Soest RWM, Kelly M, Travers SA, Bradshaw B, Vartia S, Stephens KM, and McCormack GP. 2011. Phylogenetic relationships of the marine Haplosclerida (Phylum Porifera) employing ribosomal (28S rRNA) and mitochondrial (cox1, nad1) gene sequence data. *PLoS One.* 6, e24344.

Reiss H, Kröncke I, and Ehrich S. 2006. Estimating the catching efficiency of a 2-m beam trawl for sampling epifauna by removal experiments. *ICES Journal of Marine Science*. 63, 1453-1464.

Ridley SO, and Dendy A. 1886. Preliminary report on the Monaxonida collected by H.M.S. Challenger. Part I. *Annals and Magazine of Natural History*. 18, 325-351, 470-493.

Riesgo A, Taboada S, Pérez-Portela R, Melis P, Xavier J. R, Blasco G, and López-Legentil S. 2019. Genetic diversity, connectivity and gene flow along the distribution of the emblematic Atlanto-Mediterranean sponge *Petrosia ficiformis* (Haplosclerida, Demospongiae). *BMC evolutionary biology*. 191, 1-18.

Ríos P, Altuna Á, Frutos I, Manjón-Cabeza E, García-Guillén L, Macías-Ramírez A, Ibarrola T.P, Gofas S, Taboada S, Souto J, Álvarez F, Saiz-Salinas JI, Cárdenas P, Rodríguez-Cabello P, Lourido A, Boza C, Rodríguez-Basalo A, Prado E, Abad-Uribarren E, Parra S, Sánchez F, and Cristobo J. 2022. Aviles Canyon System: Increasing the benthic biodiversity knowledge. *Estuarine, Coastal and Shelf Science*. 274, 107924.

Rix L, de Goeij JM, van Oevelen D, Struck U, Al-Horani FA, Wild C, and Naumann MS. 2018. Reef sponges facilitate the transfer of coral-derived organic matter to their associated fauna via the sponge loop. *Marine Ecology Progress Series*. 589, 85-96.

Roberts EM, Bowers DG, Meyer HK, Samuelsen A, Rapp HT, and Cárdenas P. 2021. Water masses constrain the distribution of deep-sea sponges in the North Atlantic Ocean and Nordic Seas. *Marine Ecology Progress Series*. 659, 75-96.

Rodríguez MG, and Esteban A. 1999. On the biology and fishery of *Aristeus antennatus* (Risso, 1816), (Decapoda, Dendrobranchiata) in the Ibiza Channel (Balearic Islands, Spain). *Scientia Marina*. 63, 27-37.

Rodríguez MG, Esteban A, Gil JLP. 2020. Considerations on the biology of *Plesionika edwardsi* (Brandt, 1851) (Decapoda, Caridea, Pandalidae) from experimental trap catches in the Spanish western Mediterranean Sea. *Scientia Marina*, 64, 369-379.

Rogers AD. 2018. The biology of seamounts: 25 Years on. In: *Advances in marine biology* Vol. 79, pp. 137-224. Academic Press.

Ronquist F, Teslenko M, Van Der Mark P, Ayres DL, Darling A, Höhna S, and Huelsenbeck JP. 2012. MrBayes 3.2: efficient Bayesian phylogenetic inference and model choice across a large model space. *Systematic biology*. 613, 539-542.

Rosenberg R. 1995. Benthic marine fauna structured by hydrodynamic processes and food availability. *Netherlands Journal of Sea Research*, 34, 4, 303-317.

Rot C, Goldfarb I, Ilan M. and Huchon D. 2006. Putative cross-kingdom horizontal gene transfer in sponge (Porifera) mitochondria. *BMC Evolutionary Biology*. vol. 6, pp 71.

Rueda JL, Gofas S, Aguilar R, Torriente ADL, García Raso JE, Lo Iacono C, Luque AA, Marina P, Mateo-Ramírez A, Moya-Urbano E, Moreno D, Navarro-Barranco C, Salas C, Sánchez-Tocino L, Templado J, and Urra J. 2021. Benthic fauna of littoral and deep-sea habitats of the Alboran Sea: a hotspot of biodiversity. In: *Alboran Sea-Ecosystems and Marine Resources,* pp. 285-358. Springer, Cham.

Rützler K. 1965. Systematik und Ökologie der Poriferen aus Litoral-schattengebieten der Nordadria. *Zeitschrift für Morphologie und Ökologie der Tiere*, 55 1, 1-82.

Rützler K. 1990. Association between Caribbean sponges and photosynthetic organisms. In: *New Perspective in Sponge Biology: 3d International Sponge Conference, 1985*. Smithsonian Institution Press.

Samadi S, Bottan L, Macpherson E, De Forges BR, and Boisselier M-C. 2006. Seamount endemism questioned by the geographic distribution and population genetic structure of marine invertebrates. *Marine Biology.* 1496,1463-1475

Samadi S, Schlacher T, and Richer de Forges B. 2007. Seamount benthos. In: *Seamounts: Ecology, Fisheries and Conservation*. Blackwell, 119-140.

Sandford F. 1995. Sponge/shell switching by hermit crabs, *Pagurus impressus*. *Invertebrate Biology*. 73-78.

Santín, A. 2022. Exploration and discovery of sponge assemblages on the continental shelf and slope of the Catalano-Balearic Sea by means of non-invasive techniques. Phd Thesis. Universidad de Barcelona. 511 pp.

Santín A, Grinyó J, Ambroso S, Uriz MJ, Gori A, Dominguez-Carrió C, and Gili JM. 2018. Sponge assemblages on the deep Mediterranean continental shelf and slope (Menorca Channel, Western Mediterranean Sea). *Deep Sea Research Part I: Oceanographic Research Papers*. 131, 75-86.

Santín A, Grinyó J, Ambroso S, Uriz MJ, Dominguez-Carrió C, Gili JM. 2019. Distribution patterns and demographic trends of demosponges at the Menorca Channel (Northwestern Mediterranean Sea). *Progress in Oceanography*. 173: 9-25.

Santinelli C. 2015. DOC in the Mediterranean Sea. In: *Biogeochemistry of marine dissolved organic matter.* pp. 579-608. Academic Press.

Santos GG, Sandes J, Cabral A, and Pinheiro U. 2016. *Neopetrosia* de Laubenfels, 1949 from Brazil: description of a new species and a review of records (Haplosclerida: Demospongiae: Porifera). *Zootaxa.* 4114, 331-340.

Sarà M. 1958a. Contributo all consoscenza dei Poriferi del Mar Ligure. *Annali di Museo Civico di Storia Naturale Genova*. 70, 207-244.

Sarà M. 1958b. Studio sui Poriferi di una grotta di marea del Golfo di Napoli. *Archivo Zoologico Italiano*. 43, 203-281.

Sarà M, and Siribelli L. 1960. La fauna di Poriferi delle 'secche' del Golfo di Napoli. 1. La 'secca' della Gaiola. *Annuario dell'Istituto e Museo de Zoologia dell'Università di Napoli*. 123, 1-93.

Sarà M. 1961. La fauna di Poriferi delle grotte delle isole Tremiti. Studio ecologico e sistematico. *Archivio zoologico italiano*. 46, 1-59.

Sarà M. 1962. Distribuzione ed ecologia dei Poriferi in acque superficiali del Golfo di Policastro (Mar Tirreno). *Annali del Pontificio Istituto Superiore di Scienze e Lettere S. Chiara*. 12, 191-215.

Saritas MÜ. 1972. A preliminary study on the silicious Sponge (Porifera) Fauna of Engeceli Limani in the Gulf of Izmir (Aegean Sea). *Scientific reports of the Faculty of Science, Ege University*. 143, 1-25 (in Turkish).

Schindelin J, Arganda-Carreras I, Frise E, Kaynig V, Longair M, Pietzsch T, Preibisch S, Rueden C, Saalfeld S, Schmid B, Tinevez J-Y, White D.J, Hartenstein V, Eliceiri K, Tomancak P, and Cardona A. 2012. Fiji: An open-source platform for biological image analysis. *Nature Methods.* 9, 676-682.

Schmidt O. 1862. Die Spongien des Adriatischen Meeres. Leipzig: Wilhelm Engelmann.

Schmidt O. 1864. Supplement der Spongien des Adriatischen Meeres. Enthaltend die Histologie und systematische Ergänzungen. Wilhelm Engelmann.

Schmidt O. 1868. Die Spongien der Küste von Algier. Mit Nachträgen zu den Spongien des Adriatischen Meeres Drittes Supplement. Leipzig: Wilhelm Engelmann.

Schmidt O. 1870. Grundzüge einer Spongien-Fauna des atlantischen Gebietes. Leipzig: Wilhelm Engelmann.

Schmidt O. 1875. Spongien. Die Expedition zur physikalisch-chemischen und biologischen Untersuchung der Nordsee im Sommer 1872. *Jahresbericht der Commission zur Wissenschaftlichen Untersuchung der Deutschen Meere in Kiel*. 2-3, 115-120.

Schmitt S, Hentschel U, Zea S, Dandekar T, and Wolf M. 2005. ITS-2 and 18S rRNA gene phylogeny of Aplysinidae (Verongida, Demospongiae). *Journal of Molecular Evolution*. 60, 3, 327-336.

Schuster A, Erpenbeck D, Pisera A, Hooper J, Bryce M, Fromont J, and Wörheide G. 2015. Deceptive desmas: molecular phylogenetics suggests a new classification and uncovers convergent evolution of lithistid demosponges. *PloS one*. 101, e116038.

Schuster A, Lopez JV, Becking LE, Kelly M, Pomponi SA, Wörheide G, Erpenbeck D, and Cárdenas P. 2017. Evolution of group I introns in Porifera: new evidence for intron mobility and implications for DNA barcoding. *BMC Evolutionary Biology*. 17, 82.

Schuster A, Pomponi SA, Pisera A, Cárdenas P, Kelly M, Wörheide G, and Erpenberk D. 2021. Systematics of 'lithistid' tetractinellid demosponges from the Tropical Western Atlantic - implications for phylodiversity and bathymetric distribution. *PeerJ*. 9, e10775.

Shaffer MR, Luter HM, Webster NS, Wahab MAA, and Bell JJ. 2020. Evidence for genetic structuring and limited dispersal ability in the Great Barrier Reef sponge *Carteriospongia foliascens*. *Coral Reefs*. 39 1, 39-46.

Simpson TL. 1978. The biology of the marine sponge *Microciona prolifera* (Ellis and Sollander). III. Spicule secretion and the effect of temperature on spicule size. *Journal of Experimental Marine Biology and Ecology.* 35, 31-42.

Simpson TL. 1984. The cell biology of sponges. Springer-Verlag, New York.

Sitjà C. 2020. *The bathyal connections between the Mediterranean Sea and the Northeastern Atlantic Ocean: an assessment using deep-water sponges as a case study.* Ph.D. thesis. Barcelona: Universitat de Barcelona, 360.

Sitjà C, and Maldonado M. 2014. New and rare sponges from the deep shelf of the Alboran Island (Alboran Sea, Western Mediterranean). *Zootaxa.* 37602, 141-179.

Sitjà C, Maldonado M, Farias C, and Rueda JL. 2019. Deep-water sponge fauna from the mud volcanoes of the Gulf of Cadiz (North Atlantic, Spain). *Journal of the Marine Biological Association of the United Kingdom.* 994, 807-831.

Soares MDO*,* Tavares TCL, and Carneiro PBDM. 2019. Mesophotic ecosystems: Distribution, impacts and conservation in the South Atlantic. *Diversity and Distributions* 25, 255-268.

Sollas WJ. 1885. A Classification of the Sponges. *Annals and Magazine of Natural History*. (5) 16, 95: 395.

Sollas WJ. 1886. Preliminary account of the Tetractinellid sponges dredged by H.M.S. 'Challenger' 1872-76. *Part I. The Choristida. Scientific Proceedings of the Royal Dublin Society new series*. 5, 177-199.

Sollas WJ. 1888. Report on the Tetractinellida collected by H.M.S. Challenger, during the years 1873-1876. Report on the Scientific Results of the Voyage of H.M.S. Challenger during the years 1873-76. *Zoology*. 25 part 63: 1-458, pl. 1-44

Solórzano MR. 1990. *Poríferos del litoral gallego: estudio faunístico, distribución e inventario*. Phd Thesis. Unversidad de Santiago de Compostela. 1036 pp.

Spedicato MT, Massutí E, Mérigot B, Tserpes G, Jadaud A, and Relini G. 2019. The MEDITS trawl survey specifications in an ecosystem approach to fishery management. *Scientia Marina*. 83, 9-20.

Stamatakis A. 2014. RAxML version 8: a tool for phylogenetic analysis and post-analysis of large phylogenies. *Bioinformatics.* 309, 1312-1313.

Steffen, K, Laborde Q, Gunasekera S, Payne CD, Rosengren KJ, Riesgo A, Göransson U, and Cárdenas P. 2021. Barrettides: A Peptide Family Specifically Produced by the Deep-Sea Sponge *Geodia barretti*. *Journal of Natural Products*. 84,12, 3138-3146

Steffen K, Indraningrat AAG, Erngren I, Haglöf J, Becking LE, Smidt H, Yashayaev I, Kenchington E, Pettersson C, Cárdenas P, Sipkema D. 2022. Oceanographic setting influences the prokaryotic community and metabolome in deep-sea sponges. *Scientific Reports*. 12, 1, 3356

Tabachnick KP. 2002. Family Rossellidae Schulze, 1885. In: Hooper JNA and van Soest RWM. (eds), *Systema Porifera. A Guide to the Classification of Sponges*, vol. 2. New York, NY: Kluwer Academic/Plenum, pp. 1441-1505.

Teichert S. 2014. Hollow rhodoliths increase Svalbard' shelf biodiversity. *Scientific Reports*, 4, 6972.

Terrasa B. and Oliver P. 2024. Les Barques del bou a Mallorca. Edicions UIB, Palma. In press.

Thompson JD, Higgins DG, and Gibson TJ. 1994. CLUSTAL W: improving the sensitivity of progressive multiple sequence alignment through sequence weighting, position-specific gap penalties and weight matrix choice. *Nucleic acids research.* 22, 4673-4680.

Tintoré J, Vizoso G, Casas B, Heslop E, Pascual A, Orfila A, Ruiz S, Martínez-Ledesma M, Torner M, Cusi S, Diedrich A, Balaguer-Huguet P, Gómez-Pujol L, Álvarez-Ellacuria A, Gómara S, Sebastian K, Lora S, Beltrán JP, Renault L, Melanie J, Alvarez-Berastegui D, March D, Garau B, Castilla C, Cañellas T, Roque D, Lizarán I, Pitarch S, Carrasco MA, Lana A, Mason E, Escudier R, Conti-Sampol D, Sayol JM, Barceló-Llull B, Alemany F, Reglero P, Massutí E, Velez-Belchi P, Ruiz J, Oguz T, Gómez M, Alvarez E, Ansorena L. & Manriquez, M. 2013. SOCIB: The Balearic Islands Coastal Ocean Observing and Forecasting System Responding to Science, Technology and Society Needs. *Marine Technology Society Journal*, 47, 1, 101-117.

Topsent E. 1890. Notice préliminaire sur les spongiaires recueillis durant les campagnes de l'Hirondelle. *Bulletin de la Société zoologique de France*. 15, 26-32, 65-71.

Topsent E. 1892. Contribution à l'étude des Spongiaires de l'Atlantique Nord (Golfe de Gascogne, Terre-Neuve, Açores). Résultats des campagnes scientifiques accomplies par le Prince Albert I. Monaco. 2, 1-165, pls I-XI.

Topsent E. 1892. Diagnoses d'éponges nouvelles de la Méditerranée et plus particulièrement de Banyuls. *Archives de Zoologie expérimentale et générale*. 2. 10 Notes et Revue 6. xvii-xxviii.

Topsent E. 1893. Nouvelle série de diagnoses d'éponges de Roscoff et de Banyuls. *Archives de Zoologie expérimentale et générale*. 3. 1 Notes et Revue 10, xxxiii-xliii.

Topsent E. 1894. Étude monographique des Spongiaires de France. I. Tetractinellida. *Archives de Zoologie expérimentale et générale*. 3. 2, 259-400, pls XI-XVI.

Topsent E. 1895. Campagnes du yacht Princess Alice. Notice sur les spongiaires recueillis en 1894 et 1895. *Bulletin de la Société Zoologique de France*. 20, 213-216.

Topsent E. 1895. Étude monographique des spongiaires de France II. Carnosa. *Archives de Zoologie expérimentale et générale*, 33, 493-500, pls. XXI-XXIII.

Topsent E. 1901. Considérations sur la faune des spongiaires des côtes d'Algérie. Eponges de La Calle. *Archives de Zoologie expérimentale et générale*. 3. 9, 327-370, pls XIII-XIV.

Topsent E. 1904. Spongiaires des Açores. *Résultats des campagnes Scientifiques accomplies par le Prince Albert I. Monaco*, 25, 1-280.

Topsent E. 1925. Etude des Spongiaires du Golfe de Naples. *Archives de Zoologie expérimentale et générale*. 635, 623-725

Topsent E. 1927. Diagnoses d'Éponges nouvelles recueillies par le Prince Albert ler de Monaco. *Bulletin de l'Institut océanographique Monaco*. 502, 1-19.

Topsent E. 1928. Spongiaires de l'Atlantique et de la Méditerranée provenant des croisières du Prince Albert ler de Monaco. *Résultats des campagnes scientifiques accomplies par le Prince Albert I. Monaco*, 74, 1-376, pls I-XI.

Topsent E. 1934. Eponges observées dans les parages de Monaco. Première partie. *Bulletin de l'Institut océanographique*. Monaco. 650, 1-42.

Topsent E. 1938. Contribution nouvelle à la connaissance des Eponges des côtes d'Algérie. Les espèces nouvelles d'O. Schmidt, 1868. *Bulletin de l'Institut océanographique, Monaco*. 758, 1-32.

Trainito E, Baldacconi R, and Mačić V. 2020. All-around rare and generalist: countercurrent signals from the updated distribution of *Calyx nicaeensis* (Risso, 1826) (Porifera, Demospongiae). *Studia Marina*. 33, 1

Traveset A. 1991. Presencia d'*Ephydatia fluviatilis* (Porifera: Spongillidae) en un torrent de Mallorca. *Bolletí de la Societat d'Història Natural de les Balears*. 97-98.

Uitz J, Stramski D, Gentili B, D'Ortenzio F, and Claustre H. 2012. Estimates of phytoplankton class-specific and total primary production in the Mediterranean Sea from satellite ocean color observations. *Global Biogeochemichal Cycles*. 26, GB2024.

Uriz MJ. 1981. Systematic study of sponges Astrphorida (Demospongia) from the bottoms of dragging fishing, between Tossa and Calella (Catalonia) Spain. [Spanish]. *Boletin del Instituto Español de Oceanografía*.

Uriz MJ. 1983. Monografía I. Contribución a la fauna de esponjas (Demospongia) de Cataluña. *Anales de la Sección Ciencias del Colegio Universitario de Gerona*. 7, 1-220.

Uriz MJ. 1984. Material para la fauna de esponjas ibéricas: nuevas señalizaciones de Demosponjas en nuestras costas. *Actas do IV Simposio ibérico de estudos do benthos marinho*, 3, 131-140.

Uriz MJ. 2002. Family Geodiidae Gray, 1867. *Systema Porifera: a guide to the classification of sponges*, pp. 134-140. New York: Kluwer Academic/Plenum Publishers.

Uriz MJ, and Rosell D. 1990. Sponges from bathyal depths (1000-1750 m) in the Western Mediterranean Sea. *Journal of Natural History.* 24, 373-391.

Uriz MJ, Rosell D, and Martín D. 1992. The sponge population of the Cabrera Archipelago Balearic Islands: characteristics, distribution, and abundance of the most representative species. *Marine Ecology*. 132, 101-117.

Uriz MJ, Turon X, and Becerro MA. 2003a. Silica deposition in demosponges. p. 163-193. In: *Silicon biomineralization*. Springer, Berlin, Heidelberg.

Uriz MJ, Turon X, Becerro MA, and Agell G. 2003b. Siliceous spicules and skeleton frameworks in sponges: Origin, diversity, ultrastructural patterns, and biological functions. *Microscopy Research and Technique.* 62, 279-299.

Vacelet J. 1960. Eponges de la Méditerranée Nord-Occidentale récoltées par le "Président-Théodore-Tissier" 1958. *Revue des Travaux de l'Institut des Pêches maritimes.* 24, 257-272.

Vacelet J. 1961. Spongiaires Démosponges de la région de Bonifacio (Corse). Recueil des Travaux de la Station marine d'Endoume. 22, 36, 21-45.

Vacelet J. 1969. Eponges de la Roche du Large et de l'étage bathyal de Méditerranée récoltes de la soucoupe plongeante Cousteau et dragages. *Mémoires du Muséum national d'Histoire Naturelle.* 59, 145-219.

Vacelet J. 1976. Inventaire des Spongiaires du Parc national de Port-Cros Var. Travaux scientifiques du Parc national de Port-Cros. 2, 167-186.

Vacelet J. 2007. Diversity and evolution of deep-sea carnivorous sponges. In: Custódio MR, Lôbo-Hajdu G, Hajdu E, Muricy G, editors. *Porifera research: biodiversity, innovation and sustainability.* Série Livros 28. Rio de Janeiro: Museu Nacional. pp. 107–115.

Vacelet J, and Uriz MJ. 1991. Deficient spiculation in a new species of *Merlia* (Merliida, Demospongiae) from the Balearic Islands. p. 170-178. In: *Fossil and recent sponges*. Reitner, J, Keupp, H, Eds. Springer-Verlag, Berlin.

Vacelet J, and Boury-Esnault N. 1996. A new species of carnivorous sponge (Demospongiae: Cladorhizidae) from a Mediterranean cave. In: Willenz, Ph. Ed, Recent Advances in Sponge Biodiversity Inventory and Documentation. *Bulletin de l'Institut royal des Sciences naturelles de Belgique*. Biologie. 66, 109-115.

Vacelet J*,* Bitar G*,* Carteron S*,* Zibrowius H, and Perez T. 2007. Five new sponge species (Porifera: Demospongiae) of subtropical or tropical affinities from the coast of Lebanon eastern Mediterranean. *Journal of the Marine Biological Association of the United Kingdom.* 87, 1539-1552.

Vacelet J, Boury-Esnault N, and Harmelin JG. 1994. Hexactinellid cave, a unique deep-sea habitat in the scuba zone. *Deep Sea Research Part I: Oceanographic Research Papers*. 417, 965-973.

Valisano L, Pozzolini M, Giovine M, and Cerrano C. 2012. Biosilica deposition in the marine sponge *Petrosia ficiformis* (Poiret, 1789): the model of primmorphs reveals time dependence of spiculogenesis. In: Maldonado M, Becerro MA, Turon X, and Uriz MJ. (eds). *Ancient Animals, New Challenges*. Dordrecht: Springer, pp. 259-273.

Vamvakas C. 1971. Contribution to the study of soft substrata benthic biocoenoses of Greek Seas. Area W. Saronikos Gulf. *Hellenic Oceanology and Limnology*. 10, 1-152.

Vân Le HL, Lecointre G, and Perasso R. 1993. A 28S rRNA-based phylogeny of the gnathostomes: first steps in the analysis of conflict and congruence with morphologically based cladograms. *Molecular phylogenetics and evolution*. 21, 31-51.

Van Soest RWM. 1980. Marine sponges from Curaçao and other Caribbean localities. Part II. Haplosclerida. In: Hummelinck PW and Van der Steen LJ eds, *Studies on the Fauna of Curaçao and other Caribbean Islands.* 62, 1-173.

Van Soest RWM. 1984. Marines sponges from Curaçao and other Caribbean localities Part III. Poecilosclerida. In: Hummelinck PW and Van der Steen LJ (eds). *Studies on the Fauna of Curaçao and other Caribbean Islands.* 66, 1-167.

Van Soest RWM. 1993. Affinities of the Marine Demospongiae Fauna of the Cape Verde Islands and Tropical West Africa. *Courier Forschungsinstitut Senckenberg*. 159, 205-219.

Van Soest RWM. 2017. *Flagellia*, a new subgenus of *Haliclona* (Porifera, Haplosclerida). *European Journal of Taxonomy.* 351, 1-48.

Van Soest RWM, and Hooper JNA. 1993. Taxonomy, phylogeny and biogeography of the marine sponge genus Rhabderemia Topsent,1890 (Demospongiae, Poecilosclerida). Pp. 319-351. In: Uriz MJ, and Rützler K. (eds), *Recent Advances in Ecology and Systematics of Sponges*. *Scientia Marina*. 57, 4, 273-432.

Van Soest RWM, Hooper JNA, and Hiemstra F. 1991. Taxonomy, phylogeny and biogeography of the marine sponge genus *Acarnus* (Porifera: Poecilosclerida). *Beaufortia.* 42, 49-88.

Van Soest RWM, Cleary DFR, de Kluijver MJ, Lavaleye MSS, Maier C, and van Duyl FC. 2007. Sponge diversity and community composition in Irish bathyal coral reefs. *Contributions to Zoology*. 76, 121-142.

Van Soest RWM, Beglinger EJ, and de Voogd NJ. 2010. Skeletons in confusion: a review of astrophorid sponges with dicho-.calthrops as structural megascleres (Porifera, Demospongiae, Astrophorida). *Zookeys*. 68, 1-88.

Van Soest RWM, Boury-Esnault N, Vacelet J, Dohrmann M, Erpenbeck D, De Voogd NJ, Santodomingo N, Vanhoorne B, Kelly M, and Hooper JNA. 2012. Global Diversity of Sponges Porifera. *PLoS One.* 7 4, e35105.

Van Soest RWM, Meesters EH, and Becking LE. 2014. Deep-water sponges (Porifera) from Bonaire and Klein Curaçao, Southern Caribbean. *Zootaxa*. 38785, 401-443.

Vasquez, M, Allen, H, Manca, E, Castle, L, Lillis, H, Agnesi, S, Al Hamdani Z, Annunziatellis A, Askew N, Bekkby T, Bentes L, Doncheva V, Drakopoulou V, Duncan G, Gonçalves J, Inghilesi R, Laamanen L, Loukaidi V, Martin S, McGrath F, Mo G, Monteiro P, Muresan M, Nikilova C, O'Keeffe E, Pesch R, Pinder J, Populus J, Ridgeway A, Sakellariou D, Teaca A, Tempera F, Todorova V, Tunesi L & Virtanen, E. 2021. EUSeaMap 2021. A European broad-scale seabed habitat map.

Vicens D, Gràcia F, Balaguer P, Ginard A, Crespí D, and Bover P. 2011. Cavitats litorals de gènesi marina a les Illes Balears. *Endins: publicació d'espeleologia*. 227-236.

Vicente J, Ríos JA, Zea S, and Toonen RJ. 2019. Molecular and morphological congruence of three new cryptic *Neopetrosia* spp. in the Caribbean. *PeerJ.* 7, e6371.

Vieira de Barros L, Santos G, and Pinheiro U. 2013. *Clathria (Clathria)* Schmidt, 1862 from Brazil with description of a new species and a review of records (Poecilosclerida: Demospongiae: Porifera). *Zootaxa.* 3640, 284-295.

Von Lendenfeld R. 1894. Die Tetractinelliden der Adria. Mit einem Anhange über die Lithistiden. Denkschriften der Kaiserlichen Akademieder Wissenschaften.Wien. Mathematisch-Naturwissenschaften Klasse, 61, 91- 204, pls I-VIII.

Vosmaer GCJ. 1894. Preliminary notes on some tetractinellids of the Bay of Naples. Tijdschrift der Nederlandsche Dierkundige Vereeniging. 2. 4, 269-286.

Vosmaer GCJ. 1933. The Sponges of the Bay of Naples. Porifera. In: Calcaria, vol. 1. Martinus Nijhoff, The Hague.

Voultsiadou E. 2005. Sponge diversity in the Aegean Sea: Check list and new information. *Italian Journal of Zoology*. 72, 1, 53-64.

Voultsiadou E. 2009. Reevaluating sponge diversity and distribution in the Mediterranean Sea. *Hydrobiologia.* 628, 1-12.

Watling L, & Auster PJ. 2017. Seamounts on the high seas should be managed as vulnerable marine ecosystems. *Frontiers in Marine Science*. 4,14.

White M, and Mohn C. 2004. Seamounts: a review of physical processes and their influence on the seamount ecosystem. OASIS EU Project Report, 37 pp.

Wiedenmayer F. 1977. Shallow-water sponges of the western Bahamas. *Experientia Supplementum.* 28, 1-287.

Wiens M, Belikov SI, Kaluzhnaya OV, Adell T, Schröder HC, Perovic-Ottstadt S, Kaandorp JA, Müller WEG. 2008. Regional and modular expression of morphogenetic factors in the demosponge *Lubomirskia baicalensis*. *Micron*. 39, 4, 447-460.

Wörheide G. 2006. Low variation in partial cytochrome oxidase subunit I COI mitochondrial sequences in the coralline demosponge *Astrosclera willeyana* across the Indo-Pacific. *Marine Biology.* 148, 907-912.

Würtz M, and Rovere M. 2015. Atlas of the Mediterranean seamounts and seamount-like structures. Gland, Switzerland: IUCN.

Xavier J, and van Soest R. 2007. Demosponge fauna of Ormonde and Gettysburg Seamounts (Gorringe Bank, north-east Atlantic) diversity and zoogeographical affinities. *Journal of the Marine Biological Association of the United Kingdom*. 876, 1643-1653.

Xavier JR, and Van Soest RW. 2012. Diversity patterns and zoogeography of the Northeast Atlantic and Mediterranean shallow-water sponge fauna. *Hydrobiologia.* 687, 107-125.

Zabala M, and Ballesteros E. 1989. Surface-dependent strategies and energy flux in benthic marine communities or, why corals do not exist in the Mediterranean. *Scientia Marina*. 53, l-15.

ANNEX

Supplementary table S4.1.1. Sequences used in chapter 4.1.

SPECIES	GENBANK ID
MICROCIONIDAE	
Clathria armata	KC869418
Artemisina tubulosa	LN850173
Artemisina melana	EF519575
Clathria cancellaria	HE611597
Clathria reinwardti	MH784605
Clathria reinwardti	KY947264
Clathria reinwardti	KX894489
Clathria reinwardti	HE611598
Clathria schoenus	EF519607
Clathria oxeota	EF519605
Ophlitaspongia papilla	KY492547
Ophlitaspongia papilla	KY492544
Ophlitaspongia papilla	KY492542
Clathria kylista	HE611600
Clathria kylista	HE611599
Clathria abietina	HE611593
Ophlitaspongia papilla	KY492538
Antho sp	MH784604
Clathria barleei	KC883682
Ophlitaspongia papilla	KY492543
Ophlitaspongia papilla	KY492541
Ophlitaspongia papilla	KY492540
Ophlitaspongia papilla	KY492539
Microciona prolifera	AJ843888
Ophlitaspongia papilla	KY492546
Ophlitaspongia papilla	KY492549
Ophlitaspongia papilla	KY492545
Clathria prolifera	KU906059
Clathria prolifera	KU905733
Clathria prolifera	KJ546353
Microciona prolifera	DQ087475
Microciona prolifera	AJ704978
Clathria toxitenuis	KX866770
Clathria kylista	HE611601
Clathria cervicornis	HE611596
Clathria conectens	HE611602
Clathria abietina	HE611595
Clathria pauper	LN850182
ACARNIDAE	

*Acarnus levii**	MN508967
*Acarnus levii **	MN508969
Iophon methanophila	KU659138
Acanthorhabdus fragilis	LN850167
Acanthorhabdus fragilis	LN850168
Acanthorhabdus fragilis	LN850166
Iophon sp	LN850195
Paracornulum dubium	HE611605
Paracornulum sp	HE611606
IOTROCHOTIDAE	
Iotrochota acerata	HE611625
Iotrochota birotulata	EF519633
Iotrochota birotulata	EU237486
Iotrochota birotulata	AY561963
Iotrochota coccinea	HE611623
Iotrochota coccinea	HE611624
Iotrochota baculifera	HE611621
Iotrochota baculifera	JQ034566
HYMEDESMIIDAE	
Phorbas plumosus	KY492535
Phorbas plumosus	KY492534
Phorbas plumosus	KY492532
ISODICTYIDAE	
Isodictya erinacea	LN850199
Isodictya kerguelenensis	LN850198
PODOSPONGIIDAE	
Neopodospongia cf normani	JF440339
RASPAILIIDAE	
Acantheurypon pilosella	JF440337
AXINELLIDAE	
Axinella polypoides	LN868209
HAPLOSCLERIDA	
Haplosclerida sp	MK833931
CHALINIDAE	
*Haliclona poecillastroides**	MN508968
Haliclona elegans	JX999087
Haliclona (Soestella) xena	JN242209
Haliclona (Reniera) tubifera	KR707690
Haliclona (Haliclona) oculata	JN242199
Haliclona (Reniera) tubifera	KR707694
Haliclona (Reniera) implexiformis	KJ729034
Haliclona (Reniera) implexiformis	EF519623

Haliclona (Reniera) manglaris	EF519626
Haliclona amphioxa	AJ843892
Haliclona cnidata	MH396488
Cladocroce burapha	KY565331
CALLYSPONGIIDAE	
Callyspongia (Cladochalina) diffusa	KX454494
Callyspongia (Callyspongia) fallax	JN242193
Callyspongia (Callyspongia) nuda	JN242194
Callyspongia (Callyspongia) siphonella	JX999082
Callyspongia (Cladochalina) plicifera	EU237477
PETROSIIDAE	
Xestospongia muta	MH285814
Xestospongia muta	HQ452958
Xestospongia muta	HQ452957
Xestospongia testudinaria	HQ452961
Xestospongia testudinaria	HQ452959
Xestospongia deweerdtae	KX668524
Xestospongia bergquistia	JN242221
Neopetrosia seriata	JN242213
Neopetrosia dendrocrevacea	MK105442
Neopetrosia cristata	MK105441
Neopetrosia sigmafera	MK105446
Neopetrosia próxima	MK105445
Neopetrosia próxima	MK105443
Neopetrosia próxima	MK105444
Neopetrosia próxima	AM076980
Petrosia (Petrosia) ficiformis	KX866751
Petrosia (Petrosia) ficiformis	JX999088
Petrosia sp A	JN242214
Petrosia sp E	JN242217
Petrosia sp C	JN242216
Petrosia sp B	JN242215
Petrosia sp G	JN242218
Petrosia sp J	JN242220
Petrosia sp	JN242219
PHLOEODICTYDAE	
Calyx podatypa	JX999086
Calyx arcuarius	LN850179
Calyx nicaeensis	KX866755
Oceanapia sp	JN242224
Oceanapia sp	JN242223
NIPHATIDAE	

Gelliodes aff carnosa	KY565325
Gelliodes wilsoni	KY565327
Amphimedon queenslandica	DQ915601
Amphimedon compressa	EU237474
Cribrochalina dura Petrosia dura	EF519663
Cribrochalina vasculum	EF519664
GEODIIDAE	
Geodia barretti	KC574389
LUBOMIRSKIIDAE	
Baikalospongia intermedia	EU000567

**Barcodes sequenced by the authors.*

Supplementary table S4.2.1. Field and CFM-IEOMA collection codes for specimens studied in chapter 4.2.

Species	**Field code**	**CFM-IEOMA Code**	**Observations**
Foraminospongia balearica	i802	7356	Bushy-tubular fragment
Foraminospongia balearica	i144	7357	Bushy-tubular fragment
Foraminospongia balearica	i293_1	7358	Bushy-tubular fragment
Foraminospongia balearica	i239	7359	Bushy-tubular fragment
Foraminospongia balearica	i745	7360	Bushy-tubular fragment
Foraminospongia balearica	i824_4	7361	Bushy-tubular fragment
Foraminospongia minuta	i439	7362	Small encrusting
Foraminospongia minuta	i474	7363	Small encrusting
Axinella spatula	i338_A	7364	Small erect
Axinella spatula	i338_B	7365	Small erect
Axinella spatula	i338_C	7366	Small erect
Phakellia robusta	i347_2	7367	Small, fan shaped, 1 cm^2
Phakellia robusta	i405	7368	Small, fan shaped, 1 cm^2
Phakellia robusta	i409	7369	Small, fan shaped, 1 cm^2
Phakellia robusta	i414_2	7370	Small, fan shaped, 1 cm^2
Phakellia robusta	i417	7371	Small, fan shaped, 1 cm^2
Phakellia robusta	i712	7372	Small, fan shaped, 1 cm^2
Phakellia robusta	i731	7373	Small, fan shaped, 2 cm^2
Phakellia robusta	POR760	7374	Small, fan shaped, 3 cm^2
Phakellia robusta	POR762	7375	Small, fan shaped, 3 cm^2
Phakellia ventilabra	i822_1	7376	Small, fan shaped, 3 cm^2
Phakellia hirondellei	i353	7377	Small, fan shaped, 3 cm^2
Phakellia hirondellei	i623	7378	Small, fan shaped, 3 cm^2
Heteroxya cf. beauforti	i727	7379	Small encrusting and circular
Heteroxya cf. beauforti	i726	7380	Small encrusting and circular
Heteroxya cf. beauforti	i444	7381	Small encrusting and circular
Heteroxya cf. beauforti	i461	7382	Small encrusting and circular
Heteroxya cf. beauforti	i487	7450	Small encrusting and circular
Paratimea massutii sp nov	i403	7383	Massive fragment 4 cm in diameter
Paratimea massutii sp nov	i420	7384	Spicule preparation
Rhabdobaris implicata	i338_2	7385	Small, fan shaped, 1 cm^2
Rhabdobaris implicata	i698	7386	Small, fan shaped, 1 cm^2
Dragmatella aberrans	i52_b1	7387	Small encrusting fragment with papillae
Dragmatella aberrans	i175	7388	Small encrusting fragment with papillae
Haliclona (Soestella) fimbiata	i825_1	7389	Erect, 2 cm^2
Petrosia (Strongylophora) vansoesti	i192_A	7390	Massive fragment 3-4 cm3

Petrosia (Strongylophora) vansoesti	i192_B	7391	Massive fragment 3-4 cm3
Petrosia (Strongylophora) vansoesti	i313_P	7392	Massive fragment 3-4 cm3
Petrosia (Strongylophora) vansoesti	i313_G	7393	Massive fragment 3-4 cm3
Petrosia (Strongylophora) vansoesti	i351	7394	Massive fragment 3-4 cm3
Petrosia (Strongylophora) vansoesti	i694	7395	Massive fragment 3-4 cm3
Petrosia (Petrosia) raphida	POR406	7396	Massive fragment 1-3 cm3
Petrosia (Petrosia) raphida	i178_3	7397	Massive fragment 1-3 cm3
Petrosia (Petrosia) raphida	i242	7451	Massive fragment 1-3 cm3
Petrosia (Petrosia) raphida	i254_2	7398	Massive fragment 1-3 cm3
Petrosia (Petrosia) raphida	i305	7399	Massive fragment 1-3 cm3
Petrosia (Petrosia) raphida	i312	7400	Massive fragment 1-3 cm3
Calyx cf. tufa	i75	7401	Massive fragment 3 cm3, circular pores
Calyx cf. tufa	i515	7402	Massive fragment 3 cm3, circular pores
Calyx cf. tufa	i525	7403	Massive fragment 3 cm3, circular pores
Melonanchora emphysema	i573	7404	Encrusting fragment with papillae
Polymastia polytylota	i810	7405	Circular sponge with a papillae at its upper side. 2 cm in diameter
Pseudotrachya hystrix	i303_A	7406	Small hispid sponge
Pseudotrachya hystrix	i613	7407	Small hispid sponge
Hemiasterella elongata	i149_4	7408	Erect sponge 1cm^3
Hemiasterella elongata	i337	7409	Erect sponge 1cm^3
Hemiasterella elongata	i531	7410	Erect sponge 1cm^3
Hemiasterella elongata	POR1066	7411	Erect sponge 1cm^3
Lanuginella pupa	i286_1	7412	Tubular sponge 1 cm2
Lanuginella pupa	i286_2	7413	Tubular sponge 1 cm2
Lanuginella pupa	i286_3	7414	Tubular sponge 1 cm2
Rhabderemia sp	i729_1	7415	Spicule preparation

Supplementary table S4.2.2. Genbank sequences used in Chapter 4.2.

Species	**Genbank ID's**
COI	
Agelas cerebrum	DQ075692
Agelas cervicornis	DQ075753
Agelas citrina	MH285788
Agelas citrina	MH285789
Agelas citrina	MH285787
Agelas citrina	MH285786
Agelas clathrodes	DQ075740
Agelas clathrodes	DQ075743
Agelas clathrodes	DQ075719
Agelas conifera	DQ075699
Agelas conifera	DQ075712
Agelas dilatata	DQ075693
Agelas dispar	DQ075710
Agelas dispar	DQ075715
Agelas dispar	DQ075736
Agelas dispar	DQ075707
Agelas gracilis	DQ069300
Agelas mauritania	DQ069302
Agelas nemoechinata	DQ069306
Agelas novacaledoniae	DQ069301
Agelas oroides	LN868208
Agelas repens	DQ075756
Agelas sceptrum	DQ075739
Agelas schmidti	DQ075711
Agelas sp.	MK833917
Agelas sp.	MK503382
Agelas sventres	DQ075746
Agelas sventres	DQ075695
Agelas sventres	DQ075731
Agelas sventres	MH285799
Agelas sventres	MH285794
Agelas sventres	MH285790
Agelas sventres	MH285785
Agelas sventres	DQ075772
Agelas sventres	MH285798
Agelas sventres	MH285797
Agelas sventres	MH285792
Agelas sventres	MH285791
Astrosclera willeyana	AY561969

Axinella arctica	MK570860
Axinella aruensis	JQ034547
Axinella aruensis	JQ034548
Axinella aruensis	JQ034549
Axinella aruensis	JQ034550
Axinella aruensis	JQ034551
Axinella cannabina	KX866735
Axinella corrugata	AY791693
Axinella polypoides	LN868209
Biemna fistulosa	MT586737
Biemna fistulosa	KY565306
Biemna fistulosa	AM076982
Biemna fistulosa	KU060567
Biemna fistulosa	KU060563
Biemna megalosigma var. Sigmodragma	MT491474
Biemna megalosigma var. Sigmodragma	MT491471
Biemna megalosigma var. Sigmodragma	MT491470
Biemna megalosigma var. Sigmodragma	MT491468
Biemna saucia	JF773146
Biemna sp.	MT491478
Biemna sp.	MT491477
Biemna sp4	MT491479
Biemna sp4	MT491472
Biemna sp4	MT491467
Biemna variantia	HQ379424
*Calyx cf. tufa**	MW858349
Ceratoporella nicholsoni	DQ075747
Ceratoporella nicholsoni	DQ075775
Cinachyra sp.	KX454495
Cymbaxinella verrucosa	LN868210
Eurypon cf. clavatum	AJ843893
Heteroxya cf. beauforti	MW858350
Hymerhabdia typica	KC869425
Neofibularia hartmani	JF773145
Neofibularia hartmani	MH784610
Neofibularia hartmani	HE611587
Neofibularia hartmani	JQ034574
Neofibularia irata	HE611588
Neofibularia irata	JQ034576
Neofibularia nolitangere	EF519653

Paratimea massutii ***sp. nov.*** *(Holotype)**	MW858351
Prosuberites laughlini	AY561960
Foraminospongia balearica ***sp. nov.*** *(Holotype)**	MW858346
Foraminospongia balearica ***sp. nov.*** *(Paratype)**	MW858347
Foraminospongia minuta ***sp. nov.*** *(Holotype)**	MW858348
Rhabderemia sorokinae	HE611607
*Rhabderemia sp1**	MZ570433
Sigmaxinella hipposiderus	JF773147
Sigmaxinella sp1	MT491533
Sigmaxinella sp1	MT491535
Sigmaxinella sp1	MT491532
Sigmaxinella sp2	MT491534
Sigmaxinella sp2	MT491531
Stylissa carteri	MK833941
Stylissa carteri	KY263266
Stylissa carteri	KY263105
Stylissa carteri	KY262960
Stylissa carteri	JQ034580
Stylissa carteri	JQ034581
Stylissa carteri	MK833942
Stylissa massa	JQ034582
Stylissa massa	JQ034583
Suberites domuncula	JX999078
Suberites ficus	HQ379429
28S	
Acanthostylotella cornuta	KC869600
Agelas clathrodes	AY864739
Agelas conifera	KC869634
Agelas conifera	AY864738
Agelas dispar	AY864740
Agelas oroides	KX688750
Agelas oroides	KX688753
Agelas sp.	AY561929
Astrosclera willeyana	KC869525
Axinella corrugata	KC869523
Axinella corrugata	KC869458
Axinella damicornis	AF062605
Axinella damicornis	KX688743
Axinella damicornis	GQ466058
Axinella damicornis	HQ379198

Axinella damicornis	KX688749
Axinella verrucosa	GQ466063
Biemna fistulosa	MT452534
Biemna variantia	HQ379224
*Calyx cf. tufa**	MW881149
Cymbastela cantharella	GQ466064
*Heteroxya cf. beauforti**	MW881150
Hymerhabdia typica	HQ379289
Hymerhabdia typica	HQ379398
Hymerhabdia typica	HQ379357
Hymerhabdia typica	HQ379223
Prosuberites laughlini	AY626320
Prosuberites longispinus	HQ379245
Foraminospongia balearica ***sp. nov*** *(Holotype)**	MW881153
Foraminospongia minuta ***sp. nov.*** *(Holotype)**	MW881151
Rhabderemia acanthostyla	MN386047
Rhabderemia indica	MK372889
Sigmaxinella sp	KC869491
Stylissa carteri	KU060553
Stylissa carteri	KU060402
Stylissa carteri	KU060396
Stylissa carteri	AY618720
Stylissa carteri	AY618718
Stylissa carteri	AY618719
Stylissa massa	AY618722
Stylissa massa	AY618721
Suberites domuncula	AJ620113
Suberites ficus	HQ379247

Supplementary table S4.3.1. Museum and field codes from chapter 4.3.

Species (alphabetical order)	**Field#**	**Museum#**
Calthropella (Calthropella) pathologica	i693	UPSZMC 190806
Calthropella (Calthropella) pathologica	i682	UPSZMC 190807
Caminella intuta	LIT05	UPSZMC 190808
Caminus vulcani	i142_C	UPSZMC 190809
Caminus vulcani	i254_4	UPSZMC 190810
Caminus vulcani	i391_2	UPSZMC 190811
Caminus vulcani	i526	UPSZMC 190812
Caminus xavierae **sp. nov.** holotype	CAN.07.05	UPSZTY 190813, ZMAPOR 20422
Caminus xavierae **sp. nov.** paratype	CAN.O7.O6	UPSZTY 190814
Characella pachastrelloides	i527	UPSZMC 190815
Characella tripodaria	i153_1B	UPSZMC 190816
Characella tripodaria	i153_4B	UPSZMC 190817
Characella tripodaria	i777	UPSZMC 190818
Craniella cf. *cranium*	i172_1A	UPSZMC 190819
Craniella cf. *cranium*	i151_1B	UPSZMC 190910
Craniella cf. *cranium*	i153_4_1	UPSZMC 190873
Craniella cf. *cranium*	i339_5	UPSZMC 190820
Craniella cf. *cranium*	i409_1_1	UPSZMC 190821
Craniella cf. *cranium*	i416_D	UPSZMC 190822
Craniella cf. *cranium*	i826_7_1(G)	UPSZMC 190823
Discodermia polymorpha	i141_1	UPSZMC 190824
Discodermia polymorpha	i141_2	UPSZMC 190825
Discodermia polymorpha	i141_3	UPSZMC 190826
Discodermia polymorpha	i196_1	UPSZMC 190827
Discodermia polymorpha	i196 (x3)	UPSZMC 190828
Discodermia polymorpha	i277_1	UPSZMC 190829
Discodermia polymorpha	i277 (x4)	UPSZMC 190830
Discodermia polymorpha	i294	UPSZMC 190831
Discodermia polymorpha	i308	UPSZMC 190832
Discodermia polymorpha	i320	UPSZMC 190833
Discodermia polymorpha	i321	UPSZMC 190834
Discodermia polymorpha	i322	UPSZMC 190835
Discodermia polymorpha	i354	UPSZMC 190836
Discodermia polymorpha	i606	UPSZMC 190837
Erylus cf. *deficiens*	LIT10	UPSZMC 190838
Erylus corsicus	i140_2B	UPSZMC 190839
Erylus corsicus	i356_A	UPSZMC 190840
Erylus corsicus	i389_1	UPSZMC 190841
Erylus corsicus	i402_A	UPSZMC 190842

Erylus corsicus	i402_B	UPSZMC 190843
Erylus corsicus	i402_C	UPSZMC 190844
Erylus corsicus	i707	UPSZMC 190845
Erylus discophorus	POR785	UPSZMC 190846
Erylus discophorus	LIT71	UPSZMC 190847
Erylus discophorus	LIT72	UPSZMC 190848
Erylus discophorus	LIT74	UPSZMC 190849
Erylus cf. *mamillaris*	i142_B	UPSZMC 190850
Erylus cf. *mamillaris*	i179_A	UPSZMC 190851
Erylus cf. *mamillaris*	i179_B	UPSZMC 190852
Erylus cf. *mamillaris*	i314	UPSZMC 190853
Erylus cf. *mamillaris*	i329_A	UPSZMC 190854
Erylus cf. *mamillaris*	i329_B	UPSZMC 190855
Erylus cf. *mamillaris*	i329_C	UPSZMC 190856
Geodia bibilonae **sp. nov.** holotype	i715_1	UPSZTY 190857
Geodia bibilonae **sp. nov.** paratype	i780	UPSZTY 190858
Geodia bibilonae **sp. nov.** paratype	i781	UPSZTY 190859
Geodia bibilonae **sp. nov.** paratype	i674	UPSZTY 190860
Geodia bibilonae **sp. nov.** paratype	i675	UPSZTY 190861
Geodia geodina	i140_A	UPSZMC 190862
Geodia geodina	i140_B	UPSZMC 190863
Geodia geodina	i151-3	UPSZMC 190864
Geodia geodina	i153_1A	UPSZMC 190865
Geodia geodina	i153_5B	UPSZMC 190866
Geodia geodina	i391_1	UPSZMC 190867
Geodia geodina	i391_3	UPSZMC 190868
Geodia geodina	i401_4	UPSZMC 190869
Geodia geodina	i575	UPSZMC 190870
Geodia geodina	i576	UPSZMC 190871
Geodia geodina	i708	UPSZMC 190872
Geodia matrix **sp. nov.** paratype	i146_1A	UPSZTY 190876
Geodia matrix **sp. nov.**	i146_1B	UPSZMC 190877
Geodia matrix **sp. nov.**	i146_1C	UPSZMC 190878
Geodia matrix **sp. nov.** paratype	i244_B1	UPSZTY 190879
Geodia matrix **sp. nov.** paratype	i545	UPSZTY 190880
Geodia matrix **sp. nov.** holotype	i577_1	UPSZTY 190881
Geodia matrix **sp. nov.** paratype	i577_2	UPSZTY 190882
Geodia microsphaera **sp. nov.** holotype	i589_2	UPSZTY 190883
Geodia microsphaera **sp. nov.** paratype	i589_3	UPSZTY 190884
Geodia microsphaera **sp. nov.** paratype	i589_8	UPSZTY 190885
Geodia phlegraeioides **sp. nov.** holotype	P224-11BT25	UPSZTY 190886, MNCN/1.01/1026

Geodia phlegraeioides **sp. nov.** paratype	DR15-972	UPSZTY 190887
Geodia phlegraeioides **sp. nov.**	DR15-862c	CPORCANT DR15-862c
Geodia phlegraeioides **sp. nov.**	DR15-869c	CPORCANT DR15-869c
Geodia phlegraeioides **sp. nov.**	DR15-882	CPORCANT DR15-882
Geodia phlegraeioides **sp. nov.**	DR10-490	CPORCANT DR10-490
Geodia phlegraeioides **sp. nov.**	DR10-500	CPORCANT DR10-500
Geodia phlegraeioides **sp. nov.**	COLETA#5803	COLETA#5803
Geodia phlegraeioides **sp. nov.**	COLETA#6243	COLETA#6243
Nethea amygdaloides	POR347_B	UPSZMC 190888
Nethea amygdaloides	POR7_15	UPSZMC 190889
Nethea amygdaloides	i215_b	UPSZMC 190890
Pachastrella monilifera	i139_A	UPSZMC 190891
Pachastrella monilifera	i139_B	UPSZMC 190892
Pachastrella monilifera	i153_3	UPSZMC 190893
Pachastrella monilifera	i157	UPSZMC 190894
Pachastrella monilifera	i278_A	UPSZMC 190895
Pachastrella monilifera	i278_C	UPSZMC 190896
Pachastrella monilifera	i352_4	UPSZMC 190897
Pachastrella monilifera	i650	UPSZMC 190898
Pachastrella monilifera	i687	UPSZMC 190899
Pachastrella monilifera	i688	UPSZMC 190900
Pachastrella monilifera	i771	UPSZMC 190901
Pachastrella monilifera	i824_1	UPSZMC 190903
Pachastrella monilifera	i827_2	UPSZMC 190904
Pachastrella ovisternata	i219_A	UPSZMC 190905
Pachastrella ovisternata	i278_B	UPSZMC 190906
Pachastrella ovisternata	i278_D	UPSZMC 190907
Pachastrella ovisternata	i394_1	UPSZMC 190908
Pachastrella ovisternata	i628	UPSZMC 190909
Pachastrella ovisternata	i808	UPSZMC 190902
Pachastrella ovisternata	i818_1	UPSZMC 190911
Pachastrella ovisternata	i820_1	UPSZMC 190912
Penares candidatus	i143_G	UPSZMC 190913
Penares candidatus	i315_A	UPSZMC 190914
Penares candidatus	i315_B	UPSZMC 190915
Penares candidatus	i315_C	UPSZMC 190916
Penares cavernensis **sp. nov.** paratype	LIT45	UPSZTY 190917
Penares cavernensis **sp. nov.** holotype	LIT55	UPSZTY 190918
Penares cavernensis **sp. nov.** paratype	LIT65	UPSZTY 190919
Penares euastrum	i530	UPSZMC 190920
Penares euastrum	i142_A	UPSZMC 190921
Penares euastrum	i146_4	UPSZMC 190922
Penares euastrum	i244_A	UPSZMC 190923
Penares euastrum	i524_b	UPSZMC 190924

Penares euastrum	i508	UPSZMC 190925
Penares euastrum	i528	UPSZMC 190926
Penares euastrum	i529	UPSZMC 190927
Penares euastrum	POR469	UPSZMC 190928
Penares euastrum	POR932_1	UPSZMC 190929
Penares euastrum	POR975	UPSZMC 190930
Penares euastrum	POR1141	UPSZMC 190931
Penares euastrum	POR1253	UPSZMC 190932
Penares helleri	i142_D	UPSZMC 190933
Penares helleri	i152	UPSZMC 190934
Penares helleri	i233	UPSZMC 190935
Penares helleri	i739	UPSZMC 190936
Penares helleri	POR946	UPSZMC 190937
Penares isabellae **sp. nov.** holotype	LIT48	UPSZTY 190938
Penares isabellae **sp. nov.** paratype	LIT40_1	UPSZTY 190939
Penares isabellae **sp. nov.** paratype	LIT66	UPSZTY 190940
Poecillastra compressa	i808_9	UPSZMC 190941
Poecillastra compressa	i809	UPSZMC 190942
Stelletta mediterranea	i757	UPSZMC 190943
Stelletta dichoclada	i589_1	UPSZMC 190944
Stelletta dichoclada	i715_2	UPSZMC 190945
Stelletta dichoclada	i416_A	UPSZMC 190946
Stelletta dichoclada	i416_B	UPSZMC 190947
Stelletta dichoclada	i416_F	UPSZMC 190948
Stelletta lactea	ATL01	UPSZMC 190949
Stelletta mortarium **sp. nov.** paratype	i352_1	UPSZTY 190950
Stelletta mortarium **sp. nov.** paratype	i352_2	UPSZTY 190951
Stelletta mortarium **sp. nov.** paratype	i401_2	UPSZTY 190952
Stelletta mortarium **sp. nov.** paratype	i406_A	UPSZTY 190953
Stelletta mortarium **sp. nov.** paratype	i406_B	UPSZTY 190954
Stelletta mortarium **sp. nov.**	i582	UPSZMC 190955
Stelletta mortarium **sp. nov.**	i594	UPSZMC 190956
Stelletta mortarium **sp. nov.** holotype	i714_1	UPSZTY 190957
Stelletta stellata	PC1140	UPSZMC 190958
Stryphnus mucronatus	i827_1	UPSZMC 190959
Stryphnus mucronatus	POR1196	UPSZMC 190960
Stryphnus mucronatus	POR715	UPSZMC 190961
Stryphnus ponderosus	i208_a	UPSZMC 190962
Stryphnus ponderosus	i208_b	UPSZMC 190963
Stryphnus ponderosus	POR778_1	UPSZMC 190964
Stryphnus ponderosus	POR778_2	UPSZMC 190965
Stryphnus ponderosus	POR798	UPSZMC 190966
Thenea muricata	i232_1	UPSZMC 190967
Thrombus abyssi	i391_5_1	UPSZMC 190968
Thrombus abyssi	i391_6	UPSZMC 190969

Thrombus abyssi	i470	UPSZMC 190970
Vulcanella aberrans	i139_B1	UPSZMC 190971
Vulcanella cf. *gracilis*	i279_A	UPSZMC 190972
Vulcanella cf. *gracilis*	i279_B	UPSZMC 190973
Vulcanella gracilis	i303_b	UPSZMC 190974
Vulcanella gracilis	i303_c	UPSZMC 190975
Vulcanella gracilis	i416_c	UPSZMC 190976
Vulcanella gracilis	i818_2	UPSZMC 190977

Supplementary table S4.3.2. Chapter 4.3 genbank and Sponge Barcoding Project sequence accession numbers with its correspondence species and specimen field code.

		COI Full Folmer	COI Folmer+Erpenbeck	COI minibarcodes (130 bp)	28S C1-C2	28S C1-D2
Species	**Field#**	**Genbank ID**	**Genbank ID**	**Sponge Barcoding Project ID**	**Genbank ID**	**Genbank ID**
Geodia geodina	i575	ON130519			ON133879	
Geodia geodina	i708	ON130520			ON133880	
Geodia geodina	i576	ON130521				
Geodia geodina	i140_A	ON130522				
Geodia phlegraeioides **sp. nov.**	COLETA5803	OR045842				
Geodia phlegraeioides **sp. nov.**	COLETA6243	OR045843				
Geodia phlegraeioides **sp. nov.**	DR15-869c (CPORCANT)	OR045845				
Geodia phlegraeioides **sp. nov.**	P224-11BT25	OR045844				
Geodia matrix **sp. nov**	i244_B	ON130523			ON133885	
Geodia matrix **sp. nov**	i577_1	ON130524			ON133886	
Geodia matrix **sp. nov**	i577_2	ON130525			ON133887	
Geodia bibilonae **sp. nov.**	i780	ON130526			ON133882	
Geodia bibilonae **sp. nov.**	i674	ON130527			ON133883	
Geodia bibilonae **sp. nov.**	i715_1	ON130528			ON133881	
Geodia microsphaera **sp. nov.**	i589_2	ON130529			ON133884	
Erylus cf. *mamillaris*	i329_B	ON130530			ON133855	
Erylus discophorus	POR785	ON130531			ON133854	
Erylus discophorus	LIT71	ON130532				
Erylus discophorus	LIT72	ON130533				
Erylus discophorus	LIT74	ON130534				
Erylus cf. *deficiens*	LIT10	ON130535			ON133853	
Erylus corsicus	i707	ON130536			ON133851	

Erylus corsicus	i402_B	ON130537				
Penares helleri	i739	ON130538			ON133859	
Penares helleri	POR946	ON130539			ON133858	
Penares euastrum	i530			SBP#2683	ON133852	
Penares euastrum	POR932_1			SBP#2684		
Penares cavernensis **sp. nov.**	LIT55			SBP#2685		
Penares isabellae **sp. nov.**	LIT40_1	ON130540			ON133860	
Penares isabellae **sp. nov.**	LIT48	ON130541				
Penares isabellae **sp. nov.**	LIT66	ON130542				
Penares candidatus	i315_B	ON130543			ON133857	
Nethea amygdaloides	POR347_B	ON130544				
Nethea amygdaloides	POR7_15	ON130545				
Nethea amygdaloides	i215_b			SBP#2686	ON133878	
Caminus vulcani	i526	ON130546			ON133892	
Caminella intuta	LIT05	ON130547			ON133877	
Calthropella (Calthropella) pathologica	i693	ON130548			ON133856	
Calthropella (Calthropella) pathologica	i682			SBP#2687		
Discodermia polymorpha	i606	ON130549			ON133891	
Discodermia polymorpha	i321	ON130550			ON133890	
Discodermia polymorpha	i320				ON133889	
Characella pachastrelloides	i527	ON130551			ON133873	
Characella tripodaria	i777	ON130552			ON133871	
Characella tripodaria	i153_1B			SBP#2690	ON133872	
Poecillastra compressa	i808_9	ON130553				
Poecillastra compressa	i809	ON130554			ON133870	
Vulcanella gracilis	i818_2	ON130555			ON133869	
Stryphnus mucronatus	i827_1	ON130556				

Stryphnus mucronatus	POR1196	ON130557				
Stryphnus mucronatus	POR715			SBP#2688		
Stryphnus ponderosus	i208_b			SBP#2689		
Pachastrella ovisternata	i820_1				ON133875	
Pachastrella monilifera	i688	ON130559			ON133874	
Pachastrella monilifera	i771	ON130560				
Pachastrella monilifera	i808	ON130558			ON133876	
Thrombus abyssi	i470	ON130561			ON133868	
Stelletta mortarium **sp. nov.**	i352_1	ON130562			ON133861	
Stelletta mortarium **sp. nov.**	i594	ON130563			ON133862	
Stelletta mortarium **sp. nov.**	i714_1	ON130564			ON133863	
Stelletta lactea	ATL01	ON130565			OR044718	
Stelletta dichoclada	i589_1	ON130566				ON133864
Stelletta dichoclada	i715_2	ON130567				ON133866
Stelletta dichoclada	i416_A					ON133865
Stelletta mediterranea	i757	ON130568				ON133867
Thenea muricata	i232_1	ON130569			ON133888	
Craniella cf. *cranium*	i172_1A		OR045914		ON133849	
Craniella cf. *cranium*	i416_D		OR045913		ON133850	

Supplementary Table S4.6.1. Total taxa identified to the lowest taxonomic level possible, indicating the zone, depth range and assemblage where collected as well as the sampling device used.

	Seamounts			**Depth range**	**Assemblage**	**Sampling device**	**Fishing grounds**	**Depth range**	**Assemblage**	**Sampling device**
	SO	**AM**	**EB**							
Class CALCAREA										
Calcarea sp1							X	56-83	BtC, BtD, BtE, BtF, GocB, GocD	GOC, BT
Calcarea sp2							X	66-70	BtF	BT
Calcarea sp3							X	70	BtF	BT
Calcarea sp4							X	57-61	BtF, GocA, GocD, GocE	BT, GOC
Calcarea sp5							X	62	GocD	GOC
Calcarea sp6	X	X	X	98-395	SB, SC, SF	BT, RD	X	93	BtF	BT
Calcarea sp7		X	X	105-151	SB, SC	BT, RD				
Calcarea sp9		X		99	SD	BT				
Calcarea sp10							X	61	GocA	GOC
Sycon sp1							X	54-73	GocE, GocD, BtF	GOC, BT

Class DEMOSPONGIAE										
Order AGELASIDA										
Foraminospongia balearica Díaz, Ramírez-Amaro & Ordines, 2021		X	X	98-511	sB, sC, sD, sF	RD, BT, ROV	X	131	GocH	GOC
Foraminospongia minuta Díaz, Ramírez-Amaro & Ordines, 2021	X			298-318	sA	RD				
Foraminospongia sp.							X	66	GocD	GOC
Prosuberites longispinus Topsent, 1893		X		99	sD	BT	X	62-93	BtD, BtE, BtF, GocD	BT, GOC
Prosuberites sp1		X		105	Not included	RD	X	63	GocD	GOC
Prosuberites sp2			X	126-193	sD	RD				
Hymerhabdia sp1		X		104-138	Not included	RD				
Hymerhabdiidae sp1		X		112	sC	BT				
Order AXINELLIDA										
Axinella damicornis (Esper, 1794)							X	50-93	BtD, BtE, BtF, GocA, GocB, GocC, GocD, GocF	BT, GOC
Axinella minuta Lévi, 1957		X	X	104-430	sB, sD, sF	BT, RD				

Axinella polypoides Schmidt, 1862		X		98-99	sD, sC	BT	X	54-80	GocB, GocC, GocD, BtE, BtF	BT, GOC
Axinella spatula Sitjà & Maldonado, 2014			X	145-147	sB					
Axinella vaceleti Pansini, 1984			X	108-118	sD	RD	X	67-84	GocA, GocB, GocD, Bt	BT, GOC
Axinella vellerea Topsent, 1904							X	148	Not included	GOC
Axinella verrucosa (Esper, 1794)		X		98-127	sC	BT, RD	X	54-83	GocB, GocC, GocD, BtE, BtF	BT, GOC
Axinella sp1							X	652	Not included	GOC
Axinella sp2		X	X	97-395	sB, sC, sD, sF	BT, RD	X	122	GocH	GOC
Axinella sp3							X	72	BtF	BT
Axinella sp4							X	75-79	GocD	GOC
Axinella sp5							X	75	GocD	GOC
Axinella sp6							X	84	BtD	BT
Axinella sp7		X	X	97-207	sC, sD	BT, RD	X	93	BtF	BT
Axinella sp8		X	X	98-147	sB, sC, sD	BT, RD				
Axinella sp9							X	70	BtE	
Axinella sp10			X	395	sF	BT				

Axinella sp11		X	X	99-193	sD	BT, RD				
Axinella sp12			X	102-108	sD	RD	X	109	GocH	GOC
Axinella sp13							X	83	GocB	GOC
Axinella sp14			X	102-118	sD	RD				
Ceratopsion minor Pulitzer-Finalli, 1983							X	56-77	BtE, BtF, GocB	BT, GOC
Endectyon (Hemectyon) sp.							X	78	GocB	GOC
Eurypon major Sarà & Siribelli, 1960							X	57-84	GocB, GocD, GocE, BtD	BT, GOC
Eurypon sp1		X		98-99	sD, sC	BT				
Eurypon sp2							X	70	BtE	BT
Eurypon sp3							X	140-142	BtA, GocG	BT, GOC
Eurypon sp4		X	X		sA, sF	BT, RD				
Eurypon sp5		X		220-275	sA	RD				
Halicnemia sp1							X	84	BtD	BT
Heteroxya cf. *beauforti* Morrow, 2019	X	X	X	195-325	sA	RD				
Heteroxya sp.			X	126-193	sD	RD				

Myrmekioderma sp1							X	59	GocE	GOC
Paratimea massutii Díaz, Ramírez-Amaro & Ordines, 2021			X	147-150	sB	BT				
Paratimea sp.							X	69-84	BtD, BtF	BT
Phakellia robusta Bowerbank, 1866	X	X	X	102-458	sA, sB, sD, sF	BT, RD, ROV	X	257-756	GocG, GocH	GOC
Phakellia ventilabrum (Linnaeus, 1767)			X	¿?	Not included	ROV	X	361	Not included	GOC
Phakellia sp	X		X	151-511	sA, sF	BT, RD, ROV				
Raspaciona aculeata (Johnston, 1842)							X	50-86	GocA, GocB, GocC, GocD, GocE, BtB, BtD, BtE, BtF	BT, GOC
Raspailia (Raspailia) viminalis Schmidt, 1862							X	57-84	GocB, GocD, BtD, BtE, BtF	BT, GOC
Raspailia sp.							X	62-72	BtF	BT
Stelligera sp1							X	113	GocH	GOC
Raspailidae sp1			X	189-321	sF	BT				
Axinellidae sp1							X	64-76	GocA, GocD, BtD, BtE	BT, GOC

Order BIEMNIDA										
Biemna sp2		X		97-112	sC	BT, RD				
Rhabderemia sp1			X	280-306	sA	RD				
Order BUBARIDA										
Acanthella acuta Schmidt, 1862							X	55-70	GocD, BtE	BT, GOC
Acanthella sp1							X	66	BtF	BT
Bubaris carcisis Vacelet, 1969			X	145-333	sB	BT, RD				
Bubaris sp1	X	X	X	141-523	sB, sE, sF	BT	X	142-254	BtA	BT
Bubaris sp2	X			270-325	sA	RD				
Bubaris sp3	X		X	149-405	sB, sE, sF	BT	X	142	BtA	BT
Bubaris sp4		X		225	sF	BT	X	217-221	BtA	BT
Bubaris sp5			X	145-430	sB, sF	BT				
Bubaris sp6			X	394-430	sF	BT				
Bubaris vermiculata (Bowerbank, 1866)		X		98	sC	BT	X	50-93	GocC, GocD, GocE, BtD, BtE, BtF	BT, GOC

Dictyonella incisa (Schmidt, 1880)		X		98	sC	BT	X	50-82	GocB, GocC, GocD, GocE, BtE, BtF	BT, GOC
Dictyonella cf *marsilii* (Topsent, 1893)							X	53-78	GocB, GocC, GocD, GocE, BtF	BT, GOC
Dictyonella sp1							X	56-68	BtF	BT
Dictyonella sp2							X	45-83	GocB, GocC, GocD, GocE, BtE, BtF	BT, GOC
Dictyonella sp3							X	58-79	GocD	GOC
Dictyonella sp4		X	X	102-108	sC, sD	BT, RD	X	66-67	GocD, BtE	BT, GOC
Dictyonella sp5			X	116-395	sB, sD, sF	BT, RD				
Dictyonella sp6							X	82	Not included	BT
Dictyonella sp7							X	66-70	BtE	BT
Dictyonella sp8							X	66	BtE	BT
Monocrepidium sp1							X	76	BtD	BT
Monocrepidium sp2	X	X	X	267-430	sF	BT, RD				
Rhabdobaris implicata Pulitzer-Finalli, 1983	X		X	116-325	sA, sD	RD				

Rhabdobaris sp.			X	145-147	sB	BT				
Dyctionellidae sp1							X	321	GocG	GOC
Dyctionellidae sp2							X	45	BtF	BT
Order CLIONAIDA										
Cliona celata Grant, 1826							X	67-81	BtC, BtD, BtF	BT
Diplastrella bistellata (Schmidt, 1862)		X		98-105	sC	BT	X	64-84	GocC, GocD, BtD, BtE	BT, GOC
Dotona sp.		X		99	sD	BT				
Spirastrella sp.							X	81	BtC	BT
Order DESMACELLIDA										
Desmacella annexa Schmidt, 1870	X	X	X	112-740	sB, sC, sE, sF	BT	X	82-754	GocG, GocF, BtA	BT, GOC
Desmacella inornata (Bowerbank, 1866)	X	X	X	118-756	sB, sC, sE, sF	BT, RD	X	140-361	GocG, BtA	BT, GOC
Desmacella sp1							X	75	BtF	BT
Desmacella sp2							X	66-72	BtF	BT
Desmacella sp3	X			607	sC	BT	X	758	Not included	GOC
Desmacella sp4		X		112	sC	BT				
Desmacella sp5		X	X	105-118	sC	RD, ROV				

Desmacella sp6		X		127	sC	BT				
Dragmatella aberrans (Topsent, 1890)	X	X	X	127-430	sA, sB, sC, sE, sF	BT, RD	X	139-221	GocG, BtA	BT, GOC
Microtylostylifer sp1			X	145-147	sB	BT				
Order HAPLOSCLERIDA										
Calyx cf. *tufa* (Ridley & Dendy, 1886)		X		112	sC	BT	X	133	GocH	GOC
Callyspongia septimaniensis Griessinger, 1971							X	50-93	GocA, GocB, GocC, GocD, GocE, BtB, BtC, BtD, BtE, BtF	BT, GOC
Cladocroce sp.			X	267-733	Not included	ROV				
Haliclona (Flagellia) hiberniae Van Soest, 2017			X	145-147	sB	BT	X	82	Not included	BT
Haliclona (Gellius) sp1							X	75	BtF	BT
Haliclona (Gellius) sp2			X	145-148	sB	BT	X	66-217	GocH, BtA, BtE, BtF	BT, GOC
Haliclona (Gellius) sp3			X	152-154	sB	BT				
Haliclona (Halichoclona) sp.			X	139-154	sB	BT				

Haliclona (Rhizoniera) rhizophora (Vacelet, 1969)	X	X	X	145-430	sB, sF	BT				
Haliclona (Soestella) fimbriata Bertolino & Pansini, 2015			X	134-150	Not included	ROV				
Haliclona poecillastroides (Vacelet, 1969)		X	X	94-154	sB, sC, sD	BT, RD, ROV	X	106-257	GocG, GocH, BtA	BT, GOC
Haliclona (Reniera) mediterranea Griessinger, 1971		X		105	sC	BT	X	45-93	GocA, GocB, GocC, GocD, GocE, BtD, BtE, BtF	BT, GOC
Haliclona sp1			X							
Haliclona sp2		X		76-81			X	97-102		
Haliclona sp3							X	45-93	GocA, GocB, GocC, GocD, GocE, BtC, BtD, BtE, BtF	BT, GOC
Haliclona sp4							X	62-72	GocC, GocD, BtE, Btc, BtF	BT, GOC
Haliclona sp5							X	54-69	GocD, GocE, BtE, BtF	BT, GOC
Haliclona sp6							X	69	BtF	BT
Haliclona sp7							X	62-79	GocD	GOC

Haliclona sp8							X	72-83	GocB, GocC, GocD	GOC
Haliclona sp9		X		98-105	sC	BT	X	54-82	GocB, GocC, GocD, GocE, BtE	BT, GOC
Haliclona sp10							X	57-93	GocD, BtE, BtF	BT, GOC
Haliclona sp11		X		97-102	sC	RD				
Haliclona sp12		X		99	sD	BT				
Haliclona sp13			X	141-294	sB, sF	BT				
Haliclona sp14			X	128-151	sB, sD	BT, RD				
Haliclona sp15		X	X	105-151	sB, sC	BT	X	54-67	GocD, GocE	GOC
Haliclona sp16							X	57	GocD	GOC
Haliclona sp17								54	GocD	GOC
Haliclona sp18			X	141-154	sB	BT				
Oceanapia sp1							X	82	Not included	BT
Petrosia (Strongylophora) vansoesti Boury-Esnault, Pansini & Uriz, 1994		X	X	98-297	sB, sC, sD, sF	BT, RD				
Petrosia (Petrosia) ficiformis (Poiret, 1789)		X	X	98-151	sB, sC, Sd	BT, RD, ROV	X	57-81	GocA, GocC, GocD, BtE	BT, GOC

Petrosia (Petrosia) raphida Boury-Esnault, Pansini & Uriz, 1994		X	X	98-395	sB, sC, sD, sF	BT, RD	X	109-142	GocH, GocF, BtA	BT, GOC
Petrosia sp.							X	75	GocD	GOC
Siphonochalina balearica Ferrer-Hernandez, 1916							X	45-78	GocB, GocC, GocD, GocE, BtE, BtF	BT, GOC
Siphonochalina sp.							X	50-80	GocB, GocC, GocD, GocE, BtB, BtE, BtF	BT, GOC
Haplosclerida sp1	X		X	270-325	sA	RD				
Haplosclerida sp2		X		105	sC	BT				
Haplosclerida sp3			X	280-306	sA	RD				
Haplosclerida sp4		X		99-111	sC, sD	BT, RD	X	62-79	GocD, BtE	BT, GOC
Haplosclerida sp5	X									
Haplosclerida sp6			X							
Haplosclerida sp7							X	121	Not included	BT
Order MERLIIDA										
Hamacantha (Hamacantha) sp1	X		X	147-473	sB, sF	BT				
Hamacantha (Hamacantha) sp2	X	X		195-458	sA	RD				
Hamacantha (Hamacantha) sp3	X			255-325	sA	RD				

Hamacantha (Vomerula) falcula (Bowerbank, 1874)		X	X	102-193	sC, sD	BT, RD	X	109-252	GocG, GocH, BtA	BT, GOC
Hamacantha (Vomerula) sp1		X	X	98-511	sA, sC, sF	BT, RD				
Hamacantha (Vomerula) sp2		X	X	518-638	Not included	RD				
Hamacantha (Vomerula) sp3			X	126-193	sD	RD				
Hamacantha (Vomerula) sp4			X	672	sE	BT				
Hamacantha (Vomerula) sp5	X	X	X	141-511	sA, sB, sE, sF	BT, RD	X	142-254	BtA	BT
Order POECILOSCLERIDA										
Acarnus levii (Vacelet, 1960)							X	45-78	GocB, GocD, GocE, BtE, BtF	BT, GOC
Antho (Antho) oxeifera (Ferrer-Hernandez, 1921)								55-81	GocB, GocD, GocE, BtE, BtF	BT, GOC
Antho (Antho) sp.			X	126-193	sD	RD				
Batzella inops (Topsent, 1891)							X	45-81	GocA, GocC, GocD, GocE, BtD, BtE, BtF	BT, GOC
Cladorhiza abyssicola Sars, 1872	X	X	X	145-715	sB, sE, sF	BT				
Clathria (Microciona) sp1							X	81	BtC	BT

Clathria (Clathria) coralloides (Scopoli, 1772)							X		Not included	GOC
Clathria (Microciona) sp2							X	62	GocD	GOC
Clathria (Thalysias) sp.							X	63-75	GocD	GOC
Coelosphaera sp.							X	76	BtD	BT
Coelosphaera (Histodermion) sp.		X	X	102-154	sB, sC, sD	BT, RD				
Crella (Grayella) sp.							X	72	GocC	GOC
Crella (Crella) sp.		X		105	sC					
Crella (Yvesia) sp.		X		94-112	sC, sD	BT, RD				
Crellidae sp.							X	78	GocB	GOC
Forcepia (Leptolabis) luciensis (Topsent, 1888)							X	142	BtA	BT
Hamigera sp.		X	X	139-143	Not included	RD				
Hemimycale columella (Bowerbank, 1874)							X	54-79	GocD, GocE, BtF	BT, GOC
Hymedesmia (Hymedesmia) sp1		X		112	sC	BT				
Hymedesmia (Hymedesmia) sp2		X	X	97-193	sC, sD	BT, RD				
Hymedesmia (Hymedesmia) sp3			X	473	sF	BT				
Hymedesmia (Hymedesmia) sp4							X	57-375	GocE	GOC

Hymedesmia (Hymedesmia) sp5							X	67-375	GocD	GOC
Hymedesmia (Hymedesmia) sp6							X	61	GocA	GOC
Hymedesmia (Hymedesmia) sp7	X			151-230	sA	RD				
Hymedesmia (Hymedesmia) sp8		X		124-207	Not included	RD				
Hymedesmia (Stylopus) sp1							X	56-78	GocA, GocC, GocD, BtD, BtE, BtF	BT, GOC
Hymedesmia (Stylopus) sp2							X	109	GocH	GOC
Hymedesmia sp1							X	56	BtF	BT
Latrunculia sp1		X	X	104-222	sA, sD	RD	X	84	BtD	BT
Latrunculia sp2			X	126-193	sD	RD				
Latrunculia sp3			X	104-193	sD	RD				
Lissodendoryx (Ectyodoryx) sp1							X	57-77	GocD, GocE, BtC, BtD	BT, GOC
Lissodendoryx (Anomodoryx) cavernosa (Topsent, 1892)							X	51-109	GocA, GocB, GocC, GocD, GocE, GocH, BtC, BtE, BtF	BT, GOC
Lissodendoryx sp1							X	50-66	GocE, BtE	BT, GOC
Lissodendoryx sp2							X	84	BtD	BT

Microcionidae sp1							X	57-83	GocB, BtE, BtF	BT, GOC
Microcionidae sp2							X	76	BtE	BT
Microcionidae sp3			X	126-193	sD	RD				
Mycale (Aegogrophila) contarenii (Lieberkühn, 1859)							X	50-78	GocC, GocD, GocE, BtB, BtF	BT, GOC
Mycale (Aegogropila) syrinx (Schmidt, 1862)							X	45-83	GocB, GocD, GocE, BtC, BtE, BtF	BT, GOC
Mycale (Mycale) massa (Schmidt, 1862)							X	142	BtA	BT
Mycale (Aegogropila) rotalis (Bowerbank, 1874)							X	45-81	BtE, BtF	BT
Mycale (Aegogropila) tunicata (Schmidt, 1862)							X	66	BtF	BT
Myxilla (Myxilla) sp1		X		111	Sc	BT				
Myxilla (Myxilla) rosacea (Lieberkühn, 1859)							X	119-587	Not included	GOC
Myxilla (Myxilla) iotrochotina (Topsent, 1892)							X	45-76	GocC, GocD, GocE, BtD, BtE, BtF	BT, GOC
Myxilla (Styloption) sp1							X	50	GocE	GOC

Myxilla sp.							X	61	BtF	BT
Melonanchora emphysema (Schmidt, 1875)		X		104-138	Not included	RD				
Ophlitaspongia sp1							X	45-79	GocD, GocE, BtB, BtE, BtF	BT, GOC
Phorbas sp1							X	113	GocH	GOC
Phorbas sp2		X		104-138	Not included	RD				
Phorbas sp3							X	57-84	GocA, GocB, GocC, GocD, BtD, BtE	BT, GOC
Phorbas fictitus (Bowerbank, 1866)							X	58	GocD	GOC
Phorbas tenacior (Topsent, 1925)							X	45-82	GocC, GocD, GocE, BtB, BtE, BtF	BT, GOC
Phorbas taillezi Vacelet & Pérez, 2008							X	50-69	GocC, GocD, GocE, BtC, BtF	BT, GOC
Plocamionida sp1							X	58-73	GocD, GocA	GOC
Spanioplon sp1							X	67	GocD	GOC
Terpios sp1							X	57-59	GocD, GocE	GOC
Poecilosclerida sp1							X	76	BtD	BT

Order POLYMASTIDA										
Polymastia polytylota Vacelet, 1969		X	X	145-458	sB	BT, ROV				
Polymastia sp1							X	67-77	GocD, BtE	BT, GOC
Polymastia sp2		X	X	94-473	sD, sF	BT, RD	X	142	GocA	GOC
Polymastia sp3		X	X	94-193	sD	BT, RD	X	66-93	BtE, BtF	BT
Polymastia sp4							X	79-93	BtE, BtF	BT
Polymastia sp5							X	66-142	BtA, BtE	BT
Polymastia sp6							X	142-221	BtA	BT
Polymastia sp7		X	X	195-395	sF	BT				
Polymastia tissieri (Vacelet, 1961)	X		X	297-688	sF	BT, RD				
Pseudotrachya hystrix (Topsent, 1890)		X	X	135-267	sA, sB, sF	BT, RD				
Radiella sp1			X	395-672	sE, sF	BT	X	738	GocG	GOC
Radiella sp2			X	395	sF	BT				
Spinularia sarsi (Ridley & Dendy, 1886)		X	X	267-511	sE, sF	BT, RD				
Order SCOPALINIDA										
Scopalina sp1							X	70	BtE	BT

Scopalinidae sp1		X	X	99-193	sC, sD	BT, RD				
Order SUBERITIDA										
Aaptos aaptos (Schmidt, 1864)		X	X	105-118	sC, sD	BT, RD, ROV	X	79-131	GocD, GocH	BT, GOC
Aaptos sp1							X	55-78	GocB, GocD, BtE, BtF	BT, GOC
Aaptos sp2							X	54-62	GocD, GocE	BT, GOC
Ciocalypta penicillus Bowerbank, 1822			X	102-108	sD	RD	X	67	BtC	BT
Halichondria (Halichondria) sp1							X	50-109	GocB, GocC, GocD, GocE, GocH, BtD, BtE, BtF	BT, GOC
Phakellia hirondellei Topsent, 1890			X	135-154	sB	BT, RD				
Protosuberites rugosus (Topsent, 1893)			X	141-430	sB, sF	BT				
Protosuberites sp1							X	72	BtF	BT
Protosuberites sp2							X	70-140	GocC, GocG, GocE, BtE	BT, GOC
Protosuberites sp3			X	394-430	sF	BT				

Pseudospongosorites sp1			X	147	sB	BT				
Rhizaxinella pyrifera (Delle Chiaje, 1828)		X		225-352	sE, sF	BT	X	110-361	GocG, GocH, BtA	BT, GOC
Rhizaxinella sp1		X		348-365	sE, sF	BT				
Rhizaxinella sp2							X	82-93	BtF	BT
Spongosorites sp1		X	X	94-193	sC, sD	BT, RD, ROV	X	79-131	GocH, BtE	BT, GOC
Spongosorites sp2		X	X	116-127	sC, sD	BT, RD, ROV				
Spongosorites sp3		X		127	sC	BT				
Suberites domuncula (Olivi, 1792)							X	45-83	GocA, GocB, GocC, GocD, GocE, BtB, BtE, BtF	BT, GOC
Suberites sp1							X	75-112	GocG, BtF	BT, GOC
Suberites sp2							X	80-149	GocB, GocG, GocH, BtA	BT, GOC
Stylocordyla pellita (Topsent, 1904)		X	X	204-638	sA, sF	BT, RD				
Topsentia sp1		X		112	sC	BT				
Topsentia sp2		X		97-102	sC	RD	X	93	BtF	BT

Topsentia sp3		X	X	102-108	sC, sD	BT, RD				
Halichondriidae sp1			X	152-154	sB	BT				
Halichondriidae sp2		X	X	98-287	sB, sC, sD, sF	BT, RD				
Halichondriidae sp3			X	511	sF	BT				
Halichondriidae sp4			X	141-150	sB	BT	X	122	GocH	GOC
Order TETHYIDA										
Hemiasterella elongata Topsent, 1928		X	X	105-473	sB, sC, sF	BT, RD	X	109-142	GocG, GocH, BtA	BT, GOC
Hemiasterella sp.							X	93	BtF	BT
Tethya sp1							X	45-92	GocC, GocD, GocE, BtD, BtE, BtF	BT, GOC
Tethya sp2							X	45-84	GocB, GocD, GocE, BtC, BtD, BtE, BtF	BT, GOC
Tethya sp3							X	67-80	GocB, GocD, BtC, BtF	BT, GOC
Tethya sp4		X		105-111	sC, sD	BT, RD				
Tethya sp5							X	70	BtF	BT
Tethya sp6							X	113	GocH	GOC

Timea chondrilloides (Topsent, 1904)			X	274-315	sA	RD				
Timea sp1		X	X	94-127	sC, sD	BT, RD				
Timea sp2							X	72	BtF	BT
Timea sp3		X		352-365	sE	BT	X	122-149	GocH	BT, GOC
Tethyidae sp.	X	X	X	152-715	sB, sE	BT, RD				
Tethyida sp1							X	142	BtA	BT
Order TETRACTINELLIDA										
Calthropella (Calthropella) sp.		X	X	97-118	sC, sD	RD				
Caminus sp.		X	X	98-151	sB, sC, sD	BT, RD, ROV				
Characella sp1		X	X	112	sC	BT				
Characella sp2			X	102-108	sD	RD				
Craniella sp.			X	147-154	sB	BT, ROV				
Discodermia sp.		X	X	112-151	sB, sC	BT				
Erylus sp1			X	141-151	sB	BT				
Erylus sp2			X	141-147	sB	BT				

Penares euastrum (Schmidt, 1868)		X	X	97-127	sC, sD	BT, RD	X	54-79	GocB, GocC, GocD, BtE	BT, GOC
Penares helleri (Schmidt, 1864)		X	X	97-154	sB, sC, sD, sF	BT, RD	X	109-625	GocH, BtA	GOC, BT
Penares sp.			X	128-147	sB	BT				
Geodia sp1		X	X	105-151	sB, sC	BT				
Geodia sp2		X	X	124-207	Not included	RD	X	70-125	GocC, GocH	GOC
Geodia sp3		X	X	94-111	sC, sD	BT, RD				
Geodia sp4		X		105	sC	BT				
Jaspis sp1		X	X	102-395	sA, sB, sC, sD, sF	BT, RD, ROV				
Jaspis sp2	X	X	X	135-511	sA, sC, sF	BT, RD, ROV				
Nethea sp.	X			255-293	sA	RD	X	142-148	Not included	GOC
Pachastrella monilifera Schmidt, 1868		X	X	102-265	sA, sB, sD	BT, RD, ROV				
Pachastrella sp.	X	X	X	135-550	sA, sC	BT, RD, ROV				
Poecillastra compressa (Bowerbank, 1866)	X	X	X	98-511	sA, sB, sC, sD, sF	BT, RD, ROV	X	106-257	GocH	GOC

Stelleta sp1		X	X	105-151	sB, sC	BT				
Stelleta sp2		X	X	105-151	sB, sC	BT				
Stelletta sp3			X	102-108	sD	RD				
Stryphnus ponderosus (Bowerbank, 1866)			X	135	Not included	RD				
Stryphnus sp.			X	100	Not included	ROV	X	50-63	GocE	GOC
Thenea muricata (Bowerbank, 1858)	X	X	X	122-740	sB, sE, sF	BT, RD	X	112-738	GocH, BtA	GOC, BT
Thrombus sp.			X	141-315	sB	BT, RD				
Vulcanella sp.	X	X	X	124-725	sA, sB, sC, sD, sF	BT, RD, ROV				
Subclass KERATOSA										
Order DENDROCERATIDA										
Dendroceratida sp1							X	50-62	GocE, BtB, BtE	GOC, BT
Dendroceratida sp2			X	147	sB	BT				
Dendroceratida sp3			X	102-193	sB, sD	BT, RD				
Spongionella sp1							X	57-84	GocD, BtD, BtE, BtF	GOC, BT
Order DICTYOCERATIDA										

Scalarispongia scalaris (Schmidt, 1862)							X	57-61	GocB, GocD, GocE	GOC
Chelonaplysilla sp.		X	X	98-294	sB, sC, sD, sF	BT, RD	X	57-221	GocA, GocD, GocH, BtA, BtC, BtE, BtF	GOC, BT
Dysidea avara (Schmidt, 1862)							X	53-78	GocC, GocD, GocE, BtE, BtF	GOC, BT
Dysidea sp1							X	45-93	GocA, GocB, GocD, GocE, BtD, BtE, BtF	GOC, BT
Dysidea sp2							X	54-77	GocD, BtE, BtF	GOC, BT
Dysidea sp3							X	59-82	GocD, GocE	GOC
Hippospongia sp.							X	57	GocE	GOC
Ircinia variabilis (Schmidt, 1862)							X	59	GocE	GOC
Pleraplysilla spinifera (Schulze, 1879)							X	59-61	GocA, GocE	GOC
Pleraplysilla sp.							X	66	BtF	BT
Sarcotragus sp1			X	102-145	sB, sD	BT, RD				
Sarcotragus sp2							X	67-81	GocD, BtE	GOC, BT
Sarcotragus sp3							X	55-86	GocD, GocE	GOC

Spongia (Spongia) lamella (Schulze, 1879)							X	57-58	GocD	GOC
Irciniidae sp1							X	53-75	GocD, GocE, BtF	GOC, BT
Irciniidae sp2							X	57-61	GocD, GocE	GOC
Irciniidae sp3							X	174-375	Not included	GOC
Irciniidae sp4							X	53-81	GocD, GocE	GOC
Irciniidae sp5							X	59	GocE	GOC
Dictyoceratida sp1			X	116-151	sB, sD	BT, RD				
Dictyoceratida sp2			X	128-143	sD	RD				
Dictyoceratida sp3		X	X	102-118	sC, sD	BT, RD	X	67-121	GocD, GocH, BtD, BtE, BtF	GOC, BT
Dictyoceratida sp4							X	58	GocD	GOC
Dictyoceratida sp5		X								
Dictyoceratida sp6							X	63	GocD	GOC
Subclass VERONGIMORPHA										
Order VERONGIIDA										
Aplysina aerophoba (Nardo, 1833)							X	53-77	GocD, GocE	GOC

Aplysina cavernícola (Vacelet, 1959)							X	¿¿¿?	Not included	GOC
Hexadella sp1		X	X	97-294	sB, sC, sD, sF	BT, RD	X	69	BtD	BT
Hexadella sp2			X	126-193	sD	RD				
Order CHONDROSIIDA										
Chondrosia reniformis Nardo, 1833							X	54-75	GocD, BtF	GOC, BT
Order CHONDRILLIDA										
Halisarca dujardinii Johnston, 1842							X	59-81	GocB, GocD, GocE, BtC,	GOC, BT
Class HEXACTINELLIDA										
Order LYSSACINOSIDA										
Lanuginella cf. *pupa* Schmidt, 1870		X		220-275	sA	RD				
Sympagella sp1		X	X	352-430	sE, sF	BT	X	254	BtA	BT
Order SCEPTRULOPHORA										
Tretodictyum reiswigi Boury-Esnault, Vacelet & Chevaldonné, 2017	X	X	X	147-511	sA, sB, sF	BT, RD, ROV	X	252	GocG	GOC
Hexactinellida sp1	X			297-298	sF	BT				

Supplementary table S5.1. List of Sponge species reported in the Balearic Islands, including previous works, and list of taxa reported in this phd but not identified to species level. In bold are the taxa reported this phd.

	Reported species	**Taxa not identified to species level**
Class DEMOSPONGIAE		
Order AGELASIDA		
Family AGELASIDAE		
	Agelas oroides (Schmidt, 1864)	
Family HYMERHABDIIDAE		
	Hymerhabdia oxytrunca Topsent, 1904	***Prosuberites* sp1**
	***Prosuberites longispinus* Topsent, 1893**	***Prosuberites* sp2**
	Foraminospongia balearica* Díaz, Ramírez-Amaro & Ordines, 2021	***Hymerhabdia* sp1**
	Foraminospongia minuta* Díaz, Ramírez-Amaro & Ordines, 2021	***Hymerhabdiidae* sp1**
Order AXINELLIDAE		
Family AXINELLIDAE		
	Axinella cannabina (Esper, 1794)	***Axinella* sp1**
	***Axinella damicornis* (Esper, 1794)**	***Axinella* sp2 (reported as Axinella sp3 in Chapter 4.5)**
	Axinella guiteli Topsent, 1896	***Axinella* sp3 (reported as Axinella sp4 in Chapter 4.5)**
	Axinella mahonensis Ferrer-Hernández, 1916	***Axinella* sp4 (reported as Axinella sp5 in Chapter 4.5)**
	***Axinella minuta* Lévi, 1957**	***Axinella* sp5 (reported as Axinella sp6 in Chapter 4.5)**
	Axinella perlucida Topsent, 1896	***Axinella* sp6 (reported as Axinella sp7 in Chapter 4.5)**
	***Axinella polypoides* Schmidt, 1862**	***Axinella* sp7 (reported as Axinella sp8 in Chapter 4.5)**
	Axinella pseudominutla Bibiloni, 1993	***Axinella* sp8 (reported as Axinella sp9 in Chapter 4.5)**

	Axinella rugosa (Bowerbank, 1866)	***Axinella* sp9 (reported as Axinella sp10 in Chapter 4.5)**
	Axinella spatula* Sitjà & Maldonado, 2014*	***Axinella* sp10 (reported as Axinella sp11 in Chapter 4.5)**
	***Axinella vaceleti* Pansini, 1984**	***Axinella* sp11 (reported as Axinella sp12 in Chapter 4.5)**
	Axinella vellerea* Topsent, 1904	***Axinella* sp12 (reported as Axinella sp13 in Chapter 4.5)**
	***Axinella verrucosa* (Esper, 1794)**	***Axinella* sp13 (reported as Axinella sp14 in Chapter 4.5)**
	Axinella venusta* Idan, Shefer, Feldstein & Ilan, 2021* (reported as *Axinella* sp2 in Chapter 4.5)	***Axinellidae* sp1**
Family HETEROXYIDAE		
	Myrmekioderma spelaeum (Pulitzer-Finali, 1983)	***Heteroxya* sp.**
	Heteroxya* cf. *beauforti* Morrow, 2019*	***Myrmekioderma* sp1**
Family RASPAILIIDAE		
	***Ceratopsion minor* Pulitzer-Finalli, 1983**	***Endectyon (Hemectyon)* sp.**
	Eurypon clavatum (Bowerbank, 1866)	***Eurypon* sp1**
	Eurypon lacazei (Topsent, 1891)	***Eurypon* sp2**
	***Eurypon major* Sarà & Siribelli, 1960**	***Eurypon* sp3**
	Eurypon pulitzeri Cavalcanti, Santos & Pinheiro, 2018	***Eurypon* sp4**
	Eurypon viride (Topsent, 1889)	***Eurypon* sp5**
	Plocamione dirrhopalina Topsent, 1927	***Raspailia* sp.**
	Rhabdeurypon spinosum Vacelet, 1969	***Raspailidae* sp1**
	***Raspaciona aculeata* (Johnston, 1842)**	
	***Raspailia (Raspailia) viminalis* Schmidt, 1862**	
Family STELLIGERIDAE		

	Halicnemia patera Bowerbank, 1864	***Halicnemia* sp1**
	Paratimea massutii* Díaz, Ramírez-Amaro & Ordines, 2021	***Paratimea* sp.**
		***Stelligera* sp1**
Order BIEMNIDA		
Family BIEMNIDAE		
	Biemna variantia (Bowerbank, 1858)	***Biemna* sp2**
Family RHABDEREMIIDAE		
	Rhabderemia topsenti van Soest & Hooper, 1993	***Rhabderemia* sp1**
Order BUBARIDA		
Family BUBARIDAE		
	***Bubaris carcisis* Vacelet, 1969**	***Bubaris* sp1**
	Bubaris subtyla Pulitzer-Finali, 1983	***Bubaris* sp2**
	***Bubaris vermiculata* (Bowerbank, 1866)**	***Bubaris* sp3**
	Cerbaris curvispiculifer (Carter, 1880)	***Bubaris* sp4**
	Monocrepidium vermiculatum Topsent, 1898	***Bubaris* sp5**
	Phakellia hirondellei Topsent, 1890	***Bubaris* sp6**
	***Phakellia robusta* Bowerbank, 1866**	***Monocrepidium* sp1**
	Phakellia ventilabrum* (Linnaeus, 1767)*	***Monocrepidium* sp2**
	Rhabdobaris implicata* Pulitzer-Finalli, 1983*	***Rhabdobaris* sp.**
		***Phakellia* sp**
Family DICTYONELLIDAE		
	***Acanthella acuta* Schmidt, 1862**	***Acanthella* sp1**
	Dictyonella alonsoi Carballo, Uriz & García-Gómez,1996	***Dictyonella* sp1**
	***Dictyonella incisa* (Schmidt, 1880)**	***Dictyonella* sp2**
	Dictyonella marsilii (Topsent, 1893)	***Dictyonella* sp3**
	Dictyonella obtusa (Schmidt, 1862)	***Dictyonella* sp4**

		***Dictyonella* sp5**
		***Dictyonella* sp6**
		***Dictyonella* sp7**
		***Dictyonella* sp8**
		***Tethyspira* sp.**
		***Dyctionellidae* sp1**
		***Dyctionellidae* sp2**
Order CHONDRILLIDA		
Family HALISARCIDAE		
	***Halisarca dujardinii* Johnston, 1842**	
Order CHONDROSIDA		
Family CHONDROSIIDAE		
	***Chondrosia reniformis* Nardo, 1833**	
Order CLIONAIDA		
Family CLIONAIDAE		
	***Cliona celata* Grant, 1826**	***Dotona* sp.**
	Cliona schmidtii (Ridley, 1881)	
	Cliona viridis (Schmidt, 1862)	
	Pione vastifica (Hancock, 1849)	
	Spiroxya corallophila (Calcinai, Cerrano & Bavestrello, 2002)	
	Spiroxya levispira (Topsent, 1898)	
Family PLACOSPONGIIDAE		
	Placospongia decorticans* (Hanitsch, 1895)*	
Family SPIRASTRELLIDAE		
	***Diplastrella bistellata* (Schmidt, 1862)**	***Spirastrella* sp.**
	Spirastrella cunctatrix Schmidt, 1868	
Order DENDROCERATIDA		

		***Dendroceratida* sp1**
		***Dendroceratida* sp2**
		***Dendroceratida* sp3**
Family DARWINELLIDAE		
	Aplysilla rosea (Barrois, 1876)	***Chelonaplysilla* sp.**
	Aplysilla sulfurea Schulze, 1878	
	Chelonaplysilla noevus (Carter, 1876)	
Family DYCTYODENDRILLIDAE		
	Spongionella pulchella (Sowerby, 1804)	***Spongionella* sp1**
Order DESMACELLIDA		
Family DESMACELLIDAE		
	***Desmacella annexa* Schmidt, 1870**	***Desmacella* sp1**
	Desmacella infundibuliformis (Vosmaer, 1885)	***Desmacella* sp2**
	***Desmacella inornata* (Bowerbank, 1866)**	***Desmacella* sp3**
	Dragmatella aberrans* (Topsent, 1890)*	***Desmacella* sp4**
		***Desmacella* sp5**
		***Desmacella* sp6**
		***Microtylostylifer* sp1**
Order DYCTIOCERATIDA		
		***Dictyoceratida* sp1**
		***Dictyoceratida* sp2**
		***Dictyoceratida* sp3**
		***Dictyoceratida* sp4**
		***Dictyoceratida* sp5**
		***Dictyoceratida* sp6**
Family DYSIDEIDAE		

	***Dysidea avara* (Schmidt, 1862)**	***Dysidea* sp1**
	Dysidea fragilis (Montagu, 1918)	***Dysidea* sp2**
	Dysidea pallescens (Schmidt, 1862)	***Dysidea* sp3**
	Dysidea tupha (Pallas, 1766)	***Pleraplysilla* sp.**
	***Pleraplysilla spinifera* (Schulze, 1879)**	
Family IRCINIIDAE		
	Ircinia dendroides (Schmidt, 1862)	***Sarcotragus* sp1**
	Ircinia oros (Schmidt, 1864)	***Sarcotragus* sp2**
	Ircinia strobilina (Lamarck, 1816)	***Sarcotragus* sp3**
	***Ircinia variabilis* (Schmidt, 1862)**	***Irciniidae* sp1**
	Ircinia fasciculata sensu Vacelet 1959	***Irciniidae* sp2**
	Sarcotragus foetidus Schmidt, 1862	***Irciniidae* sp3**
	Sarcotragus spinosulus Schmidt, 1862	***Irciniidae* sp4**
		***Irciniidae* sp5**
Family SPONGIIDAE		
	Hippospongia communis (Lamarck, 1814)	***Hippospongia* sp.**
	***Spongia (Spongia) lamella* (Schulze, 1879)**	
	Spongia (Spongia) nitens (Schmidt, 1862)	
	Spongia (Spongia) officinalis Linnaeus, 1759	
	Spongia (Spongia) virgultosa (Schmidt,1868)	
Family THORECTIDAE		
	Cacospongia mollior Schmidt, 1862	
	Fasciospongia cavernosa (Schmidt, 1862)	
	Hyrtios collectrix (Schulze, 1880)	
	***Scalarispongia scalaris* (Schmidt, 1862)**	
Order HAPLOSCLERIDA		
		***Haplosclerida* sp1**

		***Haplosclerida* sp2**
		***Haplosclerida* sp3**
		***Haplosclerida* sp4**
		***Haplosclerida* sp5**
		***Haplosclerida* sp6**
		***Haplosclerida* sp7**
Family CALLYSPONGIIDAE		
	Callyspongia subcornea (Griessinger, 1971)	***Siphonochalina* sp.**
	Callyspongia septimaniensis* Griessinger, 1971*	
	***Siphonochalina balearica* Ferrer-Hernandez, 1916**	
	Siphonochalina coriacea Schmidt, 1868	
Family CHALINIDAE		
	Chalinula limbata (Montagu, 1814)	***Cladocroce* sp.**
	Cladocroce fibrosa (Topsent, 1890)	***Haliclona (Gellius)* sp1**
	Dendroxea lenis (Topsent, 1892)	***Haliclona (Gellius)* sp2**
	Haliclona tenuiderma (Lundbeck, 1902)	***Haliclona (Gellius)* sp3**
	Haliclona (Flagellia) flagellifera (Ridley & Dendy, 1886)	***Haliclona (Halichoclona)* sp.**
	***Haliclona (Flagellia) hiberniae* Van Soest, 2017**	***Haliclona* sp1**
	Haliclona (Gellius) angulata (Bowerbank, 1866)	***Haliclona* sp3**
	Haliclona (Gellius) lacazei (Topsent, 1893)	***Haliclona* sp4**
	Haliclona (Gellius) uncinata (Topsent, 1892)	***Haliclona* sp5**
	Haliclona (Halichoclona) fistulosa (Bowerbank, 1866)	***Haliclona* sp6**
	Haliclona (Halichoclona) fulva (Topsent, 1893)	***Haliclona* sp7**
	Haliclona (Halichoclona) magna (Vacelet, 1969)	***Haliclona* sp8**
	Haliclona (Haliclona) michelei van Soest & Hooper, 2020	***Haliclona* sp9**
	Haliclona (Haliclona) simulans (Johnston, 1842)	***Haliclona* sp10**

	Haliclona (Haliclona) urceolus (Rathke & Vahl, 1806)	***Haliclona* sp11**
	Haliclona (Reniera) aqueductus (Schmidt, 1862)	***Haliclona* sp12**
	Haliclona (Reniera) cinerea (Grant, 1826)	***Haliclona* sp13**
	Haliclona (Reniera) cratera (Schmidt, 1862)	***Haliclona* sp14**
	***Haliclona (Reniera) mediterranea* Griessinger, 1971**	***Haliclona* sp15**
	Haliclona (Reniera) subtilis Griessinger, 1971	***Haliclona* sp16**
	Haliclona (Rhizoniera) grossa (Schmidt, 1864)	***Haliclona* sp17**
	***Haliclona (Rhizoniera) rhizophora* (Vacelet, 1969)**	***Haliclona* sp18**
	Haliclona (Rhizoniera) rosea (Bowerbank, 1866)	
	Haliclona (Rhizoniera) sarai (Pulitzer-Finali, 1969)	
	Haliclona (Rhizoniera) viscosa (Topsent, 1888)	
	Haliclona (Soestella) arenata (Griessinger, 1971)	
	Haliclona (Soestella) fimbriata* Bertolino & Pansini, 2015*	
	Haliclona (Soastrella) implexa (Schmidt, 1868)	
	Haliclona (Soastrella) mucosa (Griessinger, 1971)	
	Haliclona (Soestella) valliculata (Griessinger, 1971)	
Family NIPHATIDAE		
	Pachychalina debuenii Ferrer-Hernández, 1921	
Family PHLOEODICTYIDAE		
	Calyx* cf. *tufa* (Ridley & Dendy, 1886)*	***Oceanapia* sp1**
Family PETROSIIDAE		
	***Petrosia (Petrosia) ficiformis* (Poiret, 1789)**	***Petrosia* sp.**
	Petrosia (Petrosia) raphida* Boury-Esnault, Pansini & Uriz, 1994*	
	Petrosia (Strongylophora) vansoesti* Boury-Esnault, Pansini & Uriz, 1994*	
	Xestospongia friabilis (Topsent, 1892)	
	Xestospongia plana (Topsent, 1892)	

	Haliclona poecillastroides **(Vacelet, 1969)**	
Order MERLIIDA		
Family HAMACANTHIDAE		
	Hamacantha (Vomerula) falcula **(Bowerbank, 1874)**	***Hamacantha (Hamacantha)*** **sp1**
		Hamacantha (Hamacantha) **sp2**
		Hamacantha (Hamacantha) **sp3**
		Hamacantha (Vomerula) **sp1**
		Hamacantha (Vomerula) **sp2**
		Hamacantha (Vomerula) **sp3**
		Hamacantha (Vomerula) **sp4**
		Hamacantha (Vomerula) **sp5**
Family MERLIIDAE		
	Merlia lipoclavidisca Vacelet & Uriz, 1991	
	Merlia normani Kirkpatrick, 1908	
Order POECILOSCLERIDA		
		Poecilosclerida **sp.**
Family ACARNIDAE		
	Acarnus levii **(Vacelet, 1960)****	
	Acarnus tortilis Topsent, 1892	
Family CLADORHIZIDAE		
	Cladorhiza abyssicola **Sars, 1872**	
	Lycopodina hypogea (Vacelet & Boury-Esnault, 1996)	
Family CHONDROPSIDAE		
	Batzella inops **(Topsent, 1891)**	
Family COELOSPHAERIDAE		
	Lissodendoryx (Anomodoryx) cavernosa **(Topsent, 1892)**	***Coelosphaera*** **sp.**

	Lissodendoryx (Lissodendoryx) basispinosa Sarà, 1958b	***Coelosphaera (Histodermion)* sp.**
	Lissodendoryx (Lissodendoryx) isodictyalis (Carter, 1882)	***Lissodendoryx (Ectyodoryx)* sp1**
	Forcepia (Leptolabis) luciensis* (Topsent, 1888)*	***Lissodendoryx* sp1**
		***Lissodendoryx* sp2**
Family CRAMBEIDAE	*Crambe crambe* (Schmidt, 1862)	
	Crambe tailliezi Vacelet & Boury-Esnault, 1982	
Family CRELLIDAE		
	Anisocrella hymedesmina Topsent, 1927	***Crella (Grayella)* sp.**
	Crella (Crella) elegans (Schmidt, 1862)	***Crella (Crella)* sp.**
	Crella (Grayella) pulvinar (Schmidt, 1868)	***Crella (Yvesia)* sp.**
	Crella (Pytheas) sigmata Topsent, 1925	**Crellidae sp.**
	Crella (Yvesia) rosea (Topsent, 1892)	
Family ESPERIOPSIDAE		
	Amphilectus fucorum (Esper, 1794)	
	Ulosa digitata (Schmidt, 1866)	
Family HYMEDESMIIDAE		
	Hamigera hamigera (Schmidt, 1862)	***Hamigera* sp.**
	***Hemimycale columnella* (Bowerbank, 1874)**	***Hymedesmia (Hymedesmia)* sp1**
	Hymedesmia (Hymedesmia) baculifera (Topsent, 1901)	***Hymedesmia (Hymedesmia)* sp2**
	Hymedesmia (Hymedesmia) pansa Bowerbank, 1882	***Hymedesmia (Hymedesmia)* sp3**
	Hymedesmia (Hymedesmia) peachii Bowerbank, 1882	***Hymedesmia (Hymedesmia)* sp4**
	Hymedesmia (Hymedesmia) versicolor (Topsent,1893)	***Hymedesmia (Hymedesmia)* sp5**
	Hymedesmia (Stylopus) coriacea (Fristedt, 1885)	***Hymedesmia (Hymedesmia)* sp6**
	Phorbas dendyi (Topsent, 1890)	***Hymedesmia (Hymedesmia)* sp7**
	Phorbas dives (Topsent, 1891)	***Hymedesmia (Hymedesmia)* sp8**
	Phorbas ferrerhernandezi van Soest, 2002	***Hymedesmia (Stylopus)* sp1**

	Phorbas fibulatus (Topsent, 1893)	***Hymedesmia (Stylopus)* sp2**
	***Phorbas fictitus* (Bowerbank, 1866)**	**Hymedesmia sp1**
	***Phorbas taillezi* Vacelet & Pérez, 2008**	***Phorbas* sp1**
	***Phorbas tenacior* (Topsent, 1925)**	***Phorbas* sp2**
	Phorbas topsenti Vacelet & Perez, 2008	***Phorbas* sp3**
	Plocamione dirrhopalina Topsent, 1927	***Plocamionida* sp1**
	Plocamionida ambigua (Bowerbank, 1866)	***Spanioplon* sp1**
	Spanioplon armaturum (Bowerbank, 1866)	
Family LATRUNCULIIDAE		
	Latrunculia (Biannulata) citharistae Vacelet, 1969	***Latrunculia* sp1**
	Sceptrella insignis (Topsent, 1890)	***Latrunculia* sp2**
		***Latrunculia* sp3**
Family MICROCIONIDAE		
	Antho (Antho) inconstans (Topsent, 1925)	***Antho (Antho)* sp.**
	Antho (Antho) involvens (Schmidt, 1864)	***Clathria (Microciona)* sp1**
	***Antho (Antho) oxeifera* (Ferrer-Hernandez, 1921)**	***Clathria (Microciona)* sp2**
	***Clathria (Clathria) coralloides* (Scopoli, 1772)**	***Clathria (Thalysias)* sp.**
	Clathria (Microciona) armata (Bowerbank, 1862)	**Microcionidae sp1**
	Clathria (Microciona) ascendens (Cabioch, 1968)	**Microcionidae sp2**
	Clathria (Microciona) atrasanguinea (Bowerbank, 1862)	**Microcionidae sp3**
	Clathria (Microciona) duplex Sarà, 1958b	***Ophlitaspongia* sp1**
	Clathria (Microciona) gradalis Topsent, 1925	
	Clathria (Microciona) spinarcus (Carter & Hope, 1889)	
	Clathria (Microciona) tenuissima (Stephens, 1916)	
Family MYCALIDAE		
	***Mycale (Aegogrophila) contarenii* (Lieberkühn, 1859)**	

	***Mycale (Aegogropila) rotalis* (Bowerbank, 1874)**	
	***Mycale (Aegogropila) syrinx* (Schmidt, 1862)**	
	***Mycale (Aegogropila) tunicata* (Schmidt, 1862)**	
	***Mycale (Mycale) massa* (Schmidt, 1862)**	
Family MYXILLIDAE		
	Myxilla (Myxilla) macrosigma Boury-Esnault, 1971	***Myxilla (Myxilla)* sp1**
	***Myxilla (Myxilla) rosacea* (Lieberkühn, 1859)**	***Myxilla (Styloption)* sp1**
	Melonanchora emphysema* (Schmidt, 1875)*	***Myxilla* sp.**
	***Myxilla (Myxilla) iotrochotina* (Topsent, 1892)**	
Family TEDANIIDAE		
	Tedania (Tedania) anhelans (Vio in Olivi, 1792)	
Order POLYMASTIIDA		
Family POLYMASTIIDAE		
	Polymastia penicillus (Montagu, 1814)	***Polymastia* sp1**
	***Polymastia polytylota* Vacelet, 1969**	***Polymastia* sp2**
	***Polymastia tissieri* (Vacelet, 1961)**	***Polymastia* sp3**
	Quasillina brevis (Bowerbank, 1861)	***Polymastia* sp4**
	***Spinularia sarsi* (Ridley & Dendy, 1886)**	***Polymastia* sp5**
	Weberella verrucosa Vacelet, 1960	***Polymastia* sp6**
	Pseudotrachya hystrix* (Topsent, 1890)*	***Polymastia* sp7**
		***Radiella* sp1**
		***Radiella* sp2**
Order SCOPALINIDA		
Family SCOPALINIDAE		
	Scopalina azurea Bibiloni, 1993	***Scopalina* sp1**
	Scopalina blanensis Blanquer & Uriz, 2008	**Scopalinidae sp1**

	Scopalina lophyropoda Schmidt, 1862	
Order SUBERITIDA		
Family HALICHONDRIIDAE		
	Amorphinopsis pallescens (Topsent, 1892)	***Halichondria (Halichondria)* sp1**
	Axinyssa aurantiaca (Schmidt, 1864)	***Spongosorites* sp1**
	Axinyssa digitata (Cabioch, 1968)	***Spongosorites* sp2**
	***Ciocalypta penicillus* Bowerbank, 1862**	***Spongosorites* sp3**
	Halichondria (Halichondria) contorta (Sarà, 1961)	***Topsentia* sp1**
	Halichondria (Halichondria) genitrix (Schmidt, 1870)	***Topsentia* sp2**
	Halichondria (Halichondria) panicea (Pallas, 1766)	***Topsentia* sp3**
	Halichondria (Halichondria) semitubulosa (Lamarck, 1814)	**Halichondriidae sp1**
	Hymeniacidon perlevis (Montagu, 1814)	**Halichondriidae sp2**
	Hymeniacidon rugosa (Schmidt, 1868)	**Halichondriidae sp3**
	Spongosorites cavernicola Bibiloni, 1993	**Halichondriidae sp4**
	Spongosorites flavens Pulitzer-Finali, 1983	
	Spongosorites intricatus (Topsent, 1892)	
	Topsentia calabrisellae Bertolino & Pansini, 2015	
	Topsentia garciae Bibiloni, 1993	
	Phakellia hirondellei* Topsent, 1890*	
Family STYLOCORDYLIDAE		
	***Stylocordyla pellita* (Topsent, 1904)**	
Family SUBERITIDAE		
	***Aaptos aaptos* (Schmidt, 1864)**	***Aaptos* sp1**
	Aaptos papillata (Keller, 1880)	***Aaptos* sp2**
	Protosuberites denhartogi van Soest & de Kluijver, 2003	***Protosuberites* sp1**
	Protosuberites ectyoninus (Topsent, 1900)	***Protosuberites* sp2**

	***Protosuberites rugosus* (Topsent, 1893)**	***Protosuberites* sp3**
	Pseudosuberites hyalinus (Ridley & Dendy, 1887)	***Pseudospongosorites* sp1**
	Pseudosuberites sulphureus (Bowerbank, 1866)	***Rhizaxinella* sp1**
	***Rhizaxinella pyrifera* (Delle Chiaje, 1828)**	***Rhizaxinella* sp2**
	Suberites carnosus (Johnston, 1842)	***Suberites* sp1**
	Suberites carnosus var. *Incrustans* (Topsent, 1910)	***Suberites* sp2**
	***Suberites domuncula* (Olivi, 1792)**	***Terpios* sp1**
	Suberites ficus (Johnston, 1842)	
	Suberites massa Nardo, 1847	
	Suberites syringella (Schmidt, 1868)	
	Terpios gelatinosus (Bowerbank, 1866)	
ORDER TETHYIDA		
Family TETHYIDAE		
	Tethya aurantium (Pallas, 1766)	***Tethya* sp1**
	Tethya citrina Sarà & Melone, 1965	***Tethya* sp2**
		***Tethya* sp3**
		***Tethya* sp4**
		***Tethya* sp5**
		***Tethya* sp6**
		Tethyida sp1
		Tethyidae sp.
Family TIMEIDAE		
	Timea fasciata Topsent, 1934	
	Timea hallezi (Topsent, 1894)	***Timea* sp1**
	Timea mixta (Topsent, 1896)	***Timea* sp2**
	Timea unistellata (Topsent, 1892)	***Timea* sp3**

	Timea chondrilloides* (Topsent, 1904)*	
Family HEMIASTERELLIDAE		
	***Hemiasterella elongata* Topsent, 1928**	***Hemiasterella* sp.**
Order TETRACTINELLIDA		
Family ANCORINIDAE		
	Dercitus (Stoeba) plicatus (Schmidt, 1868)	***Jaspis* sp1**
	Jaspis johnstonii (Schmidt, 1862)	***Jaspis* sp2**
	Stelletta dichoclada* Pulitzer-Finali, 1983*	
	***Stryphnus mucronatus* (Schmidt, 1868)**	
	***Stryphnus mucronatus* (Schmidt, 1868)**	
	***Stryphnus ponderosus* (Bowerbank, 1866)**	
Family AZORICIDAE		
	Leiodermatium pfeifferae (Carter, 1873)	
Family CALTHROPELLIDAE		
	Calthropella (Calthropella) pathologica* (Schmidt, 1868)*	
	Calthropella (Corticellopsis) stelligera (Schmidt, 1868)	
Family CORALLISTIDAE		
	Neophrissospongia nolitangere (Schmidt, 1870)	
Family GEODIIDAE		
	Caminella intuta* (Topsent, 1892)*	
	***Penares euastrum* (Schmidt, 1868)**	
	***Penares helleri* (Schmidt, 1864)**	
	Erylus discophorus* (Schmidt, 1862)*	
	Penares candidatus* (Schmidt, 1868)*	
	Penares cavernensis* Díaz & Cárdenas, 2024	
	Penares deficiens* Topsent, 1927*	

	Penares isabellae* Díaz & Cárdenas, 2024	
	Erylus corsicus* Pulitzer-Finali, 1983*	
	Erylus mamillaris* (Schmidt, 1862)*	
	Geodia bibilonae* Díaz & Cárdenas, 2024	
	Geodia cydonium (Linnaeus, 1767)	
	Geodia matrix* Díaz & Cárdenas, 2024	
	Geodia microsphaera* Díaz & Cárdenas, 2024	
	Geodia geodina* (Schmidt, 1868)*	
	Caminus vulcani* Schmidt, 1862*	
	Stelletta mortarium* Díaz & Cárdenas, 2024	
Family PACHASTRELLIDAE		
	***Pachastrella monilifera* Schmidt, 1868**	
	Pacahstrella* cf. *ovisternata* Lendenfeld, 1894*	
	Characella pachastrelloides* (Carter, 1876)*	
	Characella tripodaria* (Schmidt, 1868)*	
	Nethea amygdaloides* (Carter, 1876)*	
Family TETILLIDAE		
	***Craniella cranium* (Müller, 1776)**	
Family THENEIDAE		
	***Thenea muricata* (Bowerbank, 1858)**	
Family THEONELLIDAE		
	Discodermia polymorpha* Pisera & Vacelet, 2011*	
Family THROMBIDAE		
	Thrombus abyssi* (Carter, 1873)*	
Family VULCANELLIDAE		
	***Poecillastra compressa* (Bowerbank, 1866)**	
	Vulcanella gracilis* (Sollas, 1888)*	

	Vulcanella aberrans* (Maldonado & Uriz, 1996)*	
Order TRACHYCLADIDA		
Familiy TRACHICLADIDAE		
	Trachycladus minax (Topsent, 1888)	
Order VERONGIIDA		
Family APLYSINIDAE		
	***Aplysina aerophoba* (Nardo, 1833)**	
	***Aplysina cavernícola* (Vacelet, 1959)**	
Family IANTHELLIDAE		
	Hexadella cf. *dedritifera* Topsent, 1913	
	Hexadella pruvoti Topsent, 1896	***Hexadella* sp1**
	Hexadella racovitzai Topsent, 1896	***Hexadella* sp2**
	Hexadella topsenti Reveillaud, Allewaert, Pérez, Vacelet, Banaigs & Vanreusel, 2012	
DEMOSPONGIAE INCERTAE SEDIS		
	Myceliospongia araneosa Vacelet & Pérez, 1998	
Class Calcarea		
		Calcarea sp1
		Calcarea sp2
		Calcarea sp3
		Calcarea sp4
		Calcarea sp5
		Calcarea sp6
		Calcarea sp7
		Calcarea sp9
		Calcarea sp10
Order BAERIDA		
Family BAERIIDAE		

	Leuconia nivea (Grant, 1826)	
Order LEUCOSOLENIDA		
Family AMPHORISCIDAE		
	Paraleucilla magna Klautau, Monteiro & Borojevic, 2004	
Family LEUCOSOLENIIDAE		
	Leucosolenia botryoides (Ellis & Solander, 1786)	
	Leucosolenia variabilis Haeckel, 1870	
Family GRANTIIDAE		
	Aphroceras caespitosa (Haeckel, 1872)	
	Aphroceras corticata Lendenfeld, 1891	
	Grantia capillosa (Schmidt, 1862)	
	Leucandra aspera (Schmidt, 1862)	
	Leucandra balearica Lackschewitz, 1886	
	Leucandra bolivari Ferrer-Hernández, 1916	
	Leucandra crambessa Haeckel, 1872	
	Leucandra gossei var. mahonica Topsent,1937	
	Leucandra pumila (Bowerbank, 1866)	
	Leucandra rodriguezi (Lackschewitz, 1886)	
Family HETEROPIIDAE		
	Vosmaeropsis gardineri Ferrer-Hernández, 1916	
Family SYCETTIDAE		
	Sycon ciliatum (Fabricius, 1780)	***Sycon* sp1**
	Sycon elegans (Bowerbank, 1845)	
	Sycon humboldti Risso, 1827	
	Sycon raphanus Schmidt, 1862	
	Sycon schmidti (Haeckel, 1872)	
	Sycon setosum Schmidt, 1862	

Order CLATHRINIDA		
Family CLATHRINIDAE		
	Arturia canariensis (Miklucho-Maclay, 1868)	
	Ascandra contorta (Bowerbank, 1866)	
	Borojevia cerebrum (Haeckel, 1872)	
	Clathria blanca (Miklucho-Maclay, 1868)	
	Clathrina clathrus (Schmidt, 1864)	
	Clathrina coriacea (Montagu, 1914)	
	Clathrina primordialis (Haeckel, 1872)	
	Clathrina rubra Sarà, 1958b	
	Ernstia minoricensis (Lackschewitz, 1886)	
Family LEUCASCIDAE		
	Ascaltis reticulum (Schmidt, 1862)	
Family LEUCETTIDAE		
	Leucetta solida (Schmidt, 1862)	
Class HOMOSCLEROMORPHA		
Order HOMOSCLEROPHORIDA		
Family PLAKINIDAE		
	Corticium candelabrum Schmidt, 1862	
	Plakina dilopha Schulze, 1880	
	Plakina trilopha Schulze, 1880	
Class HEXACTINELLIDA		
		Hexactinellida sp1
Order AMPHIDISCOSIDA		
Family HYALONEMATIDAE		
	Hyalonema (Cyliconema) thomsoni Marshall, 1875	

Family PHERONEMATIDAE		
	Pheronema carpenteri (Thomson, 1869)	
Order LYSSACINOSIDA		
Family ROSSELLIDAE		
	Lanuginella* cf. *pupa* Schmidt, 1870*	***Sympagella* sp1**
Order SCEPTRULOPHORA		
Family FARREIDAE		
	Farrea bowerbanki Boury-Esnault, Vacelet & Chevaldonné, 2017	
Family TRETODICTYIDAE		
	***Tretodictyum reiswigi* Boury-Esnault, Vacelet & Chevaldonné, 2017**	

**Taxa described in this phD*

*** New geographical reports documented in this phD.*

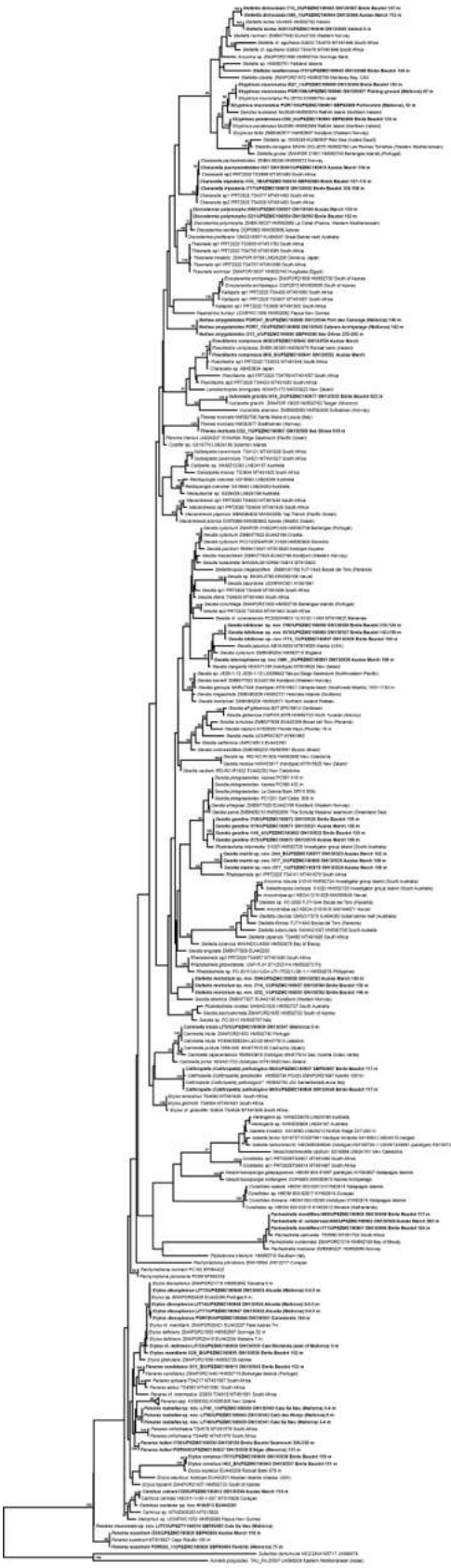

Supplementary Fig. 1. Tetractinellid COI maximum likelihood (ML) tree reconstructed with RAxML. ML bootstrap supports (1,000 bootstrap replicates) > 80 are indicated. Specimen codes are written as "field number/museum number" followed by Genbank accession number. In bold are new sequences produced in this study.

Supplementary Fig. 2. Tetractinellid 28S maximum likelihood (ML) tree reconstructed with RAxML. ML bootstrap supports (1,000 bootstrap replicates) > 80 are indicated. Specimen codes are written as "field number/museum number" followed by Genbank accession number. In bold are new sequences produced in this study.

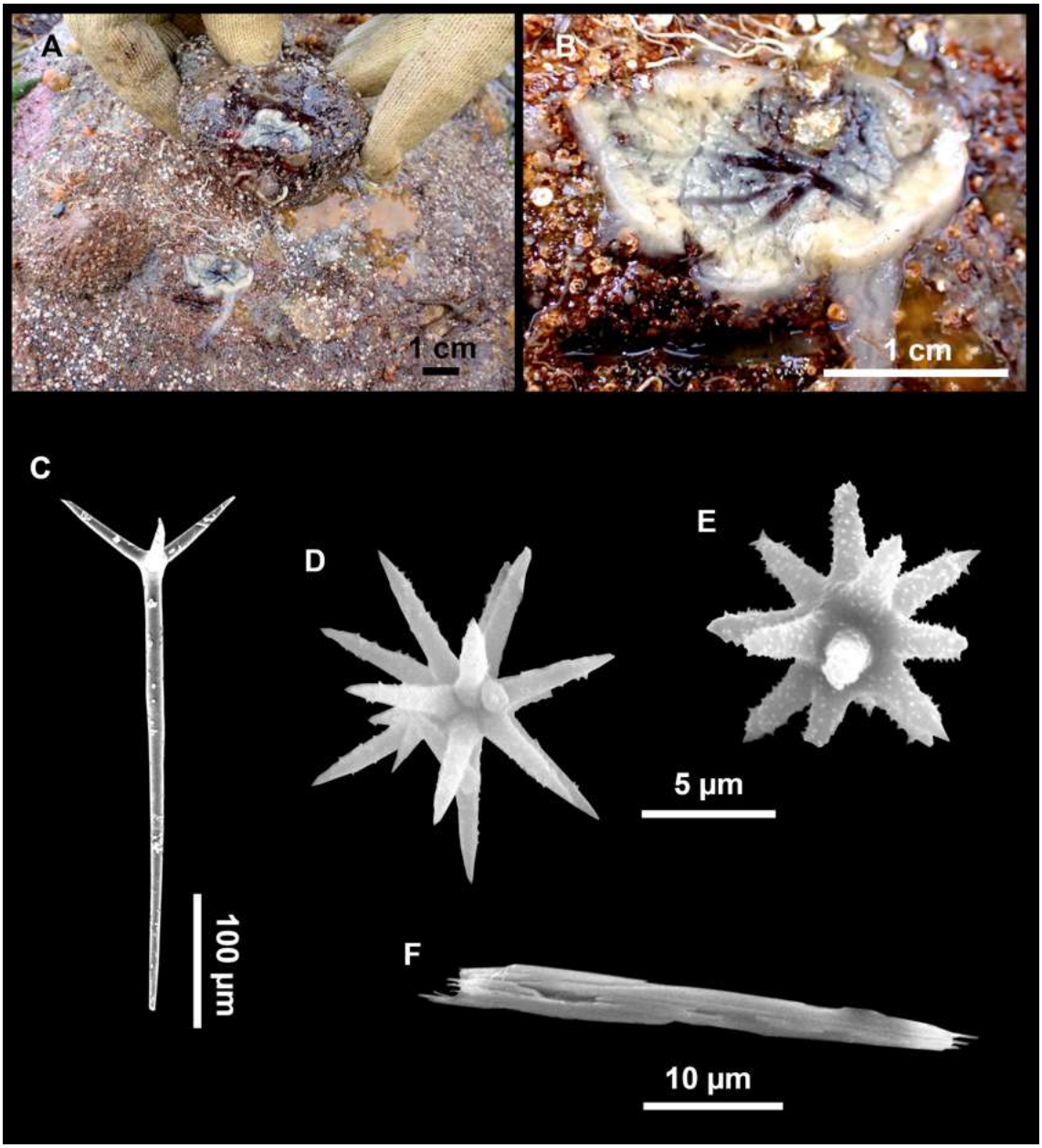

Supplementary Fig. 3. *Stelletta lactea* Carter, 1871, UPSZMC 190949. (A-B) In situ images (image courtesy of Christine Morrow). (C) Plagiotriaene. (D-E) Oxyasters to strongylasters. (F) Trichodragmas.

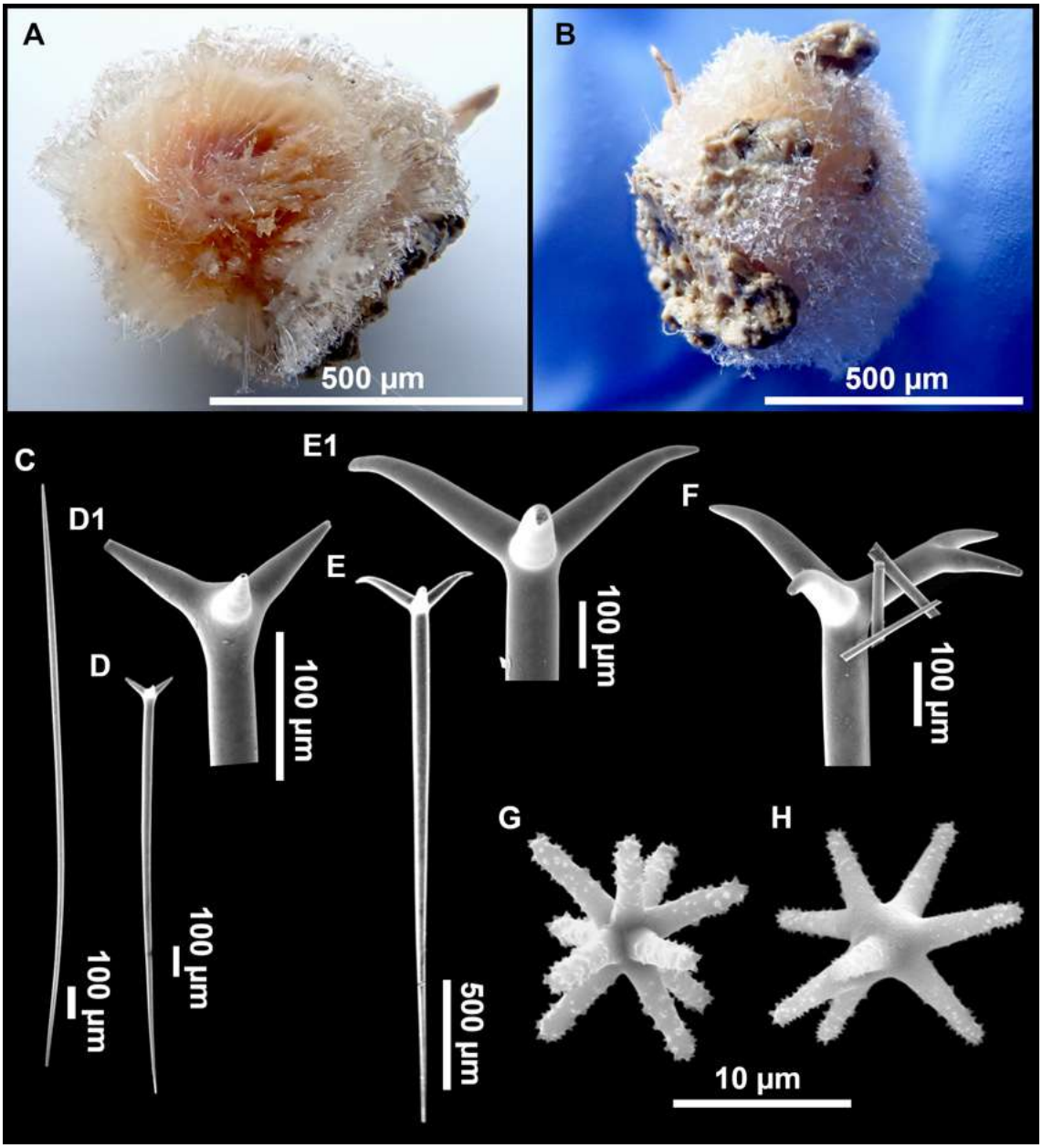

Supplementary Fig. 4. Holotype of Stelletta defensa (Pulitzer-Finali, 1983), MSNG 47153.
(A-B) Habitus, on a transversal and an upper-body view. (C-H) SEM images of the spicules. (C) Oxeas, (D-D1 and E-E1) Protriaenes with outwards-pointed and curved tips, respectively. (F) Dichotriaene, (G-H) Strongylasters.